

Foundations of Biochemical Engineering

Foundations of Biochemical Engineering

Kinetics and Thermodynamics in Biological Systems

Harvey W. Blanch, EDITOR
University of California, Berkeley

E. Terry Papoutsakis, EDITOR
Rice University

Gregory Stephanopoulos, EDITOR
California Institute of Technology

Based on the 1982 Winter Symposium
of the ACS Division of Industrial
and Engineering Chemistry jointly
sponsored by the Division of Microbial
and Biochemical Technology,
Boulder, Colorado,
January 17–20, 1982

A C S S Y M P O S I U M S E R I E S **207**

AMERICAN CHEMICAL SOCIETY
WASHINGTON, D.C. 1983



Library of Congress Cataloging in Publication Data

American Chemical Society. Division of Industrial and Engineering Chemistry. Winter Symposium (1982: Boulder, Colo.)

Foundations of biochemical engineering.

(ACS symposium series, ISSN 0097-6156; 207)

Includes bibliographies and index.

1. Biochemical engineering—Congresses.

I. Blanch, Harvey W., 1947- . II. Papoutsakis, E. Terry, 1951- . III. Stephanopoulos, G. IV. American Chemical Society. Division of Industrial and Engineering Chemistry. V. American Chemical Society. Division of Microbial and Biochemical Technology. VI. Title. VII. Series.

TP248.3.A48 1982 660'.63 82-20694
ISBN 0-8412-0752-6

Copyright © 1983

American Chemical Society

All Rights Reserved. The appearance of the code at the bottom of the first page of each article in this volume indicates the copyright owner's consent that reprographic copies of the article may be made for personal or internal use or for the personal or internal use of specific clients. This consent is given on the condition, however, that the copier pay the stated per copy fee through the Copyright Clearance Center, Inc. for copying beyond that permitted by Sections 107 or 108 of the U.S. Copyright Law. This consent does not extend to copying or transmission by any means—graphic or electronic—for any other purpose, such as for general distribution, for advertising or promotional purposes, for creating new collective work, for resale, or for information storage and retrieval systems. The copying fee for each chapter is indicated in the code at the bottom of the first page of the chapter.

The citation of trade names and/or names of manufacturers in this publication is not to be construed as an endorsement or as approval by ACS of the commercial products or services referenced herein; nor should the mere reference herein to any drawing, specification, chemical process, or other data be regarded as a license or as a conveyance of any right or permission, to the holder, reader, or any other person or corporation, to manufacture, reproduce, use, or sell any patented invention or copyrighted work that may in any way be related thereto.

PRINTED IN THE UNITED STATES OF AMERICA

**American Chemical
Society Library
1155 16th St., N.W.**

In Foundations of Biochemical Engineering; Blanch, H., et al.;
ACS Symposium Series; American Chemical Society: Washington, DC, 1983.

Washington, D.C. 20036

ACS Symposium Series

M. Joan Comstock, *Series Editor*

Advisory Board

David L. Allara

Robert Baker

Donald D. Dollberg

Brian M. Harney

W. Jeffrey Howe

Herbert D. Kaesz

Marvin Margoshes

Donald E. Moreland

Robert Ory

Geoffrey D. Parfitt

Theodore Provder

Charles N. Satterfield

Dennis Schuetzle

Davis L. Temple, Jr.

Charles S. Tuesday

C. Grant Willson

FOREWORD

The ACS SYMPOSIUM SERIES was founded in 1974 to provide a medium for publishing symposia quickly in book form. The format of the Series parallels that of the continuing ADVANCES IN CHEMISTRY SERIES except that in order to save time the papers are not typeset but are reproduced as they are submitted by the authors in camera-ready form. Papers are reviewed under the supervision of the Editors with the assistance of the Series Advisory Board and are selected to maintain the integrity of the symposia; however, verbatim reproductions of previously published papers are not accepted. Both reviews and reports of research are acceptable since symposia may embrace both types of presentation.

PREFACE

THIS VOLUME IS BASED on the 1982 Winter Symposium. Following recent tradition, this Winter Symposium was organized to provide a forum for expression of new ideas and new research approaches.

This volume discusses the fundamentals of biotechnology; that is, kinetics and thermodynamics in biological systems. State-of-the-art keynote chapters by established researchers are employed to provide the proper perspective and direction. Other chapters present new, less settled research approaches.

In the last few years biotechnology has grown tremendously in scope and significance, both as an active research area and as an industrial activity. There has also been a clear trend toward the exploration of the most sophisticated aspects of biological growth: tissue cultures, active biomolecules, antitumor compounds, chemical feedstocks from biomass, and gene cloning, to mention only a few. This trend has been accompanied by the increased use of computers in the design and control of the biological reactor.

The explosive growth of the field and the use of computers have magnified, however, a fact that had been realized for quite some time by a few. That is, that the kinetics and thermodynamics of biochemical reactions and biological growth are understood only primitively. We should remind ourselves that biological systems are immensely more complicated than the nonbiological systems upon which most of chemical technology is based. We should not forget that until quite recently there were relatively few active investigators in biotechnology throughout the world, and that most of these were microbiologists by training. This has changed dramatically, however, as biotechnology has become a common word among biochemists, cell geneticists, molecular biologists, gene cloners, engineers, protein chemists, and others.

In preparing this book, we strived to stress two things:

- the interdisciplinary nature of biotechnology. We thus made every effort to bring together prominent researchers from both the life sciences and biochemical engineering.
- the need to examine the fundamentals of biotechnology more systematically and vigorously. We believe that no structure can grow well and last long without good foundations.

The topics in this volume represent both keynote chapters and chapters on new research. They have been arranged in six sections, such that each section builds on the preceding one. The volume begins with an examination of fundamental biochemical events in the cells. It proceeds with the examination of the interaction of the biochemical events that constitute the growth of an individual cell; then it examines homogeneous and heterogeneous cell populations. The book continues with thermodynamic aspects of biological growth, and ends with the application of all of the above to bioreactor design.

Obviously, completeness has been sacrificed to diversity. We felt that the examination of the interactions among these fundamental aspects was more important than looking in depth at only a few of these aspects. Most of you would agree that ongoing research is a vital and exciting process, consisting of active and often heated interactions of data, ideas, and minds. We hope that the readers of this book will feel that they are participating in this process.

In putting together the symposium on which this book is based, we relied on the judgement, help, and advice of many colleagues, to whom we express our sincere thanks. We also thank the organizing committee of the Winter Symposia of the Division of Industrial and Engineering Chemistry and, in particular, the former chairman of the committee, Nicholas A. Peppas. Thanks are also due to R. W. Eltz, chairman of the Division of Microbial and Biochemical Technology of the American Chemical Society, joint sponsor of the symposium. We are sincerely indebted to Steve Drew of Merck, Sharp & Dohme Research Laboratories for bringing us the private sector's views on the symposium's theme.

HARVEY W. BLANCH
University of California
Berkeley, CA

E. TERRY PAPOUTSAKIS
Rice University
Houston, TX

GREGORY STEPHANOPOULOS
California Institute of Technology
Pasadena, CA

June 1, 1982

ACKNOWLEDGMENTS

Financial assistance for the 1982 Winter symposium was received from
National Science Foundation

and

Abbott Laboratories
Beckman Instruments, Inc.
Becton Dickinson and Company
Carnation Company
Chevron Research Company
E.I. du Pont de Nemours & Company, Inc.
Eastman Kodak Company
Exxon Research and Engineering Company
General Mills, Inc.
Gist-Brocades NV Research & Development
Glaxo Operations UK Limited
W. R. Grace & Company
Gulf Research and Development Company
Hoffmann-La Roche, Inc.
Kraft, Inc.
Merck Sharp and Dohme Research Laboratories
Monsanto Company
PPG Industries, Inc.
Pfizer, Inc.
Phillips Petroleum Company
The Procter and Gamble Company
Stauffer Chemical Company
Syntex Corporation
Weyerhaeuser Company

Models of Gene Function

General Methods of Kinetic Analysis and Specific Ecological Correlates

MICHAEL A. SAVAGEAU

University of Michigan, Department of Microbiology and Immunology,
Ann Arbor, MI 48109

Alternative molecular designs for gene control involving positive or negative elements are directly related to the natural environment of the organism that harbors them: positive elements are associated with high demand for expression of the regulated structural genes; while negative elements are associated with low demand for their expression. This is called the demand theory of gene regulation. These results are based on a mathematical analysis of the alternative models. The formalism used is a general one involving power-law functions that has been developed previously for the mathematical analysis of complex biological systems. This formalism, which is of interest in its own right, is briefly reviewed, although details of the analysis are not presented. The principal steps in the development of the demand theory are presented and the molecular, physiological and ecological implications are made explicit. This theory is supported by experimental evidence from more than 40 different systems and is used to make testable experimental predictions for more than 14 additional systems.

The primary purpose of this symposium is to have biologists and engineers examine the interdisciplinary area of biotechnology from the fundamental perspective of kinetics and thermodynamics. As with any interdisciplinary area, particularly one undergoing rapid change and intellectual ferment, biotechnology means different things to different people. It is therefore appropriate to give a thumb-nail sketch of this area as I see it.

Biotechnology is as old as recorded history. The early domestication of microorganisms for wine making, brewing, baking and food preservation is a prime example graphically depicted on

0097-6156/83/0207-0003\$06.75/0

© 1983 American Chemical Society

Egyptian tombs (1). Of course, this was a very empirical art that advanced only slowly. Even in more recent times, during the post-war expansion of modern industrial technology, there has been important biotechnology, e.g., as a sector of modern pharmaceutical and chemical industries. Throughout this past, the biological component has often been the weakest link in the overall bio-technology chain. To be sure, there was mass balance and the Monod growth law, which helped to predict the behavior of the biological component, but that was about all. One generally had to live with the uncertainties inherent in the biological component of the overall system.

Recent developments in biology have ushered in a "revolution" in our knowledge of the cell, particularly the microbial cell. For the familiar bacillus Escherichia coli 3/5 to 4/5 of all its molecular elements are known and new protein separation techniques are speeding this identification process to a conclusion. Thus, we shall soon have the complete catalogue of E. coli parts. However, we still know relatively little about the integrated behavior of the cell, how it will behave when its molecular elements are changed or when it finds itself in a novel environment.

The full potential of biotechnology will be realized, in my view, only when (a) the biological component is brought within the realm of engineering design and (b) engineering methods of systems analysis and prediction are brought within the realm of cell and molecular biology. Only then will there be a strong unitary biotechnology. In the last few years developments in recombinant DNA methodology have shown that the first of these objectives is now feasible. There also has been progress toward the second objective, but there is still much to be done here.

In this paper I shall first review briefly some of our own attempts to develop general methods of kinetic analysis that are appropriate for complex biological systems. Next I shall discuss the application of these methods to alternative models of gene regulation. The result of such an analysis is the demand theory of gene regulation in which the molecular nature of genetic regulatory systems is directly related to the demand for gene expression, as determined by the organism's ecological niche.

Power-law Formalism

Early efforts to analyze biological systems were blinded by the success that engineers have had in analyzing complex technological (often electrical and mechanical) systems and by the power and elegance of the mathematical methods at their disposal. Over a period of years the effort to make biological phenomena fit into the same mold became increasingly frustrated. Biological phenomena are highly nonlinear and cannot be made to wear the linear straight jacket that technological systems often submit to willingly. Furthermore, the types of nonlinearities that are

found in technological systems are very different from those found in biological systems. On the other hand, disenchantment set in with the then fashionable approach of piecing together in an ad hoc manner complex computer models that could be "adjusted" until they came to mimic some aspect of the biological phenomenon under study. In formulating our approach to these problems, we decided to go back and start from scratch. This required going back to fundamental kinetics, identifying the essential character of biological nonlinearities, and attempting the development of a mathematical formalism rooted in basic biology and specifically designed to deal with these types of systems.

The fundamental kinetic description of the underlying mechanisms in biological systems involves rational-function nonlinearities (2-4). Although in principle these functions can accurately represent any mechanism of interest, they are mathematically much too complicated for use in analyzing biological systems composed of many such mechanism (3). Thus, some form of simplifying approximation is required for these systems; such methods must capture the essential nonlinear attributes of biological phenomena and yet be sufficiently simple so that complex biological systems can be handled mathematically. These methods also should yield a standard or canonical form to facilitate comparisons of alternative models and to allow analysis of a priori as well as ad hoc models. Although these are ideals and no currently available method of kinetic analysis fully satisfies all of these requirements, a method based on power-law functions is particularly promising.

Derivation of the Basic Equations. The basic equations are obtained by forming the Taylor series expansion of the rational function in a logarithmic space and then retaining only the constant and linear terms (2,5,6,3). This procedure yields a product of power functions in the corresponding Cartesian space.

The functional equations describing a general system of n elements different in kind and/or location are composed of sums and differences of rational functions, but since the sum of two rational functions is also a rational function, the system of equations can be rewritten as a simple difference between two composite rational functions that are each positive.

When these composite rational functions are approximated by power-law functions, the description of the entire system can be written (5,7,3,4):

$$dX_i/dt = \alpha_i \prod_{j=1}^n X_j^{g_{ij}} - \beta_i \prod_{j=1}^n X_j^{h_{ij}} \quad (1)$$

$$i = 1, 2, \dots, n$$

The behavior of complex biological systems is determined by the nature of the underlying mechanisms and their abundant interrelationships, as expressed mathematically in Eqn. (1).

Exact Representation. Although the power-law formalism was originally derived as an approximation, one can often obtain an exact representation of rational-function nonlinearities by introducing additional variables (8). This obviously extends the generality and utility of the power-law formalism. Any disadvantage caused by the increase in number of variables is more than offset by the decrease in complexity of the nonlinearities. The number of parameter values plus initial conditions necessary to characterize a system remains the same in either representation.

This procedure allows a set of differential equations involving rational functions, which in general have no standard form, to be transformed into an equivalent set involving power functions, which do have a standard form. This greatly facilitates modeling and analysis. One can easily alter the model or change conditions without rewriting equations, functions, or subroutines. One simply inserts an alternative set or subset of parameter values into the standard format. This has allowed us to develop a standardized set of efficient computer algorithms for graphical interactive modeling and analysis of biological systems.

Justification. The power-law formalism is justified by four types of evidence. First, its validity rests on theoretical grounds. Because the approximation is derived using Taylor's theorem, it is guaranteed to be an accurate representation at least over a certain range of values for the concentration variables. Because the approximation is nonlinear, the range of validity is considerably greater than that for the corresponding linear approximation. Second, the power-law formalism has been justified by direct experimental observation of reactions in situ. Kohen et al. (9) have examined the kinetics of individual biochemical reactions within living cells and found that these are best described by power-law functions of the reactant concentrations. Third, this formalism predicts that in a series of steady states the concentration variables should be related to one another by a straight line in a log-log plot. The range of concentration values for which a straight-line relation holds corresponds to the range of validity for the approximation. A number of different systems have been examined previously in this regard and the approximation was found to be valid for more than a 100-fold change in concentration variables (3). Finally, one can derive a general growth law (4,10) in this formalism and ask to what extent real systems adhere to the law. As it turns out, all of the well-established growth laws that one finds in the biological literature are special cases of this general growth law (4,10). There are a number of other implications that have been

deduced with this formalism and tested against experimental evidence, and agreement has been found (e.g., see Ref. 11). Thus, the agreement between theoretical predictions and a large number of independent experimental observations provides a wealth of evidence justifying use of the power-law formalism.

Principal Advantages. There are a number of difficulties associated with the modeling and analysis of complex nonlinear systems. (a) The functional form of the nonlinearities is often unknown, as are the numbers of interactions and parameters that must be specified. (b) Once one has assumed a functional form there is still difficulty in extracting statistical estimates of the parameter values from experimental data. (c) The amount of experimental data itself that is required to characterize many nonlinear mechanisms increases exponentially with the dimensions of the problem. (d) General methods for analyzing the resulting system of nonlinear equations are not available.

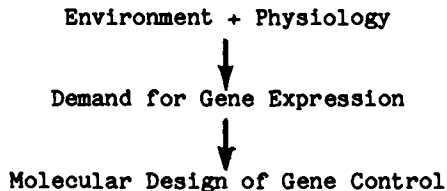
Linear analysis largely overcomes these difficulties. However, there is a considerable cost. It is valid for only small variations in the concentration variables and this is usually unrealistic for most biological systems of interest.

The power-law formalism provides a judicious compromise that has many of the advantages of linear analysis without its severe limitations. (a) The functional form is known and the interactions and parameters are readily specified. (b) From experimental data one can extract parameter values for the individual rate laws by linear regression in a logarithmic space. (c) The data necessary for such an analysis has a polynomial (rather than exponential) increase with the dimensions of the problem. (d) General methods for obtaining steady-state solutions are available by transforming the problem into linear terms. General purpose computer algorithms have been developed for dynamic solutions, and parameter estimation from integrated system behavior is also possible. (For more detailed discussion of the advantages and disadvantages of this and other approaches to the modeling and analysis of nonlinear systems, see Ref. 3.)

This concludes my brief review of the kinetic methods that we have developed for dealing with complex biological systems. These methods already have been applied to a variety of biochemical and genetic systems (e.g., see Ref. 3). However, for the remainder of this paper I shall treat one particular application in some detail.

Demand Theory of Gene Regulation

The central theme that I would like to emphasize in this application is summarized graphically as follows:



By the conclusion of this paper you will come to appreciate the logic and implications of this diagram, and, as you will see, the message is a simple but general one.

Alternative Molecular Designs. Let us begin with the influential model of Jacob and Monod (12) shown in Figure 1. Note that control is exercised by a repressor protein that affects the initiation of transcription. For many years this was the favorite paradigm of biologists concerned with the normal processes of homeostasis, growth and differentiation, as well as their pathological manifestations--infectious diseases, inborn genetic errors and cancer. By almost any criterion this has been one of the most fruitful ideas in modern biology.

What is the evidence for its validity? Bacterial systems were the first to be understood in sufficient molecular detail to test these ideas. There is now good evidence supporting this mode of regulation in many prokaryotic systems (13). However, in recent years evidence for alternative molecular designs also has been accumulated.

In some systems the regulatory protein is not a repressor but an activator that is necessary for the initiation of transcription. The example most often cited is the arabinose catabolic operon of E. coli (14). A schematic model is shown in Figure 2. The N-gene product of bacteriophage lambda is another example of a positive-acting regulator protein, but in this case it acts as an antiterminator modulating the termination of RNA transcripts before they can be extended into the regulated structural genes (15-19). A schematic model of this mechanism is given in Figure 3. We can predict a third alternative in which the regulatory protein is a negative-acting proterminator affecting the termination of RNA transcripts at a site that precedes the regulated structural genes (see Figure 4).

Details of these alternatives, and the terminology that I shall adopt in discussing them, are given in the captions of Figures 1-4 and summarized in Table I. There are a number of established variations on these themes. Although we are currently at a loss to rationalize the entire variety of molecular designs, some success in understanding the role of positive vs negative elements has been achieved with the demand theory of gene regulation (20).

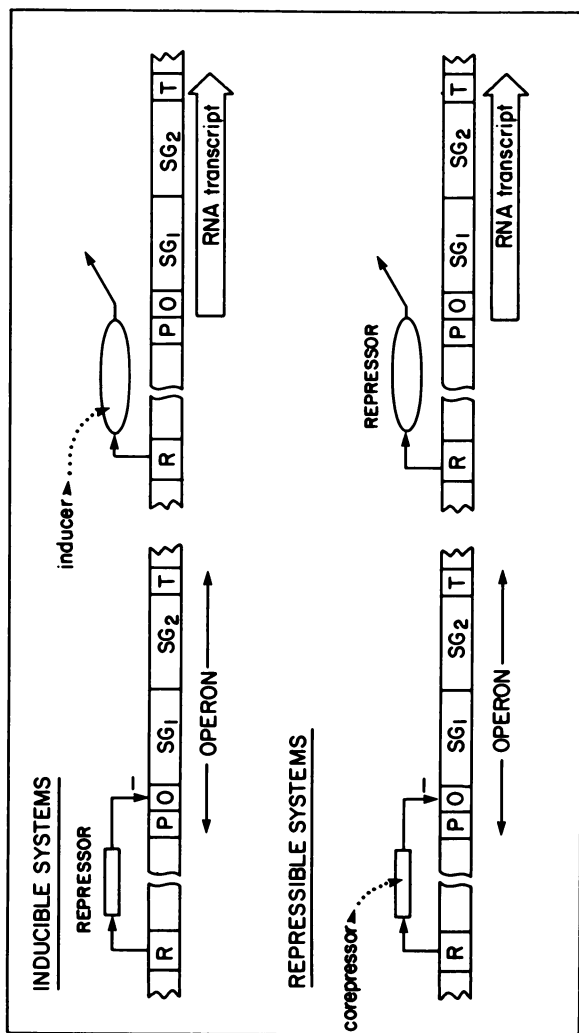


Figure 1. Repressor control of transcription initiation. A regulatory gene, R, codes for a repressor protein. Structural genes, SG, are preceded by a control region in the DNA consisting of a promoter site, P, and a modulator site, O.

In an inducible system, the repressor protein normally binds to a modulator site called the operator, O, and consequently blocks transcription of the adjacent structural genes. However, when the specific inducer for the system is present in an appropriate environment, inducer binds to the repressor and alters its conformation so that the repressor is released from the operator site. The promoter site is thereby freed, and the transcription machinery can initiate synthesis of mRNA. The mRNA, in turn, is translated to yield the protein products of the operon. In a repressible system, the operon is normally expressed because the repressor protein normally has a conformation that prevents its binding to the operator site. However, when the specific corepressor for the system is present, corepressor binds to the (apo)repressor protein and alters its conformation so that repressor now binds the operator and blocks the initiation of transcription at the promoter site.

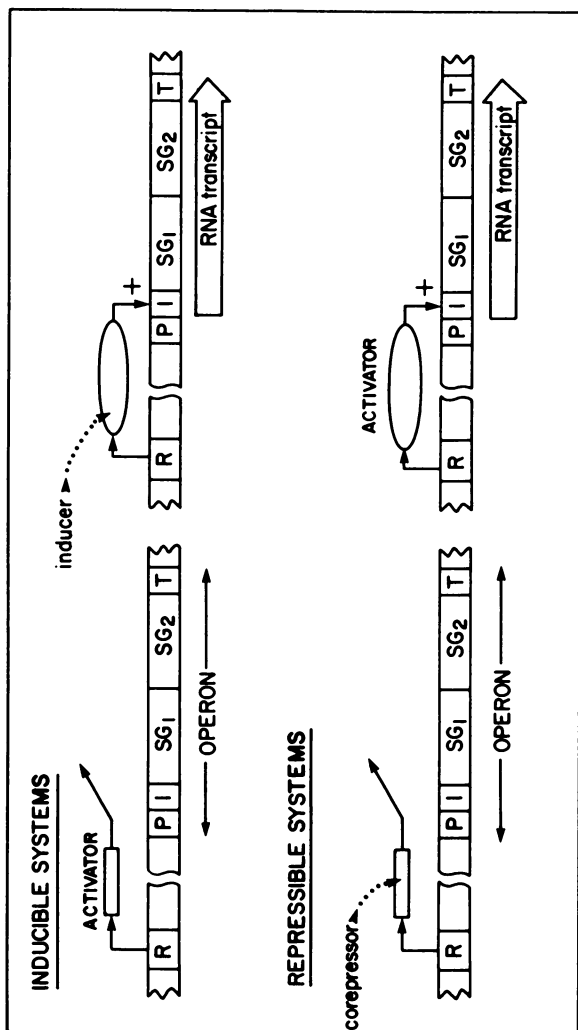


Figure 2. Activator control of transcription initiation. A regulatory gene, R, codes for an activator protein. Structural genes, SG, are preceded by a control region in the DNA consisting of a promoter site, P, and a modulator site, I.

In an inducible system, the activator protein normally has a conformation that prevents it from interacting with a modulator site called the initiator, I. Without this specific interaction, transcription is not initiated and there is no expression of the operon. However, when inducer is present in an appropriate environment, activator is converted to a conformation that can bind the initiator site and facilitate the initiation of transcription at the promoter. In a repressible system, the activator protein normally interacts with the initiator site to facilitate initiation of transcription. However, when the specific corepressor (antagonist) is present, activator is no longer able to facilitate the initiation of transcription at the promoter site and expression of the operon is turned off. See also Figure 1.

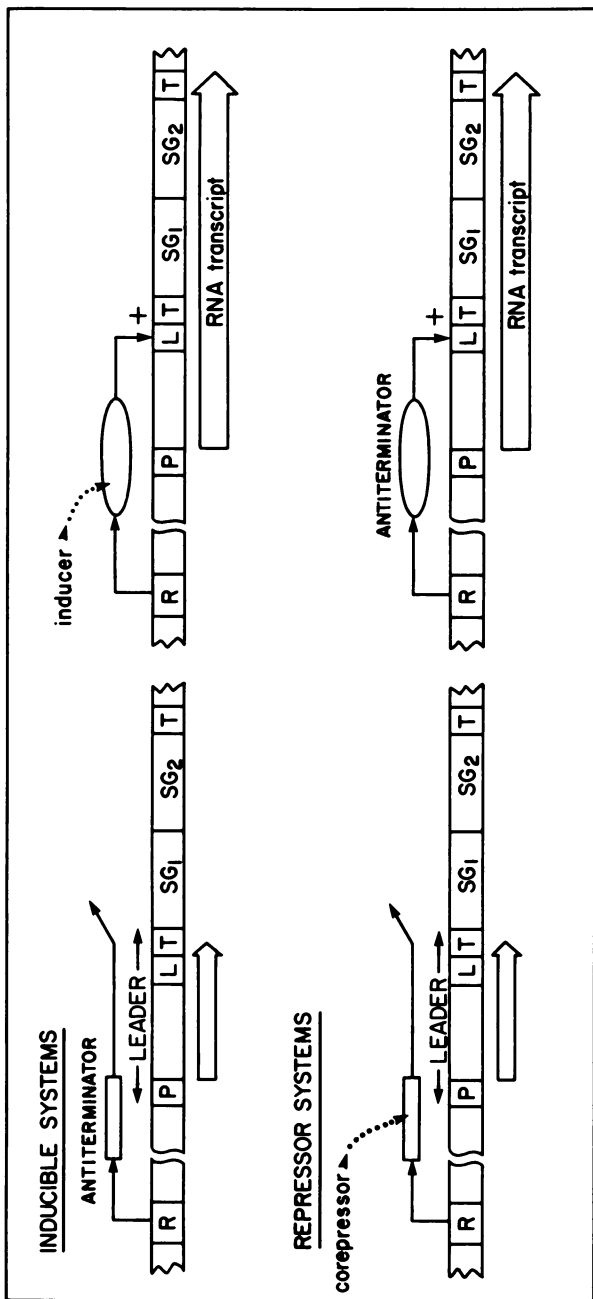


Figure 3. Antiterminator control of transcription termination. A regulatory gene, R, codes for an antiterminator protein. The control region of DNA preceding the structural genes, SG, which in Figures 1 and 2 consisted of modulator and promoter sites, has been expanded and redefined as the "leader region," which begins with a promoter, P, and ends with a terminator, T. (For simplicity, initiation of transcription is assumed to occur constitutively at the promoter.)

In an inducible system, the antiterminator protein normally is not able to interact with a modulator site (called the liberator, L) and transcripts initiated at P terminate at T. However, under inducing conditions when the antiterminator protein interacts with the liberator site, the transcription machinery is freed from the influence of the terminator T, and the transcripts initiated at P continue on through the adjacent structural genes. In a repressible system, the antiterminator protein normally interacts with the liberator site and there is expression of the adjacent structural genes. However, under repressing conditions when the antiterminator protein no longer interacts with the liberator, transcripts initiated at the promoter, P, terminate at the terminator, T.

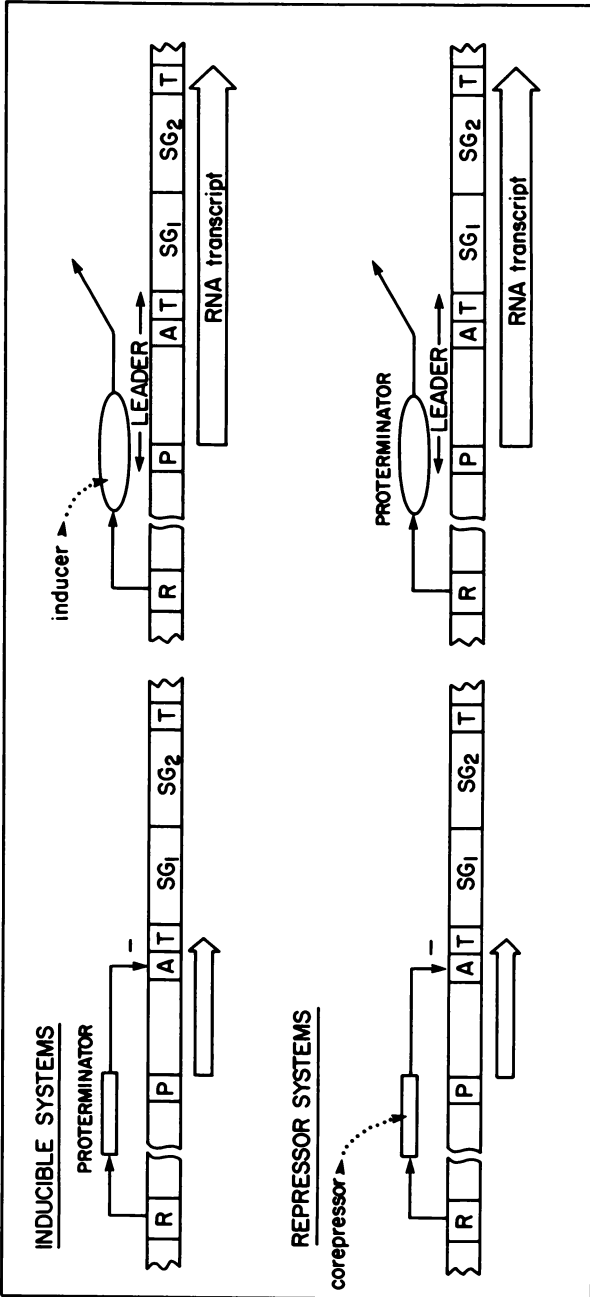


Figure 4. Proterminator control of transcription termination. A regulatory gene, R, codes for a proterminator protein. The leader region preceding the structural genes, SG, extends from the promoter, P, to the terminator, T, with its associated modulator site, A.

In an inducible system, the proterminator protein normally interacts with a modulator site called the arrestor, A, to facilitate termination of transcription at T. However, under inducing conditions the proterminator is unable to interact with the arrestor site and transcripts initiated at the promoter, P, can be extended beyond the terminator, T, through the adjacent structural genes. In a repressible system, the proterminator protein normally is unable to interact with the arrestor site, and there is transcription through the structural genes resulting in expression of the operon. However, under repressing conditions, when the proterminator protein interacts with the arrestor site to facilitate termination of transcripts at T, expression of the operon is turned off. See also Figure 3.

Why are there positive and negative mechanisms of regulating gene expression? Are these differences simply historical accidents representing equivalent evolutionary solutions to the same regulatory problem, as some have claimed? Alternatively, have they been selected for their ability to perform specific functions and, if so, can we discover what these may be?

These are important biological questions that are difficult to answer by using only the direct experimental approach. For example, one can not simply compare representative examples of systems regulated by positive (e.g., the maltose operon) and negative (e.g., the lactose operon) elements. This is not a well-controlled experiment. In other cases, an alternative may not be available for such a comparative test because it may exist in an undiscovered state. Ideally one would like a well-controlled comparison. For some systems, this may soon be possible through the imaginative use of genetic engineering. However, when there are a large number of logical alternatives to test, as there generally are, this approach becomes impractical. At the present time, it is much more practical to simulate such experiments by appropriate mathematical analysis and, ultimately, this may be the only acceptable approach for dealing with more general questions.

I have used such an approach in an attempt to answer the question, why positive and negative mechanisms of gene regulation? In what follows I shall not be concerned with the mathematical methods per se. Instead, my approach will be to outline the principal steps in the development of the theory and then emphasize the most important results.

Development of the Theory. What I have called the demand theory of gene regulation may be summarized as follows. The regulatory element will be positive (e.g., activator; antiterminator) when in the natural environment there is a high demand for expression of the regulated structural genes; it will be negative (e.g., repressor, proterminator) when there is a low demand (20-22). The development of this theory begins with an assessment of the functional differences between positive and negative mechanisms of regulation. Detailed analysis of the alternative mechanisms has shown that in most respects they behave identically. The inherent differences appear in response to common regulatory mutations (3). To discern the implications of these functional differences one asks how frequently these mutations arise and how the mutant organisms fare in their natural environment when competing with the wild-type parent organism. An analysis of the relevant population dynamics yields the results shown in Table II. Thus, a correlation is predicted between the (positive or negative) nature of the regulator and the normal demand for expression of the regulated structural genes: positive with high demand; negative with low demand.

Table I. Terminology

Nature of control	Regulator molecule	Modulator site	Transcript delimiter
Negative	Repressor	Operator	Promoter
Positive	Activator	Initiator	Promoter
Negative	Proterminator	Arrestor	Terminator
Positive	Antiterminator	Liberator	Terminator

Table II. Predicted correlation between regulatory mechanism and demand

Demand	Regulatory mechanism	
	Positive	Negative
High	Functional regulatory mechanism selected	Regulation lost through genetic drift
Low	Regulation lost through genetic drift	Functional regulatory mechanism selected

Physiology and Demand. In order to make this correlation useful, we need to know what high/low demand means in different physiological contexts. Table III lists several different types of physiological functions that have been identified in microorganisms and their phages, and the associated environmental condition corresponding to high demand. For example, when an amino acid is absent from an organism's environment, the organism must synthesize that amino acid endogenously. Thus, expression of the corresponding amino acid biosynthetic operon is in high demand. When a given carbon source is absent from an organism's environment and, therefore, cannot be utilized, expression of the corresponding catabolic operon is in low demand. If gene exchange between organisms occurs infrequently, then expression of the genes coding for the exchange machinery itself will be in low demand.

Ecology and Demand. Physiology and demand ultimately relate to the natural environment of the organism. Since most well-studied systems are found in enteric bacteria and their phages, I shall focus on their environment. This has the advantage of providing a large number of experimental results with which to test the theory.

The lower intestinal tract of warm-blooded animals is the principal habitat of these microbes. It is a rather complex ecosystem that is poorly understood. The local environment to which the microbes are exposed depends upon the diet, physiology and immunological state of the host, the microorganisms that share the same general habitat, as well as complex physical and geometrical factors. Nevertheless, one can estimate the levels of certain constituents of this microenvironment. I shall describe two types of estimates: those made indirectly from measurements of absorption by the host and those made directly from measurements of intestinal contents.

The host enzymes that cleave various dietary substances to allow absorption by the host are not uniformly distributed along the intestinal tract. Some are located in the proximal portion of the small intestine (e.g., the lactase enzymes); others are located in the distal portion of the small intestine and in the colon itself (e.g., the maltase enzymes). This localization alone allows one to make certain inferences about the presence or absence of the substrates for these cleavage and absorption enzymes. Furthermore, the different absorption systems within the same general region often exhibit very different activities. For example, the host's transport system for the absorption of galactose is very active and nearly impossible to saturate under physiological conditions; whereas that for the absorption of arabinose is relatively ineffective. Thus, from indirect information concerning the relative abundance of various substances in the diet, the localization of host enzyme systems that permit absorption of these, and the rates at which absorption

Table III. Physiology and demand

Type of system	Condition corresponding to high demand for expression
Repressible scavenging pathway	Substrate seldom present in high concentrations
Repressible drug sensitivity	Drug frequently present in high concentrations
Repressible biosynthetic pathway	End product seldom present in high concentrations
Inducible biosynthetic enzymes	End product seldom present in high concentrations
Inducible catabolic pathways	Substrate frequently present in high concentrations
Inducible detoxification pathway	Substrate frequently present in high concentration
Inducible genetic exchange	Genetic exchange frequently occurs
Inducible repair response	Repair response frequently required
Inducible toxin production	Toxin frequently produced
Inducible biosynthesis of surface antigens	Antigenic determinants frequently required

by the host occurs, one can estimate the relative concentrations of substances to which the enteric microorganisms are exposed in the colon (21,3). For example, the affinities of various sugars for transport systems in the intestine can be ranked as follows: (High) D-glucose > D-galactose > glycerol; (Low) D-xylose > L-glucose > L-mannose > L-fucose > L-rhamnose > L-arabinose. It should be emphasized that this ranking is only sufficient (at least in the extreme cases) to determine whether a given sugar has a "high" or "low" relative concentration in the colon.

Amino acid levels in the colon have been measured more directly. Samples were removed from various locations along the intestinal tract with a catheter and their amino acid content was analyzed (23). The pattern of relative concentrations, which is independent of diet, can be summarized as follows: (High) lysine > glutamate > arginine > tyrosine > tryptophan; (Low) glycine > leucine > phenylalanine > histidine > alanine > serine > valine > aspartate > proline > threonine > cysteine > isoleucine > methionine. Again, the ranking is only sufficient to determine whether a given amino acid has a "high" or "low" relative concentration in the colon.

Experimental Implications

The predictions of demand theory (Table II) can be tested with systems for which the positive or negative nature of the regulatory element is known at the molecular level and for which the physiological function and ecological context also are known. The results for 40 such systems representing 11 different types of physiological functions are summarized in Table IV. Five predictions regarding the molecular nature of the regulator and nine predictions regarding the demand for gene expression also are given in Table IV for cases in which partial experimental evidence is available. Evidence for some of these examples has been presented elsewhere (24). Since a complete review of the material (25) is beyond the scope of this article, only a few cases will be treated here as examples.

Repressible Biosynthetic Systems. In enteric bacteria the repressible systems for histidine and tryptophan biosynthesis provide examples of systems controlled by positive and negative elements, respectively (see Table IV). Since the level of histidine in the colon is among the lowest of all amino acids, expression of the histidine biosynthetic operon in the bacterium will be in high demand (Table III). Thus, demand theory predicts that the histidine biosynthetic operon will be positively regulated (Table II). In fact, there is good evidence to show that this operon is controlled primarily by an antiterminator mechanism (26,27). On the other hand, the level of tryptophan in the colon is among the highest of the amino acids and, therefore, expression of the tryptophan biosynthetic operon in the bacterium

Table IV. Nature of regulator
correlates with demand for expression

System ⁺	Nature of regulator	Demand for expression
<u>Repressible biosynthetic systems:</u>		
Arginine	Negative	Low
Cysteine	Positive	High
Histidine	Positive	High
Isoleucine-valine	Positive	High
Leucine	Positive	High
Lysine	Negative	Low
Phenylalanine	Positive	High
Threonine	Positive	High
Tryptophan	Negative	Low
Biotin	Negative	Low [#]
<u>Inducible catabolic systems:</u>		
Arabinose	Positive	High
Deoxyribonucleotides	Negative	Low
Galactose	Negative	Low
Glycerol	Negative	Low
Histidine	Negative	Low
Lactose	Negative	Low
Maltose	Positive	High
Nitrogen fixation (<u>K. pneumoniae</u>)	Positive	High
Octopine (<u>A. tumefaciens</u>)	Negative	Low

Table IV. Continued.

System ⁺	Nature of regulator	Demand for expression
Rhamnose	Positive	High
Xylose	Positive	High
Tryptophanase	Positive [*]	High
<u>Inducible genetic movement:</u>		
Prophage induction		
λ	Negative	Low
P1	Negative	Low
P2	Negative	Low
P22	Negative	Low
Transposition		
Tn3	Negative	Low
Tn5	Negative	Low
Tn10	Negative	Low
Conjugation		
Ti (<u>A. tumefaciens</u>)	Negative	Low
F	Negative	Low
R100	Negative	Low
<u>Inducible resistance/ detoxification systems:</u>		
Alcohol (yeast)	Positive	High
Mercury	Positive	High
Penicillinase (<u>S. aureus</u>)	Negative	Low

Continued on next page.

Table IV. Continued.

System ⁺	Nature of regulator	Demand for expression
Tetracycline	Negative	Low
Chloramphenicol (<u>S. aureus</u>)	Negative [*]	Low
Erythromycin (<u>S. aureus</u>)	Negative [*]	Low
D-serine	Positive	High [*]
Toluene (<u>P. putida</u>)	Positive	High [*]
<u>Inducible repair systems:</u>		
SOS (<u>lexA-recA</u>)	Negative	Low
Adaptive response to alkylating agents	Negative [*]	Low
<u>Inducible biosynthetic systems:</u>		
Isoleucine-valine	Positive	High
Tryptophan (<u>P. putida</u>)	Negative	Low [*]
<u>Repressible scavenging systems:</u>		
Alkaline phosphatase	Positive	High
General aromatic AA transport	Negative	Low
Tyrosine-specific transport	Negative	Low
Iron	Positive [*]	High
Sulfate	Positive	High [*]
<u>Inducible toxin production:</u>		
Colicine E1	Negative	Low
Cholera (<u>V. cholerae</u>)	Negative	Low [*]
Diphtheria (<u>C. diphtheriae</u>)	Negative	Low [*]

Table IV. Continued.

System ⁺	Nature of regulator	Demand for expression
<u>Inducible surface antigens:</u>		
Outer cell wall protein 1b	Positive	High [*]
K88 (K)	Positive	High [*]

⁺ Enteric bacteria unless indicated otherwise

^{*} Predicted

will be in low demand. Here demand theory predicts negative control, which is in agreement with the wealth of evidence showing that regulation of this operon is accomplished primarily through the classical repressor mechanism (18).

Inducible Catabolic Systems. Among the inducible catabolic systems in enteric bacteria, the galactose and arabinose operons are examples of systems controlled by negative and positive elements, respectively (see Table IV). Galactose is absorbed early in the small intestine at a very rapid rate and is unlikely to survive transit through the intestine to the colon (21). Expression of the bacterial galactose operon, therefore, will be in low demand (Table III), and demand theory predicts that it will be negatively controlled. This agrees with the finding of classical repressor control for the galactose operon (28). Arabinose, on the other hand, is poorly absorbed by the small intestine and is likely to survive transit to the colon without attenuation in concentration (21). Arabinose in the colon at relatively high levels implies that expression of the arabinose catabolic operon in the bacterium will be in high demand. The prediction by demand theory of positive control for the arabinose operon is consistent with the experimental evidence for activator control of this system (14).

Inducible Gene Movement. Induction of gene movement appears to be a relatively rare event in nature. Demand for expression of the machinery for movement is consequently in low demand and its regulation will be under the control of a negative-acting element (see Table IV). For example, most natural isolates of coliform organisms are lysogenic for one or more temperate phages (29) and spontaneous induction of the prophage is a relatively infrequent event in nature (30). These facts imply that the lytic functions of the prophage are normally in low demand, which is consistent with the classical repressor control established for a number of prophages (31-34). Transposition of genes also must occur infrequently in nature. Otherwise, the genome of a bacterium like *E. coli* would have become scrambled to the point where genetic maps as we know them would not exist. The transposition machinery will be in low demand and its induction will be under the control of a negative-acting element. Again, this is consistent with the finding of classical repressor control for a number of transposons (35-38).

Similar arguments can be made with regard to bacterial conjugation and, again, there is evidence for classical repressor control in these cases (39-41). The case of *Agrobacterium tumefaciens* is particularly interesting. This organism is widely found in nature. When present at the site of a fresh wound in a dicotyledonous plant under appropriate circumstances, the bacterium can transform the normal plant tissue into a disorganized tumor. This occurs when specific DNA located on a

bacterial plasmid becomes incorporated into the plant genome. This specific DNA also codes for a biosynthetic system that causes the plant to produce a rare amino acid, octopine in this example. Octopine in turn acts as a specific inducer upon the bacteria that harbor the tumor-inducing plasmid to cause expression of an octopine catabolic pathway and expression of a specific system of bacterial conjugation for plasmid transfer (see Refs. 39,40). Since octopine is only rarely found in nature, expression of the octopine catabolic system and the bacterial conjugation system will be in low demand. Demand theory predicts that these systems will be under the control of a negative-acting element. The experimental evidence showing that these systems are under the control of a repressor protein (40) is entirely consistent with these expectations.

Discussion

Our interest in the integrated behavior of complex biological systems has been pursued on two levels. On the first, we have concentrated on the development of mathematical methods specifically appropriate for complex biological systems. On the second, we have applied these methods to a number of cases representing several classes of systems.

The development of the power-law formalism, reviewed briefly in the first portion of this paper, began with a consideration of the fundamental nonlinearities that characterize the kinetic behavior of biological systems at the molecular level (2,5). From this molecular-biological context a "dynamical systems" approach to biochemical and genetic networks was developed (3-7,11,42).

The justification for this formalism is based solidly on theoretical grounds (5,6,3) as well as agreement with direct experimental observations (42,9,4). An appreciation of its utility is perhaps best gained by an examination of successful applications. Numerous examples can be found elsewhere (43-48,10,6,3,24), but the limitations of space have precluded discussing more than one example, the development of the demand theory of gene regulation.

This demand theory is now supported by experimental evidence from more than 40 systems representing more than a dozen different types of physiological functions. This theory provides a simple unified explanation for what otherwise would be unconnected and disparate observations. Furthermore, it provides a wealth of specific, testable predictions that can serve as a guide for experimental investigation (e.g., see Refs. 49,50 and Table IV).

This theory also predicts the nature of the regulatory mechanisms that govern cell-specific functions in organisms with differentiated cell types and that these mechanisms will "switch" in accordance with the demand regime during the process of differentiation (22,51). Experimental evidence consistent with these predictions is presented elsewhere (51).

In summary, the results presented in this paper illustrate the use of kinetic methods to achieve fundamental understanding of gene function. There also are practical implications that have yet to be fully explored. Clearly, if one wishes to optimally exploit the product of a particular gene, then one must know the physiology and natural ecosystem of its host organism as intimately as its molecular genetics.

Acknowledgments

This work was supported in part by grants from the National Science Foundation.

Literature cited

1. Wilkins, J.G. "Manners and Customs of the Ancient Egyptians"; John Murray: London, 1837; vol. 2, p. 155.
2. Savageau, M.A. J. Theoret. Biol. 1969, 25, 365-369.
3. Savageau, M.A. "Biochemical Systems Analysis: A Study of Function and Design in Molecular Biology"; Addison-Wesley: Reading, Mass., 1976.
4. Savageau, M.A. Proc. Natl. Acad. Sci. USA 1979, 76, 5413-5417.
5. Savageau, M.A. J. Theoret. Biol. 1969, 25, 370-379.
6. Savageau, M.A. Curr. Topics in Cell. Reg. 1972, 6, 63-130.
7. Savageau, M.A. J. Theoret. Biol. 1970, 26, 215-226.
8. Savageau, M.A.; Voit, E.O. J. Ferment. Technol. 1982, 60, in press.
9. Kohen, E.; Thorell, B.; Kohen, C.; Solmon, J.M. Adv. Biol. Med. Phys. 1974, 15, 271-297.
10. Savageau, M.A. Math. Biosci. 1980, 48, 267-278.
11. Savageau, M.A. Proc. Natl. Acad. Sci. USA 1979, 76, 6023-6025.
12. Jacob, F.; Monod, J. J. Mol. Biol. 1961, 3, 318-356.
13. Miller, J.H.; Reznikoff, W.S. "The Operon"; Cold Spring Harbor Laboratory: Cold Spring Harbor, N.Y., 1978.
14. Englesberg, E. ; Wilcox, G. Ann. Rev. Genetics 1974, 8, 219-242.
15. Roberts, J. "RNA Polymerase"; Losick, R.; Chamberlin, M., Eds.; Cold Spring Harbor Laboratory: Cold Spring Harbor, N.Y., 1976; pp. 247-271.
16. Adhya, S. ; Gottesman, M. Ann. Rev. Biochem. 1978, 47, 967-996.
17. Rosenberg, M.; Court, D. Ann. Rev. Genetics 1979, 13, 319-353.
18. Yanofsky, C. Nature 1981, 289, 751-758.
19. Platt, T. Cell 1981, 24, 10-23.
20. Savageau, M.A. Proc. Natl. Acad. Sci. USA 1977, 74, 5647-5651.
21. Savageau, M.A. Proc. Natl. Acad. Sci. USA 1974, 71, 2453-2455.

22. Savageau, M.A. Proc. 24th Annual North American Meeting of the Society for General Systems Research with the American Association for the Advancement of Science, San Francisco, California, 1980, pp. 125-133.
23. Nixon, S.E.; Mawer, G.E. Brit. J. Nutrition 1970, 24, 241-258.
24. Savageau, M.A. "Biological Regulation and Development"; Goldberger, R.F., Ed.; Plenum Press: N.Y., 1979; pp. 57-108.
25. Savageau, M.A. in preparation.
26. DiNocera, P.P.; Blasi, F.; DiLauro, R.; Frunzio, R.; Bruni, C.B. Proc. Natl. Acad. Sci. USA 1978, 75, 4276-4280.
27. Barnes, W.M. Proc. Natl. Acad. Sci. USA 1978, 75, 4281-4285.
28. Nakanishi, S.; Adhya, S.; Gottesman, M.E.; Pastan, I. Proc. Natl. Acad. Sci. USA 1973, 70, 334-338.
29. Reanney, D. Bacteriol. Rev. 1976, 40, 552-590.
30. Barksdale, L.; Arden, S.B. Ann. Rev. Microbiol. 1974, 28, 265-299.
31. Ptashne, M.; Backman, K.; Humayun, M.Z.; Jeffrey, A.; Maurer, R.; Meyer, B.; Sauer, R.T. Science 1976, 194, 156-161.
32. Scott, J.R. Virology 1970, 41, 66-71.
33. Bertani, L.E.; Bertani, G. Adv. Genet. 1971, 16, 199-237.
34. Levine, M. Curr. Top. Microbiol. Immunol. 1972, 58, 135-156.
35. Gill, R.E.; Hefron, F.; Falkow, S. Nature 1979, 282, 797-801.
36. Chou, J.; Lemaux, P.G.; Casadaban, M.J.; Cohen, S.N. Nature, 1979, 282, 801-806.
37. Biek, D.; Roth, J.R. Proc. Natl. Acad. Sci. USA 1980, 77, 6047-6051.
38. Beck, C.F.; Moyed, H.; Ingraham, J.L. Molec. Gen. Genet. 1980, 179, 453-455.
39. Chilton, M.-D.; Drummond, M.H.; Merlo, D.J.; Sciaky, D.; Montoya, A.L.; Gordon, M.P.; Nester, E.W. Cell 1977, 11, 263-271.
40. Klapwijk, P.M.; Schilperoort, R.A. J. Bacteriol. 1979, 139, 424-431.
41. Willetts, N.; Skurray, R. Ann. Rev. Genetics 1980, 14, 41-76.
42. Savageau, M.A. Arch. Biochem. Biophys. 1971, 145, 612-621.
43. Savageau, M.A. J. Mol. Evol. 1974, 4, 139-156.
44. Savageau, M.A. J. Mol. Evol. 1975, 5, 199-214.
45. Savageau, M.A. Nature 1974, 252, 546-549.
46. Savageau, M.A. Nature 1975, 258, 208-214.
47. Savageau, M.A. J. Theoret. Biol. 1979, 77, 385-404.
48. Savageau, M.A.; Jacknow, G. J. Theoret. Biol., 1979, 77, 405-425.
49. Shamanna, D.K.; Sanderson, K.E. J. Bacteriol. 1979, 139, 71-79.
50. Foster, T.J.; Nakahara, H.; Weiss, A.A.; Silver, S. J. Bacteriol. 1979, 140, 167-181.
51. Savageau, M.A. submitted for publication.

RECEIVED June 1, 1982

Kinetics of Enzyme Systems

DAVID F. OLLIS

University of California, Chemical Engineering Department, Davis, CA 95616

The many circumstances leading to the Henri equation for enzyme conversion of soluble substrates are first noted, followed by some kinetic forms for particulate and polymer hydrolysis. Effects common to immobilized enzyme systems are summarized. Illustrative applications discussed include metabolic kinetics, lipid hydrolysis, enzymatic cell lysis, starch liquefaction, microenvironment influences, colloidal forces, and enzyme deactivation, all topics of interest to the larger themes of kinetics and thermodynamics of microbial systems.

Enzyme kinetics is by now a classical field, even in the arena of immobilized enzymes, and detailed transient as well as steady state kinetic models of cellular and subcellular functions have been advanced frequently which hinge heavily on the kinetic forms appropriate to single enzyme systems. (See later conference papers of Umbarger, Shuler and Domach, Bailey, Agathos and Demain, Marc and Engasser, Costa and Moreira, and Frederickson, for examples.) We open this discussion with a review of causes for success and uncertainty regarding the single enzyme rate equation, following which we will touch upon results for particulate substrates, and close with some results for immobilized enzyme systems.

1. Soluble substrates

The Henri form¹ for reaction velocity, v , of an enzyme catalyzed reaction was proposed in 1902 as eqn (1.1):

$$v = v_{\max} \left[\frac{S}{K+S} \right] \quad (1.1)$$

0097-6156/83/0207-0027\$07.50/0

© 1983 American Chemical Society

where v_{\max} = maximum velocity, K = constant, and S = concentration of free (uncomplexed) substrate. This form was later derived by Michaelis and Menten² in 1913 using an equilibrium assumption in eqn (1.2a) and an assumed single slow step, eqn (1.2b), which yields form (1.1) above:



where

Michaelis-Menten: $K \equiv k_2/k_1$ = dissociation constant of ES (1.3a)

$$v_{\max} = k_3 E_0 \quad \text{where } E_0 = \text{total enzyme concentration (E + ES)} \quad (1.3b)$$

The subsequent Briggs-Haldane treatment³ recognized that in general the rate constants (k_1 , k_2) and k_3 could be of arbitrary relative magnitudes, rather than only (k_1 , k_2) \gg k_3 assumed implicitly by eqns (1.2a,b), leading to the form (1.1) again but with K and v_{\max} given by eqns. (1.4a,b):

$$\text{Briggs-Haldane: } K = \frac{k_2 + k_3}{k_1} \quad (1.4a)$$

$$v_{\max} = k_3 E_0 \quad (1.4b)$$

Thus, the constant K is no longer a simple equilibrium constant,⁴

Extensions of form (1.1) are apparently endless in number. For example, for a common case of a (two substrate)-(one enzyme) system given below,

Reaction Dissociation Equilibrium Constant



eqn (1.1) is again recovered where v_{\max} and K are indicated in eqns (1.6a,b);

$$v_{\max} = \frac{kE_0 S_2}{K_{12} + S_2} \quad (1.6a)$$

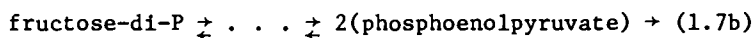
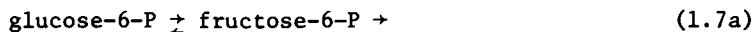
Two
substrate

$$K = \frac{K_{21}S_2 + K_1K_{12}}{S_2 + K_{12}} \quad (1.6b)$$

Thus, if S_2 is approximately constant as expected for $S_2 =$ solvent or $S_2 =$ buffered H^+ or OH^- , the Henri form of constant parameters v_{\max} and K will appear to fit the data for S_1 . Similarly, if the order of substrate binding reactions (5a) and (5b) is obligatory, form (1.1) is again obtained (e.g., by elimination of eqn (1.5d)).

When the second binding entity, S_2 is not a substrate, but instead an enzyme activator or competitive inhibitor, form (1.1) is again regained with both v_{\max} and K dependent upon activator/inhibitor level as indicated by eqns (1.6a,b).

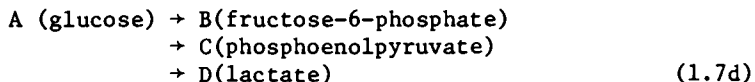
The extension of the network in eqns (1.5 a-e) to multiple intermediates is important in devising plausible multi-enzyme rate forms for microbial metabolism. The Henri form obtained in eqns (1.5a-e) involves three different enzyme complexes, all equilibrated with each other "upstream" to the kinetically slow step (eqn (1.3)). The negligible free energy changes evident for many of the steps in the Embden-Meyerhof glycolytic sequence⁶ (Figure 1) indicate that the three reaction sequences (1.7a,b,c),



and



will behave kinetically like the simpler reaction sequence (1.7d):



Moreover, the actual feedback inhibition on the conversion of B by the (later) products citrate and ATP (not shown) leads to the yet further simplification given by the network below:

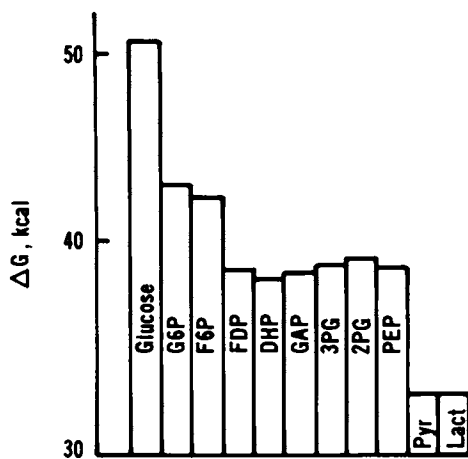
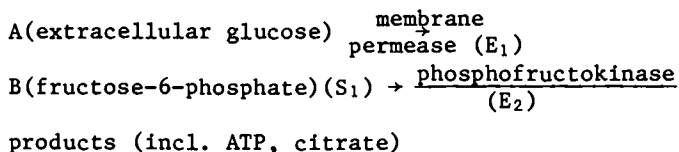


Figure 1. Free energy of intermediates of Embden-Meyerhoff glycolytic sequence in human erythrocytes. Reproduced, with permission, from Ref. 6. Copyright 1970, Worth Publishers.



Thus, the kinetics of conversions in metabolic cellular sequences, and even in whole cell kinetics, at or near steady state may be expected to resemble the kinetic rate form appropriate to one or a very small number of sequential enzyme catalyzed steps. The implications of this point in kinetic models of structured cell systems are reflected in later contributions in this conference.

The Henri form thus has a nearly universal appeal and utility in representing the variation of reaction velocity v with S_1 . The interpretive ambiguity accompanying the success of this universal "fitting" function leads us to recall Gileadi's characterization⁵ of the Langmuir form, identical to (eqn(1.)) in non-biological heterogeneous catalysis:

The Langmuir adsorption isotherm may now be regarded as a classical law in physical chemistry. It has all the ingredients of a classical equation: it is based on a clear and simple model, can be derived easily from first principles, is very useful now, about 50 (now 60) years after it was first derived and will probably be useful for many years to come, and is rarely ever applicable to real systems, except as a first approximation.

All reactions, catalyzed or otherwise, are reversible at the molecular level. This fact is most important in kinetics when overall conversion is limited thermodynamically. For example, the isomerization of glucose to fructose by glucose isomerase^{2,5}



gives (glucose) \sim (fructose) at equilibrium. Applying the pseudo-steady state assumption to the single intermediate gave eqn (1.9a)

$$v = \frac{v_{\max} [G - G^*]}{K + [G - G^*]} \quad (1.9a)$$

where the parameters v_{\max} and K are found in eqns (1.9b,c)

$$v_{\max} = \left[\frac{K^* + 1}{K^*} \right] \left[\frac{K_F}{K_F - K_G} \right] k_2 \cdot E_0 \quad (1.9b)$$

$$K = \left[\frac{1}{K_F - K_G} \right] [K_F + K_G \cdot K^*] \cdot G^* + K_F \cdot K_G \quad (1.9c)$$

and $K^* =$ glucose/fructose equilibrium constant

$K_F, K_G =$ Briggs-Haldane constants for fructose to glucose and glucose to fructose, i.e.,

$$K_F = (k_{-1} + k_2) / k_{-2} \quad \text{and} \quad K_G = (k_{-1} + k_2) / k_1$$

$G =$ glucose concentration at equilibrium.

Here we note that, even when starting with $G \gg G^*$, the equation (1.9a) will still reflect a reversible kinetic form through eqn (1.9c) where $K = f(G^*)$, although the initial rate will appear to satisfy eqn (1.1), with $K_{\text{apparent}} = (K - G^*)$.

2. Particulate substrates

The use of enzymes to lyse cells, hydrolyze fat emulsions, solubilize proteinaceous colloids, liquify or saccharify starch gels and granules, and degrade various components of cellulosic substrates indicates that many substrates are present in a particulate form. Kinetic forms for such enzyme catalyzed reaction rates are here noted, and will be revisited in the subsequent discussion of immobilized enzyme kinetics.

A first example is the hydrolysis of a uniform substrate, in the form of a given triglyceride emulsion, by a lipase. Thus, the data of Sarda and Desneuelle^{7,8} (Figure 2a,b) indicate clearly that purified pancreatic lipase preparations provide activity only when a substrate:water interface is present. The corresponding reaction velocity vs. substrate surface area function (Figure 2a,b) can be described by the form (2.1), which is the analog to (1.1) for the case where the initial enzyme level E_0 is much larger than the initial substrate level (surface area).

$$v = v_{\text{max}} \cdot \left[\frac{E}{K+E} \right]; \quad v_{\text{max}} = kS_0 \quad (2.1)$$

where $E =$ free (uncomplexed) enzyme concentration and v_{max} , $K =$ constants as for eqn. (1.1). In contrast to soluble substrates where a single reaction product is typically identifiable, multiple reaction products routinely occur in particulate degradation and/or enzymatic depolymerizations. A parallel/sequential conversion network appears to be provided for triglycerides by the data of Constantin et al.⁹ (Figure 3) which are consistent with the following network (2.2):

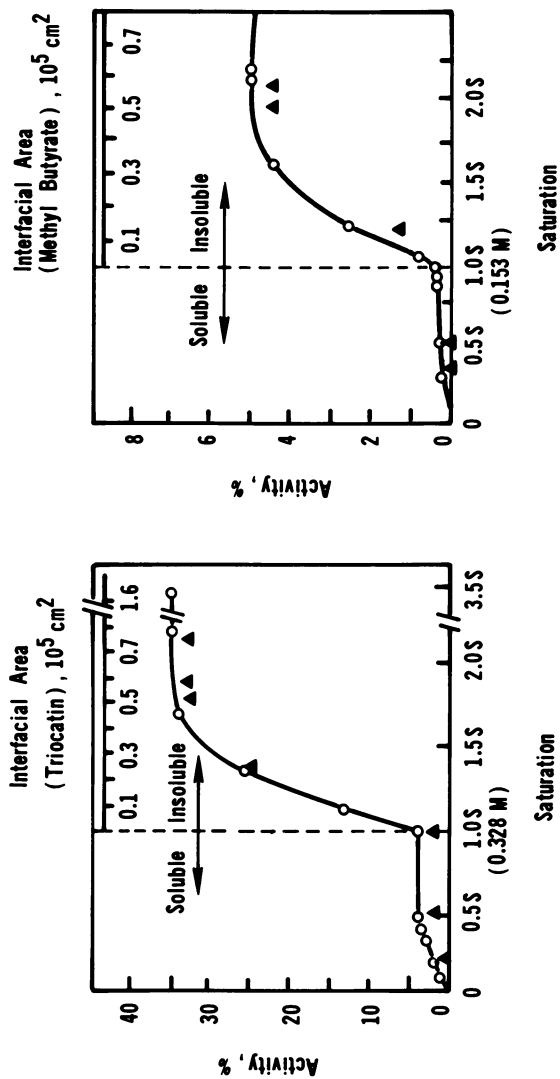


Figure 2. Variation of the rate of lipase hydrolysis of triacetin and methyl butyrate with the concentration of the substrate. The concentration is expressed as a fraction of the saturation concentration (S) and the hydrolysis rate as a percentage of the rate of triolein hydrolysis under optimal conditions. Key: ○, impure lipase plus esterolytic activity; ▲, lipase purified by electrophoresis. Reproduced, with permission, from Ref. 8. Copyright 1965, Academic Press.

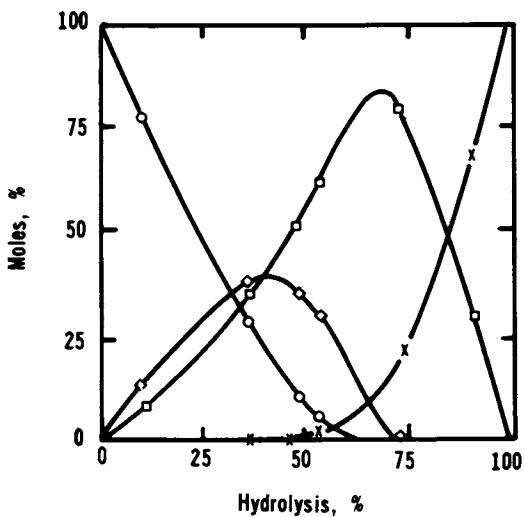
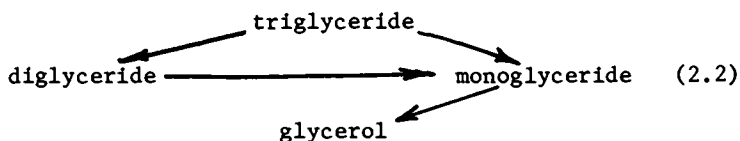
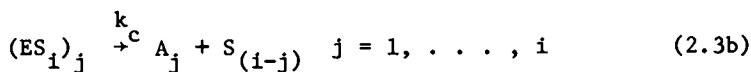
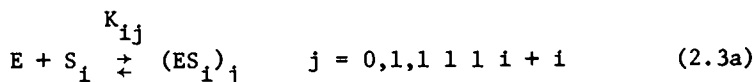


Figure 3. Liberation of diglycerides, monoglycerides, and glycerol during hydrolysis of a triglyceride by pancreatic lipase in the presence of sodium taurocholate and calcium ions. Key: \circ , triglyceride; \diamond , diglyceride; \square , monoglyceride; \times , glycerol. Reproduced, with permission, from Ref. 8. Copyright 1965, Academic Press



The simplicity of kinetic results (Figure 3) is aided by the presence of surfactant (deoxycholate) and divalent cation Ca^{++} which assists in removal of fatty acid product from the reaction interface. Lacking Ca^{++} presence, fatty acid will accumulate at the interface and compete with enzyme E for the limited substrate surface area; the reaction will consequently exhibit product inhibition. Further, the extent of triglyceride decomposition is strongly dependent upon solution composition: lacking calcium, only tri-to diglyceride conversion was noted, and even with Ca^{++} present and high enzyme levels, monoglyceride is not converted to glycerol until the triglyceride is consumed.⁹

A simple depolymerization of cell wall material apparently occurs in lysis of *Micrococcus lysodeikticus* by lysozyme. The homogenous reaction kinetics of enzyme attack of using oligomers of this monopolymeric cell wall example are conveniently studied by using oligomers of the monomer [disaccharide:(GlcNac-MurNac) (N-acetyl-D-glucosamine-N-acetylmuramic acid)]. The endoenzyme can cleave an oligomer of i units, S_i , at any of the susceptible bonds measured from a reference (e.g., non-reducible) end. A model reaction network allowing for such random internal cleavage (but forbidding cleavage of the first site from either end) was proposed¹⁰ by Chipman:



Here, the $(i+2)$ -mer S_i is complexed at the j^{th} site, numbered 0 to $i+1$, but only binding at sites $1 \leq j \leq i$ can result in reaction, as a site at an end is unreactive. The model fit kinetic data from experiments¹¹ starting with (uncleavable) dimer only. Other measures of reaction rate for cell lysis are typically more convenient: optical density of partially lysed cells

in a whole cell reaction mixture may suffice to represent the overall conversion.^{20,22}

The hydrolysis of starches by amylases is most conveniently considered in terms of sugar production (for saccharification) or viscosity reduction (for liquefaction). Starch pastes are characteristically pseudoplastic (shear thinning), and thus satisfy, over an intermediate range of shear rates, a power law relationship between shear stress, τ , and shear rate, $\dot{\gamma}$, of the form (2.4):

$$\tau = K(\dot{\gamma})^N \quad (2.4)$$

where K = apparent unit shear viscosity

N = power law index (<1 pseudoplastic)
($=1$ Newtonian)

As starch pastes were hydrolyzed by α -amylase¹², the parameters K and N were observed to change with reaction progress in a coupled manner according to the equation (2.5):

$$\log K - \log \tau_{\infty} - N \log \dot{\gamma}_{\infty} \quad (2.5)$$

Here the points $(\tau_{\infty}, \dot{\gamma}_{\infty})$ have the significance of being a limiting high shear rate (and shear stress) at which the solution is predicted to achieve the Newtonian high shear limit.

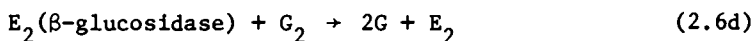
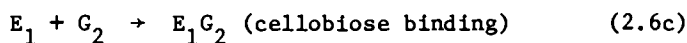
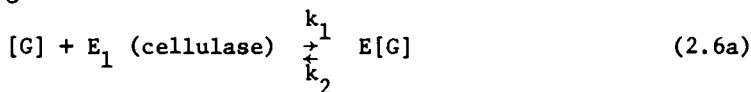
Thus, if reducing ends of product were measured to provide an average molecular weight of remaining starch molecules, it would be possible to relate K to the extent of reaction and, through eqn (2.5), the consequent rheology of the partially liquefied product. (See later paper of Rollings, Okos, and Tsao for a discussion of starch hydrolysis products.)

The action of the enzyme rennet on milk, known to destabilize a K -casein and trigger agglomeration of a multi-casein micellar suspension ($\alpha, \beta, \gamma, \epsilon, \kappa$) to produce coagulated milk for cheese-making,¹³ has been shown to produce a reaction suspension with power law behavior also described by eqns (2.4-2.5) (Tucznicki and Scott Blair).¹⁴

Where production of particular mono- or disaccharides is desired, employment of an appropriate exoenzyme, such as β -amylase is noted. The rate of depolymerization is again essentially an Henri form, unless modified by a product inhibition term.

Non-productive binding, leading to apparent inhibition, occurs frequently for endoenzymes. For example, lysozyme hydrolysis of poly (GlcNac-MurNac) yields dimer (GlcNac-MurNac)₂ which cannot be cleaved (being an end bond), $j = 0$, in eqn 2.3b above), but its non-productive binding decreases the number of enzyme sites available for acquiring a cleavable oligomer or polymer. Similarly, the hydrolysis of (insoluble) cellulose [G]

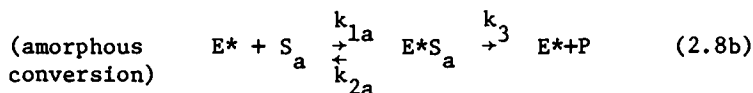
to cellobiose, G_2 , in eqns 2.6a-d and thence to glucose, G , involves a cellobiose noncompetitive binding to the cellulase; this inhibition is relieved by cellobiose conversion to glucose by β -glucosidase¹⁵:

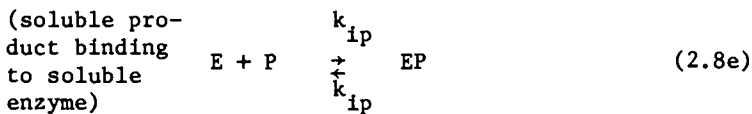
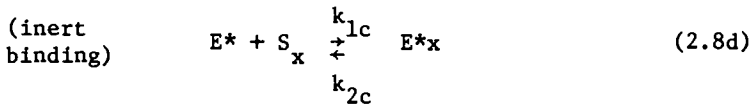
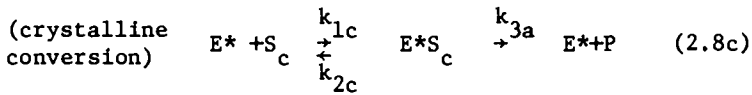


The form of the inhibition is non-competitive¹⁵ for cellobiose, thus K is unaffected (original substrate still binds with same K) but the maximal velocity is diminished according to eqn (2.7):

$$N_{\max} = k_3 E_0 \left[\frac{1 + \left(\frac{i}{K_i}\right) \frac{k_3}{k_3}}{1 + i/K_i} \right] \quad (2.7)$$

Cellulosic residues characteristically consist of a mixture of cellulose, hemicellulose, and lignin. Even the individual components are heterogeneous: the insoluble cellulose itself consists of a structured material of varying degrees of crystallinity. An illustrative structured substrate description including a kinetic model and supporting data was provided by Ryu, Lee, Tassinari and Macy.¹⁶ These investigators modelled the substrate heterogeneity by assuming that the cellulose consisted primarily of two phases: "an impermeable, denser, and highly ordered paracrystalline or amorphous phase." Correspondingly, each phase possesses a different reactivity. With S_a (amorphous), S_c (crystalline) and S_x (residual inert, including lignin) making up the total cellulose mass, S_0 , the kinetic model including binding of soluble product P to the enzyme is the system of reactions given by eqns (2.8a-3):





These authors determined crystallinity (and thus S_c) from x-ray diffraction data; molecular accessibility and surface area of variously milled samples were obtained from iodine adsorption and BET measurements. Degree of cellulose polymerization was determined from viscometry of cadoxen-dissolved solutions, with the specific viscosity extrapolated to zero concentration to obtain the intrinsic viscosity, $[\eta]$, from which in turn the viscosity average molecular weight M was estimated from the Mark-Houwink equation:

$$[\eta] = 38.5 \times 10^{-5} M^{0.76} \quad (2.9)$$

The experimental results supported both the partition of substrate into three sub-classes, and the product inhibition as well.

Immobilized Enzymes

The attachment of catalytically active sites to materials which may be easily recovered from a reaction mixture has been the sine qua non of most useful examples of catalysis outside of enzymology, and this latter area has begun to follow suit (see for example, the six Enzyme Engineering Conferences,¹⁷ as well as several summary texts¹⁸). In a pleasantly exhaustive review of the kinetics of immobilized enzyme systems, Goldstein¹⁹ several years ago assigned "the effects of immobilization on the kinetic behavior of an enzyme" to four situations:

"1. Conformational and steric effects: the enzyme may be conformationally different when fixed on a support; alternatively it may be attached to the solid carrier in a way that would render certain parts of the enzyme molecule less accessible to substrate or effector. These effects are (in 1976) well understood."

"2. Partitioning effects: the equilibrium substrate, or effector concentrations within the support may be different from those in the bulk solution. Such effects, related to the chemical nature of the support material, may arise from electrostatic or hydrophobic interactions between the matrix and low-molecular weight species present in the medium, leading to a modified microenvironment, i.e., to different concentrations of substrate, product or effector, hydrogen and hydroxyl ions, etc., in the domain of the immobilized enzyme particle.

"3. Microenvironmental effects on the intrinsic catalytic parameters of the enzyme: such effects due to the perturbation of the catalytic pathway of the enzymic reaction would reflect events arising from the fact that enzyme-substrate interactions occur in a different microenvironment when an enzyme is immobilized on a solid support.

"4. Diffusional or mass-transfer effects: such effects would arise from diffusional resistances to the translocation of substrate, product, or effector to or from the site of the enzymic reaction and would be particularly pronounced in the case of fast enzymic reactions and configurations, where the particle size or membrane thickness are relatively large. An immobilized enzyme functioning under conditions of diffusional restrictions would hence be exposed, even in the steady state, to local concentrations of substrate product or effector different from those in the bulk solution."¹⁹

These influences have been evaluated successfully, indicating a pleasant grasp of these fundamental influences on enzyme kinetics. We consider several illustrative results. The influence of the number of covalent couplings to an enzyme on its activity is shown for lysozyme, lipase, and chymotrypsin for soluble enzyme (Figure 4a) and immobilized enzyme (Figure 4b).²⁰ Here, the similarity in activity pattern changes for all three enzymes, as the ratio of soluble or insolubilized coupling groups (Figures 4a and 4b, respectively) to enzyme is increased, suggests clearly that alteration of relative enzyme activity upon immobilization (on only the external surfaces of these polyacrylamide supports) is governed by conformation or steric changes effected by the extent of enzyme covalent coupling.

The microenvironment effect due to Donnan equilibria is shown by the now classic results (Figure 5) for pH-activity profiles of chymotrypsin on polycationic, and polyanionic supports vs. that of the soluble enzyme.

Here, the charged substrate partitioning in bulk solution (S_0) and in the porous support (S_1) is given by

$$S_1 = S_0 \exp(-ze\psi/k_B T) \quad (3.1a)$$

where ze = substrate charge, ψ = electrostatic potential of

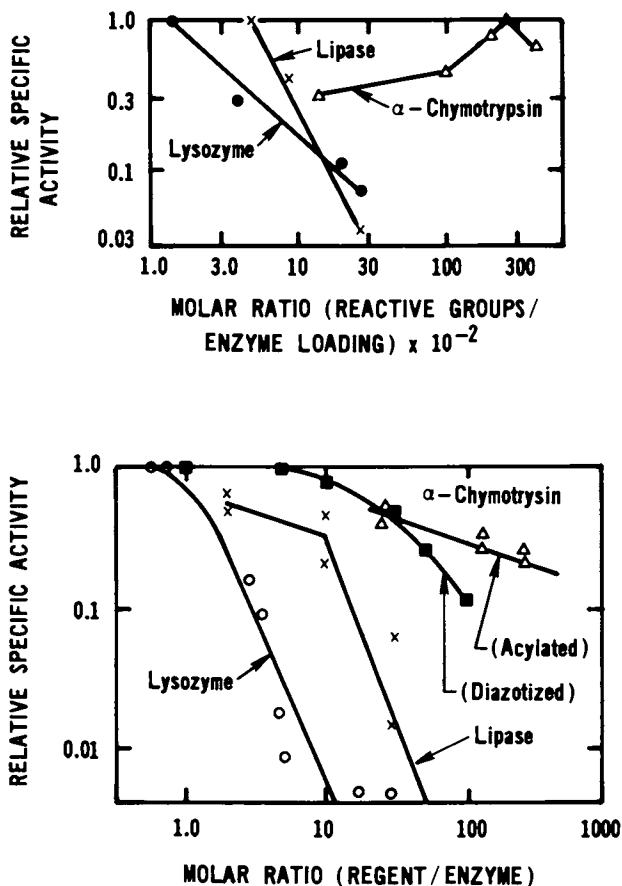


Figure 4. Top, relative specific activity of immobilized enzyme versus the molar ratio (ratio of immobilized surface coupling groups to enzyme immobilized). Key: ●, diazotized lysozyme; ×, diazotized lipase; △, acylated α -chymotrypsin. Bottom, relative specific activity of modified soluble enzymes versus the molar ratio (ratio of soluble coupling reagent to enzyme). Key: ○, diazobenzenesulfonic acid lysozyme; ×, diazobenzenesulfonic acid-lipase; ■, diazobenzene-sulfonic acid-chymotrypsin; △, acetic anhydride-chymotrypsin. Reproduced, with permission, from Ref. 20.

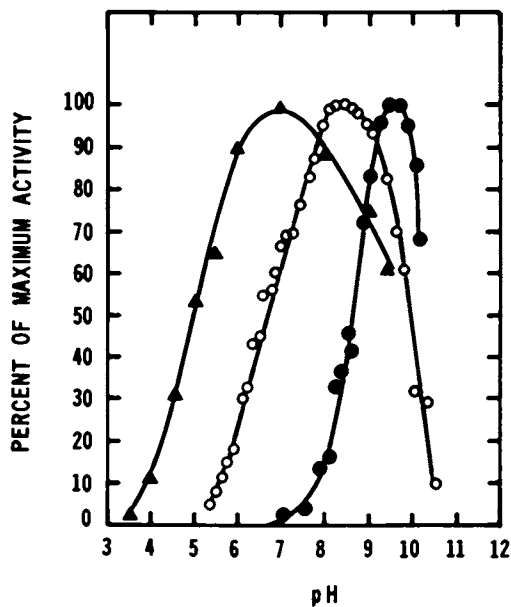


Figure 5. Activity-pH curves. Key: ○, chymotrypsin; ●, a polyanionic ethylene-maleic acid (EMA) copolymer derivative of chymotrypsin, and ▲, a polycationic derivative, polyornithyl chymotrypsin. Substrate is acetyl-L-tryrosine ethyl ester. Ionic strength is 0.01 mol/L. Reproduced, with permission, from Ref. 19. Copyright 1976, Academic Press, Inc.

support, and k_B = Boltzman constant. With Henri's eqn (1.1) assumed to apply for the actual internal concentration S_i adjacent to the enzyme, the observed rate expressed in terms of the measurable S_o value is still in agreement with the Henri form, but the apparent K' is given by eqn (3.1b).

$$K' = K \exp(z\psi/k_B T) \quad (3.1b)$$

as seen from using eqn (3.1a) in eqn (1.1):

$$v = \frac{v_{\max} S_i}{K + S_i} = \frac{v_{\max} S_o}{K \exp(z\psi/k_B T) + S_o} \quad (3.1c)$$

Donnan equilibrium, being an example of charge-charge interaction, is also influenced by ionic strength; the apparent Michaelis constant K' of the Henri form (1.1) was shown²¹ to vary with ionic strength according to eqn (3.2)

$$K' = \gamma K [1 - K' Z_m_c / KI]^{1/2} \quad (3.2)$$

where the activity coefficient ratio is $\gamma = \gamma^{\text{inner}} / \gamma^{\text{bulk}}$, Z_m_c is the effective fixed charge concentration inside the support, and I the bulk solution ionic strength.

The influence of colloidal forces on reactions involving immobilized enzymes acting on insoluble substrates has received less attention, yet it appears to offer some clear examples of fundamental phenomena important in enzyme kinetics. Datta²² examined lysis of *Micrococcus lysodeikticus* by soluble and (polyacrylamide) immobilized lysozyme. He noted that the decrease in soluble enzyme activity with decreasing ionic strength (Table 1) paralleled the measured decrease in cell lysis measured in flow through a packed bed reactor of immobilized enzyme.

Table 1²²

Ionic Strength [M]	Soluble Enzyme Activity	Immobilized Enzyme Relative Activity exp't (theory)	Cell Surface Potential ψ_p (mV)
10^{-4}	1700	~ 0 (~ 0)	+83.5mV
10^{-3}	4000	2.3 (~ 4.3)	81.0mV
10^{-2}	12000	13.3 (~ 8.3)	-36mV
10^{-1}	12000	22.6 (~ 8.3)	-37.3mV

*(first numbers are experimental results, second (in parentheses) are values predicted by particle collector theory, including influence of interception (particle size) and Brownian motion on mass transfer of particles to immobilized enzyme surface.)

The decline in rate with decreasing ionic strength is evidently associated with a sign reversal in net cell charge, from attractive ($\psi_{\text{enz. surface}} = +44.5\text{mV}$, $\psi_{\text{cell}} = -(36 \text{ to } 37.3\text{mV})$) to repulsive ($\psi_{\text{cell}} = +81 \text{ to } 83.5\text{mV}$) as determined from electrophoretic mobility measurements. A Michaelis constant (K) modification may also be involved (eqn 3.2 above). The agreement between observed rate and the calculated mass transfer limited rate (last column in parenthesis) means that the fluid mechanical and colloidal forces which act to attract/repel enzyme and cell particles are, at the highest ionic strengths, dominating the slow step kinetics, i.e., that every cell which encountered the immobilized enzyme surface was subsequently hydrolyzed.²² Similarly, the decline in rate for soluble enzyme is to be associated with a more difficult binding or lessened substrate affinity occasioned in part by the shift from attractive to repulsive colloidal force between enzyme and cell.

The mass transfer of a cell to an immobilized enzyme particle brings a relatively modest number of hydrolyzable bonds per cell particle to the catalyst. The above lysozyme data indicate that the reaction rate is essentially mass transfer controlled, i.e., the enzyme can cleave the small number of cell wall bonds per unit volume of cell rather rapidly. Solid and emulsion particles of similar size, such as cellulase particles or lipid emulsion droplets, bring a much larger number of cleavable bonds per particle to the immobilized enzyme. Immobilized pancreatic lipase²³ shows an observed reaction rate which is 10 to 100 times less than that predicted from colloidal particle transport (Figure 6). The particle collection efficiency utilized in calculation of the particle mass transfer coefficient is composed of only two important terms, interception and Brownian motion (gravitational settling and inertial impactions are negligible).²³ Thus, the particle mass efficiency of collection, η , is the simple sum of two terms:^{23,24}

$$\begin{aligned} \eta_{\text{overall}} &= \eta_{\text{Brownian}} + \eta_{\text{interception}} \\ &= 0.9 \left(\frac{k_B T}{\pi d_e d_{\text{enz}} N_o} \right)^{2/3} + 1.5 \left(\frac{d_e}{d_{\text{enz}}} \right)^2 \quad (3.3) \end{aligned}$$

where d_e , d_{enz} are substrate and immobilized enzyme particle diameter, respectively, and N_o is the fluid velocity entering the enzyme reactor.

The observed rate of reaction (Figure 6) is also orders of magnitude higher than the rate calculated by assuming that only a few molecules of product are formed per emulsion particle collision with the enzyme surface. Thus, particle-catalyst encounters result, on the average, in the cleavage of thousands to millions of lipid bonds per particle-catalyst collision event.

The above particulate examples involving lysozyme and pancreatic lipase concerned substrates with uniform reactant

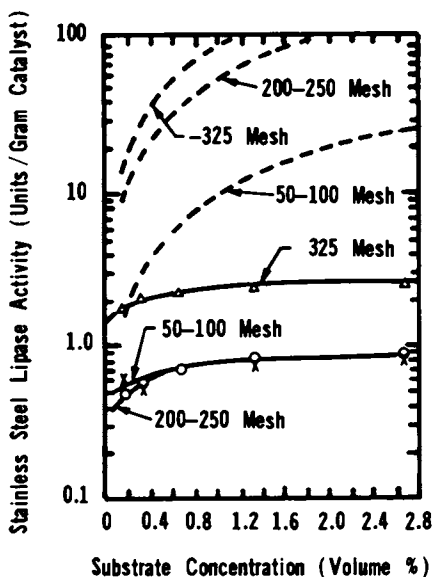
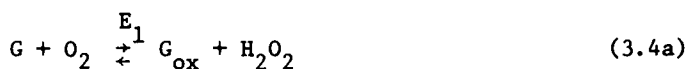


Figure 6. Comparison of calculated mass transfer rate and experimentally observed reaction rates at various substrate concentrations. Broken lines are calculated values. Experimentally observed values for stainless steel are: \times , 50-100 mesh; \circ , 200-250 mesh; and \triangle , 325 mesh. Reproduced, with permission, from Ref. 23. Copyright 1975, John Wiley and Sons, Inc.

structure: Micrococcus lysodeikticus (procaryotic) and tributyrin, respectively. More complex particulate structures provide a variety of hydrolysable bonds per particle, leading to a greater difficulty in reaching a description of enzyme hydrolytic kinetics. Examples here include eucaryotic cell walls (e.g., yeast, with cross linked mannan and glucan components), and the cellulosic substrates discussed in the earlier section.

Enzyme immobilization leads always to the need to consider diffusional limitations, as the latter can give rise to rate limitations and disguises. The general kinetic results are well established, and we touch on only a few illustrative examples in this short paper; diffusional limitations, enzyme electrode design, and polystep conversions.

Internal diffusional resistance is widely appreciated now, and tests for freedom from such internal disguises are commonly used in kinetic studies. The level of complexity of diffusional intrusions is illustrated with consideration of an immobilized dual system: glucose oxidase (E_1) and catalase (E_2) are used to oxidize glucose (G) to oxidized glucose (G_{ox}), and to decompose hydrogen peroxide (H_2O_2):



(In a developing commercial process, the oxidized glucose is reduced subsequently to fructose using a third catalyst.) The enzymes E_1 and E_2 are both deactivated by hydrogen peroxide, leading to a diffusion-reaction situation which changes slowly in time. Kinetic equations for this system have been widely studied;²⁶ the equations (3.5 a,b,c,d,e,f) used recently by Chang²⁷ are characteristic of the literature phenomena examined:

[G = glucose, A = oxygen, B = H_2O_2 , and P = oxidized glucose]

Glucose consumption rate (by oxidase (ox)):

$$= V_1 = V_1^{\max} E_{ox} / (1 + K_G/C_G + K_A/C_A) \quad (3.5a)$$

Peroxide conversion rate (by catalase (ca)):

$$= V_2 = k_{ca} E_{ca} C_B \quad (3.5b)$$

Oxidase deactivation:

$$\frac{dE_{ox}}{dt} = -k_3 C_B E_{ox} \quad (3.5c)$$

Catalase activity:

$$\frac{dE_{ca}}{dt} = -k_4 C_B E_{ca} \quad (3.5d)$$

Product formation (at pseudo-steady state):

$$\frac{dP}{dt} = \frac{-dG}{dt} \quad (3.5e)$$

In commercial large scale catalytic conversions, activity maintenance is important. Calculations by Chang²⁷ indicating the glucose oxidase activity profiles vs. distance in the catalyst pellet are shown in Figure 7 for various catalase enzyme loadings E_{20} , as represented by the Thiele parameter value,

$$\phi = \sqrt{R k_{ca} E_{ca} / D_A}$$

in Figs. 7a ($t=0$), 7b ($t=100$), 7d ($t=150$), 73 ($t=200$), and 7f ($t=300$). Lack of any catalase ($\phi_2 = 0$, Figs. 7a-3, curve a) results in the most rapid deactivation of E_1 , while the highest E_2 loading, case d, results in longest maintenance of E_1 catalyst. Additionally, in the absence of E_2 , the H_2O_2 concentration is largest in the center of the pellet, giving most rapid deactivation at $r = 0$, while with appreciable E_2 levels, the H_2O_2 is maximal at the location where the rate is largest, which is near $r = .75$ to $.9$, and falls toward zero near the pellet center since most of the original dissolved oxygen has been consumed by $r = 0.5$ and the inner part of the pellet acts primarily as a peroxide sink (and oxygen source).

The glucose \rightarrow glucose oxidase system is probably the best studied example of catalyst activity maintenance. Evaluation of system behavior, based upon Henri-related reactions (3.5a, 3.5b) and deactivations (eqns 3.5c, 3.5d) occurring simultaneously with internal (eqns 3.5a,b) diffusion and external mass transfer presents as complete a kinetic analysis as is conventionally available in other well studied commercial examples of catalysis.

A second application of immobilized enzymes involves enzyme electrodes. An illustrative example of kinetic fundamentals is provided by the urease electrode, which uses a urease membrane to cleave urea into bicarbonate and ammonium ion, coupled to an ammonium ion specific potentiometric electrode. As with the glucose oxidase/catalase example above, the homogeneous phase kinetics can be applied to describe the response of the immobilized urease:²⁸

in "planar" membrane:

diffusion + reaction of urea substrate:

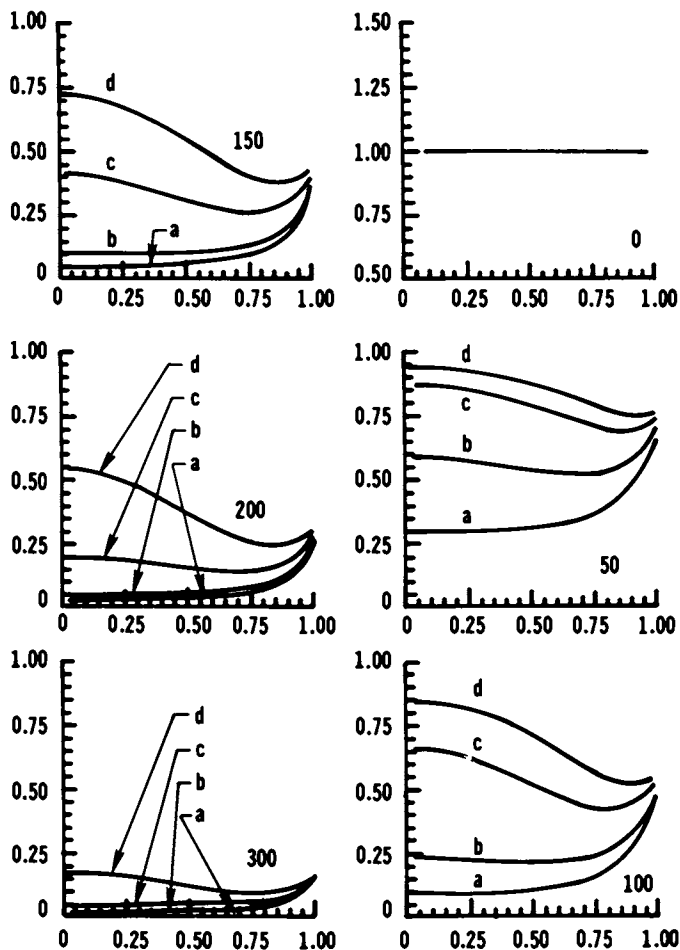


Figure 7. Activity profiles for glucose oxidase (E_1) coimmobilized with catalase (E_2) in an initially uniform concentration. The glucose oxidase loading is constant; the catalase loading increases as reflected by increased Thiele modulus, $\phi_2 = R\sqrt{E_{20}/DS_{0_2}}$, from Curve a ($E_{20} = 0$) to Curve d ($E_{20}(\max)$). Dimensionless time appears at the lower right-hand corner of each graph (27).

American Chemical
Society Library
1155 16th St., N.W.

$$D_s \frac{d^2 S}{dz^2} - \frac{k_3 k_E S}{(1+KS)(1+K'[\text{NH}_4^+])} = 0 \quad (3.6a)$$

production of ammonium ion product

$$D_{\text{NH}_4^+} \frac{d^2 [\text{NH}_4^+]}{dz^2} + \frac{2k_3 k_E S}{(1+KS)(1+K'[\text{NH}_4^+])} = 0 \quad (3.6b)$$

with boundary conditions (at steady state)

$$\frac{d[\text{NH}_4^+]}{dz} = 0 = \frac{dS}{dz} \text{ at } z = L \text{ (ammonium ion electrode)} \quad (3.6c)$$

$$D_s \frac{dS}{dz} = k_2(S - S_b) \text{ at } z = 0 \text{ (external surface)} \quad (3.6d)$$

$$D_{\text{NH}_4^+} \frac{d[\text{NH}_4^+]}{dz} = k_{\text{NH}_4^+} ([\text{NH}_4^+] - [\text{NH}_4^+]_b) \quad (3.6e)$$

Using published data of Laidler *et al.*,²⁹ the calculated ammonium ion concentration profile is presented in Figure 8 for various urease loadings in the thin "planar" membrane gel surrounding the tip of the ammonium ion electrode. These results contain useful design information. If we wish to use the electrode to measure substrate (urea), the NH_4^+ signal at the ammonium electrode surface ($z/L = 1.0$, Fig. 8) should be independent of E_o , thus we should produce an electrode with $E_o > 20\text{-}30$ mg urease per ml of gel. If we wish to detect an inhibitor, then we should load the enzyme membrane electrode very lightly (e.g., $E_o = 2$ mg/ml) so that a 50% activity inhibition, corresponding to $E' = E_o/2$, produces a considerable drop in NH_4^+ signal. The experimental voltage response of an urease enzyme electrode with various urease loadings was determined by Guilbault and Montalvo;³⁰ Fig. 9 indicates that the initial loading of 20-30 mg calculated above is in reasonable agreement with the experimental results (note that calculation gives NH_4^+ ($Z=0$) while measurement is reported as ammonium ion electrode voltage.) Many other substances have been analyzed experimentally with similar enzyme electrode probes (Guilbault)³², indicating major potential for analogs of eqns (3.6a-e).

Summary

The kinetics of soluble and immobilized enzymes, involved in reactions of soluble and insoluble substrates appears to be sufficiently well studied over the last 20 years that reactor design procedures based on fundamental kinetics rate equations may be executed with considerable confidence. The application of such enzyme kinetics forms to structured models of microbial metabolism has also progressed, as this book documents.

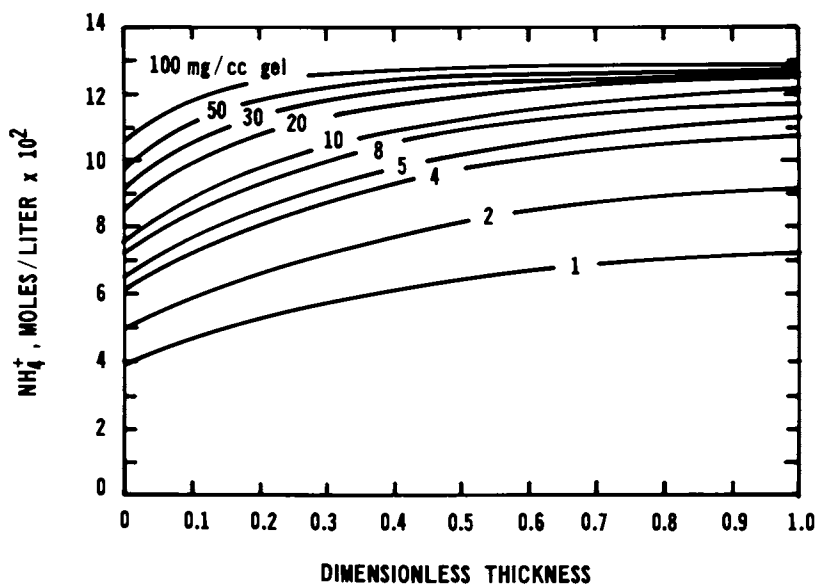


Figure 8. Influence of enzyme loading (mg enzyme/cc gel) on product profiles for 50μ membrane; bulk urea concentration, 0.0833 M ; bulk ammonium ion, negligible (10^{-7} M). Reproduced, with permission, from Ref. 28. Copyright 1972, Plenum Publishing Corp.

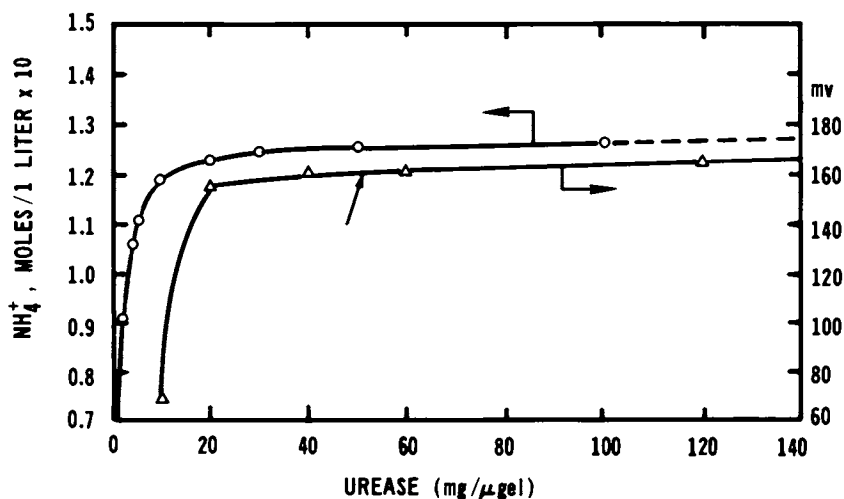


Figure 9. Comparison of experimental and calculated electrode steady-state responses versus enzyme loading. Key: Δ , experimental data ($L = 350\mu$, bulk urea = 0.0833 M, bulk ammonium ion negligible); \circ , calculation from model given in text ($L = 50\mu$, bulk urea = 0.0833 M, bulk ammonium ion negligible (10^{-7} M)). Reproduced, with permission, from Ref. 28. Copyright 1972, Plenum Publishing Corp.

Literature Cited

1. Henri, V. Comptes Rendus Acad. Sci., Paris, 1902, 135, 916.
2. Michaelis, L.; Menten, M. L., Biochem. Z., 1913, 333, 49.
3. Briggs, G. E.; Haldane, J. B. S. Biochem. J., 1925, 19, 338.
4. Dixon, M.; Webb, E. C. "Enzymes", Academic Press, 1964; Chapter IV).
5. Gileadi, E. (ed), "Electrosorption", Plenum Press, New York, 1967.
6. Lehninger, A. L. "Biochemistry", Worth Publishers, New York, 1970, p. 327.
7. Sarda, L.; Desnuelle, P. Biochim. Biophys. Acta, 1958, 30, 513.
8. Wills, E. D. Adv. in Lipid Research, 1965, 3, 219.
9. Constantin, M. J.; Pasero, L.; Desnuelle, P. Biochim. Biophys. Acta, 1960, 43, 103.
10. Chipman, D. M. Biochemistry, 1971, 10, 1714.
11. Chipman, D. M.; Pollock, J. J.; Sharon, N. J. Biol. Chem., 1968, 243, 481.
12. Cruz, A., Russel; W. B.; Ollis, D. F. AIChE J., 1976, 22, 832.
13. Whitaker, J. "Enzymology of Foods", John Wiley and Sons, New York.
14. Tuczinski, W.; Scot Blair, G. W. Nature, 1967, 216, 367.
15. Howell, J. A.; Stuck, J. D. Biotech. Bioeng., 1975, 17, 873.
16. Ryu, D. D. Y.; Lee, S. F.; Tassinari, T.; Macy, C. "Effect of Compression Million on Cellulose Structure and on Enzymatic Hydrolysis Kinetics", private communication, 1981.
17. "Enzyme Engineering I", L. B. Wingard (ed.), Plenum Press, 1972; II, Pye E. K. and L. B. Wingard (eds), Plenum Press, New York, 1974; III, Pye E. K. and Weetall, H. H. (eds), Plenum Press, New York, 1977; IV, Brown, G. and Mannecke, G. (eds), Plenum Press, New York; V, Plenum Press, New York, 1980; VI, 1982 (in press).
18. Zaborsky, O. "Immobilized Enzymes", CRC Press, 1973; Chibata, (ed), "Immobilized Enzymes: Research and Development", Kodansha Press, Tokyo, 1978.
19. Goldstein, L. "Adv. In Enzymology, XLIV, (K. Mosbach (ed.)), Academic Press, New York, 1976, pp. 397-443.
20. Datta, R.; Ollis, D. F., "Immobilized Biochemicals and Affinity Chromatography, (R.B. Dunlap (ed.)), Plenum Press, New York, 1974, p. 293; "Adv. in Enzymol.", XLIV, pp. 444-450 (K. Mosbach (ed.)).
21. Wharton, C. M.; Crook, E. M.; Brocklehurst, K. Eur. J. Biochem., 1968, 6, 572.
22. Datta, R., PhD Thesis, Princeton Univ., 1974.
23. Lieberman, R.; Ollis, D. F., Biotech. Bioengig, XVII, 1401 (1975).
24. Bailey, J. B.; Ollis, D. F. "Biochemical Engineering Fundamentals", McGraw Hill, 1977, p. 469.

25. Fratzke, A. R.; Lee, Y. Y.; Tsao, G. T. G.V.C./AIChE - Joint Meeting, Munich, 1974, 4, F2-1.
26. Prenosil, J. F., Biotech. Bioeng., 1979, 21, 89; Buchholz, K.; Godelman, . Biotech. Bioeng., 1978, 20, 1201; Reuss, M.; Buchholz, K. Biotech. Bioeng., 1975, 17, 211.
27. Chang, T. MSE Thesis, Univ. of California, Davis, March, 1982.
28. Ollis, D. F.; Carter, R. "Kinetic Analysis of a Urease Electrode: in "Enzyme Engineering II", F. K. Pye and L. B. Wingard (eds), Plenum Publishing Corp., New York, 1972, p. 271.
29. Hoare, J. G.; Laidler, K. J. J. Am. Chem. Soc., 1950, 72, 2487; Wall, M. C.; Laidler, K. J. Arch. Biochem. Biophys., 1953, 43, 299; Wall, M. C.; Laidler, K. J., Arch. Biochem. Biophys., 1953, 43, 307.
30. Guilbault, G. C. and Montalvo, J., J. Am. Chem. Soc., 1970, 92, 2533.
31. Wills, E. D. Adv. In Lipid Research, 1965, 3, 197.
32. Guilbault, G. C. "Biochemical Engineering II, A. Constantinides, W. R. Vieth and K. Venkatasubraminian (eds), Ann. N. Y. Acad. Sci., 1981, 309, 285.

RECEIVED July 7, 1982

Optimization of Fermentation Processes Through the Control of In Vivo Inactivation of Microbial Biosynthetic Enzymes

SPYRIDON N. AGATHOS and ARNOLD L. DEMAIN

Massachusetts Institute of Technology, Department of Nutrition and Food Science, Fermentation Microbiology Laboratory, Cambridge, MA 02139

Prolonged production of antibiotics could be achieved by in vivo stabilization of biosynthetic enzymes. As a model system we have focused on the gramicidin S synthetase complex in Bacillus brevis. Our group previously reported an O₂-dependent loss of total biosynthetic activity preventable by anaerobiosis. We further found this inactivation to be independent of aerobic energy-yielding metabolism and of de novo protein synthesis through inhibitor studies. However, retardation of inactivation was achieved upon addition of utilizable carbon sources to aerated cell suspensions, the degree of stabilization being proportional to the ease of uptake and to the concentration of each C-source. Dithiothreitol contributed to retardation and partial reversal of the inactivation. These results suggest that the in vivo inactivation may be due to an energy deficiency at the end of exponential growth with a concomitant exposure of sulfhydryl groups on the synthetases to autoxidation.

Important commodity chemicals are currently being produced by microorganisms in a variety of fermentation and bioconversion processes. The efficient production of these substances requires considerable enzyme levels catalyzing the biosynthesis of metabolites, as well as good catalytic activities and adequate operational stabilities. This is certainly true of both primary and secondary metabolites.

Until recently, most work aimed at optimizing production of valuable secondary metabolites such as antibiotics has consisted of environmental and genetic approaches affecting almost exclusively the levels and catalytic activities of the relevant biosynthetic enzymes, rather than their operational stability. Environmental manipulations have included: (a) the addition of appropriate precursors; (b) the disruption of regulatory mechanisms

0097-6156/83/0207-0053\$06.00/0
© 1983 American Chemical Society

controlling the initiation of antibiotic synthesis, such as repression and inhibition of their synthetases. For example, carbon catabolite regulation is relieved through addition of a slowly utilized carbon source at the beginning of a batch fermentation or through the slow addition of the otherwise readily consumed carbon source in various fed-batch type operations. Similarly, nitrogen and phosphate regulation are bypassed either through restriction of the respective N- or P- source or through addition of a slowly metabolized alternative source of those nutrients. Feedback inhibition of antibiotic synthetases has been minimized by appropriate bioreactor design, e.g., a dialysis culture in which the end product is continuously removed; (c) finally, the specific growth rate of the antibiotic-producing microorganism is optimized during the idiophase (e.g., through limitation of a key nutrient, pH control, etc.) since initiation and maintenance of idiophase production is favored at low growth rates.

Genetic solutions to the problems of the above mentioned regulatory mechanisms have also been applied successfully for the efficient production of secondary metabolites. Mutation and selection for superior producing mutants can account for much of the success of the modern antibiotic industry.

However, even with superior producer strains and rational environmental strategies for adequate expression and activity of the synthetases, these biosynthetic enzymes usually decay quickly during the idiophase. Thus, the in vivo inactivation of biosynthetic enzymes is widespread and appears to be a limiting factor in the prolonged production of antibiotics and related secondary metabolites. Despite its importance, in vivo enzyme inactivation of secondary metabolism has not received any attention as a distinct biological phenomenon, although a fundamental understanding of the process(s) could hold the key to its successful circumvention as is the case with other types of cellular enzyme regulation.

We have reasoned that a novel approach to prolong the production phase of secondary metabolites should be based on an attempt to prevent or retard the process of in vivo inactivation of the enzymes (synthetases) catalyzing their formation in fermentations. Such an attempt would require an understanding of the chemical nature of the inactivation. This knowledge could be subsequently translated into process development and control in actual fermentations, which, for the most part, are carried out in batch reactors. If the object of the fermentation is the recovery of the enzymes for further use in a cell-free system or the acquisition of active whole cells for repeated use in a fixed bed-type bioreactor, the prevention or retardation of the inactivation process would ensure both an adequate margin of time for primary harvesting and a longer half-life of the activity for the biocatalysts in the cells.

The purpose of this communication is to illustrate the potential of the above-mentioned approach by focusing on our

investigation of the in vivo inactivation of the enzyme (synthetase) complex responsible for the formation of gramicidin S (GS), a cyclic peptide antibiotic in Bacillus brevis ATCC 9999. This investigation represents the first attempt, to our knowledge, to understand and to control in vivo inactivation of a synthetase involved in the production of a secondary metabolite. The choice of GS synthesis, as our model system, was influenced by the relatively large amount of information in the literature about the enzymology of GS formation, the participation of only two polyenzymes in its biosynthesis and the existence of a cell-free biosynthetic system. Also the pattern of appearance and disappearance of the enzyme complex (GS synthetase) is typical of a large number of antibiotic fermentations. In addition, the producing organism, Bacillus brevis, is a non-filamentous, rapidly growing prokaryote and only a single antibiotic is produced in this fermentation.

Investigators have noted that after the appearance of the two soluble GS synthetases at the end of exponential growth, they rapidly disappear as the cell population moves into stationary phase (12,13) (Fig. 1). These changes have been observed using the assay which measures the total synthetase activity as well as both L-ornithine and L-phenylalanine-dependent ATP-PP_i exchange reactions (assays for the individual heavy and light GS synthetases respectively).

Friebel and Demain (4,5) found that inactivation of soluble GS synthetase in vivo is oxygen-dependent and irreversible. They also found that N₂ gas prevented in vivo inactivation of the enzyme complex under otherwise fermentation conditions. However, under these conditions no GS was produced, presumably due to the need of oxygen for ATP production in this aerobic organism.

It is useful to review briefly some of the current motions on in vivo inactivation of microbial enzymes:

In Vivo Enzyme Inactivation. Enzyme levels in microorganisms are known to be controlled through regulation of the rate of their synthesis (induction/repression) whereas enzyme activities are controlled by non-covalent binding of various ligands (activation/inhibition). However, through studies that have focused almost exclusively on the disappearance of enzymes of primary metabolism, it is now apparent that an additional type of enzyme regulation is operative in microorganisms, i.e., the control of enzymatic activity by selective inactivation. This inactivation of particular enzymes is widespread among microorganisms, is brought about by several mechanisms, and is observed under specific physiological conditions (7,11). In vivo inactivation is defined as the irreversible loss of an enzyme's catalytic activity in the cell. This definition is designed to contrast inactivation from inhibition, which is the reversible loss of enzyme activity through usually non-covalent binding of an inhibitor that can be dialyzed or diluted away to restore activity. In vivo enzyme inactivation can

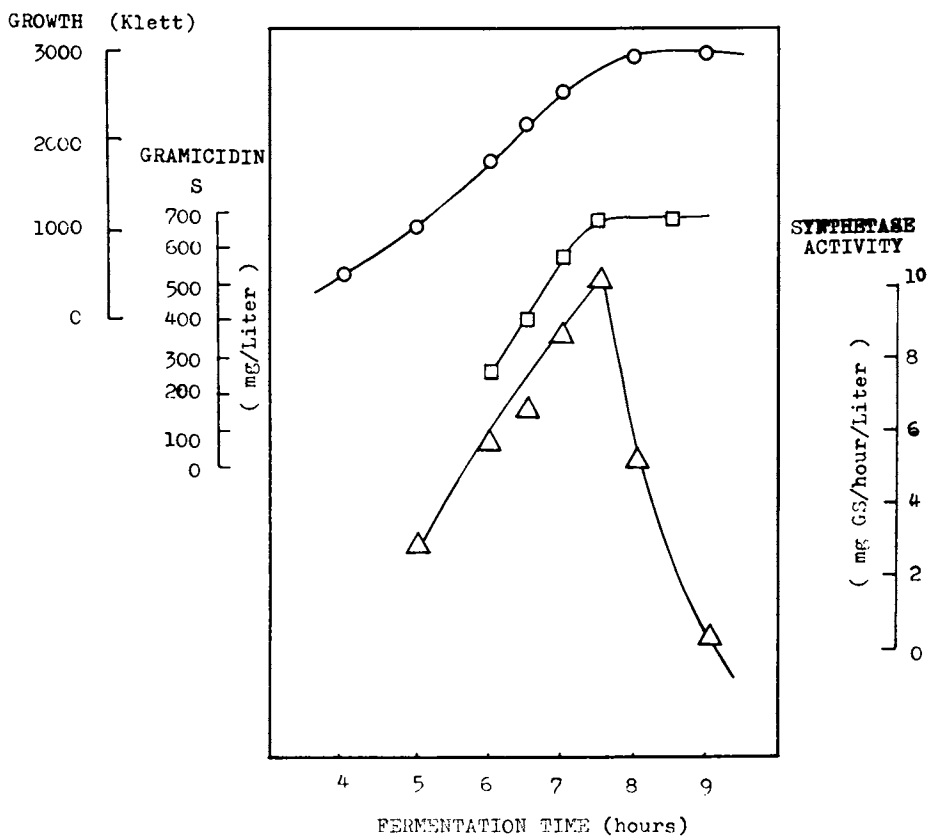


Figure 1. Dynamics of appearance and disappearance of GS synthetases. Key: \circ , growth; \square , GS; and \triangle , total GS biosynthetic activity (Synthetase scale).

be classified into modification inactivation, which involves usually a covalent modification of the protein molecule and degradative inactivation, which involves cleavage of at least one peptide bond of the enzyme protein. The in vivo inactivation of microbial enzymes is usually observed as the cells approach or enter stationary phase in a batch reactor. It occurs mainly at a point in which the microbe's nutritional/energetic state changes upon exhaustion of nutrients or a shift in carbon or nitrogen source. Possibly, it is a general regulatory mechanism aimed at phasing out a particular enzyme when a metabolic shift renders it wasteful of metabolites and/or directly harmful to the cell.

Materials and Methods

The culture used in these experiments was Bacillus brevis ATCC 9999. The preparation of spores and inoculum and the determination of growth were as previously described (9). Protein was determined by the biuret method (6).

In order to study the in vivo disappearance of GS synthetase, we have used a system that exhibits inactivation kinetics in short-term experiments. The system utilizes frozen and thawed cells of B. brevis harvested after growth in yeast extract-peptone (YP) medium in a 180-1 fermentor and frozen at -20°C immediately after harvesting. Small batches of cells were thawed just before performing in vivo inactivation studies according to the methodology of Friebel and Demain (4). In brief, these cells are agitated under air in buffer for various periods of time in the presence of appropriate compound vs. nitrogen-covered controls, crude cell-free extracts are subsequently prepared using lysozyme, and the extracts are assayed by the overall GS synthetase assay (incorporation of L-[^3H]ornithine into GS).

Results and Discussion

A typical kinetic pattern of the in vivo loss of GS synthetase in our frozen-thawed cell system is shown in Figure 2. The enzyme survives over 8 hours under nitrogen gas, but is usually lost at the end of 2-3 hours under conditions of agitation at 250 rpm, 37°C in air (simulated aerobic fermentation conditions). The time scale should not be taken as an absolute measure of the enzyme's survival, because the rate of the inactivation depends upon the previous growth history of the cells. Therefore, comparisons are made only between experiments performed with cells from the same batch of cells.

Lack of Inactivation by Energy-yielding Cellular Metabolism. We first examined whether the dependence of synthetase inactivation on oxygen reflects a requirement for aerobic energy-yielding metabolism. Some enzymes are inactivated in vivo in the presence of O_2 due to the operation of energy-yielding circuits in the cell,

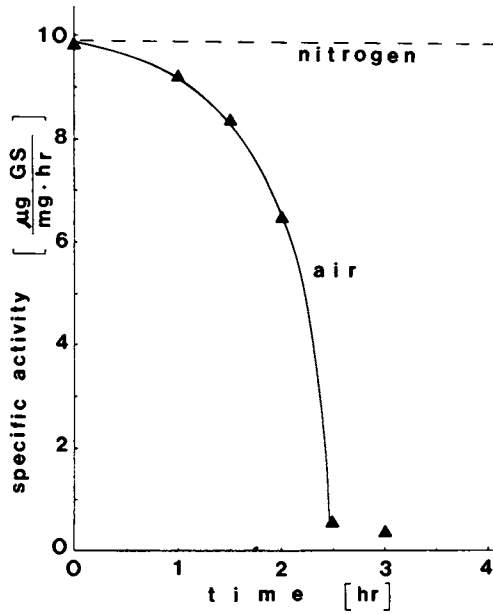


Figure 2. Typical kinetic pattern of *in vivo* inactivation of GS synthetase complex in frozen-thawed cells of *B. brevis*. Standard conditions for inactivation: agitation at 250 rpm, 37°C under air, vs. N_2 -covered control.

such as glycolysis, the citric acid cycle, electron transport, etc (11). Especially in Bacillus subtilis, it has been demonstrated that inhibitors of such energy-yielding pathways prevent the in vivo inactivation of aspartase transcarbamylase, a process requiring oxygen and entry into the stationary phase (15). In our case, inhibitors of glycolysis (NaF), the citric acid cycle (malonate) and oxidative phosphorylation (DNP), in concentrations known to inhibit their respective metabolic circuits, were not effective in preventing enzyme inactivation (Table I). Therefore, it appears as if the inactivation is not due to energy-yielding metabolic cell activity.

Table I.

Effect of Energy Metabolism Inhibitors on
in vivo Stability of GS Synthetase^a

Atmosphere	Additive	Activity %
Nitrogen	None	100
Air	None	4
Air	50 mM NaF	2
Air	50 mM Malonate	0
Air	0.2 mM DNP	6
Nitrogen	50 mM NaF	77
Nitrogen	50 mM Malonate	85
Nitrogen	0.2 mM DNP	103

^aIncubation with shaking for 90 min at 250 rpm, 37°C.

Independence of Inactivation from Protein Synthesis. A similar experiment was carried out to determine whether the inactivation was dependent upon protein synthesis. Conceivably the process of in vivo synthetase inactivation could be enzymatic, involving the mediation of an enzyme that is derepressed at some point during late exponential growth in actively growing cultures of B. brevis, e.g., a protease with an unusual requirement for oxygen or an oxygenase or an unknown "inactivase". Nevertheless, when a protein synthesis inhibitor (chloramphenicol) was included in the aerated cell suspensions of our system in a concentration known to inhibit de novo protein synthesis in B. brevis, no prevention or slow-down of the inactivation process was noted, thus suggesting that the process is not protein-synthesis dependent.

Carbon Source-mediated Retardation of Inactivation. As mentioned previously, a shift in C-metabolism is one of the physiological conditions most commonly associated with in vivo inactivation of

microbial enzymes. It might be assumed that as *B. brevis* moves into the stationary phase, the operation of the GS synthetase for continued formation of the antibiotic from its constituent amino acids becomes wasteful of protein precursors. Thus enzyme inactivation may spare building blocks and energy and may be brought about by signals of progressive depletion of carbon and energy source and/or the intracellular ATP pool. To determine whether carbon sources have any effect on inactivation of GS synthetase, various utilizable (glycerol, fructose, inositol) and nonutilizable (glucose, sorbitol) carbon sources were added to frozen-thawed cell suspensions agitated under air. As shown in Table II, several C-sources were able to partially stabilize the enzyme.

Table II.

Effect of Carbon Sources on in vivo
Stability of GS Synthetase^a

Atmosphere	Additive	Overall synthetase specific activity $\left[\frac{\mu\text{g GS}}{\text{mg}\cdot\text{hr}} \right]$	Activity (%)
Nitrogen	None	7.8	100
Air	None	0.5	6
Air	1% Glycerol	7.0	90
Air	1% Fructose	5.4	69
Air	1% Glucose	3.6	46
Air	1% Inositol	3.1	40
Air	1% Sorbitol	0.4	5

^aIncubation with shaking for 90 min at 250 rpm, 37°C.

The best stabilization was obtained with glycerol, followed by fructose, glucose, and inositol in decreasing order of effect. Sorbitol was included in this experiment since it is not a source of carbon for growth but is known to stabilize at high concentrations (~20%) some cell-free enzymes. In our case it was inactive. The results suggest that in vivo synthetase stabilization by carbon sources is linked with the utilization of these compounds by the cells under the conditions of aeration used here. Studies by Asatani and Kurahashi (1) have revealed that there exist systems of active uptake for both glycerol and fructose in *B. brevis*. The uptake of glycerol is considerably faster than that of fructose and they are both catabolized through the glycolytic (EMP) pathway. The same workers have reported that glucose, while not able to support growth as sole C-source for *B. brevis*, can diffuse

passively and very slowly into the cells and, once inside, it can be catabolized through the EMP pathway. In our frozen-thawed cells we are evidently experiencing increased permeability of the cell membrane to glucose as a result of the freeze-thaw treatment. Inositol has been found by Vandamme and Demain (14) to be a poor source of carbon for this organism. Our results indicate that there is a direct relationship between magnitude of the stabilization effect brought about by the C-sources in question and their utilization. This correlation favors the idea of a metabolic basis for the observed stabilization *in vivo*. It is possible that the cells of *B. bevis* are starved for a C- (and energy) source at the point of the *in vivo* inactivation and that such nutrients must be added to retard the inactivation process occurring under air. An experiment was carried out in which 1% glycerol was added to a cell suspension after it had been subjected to inactivating conditions (i.e., shaking in air at 37°C). Table III shows that the inactivated synthetase in these cells failed to be reactivated by glycerol, demonstrating that glycerol is effective in retarding synthetase inactivation in air but cannot restore activity after it has been lost.

Table III.

Failure of Carbon Source to Re-activate
inactivated GS Synthetase^a

Atmosphere	Additive	Overall Synthetase specific activity $\left[\frac{\mu\text{g GS}}{\text{mg}\cdot\text{hr}} \right]$
Nitrogen	None	10.3
Air	None	0.4
Air	None, initially; 1% glycerol added after inactivation	0.4

^aIncubation with shaking for 90 min at 250 rpm, 37°C.

Given the immediate implications of a simple step, such as an addition or pulsing of carbon source for prolonged preservation of the synthetase activity in whole cells, further experiments were conducted over several hours, to examine the time course of the enzyme activity in the presence of several levels of glycerol. Figure 3 shows that progressively higher levels of carbon source from 1 to 4% are able to proportionately retard the inactivation

process. In the same experiment, the dissolved oxygen (D.O.) concentrations were also monitored intermittently in the vessels containing various glycerol levels. It can be seen (Fig. 3) that there exists a correlation between enzyme activity, levels of C-source and D.O. concentration. The retention of enzyme activity is generally compatible with "lower" D.O. levels. This could mean that the lower D.O. levels are maintained, at least partly, through increased respiratory activity in the earlier domains of such time-course experiments, and that, in the presence of C-source such as glycerol, respiratory activity depleting the D.O. in the cell suspension is maintained for a longer period of time thus preventing premature O_2 -mediated inactivation. It is also possible that the catabolism of the C-source is required to continue furnishing both ATP (a co-substrate and possible positive allosteric effector of the enzyme's structural integrity) as well as reduced pyridine nucleotides, NADH/NAD(P)H (whose likely role in retarding inactivation is discussed below). On the other hand, correlation of D.O. with remaining level of enzyme activity is a significant result not only because it immediately suggests ways of engineering intervention (e.g., through a controlled regime of D.O. during production phase) in a batch antibiotic fermentation to achieve optimal GS production, but also because it might suggest a general model of regulatory action of oxygen upon enzymes in aerobic microorganisms producing secondary metabolites. A case in point is the secondary metabolic process of cyanogenesis (production of HCN) by *Pseudomonas* species described by Castric and his colleagues (2,3) which is also subject to oxygen-mediated inactivation. It is possible that oxygen becomes harmful to biosynthetic enzymes of secondary metabolism in obligate aerobes at the point of C- and energy source depletion partly by virtue of the fact that D.O. levels are kept low only during aerobic C-source catabolism.

A possible mechanistic scheme that would link directly the C-source catabolism with the molecular events constituting the inactivation of the synthetase via oxygen, could be formulated as follows: the actual target of the inactivation could well be labile sulfhydryl (SH-) active groups on the enzyme surface. According to Laland and Zimmer (8) it seems that at least seven SH- groups are directly required for activity and possibly some more are involved in ensuring the structural integrity of the enzyme macromolecule. It is then plausible to assume that while such SH- groups are susceptible to autoxidation by D.O. the presence of an actively metabolized C-source could lead to a low intracellular redox potential which is conducive to maintaining the intracellular protein cysteine residues in the SH- (i.e., reduced) state. Conceivably NAD(P)H produced under such conditions may be coupled to regeneration of SH- groups on the enzyme via thiol interchange (nucleophilic substitution) with glutathione (reduced) or lipoamide or thioredoxin. For example, glutathione, the most abundant intracellular thiol in most types of cells may interchange with the enzyme as shown in Figure 4.

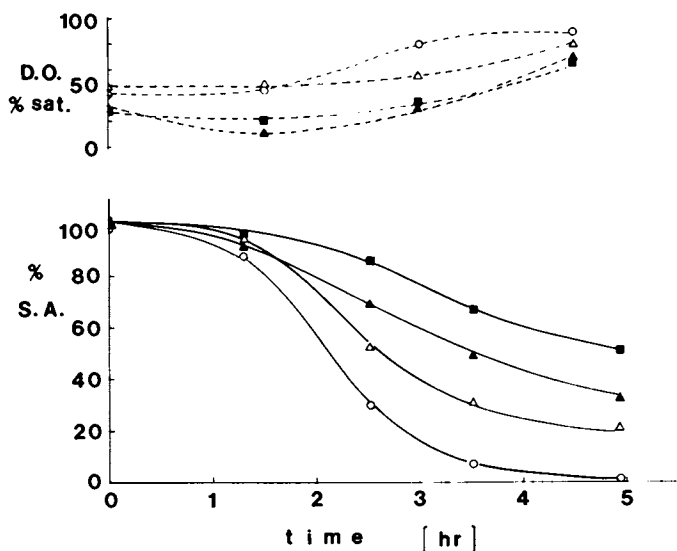


Figure 3. Time course of specific activity of GS synthetase under air in the presence of various levels of utilizable carbon source (glycerol). Shown also are the corresponding levels of dissolved oxygen (DO). Standard conditions for inactivation: agitation at 250 rpm, 37°C. Glycerol levels: ■, 4%; ▲, 2%; △, 1%; ○, 0%.

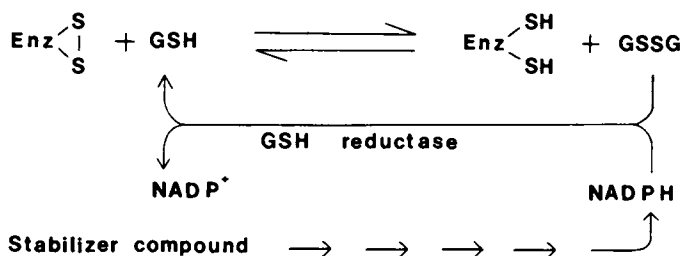


Figure 4. Hypothetical scheme illustrating the action of a stabilizer compound (e.g., utilizable carbon source) on an enzyme containing O_2 -sensitive SH—groups. GSH, reduced glutathione; GSSG, oxidized glutathione.

Inactivation Through Autoxidation of Sulfhydryl Groups. To examine further the possibility that SH- groups are oxidized and inactivated by O_2 in vivo we checked the effect of an organic thiol (DTT) on the activity of the synthetase in long-term experiments. Because hydrogen peroxide and superoxide free radicals are generated during most oxidations of organic thiols, such as DTT, in air (10), such reagents cannot be used as additives in forcibly aerated cell suspensions, but only under N_2 gas. Results from long-term incubations are shown in Figure 5. The experiment was carried out in a way which only assumes a lack of forced O_2 transfer to all cell suspensions [both experimental (with DTT) and controls (without DTT)]. This was achieved through a partial atmosphere of N_2 gas in rubber-capped vials, which, however, permit the gradual entry of air later in the incubation. DTT at 15 mM preserved practically the entire initial activity of the enzyme during 16 hours of incubation, whereas by that time the control vessel (no DTT) had lost all enzyme activity. It appears as if the slow return to aerobiosis in the control vessels (no DTT) lead to autoxidation and inactivation faster than in the vessels containing DTT.

Still another approach to determine the possible involvement of SH- groups as targets of oxidative inactivation of the enzyme was to incubate cells, having already been exposed to various degrees of O_2 -dependent inactivation, under N_2 in the presence of dithiothreitol (DTT). If the hypothesis is correct then the synthetase activity should increase under these conditions. It is of course assumed that the postulated SH- autoxidation has led to sulfur derivatives of the enzyme, which are amenable to reduction back to the thiol state (SH-) in the presence of excess dithiothreitol. An initial experiment along these lines is shown in Figure 6. It can be noted that moderate reactivation was achieved even from states that assume total loss of activity under air. In this experiment a 45-minute additional incubation of the previously exposed cell suspensions was carried out under N_2 in the presence of 15 mM DTT. The results of this experiment strongly implicate SH- groups on the synthetase as the actual targets of the O_2 -dependent inactivation.

Conclusions

It seems that utilizable C-sources are able to retard in vivo inactivation of the synthetases of GS and it also appears as if the inactivation is brought about by autoxidation of SH- groups on the enzyme complex. Moreover the loss of synthetase activity is, at least partially, reversible through externally added dithiothreitol. These results throw considerable light on the process of in vivo inactivation of the biosynthetic enzyme complex catalyzing the formation of GS in B. brevis. We believe that these findings not only suggest fresh ways of optimizing the GS fermentation by controlling the rate of synthetase inactivation, but

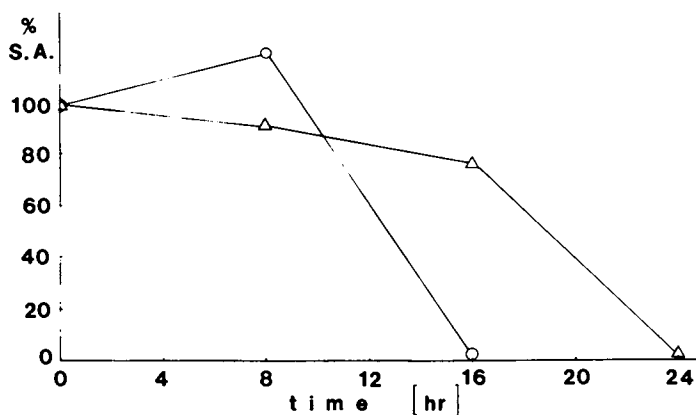


Figure 5. Long-term incubation of frozen-thawed cells of *B. brevis* under N_2 in the presence and absence of an organic thiol (DTT). Standard conditions: agitation at 250 rpm, 37°C. Key: \circ , N_2 present; \triangle , N_2 + 15 mM DTT present.

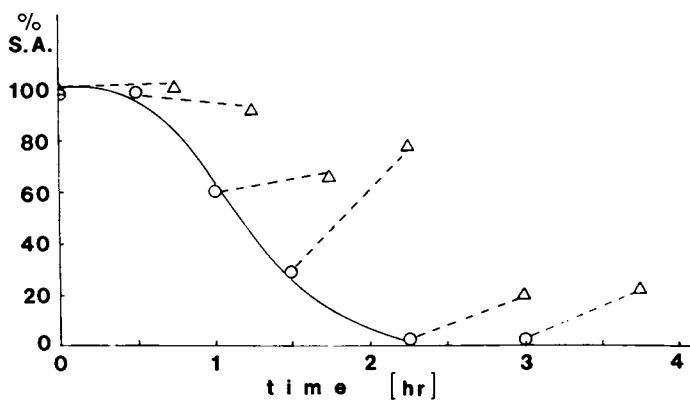


Figure 6. Effect of DDT on specific activity of GS synthetase at various degrees of prior exposure to standard inactivating conditions (air, 250 rpm, 37°C). The subsequent incubation of the cell suspensions was under N_2 in the presence of 15 mM DTT at 37°C for 45 min. Key: \circ , air only; \triangle , air, then N_2 + 15 mM DTT.

also that such knowledge should be directly applicable to the efficient production of closely related antibiotics of commercial significance, such as bacitracin. The methodology outlined in this investigation and possibly specific findings may also be extendable to different processes calling for in vivo stabilization of biosynthetic enzymes, particularly of oxygen-labile enzymes in aerobic organisms. Furthermore a fundamental understanding of the in vivo inactivation of such synthetases appears to hold the promise for a more rational intervention on the part of the biochemical engineer in making efficient use of the biosynthetic potential of a wide variety of industrially significant microorganisms. While the immediate benefit from such an understanding would be an extended production phase in batch fermentations, this knowledge should also be central in designing alternative whole-cell processes (e.g., immobilized cell reactors), in which keeping the enzymes "alive" in their native intracellular micro-environment could be the optimal approach in the operational transition from a batch to a continuous process.

Acknowledgements

We thank the Greek Ministry of Coordination and Planning for a NATO Science Fellowship for S. N. Agathos.

Literature Cited

1. Asatani, M.; Kurahashi, K. J. Biochem. (Tokyo) 1977, 81, 813-822.
2. Castric, P.A.; Ebert, R.F., Castric K.F. Current Microbiol. 1979, 287-292.
3. Castric, P.A.; Castric K.F.; Meganathan, R. "Hydrogen Cyanide Metabolism," Conn, E.E., Knowles, C.J., Vennessland, B., Wissing F., Eds.; Academic Press: New York, in press.
4. Friebel, T.E.; Demain, A.L. J. Bacteriol. 1977a, 130, 1010-1016.
5. Friebel, T.E.; Demain, A.L. FEMS Microbiol. Lett. 1977b, 1, 215-218.
6. Gornall, S.G.; Bardawill, C.J., David, M.M. J. Biol. Chem. 1949, 177, 751-766.
7. Holzer, H. Trends Biochem. Sci. 1976, 1, 178.
8. Laland, S.; Zimmer, T. Essays Biochem. 1973, 9, 31.
9. Matteo, C.C.; Glade, M.; Tanaka, A.; Piret, J.; Demain, A.L. Biotechnol. Bioeng. 1975 17, 129-142.
10. Misra, H.P. J. Biol. Chem. 1974, 249, 2151.
11. Switzer, R.L. Ann. Rev. Microbiol. 1977, 31, 135.
12. Tomino, S.; Yamada, M.; Itoh, H.; Kurahashi, K. Biochemistry 1967, 6, 2552.
13. Tzeng, C.H.; Thrasher, K.D.; Montgomery, J.P.; Hamilton, B.K.; Wang, D.I.C. Biotechnol. Bioeng., 1975, 17, 143.

14. Vandamme, E.J.; Demain, A.L. Antimicrob. Agents Chemother. 1976, 10, 265-273.
15. Waindle, L.M.; Switzer, R.L. J. Bacteriol. 1973, 114, 517.

RECEIVED June 1, 1982

Microbial Regulatory Mechanisms: Obstacles and Tools for the Biochemical Engineer

H. E. UMBARGER

Purdue University, Department of Biological Sciences, West Lafayette, IN 47907

The integration of metabolic activity of bacterial cells with the growth process can limit the extent to which a given activity can be made useful for industrial purposes. Since the mechanisms underlying this integration are genetically controlled, they can be often bypassed or compensated by judicious selection of mutants. The general physiological and molecular patterns of regulatory mechanisms that should be considered in the use of mutant methodology are briefly reviewed. Examples of the way such knowledge can be exploited to obtain valine- and isoleucine-producing strains are described.

There is today a widespread appreciation of the fact that metabolic pathways in microorganisms are remarkably well integrated with the growth process. It is further remarkable that this integration is possible under a broad range of environmental conditions — conditions that vary both chemically and physically.

This integration results from controls exerted in two ways: one, the control of enzyme activity, and the other, the control of enzyme amount. (Strictly speaking, this latter category should also include control of the amount of other macromolecules, such as the ribosomal proteins, ribosomal and transfer RNA, and membrane components.) Let me consider the physiological patterns found to affect enzyme activity, which I like to call the control of metabolite flow. (Throughout this article, the words "control" or "regulation" are meant to connote factors affecting biological functions that can be modulated, in contrast to a factor that has consequences on biological function. An analogy with a domestic water supply would be an adjustable valve that can be manipulated, in contrast to an obstruction in the supply line.)

Broadly speaking, there are three basic patterns affecting the control of metabolite flow (Table I). The simplest is end-product inhibition in which the endproduct of a pathway is an

0097-6156/83/0207-0071\$06.50/0

© 1983 American Chemical Society

Table I

Physiological Patterns of Control of Metabolite Flow

<u>Pattern</u>	<u>Example</u>	<u>Reference</u>
Endproduct inhibition	Inhibition of threonine deaminase by isoleucine (<i>E. coli</i>)	(1)
Precursor activation	Stimulation of lactate dehydrogenase by fructose-1,6-diphosphate (<i>Streptococcus fecalis</i>)	(2)
Compensatory modulation	Stimulation of carbamylphosphate synthetase by ornithine (<i>E. coli</i>)	(3)

inhibitor of the initial enzyme of the pathway. The inhibition of threonine deaminase is a well known example to which I refer later in this article (1). There are variations on this general theme in which multiple endproducts may act in concert or synergistically upon a single enzyme catalyzing the first step in a common pathway or in which a segment of a single pathway is controlled by an intermediate inhibiting an earlier step [e.g., the inhibition of phosphofructokinase of *Escherichia coli* by phosphoenolpyruvate (2)].

The reverse of endproduct inhibition is precursor activation. Although it is more difficult to cite examples in biosynthetic pathways, an example is found in the activation of certain microbial lactate dehydrogenases by fructose-1,6-diphosphate. Finally, there is another pattern of enzyme activation that I would call compensatory modulation of activity. The example that is particularly well studied is the activation of carbamyl phosphate synthetase of *E. coli* by ornithine (3). This enzyme forms carbamylphosphate needed for both pyrimidine nucleotide biosynthesis and arginine biosynthesis. The enzyme is inhibited by UMP, an indicator of the global pyrimidine pool. However, an ample supply of carbamylphosphate for arginine biosynthesis is assured by ornithine stimulating the enzyme and antagonizing the UMP-mediated inhibition. Ornithine, of course, is an intermediate that would appear only when the arginine supply was low.

This classification of regulatory patterns implies nothing with respect to the mechanisms by which regulation was achieved. The common mechanisms that have been recognized in controlling carbon flow are classified in Table II. We can recognize mechanisms that are specific in that they are related to the specific role the modulated enzyme plays and mechanisms that are general in that they may affect many enzymes or pathways that are not functionally related or have little to do with the physiological role of the enzyme.

Table II

Enzymic Mechanisms Underlying Control of Metabolite Flow

<u>Mechanism</u>	<u>Example in <i>E. coli</i></u>	<u>Reference</u>
Specific mechanisms:		
Binding at catalytic site	Inhibition of asparagine synthetase by asparagine	(4)
Binding at regulatory site	Inhibition of threonine deaminase by isoleucine and its antagonism by valine	(5)
Enzyme modification	Adenylylation of glutamine synthetase	(6)
Protein-protein interaction	Stimulation of α -subunit of tryptophan synthase by β -subunit	(7)
General mechanisms:		
Energy charge	Retardation of aspartokinase III activity at low energy charge	(8)
Reducing potential	Inhibition of pyruvate dehydrogenase at low NAD^+/NADH ratios	(9)
Substrate availability	None known	

The simplest of these mechanisms would be the action of an inhibitor binding at the active site. The inhibition of succinate dehydrogenase by oxaloacetate can be looked upon as such an example (10). It may be that tight binding of a product may also play a role in regulating the activity of an enzyme (11). The inhibition of asparagine synthetase by asparagine in microorganisms provides a likely candidate for regulation by tight binding of product (4).

Obviously more complex would be those enzymes on which a separate regulatory site has been developed for binding of either a stimulatory or an inhibitory ligand that is physiologically related to the function but not itself stoichiometrically related to the catalytic events. When such a ligand is an inhibitor, it would be an example of what Monod and Jacob (12) had defined as an allosteric inhibitor, in contrast to the previous example, which they defined as isosteric. Many examples of this kind of regulatory process have been described in both catabolic and biosynthetic pathways. However, in referring to binding of a regulatory ligand to a distinct regulatory site, I would not wish to imply a common mechanism by which the inhibition or the stimulation occurs. There probably are several mechanisms involved, and at the level of enzyme structure there is seldom complete agreement among all investigators regarding the precise details.

At the present time, we can cite more examples of enzyme modification occurring as regulatory mechanisms in animal metabolism than we can in microbial metabolism. In animal metabolism, phosphorylation by protein kinases affects many enzymes (13). There are examples of phosphorylation of bacterial proteins, but, with few exceptions, the role or even the identity of the protein is unknown. One example that has been studied is the isocitrate dehydrogenase of *E. coli*, which is phosphorylated when the cell is shifted from glucose to acetate as the carbon source and which thereby undergoes a very rapid decrease in activity (14).

The best-studied example of modification of an enzyme is that of the adenylation and deadenylation of glutamine synthase of *E. coli*, which, in effect, serves to inhibit and to activate the enzyme (6).

To some extent, the idea of protein-protein interactions affecting the activity of bacterial pathways may still be hypothetical. In yeast, we can cite at least one clearly important example. That is the inhibition of ornithine transcarbamylase upon binding to arginase, an enzyme induced by adding arginine to the medium (15). This protein-protein interaction thus prevents a futile cycle in which ornithine, formed from exogenous arginine, would be converted back to arginine. There are in vitro models that can be cited in bacterial metabolism that demonstrate the feasibility of such a mechanism, in which an activity of one protein is markedly enhanced upon binding to another. For example, the conversion of serine and indole to tryptophan is slowly catalyzed by the α subunit of tryptophan synthase alone but is

stimulated some 30-fold upon binding to β -subunit dimers.

Under the category of general controls, I have listed energy charge and reducing potential, which could be looked upon as special cases of substrate availability. The energy charge experiments of Atkinson (16) have demonstrated several examples of in vitro response to energy charge, but it is still difficult to assess the in vitro significance of such a response to energy charge, since cells do have a remarkable capacity for maintaining the energy charge within rather narrow limits (17). Similarly, the extent to which a pyridine nucleotide-linked reaction proceeds can be modulated by the NAD/NADH (or NADP/NADPH) ratio (9). The question is whether these ratios can be so changed in the growing cell to be exploited as a regulatory mechanism.

One can anticipate that the flux through a pathway might be limited not by some rate-limiting step at the beginning or within the pathway but by the rate at which the initial substrate for the pathway is supplied. To the extent that this supply of substrate is modulated, such a mechanism might play a regulatory role. That a limitation in supply can have important consequences on the extent that a pathway might function will become clear in the description of the development of an isoleucine-producing strain later in this article. However, in the sense of the word "regulation" as used here, this example would not be considered a regulatory mechanism.

Just as physiological patterns of control over metabolite flow can be recognized, so can physiological patterns of control over the amount of enzyme. Table III lists a convenient classification. Clearly, the amount of enzyme at any time is a summation of the amount formed and the amount destroyed. Two specific patterns controlling formation might be recognized: repression by endproducts and induction by substrate or a precursor. It should be stressed that the terms "repression" and "induction" are operational and should carry no connotations regarding the mechanisms.

In addition, there are general mechanisms controlling larger groups of enzymes or groups of pathways. One general mechanism is involved in repressing the formation of carbon- and energy-yielding pathways when there is a good carbon and energy source (this is better known as catabolite repression) (27). An analogous control mechanism is related to the nitrogen supply, and many inducible catabolic pathways yielding ammonia are repressed when there is already an adequate nitrogen supply (21). Another important control mechanism is that related to growth rate. At high growth rates in a rich medium, the protein-forming apparatus (ribosomes, tRNA, etc.) is high, whereas the enzymes forming the small molecule building blocks are repressed to an extent much greater than that accounted for by the presence of the endproducts in the medium (22).

Recent studies by Neidhardt and his colleagues (23) have revealed a newly recognized class of enzymes in *E. coli* that are induced at elevated temperatures.

Table III
Physiological Patterns of Regulation of Protein Amount

<u>Pattern</u>	<u>Typical examples</u> *	<u>Reference</u>
Effect on Enzyme Formation		
Specific:		
Repression by endproducts	Repression of arginine biosynthetic enzymes	(18)
Induction by substrates or precursors	Induction of <i>lac</i> operon	(19)
General:		
Related to carbon supply	Catabolite repression of <i>lac</i> induction	(20)
Related to nitrogen supply	Histidase induction in glucose-containing, NH ₃ -free media (<i>K. aerogenes</i>)	(21)
Related to growth rate	Derepression of the protein synthesizing system at fast growth rates	(22)
Related to temperature	"Thermometer" proteins, which increase or decrease in amount with growth temperature	(23)
Effect on Enzyme Destruction		
Specific:		
Stabilization by ligands	The stabilization of glutamine phosphoribosylpyrophosphate amidotransferase of <i>B. subtilis</i> by substrates	(24)
General:		
Starvation of cells for carbon or nitrogen	Increased protein turnover with onset of starvation	(25)
Inhibition of protease activity	Serine protease inhibitor of <i>B. subtilis</i>	(26)

*The examples cited are found in *E. coli*, except where indicated.

Finally, the degradation of an enzyme by proteolysis can be modulated in specific ways through substrate or product stabilization (24). These would constitute specific controls over enzyme destruction. It is also known that, when cells are starved for amino acids, nitrogen, or energy, there is increased turnover of many cell proteins (25). Such a control might be considered a general one.

Some of the mechanisms underlying the physiological responses listed in Table III are given in Table IV. Enzyme destruction, which will not be considered further, occurs of course by proteolytic breakdown and, in that it can be impeded by ligands (either substrates or inhibitors) that bind to the protein, could be subject to a specific control. Proteolysis might be enhanced by factors that activate proteases or release protease inhibitors. Such an enhancement might be considered a general control over proteolytic breakdown.

The formation of proteins can be regulated at two levels, either by affecting formation of mRNA (transcription) or its utilization as template (translation). In turn, transcription can be controlled in two ways. One is a control of initiation of transcription (i.e., whether the RNA polymerase forms an initiation complex). The other is a control over how far a polymerase travels and whether it proceeds into a structural gene or not (i.e., whether attenuation of transcription occurs). Translational control would more likely be achieved by controlling ribosome binding to the mRNA, although mechanisms affecting ribosome travel are conceivable.

Among the molecular mechanisms controlling the initiation of transcription in bacteria that might be considered specific mechanisms of control are those that involve a negative control element, or the repressor of the original model of Jacob and Monod (44). Two kinds of control were envisioned in that model. One involved a repressor protein that was active only in the presence of the endproduct of the pathway. The best-studied example is the product of the *trpR* gene, which becomes active only after binding to tryptophan. The binding of the activated repressor to the operator sites of the *trp* operon, of the *aroH* gene, or of the *trpR* gene and the binding of RNA polymerase to the corresponding promoters are mutually exclusive (28). The inverse of this pattern is the inactivation of the repressor protein by the substrate (or a derivative). The best-studied example of this pattern is the inactivation of the *lac* repressor by its binding of allolactose, a derivative of lactose formed by the action of β -galactosidase on lactose (29).

Although it was considered as one possibility by Jacob and Monod (44) in their formulation of a model for control of gene expression, regulation by positive control elements was considered a less likely mechanism for control of gene expression. There have been several examples described in which positive control

Table IV

Molecular Basis of Regulation of Protein Formation

<u>Mode of Control</u>	<u>Typical Examples</u>	<u>Reference</u>
Transcriptional Control		
Control of Transcription Initiation		
Specific:		
Negative Control Elements		
Activated by endproducts	Repression of the <i>trp</i> operon by <i>trp</i>	(28)
Inactivated by substrate or precursor	Induction of <i>lac</i> operon by allolactose	(29)
Positive Control Elements		
Activated by substrate or precursor	Induction of acetohydroxy isomeroreductase by acetohydroxy acids	(30)
(Inactivation by endproduct)	None known	
General:		
Positive Control Elements		
Activated by cAMP	Dependence of <i>lac</i> operon induction on cAMP-CRP interaction	(31)
Activated by temperature	Dependence of several heat-induced proteins on the <i>htp</i> gene product	(32)
σ -Like proteins	Shift of RNA polymerase specificity by Bacilli during sporulation	(33)
[ppGpp-mediated regulation]	Inhibition of RNA polymerase binding to <i>rnm</i> promoters.	(34)
	Enhancement of polymerase pausing in <i>rnm</i> operons	(35)
[Nitrogen-mediated regulation]	The <i>glnG</i> -dependent activation of genes involved in catabolism of nitrogen-containing compounds	(36)

Table IV, cont'd.

Control of Transcription Termination

General:

ρ -Dependent termination	<i>trp</i> ' terminator at end of <i>trp</i> operon	(37)
	t_{R1} terminator of λ	(38)
ρ -Independent termination	Termination of transcription at the end of leader sequence for amino acid biosynthetic operon	(39)
Transient termination-polymerase pausing	Polymerase pause site in <i>rrnB</i> operon	(40)

Specific:

Antitermination by specific proteins	λ <i>N</i> gene-dependent transcription beyond the t_{R1} terminator	(41)
Antitermination by ribosome halt at specific codon	Attenuation of <i>ilv</i> , <i>trp</i> , <i>his</i> , and other amino acid biosynthetic codons	(39)

Control of Translation

Specific:

Masking of ribosomal binding sites by protein binding	Binding of small ribosomal proteins at ribosome binding site for the <i>rbsL</i> (<i>str</i>) operon	(42)
By perturbation of secondary structure of message	The masking of <i>erm</i> (erythromycin resistance) ribosome binding site by retarded translation of the <i>erm</i> leader transcript	(43)

General:

(Amino acid supply)	None known
(Inhibition)	None known

Mechanisms enclosed in () may be hypothetical, since no examples have been reported. Mechanisms enclosed in [] remain unexplained, i.e., precise mechanism is unknown.

provides the primary control over expression of a gene. One example is the positive control element (upsilon, the product of the *ilvY* gene) required for the induction of acetohydroxy acid isomeroreductase, the inducible enzyme in the isoleucine and valine biosynthetic pathway of *E. coli* (30). (It should be pointed out that some regulatory elements can play both a positive and a negative control role. An example is the *araC* gene product required for induction of the arabinose-utilizing pathway (45). In the absence of arabinose, it acts as a negative control element or repressor, and in its presence it acts as a positive control element.) Again, the inverse of this pattern, inactivation of a positive control element by the endproduct of a pathway, might provide a mechanism for repression. However, this writer is aware of no example of such a mechanism.

Several of the general controls over enzyme formation appear to be achieved by affecting transcription initiation. There is no reason to assume that these general controls could not be mediated via positive or negative control elements of broad specificity, and it may be that many are. A well-studied example of a positive control element affecting many catabolic systems in bacteria is the interaction between cAMP and its binding protein (CAP), which allows binding of CAP to the DNA near the promoters of certain catabolic enzymes, after which RNA polymerase can more readily bind (31). The heat-induced proteins recently demonstrated in *E. coli* by Neidhardt's group may be considered another example (23). The induction of these enzymes appears to be dependent upon a positive control element specified by the *htp* gene (32).

Another kind of control has been found to be important in the Bacilli and might be important in other organisms as well. This is a control of large numbers of genes by altering the specificity of RNA polymerase by the binding of different sigma (σ) factors (33). Thus, during the sporulation phase, the 55-kd σ factor that is predominantly bound to RNA polymerase is replaced by a 29-kd σ factor which allows some of the spore-specific genes to be expressed. To date, at least four different σ factors have been identified in *B. subtilis*.

Two other general regulatory mechanisms have been studied that appear to affect transcription initiation. Neither, however, are well enough understood to decide whether they might constitute unique mechanisms or are special cases of positive control elements that exert a generalized control role. One is the ppGpp-mediated regulation that impedes stable (ribosomal and transfer) RNA formation and, at least in vitro, stimulates transcription of many biosynthetic and catabolic operons. While ppGpp does prevent RNA polymerase binding to stable RNA promoters, the pronounced effect of ppGpp on stable RNA formation cannot solely be explained on this basis alone (see below) (34,35). The other is the control that is an effect of nitrogen limitation and leads to the expression of genes involved in releasing NH_3 from nitrogen-

containing compounds (36). The *glnG* gene is somehow involved, but whether that product is a positive control element acting in a way analogous to that by which cAMP bound to CAP acts on carbon and energy producing pathways is not clear.

Table IV also lists some of the factors that control transcription termination. Transcription termination plays two roles. One, of course, is the termination that occurs a short distance beyond the end of a given structural gene or beyond the end of the operon. The other is a termination that serves to attenuate the transcript or to terminate transcription at a site upstream of that at which the maximal-sized transcript is terminated (39). It is the modulation of the latter kind of transcription termination that provides an important mechanism of transcriptional control.

Transcription termination is signalled by either ρ -dependent or ρ -independent sequences in the DNA (and RNA). The latter are readily recognized as regions of dyad symmetry in the DNA which yield stem and loop structures in the RNA followed by a sequence of several uridine residues in which transcription is terminated (46). ρ -Dependent termination sites seem to be characterized by transcripts with more weakly base-paired stem and loop structures near the termination site in the transcripts and with less precise points of termination than those found in ρ -independent termination sites (47,48).

Closely related to the sites of ρ -dependent and ρ -independent termination sites are sites at which pausing of RNA polymerase occurs. Pausing is also apparently characteristic of termination sites, but the "rules" for polymerase pausing are even less clear than those for termination (40,49).

Polymerase pausing and transcription termination can thus affect the extent to which the DNA downstream of the pausing or termination site are transcribed independently of the transcription initiation event. That pausing or termination can be modulated allows a control of the process. It is an enhancement by ppGpp of polymerase pausing at a site early in ribosomal RNA operons that may account for the striking effect that this nucleotide has on the synthesis of stable RNA over and above that which occurs at the polymerase binding step (40). The prolonged pausing of polymerase progress at a specific point has been termed "turnstile" attenuation.

Similarly, when termination at a site within an operon or at the end of a leader region is affected by a specific regulatory signal, an efficient control can be achieved. One of the most studied controls over a ρ -dependent termination is that which occurs at the λ tR1 site and is prevented by the λ N gene product (41). Like the activity of ρ itself, the activity of the N gene product is dependent on the elongation subunit of RNA polymerase specified by the *E. coli nusa* gene. It might be anticipated that attenuation of transcription by a specific antiterminating protein is a general pattern that will be found to occur frequently in microbial systems.

Another control over termination that has been extensively studied is the attenuation of transcription at the end of the leader regions of several amino acid biosynthetic operons (or genes) in *E. coli* and related organisms (39). The primary indication that such a mechanism is involved in the control of an amino acid biosynthetic pathway is an endproduct repression that is dependent on the amino acid being transferred to its cognate tRNA at an ample rate. Thus, derepression of the histidine biosynthetic pathway can be achieved by any mechanism that reduces the intracellular level of histidyl tRNA, for example, by limiting the supply of histidine itself or by limiting the activity of the histidyl tRNA synthetase (51).

Thus far, the amino acid biosynthetic genes controlled in this way are characterized by the presence of a leader region between the promoter and the structural gene (52,53). The leader is transcribed at a frequency dependent upon promoter strength and polymerase availability (in the case of the *trp* operon, transcription initiation itself is controlled by the *trp* repressor). The leader transcript carries the information for a short peptide that is unusually rich in the amino acid(s) for which the pathway is concerned. Whether RNA polymerase stops at the end of the leader or proceeds into the structural gene is dependent upon whether a ribosome can translate the leader transcript to the stop codon (amino acid excess) or is stalled at a codon for the amino acid for which the pathway is concerned (amino acid limitation). The mechanism underlying termination is that competing secondary structures of the leader transcript are selected by the extent of ribosomal travel and that one of these alternative secondary structures contains a typical ρ (rho)-independent termination signal. The general features have been studied best in the amino acid biosynthetic operons of several Enterobacteriaceae (39).

Although the nature of the bacterial cell makes possible specific control over transcription in ways that cannot be achieved in eukaryotic systems, control of gene expression at the level of translation is also important in bacteria. Control of translation is achieved primarily by the prevention of ribosomal binding. Such a control might be achieved by masking the binding site either by specific binding by proteins or by the secondary structure of the message itself. The best-studied examples are the ribosomal proteins (54). Although the genes for all ribosomal proteins have not yet been examined, the general pattern that seems to be emerging is that one of the ribosomal proteins specified by a multicistronic, ribosomal protein operon prevents message translation by binding at the translational start site on the message. The basis for the specific binding in the case of ribosomal proteins S4 and S7 is that the RNA in the vicinity of the ribosomal start site has a structure strongly homologous to that of the region on 16S RNA that binds to S4 (or to S7) during ribosome assembly (42).

The control over the erythromycin resistance gene, which

specifies a ribosomal methylase, is also achieved by interfering with translation of the message (43). Masking of the ribosome masking site is not by a protein binding to it but by a secondary structure occurring in the message whenever a translating ribosome is able to translate the peptide specified by the leader sequence (as could occur only if already modified ribosomes were functioning in the presence of erythromycin or if normal ribosomes were functioning in the absence of erythromycin). The ribosome binding site of the methylase message would be opened when the translating ribosome stalled in the early part of the leader (as could occur if unmodified, sensitive ribosomes were functioning in the presence of erythromycin). This mechanism, affecting accessibility of a ribosome binding site is thus reminiscent of the control of formation of a transcription termination site by the translation of the leader sequence of several amino acid biosynthetic genes described above.

These examples are a small sample of many that could be cited that make it quite clear that microbial metabolism is rather rigidly controlled for the primary function of the microbe: to grow and reproduce itself as efficiently as possible. These are what I would term obstacles to the biochemical engineer who may wish to exploit a particular enzyme reaction or a particular pathway to a function that may well be detrimental to the primary function of the organism. However, in every case, the control mechanisms that constitute these obstacles are genetically controlled and, therefore, are subject to mutation. To the extent that mutations can be selected that are advantageous to the engineer without being lethal to the organism, these control mechanisms can be considered "tools" to be manipulated and carefully honed.

It is, however, sometimes difficult to exploit the capacity of an organism to perform a useful biochemical transformation. Often Nature has selected organisms in which the strictures found in most organisms are modified, and the organism occupies a unique niche. Such organisms, if discovered, can serve useful functions. Just such organisms are those that are currently being used in the Japanese amino acid fermentation industry. In most cases, the organisms have been isolated and identified by empirical research and screening procedures. In some cases, the basis for the non-normal formation of amino acids can be explained *post facto*, but seldom does it appear that these organisms were developed by a preconceived, rational approach. I would therefore like to cite and analyze what I think provides an exception.

The exceptional case is one in which the investigators judiciously combined empirical and rational approaches to prepare an organism capable of producing large amounts of the amino acid isoleucine. The project was performed by investigation at the Tanabe Seiyaku Company in Osaka, Japan, and involved the organism *Serratia marcescens* (55). Before review of this work, it is necessary to consider briefly several aspects of the pathways by which

isoleucine and the closely related amino acid, valine, are formed.

Figure 1 shows these pathways. An important feature is that the four steps leading to valine are catalyzed by enzymes that are also needed for isoleucine formation. In addition, a fifth enzyme, threonine deaminase, is required in most plants and microorganisms for the formation of α -ketobutyrate. Several details of the pathways are given in the legend.

Also shown in Figure 1 is the arrangement of the structural genes found in *E. coli*. It should be pointed out that all of the genes, except those for the two valine-insensitive aceto-hydroxy acid synthases, are contained in the *ilv* gene cluster at the 84-minute region of the *E. coli* chromosome. It might therefore be anticipated that an *E. coli* strain carrying a plasmid with the *ilv* gene cluster would be an excellent overproducer of valine. (If the chromosomal *ilv* fragment was derived from the K-12 strain of *E. coli*, it would have to contain an *ilvO* mutation so that *ilvG* would be expressed. See Figure 1.) Such a plasmid would be even more effective if the inserted DNA carried an *ilvA* lesion, i.e., was threonine deaminase negative. Overproduction of valine would be expected, since the valine pathway derives its carbon exclusively from a key intermediate in the central metabolic route, pyruvate. Flow into the pathway would then never be restricted as long as ample carbon source was present.

An analogous condition for isoleucine overproduction would not be expected to arise if the corresponding plasmid containing an *ilvA* structural gene mutation leading to a feedback negative threonine deaminase were to be employed. As can be seen in Figure 2, carbon flow into the isoleucine pathway is dependent not only on the supply of pyruvate but also on threonine, an endproduct itself, and the synthesis of which is also stringently regulated. It is doubtful whether threonine could be formed fast enough in an otherwise normal cell to exploit fully the high level expression of the *ilv* genes carried on a plasmid as described here. The procedures followed by Komatsubara and his coworkers illustrates well how this kind of obstacle can be circumvented.

The sequence of manipulations employed by Komatsubara et al. (55) is summarized in Figure 3. The simplest step was to isolate a derivative of the parent *S. marcescens* strain, 8000, that was derepressed for the *ilvGEDA* operon and carried a lesion in the *ilvA* gene that allowed the formation of an isoleucine-insensitive (feedback negative) threonine deaminase (TD^F). This kind of isolation had earlier been accomplished by the sequential selection of an aminobutyrate-resistant strain (derepressed) followed by selection of an isoleucine hydroxamate-resistant derivative (feedback resistant) (58). The investigators were more fortunate in the selection of strain GIHVL-r6426, which arose as an isoleucine hydroxamate-resistant strain after mutagenesis by nitrosoguanidine, a mutagen known for causing closely linked mutations in the same cell. The precise nature of the mutation allowing derepression was not established, but, in analogy with what has been

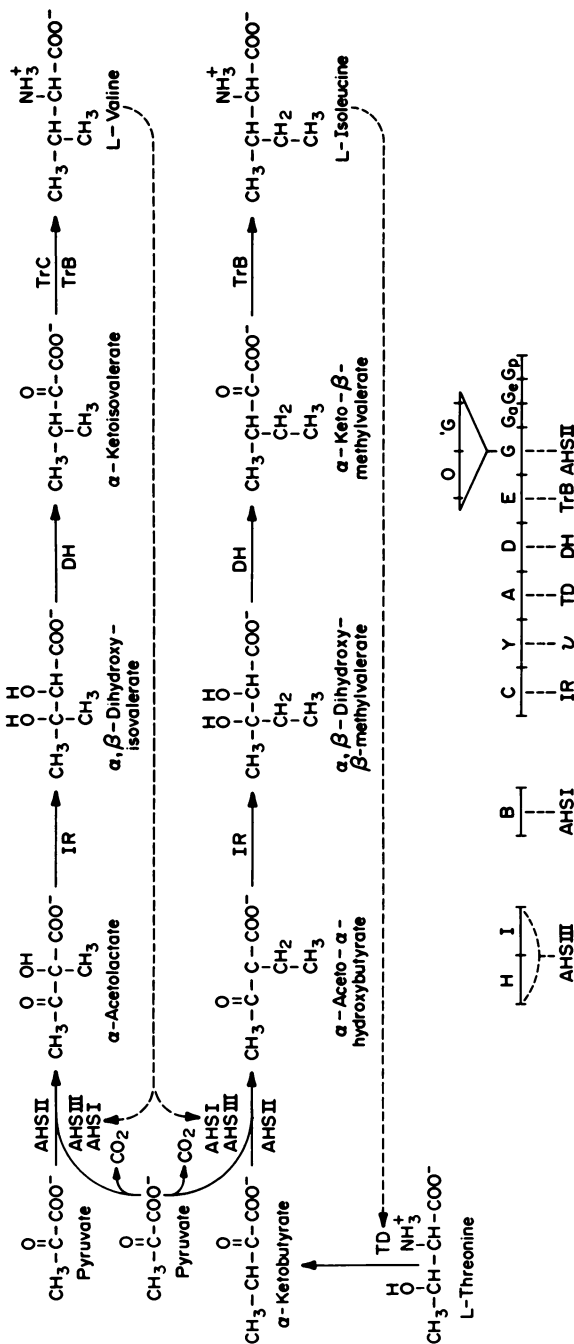


Figure 1. Biosynthesis of isoleucine and valine. The enzymes catalyzing the indicated steps are abbreviated, and the corresponding structural genes (where known) are indicated in parentheses as follows.

TD (ilvA), threonine deaminase; AHS I (ilvB) and AHS III (ilvH), valine-inhibited acetohydroxy acid synthases; AHS II (ilvG), valine-insensitive acetohydroxy acid synthase; IR (ilvC), acetohydroxy acid isomerase; DH (ilvD), dihydroxy acid dehydratase; TrB (ilvE), transaminase B; TrC, transaminase C. In *E. coli* strain K-12, ilvG exhibits no activity owing to a polar lesion in the ilvO region of the gene. Certain frameshift mutations in ilvO result in ilvG expression and increased downstream expression. Control of the ilvGEDA operon occurs by attenuation at ilvGa of transcripts initiated at the promoter ilvCp. The ilvY product, μ , is a positive control element needed for induction of ilvC by the substrates of its product, IR.

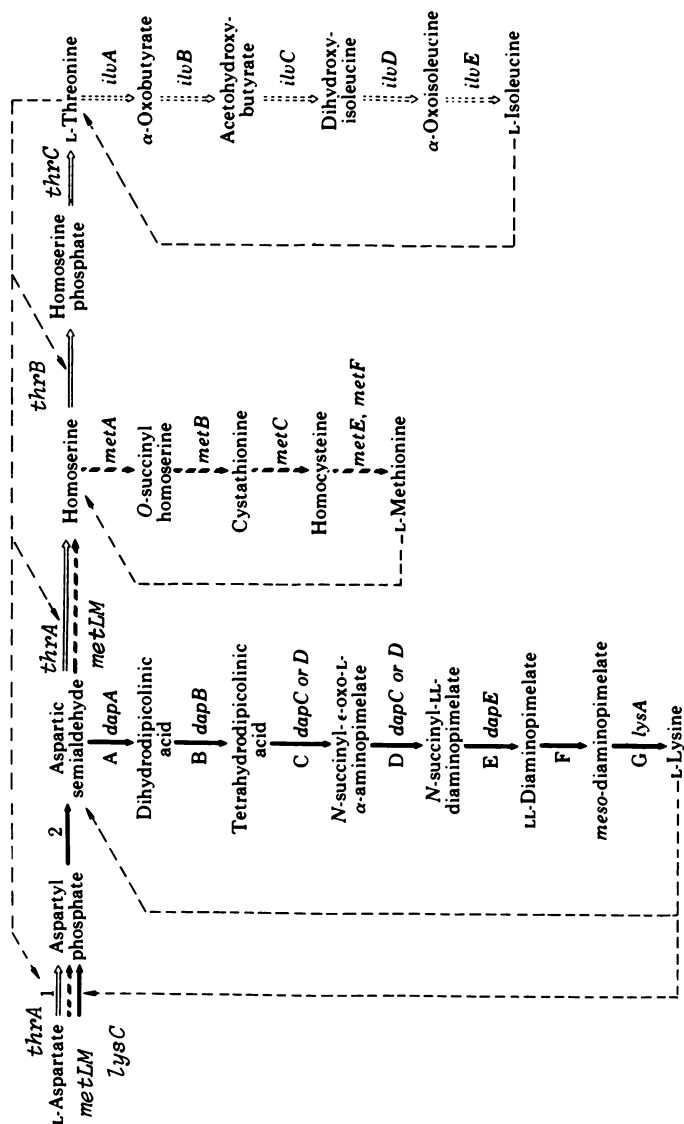


Figure 2. The biosynthesis of lysine, methionine, threonine, and isoleucine in *E. coli* and *S. marcescens*. Solid arrows, steps catalyzed by enzymes repressed by lysine. Broken arrows, steps catalyzed by enzymes repressed by methionine. Open arrows, steps catalyzed by enzymes repressed by threonine plus isoleucine. Open, dashed arrows, steps catalyzed by enzymes controlled as described in Figure 1. Structural genes indicated in italics. Dashed lines indicate reactions controlled by endproduct inhibition. Reproduced, with permission, from Ref. 57. Copyright 1975, American Society for Microbiology.

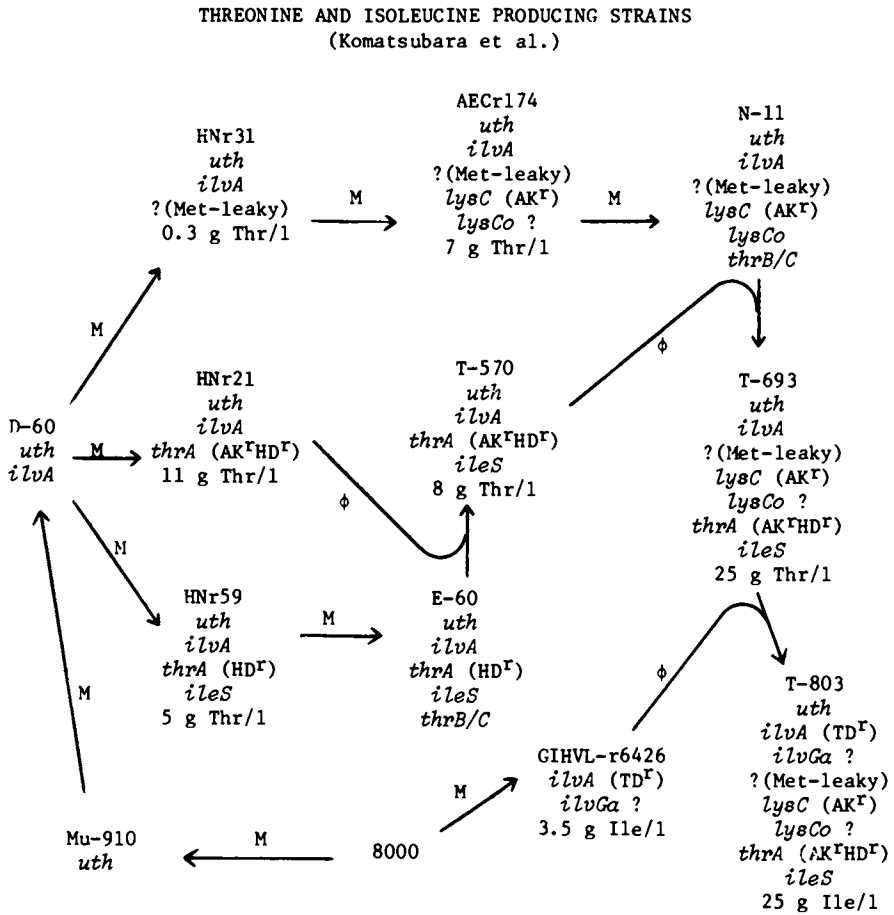


Figure 3. The development of an isoleucine-producing strain from *S. marcescens* strain 8000. Key: ϕ , phage-mediated transduction; M, nitrosoguanidine mutagenesis. See text for details.

learned about the control of the *ilvGEDA* operon in *E. coli*, it is most likely a mutation affecting the attenuator (*ilvGa*), thereby abolishing the multivalent control of the parental strain. That *ilvG*, the structural gene for the valine-insensitive acetohydroxy acid synthase, was derepressed assured that acetohydroxy acid isomeroreductase would be highly induced by substrate, even though its structural gene, *ilvC*, is not part of the derepressed operon. The resistant mutant was shown to excrete up to 3.5 gm of isoleucine per liter in a minimal medium containing 150 gm of sucrose as carbon source. That this level was limited by availability of threonine was later demonstrated by the fact that transfer of the two linked *ilv* mutations to a strain overproducing large quantities of threonine resulted in a much better isoleucine producer.

The steps used to develop the threonine producer were complex and are also outlined in Figure 3. The first of these steps was the isolation of nitrosoguanidine mutant (Mu-910) unable to utilize threonine as a nitrogen and carbon source (59). The mutation was in the *uth* gene, which specifies threonine dehydrogenase. To obtain an organism even less able to break down exogenous threonine, mutagenesis to yield an isoleucine-requiring strain lacking threonine deaminase was employed. When preformed threonine was added to fully grown cultures of the resulting strain, D-60, the rapid disappearance noted with the original parent strain was no longer observed (59).

Strain D-60 was then used to select mutants resistant to the threonine analog, β -hydroxynorvaline, following nitrosoguanidine mutagenesis (60,61). Three kinds of resistant strain were saved for subsequent use. One of these (HNr31) had an incomplete but undefined block in methionine biosynthesis, which may have accounted for the small amount of threonine that was accumulated from homoserine being funneled into the threonine pathway.

The other two mutants produced much greater amounts of threonine. One, strain HNr21, appeared to contain a single mutation in the *thrA* gene, which specifies the bicephalic enzyme, aspartokinase I-homoserine dehydrogenase I (Figure 2). Normally, both of these activities are inhibited by threonine. The mutation in strain HNr21 abolished the threonine sensitivity for both activities. This loss of feedback control resulted in an overproduction of threonine to an extent of 11 gm of threonine per liter. The other strain, HNr59, also had a *thrA* lesion, but this one appeared to abolish only the threonine sensitivity of the homoserine dehydrogenase. There was another mutation in the same strain which appeared to be in the *ileS* gene. If so, it undoubtedly caused the corresponding gene product, isoleucyl tRNA synthetase, to have a reduced affinity for its substrate. Such an enzyme would lead to reduced levels of isoleucyl tRNA and derepressed levels of the *thr* operon and the *ilvGEDA* operon. Since the mutant was an *ilvA* mutant, the concomitant derepression of the *ilvGEDA* operon was of no consequence. However, the *ilvA* mutation made it necessary for the strain to be grown in the presence of exogenous isoleucine and may

have reduced the effectiveness of the low-affinity isoleucyl tRNA synthetase in causing a derepression of the threonine biosynthetic enzymes.

In an attempt to enhance threonine production, steps were taken to replace the *thrA* gene mutation affecting only homoserine dehydrogenase I activity in strain HNr59 with that of strain HNr21, which affected both aspartokinase I and homoserine dehydrogenase I activities. This transfer was accomplished by introducing a *thrB* (or *C*) mutation in HNr59, to yield strain E-60 (62). This strain then served as recipient for phage-mediated transduction with strain HNr21 as donor. The resulting strain, T-570, contained the doubly insensitive aspartokinase I-homoserine dehydrogenase I activities of strain HNr21 but had not lost the closely linked *ileS* lesion of strain E-60 (or its parent, HNr59). Surprisingly, this strain did not produce quite as much threonine as did strain HNr21.

Attempts were therefore made to increase carbon flow into the threonine pathway by enhancing the activity of the lysine-sensitive aspartokinase. This was accomplished by selecting nitroso-guanidine-induced mutants resistant to aminoethylcysteine (61). One of these strains, AECr174, was probably another doubly mutated strain with a lysine-insensitive aspartokinase that was also derepressed. The derepression might have been either an "up" promoter or an operator mutation in the *lysC* gene (as is suggested in Figure 3). This strain accumulated 7 gm of threonine per liter. Mutagenesis to threonine auxotrophy yielded strain N-11, which allowed introduction of the *thrA* gene and *ileS* genes of strain T-570 by phage-mediated transduction (62).

The resultant strain, T-693, produced up to 25 gm of threonine per liter and provided exactly the kind of background that might feed carbon into an isoleucine pathway that had lost both feedback and repression control. This introduction was possible because strain T-693 carried the original *ilvA* lesion of strain D-60. Phage grown on strain GLHVL-6426 was therefore used to render strain T-693 isoleucine independent. In so doing, both the feedback resistance of threonine deaminase and the derepression of the *ilvGEDA* operon were introduced. The resulting strain, T-803, produced up to 25 gm of isoleucine per liter. The carbon flow into the uncontrolled threonine pathway had thus been almost completely diverted to isoleucine production with only about 3 gm of threonine now being formed by strain T-803.

This rather involved example serves perhaps as an interesting model for the way empirically generated mutations can be rationally manipulated to yield useful organisms. In the example cited, the useful tool of using analogs to select strains with altered control circuits was invaluable. There were really no unexpected mutations, yet there was no way to predict which combination of lesions would have supplemented each other to have yielded such prolific overproducers. It may be that the maximally effective combination was not obtained in strain T-803, and it is likely

that the investigators tried many more combinations than those that were reported.

Investigators are undoubtedly now being tempted to exploit the use of recombinant DNA technology to produce strains with certain biochemical activities enhanced. The lesson the model system described here has for such investigators is that, in addition to requiring elevated enzyme activities, it is also necessary to assure that the cell can provide the substrates or the carbon required for the enhanced pathway to function. The other lesson is that strain development will remain largely an empirical process but that empiricism will be more readily harnessed if the investigator has a thorough knowledge of the physiology and biochemistry of the process.

Literature Cited

1. Umbarger, H. E. Science 1956, 123, 848.
2. Kotlarz, D.; Buc, H. Biochim. Biophys. Acta 1977, 484, 35-48.
3. Anderson, P. M.; Marvin, S. V. Biochemistry 1969, 9, 171-8.
4. Cedar, H.; Schwartz, J. H. J. Biol. Chem. 1969, 244, 4112-21.
5. Hoffler, J. G.; Burns, R. O. J. Biol. Chem. 1978, 253, 1245-51.
6. Ginsburg, A.; Stadtman, E. R. "The Enzymes of Glutamine Metabolism"; Prusinev, S.; Stadtman, E. R., Ed.; Academic: New York, 1973; p. 9.
7. Crawford, I. P.; Yanofsky, C. Proc. Natl. Acad. Sci. USA 1958, 44, 1161-70.
8. Klungsøyr, L.; Hagemen, J. H.; Fall, L.; Atkinson, D. E. Biochemistry 1968, 7, 4035-40.
9. Shen, L. C.; Atkinson, D. E. J. Biol. Chem. 1970, 245, 5974-78.
10. Pardee, A. B.; Potter, V. R. J. Biol. Chem. 1948, 176, 1085-94.
11. Koch, A. L. J. Theoret. Biol. 1967, 15, 75-102.
12. Monod, J.; Jacob, F. Cold Spr. Harbor Symp. Quant. Biol. 1961, 26, 389-401.
13. Krebs, E. G.; Beavo, J. A. Annu. Rev. Biochem. 1979, 48, 923-59.
14. Garnak, M.; Reeves, H. C. J. Biol. Chem. 1979, 254, 7915-20.
15. Pennincky, M.; Simon, J. P.; Wiame, J. M. Eur. J. Biochem. 1974, 49, 429-42.
16. Atkinson, D. E. Biochemistry 1968, 7, 4030-34.
17. Chapman, A. G.; Fall, L.; Atkinson, D. E. J. Bacteriol. 1971, 108, 1072-86.
18. Vogel, R. H.; McLellen, W. L.; Hirvonen, A. P.; Vogel, H. J. "Metabolic Pathways," 3rd ed.; Vogel, H. J., Ed.; Academic: New York, 1971, vol. 5, p. 464.
19. Pardee, A. B.; Jacob, F.; Monod, J. J. Mol. Biol. 1959, 1, 165-78.
20. Nakada, D.; Magasanik, B. J. Mol. Biol. 1964, 8, 105-27.

21. Prival, M. J.; Magasanik, B. J. Biol. Chem. 1971, 246, 6288-96.
22. Pedersen, S.; Bloch, P. L.; Reeh, S.; Neidhardt, F. C. Cell 1978, 14, 179-90.
23. Herendeen, S. L.; VanBogelen, R. A.; Neidhardt, F. C. J. Bacteriol. 1979, 139, 185-94.
24. Turnbough, C. L., Jr.; Switzer, R. L. J. Bacteriol. 1975, 121, 115-20.
25. Goldberg, A. L.; St. John, A. C. Annu. Rev. Biochem. 1976, 45, 747-803.
26. Millet, J.; Gregoire, J. Biochimie 1979, 61, 385-91.
27. Magasanik, B. Cold Spring Harbor Symp. Quant. Biol. 1961, 26, 249-56.
28. Squires, C. L.; Lee, F. D.; Yanofsky, C. J. Mol. Biol. 1975, 92, 93-111.
29. Jobe, A.; Bourgeois, S. J. Mol. Biol. 1972, 69, 397-408.
30. Biel, A. J.; Umbarger, H. E. J. Bacteriol. 1981, 146, 718-24.
31. Zubay, G.; Schwartz, D.; Beckwith, J. Proc. Natl. Acad. Sci. USA 1970, 66, 104-10.
32. Neidhardt, F. C.; VanBogelen, R. A. Biochem. Biophys. Res. Commun. 1981, 100, 894-900.
33. Haldenwang, W. G.; Lang, N.; Losick, R. Cell 1981, 23, 615-24.
34. Hamming, J.; Ab, G.; Gruber, M. Nucl. Acids Res. 1980, 8, 3947-63.
35. Kingston, R. E.; Nierman, W. C.; Chamberlin, M. J. J. Biol. Chem. 1981, 256, 2787-97.
36. Backman, K.; Chen, Y.-M.; Magasanik, B. Proc. Natl. Acad. Sci. USA 1981, 78, 3743-47.
37. Wu, A. M.; Christie, G. E.; Platt, T. Proc. Natl. Acad. Sci. USA 1981, 78, 2913-17.
38. Court, D.; Brady, C.; Rosenberg, M.; Wulff, D. L.; Behr, M.; Mahoney, M.; Izumi, S. J. Mol. Biol. 1980, 38, 231-54.
39. Yanofsky, C. Nature 1981, 289, 751-58.
40. Kingston, R. E.; Chamberlin, M. J. Cell 1981, 27, 523-31.
41. Greenblatt, J.; Li, J. J. Mol. Biol. 1981, 147, 16-20.
42. Nomura, M.; Yates, J. L.; Dean, D.; Post, L. E. Proc. Natl. Acad. Sci. USA 1980, 77, 7084-88.
43. Horinouchi, S.; Weisblum, B. Proc. Natl. Acad. Sci. USA 1980, 77, 7079-83.
44. Jacob, F.; Monod, J. Cold Spring Harbor Symp. Quant. Biol. 1961, 26, 193-211.
45. Englesberg, E.; Wilcox, G. Annu. Rev. Genet. 1974, 8, 219-42.
46. Christie, G. E.; Farnham, P. J.; Platt, T. Proc. Natl. Acad. Sci. USA 1981, 78, 4180-84.
47. Calva, E.; Burgess, R. R. J. Biol. Chem. 1980, 255, 11017-22.
48. Platt, T. Cell 1981, 24, 10-23.
49. Farnum, P. J.; Platt, T. Nucl. Acids Res. 1981, 9, 563-77.

50. Umbarger, H. E. "Transfer RNA: Biological Aspects"; Söll, D.; Abelson, J. N.; Schimmel, P. R., Ed.; Cold Spring Harbor Laboratory: Cold Spring Harbor, New York, 1980; p. 453.
51. Johnston, H. M.; Barnes, W. M.; Chumley, F. G.; Bossi, L.; Roth, J. R. Proc. Natl. Acad. Sci. USA 1980, 77, 508-12.
52. Bertrand, K.; Korn, L.; Lee, F.; Platt, T.; Squires, C. L.; Squires, C.; Yanofsky, C. Science 1975, 189, 22-26.
53. Zurawski, G.; Elseviers, D.; Stauffer, G. V.; Yanofsky, C. Proc. Natl. Acad. Sci. USA 1978, 75, 5988-92.
54. Yates, J. L.; Nomura, M. Cell 1981, 24, 243-9.
55. Komatsubara, S.; Kisumi, M.; Chibata, I. J. Gen. Microbiol. 1980, 119, 51-61.
56. Leathers, T. D.; Noti, J.; Umbarger, H. E. J. Bacteriol. 1979, 140, 251-60.
57. Cassan, M.; Boy, E.; Borne, F.; Patte, J. C. J. Bacteriol. 1975, 123, 391-99.
58. Kisumi, M.; Komatsubara, S.; Sugiura, M.; Chibata, I. J. Bacteriol. 1972, 110, 761-3.
59. Komatsubara, S.; Murata, K.; Kisumi, M.; Chibata, I. J. Bacteriol. 1978, 135, 318-23.
60. Komatsubara, S.; Kisumi, M.; Murata, K.; Chibata, I. Appl. Environ. Microbiol. 1978, 35, 834-40.
61. Komatsubara, S.; Kisumi, M.; Chibata, I. Appl. Environ. Microbiol. 1979, 38, 777-82.
62. Komatsubara, S.; Kisumi, M.; Chibata, I. Appl. Environ. Microbiol. 1979, 38, 1045-51.

RECEIVED June 1, 1982

Mathematical Models of the Growth of Individual Cells

Tools for Testing Biochemical Mechanisms

M. L. SHULER and M. M. DOMACH

Cornell University, School of Chemical Engineering, Ithaca, NY 14853

The rationale for and development of mathematical models for single-cells are reviewed. The potential use of a computer model for Escherichia coli in ascertaining the plausibility of basic biological hypotheses is illustrated with respect to the control of the initiation of DNA synthesis and with respect to ammonium ion assimilation. Mechanisms postulated on the basis of in vitro enzymology can be tested for in vivo compatibility using the model. The transient behavior of single-cells to step-up and step-down in glucose or ammonium ion is shown to result in oscillatory responses and hysteresis. Methods to construct population models from single-cell models are discussed. Population models are important to engineering analysis and in relating data for experiments with large populations to the responses of a "typical cell".

Why Single-Cell Models?

The basic conceptual unit in microbiology is the single cell. Although microbiologists and biochemists work with large populations of cells, the goal is generally to understand the behavior of a "typical" cell. There is very little direct data on the growth of individual cells - and what data exists is often of questionable value because the conditions required for observations may lead to "unnatural responses". Thus, the behavior of the "typical" cell must be inferred from the aggregated behavior of the total population. Biologists usually are interested in a single aspect of cell growth (e.g. protein synthesis). Cells contain a complex, nonlinear, highly regulated series of chemical reactions. Human logic consists of a few linear steps. It is essentially impossible for the unaided mind to interrelate protein synthesis, DNA replication, nutrient transport, etc. into a coherent conceptual model of a cell.

0097-6156/83/0207-0093\$11.50/0

© 1983 American Chemical Society

Computer models of single cells act as an aid in building such conceptual models. Because such models make quantitative predictions - predictions which are experimentally verifiable - they serve as good vehicles to reveal errors in either basic mechanisms or the manner in which they are integrated in the conceptual model. Population models can be constructed from ensembles of single-cell models. Such models may be useful aids in relating the behavior of whole populations to biochemical mechanisms within a typical cell. Single-cell models are particularly well suited to the conceptual and experimental needs of biologists.

Single-cell models are also of importance to biochemical engineers. The motivation is different from biologists. Engineers are interested in manipulating a population of cells; such manipulation is facilitated by mathematical models that can predict the response of the population to perturbations in the external environment. Historically, the development of mathematical modeling in biosystems has sprung from a need to model populations of cells. Population models have inherent limitations - limitations that can be circumvented by using ensembles of single-cell models.

Population Models. To understand why single-cell models are useful it is important to review previous attempts at modeling populations. The history and philosophy of modeling as well as the virtues and faults inherent in previous models has been well described in the literature. Among these articles are those by Tsuchiya, Fredrickson, & Aris (1); Painter & Marr (2); Van Uden (3); Garfinkel, et al. (4); Fredrickson, Megee, & Tsuchiya (5); Nyiri (6); Boyle & Berthouex (7) (for waste treatment); Fredrickson (8) (for structured models only); and Bailey (9).

One method of classifying models involves the concept of "structure". Structured models have the inherent ability to describe the physiological state of a microorganism or a culture of such cells. Unless the physiological state can be specified, the dependence of a culture on its previous history cannot be accounted for. Such dependence on history is known to be important (5). Typically, structure is added to a model by considering the cell or culture to consist of two or more components (e.g. nucleic acids and protein, etc.) or to distinguish between separate cells on the basis of size or age.

Any model not incorporating the foregoing principle is unstructured--for example, the well-known Monod model. It has been shown that unstructured models are applicable only in balanced growth situations (10), which, according to Campbell's (11) definition, requires that each component of the culture be accumulated at the same rate. Unstructured models are never general, give very little insight into cellular mechanisms, and cannot be used to describe lag and decline phases in batch growth, transient

response in chemostats, or growth in multistage continuous culture. If the formation of a product is dependent on cell history and is not growth associated, then an unstructured model will be unsuitable. Unstructured models have been widely used, however, and have been successful when applied to the commonly occurring balanced growth situations of exponential phase batch culture and steady-state single-staged continuous culture.

Two of the first structured models proposed were those by Williams (12, 13) and Ramkrishna, Fredrickson, & Tsuchiya (14). Both models were deterministic and dealt with a nonsegregated biomass. A nonsegregated model is one which does not recognize explicitly the existence of individual cells. For example, the contents of a fermenter can be thought of as consisting of two phases—one biotic and the other abiotic. The biotic phase can then be treated as a homogeneous entity. Nonsegregated models, of course, cannot make any predictions about cell proliferation or the effects of cell geometry on growth. However, they are fairly easy to handle mathematically, and the overall biomass and its major components can be determined experimentally with reasonable accuracy.

It is obvious to anyone who has microscopically examined microbial cultures that cells are individuals and can vary greatly in observable properties such as cell size. Only segregated models can capture this property. Such models contain structure in the sense that changes are allowed in the distribution of states among the population in response to the external environment. Examples of models using age as a measure of the index of a cell's stage include those by Von Foerster (15); Trucco (16); Yakovlev, *et al.* (17); Fredrickson & Tsuchiya (18); Kozesnik (19); and Lebowitz & Rubinow (20). Cell size can also be utilized as suggested by Koch & Schaechter (21) and Eakman, *et al.* (22). In the above examples only one parameter was used as an index of stage; it would be impossible to insert any information about biochemical mechanisms into the model.

Models which include both structure and segregation lead to mathematical equations which are extremely difficult to solve even with the aid of modern high-speed computers. Bailey and co-workers (23, 24, 25) have made progress in circumventing some of these problems. Nonetheless it appears impossible to prepare population models which would contain a high level of structure (say more than five components) and segregation, and which still are mathematically tractable.

Population models which contain both a high-level of structure and segregation are desirable. Such models have the potential to make accurate predictions of transient responses - such predictions are important not only for process control but may be useful in designing cycled-reactors which can have product yields greater than comparable steady-state cultures (26, 27). There is also preliminary evidence that under some circumstances only a small sub-population of cells produce most of the product (24);

thus the manipulation of the distribution of sub-populations can be predicted only if a structured-segregated model is available.

Tanner (28) has made persuasive arguments for the need for more sophisticated models to optimize the design of commercial fermentation processes. He has stated that commercial fermentation processes have not been significantly optimized "because there are no simple, general, and accurate mathematical models for predicting the casual effects of control variable changes". Further, he claims that "the establishment of just one of these profiles [pH, temperature, nutrient, etc.] to optimize a batch fermentation is a nearly impossible task to perform directly on a process". The use of mathematical models in conjunction with modern quantitative optimization procedures could circumvent much of the experimental work. The need for a good model of bacterial growth which could accommodate product formation has been well recognized (e.g. 6, 23, 28-34). A structured-segregated model is sufficiently general to be used for optimization.

A way to generate highly structured-segregated models which are mathematically tractable is to build population models using an ensemble of single-cell models. Such an approach can avoid the generation of integral-differential equations which are so computationally difficult to solve. Thus, single-cell models fill certain real needs of both biologists and engineers. The advantages of single-cell models compared to normal population models are:

1. explicit accounting of cell geometry and its potential effects of nutrient transport;
 2. the ability to predict temporal events during the division cycle;
 3. the ability to consider the effects of spatial arrangements within a cell;
 4. and the ease in which details about biochemical pathways and their integration and metabolic control can be included.
- These advantages make single-cell models particularly well-suited to testing the plausibility of hypotheses about metabolic mechanisms.

Single-cell models invite complexity. Their main disadvantage is that single-cell models represent only a "typical" cell and are adequate representations of the growth of cell populations only if the moments of distribution of cellular properties higher than the first-order can be ignored. The last disadvantage is circumvented by using an ensemble of single-cell models to build a population model (i.e. each single-cell represents some small fraction of the total population).

Ideal Model. Having discussed why single-cell models may be useful, what characteristics should such models have? The following features are important:

1. the model must be consistent with experimentally confirmed observations over a wide variety of growth conditions,

2. the model must have a structure which can easily allow the incorporation of postulated biochemical mechanisms,
 3. the parameters of the model must be determined directly from independent experiments or estimated by an objective series of rules (no adjustable parameters),
 4. the effect of cell geometry and shape on nutrient uptake must be included (the external environment must be explicitly accounted for),
 5. the model must allow for the inclusion of randomness in key metabolic systems,
 6. the model must not include artificial constraints such as growth must be exponential, the cell must maintain a given shape, the cell will divide when the amount of given component doubles, etc.,
 7. the only signals that a cell can utilize are the concentrations of various biochemical species, and,
 8. the model must be mathematically tractable.
- The model should be a model - not a collection of phenomenological equations based on curve fits.

Examples of Single-Cell Models

One of the first examples of individual-cell models is that suggested by Von Bertalanffy (see 1). In his model growth was a result of competition between the process of nutrient assimilation and endogenous metabolism. Nutrient uptake was postulated to be proportional to the cell's surface area and the concentration of nutrient in the abiotic environment and the rate of endogenous metabolism was postulated to be proportional to cell mass. Heinmets (35) suggested in 1966 a model for a single cell (or the nucleus of an eucaryotic cell) that incorporated 19 differential equations. The model contained an amino acid pool, a nucleotide pool for RNA synthesis, a general intracellular metabolic pool, total protein, RNA polymerase, genes for synthesis of various RNA's, m-RNA (2 types), r-RNA, and t-RNA. The model could respond to step changes in the extracellular nutrient pools. The main purpose of the model was to examine how a cell would change from normal to abnormal growth. The mechanistic scheme reflects the general understanding of cellular biochemistry in 1965 but differs somewhat from the present conception of the cell. The constants chosen were arbitrary, and the model was not formulated to any specific organism, and no attempt was made to compare the predictions to actual experimental data. Effects of cell geometry and size on nutrient uptake were not considered. The cell division hypothesis depends on an imposed criterion to do with the concentrations of intracellular components. Cell division is not a "natural" response of the model. Davison (36) has solved Heinmets' model with only the digital computer and has compared the results with two experimental situations. The first was the

recovery of an *E. coli* for Mg^{++} starvation, and the second was the effect of split radiation doses on Chinese Hamster cells. In both cases reasonable qualitative predictions were obtained from the model.

Another example of single-cell model is that proposed by Simon (37) in 1973. He considered only steady-state balanced growth. His model cell contained enzymes involved in division initiation, in the formation of DNA precursors, and in RNA synthesis. DNA synthesis was initiated when a critical material accumulated to a threshold value; DNA initiation caused all the threshold material to be consumed. Each protein synthesis rate was made proportional to the degree of genome activation. The ratio of cell volume to protein was considered constant, and volume growth was forced to be exponential. The surface to volume ratio was considered constant (a cylinder without ends). The effects of the abiotic environment were not explicitly accounted for; the value of the growth rate was imposed on the cell. The cell was required to divide when the amount of each component is doubled. Initial cell size could be predicted. A short general qualitative comparison of the model to experimental observations was given; the model was found to be satisfactory for the parameters compared.

Weinberg, Zeigler, & Laing (38) and Zeigler & Weinberg (39) have attempted to construct a model of an *E. coli* cell. They have considered how the various components of the cell might be aggregated. Their cell contains explicit concentrations for cell wall, DNA, m-RNA, t-RNA, ribosomes, protein, amino acids, wall precursors, nucleotides, ATP, and ADP are shown (38, 39) along with a pool called glucose which includes glucose and other small metabolites made from glucose. They claim that their model of a cell differs from others in that the abstraction involved in model formulation arises from the aggregation of variables rather than the selection of subsystems. Difference and Boolean equations were used to describe the system. Hyperbolic ("saturation kinetics") rate forms were not used; for example, the rate of production of amino acids from glucose was made proportional to the product of glucose, ATP, and enzyme 2 concentrations. Enzyme activity was modified to simulate an allosteric enzyme by use of Boolean equations. Their cell was constrained to grow exponentially in volume. A mechanism for initiation of DNA replication was included but none for cell division. From the above papers (38, 39) it is not clear whether nutrient uptake was explicitly accounted for or not. They (39) describe how they evaluated rate constants from the data in the literature. A direct comparison to experimental data was made (38) for shift experiments between various media; r-RNA and DNA concentrations were satisfactorily predicted by the model if feedback controls were included.

Another approach to predicting the response of a "typical" cell to a shift in media has been suggested by Bremer and co-work-

ers (40, 41, 42). They have made extensive measurements of RNA metabolism and protein synthesis in *E. coli* and have correlated their results with phenomenological expressions. These expressions coupled with similar relationships suggested by other workers (e.g. Cooper and Helmstetter (43)) allow rather accurate calculation of cell size and composition for unrestricted growth in media of various compositions. These expressions appear to be unsatisfactory for growth restricted by a limiting nutrient as glucose (41). The above expressions do not explicitly depend on the external environment; the growth rate which a media will support must be known beforehand. These expressions are really correlations rather than a true model. They are limited to a narrow range of growth conditions and are not potentially as general as the other models discussed.

Another type of single-cell model has been considered by Nishimura and Bailey (24). The model is structured in that both cell mass and DNA content are explicitly recognized. Rules concerning DNA replication and the timing of initiation DNA synthesis are imposed on the cell; the rules are derived from the observations of Cooper and Helmstetter (43) and Donachie (44). The single-cell model was essentially the basis for the construction of a population model - a formulation among the most general currently available. The main limitation of the model is its inability to permit an explicit calculation of each cell's growth rate in terms of the external environment and the cell's physiological state.

Ho and Shuler (45) proposed a mathematical model for the growth of an individual bacterium incorporating feedback control of nutrient uptake. This simple model could predict the growth pattern for a cell of a given shape (filamentous, bacillus, or spherical). The model cell contained four components (ammonium ion, glucose, precursors, and macromolecules). An analytical solution was possible for filamentous cells, but numerical solutions were required for other cell shapes.†

More recently Shuler, Leung, and Dick (46) have presented a more complete model for the growth of a single-cell of *Escherichia coli* B/r A. The model contained 14 components. All of the cell's components were included in one of the model components. The model cell relied on chemical concentrations as control signals so that the growth pattern, timing of DNA synthesis, cell shape, cell size, cell composition, and cell division could be considered natural responses to explicit changes (e.g. glucose concentration) in the external environment. An attempt was made to evaluate kinetic parameters from independent measurements on exponentially growing cells. Four parameters, having to do with cell envelope

†The example cited in Equation B9-B14 of Ho and Shuler (45) is faulty. However, it is easy to demonstrate that the conclusion is correct. Details of the corrected example are available upon request.

and cross-wall formation were taken as adjustable. This prototype model is being further developed.

The Cornell Single-Cell Model

The prototype model has been revamped. The base model has 20 components; the additional components are necessary to allow an accurate description of the systems allowing the incorporation of ammonium ion into amino acids, to allow more accurate estimates of cellular energy expenditures, and to allow a more complete simulation of systems controlling transcription and translation. Some of the parameters in the prototype model (46) were calculated based on cell dimensions obtained for cells fixed in osmium tetroxide; these have been recalculated using size parameters obtained from glucose-limited chemostat cultures with gluteraldehyde-fixed cells.

Figure 1 and Tables I to IV describe the current model. Justification of parameter values have been given elsewhere (46-50). Almost all parameters were estimated from independent measurements on exponentially growing cells or cell-free systems. Values for η_2 and η_3 (parameters associated with the ratio of envelope used for extension and cross-wall formation) were required to be positive but were otherwise considered adjustable. Values for $K_{M_4A_2}$ and $K_{P_4A_2}$ were adjusted within the range of 0 to 0.05 gm/cc of cell volume. Values for η_2 , η_3 , $K_{M_4A_2}$, and $K_{P_4A_2}$ were estimated by comparing data to model predictions at $\mu = 0.95 \text{ hr}^{-1}$ and $\mu = 0.5 \text{ hr}^{-1}$. A parameter for unidentified energy consumption, δ_v , was included to make the predicted growth yield at $\mu = 0.95 \text{ hr}^{-1}$ match experimental measurements. Values for K_{iIF} , p , Z , and K_{ZM_4} required experimental growth data for $\mu < 0.95 \text{ hr}^{-1}$ but were evaluated independently of the model's predictions. All parameters were set based on glucose-limited growth only. No further adjustments were made for prediction of ammonium ion-limited growth.

The model makes reasonable predictions of the dependence of cell size, cell shape, cell composition, growth rate, and the timing of cellular events on external concentrations of glucose. Results for glucose-limited growth are given elsewhere (47, 50).

The current model makes use of recent observations of Fralick (51), Messer, *et al.* (52), and Fayet & Louarn (53) to construct a mechanism for the control of the initiation of DNA synthesis. The scheme is illustrated in Figure 2. The *dnaA* gene which is located near the origin makes a gene product (RP) which represses the transcription of the O-RNA gene. Initiation requires O-RNA as a primer. An anti-repressor (ARP) is made which inactivates RP. Experimental evidence for ARP exists (51), and there are indications that ARP production is related to cell envelope formation (54). In the model we have made the rate of

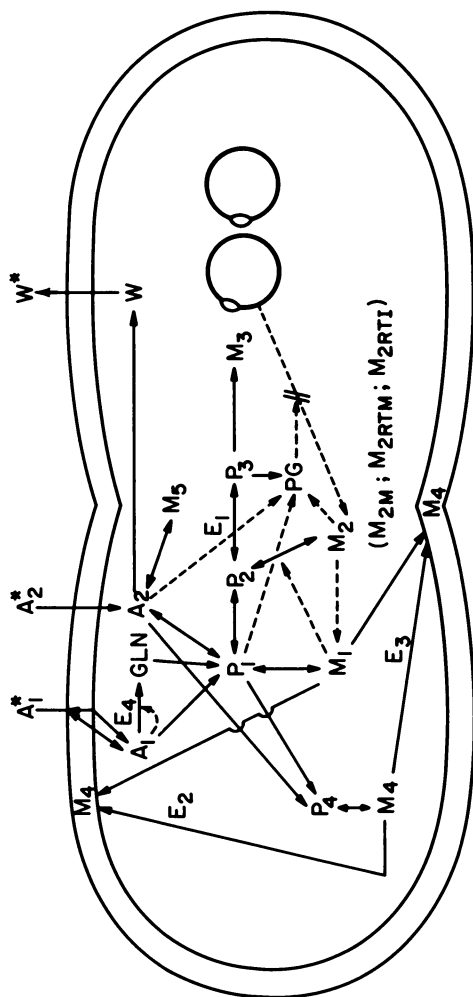


Figure 1. An idealized sketch of the model for *E. coli* B/r A growing in a glucose-ammonium salts medium with glucose or ammonia as the limiting nutrient. At the time shown the cell has just completed a round of DNA replication and initiated cross-wall formation and a new round of DNA replication. Solid lines indicate the flow of material, while dashed lines indicate flow of information.

- A_1 = ammonium ion
 A_2 = glucose (and associated compounds in the cell)
 W = waste products (CO_2 , H_2O , and acetate) formed from energy metabolism during aerobic growth
 P_1 = amino acids
 P_2 = ribonucleotides
 P_3 = deoxyribonucleotides
 P_4 = cell envelope precursors
 M_1 = protein (both cytoplasmic and envelope)
 M_{RTI} = immature "stable" RNA
 M_{RTM} = mature "stable" RNA (r-RNA and t-RNA—assume 85% r-RNA throughout)
 M_M = messenger RNA
 M_2 = DNA
 M_3 = non-protein part of cell envelope (assume 16.7% peptidoglycan, 47.6% lipid, and 35.7% polysaccharide)
 M_4 = glycogen
 PG = ppGpp
 E_1, E_2 = enzymes in the conversion of P_1 to P_2
 E_3, E_4 = molecules involved in directing cross-wall formation and cell envelope synthesis—the approach used in the prototype model was used here but more recent experimental support is available
 GLN = glutamine
 E_5 = glutamine synthetase

*—the material is present in the external environment.

TABLE I: Stoichiometric relations for the lumped energy, mass, and reductant consumptive processes represented in the cell model.

The following symbols are used:

α, β = anabolic use of ammonium ion or glucose, respectively

γ = conversion of precursor into macromolecule

ϵ = conversion of one precursor into another

ω = direct use of reducing equivalents for energetics or for biosynthesis

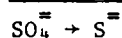
δ_{ATP} = ATP requirements to drive given reaction

X = total pool of reducing power

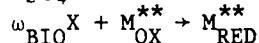
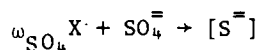
The rest of the symbols are defined in Figure 1.

Transport	*Coupled Reaction
(1) A_1^* transports in & becomes A_1	$\omega_{A_1} A_1 + \omega_{A_1} \frac{1}{2} O_2 \rightarrow \omega_{A_1} H_2O$
(2) A_2^* transports in & becomes A_2	$\delta_{A_2} \text{ATP} \rightarrow \delta_{A_2} (\text{ADP} + P_i)$
Precursor Formation	
(3) $\alpha_1 A_1 + \beta_1 A_2 + \dots \rightarrow P_1 + \dots$	$\delta_{P_1} \text{ATP} \rightarrow \delta_{P_1} (\text{ADP} + P_i)$
(4) $\epsilon_2 P_1 + \beta_2 A_2 + \dots \rightarrow P_2 + \dots$	$\delta_{P_2} \text{ATP} \rightarrow \delta_{P_2} (\text{ADP} + P_i)$
(5) $\epsilon_3 P_2 + \omega_{P_3} X + \dots \rightarrow P_3 + \dots$	$\delta_{P_3} \text{ATP} \rightarrow \delta_{P_3} (\text{ADP} + P_i)$
(6) $\epsilon_4 P_1 + \beta_4 A_2 + \dots \rightarrow P_4 + \dots$	$\delta_{P_4} \text{ATP} \rightarrow \delta_{P_4} (\text{ADP} + P_i)$
Macromolecule Formation	
(7) $\gamma_1 P_1 \xrightarrow{\uparrow} M_1 + \dots$	$\delta_{M_1} \text{ATP} \rightarrow \delta_{M_1} (\text{ADP} + P_i)$
(8) $\gamma_2 P_2 \xrightarrow{\uparrow} M_2 + \dots$	$\delta_{M_2} \text{ATP} \rightarrow \delta_{M_2} (\text{ADP} + P_i)$
(9) $\gamma_3 P_3 \xrightarrow{\uparrow} M_3 + \dots$	$\delta_{M_3} \text{ATP} \rightarrow \delta_{M_3} (\text{ADP} + P_i)$
(10) $\gamma_4 P_4 \xrightarrow{\text{E2 \& E3}} M_4 + \dots$	$\delta_{M_4} \text{ATP} \rightarrow \delta_{M_4} (\text{ADP} + P_i)$
(11) $\gamma_5 A_2 \xrightarrow{\uparrow} M_5 + \dots$	$\delta_{M_5} \text{ATP} \rightarrow \delta_{M_5} (\text{ADP} + P_i)$
Additional Direct Reductant Use	
Transport of ions	$\omega_{\text{ION}} X + \omega_{\text{ION}} \frac{1}{2} O_2 \rightarrow \omega_{\text{ION}} H_2O$
Membrane recharge to offset H^+ leakage	$\omega_M X + \omega_M \frac{1}{2} O_2 \rightarrow \omega_M H_2O$

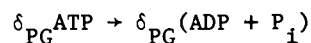
Table I, continued.

Additional Biosynthetic Reductant Use

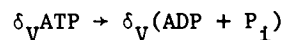
Mass use

Additional ATP Coupling

PG formation

Non-Specified ATP Use

Size linked



* Coupled to either phosphate bond energy or oxidative reactions. Products of oxidation include pmf and reducing equivalents.

** M_{OX} , M_{RED} = unreduced and reduced cell mass, respectively.

TABLE II: Equations Describing the Rate of Change of Each Component in the Cell.

The symbols are the same as listed in Figure 1 and Table I. Additional symbols used are:

- μ, k, η = maximum rates of synthesis of the macromolecules, precursors, and enzymes, respectively
 v = maximum transport rate
 K = saturation constants
 k_T = decomposition rates
 R = rate of transport
 F = number of forks in DNA molecule
 N_o = number of DNA origins
 S = cellular surface area
 V = volume
 RI = mass of idling ribosomes
 $Z = \frac{\text{moles acetate formed}}{\text{moles glucose dissimilated}}$
 GD = number of genes coding for stable RNA synthesis
 ρ = density
 f = proportionality constant between M_4 and cell surface area
 SL = septum length
 CL = length of cylindric section of the cell
 W = cell width
 $SEPF$ = mass of septum
 IF = initiation factors for protein synthesis
 RP = repressor protein
 ARP = anti-repressor protein
 $(P/O)_{\max}$ = maximum P/O ratio

When S and D are used as subscripts, they denote rate of synthesis and rate of degradation respectively. A and C as subscripts refer to anabolism and catabolism.

$$\frac{dA_1}{dt} = R_{A_1} \cdot S - \alpha_1 \left[\left(\frac{dP_1}{dt} \right)_S - \left(\frac{dP_1}{dt} \right)_D \right] - \alpha_{1, GLN} \left(\frac{dGLN}{dt} \right)_S \quad (1)$$

$$\left(\frac{dA_2}{dt} \right)_A = \beta_1 \left[\left(\frac{dP_1}{dt} \right)_S^{\text{NET}} - \left(\frac{dP_1}{dt} \right)_D \right] + \beta_2 \left[\left(\frac{dP_2}{dt} \right)_S - \left(\frac{dP_2}{dt} \right)_D \right] + \beta_4 \left(\frac{dP_4}{dt} \right)_S + \gamma_5 \left(\frac{dM_5}{dt} \right) \quad (2)$$

Table II, continued.

$$\begin{aligned}
 \left(\frac{dATP}{dt}\right)_S &= \delta_{A_2} \left(\frac{dA_2}{dt}\right) + \delta_{P_1} \left(\frac{dP_1}{dt}\right)_S + \delta_{P_2} \left(\frac{dP_2}{dt}\right)_S + \delta_{P_4} \left(\frac{dP_4}{dt}\right)_S + \\
 &\delta_{M_5} \left(\frac{dM_5}{dt}\right) + \delta_{M_1} \left(\frac{dM_1}{dt}\right)_S + \delta_{M_2} \left[\left(\frac{dM_{2RTI}}{dt}\right)_S + \left(\frac{dM_{2M}}{dt}\right)_S \right] + \\
 &\delta_{M_3} \left(\frac{dM_3}{dt}\right) + \delta_{M_4} \left(\frac{dM_4}{dt}\right)_S + \delta_{PG} \left(\frac{dPG}{dt}\right)_S + \delta_v \left(\frac{dv}{dt}\right) + \\
 &\delta_{GLN} \left(\frac{dGLN}{dt}\right)_S + \delta_{P_1}' \left(\frac{dP_1}{dt}\right)_S' \quad (3)
 \end{aligned}$$

$$\begin{aligned}
 \frac{dX}{dt} &= \omega_{A_1} \cdot R_{A_1} \cdot S + (\omega_{ION} + \omega_{BIO} + \omega_{SO_4}) [d(\sum A_i + \sum P_i + \sum M_i)/dt] + \\
 &\omega_M \cdot S + \omega_{P_3} \left(\frac{dP_3}{dt}\right)_S \quad (4)
 \end{aligned}$$

$$\left(\frac{dA_2}{dt}\right)_C = \left[\frac{\left(\frac{dATP}{dt}\right)_S + dX/dt(P/O)_{\max}}{4 + (12 - 4 \cdot Z)(P/O)_{\max}} \right] \cdot 180 \quad (5)$$

$$Z = \mu_z \left(\frac{\left(\frac{dM_4}{dt}\right)_S}{\left(\frac{dM_4}{dt}\right)_S + K_{zM_4}} \right) \quad (6)$$

$$\frac{dA_2}{dt} = R_{A_2} \cdot S - \left[\left(\frac{dA_2}{dt}\right)_A + \left(\frac{dA_2}{dt}\right)_C \right] \quad (7)$$

$$\left(\frac{dP_1}{dt}\right)_S^{\dagger} = k_1'' \left[\frac{GLN/V}{K_{P_1GLN} + GLN/V} \right] \left[\frac{A_2/V}{K_{P_1A_2} + A_1/V} \right] \cdot V \quad (8a)$$

$$\begin{aligned}
 \left(\frac{dGLN}{dt}\right) &= k_1' \cdot E \left[\frac{A_1/V}{K_{GLNA_1} + A_1/V} \right] \left[\frac{P_1/V}{K_{GLNP_1} + P_1/V} \right] \left[\frac{K_{GLN}}{K_{GLN} + (GLN/V)^q} \right] - \\
 &\left(\frac{dP_1}{dt}\right)_S' \quad (8b)
 \end{aligned}$$

[†]Term is equivalent to glutamine driven Glutamate Synthase

Continued on next page.

Table II, continued.

$$\begin{aligned}
 \left(\frac{dP_1}{dt}\right) = & \left[k_1 \left(\frac{K_{P_1}}{K_{P_1} + P_1/V} \right) \left(\frac{A_1/V}{K_{P_1 A_1} + A_1/V} \right) \left(\frac{A_2/V}{K_{P_1 A_2} + A_2/V} \right) \cdot V + \right. \\
 & \left. 2 \cdot \left(\frac{dP_1}{dt}\right)'_S - \left(\frac{dGLN}{dt}\right)_S \right]^* - k_{TP_1} \left(\frac{K_{TP_1}}{K_{TP_1} + A_2/V} \right) \cdot P_1 - \gamma_1 \left(\frac{dM_1}{dt}\right) - \\
 & \epsilon_2 \left(\frac{dP_2}{dt}\right) + \gamma_2 \frac{dM_2}{dt} + \epsilon_3 \frac{dP_3}{dt} + \epsilon_3 \gamma_3 \frac{dM_3}{dt}^{**} - \epsilon_4 \left(\frac{dP_4}{dt}\right) + \\
 & \gamma_4 \frac{dM_4}{dt}^\dagger \qquad (8c)
 \end{aligned}$$

$$\begin{aligned}
 \frac{dP_2}{dt} = & k_2 \left(\frac{K_{P_2}}{K_{P_2} + P_2/V} \right) \left(\frac{P_1/V}{K_{P_2 P_1} + P_1/V} \right) \left(\frac{A_2/V}{K_{P_2 A_2} + A_2/V} \right) \cdot V - \\
 & k_{TP_2} \left(\frac{K_{TP_2}}{K_{TP_2} + A_2/V} \right) P_2 - \gamma_3 \left[\left(\frac{dM_{2RTI}}{dt}\right) - \left(\frac{dM_{2RTM}}{dt}\right)_D + \left(\frac{dM_{2M}}{dt}\right) \right] - \\
 & \epsilon_3 \left(\frac{dP_3}{dt} + \frac{\gamma_3 dM_3}{dt}\right) \qquad (9)
 \end{aligned}$$

$$\begin{aligned}
 \frac{dP_3}{dt} = & k_3 \left(\frac{K_{P_3}}{K_{P_3} + P_3/V} \right) \left(\frac{P_2/V}{K_{P_3 P_2} + P_2/V} \right) \left(\frac{A_2/V}{K_{P_3 A_2} + A_2/V} \right) E_1 - \\
 & \gamma_3 \frac{dM_3}{dt} \qquad (10)
 \end{aligned}$$

$$\frac{dP_4}{dt} = k_4 \left(\frac{K_{P_4}}{K_{P_4} + P_4/V} \right) \left(\frac{P_1/V}{K_{P_4 P_1} + P_1/V} \right) \left(\frac{A_2/V}{K_{P_4 A_2} + A_2/V} \right) \cdot V - \gamma_4 \frac{dM_4}{dt} \qquad (11)$$

* Term is equal to net P_1 formation, $\left(\frac{dP_1}{dt}\right)_S^{NET}$, where the first term refers to A_1 incorporation via glutamate dehydrogenase, $\left(\frac{dP_1}{dt}\right)_S$.

** This term is equivalent to: $\epsilon_2 \left[\left(\frac{dP_2}{dt}\right)_S - \left(\frac{dP_2}{dt}\right)_D \right]$

† This term is equivalent to: $\epsilon_4 \left(\frac{dP_4}{dt}\right)_S$

Table II, continued.

$$\frac{dM_1}{dt} = \mu_1 \left(\frac{A_2/V}{K_{M_1A_2} + A_2/V} \right) \left(\frac{P_1/V}{K_{M_1P_1} + P_1/V} \right) 0.85 M_{2RTM} - k_{TM_1}' M_1 - k_{TM_1} \left(\frac{K_{TM_1}}{K_{TM_1} + A_2/V} \right) M_1 \quad (12)$$

$$\frac{dM_{2RTI}}{dt} = \mu_{2I} \left(\frac{P_2/V}{K_{M_2P_2} + P_2/V} \right) \left(\frac{K_{iPG}}{K_{iPG} + PG/V} \right) \cdot \left\{ \frac{K_{iIF}}{K_{iIF} + \left[\left(\frac{dM_1}{dt} \right)_{\text{Max}} \frac{M_1}{V} - \frac{(dM_1/dt)_S}{V} \right]} \right\} \cdot \text{GD} - k_{TM_2RTI} \left(\frac{K_{TM_2RTI}}{K_{TM_2RTI} + \frac{(dM_1/dt)_S}{V}} \right) M_{2RTI} - \left(\frac{dM_{2RTM}}{dt} \right)_S \quad (13)$$

$$\frac{dM_{2RTM}}{dt} = \mu_{2RTM} \cdot M_{2RTI} - k_{TM_2RTM} \left(\frac{K_{TM_2RTM}}{K_{TM_2RTM} + A_2/V} \right) \quad (14)$$

$$\frac{dM_{2M}}{dt} = \mu_{2M} \left(\frac{dM_1}{dt} \right)_S - k_{TM_2M} \cdot M_{2M} \quad (15)$$

$$\frac{dM_3}{dt} = \mu_3 \left(\frac{P_3/V}{K_{M_3P_3} + P_3/V} \right) \left(\frac{A_2/V}{K_{M_3A_2} + A_2/V} \right) \cdot F \quad (16)$$

$$\frac{dM_4}{dt} = \mu_4 \left(\frac{P_4/V}{K_{M_4P_4} + P_4/V} \right) \left(\frac{A_2/V}{K_{M_4A_2} + A_2/V} \right) \cdot (E_2 + E_3) - k_{TM_4} \left(\frac{A_2/V}{A_2/V + K_{TM_4A_2}} \right) M_4 \quad (17)$$

$$\frac{dM_5}{dt} = \mu_5 \left(\frac{A_2/V}{K_{M_5A_2} + A_2/V} \right) \cdot V - k_{TM_5} \left(\frac{K_{TM_5}}{K_{TM_5} + A_2/V} \right) M_5 \quad (18)$$

$$RI = \left[1 - \left(\frac{A_2/V}{A_2/V + K_{M_1A_2}} \right) \left(\frac{P_1/V}{P_1/V + K_{M_1P_1}} \right) \right] 0.85 M_{2RT} \quad (19)$$

Continued on next page.

Table II, continued.

$$\frac{dPG}{dt} = \mu_{PG} \left(\frac{K_{iP_1}}{K_{iP_1} + P_1/V} \right) RI - k_{TPG} \left(\frac{A_2/V}{A_2/V + K_{TPGA_2}} \right) \cdot PG \quad (20)$$

$$R_{A_1} = v_{A_1} \left[\frac{C_{A_1}^*}{K_{A_1} + C_{A_1}^*} - \frac{A_1/V}{K_{A_1} + A_1/V} \right] \left[\frac{A_2/V}{K_{A_1A_2} + A_2/V} \right] + v_{A_1} \left(\frac{C_{A_1}^*}{K_{A_1} + C_{A_1}^*} \right) \left(\frac{K_{iA_1}}{K_{iA_1} + A_1/V} \right) \left(\frac{A_2/V}{K_{A_1A_2} + A_2/V} \right) \quad (21)$$

$$R_{A_2} = v_{A_2} \left(\frac{C_{A_2}^*}{K_{A_2} + C_{A_2}^*} \right) \left(\frac{K_{iA_2}}{K_{iA_2} + (A_2/V)^n} \right) \quad (22)$$

$$\frac{dE_1}{dt} = \eta_1 N_o \frac{dM_1}{dt} \quad (23)$$

$$\frac{dE_2}{dt} = \eta_2 \frac{dM_1}{dt} \quad (24)$$

$$\frac{dE_2}{dt} = \eta_3 M_1 \quad (25)$$

$$\frac{dE_4}{dt} = \eta_4 \left[\frac{K_{E_4}}{K_{E_4} + (A_1/V)^l} \right] \left(\frac{dM_1}{dt} \right)_S - k_{TE_4} E_4 \quad (26)$$

$$V = \frac{\sum P_i + \sum A_i + \sum M_i - M_4}{\rho_{cyto}} + \frac{M_4}{\rho_{env}} \quad (27)$$

$$S = f_s M_4 \text{ and } dS = f_s dM_4 \quad (28)$$

$$S = \pi W^2 + \pi W \cdot CL + 2\pi W \cdot SL \quad (29)$$

$$V = \frac{1}{6} \pi W^3 + \frac{1}{2} \pi W^2 \cdot CL + \frac{1}{2} \pi W^2 \cdot SL - \frac{2}{3} \pi \cdot SL \quad (30)$$

$$SL = \frac{SEPF}{2\pi W} \quad (31)$$

$$SEPF|_{t+\Delta t} = SEPF|_t + \frac{E_3}{E_2 + E_3} \cdot dS \quad (32)$$

$$CL|_{t+\Delta t} = CL|_t + \frac{E_3}{E_2 + E_3} \frac{dS}{\pi \cdot W} \quad (33)$$

Table II, continued.

$$\left(\frac{dARP}{dt}\right)_S = k_{ARP} \cdot \left(\frac{dM_u}{dt}\right)_S \quad (34a)$$

$$ARP|_{t+\Delta t} = ARP|_t + \left(\frac{dARP}{dt}\right)_S \Delta t \quad (34b)$$

$$RP_{burst} = k_{RP} \cdot N_0 \cdot \frac{K_{1RP}}{K_{1RP} + \left[\left(\frac{dM_1/dt}{M_1}\right)_{Max} \frac{M_1}{V} - \frac{(dM_1/dt)_S}{V} \right]} \quad (35)$$

$$RP_{Total} = RP + RP_{burst} \quad (36)$$

TABLE III: Values of Parameters Associated with Rate Equations

ammonium ion	$v_{A_1} = 9.5 \times 10^{-7} \frac{\text{gm}}{\text{hr cm}^2}$	$K_{iA_1} = 2.3 \times 10^{-3} \frac{\text{gm}}{\text{cc}}$
	$K_{A_1}^* = 3.6 \times 10^{-6} \frac{\text{gm}}{\text{cc}}$	$K_{A_1A_2} = 7.2 \times 10^{-5} \frac{\text{gm}}{\text{cc}}$
	$v_{A_1}' = 2.056 \times 10^{-7} \frac{\text{gms}}{\text{cc hr}}$	$K_{A_1} = 1.0 \times 10^{-5} \frac{\text{gms}}{\text{cc}}$
	$K_{A_1}' = 1.0 \times 10^{-7} \frac{\text{gms}}{\text{cc}}$	$K_{A_1} = 1.0 \times 10^{-5} \frac{\text{gm}}{\text{cc}}$
glucose	$v_{A_2} = 1.7 \times 10^{-5} \frac{\text{gm}}{\text{hr cm}^2}$	$K_{A_2}^* = 1.2 \times 10^{-5} \frac{\text{gm}}{\text{cc}}$
	$K_{iA_2} = 7.8 \times 10^{-12} \left(\frac{\text{gm}}{\text{cc}}\right)^4$	$n = 4$
amino acids	$k_1 = 0.390 \frac{\text{gms}}{\text{hr cc}}$	$K_{P_1A_1} = 2.5 \times 10^{-5} \frac{\text{gm}}{\text{cc}}$
	$K_{P_1} = 5.0 \times 10^{-2} \frac{\text{gm}}{\text{cc}}$	$K_{P_1A_2} = 2.5 \times 10^{-4} \frac{\text{gm}}{\text{cc}}$
	$k_{TP_1} = 0.025 \text{ hr}^{-1}$	$K_{TP_1} = 1.1 \times 10^{-5} \frac{\text{gm}}{\text{cc}}$
	$k_1' = 475 \frac{\text{gms}}{\text{hr} \cdot \text{gm E}_4}$	$K_{GLNA_1} = 3.6 \times 10^{-6} \frac{\text{gms}}{\text{cc}}$
	$K_{GLNP_1} = 9.9 \times 10^{-4} \frac{\text{gms}}{\text{cc}}$	
	$q = 3$	$K_{P_1GLN} = 4.0 \times 10^{-5} \frac{\text{gms}}{\text{cc}}$
	$k_1'' = 0.39 \frac{\text{gms}}{\text{hr cc}}$	$K_{GLN} = 3.3 \times 10^{-12} \left(\frac{\text{gms}}{\text{cc}}\right)^3$
ribonucleotides	$k_2 = 0.19 \frac{\text{gm}}{\text{hr cc}}$	$K_{P_2P_1} = 9.9 \times 10^{-4} \frac{\text{gm}}{\text{cc}}$
	$K_{P_2} = 9.0 \times 10^{-3} \frac{\text{gm}}{\text{cc}}$	$K_{P_2A_2} = 2.5 \times 10^{-4} \frac{\text{gm}}{\text{cc}}$
	$k_{TP_2} = 0.03 \text{ hr}^{-1}$	$K_{TP_2} = 1.1 \times 10^{-5} \frac{\text{gm}}{\text{cc}}$
deoxyribonucleotides	$k_3 = 40 \frac{\text{gm}}{\text{hr gm E}_1}$	$K_{P_3P_2} = 9.9 \times 10^{-4} \frac{\text{gm}}{\text{cc}}$
	$K_{P_3} = 2.2 \times 10^{-4} \frac{\text{gm}}{\text{cc}}$	$K_{P_3A_2} = 7.2 \times 10^{-5} \frac{\text{gm}}{\text{cc}}$

Table III, continued.

cell envelope precursors	$k_4 = 0.060 \frac{\text{gm}}{\text{hr cc}}$	$K_{P_4P_1} = 9.9 \times 10^{-4} \frac{\text{gm}}{\text{cc}}$
	$K_{P_4} = 5.0 \times 10^{-3} \frac{\text{gm}}{\text{cc}}$	$K_{P_4A_2} = 1.2 \times 10^{-4} \frac{\text{gm}}{\text{cc}}$
protein	$\mu_1 = 4.6 \frac{\text{gms}}{\text{hr gm RNA}}$	$K_{M_1P_1} = 2.2 \times 10^{-4} \frac{\text{gm}}{\text{cc}}$
	$K_{M_1A_2} = 7.2 \times 10^{-5} \frac{\text{gm}}{\text{cc}}$	$k'_{TM_1} = 0.025 \text{ hr}^{-1}$
	$K_{TM_1} = 1.1 \times 10^{-5} \frac{\text{gm}}{\text{cc}}$	$k_{TM_1} = 0.025 \text{ hr}^{-1}$
RNA	$\mu_{2RTI} = 9 \times 10^{-15} \frac{\text{gm}}{\text{hr-unit}}$	$K_{M_2P_2} = 7.2 \times 10^{-5} \frac{\text{gm}}{\text{cc}}$
	$K_{1PG} = 2.0 \times 10^{-7} \frac{\text{mole}}{\text{cc}}$	$K_{1IF} = 0.009 \left(\frac{\text{gm}}{\text{cc hr}}\right)^3$
	$k_{TM_2RTI} = 21.0 \text{ hr}^{-1}$	$K_{TM_2RTI} = 0.018 \frac{\text{gm}}{\text{hr cc}}$
	$\mu_{2RTM} = 14 \text{ hr}^{-1}$	$k_{TM_2RTM} = 0.07 \text{ hr}^{-1}$
	$P = 3$	$\mu_{2M} = 0.32 \frac{\text{gm RNA}}{\text{gm Protein}}$
	$K_{TM_2RTM} = 1.1 \times 10^{-5} \frac{\text{gm}}{\text{cc}}$	$k_{TM_2M} = 21.0 \text{ hr}^{-1}$
DNA	$\mu_3 = 6.0 \times 10^{-15} \frac{\text{gms}}{\text{hr fork}}$	$K_{M_3P_3} = 4.0 \times 10^{-6} \frac{\text{gm}}{\text{cc}}$
	$K_{M_3A_2} = 2.0 \times 10^{-5} \frac{\text{gm}}{\text{cc}}$	
cell envelope	$\mu_4 = 100.0 \frac{\text{gm}}{\text{hr gm } E_{23}}$	$K_{M_4P_4} = 5.0 \times 10^{-4} \frac{\text{gm}}{\text{cc}}$
	$K_{M_4A_2} = 1.8 \times 10^{-4} \frac{\text{gm}}{\text{cc}}$	$K_{TM_4} = 0.23 \text{ hr}^{-1}$
		$K_{TM_4A_2} = 1.8 \times 10^{-4} \frac{\text{gm}}{\text{cc}}$
glycogen	$\mu_5 = 2.0 \times 10^{-2} \frac{\text{gm}}{\text{hr cc}}$	$k_{TM_5} = 0.14 \text{ hr}^{-1}$
	$K_{M_5A_2} = 2.0 \times 10^{-3} \frac{\text{gm}}{\text{cc}}$	$K_{TM_5} = 1.0 \times 10^{-3} \frac{\text{gm}}{\text{cc}}$

Continued on next page.

Table III, continued.

enzymes	$\eta_1 = 1.0 \times 10^{-3}$	$\eta_2 = 3.2 \times 10^{-3}$
	$\eta_3 = 1.6 \times 10^{-2} \text{ hr}^{-1}$	
	$K_{E_4} = 2.0 \times 10^{-10} \left(\frac{\text{gm}}{\text{cc}}\right)^2$	$\eta_4 = 0.01$
	$\ell = 2$	$k_{TE_4} = 0.05 \text{ hr}^{-1}$
ppGpp	$\mu_{PG} = 6.4 \times 10^{-3} \frac{\text{mol}}{\text{hr-gm RNA}}$	$k_{iP_1} = 12.7 \times 10^{-5} \frac{\text{gm}}{\text{cc}}$
	$k_{TPG} = 125 \text{ hr}^{-1}$	$k_{TPGA_2} = 7.2 \times 10^{-5} \frac{\text{gm}}{\text{cc}}$
acetate	$\mu_z = 0.9$	$K_{zM_4} = 1.0 \times 10^{-14} \frac{\text{gm}}{\text{cc}}$
oxidation	$\frac{P}{O} _{\max} = 1.5$	
cell shape	$\rho_{\text{cyto}} = 0.258 \frac{\text{gms}}{\text{cc}}$	$f_s = 259 \times 10^6 \frac{\text{cm}^2}{\text{gm}}$
	$\rho_{\text{env}} = 0.553 \frac{\text{gms}}{\text{cc}}$	
DNA initiation	$k_{ARP} = 2.6 \times 10^{-3} \frac{\text{gm}}{\text{gm } M_4}$	$K_{iRP} = 0.22 \frac{\text{gm}}{\text{cc-hr}}$
	$k_{RP} = 3.65 \times 10^{-17} \frac{\text{gmRP}}{\text{hr-N}_O}$	

Stoichiometric Coefficients:

α_1	= 0.179	ϵ_2	= 1.149	γ_1	= 1.167
$\alpha_{1, \text{GLN}}$	= 0.1222	ϵ_3	= 1.049	γ_2	= 1.057
β_1	= 1.128	ϵ_4	= 0.128	γ_3	= 1.053
β_2	= -0.456			γ_4	= 1.10
β_4	= 1.28			γ_5	= 1.11

Table III, continued.

glycogen	$\mu_5 = 2.0 \times 10^{-2} \frac{\text{gm}}{\text{hr cc}}$	$k_{TM_5} = 0.14 \text{ hr}^{-1}$
	$K_{M_5A_2} = 2.0 \times 10^{-3} \frac{\text{gm}}{\text{cc}}$	$K_{TM_5} = 1.0 \times 10^{-3} \frac{\text{gm}}{\text{cc}}$
enzymes	$n_1 = 1.0 \times 10^{-3}$	$n_2 = 3.2 \times 10^{-3}$
	$n_3 = 1.6 \times 10^{-2} \text{ hr}^{-1}$	
	$K_{E_4} = 2.0 \times 10^{-10} \left(\frac{\text{gm}}{\text{cc}}\right)^2$	$n_4 = 0.01$
	$l = 2$	$k_{TE_4} = 0.05 \text{ hr}^{-1}$
ppGpp	$\mu_{PG} = 6.4 \times 10^{-3} \frac{\text{mol}}{\text{hr-gm RNA}}$	$K_{iP_1} = 12.7 \times 10^{-5} \frac{\text{gm}}{\text{cc}}$
	$k_{TPG} = 125 \text{ hr}^{-1}$	$K_{TPGA_2} = 7.2 \times 10^{-5} \frac{\text{gm}}{\text{cc}}$
acetate	$\mu_z = 0.9$	$K_{zM_4} = 1.0 \times 10^{-14} \frac{\text{gm}}{\text{hr}}$
oxidation	$\frac{P_i}{O_i}_{\max} = 1.5$	
cell shape	$\rho_{\text{cyto}} = 0.258 \frac{\text{gms}}{\text{cc}}$	$f_s = 259 \times 10^6 \frac{\text{cm}^2}{\text{gm}}$
	$\rho_{\text{env}} = 0.553 \frac{\text{gms}}{\text{cc}}$	
DNA initiation	$k_{ARP} = 2.6 \times 10^{-3} \frac{\text{gm}}{\text{gm } M_4}$	$K_{iRP} = 0.22 \frac{\text{gm}}{\text{cc-hr}}$
	$k_{RP} = 3.65 \times 10^{-17} \frac{\text{gmRP}}{\text{hr-N}_O}$	

Stoichiometric Coefficients:

α_1	= 0.179	ϵ_2	= 1.149	γ_1	= 1.167
$\alpha_{1, \text{GLN}}$	= 0.1222	ϵ_3	= 1.049	γ_2	= 1.057
β_1	= 1.128	ϵ_4	= 0.128	γ_3	= 1.053
β_2	= -0.456			γ_4	= 1.10
β_4	= 1.28			γ_5	= 1.11

TABLE IV: Values of Parameters for Calculation of Energy Requirements

Compound or Process	δ_i $\frac{\text{Mole ATP}}{\text{gm}}$	ω_i $\frac{\text{Mole 'H}_2\text{'}}{\text{gm}}$
A ₁ , NH ₄ ⁺ , transport		0.028
A ₂ , glucose transport	0.0056	
+P ₁ , Amino Acids	0.0025	
P ₂ , Ribonucleotides	0.022	
P ₃ , Deoxyribonucleotides		0.0031
P ₄ , Non-Protein Envelop Precursors	0.0016	
M ₁ , protein	0.039	
M ₂ , RNA	0.0067	
M ₃ , DNA	0.0071	
M ₄ , Non-Protein Envelope	0.0081	
M ₅ , Glycogen	0.0124	

Ion Transport		$\frac{2 \times 10^{-3} \text{ mole}}{\text{gm cell}}$
Membrane Energy Recharge		$\frac{5.8 \times 10^{-4} \text{ moles}}{\text{cm}^2\text{-hr}}$
PG Formation	$\frac{3 \text{ moles}}{\text{mole}}$	
Uncoupled ATP Use	$\frac{0.0633 \text{ moles}}{\text{cm}^3}$	
SO ₄ ⁼ → S ⁼		$\frac{1.21 \times 10^{-3} \text{ mole}}{\text{gm}}$
Biosynthesis Reduction		$\frac{1.39 \times 10^{-2} \text{ mole}}{\text{gm}}$
+Glutamate dehydrogenase pathway for carbon and energy limited conditions.		
For glutamine synthetase, assume 1 mole ATP is used for every mole glutamine formed which results in a value of 0.007 for δ_{GLN} in Equation 3, Table II.		

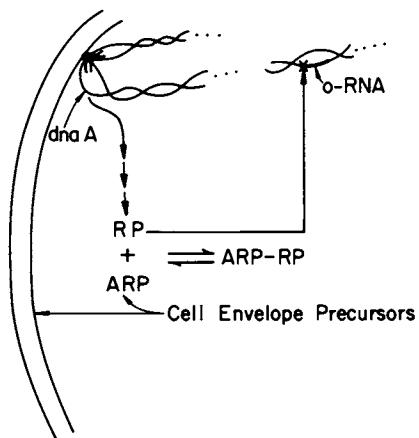


Figure 2. A potential scheme for the control of initiation of DNA synthesis. The *dnaA* gene product, RP, is a repressor protein. If a molecule of repressor protein combines with anti-repressor protein, ARP, it is inactivated. Active RP prevents the transcription of O-RNA, which is required for initiation.

ARP formation to be a constant fraction of the rate of cell envelope formation. When the level of unbound RP approaches zero, O-RNA transcription is allowed. The combining of RP with ARP is similar to a mechanism proposed by Fantes, *et al.* (55). The model mechanism requires that the *dnaA* gene be transcribed only for a short period of time so as to obtain a "burst". Pritchard, Barth, & Collins (56) have previously postulated the production of an initiation-inhibitor as a "burst" by a gene located near the origin.

The plausibility of the above mechanism was established by comparing to data the model's predictions of the length of the C period (the time to replicate a whole new DNA molecule) and D period (the time from the termination of the chromosome synthesis to the next cell division) and the timing of initiation. The results are given in Tables V and VI. Other mechanisms (e.g. positive control due to build-up of DNA precursors, to the rate of cell envelope synthesis, to the mass of the cell envelope, or to the total cell mass) have been shown to be implausible when tested for growth under glucose limitation (46). The form of the equations for the glucose-limited cell have been justified (46, 47, 50). For the case of ammonium ion limitation the equation for ammonium ion transport (Equation 21) can be justified based on the observations of Stevenson and Silver (57). They presented evidence for a dual-transport system in *E. coli*. The scheme for incorporation of ammonium ion into cellular metabolites can be described by the following equations:

- (1) L-glutamate + ATP + NH_4^+ \rightarrow L-glutamine + ADP + P_i
- (2) α -Ketoglutarate + L-glutamine + NADPH \rightarrow 2 glutamate + NADP^+
- (3) α -Ketoglutarate + NH_4^+ + NADPH \rightarrow L-glutamate + H_2O + NADP^+

Reaction 1 is mediated by glutamine synthetase while Reactions 2 and 3 are catalyzed by glutamate synthase and glutamate dehydrogenase respectively.

In Table II the series process described by Reactions (1) and (2) are represented by Equations (8a) and (8b) and Reaction (3) by the first part of Equation (8e).

Glutamate is considered a key compound because it represents the first major transformation of inorganic-N to organic; hence, nitrogen flux into the amino acid pool cannot occur any faster than glutamate-N production. This follows from glutamate's high activity with transaminases.

- (4) L-glutamate + RCO_2COOH \rightarrow $\text{RCHNH}_2\text{COOH}$ + α -Ketoglutarate

Presumably two potential routes of ammonia incorporation exist (58, 59). The high affinity route consists of glutamine synthetase activity working in conjunction with glutamate

TABLE V: Comparison of Model and Experimental Estimates of C&D Periods

μ hr^{-1}	C_{model} min.	D_{model} min.	$C^*_{\text{expt.}}$ min.	$D^*_{\text{expt.}}$ min.
0.95	41	21	42	22
0.68	47	28	42	22
0.51	59	35	56	28
0.39	75	42	73	39
0.29	99	51	~94	47
0.24	120	60	~115	~57
0.16	189	81	~178	~89

*Values from Helmstetter & Pierucci (71). No measurements were made for $\mu < 0.35 \text{ hr}^{-1}$. Values for $\mu < 0.35 \text{ hr}^{-1}$ were estimated from the suggestion (26) that $C = 2/3 \tau$ and $D = 1/3 \tau$.

TABLE VI: Comparison of Model and Experimental Estimates of the Time of Initiation of Chromosome Synthesis

μ hr^{-1}	t/τ_{Model}	$t/\tau_{\text{expt.}}^*$
0.95	0.59	0.58 ± 0.1
0.68	0.78	0.91 ± 0.1
0.51	0.86	0.96 ± 0.1
0.39	0.90	0.98 ± 0.1
0.29	0.94	0.99 ± 0.1
0.24	0.95	0.99 ± 0.1
0.16	0.99	1.0 ± 0.1

*From Helmstetter & Pierucci (71). Note that $t/\tau = 0 = 1.0$ or initiation at cell division is essentially the same as initiation at cell birth.

synthase. Glutamate dehydrogenase activity is responsible for the low affinity system which predominates under conditions of high intracellular ammonium ion levels. There is evidence (60, 61, 62) that the high affinity system is subject to ammonium ion repression and modulation of its activity by a number of mechanisms, including covalent modifications through a cascade enzyme system. In contrast the low affinity system is modulated only by large concentrations of glutamate (61, 63). Data to support this scheme has been obtained primarily with cell-free systems. Whether this scheme can function in a complete organism can be verified by comparing the computer predictions with data.

In Figure 3 the model's predictions of growth rate dependence on ammonium ion concentration is compared with chemostat data. Generally the model's predictions are quite reasonable. The model, however, suggests that the changeover from the low to high affinity region occur at $\mu \approx 0.75 \text{ hr}^{-1}$, while with the data the break appears to occur at about $\mu \approx 0.65 \text{ hr}^{-1}$. The model also predicts a lower effective saturation constant than indicated by the data. Nonetheless, the general character of the cell response is well captured by the model.

In Figure 4 the model's predictions of cell size for both glucose- and ammonium-limited growth are compared to chemostat data. In both cases the model's predictions are in close accord with the observed responses. The reason the nitrogen-limited cells are larger than the glucose-limited cells is probably due to increased storage of carbon as glycogen. The model's predictions of glycogen content of ammonium-limited cells is compared to the data of Holme (65) in Figure 5.

The predictions of the model for nitrogen-limited growth are in remarkable agreement with experiment when considering that no new adjustable parameters were introduced to describe nitrogen-limited growth. All parameter values were set with respect to glucose-limited growth. The mechanisms postulated on the basis of in vitro enzymology appear to be quite plausible upon integration into the whole cell.

Transient Response of Single-Cell Models. With the base model well-established by comparison to steady-state data, transient response predictions can be made with some minimum degree of confidence. The highly structured nature of the Cornell single-cell model should endow the single-cell model with the potential to accurately predict dynamic internal changes in composition. A computer simulated experiment is shown in Figure 6 to test transient changes in growth rate to a step change in glucose concentration. In the experiment the glucose concentration is altered suddenly from a high value permitting $\mu = 0.95 \text{ hr}^{-1}$ at steady-state to a glucose concentration permitting growth at $\mu = 0.50 \text{ hr}^{-1}$ at steady-state. The change in cell-growth rate drops dramatically and oscillates slightly. Eight cell generations are required before the new steady-state growth

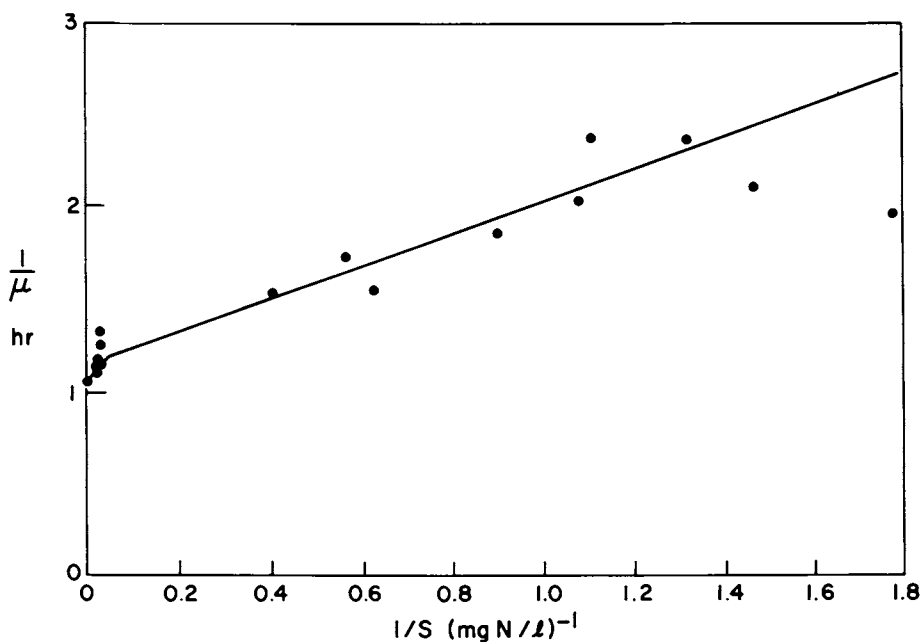


Figure 3. The model's prediction of growth-rate (solid line) dependence on ammonium-ion concentration is compared to experimental data. The data and the model predictions indicate that more than a single system is responsible for ammonium-ion uptake, assimilation, or both.

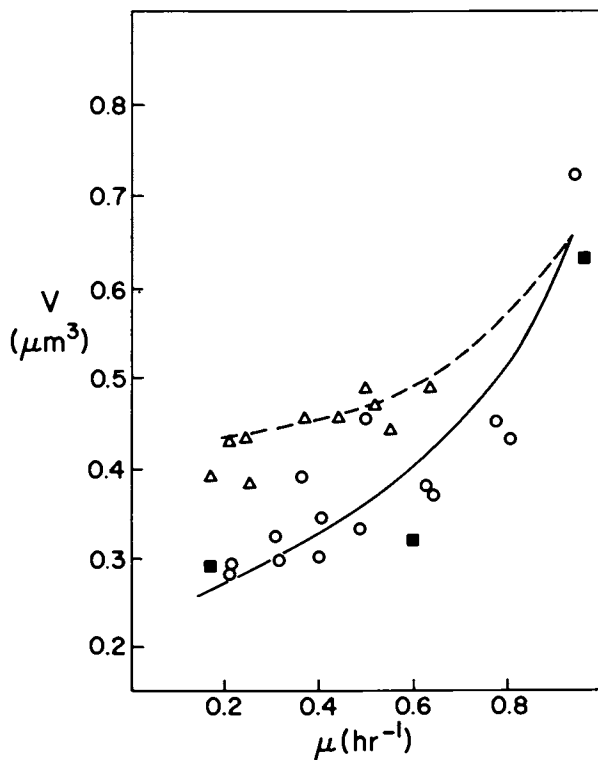


Figure 4. Variation of cell volume with growth rate. For glucose-limited cells: \circ , data from Cornell; \blacksquare , data from Ref. 64. For ammonium-limited cells: \triangle , data from Cornell. Solid line, the model's prediction for glucose-limited cells; dashed line, model's prediction for ammonium-limited cells.

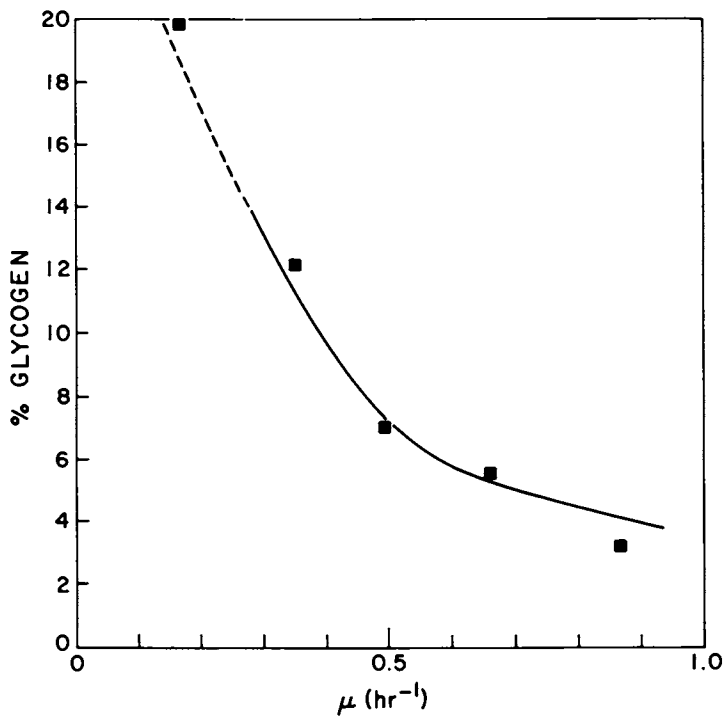


Figure 5. Model's predictions of the effects of ammonia limitation on glycogen content. Data points from Ref. 65.

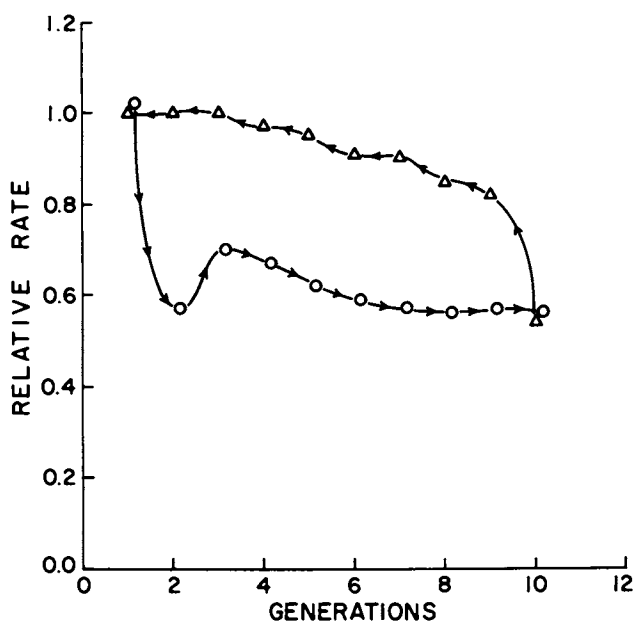


Figure 6. Transient responses of the computer cell: ○, response to step-decrease in external glucose concentration (1000 mg/L to 4.5 mg/L); △, response to a step-increase (4.5 mg/L to 1000 mg/L). Relative rate corresponds to the average growth rate during that cell generation.

rate is approximated. If the experiment is reversed and glucose is suddenly changed from the lower to the higher value, the cell responds by steadily increasing its growth rate. Again it takes about eight cell generations to get a new steady-state. The important feature here is that the cell returns to the original growth-rate via a different path. There is substantial hysteresis in the computed predicted response to these perturbations.

The explanation for the rapid response of the cell to a step down in energy availability is shown in Figure 7. The decrease in glucose causes a rapid increase in ppGpp which drastically reduces RNA synthesis and consequently reduces other cellular processes such as protein synthesis. Such responses have been observed experimentally (66, 67).

Nitrogen-limited cells also show hysteresis when subjected to an experiment analogous to the ones for glucose-limited cells. The biggest difference (see Figure 8) is the oscillatory response and overshoot during the step-up part of the experiment. The overshoot is probably due to the high level of both low and high affinity systems for converting ammonium into amino acids. The growth rate of *E. coli* in glucose-minimal medium can be enhanced by the addition of amino acids. The large decrease in growth rate during step-down is likely due to the inability of the low affinity glutamate dehydrogenase system to produce sufficient amino acids by itself with low ammonium ion concentrations and a moderately long lag in the production of the enzymes for the high affinity system.

Population Models From Single-Cell Models

The single-cell model is limited in its usefulness for engineering calculations unless a population model can be constructed from the information in the single-cell model. It is possible to build a population model using an ensemble of single-cell models to mimic the response of a large population of cells (24, 46, 68). Since computer capacity is finite, the question is really, "how few cell models can be included in a population and still allow reasonable predictions of the behavior of a natural population of cells?"

Figure 9 presents a sketch of an "ideal" size distribution and a "typical" size distribution. The "ideal" distribution would occur if there were no variation producing processes within the cell (i.e. all cells have identical cell cycles). In the ideal distribution cells automatically divide at twice the birth volume, and there are two times as many cells of birth size as division size. The frequency function of cells of intermediate size would decrease approximately exponentially from birth to fission-ready cells.

However, variation causing processes exist. Hypothetical probability functions relating birth and division to cell size are shown. Such functions will result in a "typical" size

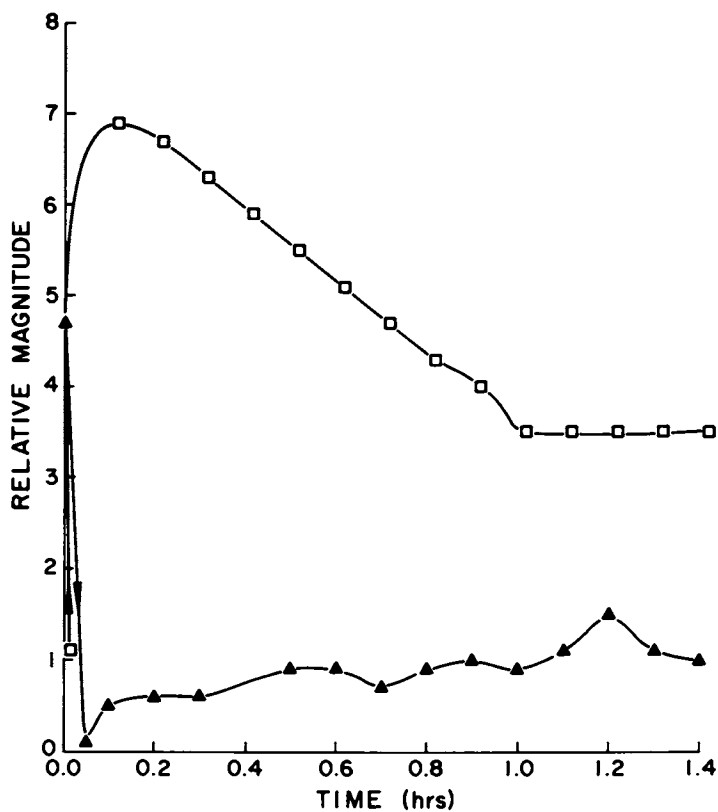


Figure 7. Changes in the relative magnitude of internal ppGpp concentration (\square) and in the rate of RNA synthesis (\blacktriangle) are given for the first division cycle after the step-down in glucose concentration (see Figure 6). The decrease in energy-availability causes a rapid increase in ppGpp that significantly reduces RNA synthesis and consequently, reduces cell metabolism and growth.

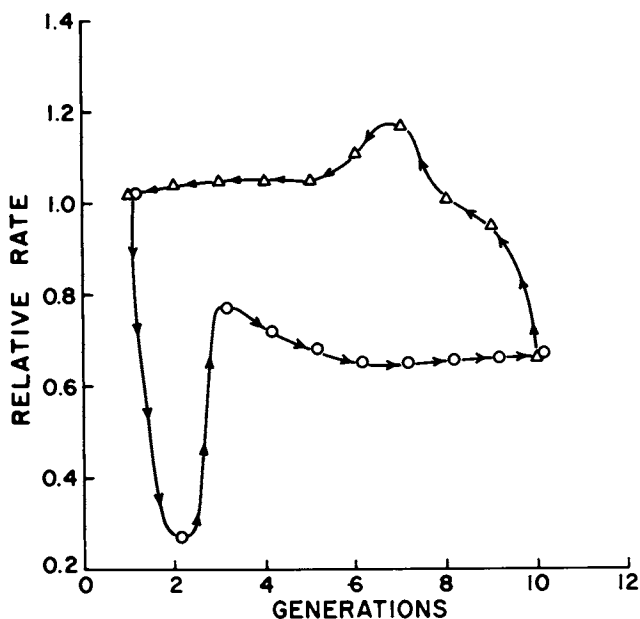


Figure 8. Transient response of the computer cell to a step-change in external ammonium-ion concentration: ○, response to step-decrease (2.5 mg/L to 1.4 mg/L); △, response to step-increase (1.4 mg/L to 2.5 mg/L). The relative rate corresponds to the average growth rate during that cell generation.

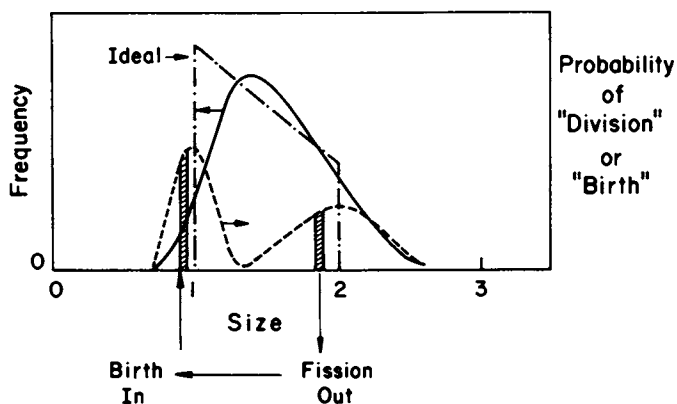


Figure 9. Sketches of ideal size distribution (---) and typical size distribution (—). The typical distribution results from random processes that cause the cell to have a significant probability of fission over a range of sizes.

distribution plot which exhibits a slight positive skewing. For each size class in the distribution cells can enter by growth or birth and may exit the size class due to further growth or division.

Consideration of "ideal" and "typical" size distributions suggests certain characteristics required to simulate a large population with a finite number of cells. The ensemble to be constructed will have some number of discreet size classes and some other number of cell models within each size class. Requirements for an accurate simulation are:

1. Sufficient number of size classes so that growth through the intervals is smooth. If the cells are spaced further apart than the mesh size of the size analyzer in use, then gaps in the frequency curve will periodically occur.

2. Mechanisms causing variations in fission size must be identified.

3. Once the variation causing processes are quantified, then sufficient cells must be put into each size class to accurately mimic the random processes within each size class (i.e. the sample must be large enough that the distribution of properties can reproduce itself for the case of steady-nutrient supply).

Factors that could contribute to variability within the cell can easily be imagined. Any time a small number of copies exist the process description becomes less deterministic and more stochastic. Some possible variation producing processes are:

1. RP "burst" size
2. RP partition upon fission
3. ARP variation
4. Replication velocity - possibly related to the number of unwinding enzymes
5. Ratio of E_2 to E_3 and consequently ratio of cross-wall formation to cell extension
6. Asymmetric division.

To more efficiently test ways of constructing population models we have simulated the simulation by using a number of structureless cells. The cells were assigned a mode of cell increase, and their variation of fission size was accomplished by selecting the next termination size on a random basis and storing it. The range and frequency of fission size was comparable to observed patterns (e.g. 10% coefficient of variation and Gaussian frequency distribution (22, 69)).

Figure 10 shows the results of a simulation with 200 cells - 20 cell classes and two cells per class. A steady-state environment was imposed. Even after 30 generations the size distribution exhibits significant instabilities. By going to 2000 cells - 20 cell classes and 100 cells per class (Figure 11) - the stability of the size distribution is greatly improved. In the above two cases equal cell sizes among daughters at division was required. Little differences in distributions were observed when

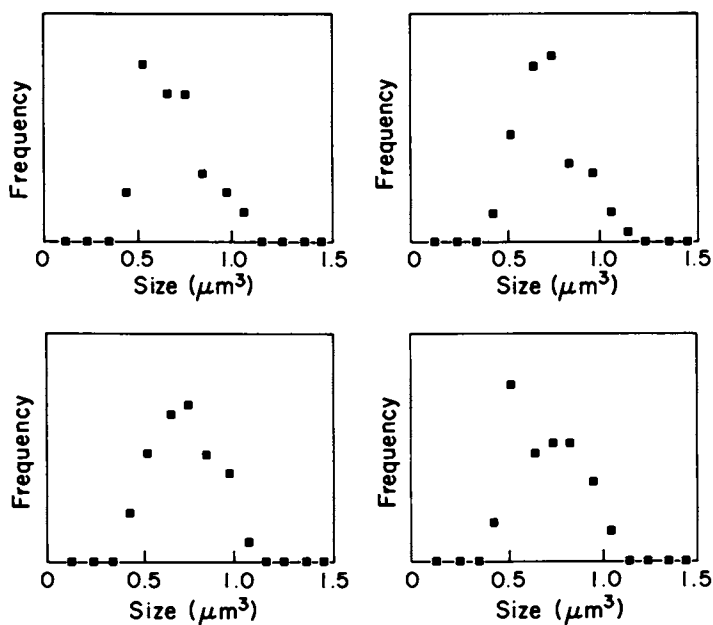


Figure 10. Computer simulation of a population using 200 unstructured cell models. There were 20 size classes with 10 cells per class in the simulation. Even at steady state the size distribution shows significant instabilities in shape.

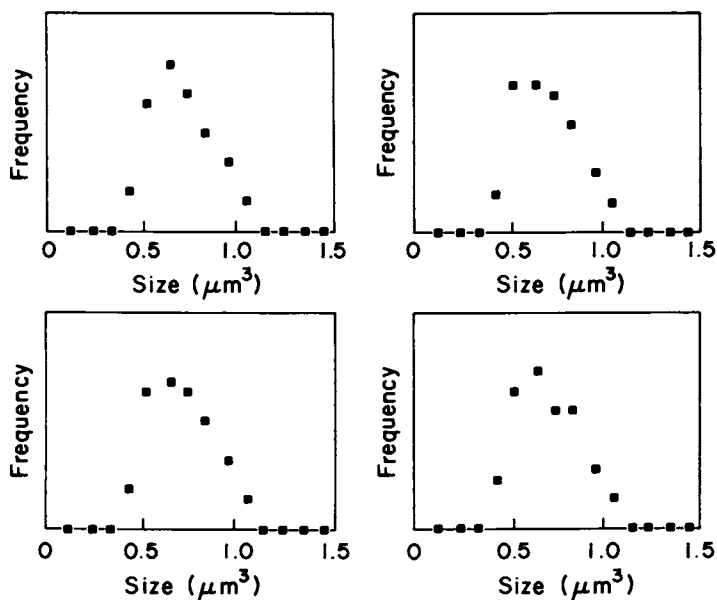


Figure 11. Computer simulation of a population using 2000 unstructured cell models. There were 20 size classes with 100 cells per class in the simulation. The steady state size distributions are considerably more stable than the simulation with 200 cells (See Figure 10).

unequal fission was allowed. The precision of fission is high (70), so its inclusion with realistic probability values was not expected to greatly alter the results. The bulk of variation in birth size (> 75%) is linked to the variation in overall fission size and not the location of the cross-wall plane. Since the assumption of equal fission greatly simplifies programming and reduces demands on computer memory, it is prudent to assume equal fission.

Figure 12 displays the steady-state stability of size-distributions generated with the structured single-cell model. Sixteen cell classes with fifteen cells per class were used. Random processes allowed were variation in "burst" size of RP (20%) and in replication velocity (10%). Variation with respect to other criteria are currently being investigated. The stability displayed by the distributions will be acceptable in most potential applications. Clearly other types of distributions (e.g. RNA, DNA, protein, etc.) can be generated from such population runs.

Summary

Single-cell models can be written that mimic very closely the responses of living cells. Such models are convenient tools for testing the plausibility of basic biochemical mechanisms. They may be particularly attractive in testing the potential in vivo compatibility of mechanisms postulated on the basis of in vitro enzymology. The single-cell models make reasonable predictions during transient conditions and are numerically stable. Since stable distributions of a population can be constructed by using an ensemble of single-cell models, it should be possible to develop population models with both high levels of segregation and structured. Such models need to be further developed and tested for their ability to predict the transient behavior of cell populations to perturbations in the abiotic environment.

Acknowledgment

This work was supported, in part, by NSF Grant CPE-7921259.

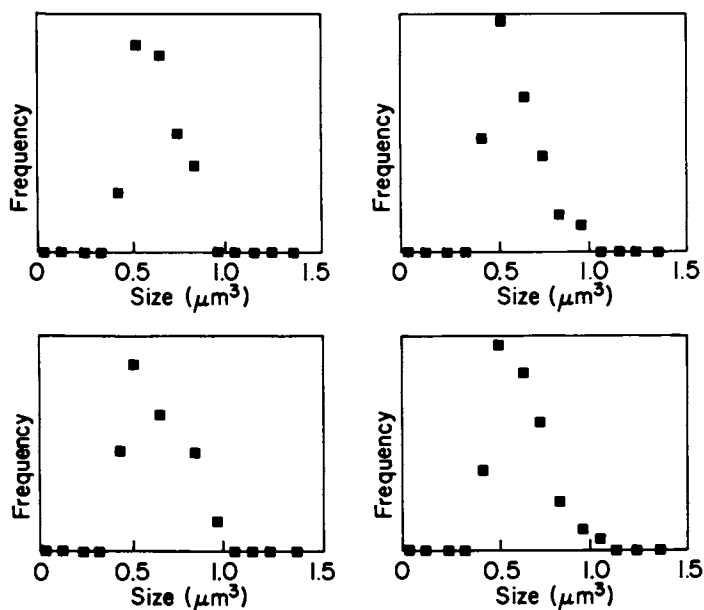


Figure 12. Computer simulation of a population using 240 structured cells (the Cornell single-cell model). There were 16 size classes and 15 cells per class in the simulation. The steady-state size distributions display a level of stability acceptable for most applications.

Literature Cited

1. Tsuchiya, H.M.; Fredrickson, A.G.; Aris, R. Adv. Chem. Eng. 1966, 6, 125-205.
2. Painter, P.R.; Marr, A.G. Ann. Rev. Microbiol. 1968, 22, 519-548.
3. Van Uden, N. Ann. Rev. Microbiol. 1969, 23, 473-486.
4. Garfinkel, D.; Garfinkel, L.; Pring, M.; Green, S.B.; Chance, B. Ann. Rev. Biochem. 1970, 39, 473-498.
5. Fredrickson, A.G.; Megee, R.D., III; Tsuchiya, H.M. Adv. Appl. Microbiol. 1970, 13, 419-465.
6. Nyiri, L.K. Adv. Biochemical Eng. 1972, 2, 49-95.
7. Boyle, W.C.; Berthouex, P.M. Biotechnol. Bioeng. 1974, 16 1139-1159.
8. Fredrickson, A.G. Biotechnol. Bioeng. 1976, 18, 1481-1486.
9. Bailey, J.E. Chem. Eng. Sci. 1980, 35, 1854-1886.
10. Fredrickson, A.G.; Ramkrisha, D.; Tsuchiya, H.M. Chem. Eng. Symp. Series 1971, 67(108), 53-59.
11. Campbell, A. Bacteriol. Rev. 1957, 21, 263-272.
12. Williams, F.M. J. Theo. Biol. 1967, 15, 190-207.
13. Williams, F.M. "Systems Analysis and Simulation in Ecology"; Patten, B.C., Ed.; Academic Press: New York, 1971, Vol. 1.
14. Ramkrishna, D.; Fredrickson, A.G.; Tsuchiya, H.M. Biotechnol. Bioeng. 1967, 9, 129-170.
15. Van Foerster, H. "The Kinetics of Cellular Proliferation"; Stohlman, F., Ed.; Grune & Stratton: New York, 1959, p. 382.
16. Trucco, E. Bull. Math. Biophys. 1965, 27, 285-304, 449-471.
17. Yakovlev, A.Y.; Zorin, A.V.; Isanin, N.A. J. Theor. Biol. 1977, 64, 1-25.
18. Fredrickson, A.G.; Tsuchiya, H.M. AIChE J. 1963, 9, 459-468.
19. Kozesnik, J. "Continuous Cultivation of Microorganisms"; Malek, I.; Beran, K.; Hospodka, J., Eds.; Academic Press: New York, 1964, p. 59.
20. Lebowitz, J.L.; Rubinow, S.I. J. Math. Biology 1974, 1, 17-36.
21. Koch, A.L.; Schaechter, M. J. Gen. Microbiol. 1962, 29, 435-454.
22. Eakman, J.M.; Fredrickson, A.G.; Tsuchiya, H.M. Chem. Eng. Prog. Symp. Series 1966, 62(69), 37-49.
23. Bailey, J.E.; Fazel-Madjlessi, J.; McQuitty, D.N.; Lee, L.Y.; Oro, J.A. AIChE J. 1978, 24, 570-576.
24. Nishimura, Y.; Bailey, J.E. Math. Biosciences 1980, 51, 305-328.
25. Nishimura, Y.; Bailey, J.E. AIChE J. 1981, 27, 73-81.
26. Pickett, A.M.; Bazin, M.J.; Topiwala, H.H. Biotechnol. Bioeng. 1980, 22, 1213-1224.
27. Pickett, A.M.; Bazin, M.J.; Topiwala, H.H. Biotechnol. Bioeng. 1979, 21, 1043-1055.
28. Tanner, R.D. Biotechnol. Bioeng. 1970, 12, 831-843.
29. Bischoff, K.B. Can. J. Chem. Eng. 1966, 44, 281-284.

30. Blanch, H.W.; Rogers, P.L. Biotechnol. Bioeng. 1972, 14, 151-171.
31. Constantinides, A.; Spencer, J.L.; Gaden, E.L., Jr. Biotechnol. Bioeng. 1970, 12, 803-830.
32. Ho, L.Y.; Humphrey, A.E. Biotechnol. Bioeng. 1970, 12 291-311.
33. Koga, S.; Burg, C.R.; Humphrey, A.E. Appl. Microbiol. 1967 15, 683-689.
34. Yamashita, S.; Hoshi, H.; Inagaki, T. "Fermentation Advances"; Perlman, D.; Academic Press: New York, 1969, p. 441.
35. Heinmets, F. "Analysis of Normal and Abnormal Cell Growth"; Plenum Press: New York, 1966.
36. Davison, E.J. Bull. Math. Biol. 1975, 37, 427-458.
37. Simon, Z. J. Theor. Biol. 1973, 38, 39-49.
38. Weinberg, R.; Zeigler, B.P.; Laing, R.A. J. Cybernetics 1971, 1, 34-48.
39. Zeigler, B.P.; Weinberg, R. J. Theor. Biol. 1970, 29, 35-56.
40. Dennis, P.P.; Bremer, H. J. Bacteriol. 1974, 119, 270-281.
41. Brunschede, H.; Dove, T.L.; Bremer, H. J. Bacteriol. 1977, 129, 1020-1033.
42. Bremer, H.; Chuang, L. J. Theor. Biol. 1981, 88, 47-81.
43. Cooper, S.; Helmstetter, C.E. J. Mol. Biol. 1968, 31, 519-540.
44. Donachie, W.D. Nature, 1968, 219, 1077.
45. Ho, S.V.; Shuler, M.L. J. Theor. Biol. 1977, 68, 415-435.
46. Shuler, M.L.; Leung, S.; Dick, C.C. Ann. N.Y. Acad. Sci. 1979, 326, 35-55.
47. Domach, M.M.; Leung, S.K.; Cahn, R.E.; Cocks, G.G.; Shuler, M.L. J. Bacteriol. (Submitted for publication)
48. Leung, S.K. M.S. Thesis, Cornell University, Ithaca, New York, 1979.
49. Dick, C.C. M.S. Thesis, Cornell University, Ithaca, New York, 1978.
50. Domach, M.M. Ph.D. Thesis, Cornell University, Ithaca, New York, 1982.
51. Fralick, J.A. "DNA Synthesis - Present and Future"; Molineux, I.; Kohiyama, M., Eds.; Plenum Press: New York, 1978, 71-83.
52. Messer, W.; Dankwork, L.; Tippe-Schindler, R.; Womack, J.E.; Zahn, G. "DNA Synthesis and Its Regulation"; Goulian, M.; Hanawalt, P., Eds.; W.A. Benjamin: Menlo Park, California, 1975, p. 602.
53. Fayet, O.; Louarn, J. "DNA Synthesis - Present and Future"; Molineux, I.; Kohiyama, M., Eds.; Plenum Press: New York, 1967, p. 27.
54. Grossman, N.; Ron, E.Z. J. Bacteriol. 1980, 143, 100-104.
55. Fantes, P.A.; Grant, W.D.; Pritchard, R.H.; Sudbery, P.E.; Wheals, A.E. J. Theor. Biol. 1975, 50, 213-244.

56. Pritchard, R.H.; Barth, P.T.; Collins, T. Symp. Soc. Gen. Microbiol. 1969, 19, 263-297.
57. Stevenson, R.; Silver, S. Biochem. Biophys. Res. Comm. 1977, 75, 1133-1138.
58. Kavanagh, B.M.; Cole, J.A. "Continuous Culture 6: Applications and New Fields"; Ellwood, D.C.; Evans, C.G.T.; Melling, J., Eds.; Ellis Horwood Ltd.: Chichester, Great Britain, 1976, Chap. 14.
59. Dalton, H. "Microbial Biochemistry"; Quayle, J.R., Ed.; University Park Press: Baltimore, 1979, Chap. 6.
60. Woolfolk, C.A.; Shapiro, B.; Stadtman, E.R. Arch. Biochem. Biophys. 1966, 116, 177-192.
61. Miller, R.E.; Stadtman, E.R. J. Biol. Chem. 1972, 247, 7407-7419.
62. Ginsburg, A.; Stadtman, E.R. "The Enzymes of Glutamine Metabolism"; Prusiner, S.; Stadtman, E.R., Eds.; Academic Press: New York, 1973, p. 9.
63. Varricchio, F. Biochim. Biophys. Acta 1969, 177, 560-564.
64. Helmstetter, C. J. Mol. Biol. 1974, 84, 21-36.
65. Holme, T. Acta Chem. Scand. 1957, 11, 763-775.
66. Cashel, M. Ann. Rev. Microbiol. 1975, 29, 301-318.
67. Gallant, J. Ann. Rev. Genetics 1979, 13, 393-415.
68. Shuler, M.L.; Domach, M. 72nd Annual AIChE Meeting, San Francisco, California, November 25-29, 1979.
69. Koppes, L.J.H.; Woldringh, C.L.; Nanninga, N. J. Bacteriol. 1978, 134, 423-433.
70. Marr, A.G.; Harvey, R.J.; Tentini, W.C. J. Bacteriol. 1966, 91, 2388-2389.
71. Helmstetter, C.; Pierucci, O. J. Mol. Biol. 1978, 102, 477-486.

RECEIVED June 29, 1982

Single-Cell Metabolic Model Determination by Analysis of Microbial Populations

JAMES E. BAILEY

California Institute of Technology, Department of Chemical Engineering,
Pasadena, CA 91125

The properties of microbial populations result from the characteristics of metabolism and its control at the level of the individual cell. Useful descriptions of population behavior may therefore be constructed based on understanding of single-cell metabolism, and, conversely, studies of population properties may be employed to extract information about single-cell operation. Population balance equations provide the primary mathematical tool for these purposes, and flow cytometry allows experimental access to the distribution of cell states in the population. Application of these methods to bacteria and yeasts is illustrated using three example systems.

The microbial populations propagated in reactors ranging from Petri dishes to fermentors to natural ecosystems are typically heterogeneous with respect to age, size, and biochemical activity. The overall rates of substrate utilization, biosynthesis and product formation in these reactors are sums, taken over the cell population, of the rates of the corresponding processes in the individual cells present (1,2). Viewed from this perspective, optimizing the performance of a microbial process requires determination of the cells' genotype and of a reactor design such that the optimal distribution of states is achieved in the process's microbial population.

Adoption of this approach to microbial process development cannot occur until methods exist for determining the influence of reactor design and operating parameters on single-cell metabolic control actions and reaction rates. If this information is available, population balance equations and associated medium conservation equations provide the required bases for reactor analysis (1,2). For example, for a well-mixed, continuous-flow isothermal microbial reactor at steady-state, the population balance equation may be written:

0097-6156/83/0207-0135\$07.50/0

© 1983 American Chemical Society

$$\frac{d}{dp} \left[r_f(p,s) f(p,s) \right] = D \left[4\phi(2p,s) - \phi(p,s) - f(p,s) \right] \quad (1.1)$$

$$f(0,s) = 0 \quad (1.2)$$

where here it has been assumed that the state of a single cell can be characterized by a single variable p (e.g., cell age, cell protein content, or cell volume) and that the effect of the environment on cell kinetics and controls can be represented by a single environmental variable s (e.g., limiting nutrient concentration, temperature). Even in this relatively simple case, the above equation shows the connection among reactor operating conditions, represented here by the dilution rate D (= mean residence time⁻¹), single-cell kinetics and controls, appearing here as $\phi(p,s)$ ($\phi(p,s)dp$ = the fraction of dividing cells with p -values between p and $p+dp$) and $r_f(p,s)$ (the time rate of change of p in a cell with a certain p -value in a certain environment s), and the distribution of states in the cell population, here written as a frequency function $f(p,s)$ for single-cell p -values ($f(p,s)dp$ = the fraction of cells in the population with p -values between p and $p+dp$).

The population balance equation for the process has an extremely important alternative application. If the frequency function or subpopulation fractions evaluated using the frequency function can be measured experimentally, the population balance equations provide a link between alternative models for regulation and single-cell kinetics and parameter values employed in those models on the one hand, and experiment on the other. That is, one may calculate, using the population balance equations, frequency functions corresponding to various single cell models and then compare the frequency functions so calculated with the experimental ones. Through this sort of comparison, qualitative features of presumed single cell models can be tested and, furthermore, parameters in those models may be evaluated. Use of this strategy will be illustrated below in several examples.

While clever experimental design may make it possible to test predictions of single-cell models without recourse to measurements of f , direct experimental access to the frequency function is often desirable and sometimes necessary in order to evaluate single-cell control and kinetic properties using the strategy just outlined. A variety of methods are available for achieving frequency function measurements. The painstaking investigations of Henrici (3) and later workers demonstrate the feasibility of measuring distributions of cell sizes and shapes from microscopic observation of cell populations. This approach is usually limited by difficulties in obtaining fine quantitative resolution and in examining a sufficiently large sample population to obtain good statistics.

The advent of single-cell measurements in flowing cell suspensions, first accomplished in the Coulter particle sizing instrument (4), has revolutionized the experimental characterization of distributions of states in cell and other particulate populations. Optical techniques, including light scattering, light absorption, and fluorescence measurements from individual cells in flow systems, have broadened the scope of cellular parameters which can be measured on an individual cell basis in a millisecond or less in a flowing cell suspension (5). As illustrated schematically in Figure 1, such instrumentation allows rapid determination, from a properly prepared and labeled sample of the cell population, of an experimental approximation to the frequency function for single-cell content of the labeled component. The sample preparation process shown in Figure 1 may be simplified greatly in cases where light scattering or light absorption are used to measure the cell size or morphology. Flow cytometry has now been applied successfully to a number of microbial systems, and fluorescent stains are available which can be used to achieve measurements of single-cell protein, DNA, double-stranded nucleic acid content and viability of some strains (e.g., 6-9).

A framework for formulating models of single-cell controls and kinetics is provided by consideration of the cell cycle of the organism (10). The cycle of chemical and morphological changes which occurs as a daughter cell ages, grows, and ultimately divides to yield new daughter cells may be decomposed into several interlocking cycles, such as the cell division cycle, which describes the cycle of growth and division, and the nuclear cycle, which concerns the processes of DNA synthesis and segregation of DNA molecules upon cell division. Previous investigations by geneticists, microbiologists and biochemists provide guidance into the basic features of these cycles and into their interrelationships and coordination.

In the examples discussed below, cell cycle properties reported in the biological sciences literature comprise the starting point of either mathematical or experimental analyses which relate single-cell operation with the resulting properties of a growing cell population. The tools of mathematical modeling of cell populations and of flow cytometry allow prediction of microbial population behavior under circumstances different from those used in the original exposition of the cell cycle models. Consequently, such simulations and experiments provide a means for evaluating the generality of the proposed cell cycle models and, in some cases, for quantitative determinations of parameters or kinetic forms which are part of the cell cycle model. This is an extremely important aspect of the studies to be described here, since, given the diversity and complexity of control systems in microorganisms and other cells, the observation of a particular phenotypic control behavior in one or a set of cell environments in no way guarantees that the same controls or results will occur when growth conditions are changed. An area of special interest here is the application of

cell cycle models based upon transient, unbalanced growth experiments to steady-state balanced growth situations and vice-versa. The value of combinations of steady-state and transient experiments in formulating and testing models of single cell kinetics and controls will be apparent in the examples which follow.

Three example organisms are considered in the following sections. These have been chosen to illustrate a variety of biological features, mathematical modeling approaches and results, and alternative experimental approaches and strategies for identifying and testing models. *Escherichia coli*, the widely-studied intestinal bacterium, is examined first. This simple procaryote divides by binary fission and exhibits a pattern of DNA synthesis during the cell cycle which is rather complex and quite different from that observed in eucaryotic microorganisms. Furthermore, it will be seen that, for this microorganism, accurate calculation of cell numbers requires attention to the DNA synthesis processes of the cell and its control (here and in the remainder of the work the term "DNA" refers only to DNA in the chromosome(s) of the cell). The next example considers the fission yeast, *Schizosaccharomyces pombe*, which divides by binary fission and which exhibits a nuclear cycle-cell separation coordination which is significantly different from that normally ascribed to eucaryotes. The final example will consider growth of *Saccharomyces cerevisiae* populations. This yeast, used widely in baking and brewing, provides an interesting third type of single-cell behavior with DNA synthesis occurring in the classical eucaryotic pattern, but with asymmetric cell division.

A Mathematical Model for Growth of *E. coli* Populations

Cooper and Helmstetter (11) have shown that, under a variety of growth conditions, many experimental observations are consistent with a model in which the time for replication of the entire chromosome of *E. coli* B/r is approximately forty minutes. During this time, the rate of replication fork advance appears to be constant. Furthermore, cell division control is related to DNA synthesis: the bacterial cell divides approximately twenty minutes after a replication fork reaches the terminus of the chromosome. These features in combination imply interesting patterns of DNA synthesis in individual bacterial cells.

As shown in Figure 2, the situation is quite simple when the organism has a doubling time of sixty minutes. DNA synthesis occurs at a constant rate for the first forty minutes of the life of a single cell (the times shown in this diagram are times remaining until division), and the cell synthesizes no DNA during its final twenty minutes of growth before division. However, the growth of an *E. coli* cell with a doubling time of fifty minutes implies a more complicated pattern of DNA synthesis, in which a new set of replication forks begins synthesizing DNA ten minutes before the cell divides.

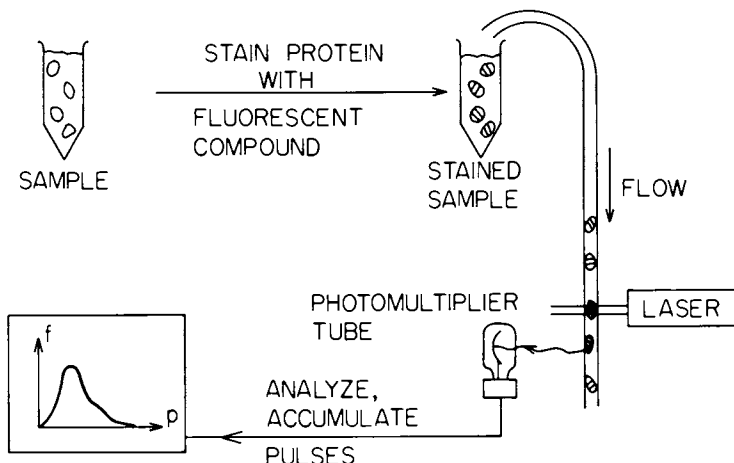
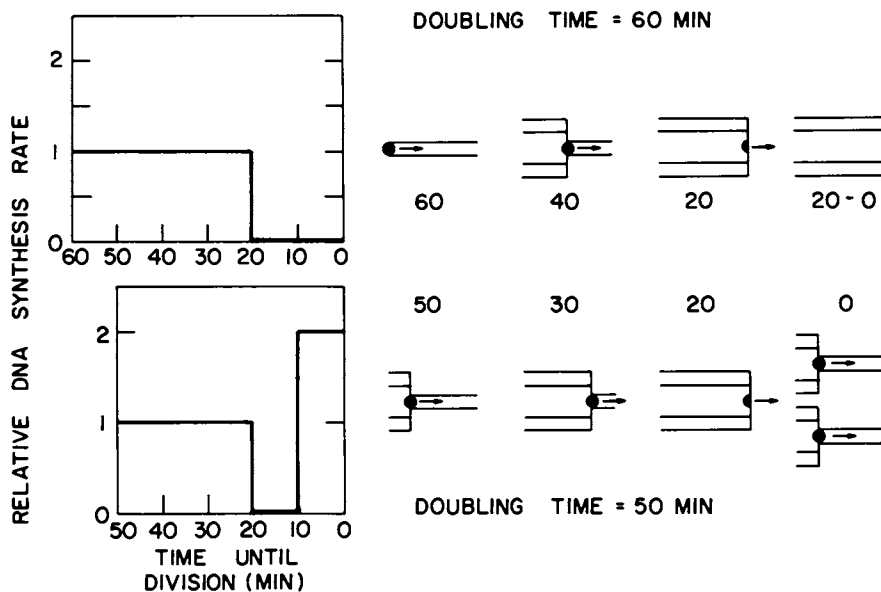


Figure 1. Schematic diagram of flow cytometry measurement of the frequency function, f , for single-cell protein content, p , in a cell population. After cellular protein is stained with a specific fluorochrome, the dilute cell suspension is analyzed in the flow cytometer. Laser radiation excites stain fluorescence in a single cell; that is measured by a photomultiplier tube. The resulting voltage pulses are sorted and stored to obtain the frequency function.



*Figure 2. DNA synthesis rates and chromosome configurations according to the Cooper-Helmstetter (11) model for *E. coli* growing at different rates. (The circular chromosome is shown here in linear form for schematic convenience.)*

Thus, during the final ten minutes of cell growth, DNA is synthesized at double the rate observed at any time during the slower growth situation. This model indicates that DNA synthesis in bacteria, far from being a continuous process, is also one that proceeds at various rates, with discontinuities in rate depending upon time elapsed in the cell cycle and the doubling time of the cell. This feature of this simple bacterium provides a dramatic example of variation in metabolic activities of cells during their life cycle.

The Cooper-Helmstetter model does not in itself provide a complete model for growth and division of a single bacterium, but such a model may be obtained by adding two additional elements. Donachie (12) has shown that DNA synthesis - growth rate - cell size data is consistent with the hypothesis that replication forks begin at every chromosome origin whenever $m = 2^n m^*$, $n = 1, 2, \dots$, where m^* is the mass of a resting cell. The model is completed by assuming that the specific rate of single cell mass synthesis $\mu(t)$ is independent of cell mass or physiological state and is a function of time that is either specified or determined by calculation using an auxiliary model (13). Figure 3 summarizes the different parts of the model and the way in which they interlock in order to provide a complete description of single-cell mass synthesis, DNA synthesis, and cell division. As noted in the figure, the Cooper-Helmstetter model allows determination not only of the amount of DNA in the individual cell, but also of the chromosome configuration; that is, position of the replication forks along the chromosome. Thus, by reference to a map of the chromosome, one may determine the numbers of all chromosomal genes in the cell at any instant of time under any growth environment and growth history.

By means of a clever transformation of variables and some ingenious reasoning, Nishimura was able to obtain analytical solutions for the distributions of mass, DNA content, chromosome configuration, and total cell numbers in populations of bacteria described by the above model (14). Figure 4 shows the model results for steady-state balanced growth of *E. coli* at a variety of doubling times. The rear panel, which shows the calculated ratio of mean DNA content to mean cell mass, exhibits a decreasing dependence on doubling time which is consistent with previous experimental observations (15). However, there are many simpler models which presumably could be derived which would also reproduce this particular result. The present model also gives the effects of population growth rate on DNA and mass frequency functions as shown in the sequences along the floor of the figure. However, experimental data on these frequency functions are not presently available. Consequently, one must find alternative situations to test the model in which the model is in some sense more severely and critically exposed.

Several lines of research in the physical sciences and engineering suggest that unsteady-state experiments are often extremely useful in exploring generality of mathematical models. For example,

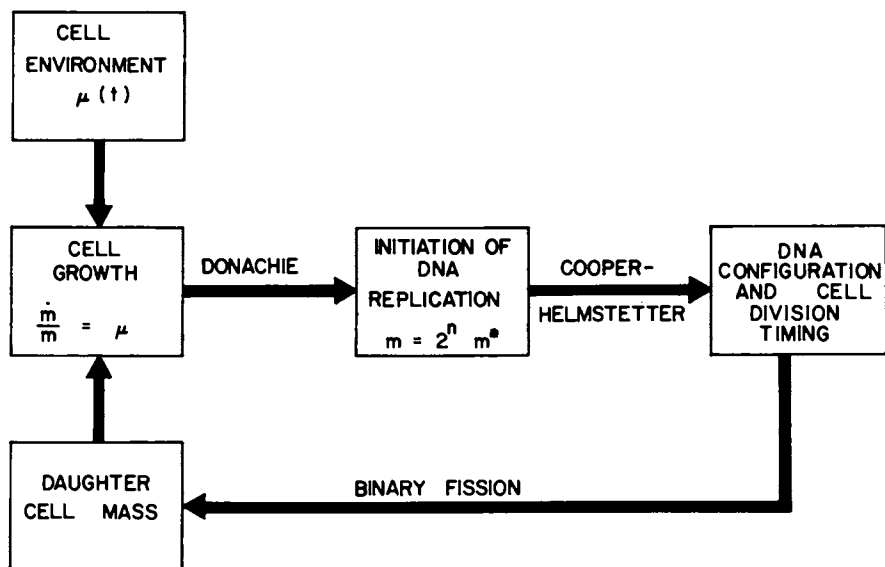


Figure 3. Summary of a model for coordinated mass and DNA synthesis and cell division for individual cells of *E. coli*. Reproduced, with permission, from Ref. 14. Copyright 1980, Elsevier North Holland, Inc.

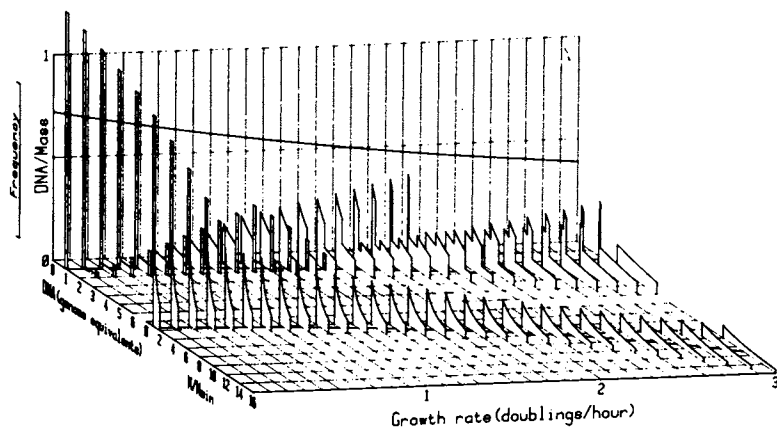


Figure 4. Calculated properties of *E. coli* populations in steady state balanced growth at different rates. Frequency functions for cell mass and DNA content are shown on the bottom panels; the rear panel shows the calculated ratio of mean cell DNA content to mean cell mass. Reproduced, with permission, from Ref. 13. Copyright 1981, American Institute of Chemical Engineers.

transient experiments were applied in the studies of Kjeldgaard *et al.* (16) in studies of *E. coli* macromolecular synthesis. In particular, the time dependence of total culture cell mass, DNA, RNA, and cell numbers were followed after a shift increase in growth rate. These experiments show clearly that cell mass, DNA, and cell numbers follow different trajectories with cell mass responding first to the new environment, DNA second, and cell numbers last. The number of cells in the population increases following the shift at a rate characteristic of the old medium until roughly one hour after the shift. The model described, when used to calculate the results of the same experiment, yields the behavior shown in Figure 5. The time-variations of total culture cell mass, DNA content, and cell numbers shown on the rear panel mimic very closely the experimental results. Consequently the model easily passes this test. It would be interesting to design new transient experiments to explore more thoroughly the ability of the model just outlined to describe transient bacterial population behavior.

This example shows how basic information from the biological sciences literature combined with facile mathematical analysis can provide useful working relationships which connect basic single-cell cycle parameters with properties of cell populations growing under different conditions. Related models of *E. coli* population dynamics have been developed extensively by Bleecken (17-19), who has structured his model and analysis to allow direct determination of the number of any particular gene present in the culture during balanced growth and during the transient following a growth rate change.

Also of interest in this connection is the elaborate model of the bacterial cell developed by Shuler and colleagues which is described in detail elsewhere in this volume. That model offers the advantages of more complete representation of basic cellular functions and, thereby, ability to simulate correctly a wider variety of responses to growth environment. Furthermore, that model does not require any supplementary or auxiliary calculations to determine growth rate of the organism as does the model outlined above. On the other hand, the structured model of Shuler and coworkers requires considerably more computational effort for its solution and less possibility of identification of certain qualitative features than does the approach outlined above. It is expected that, in the coming years, through lumping procedures guided by sensitivity analyses, a spectrum of models for this organism will become available which will allow the experimentalist or reactor designer to select the level of model complexity required for the problem under consideration.

Cell Cycle Operation and Single-Cell Protein Synthesis Kinetics for *S. pombe*

Flow cytometry provides direct qualitative insights into the

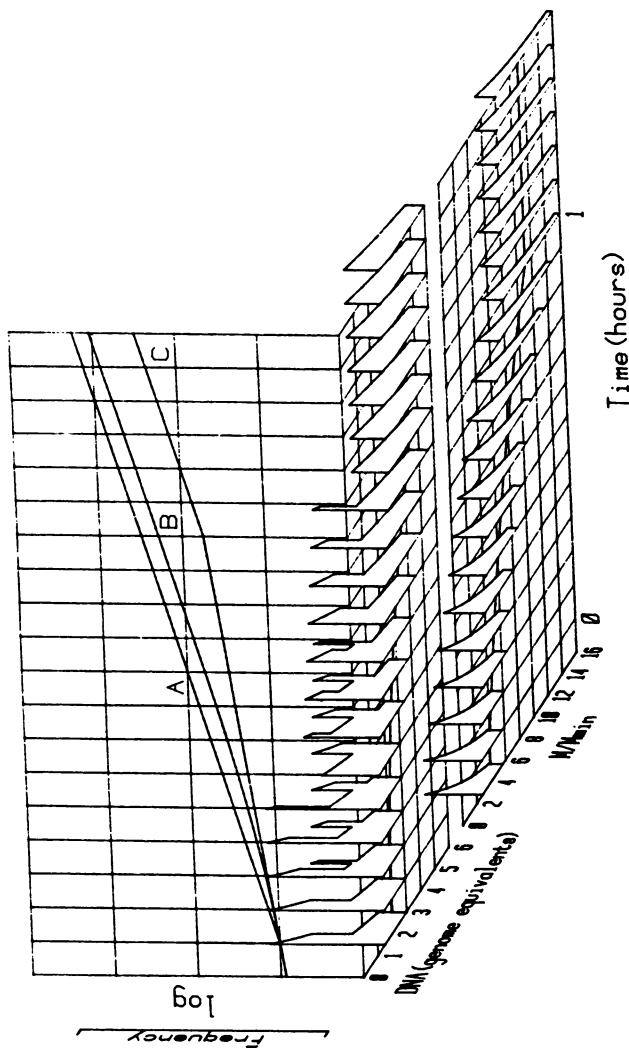


Figure 5. Calculated results of a shift in specific growth rate for an *E. coli* population ($\mu = 1.038 \text{ hr}^{-1}$ for $t < 0$, $\mu = 2.076 \text{ hr}^{-1}$ for $t > 0$). Curves A, B, and C on the rear panel are the mass, DNA content, and cell numbers in the culture, each normalized by their respective values at $t = 0$. Reproduced, with permission, from Ref. 14. Copyright 1980, Elsevier North Holland, Inc.

coordination of DNA synthesis and cell division in the fission yeast *S. pombe*. To put the experimental results into perspective, consider the composite diagram showing the interrelated cycles of DNA synthesis and separation, cell shape, and cell volume indicated schematically in Figure 6 (20-24). Here the events which occur during the cell cycle are displayed in relative position and duration along arcs of a circle, the top of which is taken arbitrarily to be coincident with the cell separation event. In this discussion, the relationship of the interval of DNA synthesis, which in this eucaryote provides duplication of all of the chromosomes in the mother cell, relative to the time of physical separation of daughter cells is of special interest.

For this organism, as in other eucaryotes, the DNA content of the cell exhibits less variation than in the bacterial case, with the content for an individual cell ranging between one complete set of genetic information; i.e., one genome or one genome equivalent (1C), and two genome equivalents (2C). However, in this organism a rather unusual feature occurs in which physiological separation of the daughter cells takes place before physical separation, so that DNA synthesis may begin in the physiologically partitioned daughter cells before those cells actually physically separate. Thus, depending upon the disposition of the interval of DNA synthesis relative to cell separation, cells will exist in the population containing up to 4C DNA content if DNA synthesis is complete before the cells separate and as little as 1C DNA if the cells separate before DNA synthesis begins (here and below, the term "cell" refers to the physically separated units which are observed in a flow cytometry measurement). Previous experiments on the coordination between DNA synthesis and cell separation in this organism are somewhat ambiguous (20-24), so that the S-phase has been shown in the above diagram as straddling the point of cell separation. Notice that, independent of the disposition of this relatively brief interval of the cell cycle, the majority of cells in a fission yeast population will possess a DNA content of 2C.

The upper four frames of Figure 7 show flow cytometer measurements of the frequency functions of individual cell DNA content in *S. pombe* (972 h⁻¹) populations grown in steady-state chemostat culture. The parameters indicated in the figure frames are the specific growth rates in units of hr⁻¹. The dominant peak in each of these measurements corresponds, as explained previously, to a DNA content of two genome equivalents (2C). An interesting feature is observed in the data obtained at lower growth rates. The frequency function for an overall population specific growth rate of 0.088 hr⁻¹ exhibits three modes, the first corresponding to a DNA content of 1C, the second to the most prevalent 2C population, and the final one to a population of cells containing a DNA content of 4C. The last mode is not believed to be the result of cell clumping, as all samples in these analyses were treated by sonication immediately prior to flow cytometric analysis. (The suitability of this procedure for providing accurate cell counts,

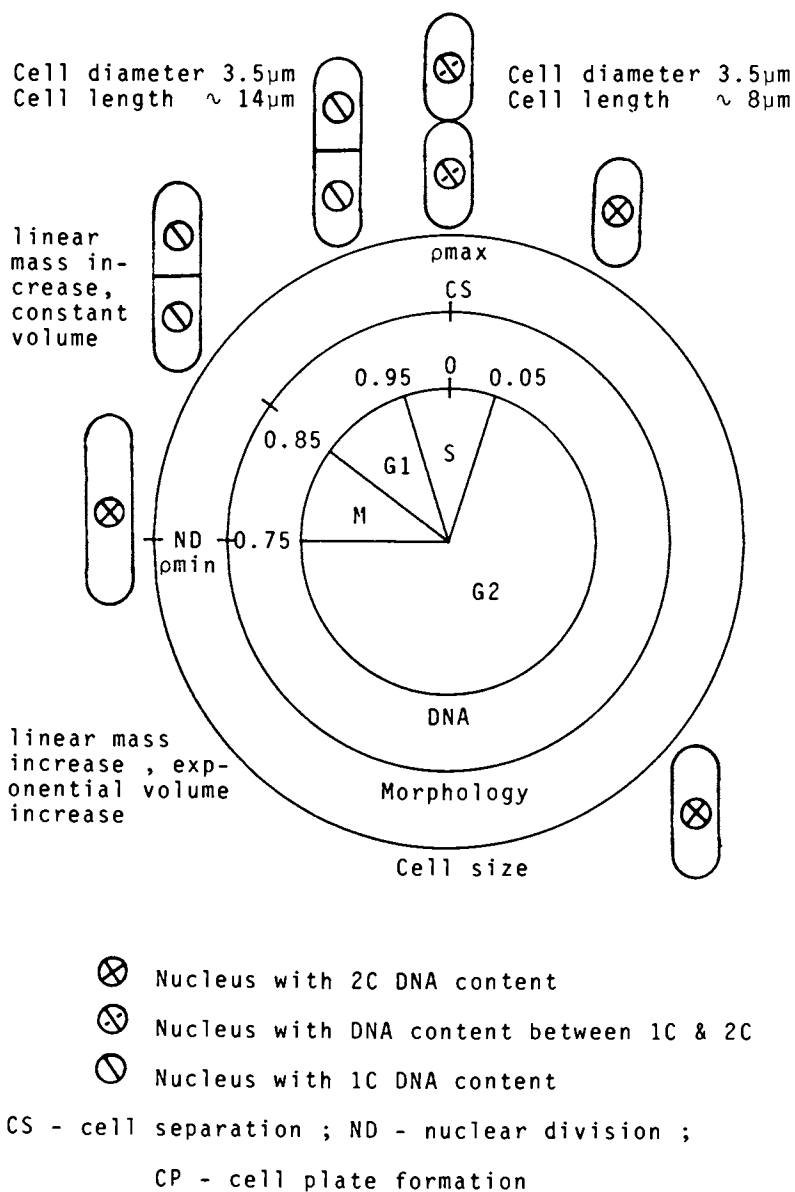


Figure 6. Schematic diagram of the nuclear and cell division cycles of fission yeast *S. pombe*.

and thereby minimum clumping, was verified in separate control experiments.)

Consequently, these data indicate that the coordination between DNA synthesis and cell separation becomes imprecise in this organism at low growth rates, with some cells dividing before initiating DNA synthesis and others completing DNA synthesis before dividing. This interesting imprecision in cell cycle operation would not have been evident by any population-average measurements upon this system. Only measurement of the frequency function provides the sensitivity and detail of information required to observe this feature.

The two frequency functions shown in the bottom two frames of Figure 7 correspond to different steady-state populations growing at approximately the same overall population growth rates as those shown in the two middle frames. These different steady states were achieved by different start-up procedures of the reactor and seem to be connected with some unusual cell clumping phenomenon when reactor start-up initiates with a significant glucose limitation of growth. Additional information on this multiple steady-state phenomenon and on its manifestation in other types of measurements is available elsewhere (9).

Figure 8 shows the frequency functions for single cell protein content obtained by the same cultivation methods as just outlined. Considering the set of steady-state results obtained by the same start-up procedure (the top four frames in Figure 8), it is apparent that there is a significant shift of the frequency function towards higher protein contents and also increased skewing to the right as the overall population specific growth rate increases.

Quantitative analysis of these measurements has been undertaken by two different strategies based upon the governing population balance equations which describe the system (25). One method employed the Collins-Richmond equation (26), the integrated form of the population balance equation, with results which are summarized in detail elsewhere (25). In the second approach, a simple functional form was chosen for the fission frequency function ϕ which contained two adjustable parameters (the results of Harvey, Marr and Painter (27) indicate that the results of population balance model solutions are not highly sensitive to the functional form of this function in the model). Then, four different function forms for the single-cell rate of protein synthesis function r_f were examined. For the following four functional forms,

$$r_f(p,s) = k_0(s), \quad \text{zero order} \quad (2.1)$$

$$r_f(p,s) = k_1(s)p, \quad \text{first order} \quad (2.2)$$

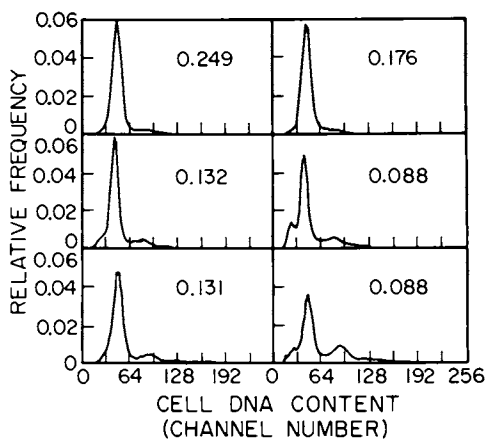


Figure 7. Frequency functions for cellular DNA content for S. pombe populations propagated in a chemostat at different dilution rates (specific growth rates shown in each frame). Channel number, one division = 6.8×10^{-4} pg DNA/cell. Reproduced, with permission, from Ref. 9. Copyright 1981, John Wiley & Sons, Inc.

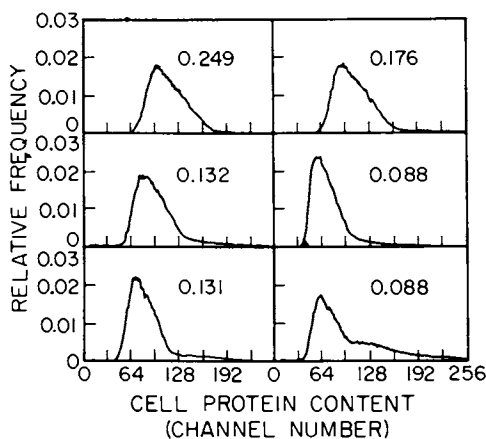


Figure 8. Protein content frequency functions for S. pombe populations grown in a chemostat. Channel number, one division = 0.078 pg protein/cell. Reproduced, with permission, from Ref. 9. Copyright 1981, John Wiley & Sons, Inc.

American Chemical
Society Library
1155 16th St., N.W.

$$r_f(p,s) = k_0(s) + k_1(s)p, \quad \text{two term} \quad (2.3)$$

$$r_f(p,s) = k_0(s) + k_1(s)p + k_2(s)p^2, \quad \text{three term} \quad (2.4)$$

a parameter search using the Marquardt algorithm was conducted to minimize in an integral least squares sense the difference between the population balance model solution and measured frequency function. The best fit calculations for each of the four different functional forms of protein synthesis kinetics are shown by solid lines in Figure 9 along with the experimental frequency function data for an overall population specific growth rate of 0.246 hr^{-1} . Clearly, even with optimally adjusted parameters, the zero order, first order, and two-term models cannot provide a satisfactory fit of the experimental data, while the three-term form which includes second-order dependence on single-cell protein content adequately represents the data.

Similar calculations seeking best fits between various models and experimental data corresponding to different overall specific growth rates provided estimates of the kinetics of single cell protein synthesis at each of the growth rates considered. These results are shown in Figure 10. The qualitative features of these results are rather surprising, indicating that the basic functional form of single cell protein synthesis kinetics changes significantly from approximately linear at the lowest growth rate considered to distinctly parabolic at the more rapid growth rates investigated.

These trends may reflect the need for inclusion of additional variables in modeling the kinetics of single cell protein synthesis. It is possible that the great difference in protein synthesis rates observed at small protein contents at different overall growth rates is because of some change in another aspect of the cell's metabolism which is not represented in this model. The minima in protein synthesis rates displayed in Figure 10 may result from a requirement that the cell engage in other biosynthetic activities during this part of the cell cycle at high growth rates. It is significant to note that an independent analysis of the same data using the Collins-Richmond equation indicated the same qualitative relationship between rate form and overall growth rate as is indicated in Figure 10 (25).

A comparison of the outcomes of this approach to single-cell protein synthesis kinetics determination with the alternative method which has been widely used in many previous studies of cell cycle and cell kinetic behavior of many organisms is instructive. In the latter methods, synchronous culture or an equivalent experimental technique are used to make measurements of the time variation of protein content or some other cellular variable versus time as the cell grows from a newborn daughter cell to a mature and dividing mother cell. Then, by estimating the slope of

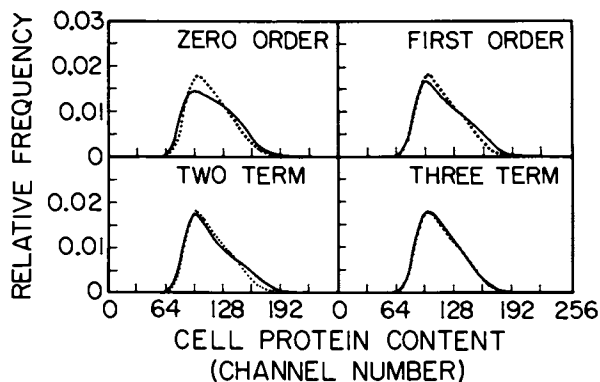


*Figure 9. Comparison of experimentally measured protein content frequency function (dots) for *S. pombe*, grown in a chemostat with $D = 0.246 \text{ hr}^{-1}$, with best fit simulations (lines) using the kinetic forms of Equation 2. Reproduced, with permission, from Ref. 25. Copyright 1981, John Wiley & Sons, Inc.*

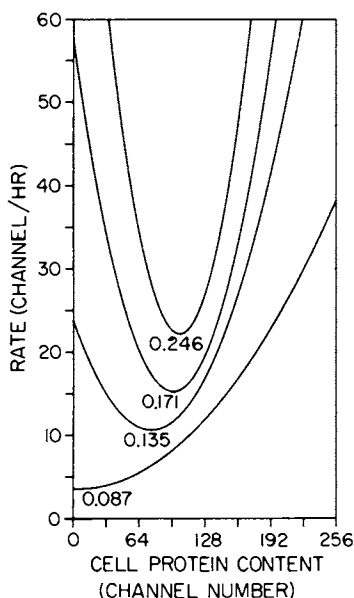


Figure 10. Rate functions for single-cell protein synthesis as determined by analysis of protein content frequency functions measured in steady state chemostat growth. Parameters near each curve indicate dilution rates employed (hr^{-1}). Reproduced, with permission, from Ref. 25. Copyright 1981, John Wiley & Sons, Inc.

this cell variable versus time trajectory, one estimates synthesis rates and established kinetics. The difficulty with this procedure is the limited range of the cell variable over which the measurement can be made, namely from a value corresponding to a newborn cell to a value corresponding to a dividing cell. Over this limited range of change of any variable, for a variable that increases monotonically during the cell cycle, it is very difficult to discriminate among alternative kinetic forms unless they are extremely different.

This insensitivity of the trajectory-tracking kinetics determination approach can be seen by inverting the procedure: assume different functional forms for the kinetics on a single-cell basis and calculate, using these kinetics, the trajectory of the cellular variable versus time. The results will show that, for quite different kinetic forms, the trajectories are very close and, considering unavoidable experimental measurement inaccuracies, very difficult to distinguish. For example, in the present case, use of a linear kinetic form and the parabolic one shown in Figure 10 for the $\mu = 0.246 \text{ hr}^{-1}$ case gives very similar p versus time trajectories; on the other hand, when these kinetic forms are used to calculate frequency functions in balanced growth, the results are quite different (compare frames B and D of Figure 9). Therefore, in this case and presumably in many others, analysis of the relationship between single-cell kinetic form and the corresponding frequency function in steady-state balanced growth provides a more sensitive tool for discrimination and identification of single-cell kinetics than do classical trajectory-tracking procedures of various kinds.

As a test of the range of applicability of the kinetics determined in the steady-state measurements, the transient population balance equation has been solved, using the kinetics determined from steady state, to simulate the sequence of protein content frequency functions obtained in synchronous growth of this organism. The simulation results are in very good qualitative agreement with the experimental measurements of the corresponding quantities (28).

Growth and Nuclear Cycle Operation in Single Cells of *S. cerevisiae*

The budding yeast *S. cerevisiae* is currently employed in a variety of applications, including brewing, baking, and genetic engineering. This organism grows on a single cell basis by, at a particular point in its growth, producing a bud which increases in size and mass as the cell grows (29-34). In fact, it has been suggested that, to a good approximation, all of the new cell mass synthesized between bud emergence and separation of the bud as a daughter cell goes into the growing bud entirely (29). The mother cell mass, at least in the simplest form of this model, is not presumed to increase at all during this stage of the cell division cycle. These features are summarized qualitatively in the sketch

of the cell division cycle for *S. cerevisiae* provided in Figure 11. As indicated in this diagram, upon cell division, the mother cell recycles to a standard point, labeled "start", and the bud, being generally smaller than the "start" cell mass, must grow for some time before it attains the "start" state and before it is prepared to form a bud and itself become a mother cell.

This view of the growth and division of individual cells of this organism is based upon a variety of experimental studies which have involved growth rate shift experiments, shifts of growing cells into starvation media, and growth of yeast populations in different media supporting different growth rates (29-34). Other measurements, often made in concert with the above experiments, suggest that the nuclear cycle for this organism is coordinated with the cell division cycle in the manner shown in Figure 11. The G_1 , or first gap, interval extends from cell "birth" until the point of bud emergence when the S-phase begins and DNA synthesis occurs. The duration of S-phase has been reported to be relatively insensitive to overall population growth rate in aerobic situations in shake flask cultures (aerobic is used here in a somewhat generous sense, since shake flask cultures cannot generally be assumed to be sufficiently aerated to eliminate oxygen limitations of growth and resulting responses of cellular controls). Following the DNA synthesis interval, the second gap and nuclear division phases occur, after which cell separation takes place. Interestingly, the experiments cited above suggest that the total time spent in the G_2 and M phases are also relatively insensitive to overall growth rate of the population. Thus, the effect of overall growth rate suggested by this model is to affect primarily the length of G_1 and correspondingly, the fraction of the population which consists of unbudded cells and the corresponding cell mass and cell DNA frequency functions.

Flow cytometry and mathematical analysis of the results has been applied to study the operation of the nuclear cycle in *S. cerevisiae* grown in steady-state chemostat culture under anaerobic conditions (36); a similar strategy was employed in the investigations of Slater *et al.* (30). It is worth noting here that experiments under these conditions have not been reported previously, and consequently these results contribute to determination of the extent of general applicability of the model suggested by experiments under different growth conditions.

Assuming that an individual cell nuclear cycle operates qualitatively as shown in Figure 11, it follows that the expected form of the frequency function of individual cell DNA content in a growing population of this budding yeast will have the following features: At a DNA content corresponding to one genome equivalent (1C), there should be an impulse which has magnitude equal to the fraction of the population in the G_1 -phase of the nuclear cycle. Similarly, a second impulse located at a fluorescence level corresponding to a DNA content of two genome equivalents (2C) will appear with a magnitude equal to the fraction of the population in

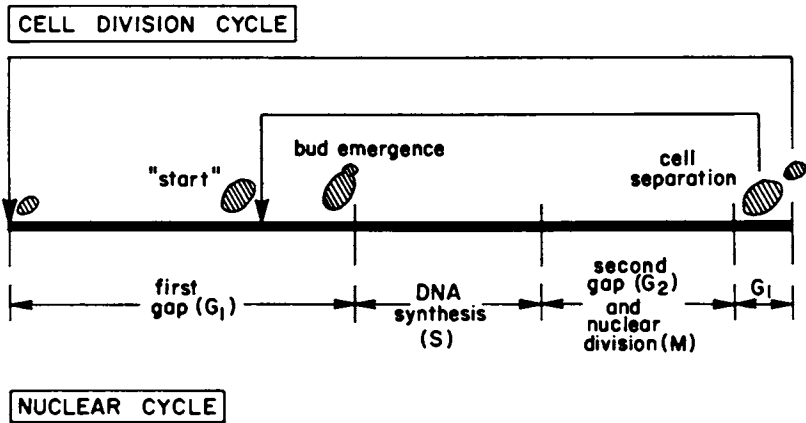


Figure 11. Schematic diagram of the nuclear and cell division cycles for the budding yeast *S. cerevisiae*. Reproduced, with permission, from Ref. 35. Copyright 1980, Pergamon Press Ltd.

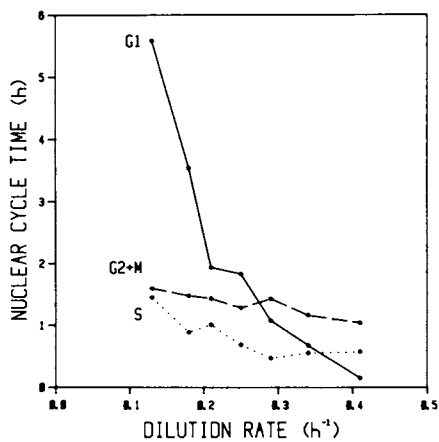
the G_2+M -phases. Between these two impulses will be a connecting curve which corresponds to cells in S-phase and with DNA contents between 1C and 2C. It must be recognized, however, that actual experimental measurements of the frequency function using flow cytometry will not have this appearance due to noise both in the organism metabolism and in the measurement procedures. Thus, one expects to see something approximating normal distributions centered where the two impulse functions are anticipated.

The results of flow cytometry frequency function measurements at different continuous culture dilution rates are illustrated in Figure 12. These possess the general forms just suggested. Unfortunately, the magnitude of the dispersion in these data is sufficiently great as to obscure the contribution of the S-phase cells. Availability of this information for this organism is hampered by the relatively small number of cells involved in this phase and by the resolution problems mentioned before. Investigations of ways to improve both measurement and data analysis techniques in this regard are in progress.

However, by adding to the expected idealized DNA frequency function a noise model, it is possible through a parameter optimization procedure to extract from the data shown in Figure 12 estimates of the fractions of the cell population at a given overall population growth rate ($= D$) which are in the G_1 , S, and G_2+M -phases of the nuclear cycle. Combining this information with the calculated age distribution in the culture, it is possible to estimate the duration of the nuclear cycle intervals under different overall growth rates of the yeast population. The results of this analysis are illustrated in Figure 12. These findings show that the nuclear cycle operation, at least as manifested by the duration of the different phases, is qualitatively identical under these culture conditions as under the different growth environments investigated in formulating the model discussed above. That is, the duration of the S-phase and the total time an individual cell spends in the G_2+M -phases is relatively insensitive to overall growth rate of the culture. On the other hand, the time spent in the G_1 -phase changes significantly with respect to overall population growth rate, decreasing dramatically as the culture growth rate is increased.

The diagram of budding yeast cell cycle operation shown in Figure 11 above is somewhat oversimplified. Important aging phenomena occur as a cell cycles around the inner loop producing buds and resulting daughter cells in each pass through the inner loop of the cell division cycle diagram. As a mother cell produces repeated offspring, it accumulates bud scars. Also, it may, through increased age and opportunity to conduct biosynthesis and construction of large organelles, gain metabolic capacity as it ages. Therefore, in formulating mathematical models of single-cell growth of this and related organisms, the possible positive effect of aging due to accumulation of organelles may need to be considered, as may the possibly inhibitory effect of the accumula-

Figure 12. Nuclear cycle time intervals estimated by analysis of DNA content frequency functions for *S. cerevisiae* ATCC 18790 populations grown at steady state at different dilution rates. Reproduced, with permission, from Ref. 36. Copyright 1981.



tion on the outer cell surface of bud scar material which is inactive for material exchange with the cell environment.

Discussion

The examples above illustrate how measurements of cell population frequency functions, fractional amounts of various cell subpopulations, and overall behavior of microbial cultures can be used to evaluate in qualitative and quantitative terms some of the fundamental processes of control and biosynthesis at the single-cell level. Population balance equations, or equivalent computer simulation techniques and mathematical analyses, connecting single-cell behavior with population properties provide the required working connection between experiments and single-cell properties. This approach appears to be extremely powerful in that it provides, for some of the cases considered, greater sensitivity to single-cell operation than do alternative methods which attempt to describe single-cell behavior directly. Furthermore, the flow cytometry experimental methods illustrated do not in general require special manipulation of culture conditions or cells for the purposes of conducting the desired experiment. Cells may be cultivated under any conditions of interest, including time-invariant environments which give rise to balanced growth, and the methods described in this paper applied. Combinations of flow cytometry measurements and computer analysis based on cell cycle models provide rapid access to qualitative and quantitative information on cell cycle operation and control.

Obviously, more research in this direction is required to enable these strategies to be applied for the design purposes described at the beginning of the paper. This will require a broader repertoire of experimental capabilities, including the ability to measure more detailed information about cell composition using flow cytometry. Furthermore, the mathematical modeling approaches described in this work must be enhanced and expanded to include more cell components and to consider relationships among substrate utilization, cell growth and the synthesis of cell components, and product formation on an individual cell basis. This general line of research is an important avenue for relating reactor design and characterization objectives of biochemical reaction engineering with basic metabolism and cellular control information in the biological sciences.

It is interesting to note that, in some of the examples above, a kinetic approach is appropriate which differs from the traditional strategy of defining composition and temperature dependence of reaction rates functions. Certain assemblies of complicated cellular reaction and regulation processes may be represented reasonably accurately under a variety of growth conditions in terms of timers, the initiation points and durations of which may be dependent upon growth conditions. However, the above examples show that certain parameters associated with starting

points and running time of these timers are invariants and thus provide a useful foundation upon which to describe the features of cell operation and cell population properties. More attention to mathematical modeling of systems which feature such clocks and which focus upon the starting and running time of these clocks is an interesting avenue for future work.

Acknowledgements

The author is extremely indebted to his colleagues and students, D. McQuitty, Y. Nishimura, D. Agar, M. Hjortso, J. Fazel-Madjlessi, M. Gilbert, A. Bartel, L. Y. Lee, and J. Oro, for their central role in the research described in this paper and to the National Science Foundation for financial support of this research.

LITERATURE CITED

1. Fredrickson, A. G.; Ramkrishna, D.; Tsuchiya, H. M. Math. Biosci. 1967, 1, 327.
2. Ramkrishna, D. Adv. Biochem. Eng. 1979, 11, 1.
3. Henrici, A. T. "Morphological Variation and the Rate of Growth of Bacteria"; Charles C. Thomas: Springfield, Ill., 1928.
4. Coulter, W. H. 1953, U. S. Patent No. 2-656-508.
5. Crissman, H. A.; Mullaney, P. F.; Steinkamp, J. A. In "Methods in Cell Biology" 1975, IX, 179.
6. Bailey, J.; Fazel-Madjlessi, J.; McQuitty, D. N.; Lee, L. Y.; Oro, J. A. AIChE J. 1978, 24, 561.
7. Hutter, K. J.; Eipel, H. E. Eur. J. Appl. Microbiol. Biotechnol. 1978, 5, 203.
8. Bailey, J. E.; Fazel-Madjlessi, J.; McQuitty, D. N.; Gilbert, M. F. Ann. N.Y. Acad. Sci. 1979, 326, 7.
9. Agar, D. W.; Bailey, J. E. Biotechnol. Bioeng. 1981, XXIII, 2217.
10. Mitchison, J. M. "The Biology of the Cell Cycle", Cambridge University Press: Cambridge, Great Britain, 1971.
11. Cooper, S.; Helmstetter, C. E. J. Molecular Biol. 1968, 31, 519.
12. Donachie, W. D. Nature, 1968, 219, 1077.
13. Bailey, J. E.; Nishimura, Y. AIChE J. 1981, 27, 73.
14. Nishimura, Y.; Bailey, J. E. Math. Biosci. 1980, 51, 305.
15. Schaechter, J.; Maaløe, O.; Kjeldgaard, N. O. J. Gen. Microbiol. 1958, 19, 592.
16. Kjeldgaard, N. O.; Maaløe, O.; Schaechter, M. J. Gen. Microbiol. 1958, 19, 607.
17. Bleecken, S. Z. Allg. Mikrobiol. 1973, 13, 3.
18. Bleecken, S. Biol. Zbl. 1977, 96, 529.

19. Bleecken, S. "Populationsdynamik einzelliger Mikroorganismen Modellbildung und -anwendung"; FEB Georg Thieme Leipzig: Leipzig, Germany 1979.
20. Bostock, C. J. Exp. Cell Res. 1970, 60, 16.
21. Mitchison, J. M. Methods in Cell Biology 1970, 4, 131.
22. Nurse, P.; Thuriaux, P. Exp. Cell Res. 1977, 107, 365.
23. Nasymth, K.; Nurse, P.; Fraser, R. S. S. J. Cell Sci. 1979, 39, 215.
24. Polanshek, M. M. J. Cell Sci. 1977, 23 1.
25. Agar, D. W.; Bailey, J. E. Biotechnol. Bioeng. 1981, XXIII, 2315.
26. Collins, J. F.; Richmond, M. H. J. Gen. Microbiol. 1962, 28, 15.
27. Harvey, R. J.; Marr, A. G.; Painter, P. R. J. Bacteriol. 1967, 93, 605.
28. Agar, D. W.; Bailey, J. E. Biotechnol. Bioeng. 1982, XXIV, 217.
29. Hartwell, L. H.; Unger, M. J. Cell Biol. 1977, 75, 422.
30. Slater, M. S.; Sharrow, S. O.; Gart, J. R. PNAS, 1977, 74, 3850.
31. Johnston, G. C.; Pringle, J. R.; Hartwell, L. H. Exp. Cell Res. 1977, 105, 79.
32. Carter, B. L. A.; Lorincz, A.; Johnston, G. C. J. Gen. Microbiol. 1978, 106, 222.
33. Tyson, C. B.; Lord, P. G.; Wheals, A. E. J. Bacteriol. 1979, 138, 92.
34. Johnston, G. C.; Ehrhardt, C. W.; Lorincz, A.; Carter, B. L. A. J. Bacteriol. 1979, 137, 1.
35. Bailey, J. E. Chem. Engr. Sci. 1980, 35, 1854.
36. Bailey, J. E.; Agar, D. W.; Hjortso, M. A. p. 157 in "Computer Applications in Fermentation Technology"; Society of Chemical Industry: London, 1982.

RECEIVED July 22, 1982

A Cybernetic Perspective of Microbial Growth

DORAISWAMI RAMKRISHNA

Purdue University, School of Chemical Engineering, West Lafayette, IN 47907

What goes by cellular metabolism is an immense class of chemical and physical rate processes within and without the cell marked most strikingly by their diversity and specificity. It forms the basis of the response of microorganisms to their environment, the modelling of which must of necessity suffer some oversimplification if it is to be of any value. In this context, kinetic models of microbial growth within the framework of interaction between lumped biochemical species and the environment have had considerable appeal in the past. However, the subtle facilities which derive from the elaborate internal machinery of the cells pose a challenge that no meager expansion of the kinetic framework will ever meet.

We examine here a cybernetic perspective of microbial growth which contends that the net asset of the cell's internal machinery is the facility to make 'rational' (optimal) decisions in responding to its environment, one that seems markedly manifest in the situation of diauxic growth. The growth of microbial cells in the presence of multiple substrates is addressed in this work within a cybernetic framework which lays emphasis on the optimal allocation of existing 'resources' among parallel enzyme-synthesis systems. The work to be presented will discuss the main issues connected with this outlook, what the chief assets of the framework might be and the interpretation of several experimental results within the cybernetic scheme.

0097-6156/83/0207-0161\$06.00/0
© 1983 American Chemical Society

Mathematical models of varying degrees of sophistication are the main instruments with which quantitative understanding has been secured of engineering processes both in analysis and design. In dealing with microbial systems, an important development in the past has been of the adoption of the chemical kinetic framework viewing the cell mass as lumped biophase (the so-called non-segregated models) and interacting as a whole with its environment. Such models have been the basis for design and analysis of industrial fermentations. Several interesting features of the methodology of chemical reaction engineering have found their way into biochemical engineering. Whether or not precisely quantitative understanding follows from modelling, an entirely useful aspect of it has been the efficient assessment of the implications of specific hypotheses concerning the behavior of a given system thus formulating new revealing experiments. It is perhaps in this sense more than any other that kinetic modelling has been a valuable tool in the investigation of microbial systems, and it is in this sense too that the ideas to be presented here must be interpreted.

In the adoption of a strictly chemical kinetic framework for modelling microbial systems, an important distinction arises. Microorganisms are not a "dead bag" of biochemical constituents responding to their environment in strict conformity with a kinetic prescription that is characteristic of reaction systems. (In this connection, it is interesting to allude to the remark of Fredrickson and Tsuchiya [1] that "... organisms ... are not tin soldiers!"). It is germane that we quote Demain [2] in this regard, "Microorganisms have evolved over the years, developing better and better mechanisms to prevent overproduction of their metabolites. Yet we microbiologists and bioengineers are dedicated to increasing the inefficiency of fermentation organisms as we continue to work toward the goal of almost complete conversion of nutrient into product with as little as possible going into the microbial protoplasm (except, of course, if we are in the single cell protein business)." Further, Demain observes that, "All microorganisms must possess regulatory (control) mechanisms in order to survive. Very efficient organisms are tightly controlled. In fermentation organisms, controls are less rigid but nevertheless present." The implications of the foregoing assertions are deep and far-reaching. The biochemical engineer's objective is in conflict with that of the organism and an attempt to 'control' the organism without familiarity with its internal control features could lead one away from projected optimal goals. (It must of course be mentioned here that there exist several instances of dramatic improvements in the formation of fermentation products through efforts based on a qualitative understanding of the regulatory processes within the cells. Some of these involve genetic variations while others do not.)

Demain points out that coordination of microbial metabolism is a necessity born out of the tremendous diversity which per-

vades cellular constitution and activity. The genetic capacity of a bacterial cell can accommodate over 1000 enzymes and that only under some strict supervision can the resources of the cell be invested frugally. Such a coordination is accomplished chiefly by (i) induction, (ii) catabolite regulation and (iii) feedback regulation. Induction provides the cell with the mechanism to form enzymes rapidly when needed. Catabolite regulation becomes useful, for example, in the inhibition of formation of certain enzymes (catabolite repression). Feedback regulation includes feedback inhibition and feedback repression. Feedback inhibition is distinguished from repression in that the former involves an end product which inhibits the action of an enzyme somewhere "upstream" the pathway, while the latter implies the prevention of the formation of one or more upstream enzymes by a derivative of the end product. The actual accomplishment of these regulatory processes requires the intervention of an elaborate genetic mechanism.

The biosynthesis of a particular enzyme is itself an elaborate and complex process involving several cellular components. The genetic information for any particular enzyme is carried in a stretch of DNA which is the 'structural gene' for that protein. The 'pattern' is transcribed in a strip of the messenger RNA that dictates the proper sequence of amino acids in the synthesis of the enzyme. Van Dedem and Moo-Young have made an interesting beginning into incorporation of the operon theory of Jacob and Monod into a kinetic model for enzyme syntheses [3]. Indeed even a relatively simple model leads to many unidentifiable kinetic constants.

Our objective in this work is to present an approach at variance from modelling of microbial response based purely on kinetic considerations. We base this approach on the viewpoint that while the detailed modelling of regulatory processes (accounting for their underlying genetic mechanisms) is intractably complicated, it may be possible to interpret them as being inspired by an optimal motive. It would seem that such facility for an optimal response of an organism to its environment would be an acquisition consistent with the theory of evolution. While this viewpoint is evident in the statement of Demain quoted earlier, it has been a popular aspect of contemporary biology (see for example [4]). This approach based on postulating the existence of an optimality criterion is what we have termed as the 'cybernetic' perspective. (*Cybernetics*, which arises from the Greek word κυβερνήτης meaning steersman, has been defined by Wiener as control and communication in the animal and the machine [5]). The basic merit of the cybernetic approach is that it adopts a mathematically simple description of a complex organism but compensates for the oversimplification by assigning an optimal control motive to its response. The implication is that the elaborate internal machinery of the cell provides the organism with the facility to implement the calculated control policy.

While a truly detailed model would actually be concerned with details of this implementation (even if it is not viewed as such) they are of no concern to the cybernetic model. There is of course no direct way of confirming an optimal strategy so that its acceptability must be based on experimental evidence pertaining to its implications. This has been the basis of some criticism of the cybernetic approach [6]. It is emphasized here that formulations of optimal policies must be construed merely as innovative description (prediction) of observed phenomena rather than as "ultimate" explanations. In this connection, it is important to recognize that the approach could lead to many new and interesting experiments. An example of the cybernetic approach to microbial growth may be found in the work of Swanson, Aris Fredrickson and Tsuchiya [7,8], who were specially concerned with the lag phase in single substrate systems.

It may be seen that the cybernetic approach is based on an invariant strategy rather than an invariant kinetic response implicit in the framework of kinetic models. Thus the approach envisaged here is more likely to describe transient semi-continuous experiments, in which the cells' environment may be varied at will, than a purely kinetic approach. There are however important constraints only within which the framework suggested here may be considered. Since the organisms are deemed to respond based on an invariant optimal strategy (i.e., the cells never lose sight of their optimal goal while experiencing the varying environment) we are not addressing situations in which any aberration in the regulatory mechanisms (leading to non-optimal goals) are encountered. Thus only environmental manipulations in which no genetic changes are brought about in the organisms can be legitimately considered, since the mutants cannot be expected to retain the optimal framework of the original genotype. Having said this, we wish to emphasize the distinction between striving for an optimal goal and actually accomplishing it. If we grant that the facility for optimal behavior has been acquired for certain types of environmental variations, then one may expect that as long as the organisms are subjected to the same class of environmental changes, they would not only strive for an optimal goal but also accomplish it. On the other hand, if we subject the microorganisms to environmental changes of a type entirely different from those with which they can cope in an optimal way, then the result could well be a non-optimal behavior even if there have occurred no genetic changes. Such aberrations from optimal behavior would seem to come within the purview of the cybernetic approach. In fact this is an important issue which we will address again at a later stage.

A classic example in which the internal regulatory processes of the cells play a very important role is the phenomenon of diauxic growth discovered by Monod [9] in multiple substrate systems. In diauxic growth there is preferential utilization of certain substrates over others, although each substrate by itself

would have been acceptable to the organism. The situation appears to fit the cybernetic approach rather well since preference for a particular substrate could well be the result of an optimal strategy. We quote again from Demain [2]. "The cell faces a problem when more than one utilizable growth substrate is present. Enzymes could be formed to catabolize all substrates, but this would be wasteful. Instead, enzymes are made which utilize the best substrate (usually glucose) and only after exhaustion of the primary substrate are enzymes formed which catabolize the poorer carbon source." That one substrate is "better" than another is unmistakably implied although a qualification as to what makes one better than the other is conspicuously absent.

THE CYBERNETIC FRAMEWORK. SOME ISSUES

Viewing the cell as a control system raises several important issues. We assume that the control system is much like that conceived for controlling industrial systems. First, an essential part of control of a process is measurement of one or more process variables. Thus the transformation of nutrient material to protoplasmic mass and also products which are released into the environment provides a spectrum of quantities for "measurement". If control is based on sensing concentrations of environmental components prior to (such as nutrients) or at early stages of transformation, it comes within the category of feedforward control. In contrast if control is based on correction of performance by measuring variables at the downstream end of the transformation process then we have feedback control. Indeed we could have both feedforward and feedback strategies. Feedback control is possible, for example, in muscular action (in higher organisms) to accomplish a particular goal. In the situations of interest to us here one is inclined towards a feedforward strategy because an efficient system would gear its internal machinery to prepare ahead in a complex process of breakdown of nutrients. It is recognized however that the possibility of feedback strategies cannot be entirely overlooked.

The next issue is that of the control objective. Prior discussions in this paper and reference to other works such as Demain [2] gravitate towards the concept of maximizing biomass productivity. Again this suggestion is more of an interesting possibility than with a view to exclude others that may appear more attractive in subsequent stages of this work. Suppose we grant that the cell's goal is in maximizing cell mass. Two basic questions arise. Is the desired maximization of the cell mass productivity at every instant, or over a finite time interval in which case the average productivity is maximized? We may refer to the first case as a "short term" (or instantaneous) perspective. In the second case, we have a "long term" perspective. In examining the relative plausibility of the two schemes we must

bear in mind that growth represents a complex sequence of reactions occurring necessarily over a finite time interval. Thus an organism evolving in certain patterns of environmental variations could conceivably account for this in formulating its optimal policy much in the spirit of "saving (its resources) for a rainy day". This argument is in favor of a 'long term' objective. Of course the organism's projection of its future could prove to be in error (since the experimenter can vary its environment at will) the result of which would then be a non-optimal response. Dhurjati [10] has investigated a 'long term' model for diauxic growth which will be discussed subsequently.

A 'short term' perspective is reflective of a decision to make the best use of the environment at the instant (without concern for the future). Here one has the option of assuming that there may or may not be a time delay in the implementation of that policy. If a small time delay exists, (a long time delay does not reflect an efficient organism) it may not greatly affect the organism's response in slowly varying environment. However, for rapid environmental changes, substantially non-optimal behavior may be expected from such models. Another interesting situation to investigate here is the effect of how limitations on control variables might affect a policy based on a short term perspective. To make this clearer, suppose the control objective is to be implemented by allocating existing resources of the cell. Suppose further that resources are constantly replenished by growth processes. A short term perspective makes no anticipation about subsequent replenishments so that it is possible to conceive of situations where, in the interest of an immediate optimal objective, an impending crisis (such as inadequate resources to utilize a later favorable environment) is not accounted for.

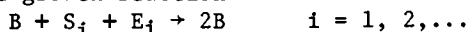
Another important issue is that of the proper control variables. We have just alluded to the possibility of viewing microbial response as a resource allocation problem. The resources might, for example, constitute only a critical resource such as ATP that is the primary source of energy for metabolic purposes. It is difficult to be any more specific about this issue at this inceptive stage of our work.

In what follows we will present two models, one based on a 'long term' perspective and another based on a 'short term' perspective both addressing the phenomenon of diauxic growth in multiple substrate systems.

Growth in Multiple Substrate Systems

Monod's pioneering work on diauxic growth [9] is an interesting situation in which internal regulatory processes appear to play an important role. Here, the cells are confronted with a mixture of two substrates (generally sugars) such as, say glucose and xylose. While growth could occur following a normal

lag phase with either of the substrates in the absence of the other, in the mixed substrate environment the cells show an exclusive preference for glucose until all of it is virtually exhausted before xylose is utilized. This preference for glucose could be interpreted as the result of an optimal decision. Dhurjati [10] has considered a cybernetic model based on a long term perspective of microbial response to a multisubstrate environment. Thus he proposes that the cells in the inoculum, on exposure to a mixture of two substrates S_1 (such as glucose) and S_2 (such as xylose), at some initial instant ($t=0$) must decide on a program of utilization of the two substrates such that all the obtainable biomass is realized in the shortest time. The optimal objective is therefore the maximization of the average biomass productivity over the entire period of growth. The tacit implication here is that a batch growth is presumed at the outset. This "projection of the future" is essential to a long term policy. Thus the internal machinery of the cell is presumed to commit itself to a policy of allocation of its resources based on the assumption that no subsequent replenishment of either substrate would be available. Of course actual experience could be otherwise since the experimenter could vary the environment at will. The question arises then as to how the model would view the growth of the culture in an environment thus manipulated. Could the cells not review the situation at any instant when there is an external manipulation and make a reallocation of its resources (i.e., revise its control policy)? If so could this occur continually regardless of the speed with which the substrate environment is varied? Dhurjati's model is predicated on a long term policy which is provoked only when a step change in substrate concentration occurs. While there are some conceptual difficulties with this model connected with the questions just raised, it does lead to the diauxic growth curve. To highlight on the model, the cell growth process is viewed as comprising the growth reaction



where B is the biomass, S_i is the i^{th} substrate, E_i is considered as a 'key enzyme' in the uptake of the i^{th} substrate. The enzyme E_i is synthesized at a rate dependent on the allocation of its resources and Dhurjati's [11] equation is reproduced here

$$\frac{de_i}{dt} = \alpha_i \dot{R} u_i - \beta_i e_i \quad (1)$$

where e_i is the enzyme concentration, α_i and β_i are rate constants, \dot{R} is a fixed rate of total resource availability the fraction of which allocated for enzyme E_i is given by u_i . The resource availability rate R is assumed to be fixed here although in a more elaborate model it is possible to include replenishment of resources during growth. Note that Eq.(1) implies a maximum level of enzyme concentration because of the first order breakdown rate. The substrate consumption rate is

assumed to involve the enzyme concentration in the following manner

$$\frac{ds_i}{dt} = -b \frac{V_i e_i s_i}{K_i + s_i} \quad i = 1, 2, \dots \quad (2)$$

while growth on the substrates is written as

$$\frac{db}{dt} = -b \sum_i Y_i \frac{ds_i}{dt} \quad (3)$$

The biomass, whose concentration is represented by b , is viewed as comprising key enzymes and the rest of the biomass. For the sake of simplicity no material resources have been explicitly included in the biomass for the present.

Dhurjati [10] based the optimal allocation of resources on minimizing the time required for realizing all of the biomass from the different substrates. Thus the control objective is given by

$$\text{Min}_u t_f \quad \sum_i u_i = 1 \quad (4)$$

where t_f is the time required for the substrate levels to drop to some preassigned values (since arbitrarily small values would lead to arbitrarily large times mathematically).

This completes Dhurjati's model. The mathematical technique of computing the optimal allocation rates to accomplish the objective (4) is contained in the well-known minimum principle of Pontryagin [11] which will not be discussed here. The linear functionality of the control variables u_i leads to what is referred to as a "bang-bang" policy which in the present context implies exclusive utilization of one of the substrates. (Dhurjati [10] has investigated the possibility of singular control which could accommodate simultaneous consumption of different substrates and finds the constraints to be implausible). The diauxic growth situation is thus described by this model. Dhurjati was able to adapt model constants to describe growth data obtained by him on *Klebsiella pneumoniae* grown on a mixture of glucose and xylose. The preference for glucose with a higher growth rate on it is consistent with the interpretations of the model. The result is displayed in Figure 1. The question arises as to whether the organism in fact consumes both glucose and xylose after the former has dropped to sufficiently low levels. While this is not readily verifiable because of the difficulties inherent in measuring small differences in small substrate concentrations some assertions can be made in regard to Dhurjati's model. The linearity in the control variable will permit only exclusive utilization of one substrate or the other. If for example 'more preferred' substrate, say S_1 drops to sufficiently low levels, the preference would switch to the 'less preferred' substrate (S_2) after which exclusive utilization of S_2 will follow until again it is profitable to switch to S_1 and so on. This did not occur in the calculations presented because of the high discrepancy between growth rates on the two substrates and

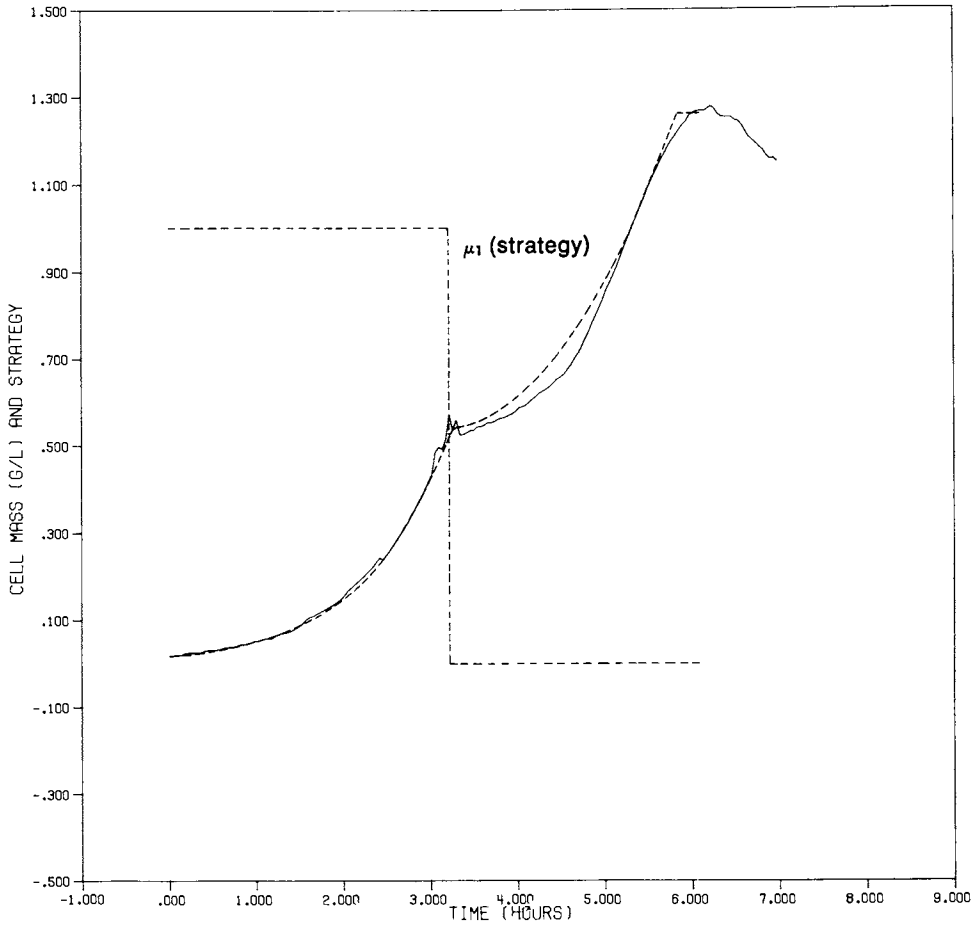


Figure 1. The diauxic growth curve predicted by Dhurjati's model for *Klebsiella pneumoniae* grown on a glucose-xylose mixture. Dashed lines, model; solid line, experimental.

the preassigned levels of substrate concentrations at t_f . Undoubtedly, for substrate pairs on which the difference in the growth rate is not very great, the model would predict alternate switching between substrates until t_f is reached. Unless nonlinear relationships are entertained in the control variables u_1 one is constrained to this sort of prediction. It will be of interest to investigate experimentally whether such alternate switching is in fact encountered. It is in this connection that the measurement of dissolved oxygen becomes a very interesting diagnostic tool. For example, a change in policy (such as switching substrates) is readily detected by a relatively abrupt change in dissolved oxygen while no corresponding change is likely to be apparent in either the biomass or the substrate concentrations. In Figure 2, are presented some results from Dhurjati's experiments. The organism's growth on xylose is interrupted by varying amounts of glucose at different instants of time. The dissolved oxygen shows an abrupt drop in oxygen concentration at the instant of glucose addition since the growth rate is higher on glucose and calls for increased oxygen consumption. The oxygen concentration shoots up again when the added glucose is exhausted. The concentration to which this upshoot occurs depends on time elapsed following glucose addition before the the organism is ready to revert to xylose again. If this time is short, growth resumes on xylose at the same level at which it was interrupted. If the time span is longer the resumption occurs at a somewhat reduced level possibly indicating that some breakdown of the key enzyme for xylose may have occurred in the interim. There appears to be little doubt that the measurement of dissolved oxygen will play a key role in the diagnosis of switching policies of the cell's internal machinery.

Kompala [12] has considered a model based on a short term perspective for the growth situation with which Dhurjati dealt. This model adopts the viewpoint that the cell optimally allocates its resources at every instant. Thus the state of the cell and its environment results in an immediate resource allocation with the objective of maximizing the acceleration (or minimizing the deceleration) in growth rate. The implication is that the cell is ever alert to environmental changes and always does the best. Some possible objections may arise. First, it is not clear, whether it is reasonable to expect that regardless of the rate at which environmental changes occur, the cells would optimally gear its enzyme synthesis rate unhampered by any metabolic inertia; for example, could control action taken at a particular instant result in an instantaneous change in enzyme synthesis rate? An attempt to cure this would in essence be a renewed quest for a 'long term' model. Second, with the imposition of a proper penalty for decision, it does not necessarily follow that what is best for each instant is best on the whole, an issue that has been raised before. Kompala's model constants do adapt to produce the diauxic curve. His model equations are virtually

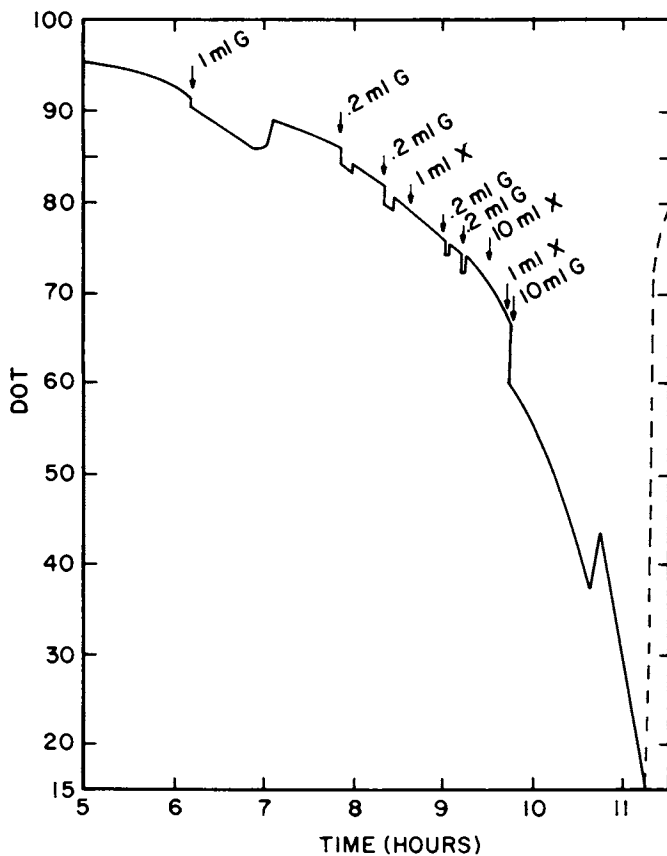


Figure 2. Dissolved oxygen curve for Klebsiella pneumoniae grown on xylose with periodic addition of glucose. G, 250 mg/mL glucose; X, 250 mg/mL xylose (t = 0, 50 mL X).

the same as those of Dhurjati [10] except for the enzyme synthesis and breakdown rates in Eq. (1) which must be replaced by

$$\frac{de_i}{dt} = \frac{\alpha'_i s_i}{K'_i + s_i} u_i - \beta_i e_i \quad (5)$$

At any instant t , the state of the biomass is determined by the concentrations b , and $\{e_i\}$ while that of the environment by $\{s_i\}$. The growth rate at this instant is determined by the above variables. However, the organism gears the enzyme synthesis rate at that instant to maximize d^2b/dt^2 by manipulating the control variables $\{u_i\}$. Because u_i occurs linearly in Eq. (5) the optimal decision is readily arrived at. By letting

$$j = \{i: \max \frac{V_i \alpha'_i s_i^2}{(K'_i + s_i)^2}\} \quad (6)$$

we find the optimal policy to be the "bang-bang" result

$$u_i = \delta_{ij} \quad (7)$$

This remarkably simple result as against the use of the Pontryagin principle required for Dhurjati's model is indeed a great asset for this model. (Parallel to the possibility of singular solutions in Dhurjati's formulation, one needs to investigate simultaneous utilization here when $V_i \alpha'_i s_i^2 / (K'_i + s_i)^2$ versus S_i intersect for different i).

Figure 3 shows the results of calculations for batch growth with two substrates. The sequential utilization of the substrates characteristic of the diauxic growth situation is reproduced by the model. This by itself is no more than establishing that the model premises are not implausible and is thus more a beginning than the end. In Figure 4, the model's perspective of an experiment in which the growth on the 'less preferred' substrate is interrupted by addition of the more preferred substrate. The immediate switch to glucose observed in Dhurjati's experiments is accommodated by this model. If it is agreed that a model based on a long term perspective such as that of Dhurjati will ignore environmental changes other than those on which the optimal policy was based, then the perturbed batch experiment just referred to cannot be described by Dhurjati's model. In this sense, Kompala's model is an improvement on Dhurjati's model.

Neither of the above models explicitly include the original claim that the resources are a part of the biomass and their availability may thus be constrained. This feature is readily built into either model. For example, we may denote the resources by R , their concentration by r , and postulate that their formation occurs by growth, and consumption by their allocation for enzyme synthesis. Admittedly this is somewhat of a narrow view of how resources may be used in metabolic processes but this simplification is virtually at the same level as that inherent in the lumped kinetic models of the past. The differential equation for r may be written as

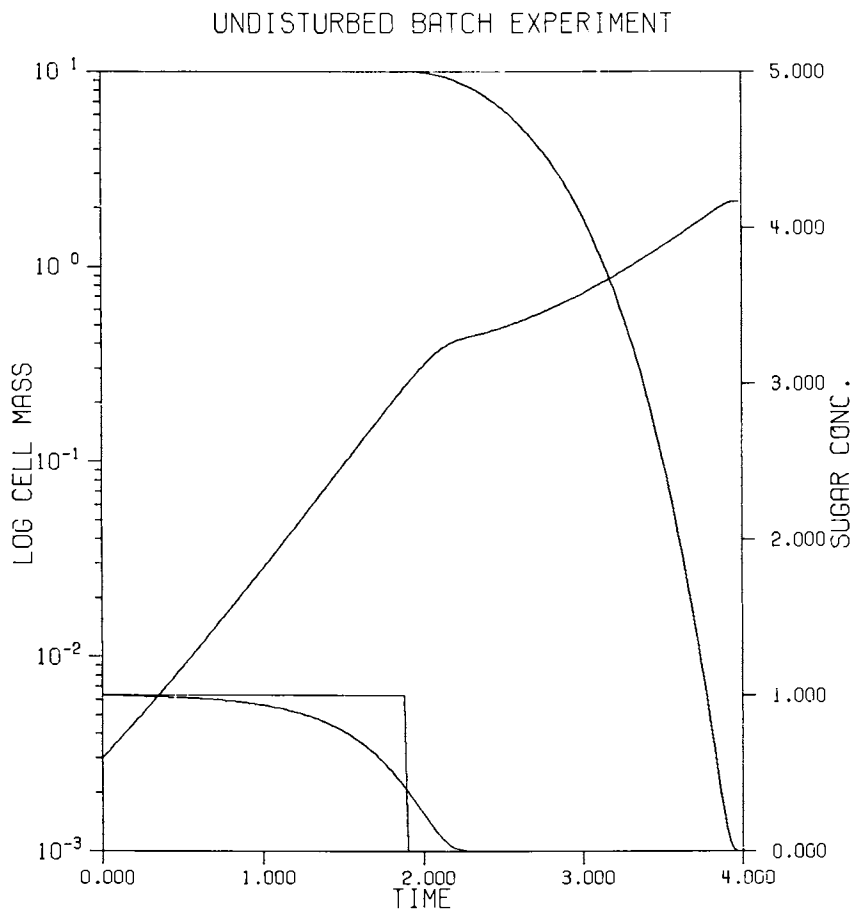


Figure 3. *The diauxic growth curve predicted by Kompala's short term model.
AG (glucose) = 90.0; AX (xylose) = 60.0.*

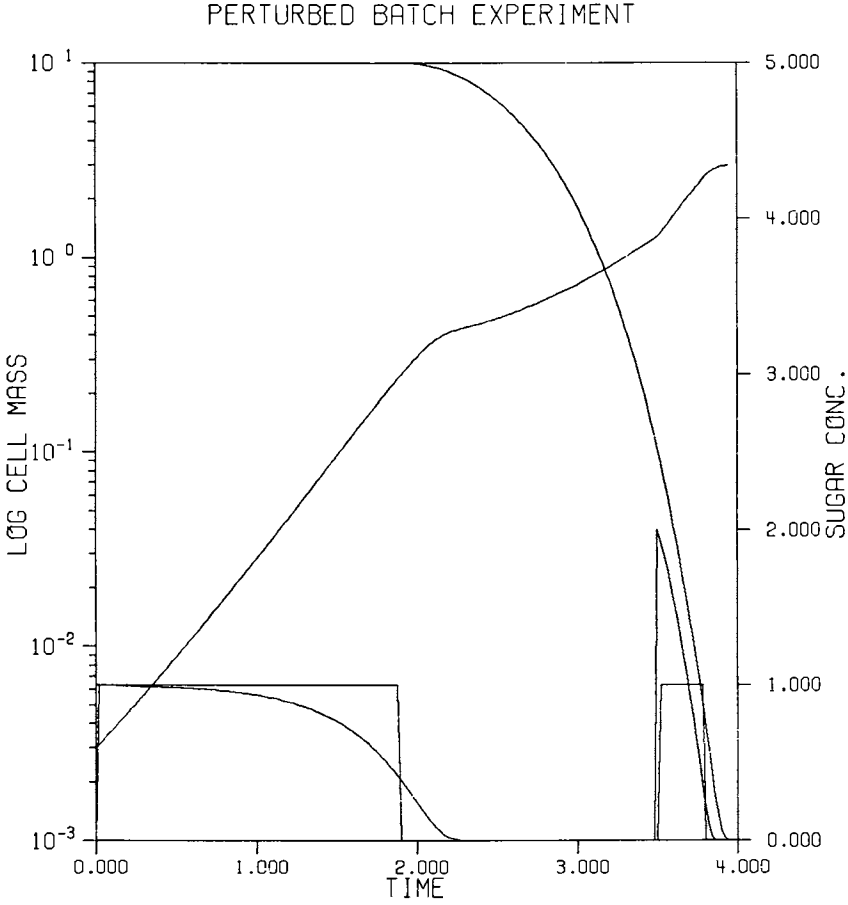


Figure 4. Growth on xylose interrupted by glucose addition as predicted by Kompala. AG = 90.0; AX = 60.0.

$$\frac{dr}{dt} = \gamma \frac{db}{dt} - \sum_i f_i(s_i, u_i r) \quad (8)$$

where $f_i(s_i, u_i r)$ is the rate of consumption of resources for the synthesis of i^{th} enzyme E_i ; it is related to the rate of synthesis of E_i to within a stoichiometric multiple. In Eq.(8) γ is a stoichiometric constant. In particular it is of interest to note that

$$\sum_i u_i \leq 1 \quad (9)$$

where the inequality sign is to account for the possibility that not all of the available resources need necessarily be invested at any instant. A model based on a long term perspective could in fact call for a policy of underutilization of resources at a given instant if a subsequent stage calls for increased resources. Propose, for example, that

$$f_i(s_i, u_i r) = \delta_i \frac{\alpha_i' s_i}{(K_i' + s_i)} \frac{u_i r}{(\kappa_i + u_i r)} \quad (10)$$

with Eq.(5) modified by

$$\frac{de_i}{dt} = \frac{\alpha_i' s_i}{(K_i' + s_i)} \frac{u_i r}{(\kappa_i + u_i r)} - \beta_i' e_i \quad (11)$$

where the δ_i in Eq.(10) represents a readily interpreted stoichiometric constant. In Eq.(11) κ_i is a Michaelis constant. The nonlinearity with respect to u_i in Eq.(11) is to be noted particularly, which may eliminate the exclusive bang-bang optimality result. Thus simultaneous utilization of substrates could also be predicted by such models. If ample resources are present, then the above Michaelis-Menten kinetic expression in Eq.(11) prevents over-allocation for any particular enzyme.

Whether the modelling be done based on a short or long term perspective, the issue raised earlier in regard to provoking non-optimal responses by suitable environmental variations is an important one. The short term models would not necessarily predict, for example, the maximum average productivity of biomass over the entire period of growth. Similarly the long term models would not predict the maximum average productivity if changes occurring in the environment are other than those which were accounted for in the optimization. Thus an interesting method of evaluating the responses predicted by the models is to compare them with those in which "perfect optimal behavior" is considered. Obviously perfect optimal behavior may be predicted by using the Pontryagin principle on the state equations in which the imposed environmental variations are built in. One need hardly point out that the superposition of the actual microbial response relative to that of the model and that based on perfect optimality would then be of the most vital interest.

Concluding Remarks

Our attempt here has been to find a mathematical framework for certain well-expressed ideas concerning microbial behavior in regard to the role of internal regulatory processes. This framework essentially draws on the formulation of kinetic models in that biomass is lumped into a small number of component masses, and growth being regarded as increase in their quantities by interaction with nutrients. The component masses include key enzymes whose synthesis is controlled by optimal allocation of certain critical resources. Various important issues have been raised connected with this cybernetic perspective. The main motivation is to evaluate the consequences of hypotheses concerning internal regulatory processes, and to find experimental situations in which they manifest in the most unambiguous ways. It is not essential that this pursuit be in consonance with precise quantitative fits of model predictions with experimental data. Rather the function of such model building is simply to develop better understanding of real systems. Unfortunately, it is not often that this aspect of modelling is perceived as such.

Acknowledgments

The work presented here owes much to the participation of graduate students Prasad Dhurjati and Dhinakar Kompala, and to my colleagues Michael C. Flickinger and George T. Tsao, and is the subject of a future joint publication under preparation. Partial support by the National Science Foundation under Grant No. Eng 7820964 is gratefully acknowledged.

Nomenclature

B	Biomass
b	Concentration of biomass
E	Key enzyme
e	Concentration of key enzyme
f	Rate of consumption of resources for synthesis of key enzyme.
K	Michaelis constant for growth
K'	Michaelis constant of enzyme synthesis
R	Total resource availability rate
r	Concentration of limiting resource
S	Substrate
s	Concentration of substrate
t	Time
u	Fractional allocation
V	Rate constant in growth

Y	Yield coefficient
Greek symbols:	
α, α'	Rate constants in enzyme synthesis
β	Rate constant for enzyme breakdown
γ	Stoichiometric constant for replenishment of resources by growth
δ	Stoichiometric constant for consumption of resources for enzyme synthesis
δ_{ij}	Kronecker delta equals unity when $i=j$ and vanishes otherwise
κ	Michaelis constant for consumption of resources for enzyme synthesis
Subscripts	
i	Refers to i^{th} substrate
f	Refers to final state of growth when substrates drop to preassigned levels

Literature Cited

1. Fredrickson, A.G., and H.M. Tsuchiya, in "Chemical Reactor Theory," E. L. Lapidus and N.R. Amundson, Prentice-Hall, N.J., 1975.
2. Demain, A.L., Adv. Biochem. Eng. Ed. T.K. Ghose, A. Fiechter; N. Blakebrough Springer Verlag, Heidelberg, 1971.
3. Van Dedem, G., and M. Moo-Young, Biotech. and Bioeng., (17), 927, 1975.
4. Rosen, R., "Foundations of Mathematical Biology," Ed. R. Rosen, Academic Press, Vol II, 1972.
5. Wiener, N., "Cybernetics or Control and Communication in the Animal and the Machine," M.I.T. Press, Mass. 1975.
6. Oster, G. and E.O. Wilson, Monographs in Population Biology 12, ch. 8. "A critique of optimization theory in evolutionary biology," Princeton U. Press, 1970.
7. Swanson, C.H., R. Aris, A.G. Fredrickson and H.M. Tsuchiya, J. Theor. Biol., (12), 228, 1966.
8. Tsuchiya, H.M., Fredrickson, A.G., and Aris, R., Adv. Chem. Eng., (6), 125, 1966.
9. Monod, J., "Recherches sur la croissance des cultures bacteriennes," Herman & Cie. Paris, 1942.

10. Dhurjati, P., Ph.D. Dissertation, Purdue University, West Lafayette, Indiana, 1982.
11. Pontryagin, L.S., V.G. Boltyanski, R.V. Gamkrelidze and E.F. Mischenko, "The Mathematical Theory of Optimal Processes," Interscience, N.Y., 1962.
12. Kompala, D.S. M.S. Dissertation, Purdue University, West Lafayette, Indiana, 1982.

RECEIVED June 29, 1982

Strategies for Optimizing Microbial Growth and Product Formation

CHARLES L. COONEY

Massachusetts Institute of Technology, Department of Nutrition and Food Science, Biochemical Engineering Laboratory, Cambridge, MA 02139

An essential element for fermentation processes, whether for cell mass or product, is the efficient growth of the organism. Optimizing the environment for growth requires balancing the economic feasibility of maintaining a suitable chemical and physical environment, while meeting the physiological needs of the organism. Using several examples of bacteria, yeast and mold fermentations, strategies for optimizing growth are examined and compared. In the first case, the objective of the fermentation is cell mass production; two examples are Baker's yeast (*Saccharomyces cerevisiae*) and single-cell protein (*Hansenula polymorpha*) production. In seeking to optimize productivity and conversion yields, carbon source and oxygen become key operating variables. The second case focuses on production of enzymes; in particular, the production of heparinase by *Flavobacterium heparinum* and α -glucosidase (maltase) by *Saccharomyces italicus*. The objective functions are maximum total activity and maximum productivity. Important variables are growth rate and composition and concentration of nutrients in the environment. The level of these enzymes is subject to metabolic regulation in response to the environment and the productivity depends also on microbial growth. Lastly, the third case to be examined is metabolite production; the production of penicillin by *Penicillium chrysogenum* is discussed. Optimization of growth must consider not only rapid accumulation of cell mass, but also conditioning of the cell to maximize the rate and extent of product formation. Maintenance of adequate nutrients in the environment, with high levels of some and low levels of others, is essential. An analysis of strategies to meet the metabolic demands provides insight into ways to improve the organism through genetic engineering, as well as the process through bioreactor design.

0097-6156/83/0207-0179\$06.00/0

© 1983 American Chemical Society

The common theme in the development of optimum fermentation strategies is "environmental management". The examples described here cover a spectrum of fermentations including cell mass, enzyme and secondary metabolite production, yet it will become apparent that there is a common need for careful environmental management with particular emphasis on carbon source management throughout the fermentation.

The objective functions important to fermentation process optimization are: volumetric productivity, product concentration, conversion yield and process reproducibility. Maintaining a high productivity will allow one to maximize return on capital investment. This is particularly important for the development of new processes, as a consequence of the capital intensity of fermentation processes. The need to achieve and maintain high product concentrations reflects the importance of recovery in the cost of production. Achievement of high conversion yields is necessary to minimize raw materials cost. Furthermore, a high conversion yield from the carbon source will minimize the demand for oxygen and the need for heat removal, thus minimizing these operating costs (1). Lastly, reproducibility is essential to minimize both capital and operating costs, as well as meet production goals. These objective functions are not equally important, however, in all fermentations as illustrated in the following brief case studies which are compiled here to illustrate the importance of environmental management in developing strategies for optimizing microbial growth and product formation.

Production of Cell Mass

The manufacturing costs for the production of microbial cell mass are dominated by: (i) the raw materials cost, especially the carbon source; (ii) capital investment, in the case of a new manufacturing facility; and, (iii) energy costs, with most of the energy being used for oxygen transfer and heat removal (1, 2). As a consequence, it is essential to achieve high conversion yields while maintaining high productivities from the bioreactor. Two approaches to these goals are illustrated by the following:

Baker's Yeast Production. One of the oldest fermentation processes for the production of cell mass is Baker's yeast production. The actual product of the fermentation is cell mass and its "baking power", or ability to generate carbon dioxide under baking conditions. This industry, which was modernized by Pasteur in the 1800's, is characterized by its high sensitivity to raw material costs variables or seasonal demand and need to maintain a

product acceptable to the baker. The objective in process development is to achieve high conversion yields of yeast from the carbon source at a high productivity while maintaining the best baking power. The solution to meet these objectives has been the evolution of the fed-batch fermentation process.

It has often been suggested that Baker's yeast could be most economically produced by a continuous process, however, there is little incentive to convert existing (and fully depreciated capital investment) from fed-batch to continuous operation. The fed-batch fermentation allows a plant containing many fermentors to operate with a variable product demand. Furthermore, the food industry producing Baker's yeast is not interested in a process change which may alter their product identity and hence desirability by the baker. For these reasons, fed-batch operation offers maximum plant operation flexibility. It is interesting to note, however, in considering new plant construction, there may be more incentive to go to a continuous process as a means of reducing the entry costs associated with this capital intensive industry.

The strategy underlying the operation of the fed-batch fermentation is based on matching the supply of carbon source with the demand by the microorganism. The rationale for this is illustrated in Figure 1 (3). In order to maximize the conversion yield, there is a narrow range of growth rates between 0.075 and 0.25 h^{-1} that can be used. It is important to stay above 0.075 h^{-1} to prevent excessive maintenance metabolism (4). In addition, the growth rate must be below 0.25 h^{-1} to prevent ethanol production which occurs in response to the Crabtree effect. In addition, it is imperative that sufficient oxygen be available to prevent anaerobic production of ethanol.

Several investigators (3, 5) have proposed the application of computer process control to this process. Using on-line measurements of air flow rate, oxygen consumption and carbon dioxide production in combination with a set of material balance equations described by Cooney *et al.* (6), it is possible to calculate on-line the cell concentration and growth rate and apply a modified feed-forward control strategy to increase (or decrease) the sugar addition rate so that the specific growth rate does not exceed a critical value while at the same time maximizing the volumetric productivity (3, 7). Results of a typical fermentation are shown in Figure 2 and a summary of results from a variety of fermentations under various operating conditions are shown in Table I.

From an analysis of these fermentations, it is clear that the key to a successful fermentation is careful management of the carbon source; this is achieved by continuous assessment of the

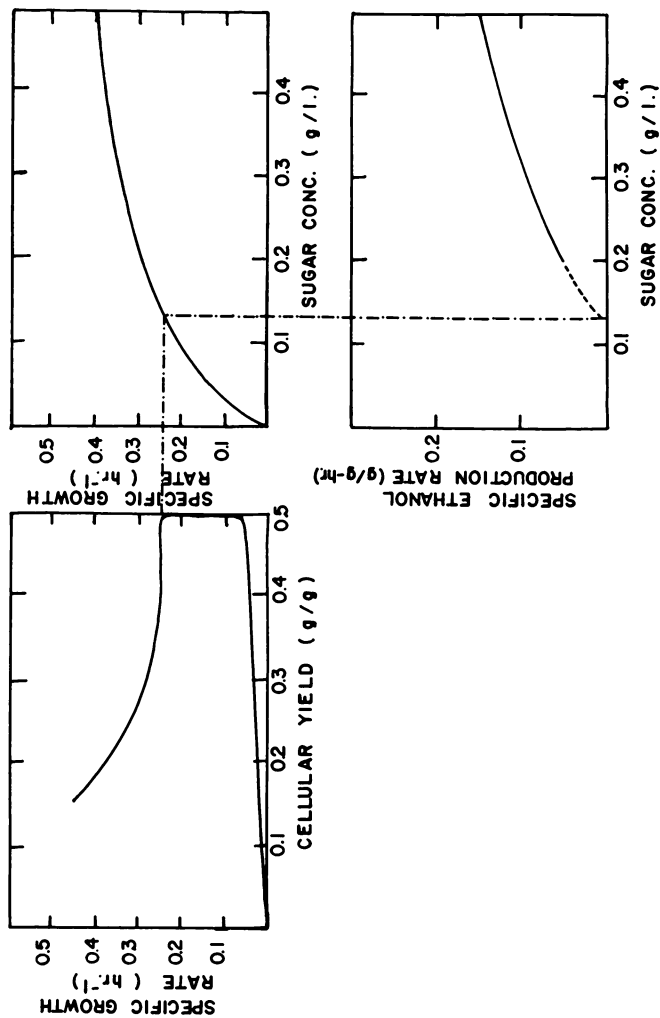


Figure 1. Relationships in baker's yeast fermentation. Left, specific growth rate and cell yield; upper right, sugar concentration and specific growth rate; and lower right, sugar concentration and ethanol production rate. Reproduced, with permission, from Ref. 3. Copyright 1979, John Wiley & Sons, Inc.

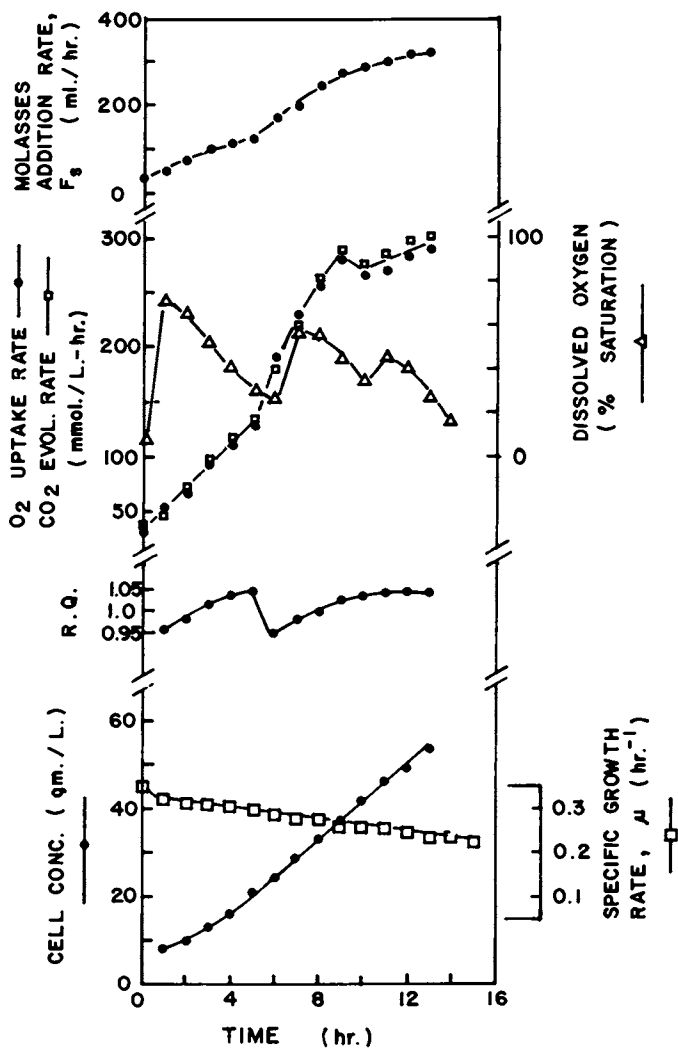


Figure 2. Kinetics of baker's yeast fermentation under feedback-modified feed-forward computer control. Reproduced, with permission, from Ref. 3. Copyright 1979, John Wiley & Sons, Inc.

Table I
 COMPARISON OF COMPUTER-CONTROLLED YEAST FERMENTATIONS WITH DIFFERENT
 INITIAL CELL CONCENTRATIONS

Initial cell conc (g/liter)	Final cell conc (g/liter)	Fermentation time (hr)	Overall cell yield (g cells/g sugar)	Volumetric productivity (g/liter-hr)
3.8	59.1	17.0	0.49	3.3
4.9	52.0	16.0	0.49	3.1
5.8	54.6	12.8	0.50	4.0
8.9	54.1	14.0	0.51	3.4
9.0	49.3	11.7	0.49	3.7
14.4	63.2	10.2	0.50	5.2

Source: Ref. 3.

demand for the carbon source and a feedback modified feedforward control strategy to match supply and demand.

Single-Cell Protein. The concept of single-cell protein, while not new in that it was utilized by both the Aztecs and various cultures in central Africa, has only recently (since 1960) been proposed as a means for producing large-scale, high quality protein to supplement traditional protein resources (8). The manufacturing cost for SCP is dominated by the raw material cost, as well as capital investment (1). As a consequence, the objective in process development is to maximize the conversion yield and the volumetric productivity. In this way, the operating and capital investment cost can be minimized. Continuous culture offers a useful approach in which cells can be grown under carbon source to protein under conditions of high volumetric productivity.

Two strategies for optimization of SCP production are suggested in Figure 3. Figure 3A shows a traditional continuous culture isotherm. The maximum productivity occurs at a value D_{\max} (9). However, this analysis does not lead to an economic optimum operating condition. It assumes that the inlet feed concentration, S_0 , is a constant under all operating conditions, and furthermore does not take into account the need to operate the fermentor at its maximum productivity, the value of which is determined by the oxygen transfer rate (or in the case of very large reactors, the heat transfer rate). This is illustrated in Equation 1:

$$W_m = DX_m = Y_{O_2} R_{O_2}^{\max} \quad (1)$$

where W_m is the maximum productivity

D is the dilution rate

X_m is the maximum cell concentration allowed by $R_{O_2}^{\max}$

$R_{O_2}^{\max}$ is the maximum oxygen transfer rate

Plotting the maximum cell density permitted at a given oxygen transfer rate (and hence constant volumetric productivity), gives the results shown in Figure 3B. In this analysis, S_0 , the feed concentration of carbon source, is not constant. Considering the strategy for operation, one will choose a dilution rate that: (1) will minimize the residual limited nutrient concentration and thus achieve highest substrate utilization and minimum waste treatment load, (2) will maximize the conversion yield of the limiting nutrient, the carbon source, and (3) will maximize the cell concentration to minimize recovery costs. The desired dilution rate is indicated by the arrow on Figure 3B. Again, the strategy relates to effective management of the carbon source. In this regard,

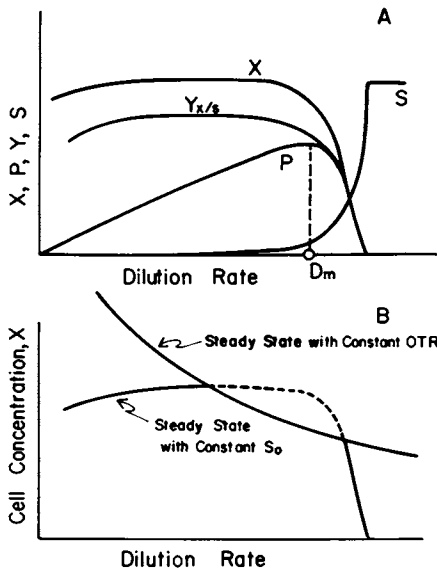


Figure 3. Strategies for optimization of continuous culture for production of single-cell protein. Top, under continuous culture isotherm with a fixed value for carbon source feed concentration. D_m is the dilution rate of maximum productivity. Bottom, comparison of isotherm for fixed substrate feed concentration, S_0 , with that for fixed oxygen transfer rate, OTR (curves show the maximum cell concentration for a given OTR and cell yield).

the use of continuous culture is an important tool for SCP production.

It is important, however, to go one step further in this analysis. One of the major carbon sources of interest for single cell protein production is methanol. The reasons for this relate primarily to its low cost and availability. It has been shown that high methanol concentrations are toxic to cell growth and more importantly lead to decreased cell yield (10). Therefore, a further objective is to maintain the residual methanol concentration low at all times. The importance of this is illustrated in Figure 4 (11), which shows the response of Hansenula polymorpha to a perturbation in methanol concentration. The perturbation was initiated by a period of oxygen starvation (achieved by reducing the agitation rate). Because methanol metabolism is obligately aerobic, under oxygen limiting conditions methanol rapidly accumulates. When the oxygen limitation is eliminated by restoring agitation, the methanol is rapidly catabolized and some formaldehyde and formic acid accumulates. Both these compounds are extremely toxic and lead to instability in culture operation. To overcome this problem, an on-line computer control strategy that would continuously assess residual methanol concentration and, should methanol accumulate, take corrective action to prevent culture instability was developed (12).

The strategy for optimizing single-cell protein production is based not only on a dilution rate that will give a low residual substrate concentration and high conversion yield, but also that will operate with the maximum cell density permitted by the oxygen transfer rate. Simultaneously, it is important to prevent accumulation of residual methanol to achieve both high yields and process stability.

Enzyme Production

The economics of enzyme production are dominated in most cases by recovery costs. For this reason, the objective functions for optimization are to maximize the specific activity (units of enzyme activity per weight of cell mass) and volumetric productivity (units per liter-h). Maximization of specific activity ensures both efficient conversion of raw materials to the desired product as well as facilitating enzyme recovery; maximization of total volumetric productivity helps to minimize recovery costs and maximize economic return on capital investment. To achieve these objectives in process development, one utilizes both genetic manipulations and environmental management to achieve a high enzyme specific activity and a high cell density.

Two case studies are examined here to illustrate the important elements in developing a strategy for optimal enzyme production.

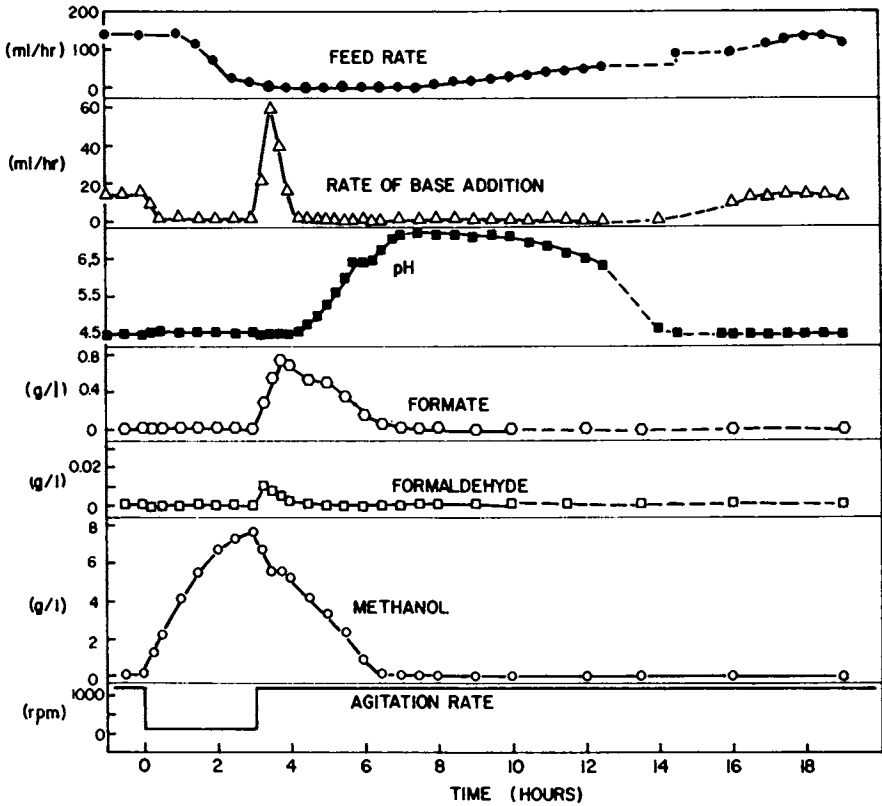


Figure 4. Response of a steady state culture of *H. polymorpha* to an interruption in agitation causing oxygen limitation. Reproduced, with permission, from Ref. 11. Copyright 1981, American Society for Microbiology.

Maltase Production

The intracellular enzyme maltase (α -glucosidase E.C. 3.2.1.20) is an important enzyme for analysis of blood amylase. The enzyme is intracellular and is subject to carbon catabolite repression by glucose as well as induction by maltose. A study was initiated with the objective of developing a lower cost process for maltase manufacture; the goals were to minimize the fermentation medium cost while maximizing the total activity and productivity of maltase formation. The starting point was a fermentation with Saccharomyces italicus grown in complex medium containing maltose as the sole carbon source. Results from this fermentation are shown in Figure 5. The problems with this fermentation are high medium cost and the point of harvest of maximum maltase activity was difficult to assess, as soon as maltose disappeared the specific activity of the enzyme rapidly decayed.

Medium optimization was achieved by developing a defined medium without maltose. Saccharomyces italicus does not use sucrose because it lacks invertase, however, maltase will hydrolyze sucrose and allow it to be used for growth. A mutation and selection program was initiated to select for mutants of S. italicus that would grow on sucrose as the sole carbon source. It was hypothesized that such mutants would have a high concentration of maltase. The results are shown in Table II, in which mutant 1-4 is compared with the wild type (13). As expected, the mutant, when grown on sucrose, has high maltase activity. When grown in defined medium with sucrose, the volumetric and specific activity of maltase are greatly enhanced.

Table II

MALTASE PRODUCTION ON VARIOUS CARBON SOURCES

<u>Carbon Source</u>	<u>Maltase (units/g-cell)</u>	
	<u>Wild Type</u>	<u>Mutant 1-4</u>
Sucrose	no growth	
Maltose	870	770
Glycerol	10	1100
Acetate	10	770
Fructose	10	380
Glucose	10	320

A comparison of alternative methods for producing this enzyme in batch and continuous culture is shown in Table III. The results are somewhat surprising. It was anticipated that in continuous culture under carbon-limited conditions the specific activity of maltase would be higher than observed in batch culture. However, for reasons that are not clear, the specific activity is substantially higher in batch culture. These results illustrate

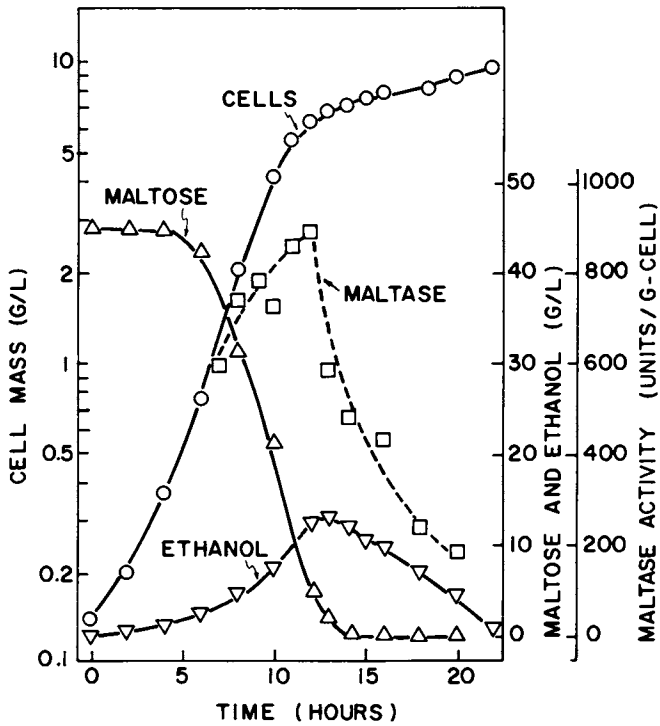


Figure 5. Batch fermentation for maltase production by *Saccharomyces italicus*. Reproduced, with permission, from Ref. 13. Copyright 1982, American Society for Microbiology.

again the importance of using good carbon source management and developing an optimal strategy for enzyme production. It is also interesting to note that by going from a complex to a defined medium one not only reduced the medium cost but also stabilized the enzyme to subsequent degradation.

Table III

MALTASE PRODUCTION BY MUTANT AND WILD TYPE

Process	Specific Activity (units/ g-cell)	Productivity	
		(units/ g-cell-hr)	(units/l-hr)
Batch (1-4)	2200	170	1300
Continuous (1-4)	1400	290	3400
Batch (wild type)	890	70	470

Heparinase Production

The enzyme heparinase is of interest as a means for degrading heparin in blood and for degrading large molecular weight heparin into smaller fragments having potential as novel anticoagulants (14). The production of heparinase by Flavobacterium heparinum in a complex medium with heparin as an inducer is shown in Figure 6. The requirement for heparin makes the medium expensive and it is difficult to pick the best harvest time because the enzyme activity rapidly decays late in the fermentation. The first step in process optimization was to develop a defined medium; results are shown in Figure 7 (15). Although heparin is still required as an inducer, this lowers medium cost and increases the stability of heparinase. It was expected that the production of this enzyme, in addition to being under induction by heparin, would be under control by carbon catabolite repression. The results showed that increasing the initial concentrations of glucose leads to both decreased growth and heparinase production (15). For this reason, we examined a fed-batch culture designed to keep the glucose low throughout the fermentation. The results showed that it is possible to achieve high enzyme activity which is relatively stable at the end of the fermentation. Again, the strategy of carbon source management has proved to be very effective in optimizing this fermentation. Currently we are in the process of looking for mutants which no longer require heparin as an inducer. We are also exploring the use of continuous cul-

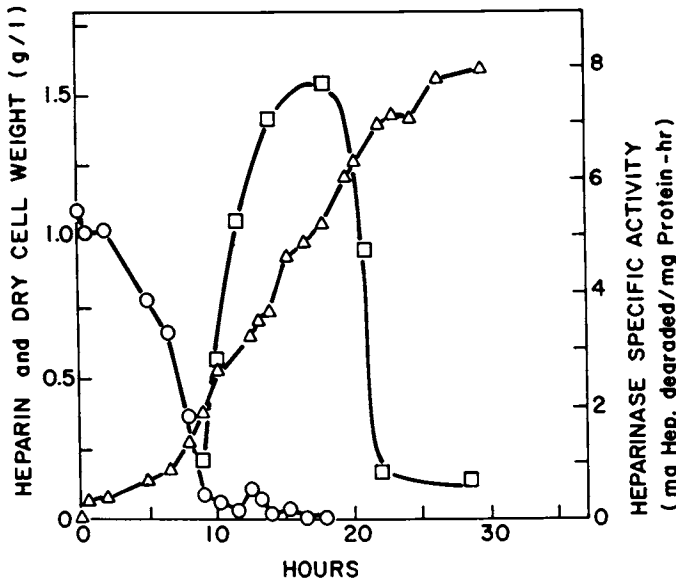


Figure 6. Batch fermentation for the production of heparinase by *Flavobacterium heparinum* on complex medium. Key: \square , heparinase specific activity; Δ , dry cell weight; \circ , heparin concentration. Reproduced, with permission, from Ref. 15. Copyright 1981, American Society for Microbiology.

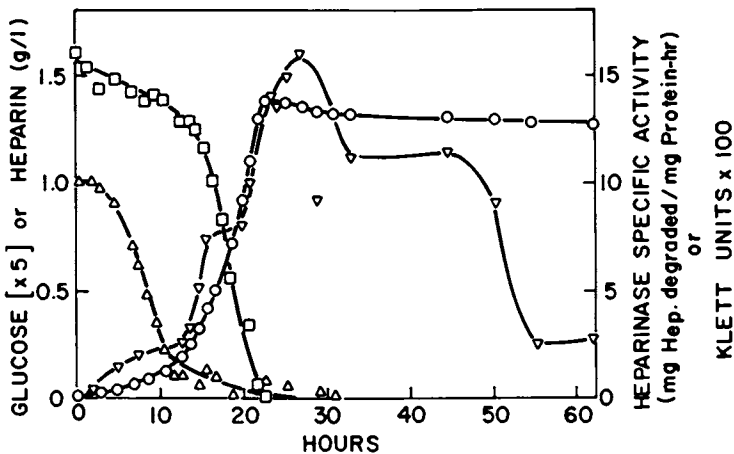


Figure 7. Batch fermentation for the production of heparinase by *F. heparinum* in defined medium. Key: \circ , dry cell weight, (D) glucose; Δ , heparin; and ∇ , heparinase activity. Reproduced, with permission, from Ref. 15. Copyright 1981, American Society for Microbiology.

ture as a means for maintaining low glucose concentrations with the hope of maximizing the specific activity of heparinase.

Metabolite Production

The primary objective functions for production of metabolites are to maximize the concentration (to minimize recovery costs) while maintaining high conversion yields of costly raw materials to the product, under conditions of high volumetric productivity (to reduce capital cost). The usual approach is to rapidly produce a high cell concentration under conditions that maximize the conversion rate of raw materials to the desired product.

The example considered here is penicillin production by Penicillium chrysogenum. Penicillin is under control of carbon catabolite repression and is typically formed as a secondary product after primary growth in the fermentation. The strategies developed in industry for this fermentation generally revolve around a fed-batch fermentation which restricts the flow of carbon to the culture to slow down growth, thus preventing carbon catabolite repression. Mou and Cooney (16) initiated a program to examine the application of on-line computer control as a means for achieving improved carbon source management for penicillin production. The rationale was to utilize on-line monitoring of growth to assess the demand of the culture for the carbon source and in this way develop a means to control the specific growth rate in the fermentation. It was reasoned that on-line computer control would prove to be more flexible in allowing one to balance supply and demand of the carbon source during this fermentation.

A series of studies were conducted in which a computer control system was utilized to control both growth phase and production phase growth rates and to ask the question, "what is the effect of changes in these growth rates on the specific productivity of penicillin?". In Figure 8 are shown results in which the production phase growth rate was manipulated from 0 to 0.015 h^{-1} while the initial growth rate was manipulated constant at its maximum value of 0.107. The specific rates of penicillin production are shown in Figure 9. It is clear that control of the production phase growth rate is important to maintaining the ability of the cells to make penicillin. While it is not clear from these results what the optimum value is, this approach does allow one to begin to design a set of experiments to answer that question. In a second set of experiments, two growth phase growth rates were compared. In the first case, the growth was controlled at 0.11 h^{-1} and in the second case at 40% of this value. The results, shown in Figure 10, indicate that cells grown more slowly during the initial growth phase have a higher specific rate of penicillin production. Again, it is not clear what the optimum values for growth phase growth rate are; it is clear, however, that carbon source management during both the growth and production phase is important to maximize the specific rate of penicillin production.

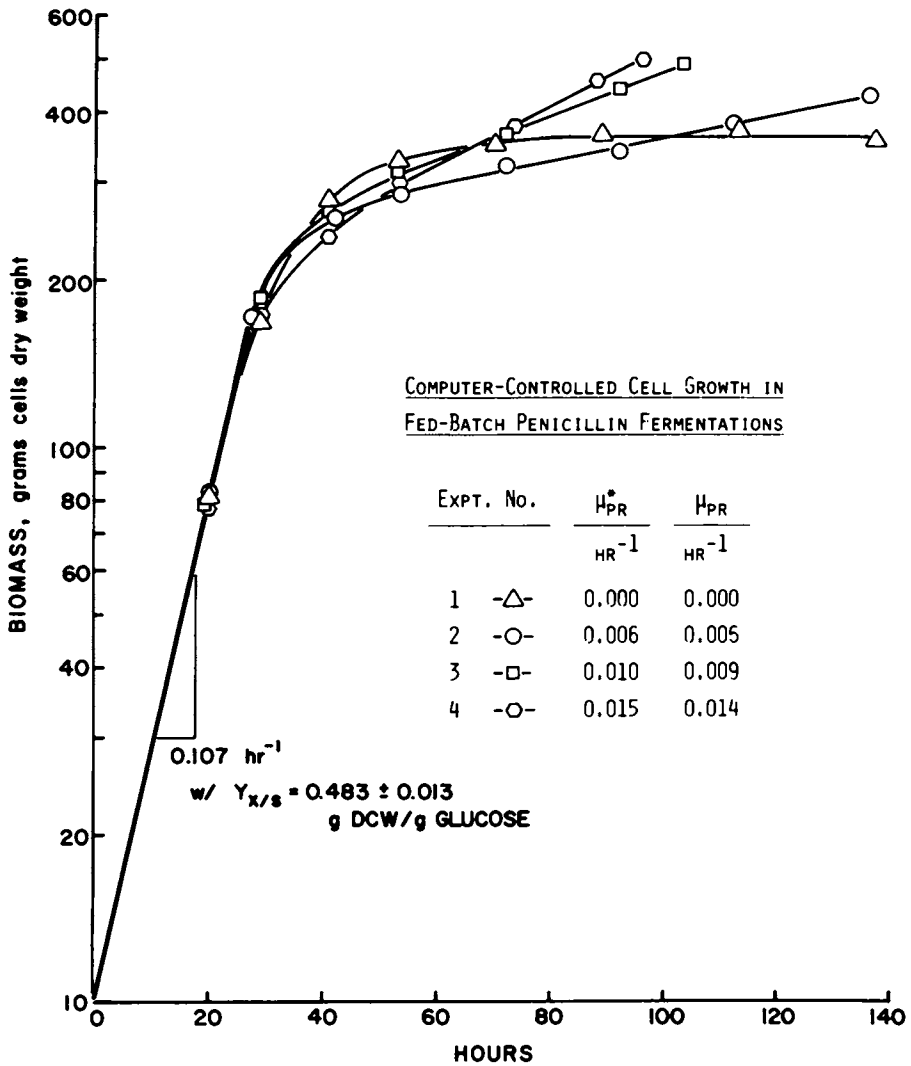


Figure 8. Growth kinetics of *P. chrysogenum* grown in computer controlled fed-batch culture (see text for details).

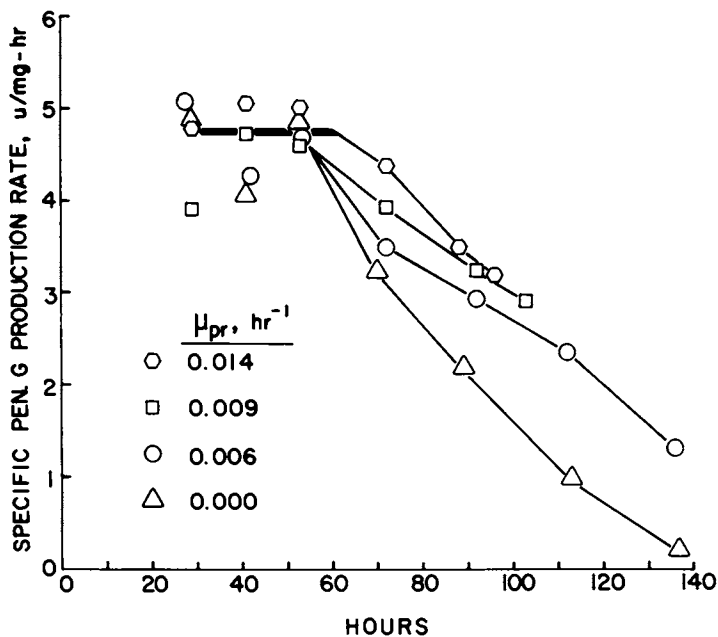


Figure 9. Specific penicillin production rate for the fermentation shown in Figure 8.

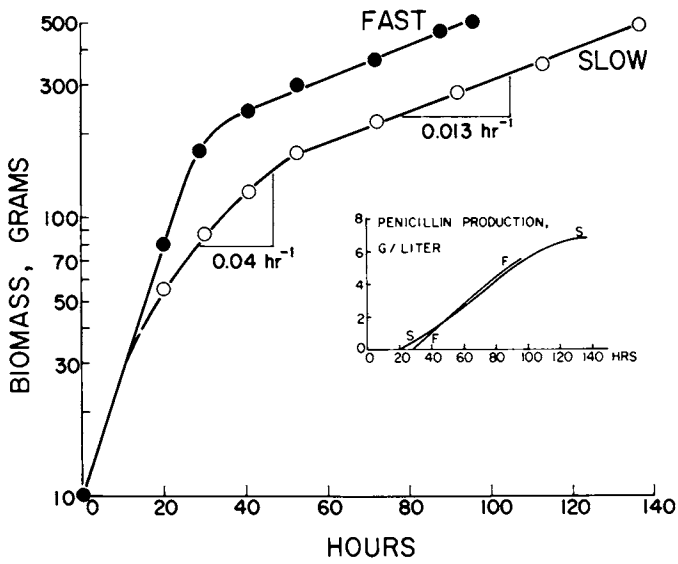


Figure 10. Growth and penicillin production by *P. chrysogenum* grown at two different growth phase growth rates.

These results suggest that further refinement of this important fermentation can be achieved through the use of on-line monitoring and control.

Conclusions

For the production of cell mass, enzymes and metabolites, it is clear from the above examples that careful carbon source management is important to achieve high cell concentrations with high yield, maximum specific enzyme activities and the efficient conversion of raw materials to products. One approach to achieve good environmental management is through the use of on-line process control. In this way, it is possible to match the supply with the demand for carbon source in a wide variety of fermentations. Another approach is to use both traditional genetics as well as genetic engineering to alter regulation and patterns of carbon source utilization to achieve better carbon source management. Genetics can be used to eliminate carbon catabolite repression, side reactions to undesired products and the need for inducers of desired enzymes. In addition, the use of recombinant DNA to increase gene dosage can be important to increasing the specific activity of desired enzymes; these may be enzymes that are desired as products or that are rate limiting enzymes in metabolic pathways. Simultaneously with optimizing the genetic constitution and the application of process control strategies, it is essential in bioreactor design and scale-up to take into account the organism's sensitivity to carbon source concentrations. In situations such as methanol fermentations where the organism may be very sensitive to small variations in carbon source concentrations, mixing time is a key parameter and novel engineering designs must often be considered to avoid this problem. Despite what appears superficially to be diversity among fermentation processes, there are several common factors important in the design of optimum process strategies. Carbon source management is key among these.

Literature Cited

1. Cooney, C.L. Microb. Growth on C₁ Compounds, 1975, pp. 183-197.
2. Cooney, C.L.; Rha, C.K.; Tannenbaum, S.R. Adv. in Food Res., 1980, 26, 1-52.
3. Wang, H.Y.; Cooney, C.L.; Wang, D.I.C. Biotech. Bioengr., 1979, 21, 975-995.
4. Pirt, S.J. "Principles of Microbe and Cell Cultivation", 1975, Blackwell Scientific Publications, London.
5. Aiba, S.; Nagai, S.; Nishizawa, Y. Biotechnol. Bioengr., 1976, 19, 1001.
6. Cooney, C.L.; Wang, H.; Wang, D.I.C. Biotech. Bioengr., 1977, 19, 55-66.

7. Wang, H.Y.; Cooney, C.L.; Wang, D.I.C. Biotech. Bioengr., 1978, 19, 67-86.
8. Cooney, C.L.; Rha, C.K.; Tannenbaum, S.R. Adv. Food Res., 1981, 26, 1-47.
9. Herbert, D.; Elsworth, R.; Telling, R.C. J. Gen. Microbiol., 1956, 14, 601-622.
10. Books, J.D.; Meers, J.L. J. Gen. Microbiol., 1973, 77, 513.
11. Swartz, J.R.; Cooney, C.L. Appl. Env. Microbiol., 1981, 41, 1206.
12. Swartz, J.R. Ph.D. Thesis, M.I.T., Cambridge, MA, 1979.
13. Schaefer, E.J.; Cooney, C.L. Appl. Environ. Microbiol., 1982, 43(1), 75-80.
14. Langer, R.; Linhardt, R.J.; Hoffberg, S.; Larsen, A.K.; Cooney, C.L.; Tapper, D.; Klein, M. Science, 1982, in press.
15. Galliher, P.M.; Cooney, C.L.; Langer, R.; Linhardt, R.J. Appl. Environ. Microbiol., 1981, 41(2), 360-5.
16. Mou, D-G.; Cooney, C.L. Biotech. Bioeng., 1982, submitted.

RECEIVED July 22, 1981

Interactions of Microbial Populations in Mixed Culture Situations

A. G. FREDRICKSON

University of Minnesota, Department of Chemical Engineering and
Materials Science, Minneapolis, MN 55455

This paper reviews the classification and dynamics of interaction between pairs of microbial populations inhabiting a common environment. A few cases of interaction between three or more populations are considered, also. The nature of the scheme of classification of interaction is described and its utility as well as its weaknesses are mentioned. Several interactions, competition for resources and feeding of one population upon another in particular, have been studied in some detail and reasonably reliable mathematical models of some simple types of these interactions are available. Other interactions have not received so much attention, however, and in some cases nothing but qualitative statements about an interaction can be made. The review is concluded with a listing of areas where research is needed to provide and improve knowledge of interspecific microbial interactions.

Probably the main reason for the predominance of pure culture techniques in the fermentation industry is that in most cases the product is a complicated, valuable organic molecule which can be made by a single microbial population, and when we have isolated and improved such a population we do not want to undo the labors of the microbiologists and geneticists by letting into our propagation apparatus other microorganisms which might compete with or be antagonistic to our producer population, or which might make substances which would have to be separated from the desired product, and so on. The reasons why most fermentation technology is pure culture technology are therefore similar to the reasons why our agriculture tends to be monoculture of plants.

Nevertheless, there are reasons for studying mixed cultures, and I will list four. First, certain industrial operations, notably waste disposals, do utilize mixed cultures. Second, invasion by contaminants or formation of mutants turn pure

0097-6156/83/0207-0201\$07.75/0

© 1983 American Chemical Society

cultures into mixed cultures. Third, mixed cultures offer some potential advantages, such as (i) ability to perform sequences of chemical transformations which no pure culture can do, (ii) ability to grow on simpler and so cheaper media, (iii) ability to continue functioning over wider ranges of environmental conditions, and (iv) ability to resist invasion by contaminants. Finally, a fourth reason for studying mixed cultures is that natural systems always involve the activities of mixed cultures.

Classification of population interactions

When several populations of microorganisms inhabit a common abiotic environment they will almost invariably interact with one another. Attempts to construct theories of the dynamics of such systems--that is, to construct theories which will predict how the systems evolve in time--must be based therefore on knowledge of what interactions occur and on the kinetics of such interactions. Hence, the rest of what I have to say will focus on what is known about interactions in simple mixed culture systems.

Economy of discussion makes it necessary to devise some scheme for naming microbial interactions. In addition, development and use of such a scheme will help organize our thinking on the subject and will even suggest research that should be done.

All schemes of naming interactions that I have seen are based on naming interactions between pairs of populations. This is perfectly understandable, since a pair of populations is the simplest unit of biological organization that can exhibit interactions other than intraspecific ones. However, the use of the basis named leads to some difficulties when we consider systems with three or more populations, as will be explained shortly.

The scheme of naming interactions between a pair of populations, say A and B, usually adopted by ecologists is based on the qualitative effects that the presence of A has on B as well as on the effects that B has on A. If the presence of A stimulates the growth of B somehow, then A is said to have a positive effect on B whereas A is said to have a negative effect on B if the presence of A represses or slows the growth of B. Nothing is said about the precise means by which one population affects the other, and thus, by this scheme, quite different mechanisms of interaction will be classified in the same way; this is not altogether undesirable, of course. A typical scheme of such classification is given by Odum (1).

I am going to retain the foregoing scheme, but in addition, as I have suggested elsewhere (2), the scheme will be combined with another that names interactions as direct or indirect. Direct interactions are those for which physical contact of individual organisms from the two different populations is a necessary part of the interaction. Indirect interactions require no such contact, but rather are those interactions which occur when changes in the abiotic environment produced by the activities of one population affect the growth rate of the other, and vice versa. Direct interactions are thus physical in nature, whereas indirect interactions are chemical in nature.

The scheme of naming binary interactions based on these two sets of criteria is shown in Figure 1. This figure is largely self explanatory and most of the names used are familiar, although not every ecologist would attach the exact same meaning to several of them that the figure does. For example, some ecologists use antagonism to refer to any interaction that has a negative effect but in the figure, antagonism means that each member of the pair exerts a negative effect on the other.

In two cases, however, I have used words which are new or deviate from common usage. The interaction which results when population B grows on products of lysis of cells of population A, the lysis being caused by exoenzymes released by population B, is called eccrinolysis. This is a word which I got from discussions with C. Takoudis, S. Pavlou, and R. Aris. Eccrinolysis is typified by the interaction of myxobacteria with certain other bacteria; see, e. g., Kaiser et al. (3). The word which deviates from common usage is feeding, which is here used in preference to predation. Predation has connotations of hunting and one-on-one action which do not characterize all of the interactions that I call feeding. I agree that feeding is too general a word to be used as Figure 1 uses it, and I hope that someone can suggest a better word to replace it.

Very often the interaction between a pair of populations will be more complicated than any one of the interactions named and described in Figure 1. When we are confronted with such situations, it seems best not to try to invent new words to describe them but rather to state what combination of the interactions of Figure 1 are involved. For example, consider a situation where a by-product of the metabolism of one population acts as a growth factor for a second population, and where the two populations consume a common substrate to supply their needs for carbon and available energy. The interaction between the populations is neither commensalism nor competition, but we do not invent a new word to describe it; instead, we say that it is commensalism plus competition. When the interaction between two populations is fully described by just one of the items listed in Figure 1, it is convenient to emphasize that fact by saying that the interaction is pure.

Effect of presence of B on growth rate of A	Effect of presence of A on growth rate of B	Qualifying remarks	Name of interaction
-	-	Negative effects caused by removal of resources	COMPETITION
-	○		
-	-	Negative effects caused by production of toxins or inhibitors	ANTAGONISM
-	○		AMENSALISM
-	+	Negative effects caused by production of lytic agents; positive effects caused by solubilization of biomass	ECCRINOLYSIS
+	○	Positive effect caused by production by B (host) of a stimulus for growth of A (commensal) or by removal by B of an inhibitor for growth of A	COMMENSALISM
+	+	See remarks for Commensalism. Also presence of both populations not necessary for growth of both	PROTO - COOPERATION
+	+	See remarks for Commensalism. Also presence of both populations is necessary for growth of either	MUTUALISM

-	+	B feeds on A	FEEDING - INCLUDES PREDATION AND SUSPENSION-FEEDING
-	+	The parasite (B) penetrates the body of its host (A) and therein converts the host's biomaterial or activities into its own	PARASITISM
+	+	A and B are in physical contact; interaction highly specific	SYMBIOSIS
-	-	Competition for space	CROWDING

Figure 1. Scheme of classification of binary population interactions. The roles of A and B may be reversed. Top, indirect interactions; bottom, direct interactions.

In a system inhabited by p different populations, there is a possibility for $p!/2!(p-2)!$ binary interactions to occur. A quantitative understanding of the dynamics of each of these interactions is necessary but not sufficient for a quantitative understanding of the dynamics of the whole system. Insufficiency may be demonstrated by considering as an example the feeding of a single protozoan population on two bacterial populations which compete for a common resource. Clearly, study of the two individual food chains involved here will not allow us to predict the behavior of the three-population system, because until the protozoans are actually presented with the choice of the two kinds of bacteria, we will not know whether and to what extent the protozoans will exercise preference in their uptake of food.

Discussion of the interactions

I will now discuss these various interactions in turn, beginning with the indirect or chemical ones; the principal objects of the discussion will be to summarize the state of knowledge about each and to point out research that needs to be done on each.

Competition. Probably the majority of studies of competition that have been published have dealt with what has been called pure and simple competition (4). In this type of competition, there is only one resource whose availability or concentration affects the growth rate of a competitor population, this resource is the same for both competitors in the interaction, and the growth rates are not affected by changes in the concentrations of other substances present in the common environment.

Pure and simple competition has a strong tendency to result in the exclusion of one of the competitors, and various attempts to formulate a competitive exclusion principle have appeared in the literature. One such formulation, which is supported by many experiments as well as by the predictions of mathematical models, is that pure and simple competitors will not coexist indefinitely in a system that is spatially homogeneous and that is subject to time-invariant external influences. For example, the prediction is that pure and simple competitors will not coexist in a well-mixed chemostat having a vanishingly small surface-to-volume ratio (so that the spatial heterogeneity due to the presence of the chemostat walls is negligible) if the dilution rate and temperature of the chemostat, the composition of feed to the chemostat, etc., are all independent of time. Moreover, the prediction is that not only will the competitors not coexist in a steady state in such a system but that they will not even coexist in a perpetually transient state, such as sustained oscillations of their population densities; see Fredrickson and Stephanopoulos (4) for a discussion of the literature on these points.

Further analysis of pure and simple competition suggests that populations which so compete can coexist if two sets of conditions are satisfied. First, the dependence of the growth rates of the populations on the concentration of the limiting resource must be such that there is a range (or set of ranges) of concentration which causes the first population to grow faster than the second, and another range (or set of ranges) of concentration which causes the second population to grow faster than the first. If one population grows faster than the other at all concentrations of the limiting resource, coexistence seems never to be possible. Second, the environment must be either spatially or temporally heterogeneous, and heterogeneous in such a way that it favors the growth of one population here (now) and of the other population there (then). Spatial heterogeneity can be imposed on a system, as for example, by using two chemostats with interstage flows (5) and temporal heterogeneity can be imposed on a single chemostat by periodic variation of dilution rate, feed composition, etc., as studied by many workers (6-11). Analyses of the competition equations used by the foregoing workers shows that so long as spatial homogeneity is imposed on systems, as by mixing in a chemostat, temporal heterogeneity is not generated by the activities of pure and simple competitors, so that temporal heterogeneity must be imposed from outside the system (12,13).

Now the competition equations just referred to are based on the hypothesis that we are dealing with a resource that is not self-renewing; that is, which is either a non-living substance or a biological resource which for some reason or other is not growing and reproducing. When this hypothesis is changed, and one assumes that the resource competed for is capable of self-renewal, it appears that the competitive exclusion principle stated above is no longer true.

Some years ago A. L. Koch (14) published computer simulations of situations in which two predator populations competed purely and simply for one prey population. Koch's simulations showed these three populations coexisting in what appeared to be limit cycles, a clear violation of the competitive exclusion principle stated above, but since his simulations were based on Lotka-Volterra type equations which I consider to be quite inappropriate for microbial populations, I disregarded his results and did not see their significance. Similar results published by Hsu *et al.* (15,16) were disregarded for the same reason. However, P. Waltman of the University of Iowa recently pointed out to me in a personal communication that even when Lotka-Volterra concepts are discarded entirely and Monod's model is used for all growth rates, the resulting competition equations for two predators and one prey seem to have limit cycle solutions for certain conditions of operation. Mr. Basil Baltzis has found that use of a so-called multiple saturation model for the predators, which seems to be more appropriate than Monod's model for protozoans at any rate (17), and of Monod's model for the prey, also leads to prediction

of coexistence of the three populations in what appear to be limit cycles. Hence, it is not the particular growth model that makes the difference here; rather, it is the presence of the additional trophic level that allows competing predators to coexist.

It seems intuitively evident that a necessary condition for coexistence (in a limit cycle) of two feeding populations that compete purely and simply for a growing and reproducing food population is that there must be a range (or set of ranges) of food concentration for which the first feeder grows faster than the second and another range (or set of ranges) of food concentration for which the second feeder grows faster than the first. If this is so, then what appears to be happening in these three-population systems is that the activities of the populations create temporal heterogeneity of the environment even when none is imposed from without, and when this heterogeneity favors in succession growth of first one feeder and then the other, coexistence in cycles of population density will in some cases be possible.

The predictions of these recent modeling studies should be tested by experimental research. This could be done by observing, say, the competition of two protozoan populations, which do not feed on each other, for a single, growing bacterial population in a chemostat. In addition, modeling and mathematical analyses of other situations where competition ends a food chain might be rewarding. An example might be a system where two populations compete for a growth factor which is released into the environment by the activities of a host population. This would not be expected to produce coexistence of the competitors if the interaction of each with the host was pure commensalism, but if the competitors also did something that influenced the host population, coexistence in limit cycles might be possible. Finally, these recent results suggest that further examination of pure and simple competition for a resource that does not renew itself might be profitable. It should be remembered in this connection that experimental devices like the chemostat impose spatial homogeneity on competition systems. If we did not impose homogeneity by mixing, is it possible that the activities of the populations could create spatial heterogeneity even where none is imposed? If this is possible, could it allow pure and simple competitors to coexist? I think that Prof. Lauffenberger has been working on questions like this, and I hope that he will provide us with some answers today.

There are several other points about competition that I would like to make before going on to other kinds of interaction. Competition between populations in certain environments might be pure--i. e., the only interaction between the populations--but it might not be simple because the concentrations of two or more nutrients competed for may affect the growth rates of the populations. "Nutrients" as used here means chemicals not produced by the competing populations or by others present, so there is no question here of competition for self-renewing resources. In nutrient-poor environments, the concentrations of several

substances which are complementary resources (fulfill different needs in the cellular economies) may become rate-limiting whereas in complex, nutrient-rich environments, the concentrations of several substances which are substitutable resources (fulfill the same need in the cellular economies) may become rate-limiting.

Many mathematical models of situations like the foregoing have been published; see (6, 18-25). Analyses of these models suggests that pure but not simple competition should often result in coexistence of competitors, even in systems in which spatial homogeneity of the environment is imposed and for which all external influences are time-invariant. Experimental data of Yoon *et al.* (22) on competition of *Bacillus cereus* and *Candida tropicalis* for the substitutable resources glucose and fructose show that coexistence in a chemostat is indeed possible here. Experimental testing of model predictions in situations of elementary but not simple competition is quite important, because the models used are necessarily those for multiple substrate limitation of growth, and all such models have low credibility, in my opinion.

Another form of elementary but not simple competition is what has been called (4) partial competition. In this, two populations compete for a resource whose availability affects both their growth rates, but in addition, the growth rate of one of the populations, at least, is also affected by the concentration of a substance which is exempt from competition, either because it is a resource which only one of the populations can use, or because it is a substance that is not used by either population but nevertheless exerts an effect, say of autoinhibition, on the growth rate of one of them. Gottschal *et al.* (26) have provided an elegant experimental example of the former situation with their mixotroph-obligate heterotroph system fed on a combination of acetate and thiosulfate; coexistence of these populations in a chemostat occurred even though the populations competed for acetate. A similar example is given by Laanbroek *et al.* (27). De Freitas and Fredrickson (28) have analyzed mathematical models of situations of the latter type, and these show that the production of autoinhibitors can allow competitors--partial competitors--to coexist. Finally, Miura *et al.* (29) have analyzed a mathematical model of a situation where partial competition for a resource is coupled with commensalism; again, coexistence is predicted to be possible. Broad as well as deep knowledge of microbial nutrition and physiology are probably necessities for creating successful experimental systems of partial competition, and one hopes that more people having such knowledge will attempt to apply it in the direction noted.

The last thing that I want to say about competition is that it might be rewarding to consider models of it that take into account some of the non-ideal factors that frequently complicate growth of microorganisms. By non-ideal factors I mean such things as the occurrence of maintenance, variability of biomass yield, time lag of metabolic process rates in response to changes in

environmental conditions, and so on. These things are usually ignored in mathematical models of competition, but it seems possible that their occurrence could have strong effects on the results of competition. For example, Alexander (30) mentions that capacity of a population to synthesize and store reserve foods when external food is abundant and then to use the stored food when the external supply dwindles is likely to be an important aspect of a population's competitive ability. The experiments of van Gernerden (31) on competition of purple sulfur bacteria grown in a chemostat subjected to a regimen of alternating light and dark seem to verify Alexander's suggestion. Wilder *et al.* (32) have considered recently a model of competition in which time lags of metabolic response were accounted for. But aside from these examples, I do not know of other papers which consider the effects that non-ideal phenomena might have on competitive situations. Mathematical models that we might make for such situations undoubtedly would not have high credibility, but they might make interesting predictions which could then be tested experimentally.

Amensalism and antagonism. A computerized literature search on these interactions will produce a large number of references, a fact which indicates that the importance of these interactions is recognized widely. However, examination of the references produced will show that very little mathematical modeling work or experimental work that is helpful in constructing such models has been done. The most important reason for this is probably that models of amensalism and antagonism have to be based on models for the kinetics of production and action of inhibitors and toxins, and current models for the kinetics of these processes are not of high credibility. Better models could, no doubt, be constructed from data from experiments on systems exhibiting amensal or antagonistic interactions, but the best remedy for the difficulty noted is the performance of autecological--meaning usually pure culture--work on organisms that produce toxins or inhibitors and also on organisms that are affected by such substances.

Use of simple models which are plausible but which have low credibility because they have not had extensive experimental testing and refinement suggests that a pair of populations which interact by amensalism or antagonism only, or by a combination of amensalism or antagonism with competition for a single resource, cannot coexist indefinitely in a common, homogeneous environment (28). An experimental system which involved competition and amensalism was devised by Adams *et al.* (33). They found that the two populations, both of which were strains of *Escherichia coli*, did not coexist in a chemostat and that the identity of the population which was excluded depended on the densities of the populations at the beginning of the experiment. Both of these results are predicted by simple models (28), and thus, the notion that populations which interact by amensalism or antagonism cannot coexist gains some plausibility.

Amensalism is probably a means by which some organisms or groups of organisms can defend their habitat against invaders who would compete with them for the resources of the habitat. If an association of organisms occurs in a habitat, then the conjectural principle stated above requires that these organisms shall not interact by amensalism; rather, amensalism comes into play when an invader appears. A relatively simple example of this sort of thing is shown in Figure 2. In this figure, A and B are the organisms of the association. They compete for the resources, S, of their habitat, but B is commensally dependent on A through the by-product, P, of the growth of A; P is required by B but cannot be synthesized by that organism from available precursors. This association leads to stable coexistence steady states, in spite of the competition; see the discussion of commensalism given below. In addition, the commensal population produces a substance, T, which is not inhibitory to itself or to its host, but which is inhibitory to many potential invaders of the habitat. When such an invader, I, appears, amensalism comes into play, and if the amensalism is strong enough, the invader will be destroyed. It would be very interesting to find an experimental realization of the scheme shown in Figure 2, and to see what its dynamics were.

Commensalism. One of the difficulties with the scheme of classification used here is that it does not recognize differences in mechanisms of interactions. This may also be one of its strengths, though I am not so sure about that. The difficulty is well illustrated by the interaction of commensalism; all of the following situations are commensalism, and all involve quite different mechanisms. (i) Population H releases a by-product of growth, P, which is required by another population, C, for its growth; (ii) population H produces a set of exoenzymes, E, which attack insoluble materials, S', to produce soluble substrates, S, which are then used by another population, C; (iii) population H consumes a substance, I, which inhibits the growth of another population, C; and (iv) population H produces an exoenzyme, E, which destroys a substance, I, that is toxic to another population, H. In all of these situations, and in

others that one can imagine, the host population (H) performs a function which changes the chemical environment in a way that favors the growth of the commensal population (C), but the activities of the commensal are such that the favor is not reciprocated.

Mechanisms (i)-(iv) above are different forms of commensalism, and we may think of them as elementary or simple forms of this interaction. Clearly, these forms may occur in combination with one another, and thus, even a situation of pure commensalism might be complex in the sense that several different mechanisms are involved in it. The same thing can be said about most of the other interactions named in Figure 1.

The nature of the commensal interactions just described is such that many of those that we might find in nature or construct

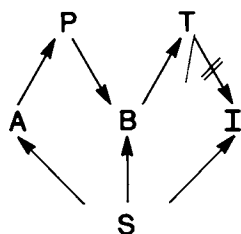


Figure 2. An association of two populations that interact by commensalism and competition, and that are protected from invasion by the production of a toxin.

in the laboratory would not be pure but would be complicated by competition of host and commensal for a substrate. Meers (34) pointed this out for mechanism (i) above and it is clear that it is likely to be true of the other mechanisms as well. The occurrence of commensalism of mechanism (i) can prevent competitive exclusion from happening, and that the association of host and commensal is stable even though they compete has been demonstrated convincingly both by experiment and by mathematical models; see Megee *et al.* (35), Gottschal *et al.* (26), Miura *et al.* (29,36). I would think that the other kinds of commensalism listed above would also permit competing host and commensal populations to coexist.

Reilly (37) pointed out another set of complications that often affect commensal systems; this was suggested by some experiments performed by Chao and Reilly (38). The complications that Reilly mentioned arise from the production of metabolic by-products by the commensal population that have effects, either stimulatory or inhibitory, on the host population. The production of such substances changes the interaction of pure commensalism into an interaction of pure mutualism or proto-cooperation, or into a combination of commensalism and amensalism. Reilly presented computer solutions of the differential equations for various model systems of this type, and more recently Sheintuch (39) made a detailed analysis of commensal systems complicated by the production of substances having inhibitory effects.

In spite of the likelihood that the foregoing complications will occur, there are probably a fair number of situations where commensalism is pure or relatively pure; that is, not much complicated by competition or by the production of substances by the commensal which affect the host. As an example, I cite the situation studied by Lee *et al.* (40). The organisms used, *Lactobacillus plantarum* and *Propionibacterium shermanii*, are associated together in the manufacture of Swiss cheese. The potential for competition of these organisms is present, for both can use, say, glucose as the source of carbon and available energy. However, *P. shermanii* can substitute lactic acid for glucose, and in fact, it was shown (41) that this organism takes up no glucose when sufficient amounts of lactic acid are present. Hence, the lactic acid produced by *L. plantarum* is used by *P. shermanii*, and by its preference for lactic acid over glucose, *P. shermanii* avoids competition with *L. plantarum*, although it does so at the expense of becoming commensally dependent on the latter organism. One would expect that many situations where a population having the capacities to use several to many substitutable resources and to exhibit substrate preference--a generalist population--forms an association with a population lacking these features but having the ability to grow rather rapidly in certain rather specialized environments--a specialist population--occur in nature.

Mutualism and Protocooperation. If the activities of two populations are such that each produces and excretes into the common environment a substance or set of substances which serves as required substrate or growth factor for the other, and if such substances are not supplied to the environment from external sources, then the interaction between the populations will involve mutualism. Other mechanisms giving rise to mutualism might be imagined also, but the one described, which is sometimes called syntrophism and sometimes cross-feeding, is likely to be the form of mutualism most often encountered. Experimental examples of it have been provided by Nurmikko (42), Wolfe and Pfennig (43), Slater (44), and Lamb and Garver (45), as well as by others.

Three remarks about this kind of mutualism seem pertinent. First, the fact that two organisms will grow together in a batch of medium in which they will not grow separately is often taken to be an indication that the organisms are exhibiting syntrophism. In many cases where this observation is made the inference is no doubt correct. But even if it is valid, it does not follow that the syntrophism can be put to use in, say, a chemostat type of apparatus. I have shown elsewhere (2) that in order for mutualistic steady states to be possible in a chemostat it is necessary that the production and consumption of the substances which produce the interaction must be such that more of them is produced than is consumed. If that is the case, the system is supercritical, and mutualism can produce a steady state of coexistence in a chemostat. But if the system is only critical or subcritical, no such steady state is possible. Hence, if we wish to exploit a situation of syntrophism in a chemostat, we have to be sure that the situation at hand is supercritical or the attempt at exploitation will fail.

The second point is that even for syntrophic pairs of organisms which are supercritical, the steady state of washout from a chemostat is always stable with respect to small perturbations (46). Therefore, the steady state of coexistence of the populations cannot be stable with respect to all large perturbations, so coexistence of the partners is always menaced by large perturbations of their system.

The third point is that there will often (always?) be two coexistence steady states for a pair of syntrophic organisms in a chemostat. In one of these, the only interaction between the populations is mutualism but in the other, some other interaction, such as competition for a nutrient supplied from outside the system, occurs also. It turns out that the steady state of pure mutualism is unstable always (46), so that if we wanted to study it we would have to try to stabilize it by adding some controls to the chemostat.

Protocooperation differs from mutualism in that in mutualism neither population can survive without the other whereas in protocooperation one or both populations can survive without the other. One could define two sub-cases of protocooperation, depending upon whether the presence of the second population is necessary for

survival of one population or neither population. The example provided by Wilkinson et al (47) seems to be of the former kind of proto-cooperation. Here, a Pseudomonas species produces methanol from methane, and is strongly auto-inhibited by the alcohol; a Hyphomicrobium species consumes the alcohol and thus releases the Pseudomonas from auto-inhibition. The interaction may be somewhat more complex, for Wilkinson et al. were unable to grow their Pseudomonas in pure culture, and two other populations, an Acinetobacter species and a Flavobacter species, were present also in their mixed culture system and may have played some role in it.

It appears that removal of inhibitory substances plays a large role in many proto-cooperative interactions that we can imagine, and when we attempt to construct mathematical models of these interactions we are faced with the difficulty that we do not have models for the kinetics of inhibitory action in which we can place a lot of confidence. Advancement of the theory of proto-cooperation therefore would seem to depend on advancement of autecological knowledge of the kinetics of inhibitor action.

Eccrinolysis. Construction of theories of this interaction is faced with difficulties similar to those facing construction of theories of proto-cooperation, but the difficulties are even more severe. In order to construct such a theory, we would need knowledge of the kinetics of formation of exoenzymes by the one population and of the kinetics of action of those enzymes on the other population of the pair. The kinetics of both processes are complex, if we may judge from some recent attempts at modeling exoenzyme production and action presented by Van Dedem and Moo Young (48), and thus, it is not surprising that attempts to make models of systems exhibiting eccrinolysis seem not to have been made. The interaction is probably of importance in some natural systems, for it must be involved in the cycling of minerals. Therefore, attempts to study it quantitatively should be made.

We turn now to direct interactions between pairs of microbial populations.

Feeding. The first thing to be said about this subject at the present time is that insufficient attention has been paid to the differences in the modes of feeding exhibited by phagotrophic microorganisms. Such differences may be illustrated by considering the feeding of Didinium nasutum, Dictyostelium discoideum, and Tetrahymena pyriformis, all organisms which have been used in laboratory studies of what is usually called microbial predation.

Didinium nasutum is a ciliated protozoan that was used by Gause (49) in his seminal studies of microbial interactions, and many subsequent studies using this organism have been made; for a resume of literature, see Berger (50). Didinium feeds by attacking and ingesting other protozoa, normally Paramecium, which it encounters during its swimming activity. Attacks are on one Paramecium cell

at a time, and chemotaxis seems to play a role in these (51,52). Feeding is selective both in regard to differences in the frequency of attacks on preferred and non-preferred food as well as in regard to differences in the percentages of unsuccessful attacks on different organisms (50,52). It seems quite appropriate to apply the term predation to this kind of feeding behavior. It should be noted that Didinium is not what Slobodkin (53) has called a "prudent predator," for it commonly makes the potentially lethal mistake of consuming all of its prey when it is inoculated into a batch of them (49,54,55).

Dictyostelium discoideum is an acellular slime mold that has been used much by biologists studying such processes as chemotaxis, cell aggregation, and morphogenesis. Feeding forms of this organism are amoebae, and in natural situations, these glide over solid surfaces and engulf bacterial cells, their food, when they encounter them. Tsuchiya et al. (56) grew this organism on bacteria in liquid culture in chemostats, and they observed the oscillations of population densities that theoreticians had been predicting for so long. Dr. Bazin has been working with this organism in recent years, and I hope he will tell us more about it.

Tetrahymena pyriformis is a ciliated protozoan whose feeding has been studied by many workers; a recent literature survey is given by Swift et al. (57). A cell of T. pyriformis has a buccal cavity which has a large undulating membrane on one side and three smaller, moving membranes on the other. The beating of these membranes directs water into the buccal cavity, and particles, especially bacteria, suspended in this water are collected by the organism if they are of appropriate size, neither too large nor too small. It would seem that this kind of food-collecting apparatus should have no ability to select particles except on the basis of properties that are hydromechanically significant, such as size, shape, and density. It is not appropriate to apply the name predation to this kind of feeding, and the term suspension-feeding advocated by Jørgensen (58) will be used instead.

The remainder of my remarks on feeding will be about suspension-feeding. This is not because I consider this to be the most important kind of microbial feeding but rather because it is the kind with which I have first hand experience.

An interesting fact which emerges from many laboratory studies of suspension-feeding of Tetrahymena and similar bacterivorous protozoans is that these organisms have not been observed to consume all of the bacteria in their habitat. Hence, they are examples of Slobodkin's "prudent predators," although I will change his term to prudent feeders.

The features of a suspension-feeder's behavior which make it "prudent" are not the same for all such organisms. For example, Bader et al. (59) studied feeding on the blue-green alga Anacystis nidulans by the ciliated protozoan Colpoda steinii. [The identi-

fication of this protozoan was challenged by Frenchel (60) on the grounds that "the real *Colpoda steinii* is about 10 times smaller than that recorded in the reference (to a new handbook of suspension-feeding by Jørgensen)." I have not yet seen Jørgensen's work. Actually, Bader *et al.* made no statement about the size of their ciliate, but they used the same culture used by Drake and Tuschiya (61), and the cell volume data reported by these workers is within, comfortably so, the range of cell sizes commonly stated for *Colpoda steinii*, as by Kudo (62), for example]. When certain conditions arise in cultures of *Colpoda steinii*, its motile, feeding cells undergo morphological change and become non-motile, non-feeding cysts. Conditions which cause encystment are by no means fully understood, but they seem to include a low density of food, a high density of feeding cells, or, at intermediate densities of the two populations, some combination of the densities. Many suspension-feeders are known to form cysts, and it seems likely that all having this capacity will be found to be "prudent" feeders.

Protozoologists have not been able to confirm a few reports that *Tetrahymena pyriformis* encysts (Corliss (63)) and so this organism must be regarded to be non-encysting. Nevertheless, it appears to be "prudent" because when it is inoculated into a batch of viable but non-growing bacteria it does not consume all of them but instead only reduces the density of viable bacteria to the order of $10^5 - 10^7 \text{ mL}^{-1}$. This observation was made by Habte and Alexander (64) and confirmed by Watson *et al.* (65). Experiments reported in these papers prove that failure to consume all of the bacteria is not due to death of the protozoa, to autoinhibition of the protozoa, to exhaustion of some essential material which the protozoa get from the liquid medium rather than from feeding on the bacteria, or to loss of the protozoan's ability to feed on the bacteria. One could try to explain the results mentioned by saying that the bacteria present initially have a distribution of sizes and that bacteria falling into some domain or domains of this distribution cannot be consumed by the protozoa. For example, Fenchel (60,66) has shown that the ability of a suspension-feeder to collect latex beads is confined to beads of a certain size range, and since the same result applies without much doubt to collection of bacteria, the argument may be made that the bacteria which comprise the residuum left after viable bacterial density in a batch ceases to fall are those that are too small, or too large, or too small and too large, to be collected by the protozoans. One cannot test this hypothesis directly by measuring the changes produced in the size distribution of viable bacteria by the feeding because the density of viable bacteria present toward the middle and end of the experiment is always much less than the density of detrital particles having sizes comparable to the bacteria and which are always produced by feeding.

The foregoing hypothesis, while plausible, is contradicted by some additional experiments done by Habte and Alexander (64). They found that *T. pyriformis* failed to start collecting bacteria when

inoculated at high density into a culture of non-growing bacteria, even though inoculation of *T. pyriformis* at low density into a culture of non-growing bacteria did result in collection (the initial bacterial densities were the same in both experiments). I do not think that the observed failure to start feeding in the high density case is an artifact to be attributed to the procedures used to prepare the protozoan inoculum, although that does need to be checked out.

An alternate working hypothesis which is suggested by the foregoing discussion is that *T. pyriformis* cells possess sensing and control mechanisms which lead to cessation of their feeding activity under certain conditions of environmental state. A corollary of this hypothesis is that *T. pyriformis* cells which do not eat bacterial cells under one set of conditions can eat these cells--the same ones--under a different set of conditions. Testing of these different hypotheses is something that we are trying to do at the present time.

Additional adaptations which make microbial feeders "prudent" or which allow microbial "predators" to coexist with their "prey" are discussed in a recent review by Alexander (67).

Cessation of feeding, whether it be caused by encystment or by some process that is not accompanied by a morphological transformation of the feeders, implies that there is some threshold density of food. The threshold density is such that feeding will stop (or fail to start) if the density falls (or is) below the threshold density. One would expect that the threshold density of food would depend on the identities of the feeding and fed-upon populations as well as on such things as the composition of the medium. However, there is some evidence that in addition to these factors the threshold density of food changes with the density of the feeders themselves. For example, in the experiment of Habte and Alexander cited above (64), *Tetrahymena* cells inoculated at high density failed to start feeding whereas *Tetrahymena* cells inoculated at a low density did start, and this is evidence that the threshold density of bacteria is raised by increase of the protozoan density. Bader *et al.* (59) reached similar conclusions about thresholds for encystment of *Colpoda steinii*, and additional evidence from the literature could be cited.

Results such as these suggest that the threshold relation between the two densities might be as shown in Figure 3. Herein, feeding will occur if the combination of densities lies above and to the left of the curve but feeding will not occur if the combination lies below and to the right of the curve.

The curve shown is drawn with a horizontal asymptote because, if the density of the feeding population is sufficiently low, there can be no effects of crowding in this population. Under such conditions, the threshold density of the fed-upon population--if there is such a threshold density--must be independent of the density of the feeding population. The curve is drawn with a vertical asymptote, also. This is because one expects that, under very

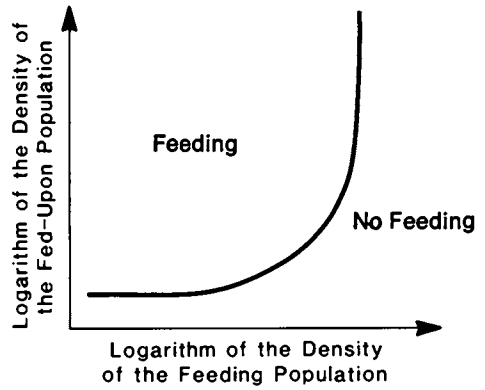


Figure 3. Conjectural relation between densities of feeding and fed-on population where cessation of feeding by a "prudent" feeder occurs.

crowded conditions, the best thing for a feeding population to do would be to stop eating and so prevent further increase of crowding. Under such conditions, there is no threshold density of the fed-upon population, of course.

Figure 3 must be regarded almost entirely as speculation, since, so far as I know, a complete figure like it has never been established for any pair of microorganisms. Salt (68) gave data for the predator-prey system Woodruffia metabolica-Paramecium aurelia, but these are of limited extent and do not show the asymptotes of Figure 3. Bader *et al.* (59) gave a figure for conditions of population densities which lead to encystment of the suspension-feeder Colpoda steinii when it feeds on Anacystis nidulans. Their data do suggest that asymptotes exist, but the data are insufficient to prove that they do, and in addition, are badly scattered. Threshold and intraspecific crowding phenomena are of fundamental biological and ecological significance, and so work to clarify the picture that we have of them now should be pursued with vigor.

If there is indeed a threshold density of bacteria below which protozoans like Tetrahymena do not feed, then it follows that growth and feeding of such organisms cannot be described by Monod's model of growth (69). A model that suggests itself for situations like this is

$$\phi(b) = \begin{cases} 0 & b \leq b_t \\ \frac{\phi_m(b - b_t)}{L + b - b_t} & b \geq b_t \end{cases} \quad (1)$$

where $\phi(b)$ is the feeding rate per protozoan cell when the bacterial density is b , b_t is the threshold density of bacteria, and ϕ_m and L are model parameters, the former being the maximum, or saturation value, of $\phi(b)$. Models like this are inconvenient from the mathematical and computational point of view, however. The multiple saturation model of Jost *et al.* (17) is

$$\phi(b) = \frac{\phi_m b^2}{(L_1 + b)(L_2 + b)} \quad (2)$$

and it avoids the mathematical and computational difficulties inherent in use of an explicit threshold model, like Equation (1). Equation (2) does not have a threshold value of b , of course, but it does predict that

$$\lim_{b \rightarrow 0} \frac{d\phi}{db} = 0 \quad (3)$$

which is characteristic of a true threshold model but not of Monod's model. It has been shown that the multiple saturation model does a much better job of correlating data for feeding of Tetrahymena on bacteria than does Monod's model (17,70,71,72).

As pointed out above, Tetrahymena pyriformis consistently fails to clear batches of water of bacteria, and the explanation for this may be that some of the bacteria are too small or too large to be captured by the protozoans. If this is the case, then there is no threshold density of the bacteria, of course, so there would be little justification for using models like Equations (1) or (2). In this circumstance, what one needs to do is to divide the bacteria into sub-populations, one which is eaten by the protozoans and one or more which is (are) not eaten by them. Monod's model might be assumed for feeding of the protozoans on the sub-population of bacteria that they can eat, and models for transfer of bacteria from one sub-population to another would be needed, also.

Actually use of models like those that we have been discussing can probably never yield better than order-of-magnitude predictions of population densities in dynamic, transient situations. Recent studies of the responses of Tetrahymena pyriformis to sudden changes in the bacterial density of its surroundings reveal phenomena (57,65) which seem to require partial differential equations rather than ordinary differential equations for their accurate description.

Finally, it should be mentioned that feeding by protozoans would be expected to exert strong regulatory effects on the bacterial populations on which they feed, especially if these latter populations compete with one another for nutrients. Jost *et al.* (17), for example, found that feeding of Tetrahymena pyriformis on Escherichia coli and Azotobacter vinelandii in a chemostat seemed to lead to coexistence of the three populations in a perpetually transient state; in the absence of the protozoans, however, Azotobacter was excluded by E. coli.

Clearly, an important factor to be considered in situations like the foregoing is the possibility that the protozoans may exhibit preference for one bacterial species over the other. As mentioned previously, it seems likely that food preference by suspension-feeding microorganisms must be based entirely, or almost entirely, on differences in hydromechanically significant properties like size, shape, and density, of the food organisms. Experiments in which protozoans are presented with choice of food, the food organisms differing in the properties noted, need to be done. We are currently presenting Tetrahymena pyriformis with E. coli and A. vinelandii, these being bacteria whose sizes are quite different. But experiments in which a suspension-feeder is presented with bacteria having the same size and shape, but differing in some properties that are not hydromechanically significant, need to be done, too. One expects no preference in such cases, and the one experiment of the kind that I know of showed no preference

(73), but more data of the same kind are needed before one can conclude that food preference by suspension-feeders is based solely on differences of hydromechanically significant properties of food organisms.

Parasitism. In this direct interaction a parasite cell or particle attaches itself to a host cell and makes a partial or total penetration into it, where it then uses the host's biomass or metabolic activities to grow and reproduce itself. Examples are provided by the parasitism of viruses on bacteria and other microorganisms, by the parasitism of the very small bacterium Bdellovibrio on other bacteria, and by the parasitism of bacteria on protozoa (30,74,75). Parasitism is characterized by a variable but always high degree of host specificity. That is, a given parasite is able to infect only a limited number of hosts, and in some cases, the number may be small indeed.

A number of mathematical models for host-parasite relations have been published. For references to literature appearing before 1977, see Fredrickson (2). A more recent model has been given by Levin et al. (76).

Parasitism can serve to regulate competition between different host populations. An example is provided by the work of Levin et al. (76). They found that parasitism by the virulent bacteriophage T2 on two strains of Escherichia coli stabilized the competition of the strains for sugar, and allowed the competitors to coexist in a chemostat. One of the strains was susceptible to infection by T2 but the other was not.

A most interesting aspect of the virus-bacteria host-parasite interaction is the tendency for genetic changes of the populations to keep altering the dynamics of the interaction. This is well illustrated by some additional work of Chao et al. (77). A host bacterium B_0 (a strain of E. coli) and a bacteriophage T_0 were introduced into a chemostat; B_0 was susceptible to infection by T_0 . Mutation of B_0 produced a new strain of bacteria, B_1 , which was not susceptible to infection by T_0 . However, mutation of the phage produced a new virus, T_1 , which was capable of infecting both B_0 and B_1 . A second mutation of the bacteria produced a third strain, B_2 , which was immune to infection by T_0 and T_1 . In these experiments, the various strains of bacteria competed with one another for sugar, but the presence of the parasites prevented competitive exclusions from occurring. When a strain of bacteria that was not susceptible to infection by any of the parasites was present, sugar concentration was low and bacterial and phage densities were high. However, when all strains of bacteria present were susceptible to infection by the phages, sugar concentration was high and bacterial and phage densities were low. These observations of Chao et al. (77) suggest that the host-parasite relation is a kind of genetic race between the two groups of organisms. Undoubtedly, analogous situations occur with other intermicrobial interactions, and efforts to detect and analyze such situations would very likely prove to be most fruitful.

Symbiosis. This is a direct interaction between two microbial populations which is characterized not only by the mutual (even if imperfectly understood) benefits which it confers upon the partners in the association but also, like parasitism, by its high degree of specificity. That is, the two partners are more or less uniquely adapted to live together, and it is impossible or very difficult to replace one of the partners in the association by another organism of similar kind. Undoubtedly, syntrophism is involved in many microbial symbioses, and perhaps models like those for this mutualistic interaction would be applicable to symbiosis. Quantitative models for symbiosis seem to be non-existent at the present time, however.

Crowding. This interaction is important when population densities become so large that the availability of space becomes a limiting factor in the growth of the populations. The inter-specific interaction of crowding is probably not of much importance in situations where the interacting populations are suspended in a liquid medium, because densities therein are not likely to become so high that availability of space becomes a rate-limiting factor for both populations. Intraspecific crowding can become important in liquid cultures, it appears; the existence of the vertical asymptote in the graph of Figure 3 is an example of an effect due to intraspecific crowding.

Interspecific crowding may be of great importance when we are dealing with systems in which much surface area, upon which the organisms attach themselves, is present. A good deal of effort has been expended in recent years to understand the mechanisms involved in attachment of organisms to surfaces. The mechanisms are complex, even when only a single population is involved, for the density of attached cells is found to depend on the identity and physiological state of the organism, the identity of the material of which the surface is made as well as the prior treatment of the surface, the composition of the liquid medium adjacent to the solid surface, the density of the organisms in the liquid medium, and the time of contact between the suspension of organisms and the surface (78). Familiar concepts that apply to adsorption of molecules on surfaces, like that of the active site, seem not to apply, and this means that the Langmuir-Hinshelwood model of adsorption, or one of its generalizations, is not likely to apply, either. Instead, it seems that we need to construct dynamic stochastic models which will make the probability of attachment of one cell to a given area of surface in a short interval of time dependent upon the number of cells already attached to that surface as well as to the density of cells present in the bulk liquid, etc. Since I am not aware that models like this have been worked out even for single populations, I cannot say anything meaningful about models for competition of two populations for

space on a solid substratum. We are trying to study this interaction in our laboratory at the present time, but it is not an easy thing to do.

It was pointed out above that "crowding" as I have used the term refers to an interspecific interaction but that biologists often use the term for an intraspecific interaction. The context will make it clear in most cases which kind of interaction is being referred to, so there should be no difficulty in using the same word for two different kinds of situations.

Summary and discussion

The foregoing discussion shows that improved understanding of interactions between microbial populations will require research in a number of related areas. A partial list is as follows.

Much work remains to be done on the autecology of microbial populations; that is, on the responses of individual populations to changes in their environment and on the changes produced in the abiotic environment by the activities of such populations. Of particular importance insofar as osmotrophic microorganisms are concerned is research aimed at providing good models for the effects of multiple nutrient limitation on growth rates, for the kinetics of subcellular processes in general, for the kinetics of formation of extracellular chemicals and enzymes, for the kinetics of action of inhibitors, toxins, and lytic enzymes, etc. More work is needed on the autecology of phagotrophic microorganisms, also. The mechanisms that make such organisms "prudent" feeders need to be established and compared and the question of the extent to which they select their food needs to be examined further.

Almost all attempts to construct mathematical models of population interactions assume that the populations present are entities of fixed genetic constitution. If they allow for the occurrence of mutation, it is almost always in the sense of assuming that a mutant of given properties has formed, and then trying to see how the system of mutant, wild organism, and any other organisms present, will evolve in time. Models which are built on some of the exciting new information that microbial geneticists have provided need to be developed and applied to systems of interacting populations. High priority should be given to producing models which take into account mechanisms of mutation and genetic recombination.

Several binary interactions have been neglected by people who take a quantitative, mathematical approach to such processes. Amensalism, antagonism, and ecrinolysis are indirect interactions which fall into this category, and there is room and motivation for much work on them. In addition, there are many elementary mechanisms of commensalism, mutualism, and protocoeperation that have been neglected. Among the direct interactions, nothing quantitative is known about crowding and symbiosis, and the former interaction, at least, should be made the object of study quite soon.

New experimental techniques and apparatus for studying population interactions need to be developed. Alternate and improved methods of obtaining census data on systems containing two or more populations are critical needs, and improved, automated means of making chemical analyses of abiotic media would be most helpful, too.

New mathematical techniques for dealing with the systems of nonlinear differential equations that result from models of population interactions need to be found. Discussions with mathematicians make it clear that techniques which would seem to be useful have not been much developed, so rapid progress is not to be expected in this difficult line of endeavor. However, some progress has been made. For example, Stephanopoulos (79,80) has shown how the theory of the Poincaré index can be applied to the equations of binary population interactions. The problem with this technique is that it works only when the problem can be reduced to two ordinary differential equations. Many situations of binary interaction fall into this category (79), but many do not and of course ternary, quaternary, etc. interactions do not, either.

Another line of research, entirely different from what has just been mentioned, concerns the applications of mixed cultures and of knowledge about interactions in mixed cultures. It seems to me that it would now be worthwhile to try to think of industrial operations where mixed cultures could be used to advantage. Development of genetic engineering techniques for making microorganisms capable of doing specific, assigned tasks would seem to have increased the likelihood that successful mixed culture processes can be developed, and work on developing them might now prove to be rewarding. There is also the additional field of application of models and theories of population interactions to problems of understanding the dynamics of natural ecosystems. Mitigation of pollution of lakes and streams, cleanup of oil and chemical spills, prevention of acid mine drainage, and so on, are all real and large problems, and it is reasonable to expect that application of the models and theories noted can be of help in solving such problems.

Acknowledgement

The support of the National Science Foundation, through grants ENG77-21632 and CPE-8020783, is acknowledged with thanks.

Literature Cited

1. Odum, P. "Fundamentals of Ecology", 3rd. ed., Saunders: Philadelphia, 1971, pp. 211-213.
2. Fredrickson, A. G. Annu. Rev. Microbiol. 1977, 31, 63.
3. Kaiser, D.; Manoil, C.; Dworkin, M. Annu. Rev. Microbiol. 1979, 33, 595.
4. Fredrickson, A. G.; Stephanopoulos, G. N. Science 1981, 213, 972.
5. Stephanopoulos, G. N.; Fredrickson, A. G. Biotechnol. Bioeng. 1979, 21, 1491.
6. Stewart, F. M.; Levin, B. R. Am. Nat. 1973, 107, 171.
7. Grenney, W. J.; Bella, D. A.; Curl, H. C., Jr. Am. Nat. 1973, 107, 405.
8. Chisholm, S. W.; Nobbs, P. A. "Modeling Biochemical Processes in Aquatic Ecosystems", Canale, R. P. Ed., Ann Arbor Science: Ann Arbor, Michigan, 1976, pp. 337-355.
9. Stephanopoulos, G. N.; Fredrickson, A. G.; Aris, R. AIChE J. 1979, 25, 863.
10. Hsu, S. B. J. Math. Biol. 1980, 9, 115.
11. Smith, H. L. SIAM J. Appl. Math. 1981, 40, 498.
12. Hsu, S. B.; Hubbell, S.; Waltman, P. SIAM J. Appl. Math. 1977, 32, 366.
13. Hsu, S. B. SIAM J. Appl. Math. 1978, 34, 760.
14. Koch, A. L. J. Theor. Biol. 1974, 44, 387.
15. Hsu, S. B.; Hubbell, S. P.; Waltman, P. SIAM J. Appl. Math. 1978, 35, 617.
16. Hsu, S. B.; Hubbell, S. P.; Waltman, P. Ecol. Monogr. 1978, 48, 337.
17. Jost, J. L.; Drake, J. F.; Fredrickson, A. G.; Tsuchiya, H. M. J. Bacteriol. 1973, 113, 834.
18. León, J. A.; Tumpson, D. B. J. Theor. Biol. 1975, 50, 185.
19. Peterson, R. Am. Nat. 1975, 109, 35.
20. Taylor, P. A.; Williams, P. J. LeB. Can. J. Microbiol. 1975 21, 90.
21. Yoon, H.; Blanch, H. W. J. Appl. Chem. Biotechnol. 1977, 27, 260.
22. Yoon, H.; Klingzing, G.; Blanch, H. W. Biotechnol. Bioeng. 1977, 19, 1193.
23. Stephanopoulos, G. N.; Schuelke, L. M.; Stephanopoulos, G. Theor. Pop. Biol. 1979, 16, 126.
24. Smouse, P. E. Theor. Pop. Biol. 1980, 17, 16.
25. Hsu, S. B.; Cheng, K-S.; Hubbell, S. P. SIAM J. Appl. Math. 1981, 41, 422.
26. Gottschal, J. C.; de Vries, S.; Kuenen, J. G. Arch. Microbiol. 1979, 121, 241.
27. Laanbroek, H. J.; Smit, A. J.; Nulend, G. M.; Veldkamp, H. Arch. Microbiol. 1979, 120, 61.
28. DeFreitas, M.; Fredrickson, A. G. J. Gen. Microbiol. 1978, 106, 307.

29. Miura, Y.; Tanaka, H.; Okazaki, M. Biotechnol. Bioeng. 1980, 22, 929.
30. Alexander, M. "Microbial Ecology", Wiley: New York, 1971, pp. 290; 327-368.
31. van Gernerden, H. Microbial Ecol. 1974, 1, 104.
32. Wilder, C. T.; Cadman, T. W.; Hatch, R. R. Biotechnol. Bioeng. 1980, 22, 89.
33. Adams, J.; Kinney, T.; Thompson, S.; Rubin, L.; Hellin, R. B. Genetics 1979, 91, 627.
34. Meers, J. L. CRC Critical Rev. Microbiol. 1973, 2, 139.
35. Megee, R. D., III; Drake, J. F.; Fredrickson, A. G.; Tsuchiya, H. M. Can. J. Microbiol. 1972, 18, 1733.
36. Miura, Y.; Sugiura, K.; Yoh, M.; Tanaka, H.; Okazaki, M.; Komenmushi, S. J. Ferment. Technol. 1978, 56, 339.
37. Reilly, P. J. Biotechnol. Bioeng. 1974, 16, 1373.
38. Chao, C.-C.; Reilly, P. J. Biotechnol. Bioeng. 1972, 14, 75.
39. Sheintuch, M. Biotechnol. Bioeng. 1980, 22, 2557.
40. Lee, I. H.; Fredrickson, A. G.; Tsuchiya, H. M. Biotechnol. Bioeng. 1976, 18, 513.
41. Lee, I. H.; Fredrickson, A. G.; Tsuchiya, H. M. Appl. Microbiol. 1974, 28, 831.
42. Nurmikko, V. Experientia 1956, 12, 245.
43. Wolfe, R. S.; Pfennig, N. Appl. Env. Microbiol. 1977, 33, 427.
44. Slater, J. H. "The Oil Industry and Microbial Ecosystems", Chater, K. W. A.; Somerville, H. S. Eds., Heyden and Son, London, pp. 137-154.
45. Lamb, S. C.; Garver, J. C. Biotechnol. Bioeng. 1980, 22, 2119.
46. Meyer, J. S.; Tsuchiya, H. M.; Fredrickson, A. G. Biotechnol. Bioeng. 1975, 17, 1065.
47. Wilkinson, T. G.; Topiwala, H. H.; Hamer, G. Biotechnol. Bioeng. 1974, 16, 41.
48. Van Dedem, G.; Moo-Young, M. Biotechnol. Bioeng. 1973, 15, 419.
49. Gause, G. F. "The Struggle For Existence", Williams & Wilkins, Baltimore, 1934, pp. 114-140.
50. Berger, J. Trans. Am. Micros. Soc. 1979, 98, 487.
51. Seravin, L. N.; Orlovskaja, E. E. Acta Protozool. 1977, 16, 309.
52. Berger, J. Gen. Microbiol. 1980, 118, 397.
53. Slobodkin, L. B. Am. Zool. 1968, 8, 43.
54. Luckinbill, L. S. Ecology 1973, 54, 1320.
55. Luckinbill, L. S. Ecology 1974, 55, 1142.
56. Tsuchiya, H. M.; Drake, J. F.; Jost, J. L.; Fredrickson, A. G. J. Bacteriol. 1972, 110, 1147.
57. Swift, S. T.; Najita, I. Y.; Ohtaguchi, K.; Fredrickson, A. G. paper in preparation, 1982.
58. Jørgensen, C. B. "Biology of Suspension Feeding", Pergamon: Oxford, 1966.
59. Bader, F. G.; Tsuchiya, H. M.; Fredrickson, A. G. Biotechnol. Bioeng. 1976, 18, 311.

60. Fenchel, T. Microbial Ecol. 1980, 6, 13.
61. Drake, J. F.; Tsuchiya, H. M. Appl. Env. Microbiol. 1977, 34, 18.
62. Kudo, R. "Protozoology", 5th. ed., Thomas: Springfield, Ill., 1966, p. 870.
63. Corliss, J. O. J. Protozool. 1970, 17, 198.
64. Habte, M.; Alexander, M. Ecology 1978, 59, 140.
65. Watson, P. J.; Ohtaguchi, K.; Fredrickson, A. G. J. Gen. Microbiol. 1981, 122, 323.
66. Fenchel, T. Microbial Ecol. 1980, 6, 1.
67. Alexander, M. Annu. Rev. Microbiol. 1981, 35, 113.
68. Salt, G. W. Ecol. Monogr. 1967, 37, 113.
69. Monod, J. "Recherches sur la croissance des cultures bactériennes", Hermann: Paris, 1942.
70. Bader, F. G.; Fredrickson, A. G.; Tsuchiya, H. M. "Modeling Biochemical Processes in Aquatic Ecosystems", Canale, R. P. Ed., Ann Arbor Science: Ann Arbor, Michigan, 1976, pp. 257-279.
71. Stephanopoulos, G. N.; Fredrickson, A. G. Bull. Math. Biol. 1981, 43, 165.
72. Ratnam, D. A.; Pavlou, S.; Fredrickson, A. G. paper in preparation, 1982.
73. Coleman, G. S. J. Gen. Microbiol. 1964, 37, 209.
74. Stainer, R. Y.; Adelberg, E. A.; Ingraham, J. "The Microbial World", 4th ed., Prentice-Hall: Englewood Cliffs, New Jersey, 1976, pp. 766-773.
75. Atlas, R. M.; Bartha, R. "Microbial Ecology", Addison-Wesley: Reading, Mass., 1981, pp. 273-276.
76. Levin, B. R.; Stewart, F. M.; Chao, L. Am. Nat. 1977, 111, 3.
77. Chao, L.; Levin, B. R.; Stewart, F. M. Ecology 1977, 58, 369.
78. Ellwood, D. C.; Melling, J.; Rutter, P., Eds., "Adhesion of Microorganisms to Surfaces", Society for General Microbiology: London, 1979.
79. Stephanopoulos, G. N. AIChE J. 1980, 26, 802.
80. Stephanopoulos, G. N. Biotechnol. Bioeng. 1981, 23, 2243.

RECEIVED June 1, 1982

The Role of Specialists and Generalists in Microbial Population Interactions

J. G. KUENEN

Delft University of Technology, Laboratory of Microbiology,
Julianalaan 67a, 2628 BC Delft, The Netherlands

In many environments highly specialized bacteria coexist with generalists, i.e. bacteria able to metabolize a large diversity of substrates. In order to understand the mechanisms of interaction between these types of bacteria, model experiments in continuous culture have been carried out with two typical specialists and one generalist. It could be shown that the generalist can compete successfully with specialists for growth limiting substrates when mixtures of substrates are available. Under these conditions the generalist can utilize these mixtures simultaneously. Another advantage of generalists might lie in their capability to continue to grow when the supply of different substrates alternate. In that case specialists would alternately grow and starve. Model-competition experiments indicate that, in general, the success of specialists was favoured by increased length of growth and starvation periods.

The breakdown of organic and inorganic compounds in nature is carried out by an enormous diversity of bacteria which are adapted to a variety of physical and chemical environmental parameters. In a given environment, many microorganisms may coexist which often have completely different metabolic capabilities, but sometimes also have overlapping properties. Typically, one can find highly specialized organisms, able to metabolize only one or a few compounds, coexisting with very versatile organisms, termed generalists. The latter are able to metabolize a great diversity of organic compounds.

From the ecological point of view one may ask how to explain this coexistence of microorganisms and how their respective physiological properties may give them an advantage or disadvantage under a given growth condition. Similarly, from the point of view of management of sewage treatment plants, one may ask how the

0097-6156/83/0207-0229\$06.75/0

© 1983 American Chemical Society

regime of a plant may select certain metabolic types and how this may have a bearing on properties of the plant such as susceptibility to pulse charges and loading capacity.

In order to understand the complicated reactions occurring between specialists and generalists within a complex mixture of other organisms, a thorough insight into their basic metabolic properties, that is their physiological behaviour, is needed. Unfortunately the physiology of most microorganisms is impossible to study in the very complicated mixtures in which they naturally occur. Therefore, as a initial approach, it has been necessary to study specialists and generalists in pure cultures, and in artificial composite-mixtures of organisms in order to obtain insight into their ecological niches.

When grown on their specific substrate in the laboratory, the specialists are characterized by very high specific growth rates (μ_{max}), whereas the generalists turn out to possess relatively low maximum specific growth rates on the substrates they can utilize. Even at very low concentrations of a substrate, as they generally occur in the environment, the versatile organisms grow relatively slowly.

Figure 1 shows a generalized picture of the relationship between the growth limiting substrate and the specific growth rate of a specialist and a generalist.

It may be asked whether the generalists might be able to grow faster than specialists in mixtures of substrates. However, under such conditions the generalists often show sequential substrate utilization, known as diauxie. A well known example is the growth of the bacterium *Escherichia coli* on mixtures of glucose and lactose. First the glucose is utilized, and only when this compound is completely metabolized, the enzymes needed for lactose utilization will be induced, allowing growth on lactose. Thus at high concentrations of mixtures of substrates, simultaneous utilization in this case is not possible.

One should realize that in many natural and seminatural environments concentrations of substrates are generally low, usually below the mM and even often below the μ M range. Under such conditions, the growth rate of microorganisms will be limited by the concentration of their substrates, and mixed substrate utilization might be possible. In the laboratory, growth under dual substrate limitation can be conveniently created in a flow-controlled chemostat, or continuous culture. In the growth medium supplied to the culture, all ingredients necessary for growth are in excess except for the two substrates in question. It has been shown for *E. coli* by Silver and Mateles (1) that under such conditions simultaneous utilization of glucose and lactose was possible. Analogous results have been obtained for other bacteria, such as *Pseudomonas oxalaticus* growing on mixtures of formate and acetate (2) and *Thiobacillus* strain A2 growing on thiosulfate and acetate (3). Our own work on the generalist *Thiobacillus* A2 may serve as

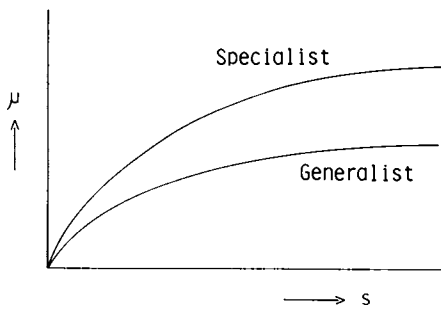


Figure 1. The relationship between the concentration (s) of the growth-limiting substrate and the specific growth rate (μ) of a typical specialist and a typical generalist bacterium growing on the same substrate.

an example. *T. A2* is a very versatile organism able to grow on at least 25-30 different organic substrates, and, in addition, also capable of autotrophic growth on inorganic reduced sulfur compounds. (See Table I). Under the latter conditions it oxidizes, for example, thiosulfate or sulfide as a source of energy while using carbon dioxide as the only carbon source for growth. When grown in batch culture in the presence of high concentrations of acetate and thiosulfate *T. A2* clearly shows a biphasic utilization of the two compounds (Figure 2). However when grown in the chemostat under growth limitation by this mixture, simultaneous utilization of acetate and thiosulfate is possible irrespective of the available ratio of thiosulfate and acetate (Figure 3). Under such conditions, acetate and thiosulfate concentrations in the culture are below the detection level. The metabolic machinery of *T. A2* adapts to the required turnover rates of the respective substrates. For example, the ability to oxidize thiosulfate is present at maximum capacity when only thiosulfate is supplied to the culture, whereas no thiosulfate respiration capacity is present when only acetate is available. Interestingly, the ability of the cells to assimilate CO₂ for cell carbon is efficiently adapted to the available organic carbon in the culture. This implies that when the ratio of thiosulfate to acetate is relatively high, acetate is used primarily as a carbon source to "save" energy for CO₂ fixation. Further work in our laboratory by others (4 and 5) has shown that simultaneous utilization of mixtures of other substrates is equally possible.

The aim of our research was then focussed on the question of whether this generalist would be able to compete successfully for growth-limiting substrates with specialists during mixotrophic growth under nutrient limitation. For our purpose we used the three model organisms shown in Table II. These included a typical generalist, namely the versatile *Thiobacillus A2*, and two specialists. The first specialist was the chemolithoautotroph, *Thiobacillus neapolitanus*, which can grow very fast in minerals-thiosulfate medium using CO₂ as its carbon source, and the second was a chemoorganoheterotroph *Spirillum G7*, which can grow very rapidly on minerals-acetate medium using acetate as carbon and energy source. (See also Table I).

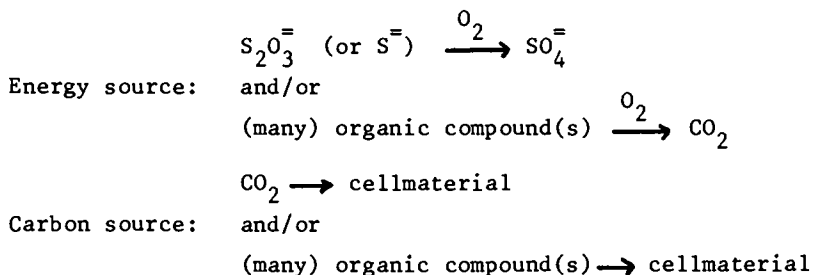
A series of experiments was carried out in continuous culture to study the competition between sets of two and three organisms. In the first experiment, *Thiobacillus A2* and *Thiobacillus neapolitanus* were each grown separately in a thiosulfate-limited chemostat. Once steady states had been established at a fixed dilution rate, the cultures were mixed one to one (v/v) and the change in the percentages of the two organisms was followed until no further change could be observed for one or two volume changes. Figure 4 shows that in minerals-thiosulfate medium, *Thiobacillus A2* was out-competed by the specialist. *T. A2* was not completely eliminated since it has been shown that the specialist excretes glycolate (6) which can be consumed by *T. A2*.

Table I

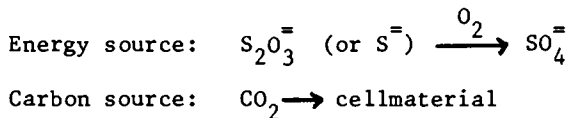
Types of metabolism of "model" bacteria used for the study of competition between "specialists" and "generalists".

GENERALIST:

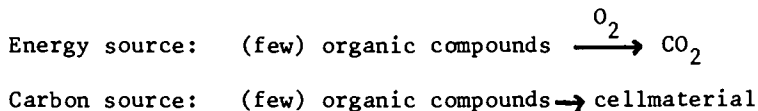
Facultative chemolitho(auto)troph ("mixotroph") (*Thiobacillus* A2)

SPECIALIST I

Obligate chemolitho(auto)troph (*Thiobacillus neapolitanus*)

SPECIALIST II

Chemo(organo)heterotroph (*Spirillum* G7)



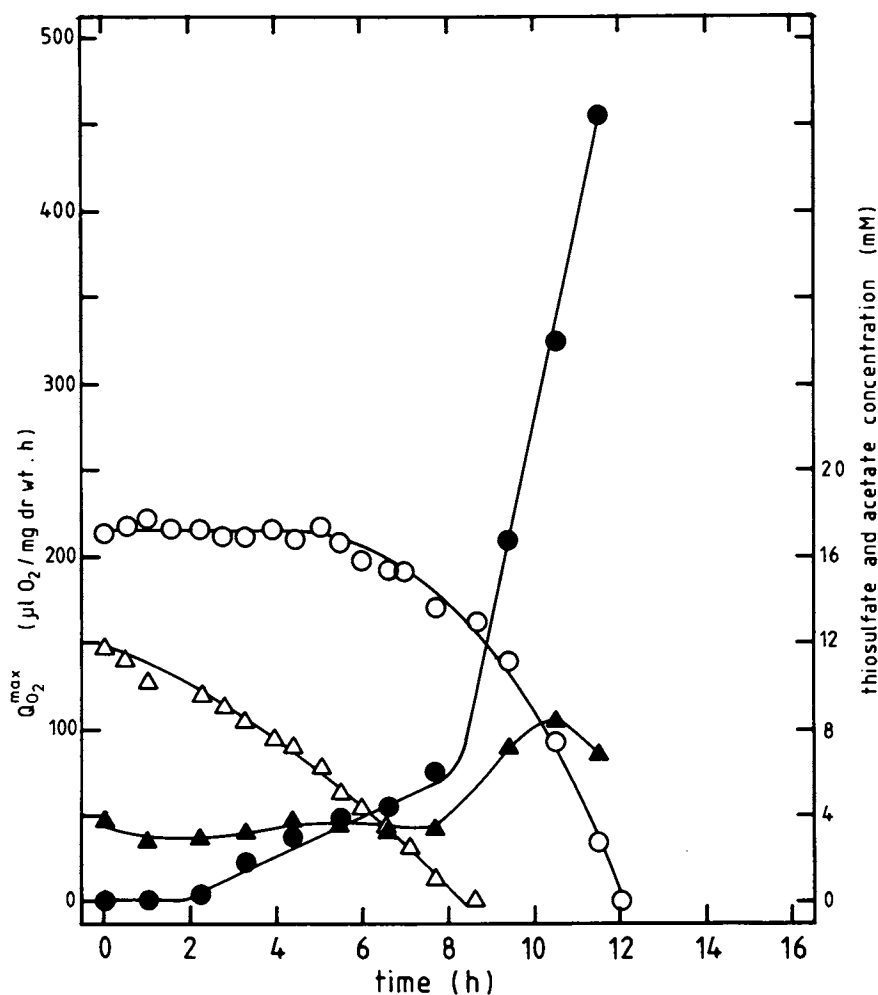


Figure 2. Maximum substrate oxidation capacities ($Q_{O_2}^{max}$) and substrate concentration during growth of *T. A2* on a mixture of acetate and thiosulfate in batch culture. The inoculum consisted of cells from an acetate-grown culture. Key: ●, $Q_{O_2}^{max}$ -thiosulfate; ▲, $Q_{O_2}^{max}$ -acetate; ○, thiosulfate concentration; △, acetate concentration. Reproduced, with permission, from Ref. 3. Copyright 1980, Springer-Verlag.

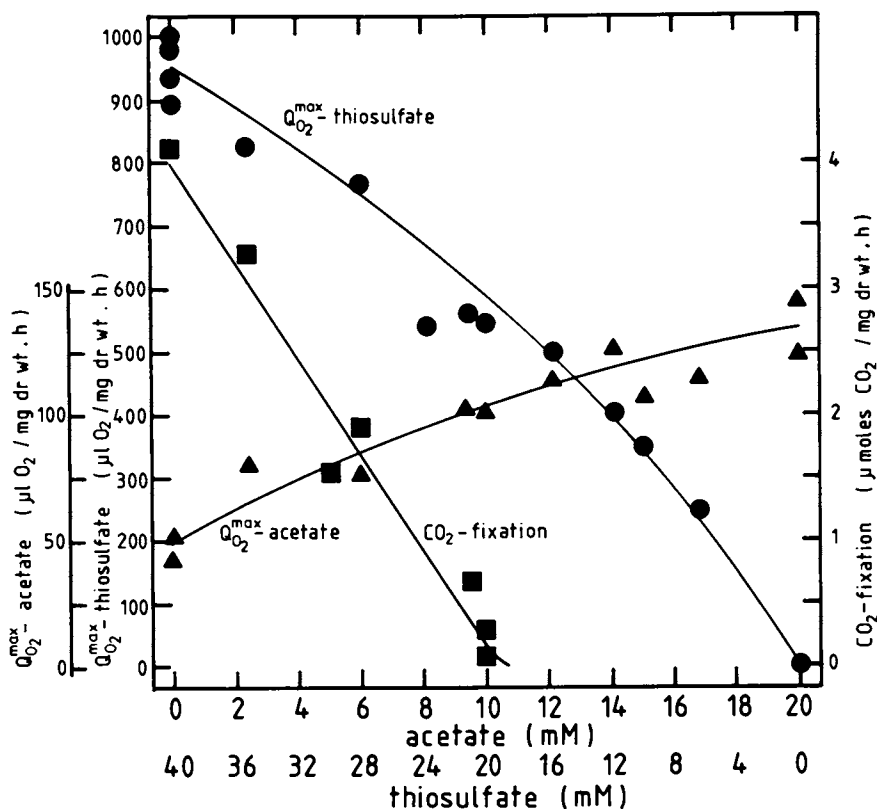


Figure 3. Maximum substrate oxidation potentials and carbon dioxide fixation potential of whole cells of *T. A2* as a function of different acetate and thiosulfate concentrations in the reservoir medium of the chemostat cultures. Key: ●, $Q_{O_2}^{max}$ -thiosulfate; ▲, $Q_{O_2}^{max}$ -acetate; ■, CO_2 -fixation potential. Reproduced, with permission, from Ref. 3. Copyright 1980, Springer-Verlag.

Data were obtained with cells from thiosulfate- and/or acetate-limited chemostat cultures in steady state at a dilution rate of 0.05 h^{-1} . Acetate and thiosulfate concentrations in the cultures were below the detection level. Cellular carbon in the cultures ranged from 110 mg C/L (40 mM thiosulfate) to 200 mg C/L (20 mM acetate).

When acetate was supplied to the inflowing medium, the number of *T. A2* cells increased since *T. neapolitanus* cannot utilize acetate. Figure 5 shows that with increasing acetate concentration the percentage of *T. A2* gradually increased and coexistence of the two organisms became possible. Above a concentration of about 10 mM acetate, the specialist was eliminated from the culture. The explanation for this lies in the ability of *T. A2* to utilize acetate and thiosulfate simultaneously under these growth conditions. With increasing acetate concentration, the absolute concentration of the *T. A2* cells increased and allowed these organisms to claim an increasingly larger share of thiosulfate. Eventually, the ratio of acetate to thiosulfate became such that *T. A2* was able to reduce the thiosulfate concentration to below the level at which *T. neapolitanus* could maintain the required growth rate, resulting in the wash out of the specialist. Very similar results were obtained with mixtures of thiosulfate and glycollate (4) or thiosulfate and glucose (5).

Competition experiments between the specialist *Spirillum G7* and *T. A2* gave analogous results. In acetate medium *Spirillum G7* out-competed *T. A2* completely. *Thiobacillus A2* out-competed the specialist when more than 10 mM thiosulfate was present in the acetate-minerals medium. Obviously, under "natural" conditions in the environment, or in sewage treatment plants, the generalist would have to compete with both specialists at the same time. Therefore, three-membered cultures were also studied. The results, as summarized in Figure 6, show that coexistence of the three organisms was possible over a large range of concentration ratio's with *T. A2* dominating the culture. The coexistence of three organisms does not agree with theoretical predictions which will be discussed below. In any case the outcome of these experiments clearly indicated that when mixed substrates are supplied, generalists have metabolic advantages which allow them to claim a "niche", that is, a right of existence in the natural environment. The validity of this generalisation was confirmed by the results of enrichment cultures carried out in the chemostat inoculated with natural samples. Table III shows the outcome of such enrichment cultures performed with different mixtures of thiosulfate and acetate. In all cases when fresh water inocula were used, a dominant culture of a generalist *Thiobacillus* was obtained. Interestingly, in 4 out of 5 cases the generalist was a facultative chemolithotroph able to grow autotrophically. However, in one case when relatively high amounts of acetate were presented to the culture, a bacterium able to obtain energy from thiosulfate but not able to fix CO₂ came to the fore. This is not surprising, since at this ratio CO₂ fixation is not required (compare Figure 3 for *T. A2*).

As mentioned before, a somewhat puzzling result of the competition experiments with the three-membered culture was that coexistence of three organisms seemed possible. In several theoret-

Table II

Maximum specific growth rates μ_{\max} (h^{-1}) of the specialized, obligately chemolitho(auto)trophic *Thiobacillus neapolitanus*, the versatile, facultatively chemolithotrophic *Thiobacillus* A2 (a generalist), and a specialized heterotrophic *Spirillum* G7, during growth in minerals medium supplemented with thiosulfate (t), acetate (a) or mixtures of both substrates (t + a). *T. neapolitanus* and *Spirillum* G7 cannot grow on acetate or thiosulfate respectively (10).

	Maximum specific growth rate μ_{\max} (h^{-1})		
	t	a	t + a
<i>T. neapolitanus</i>	0.35	-	0.35
<i>Thiobacillus</i> A2	0.10	0.22	0.22
<i>Spirillum</i> G7	-	0.43	0.43

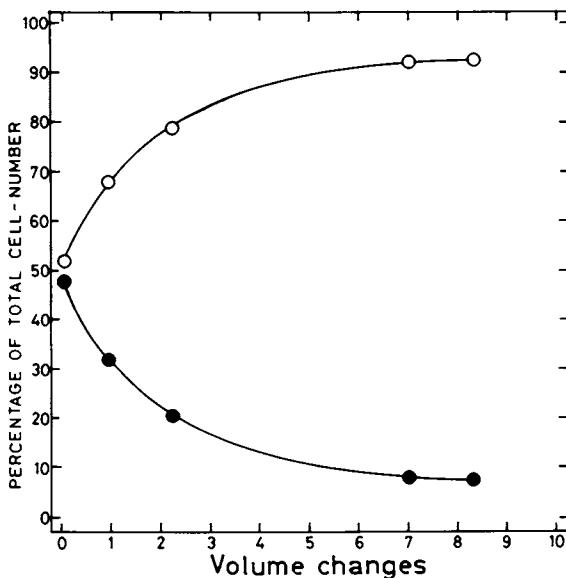


Figure 4. Competition in continuous culture between *T. neapolitanus* (the specialist) and *T. A2* (the generalist) for thiosulfate as the only growth-limiting substrate. Key: ●, relative cell number of *T. A2*; ○, *T. neapolitanus*. Reproduced, with permission, from Ref. 4. Copyright 1979, Springer-Verlag.

The chemostat was run at a dilution rate of 0.05 h^{-1} with a 40 mM thiosulfate concentration in the reservoir medium. Organisms had been pregrown separately in continuous culture at $D = 0.05 \text{ h}^{-1}$ and at zero time mixed in a 1:1 rate.

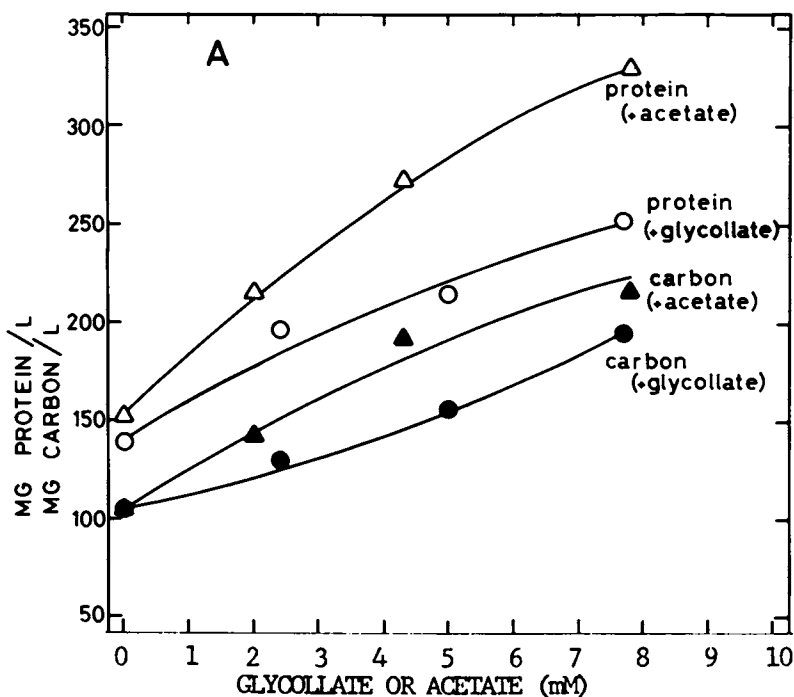


Figure 5A. Effect of different concentrations of organic substrate on the outcome of the competition between *T. A2* and *T. neapolitanus* for thiosulfate. Protein concentration and organic content in the cultures are shown, limited by thiosulfate plus acetate or glycollate. Reproduced, with permission, from Ref. 4. Copyright 1979, Springer-Verlag.

The chemostat was run at a dilution rate of 0.07 h^{-1} . The inflowing medium contained thiosulfate (40 mM) together with either acetate or glycollate at concentrations ranging from 0 – 7 mM . Relative cell numbers, protein content, and organic cell carbon in the culture were determined after steady states had been established.

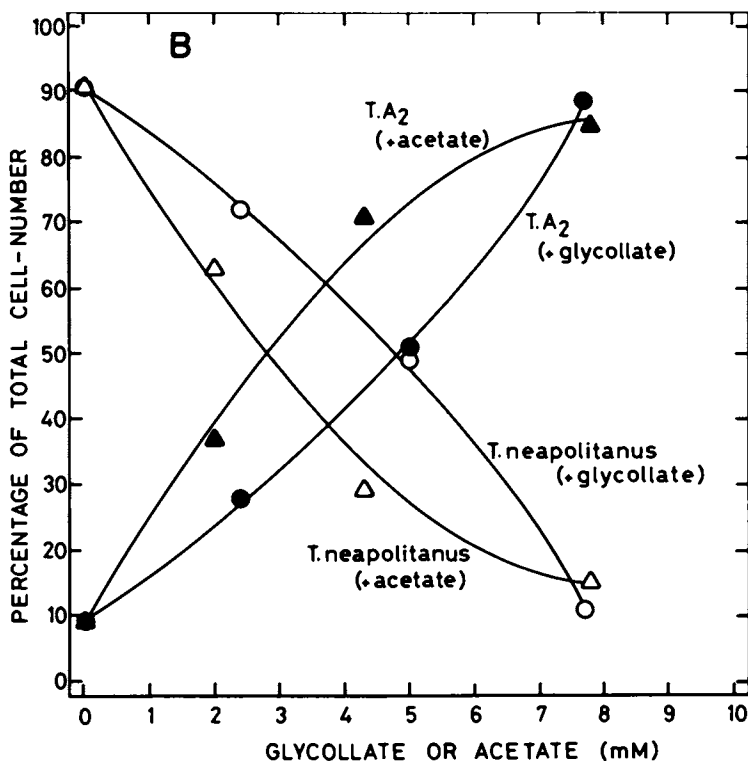


Figure 5B. Effect of different concentrations of organic substrate on the outcome of the competition between *T. A2* and *T. neapolitanus* for thiosulfate. Conditions as in Figure 2A. The percentage of *T. A2* cells and of *T. neapolitanus* cells in cultures are shown, with thiosulfate plus acetate or glycollate in the reservoir medium. Reproduced, with permission, from Ref. 4. Copyright 1979, Springer-Verlag.

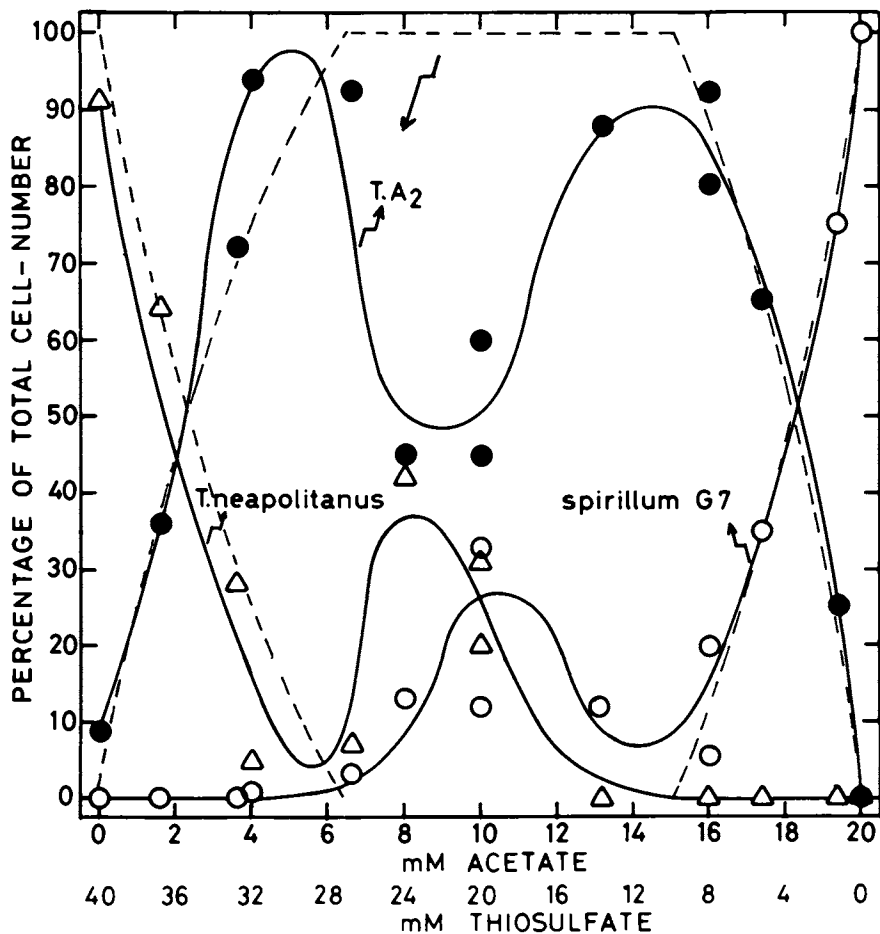


Figure 6. Results of competition between the generalist *T. A2*, and two specialists, *T. neapolitanus* and *Spirillum G7* for thiosulfate and acetate as growth-limiting substrates in the chemostat at a dilution rate of 0.07 h^{-1} . Concentrations in the inflowing medium ranged from 0–20 mM for acetate and from 0–40 mM for thiosulfate. After a steady state had been established relative cell numbers were determined. Solid line, experimental data; dashed line, outcome of the competition as predicted from mathematical modeling.

Table III

Results of enrichment cultures (I - V) from fresh water samples after 15-20 volume changes in the chemostat under dual substrate limitation of thiosulfate (t) and acetate (a) at a dilution rate of 0.05 h^{-1} , using different mixtures of t + a. Adapted from Gottschal and Kuenen, (11).

Number	sample	substrate concentration in medium (mM)	Dominant population	
			% of total	metabolic type
I	canal	30 t + 5 a	82	facultative chemolithotroph
II	canal	10 t + 15 a	75	" "
III	canal	30 t + 5 a	85	" "
IV	ditch	20 t + 10 a	50	" "
V	ditch	10 t + 15 a	86	chemolithoheterotroph

tical treatments of the growth of microbial populations on mixtures of substrates it has been predicted that the maximum number of organisms which can coexist can never be more than the number of growth-limiting substrates supplied to the culture. This holds if no interaction other than mere competition takes place in the culture. Based on previous publications of other workers Gottschal and Thingstad (7) have developed a mathematical model for growth of the three organisms in the particular case.

The model is based on simple Monod kinetics for growth. The specific growth rate of the specialist autotroph (A) on thiosulfate (s_t) is

$$\mu_{tA}(s_t) = \frac{\mu_{tA}^{\max} \cdot s_t}{K_{tA} + s_t}$$

in which s_t is the concentration of the thiosulfate and K_{tA} the substrate saturation constant of the autotroph for thiosulfate.

Similarly, for growth of the heterotroph (H) on acetate (s_a) one obtains

$$\mu_{aH}(s_a) = \frac{\mu_{aH}^{\max} \cdot s_a}{K_{aH} + s_a}$$

The growth rate for the mixotrophic generalist (M) has been taken as the sum of the two separate growth rate:

$$\mu_M(s_a, s_t) = \frac{\mu_{aM}^{\max} \cdot s_a}{K_{aM} + s_a} + \frac{\mu_{tM}^{\max} \cdot s_t}{K_{tM} + s_t}$$

As pointed out by Gottschal and Thingstad (7), this is an approximation which can only be valid at low growth rates where the relationship between μ and s is nearly linear. This model does not take into account that the generalist adapts its substrate oxidizing capacity to the ratio between the two substrates available in the mixture. This would probably lead to an over-estimation of μ_{aM}^{\max} and μ_{tM}^{\max} . It could be shown, however, that in a two-membered culture the decrease of μ_{aM}^{\max} would have a constant value since the physiological state of the generalist (M) would be constant.

Although the model allowed accurate prediction of the competition between two organisms (Figure 7 a,b), it could indeed not account for the anomaly observed in the experiments using three organisms. The dotted lines of Figure 6 describe the predicted steady state values. The parameters used in this prediction had been derived from the outcome of the results obtained from the two-membered cultures.

Several possibilities explaining this anomaly have been con-

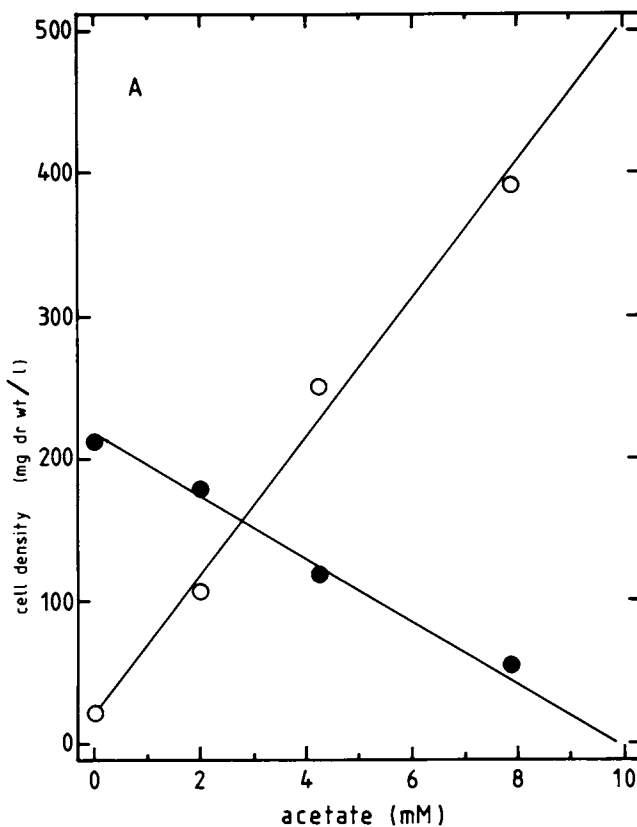


Figure 7A. Cell density of the generalist (mixotroph *T. A2*, ○) and the autotroph (specialist *T. neapolitanus*, ●) in mixed chemostat culture at steady state, growing at a dilution rate of 0.075 h^{-1} . Growth was simultaneously limited by thiosulfate (reservoir medium concentration, $S_1^\circ = 40\text{ mM}$) and by increasing concentrations of acetate in the reservoir medium ($S_a^\circ = 0\text{--}10\text{ mM}$).

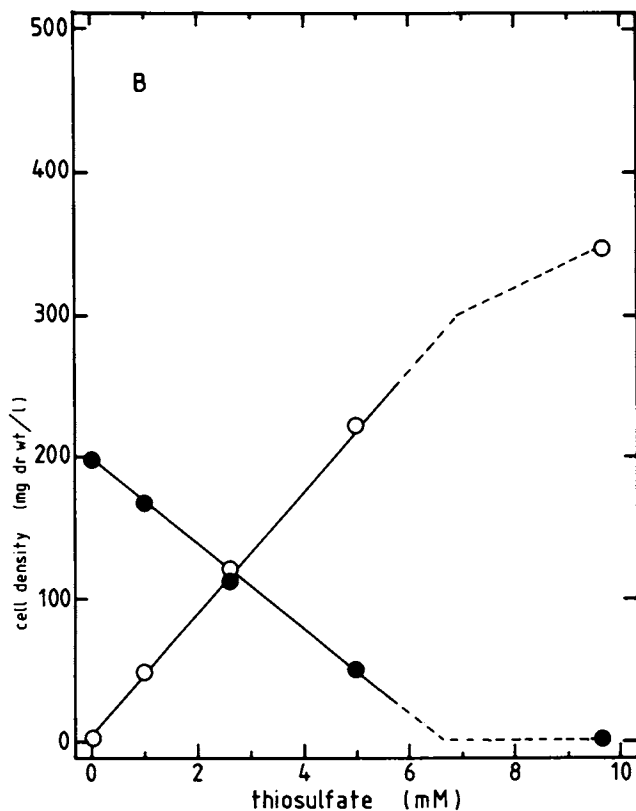


Figure 7B. Cell density of the mixotroph (○) and the heterotroph (specialist *Spirillum G7*, ●) in mixed chemostat-culture at steady state, growing at a dilution rate of 0.075 h^{-1} . Growth was simultaneously limited by acetate ($S_a^\circ = 20 \text{ mM}$) and by increasing concentrations of thiosulfate in the inflowing medium (0–10 mM).

sidered. First of all, the assumption that no interactions other than competition for the substrates occur may be incorrect. Although this possibility cannot be ruled out, it is unlikely since the spent medium from each of the pure cultures did not influence the growth of the other(s). *T. neapolitanus* did however excrete glycollate, which can be utilized by *T. A2* and by *Spirillum G7*. However, the effect of glycollate should be greatest when the concentration of *T. neapolitanus* is highest, and this is apparently not the case.

A more complicated explanation may lie in the fact, indicated above, that in the theoretical treatment, it has been assumed that the growth of *T. A2* is the sum of the separate specific growth rates on the individual substrates. As long as only two organisms are present in the culture, *T. A2* may indeed be in a constant metabolic state. However, the physiological state of *T. A2* in the presence of *T. neapolitanus* is very different from that of *T. A2* in the presence of *Spirillum G7*. At the very moment that *T. neapolitanus* is removed from the culture the metabolic state of *T. A2* will change to that found in pure culture during mixed substrate consumption (Figure 3). As a result, the assumed K_s and μ_{max} values for *T. A2* will alter and in fact it can be shown that this will make *T. A2* less competitive. As pointed out by Gottschal and Thingstad (7), it may therefore be that the rate at which the shift in population occurs in the three-membered culture is much smaller than that in the two-membered cultures. Mathematical simulation experiments show that if a shift in parameters happened, it might very well take 100 or more volume changes before a real steady state would be attained. If this were the case, changes might have taken place so slowly that they were not noticed in the actual experiments, even though, in one experiment, a measurement of ratios was made after 30 volume changes.

In spite of the discrepancy between the theoretical and practical models, it should be stressed that both models clearly indicate the ecological advantages of a generalist type of physiology.

Recent work by Laanbroek, Smit, Klein-Nulend and Veldkamp (8) shows that this phenomenon may also explain the coexistence of versatile and specialist *Clostridium* species. Furthermore, results obtained by Harder and co-workers (W. Harder, University of Groningen, unpublished) indicated that the same principle may apply to generalists and specialists among the methanol utilizing bacteria.

Mixotrophic growth of the generalists is apparently only one possible advantage of a versatile metabolism. Another possible benefit might lie in the capability of versatile organisms to grow continuously with alternating supplies of two substrates. This has also been studied in detail for the same set of three organisms shown in Table II. (9). Figure 8 gives an example of one series of experiments designed to show that the generalist can grow uninterrupted during an alternating supply of 4h thiosulfate,

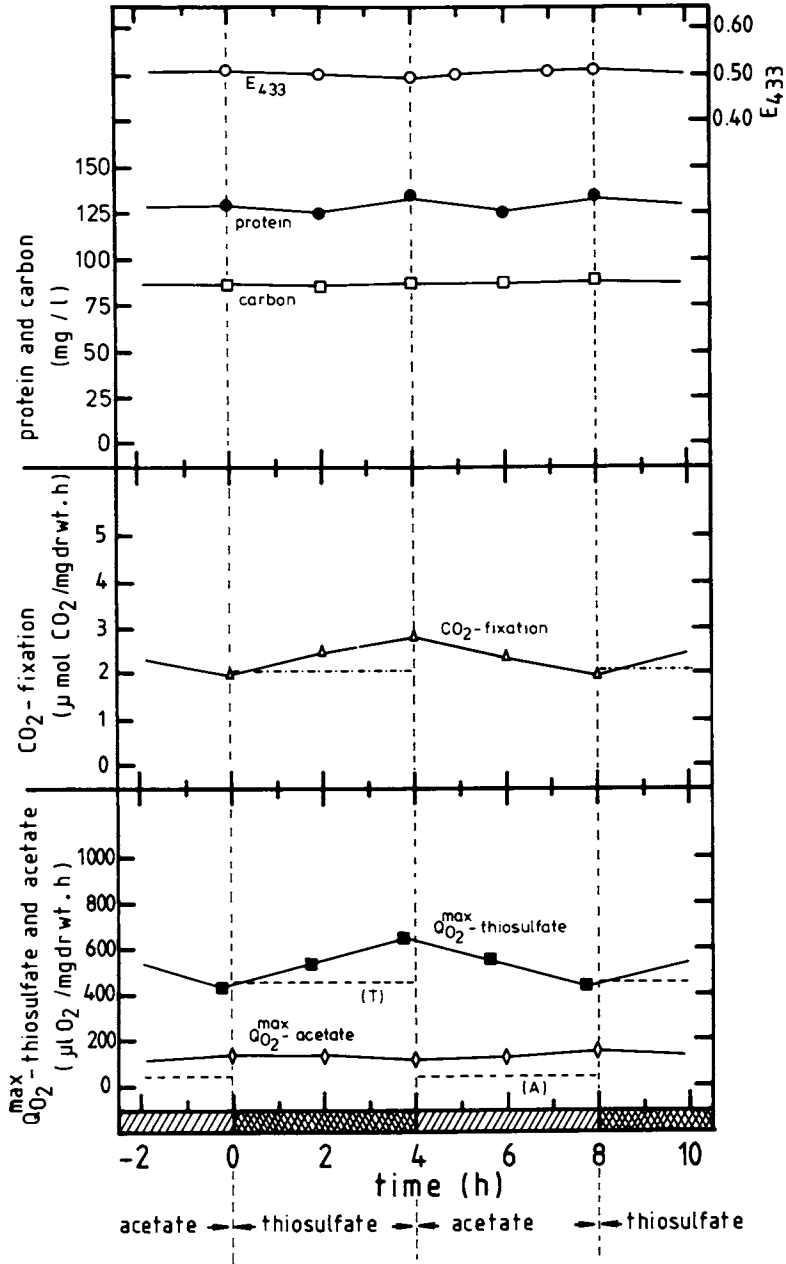


Figure 8. *T. A2* grown under alternate limitation of acetate and thiosulfate in continuous culture at a dilution rate of 0.05 h^{-1} . Thiosulfate (40 mM) or acetate (10 mM) was supplied to the culture, each for 4 h. The dashed lines indicate the minimum activities needed for uninterrupted growth. Reproduced, with permission, from Ref. 9. Copyright 1981, Society for General Microbiology.

4h acetate, in a chemostat run at a dilution rate of 0.05 h^{-1} . Under these conditions, the overcapacity of *T. A2* to oxidize either of the substrates was marginal. During the acetate period, the ability to oxidize thiosulfate was repressed more than the acetate oxidation potential was during the thiosulfate period. When the acetate period was extended relative to the thiosulfate period, *T. A2* no longer maintained a sufficiently high thiosulfate oxidation potential to permit continued growth at the same rate. As a result, population densities started to fluctuate and thiosulfate transiently accumulated.

Interestingly, the two specialist organisms grew well in pure culture on their specialist substrate under a regime of 4h substrate (thiosulfate or acetate) and 4h starvation. Of course, during the starvation period a proportion of the specialists was washed out of the chemostat, but the remaining organisms retained a very high overcapacity to oxidize the substrate, permitting them to grow instantaneously at a high rate after the starvation period.

When a competition experiment was carried out between *T. A2* and *T. neapolitanus* under alternating substrate conditions, the two organisms appeared to coexist in equal numbers. This suggested that *T. neapolitanus* would utilize practically all of the thiosulfate, whereas *T. A2* was growing on acetate only.

The explanation of this result lies in the versatility of *T. A2*. During the acetate period *T. A2* reduced its thiosulfate oxidizing capacity whilst *T. neapolitanus* was washed out but retained its high thiosulfate oxidation potential. As a result, at the beginning of the thiosulfate period, the *T. neapolitanus* population could oxidize the thiosulfate at a much higher rate than *T. A2*. Direct measurement of the substrate levels in the chemostat showed that under these conditions *T. neapolitanus* could maintain the concentration of the substrate 10 fold lower than *T. A2* was able to (Figure 9). Thus, during the thiosulfate period in the mixed culture *T. neapolitanus* could grow much faster than *T. A2*. Furthermore, the very low concentration of thiosulfate imposed by *T. neapolitanus* obviously led to a further reduction of the thiosulfate oxidizing potential of *T. A2*. In other words, the generalist was forced by the specialist to grow as a heterotroph on acetate only.

T. A2 is, however, not a specialist heterotroph and the addition of the specialist acetate-utilizing *Spirillum G7* to the two-membered culture led to wash out of *T. A2*, resulting in a coexisting population of the two specialists (Figure 10a).

Further experiments showed that an alternating supply of two different mixtures of thiosulfate and acetate led to coexistence of all three organisms (Figure 10 b,c). Obviously, under an alternating supply of specialist substrates, generalists similar to *T. A2* clearly are at a disadvantage. However, it could be shown that nature harbours organisms akin to *T. A2* which are better

American Chemical
Society Library

1155 16th St., N.W.

In Foundations of Biochemical Engineering; Blanch, H., et al.;
ACS Symposium Series; American Chemical Society: Washington, DC, 1983.

Washington, D.C. 20036

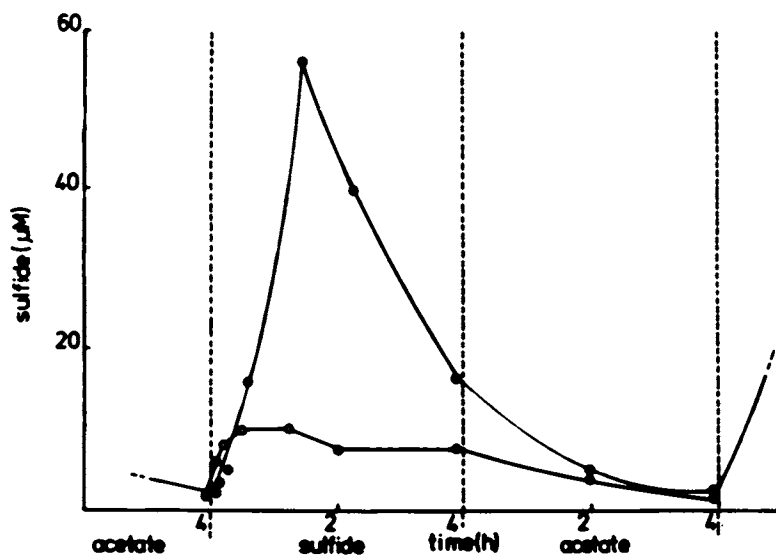


Figure 9. The accumulation of sulfide under alternate supply of 4 h acetate, 4 h sulfide to a continuous culture of *T. A2*. ○, sulfide concentration in the culture at pH 8.0; and ●, at pH 7.5. Competition experiments all had been carried out at pH 7.5. Sulfide is a substrate which, in these experiments, is entirely equivalent to thio-sulfate, but has the advantage of being detectable down to a concentration of less than 1 μM . In cultures of *T. neapolitanus* grown at pH 7.5 the sulfide concentration never increased to above 4 μM . Reproduced, with permission, from Ref. 12. Copyright 1982, H. Veenman en Zonen BV.

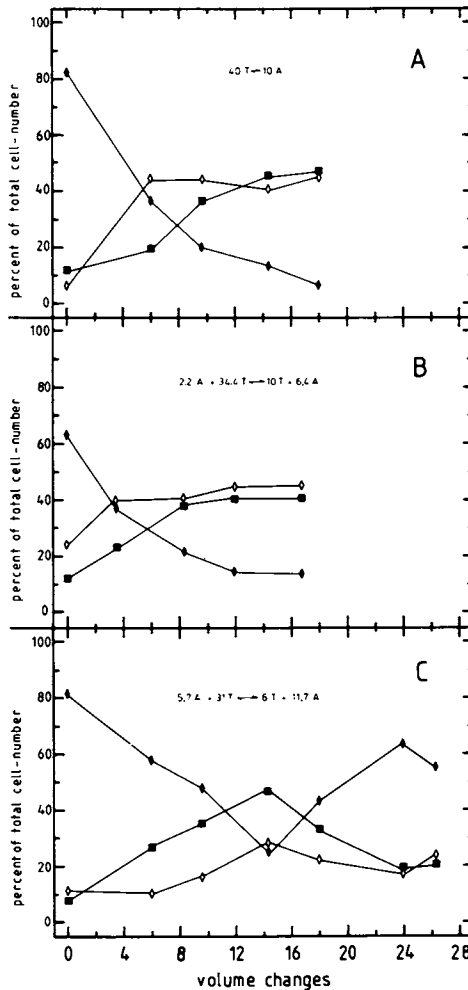


Figure 10. Competition in continuous culture between *T. A2*, *T. neapolitanus* and *Spirillum G7* for thiosulfate and acetate as growth-limiting substrates. The dilution rate was 0.05 h^{-1} with intermittent feeding of two media containing thiosulfate, or acetate, or both. These media were supplied alternately to the culture, each during 4 h. Key: ◆, *T. A2*; ■, *Spirillum G7*; and ◇, *T. neapolitanus* as percentage of the total cell number present in the culture. A: One medium contained 10 mM acetate, the other 40 mM thiosulfate. B: One medium contained 2.2 mM acetate plus 34.4 mM thiosulfate, the other 10 mM thiosulfate plus 6.4 mM acetate. C: One medium contained 5.7 mM acetate plus 31.0 mM thiosulfate, the other 6 mM thiosulfate plus 11.7 mM acetate. Reproduced, with permission, from Ref. 9. Copyright 1981, Society for General Microbiology.

adapted to the regime described in Figure 10a. When a continuous culture under this regime was inoculated with fresh water mud, a dominant population of a spirillum-shaped facultative chemolithotroph developed (9). The success of this organism was probably due to its ability to "store" acetate as a polymer (poly- β -hydroxybutyrate) in the cells. This polymer was used during the thiosulfate period as a source of carbon (J.G. Kuenen and A. Spijkerman, unpublished results). In this way, the thiosulfate utilizing spirillum could save energy for CO_2 fixation during the thiosulfate period.

The experiments described in this paper clearly show the possible advantages and disadvantages of the specialist versus generalist strategies for survival. Our present hypothesis is that specialist organisms will be successful under conditions where the turnover rate of their specialist substrate is high relative to that of other substrates. On the other hand, versatile organisms might have an advantage when the relative turnover rates of several of their growth substrates are in the same order of magnitude. Obviously when the supplies of different substrates strongly fluctuate or even alternate, the outcome of competition between specialists and generalists for growth-limiting substrates will be determined by the length of the supply periods. As yet it has not been possible to confirm these predictions with direct measurements of generalists and specialists in natural mixed cultures. At present we are developing methods for the measurement of the contributions of the different population in suitable systems, namely sewage treatment plants, which receive supplies of, for example, sulfide and organic substrates.

A better understanding of the selection of different populations in the mixed cultures of sewage treatment plants may facilitate control and management of these plants. An example may help to adstruct this point. The presence of specialist populations will improve the "resilience" of the plant to strong fluctuations, since the organisms usually possess a high overcapacity. In contrast if, during supply of sulfide and organic compounds, chemolithotrophic heterotrophs are selected, the population will become extremely sensitive to strong fluctuations of sulfide, not only because their maximum respiratory capacity is low, but also because such organisms tend to produce toxic products inhibitory for their own metabolism of sulfide. In such a case, a sudden pulse of sulfide would lead to accumulation of sulfide, subsequent formation of toxic products, and further inhibition of the sulfide oxidation, leading to even further accumulation of this compound. With prior knowledge of this selection, one might be able to absorb this peak loading, thus avoiding unsatisfactory performance of the sewage treatment plant.

Acknowledgements

Many thanks are due to my two former co-workers Dr. J.C. Gottschal and Dr. R.F. Beudeker who did most of the experimental work described in this paper. I thank Miss L.A. Robertson for correcting the English and Mrs. C.M. Paanakker-Kuipers and Mrs. I. Hagman-v.d. Bulk for typing the manuscript.

Literature Cited

1. Silver, R.S.; Mateles, R.I. J. Bacteriol. 1969, 97, 535-543.
2. Dijkhuizen, L.; Harder, W. Arch. Microbiol. 1979, 123, 47-53.
3. Gottschal, J.C.; Kuenen, J.G. Arch. Microbiol. 1980a, 126, 33-42.
4. Gottschal, J.C.; de Vries, S.; Kuenen, J.G. Arch. Microbiol. 1979, 121, 241-249.
5. Smith, A.L.; Kelly, D.P. J. Gen. Microbiol. 1979, 115, 377-384.
6. Cohen, Y.; De Jonge, I.; Kuenen, J.G. Arch. Microbiol. 1979, 122, 189-194.
7. Gottschal, J.C.; Thingstad, T.F. Biotechnology and Bioengineering 1982, in press.
8. Laanbroek, H.J.; Smit, A.J.; Klein-Nulend, G.; Veldkamp, H. Arch. Microbiol. 1979, 120, 61-67.
9. Gottschal, J.C.; Nanninga, H.; Kuenen, J.G. J. Gen. Microbiol. 1981, 126, 85-96.
10. Gottschal, J.C.; Kuenen, J.G. "Microbial Growth on C₁ Compounds"; Dalton, H., Ed.; Heyden: London, Philadelphia, Rheine, 1981, 91-104.
11. Gottschal, J.C.; Kuenen, J.G. FEMS Microbiol. Lett. 1980b, 7, 241-247.
12. Beudeker, R.F.; Kuenen, J.G. Antonie van Leeuwenhoek 1982, in press.

RECEIVED June 1, 1982

Microbial Predation Dynamics

M. J. BAZIN, C. CURDS¹, A. DAUPPE¹, B. A. OWEN, and
P. T. SAUNDERS

Queen Elizabeth College, Department of Microbiology, London, England W87AH

The specific growth rate of a microbial predator (λ) was found to be dependent upon the ratio of the prey (H) to predator (P) population densities rather than the prey density alone. Predatory amoebae of the cellular slime mould Dictyostelium discoideum were grown in single-stage and two-stage chemostat cultures with the gut bacterium, Escherichia coli as their source of food. Predator growth in the cultures was compared to each of three functions which have been proposed for λ . In addition to showing that λ changed with respect to H/P, the results indicated also that it depended explicitly on time, so that the differential equations describing the predator-prey system are probably non-autonomous.

Quite clearly, the growth of a predator population is in some way dependent upon the abundance of its prey. The most frequently cited model of predator-prey dynamics is the set of linked, non-linear differential equations known as the Lotka-Volterra equations (1). This model assumes that in the absence of predator, the prey grows exponentially, while in the absence of prey the predator dies exponentially, and that the predator growth rate is directly proportional to the product of the prey (H) and predator (P) population densities. The equations are:

$$\dot{H} = k_1 H - k_2 PH \quad (1)$$

$$\dot{P} = -k_3 P + k_4 PH \quad (2)$$

where k_i 's are constants. The specific growth rate of the

¹ Current address: British Museum (Natural History), Cromwell Road, London SW7, England

predator population (λ) according to the model is therefore directly proportional to the prey density:

$$\lambda = k_4 H \quad (3)$$

In microbiology the relationship between the specific growth rate of a microbial predator and its prey is often expressed in terms of the hyperbolic function suggested by Monod (2) for the growth of bacteria on a limiting dissolved nutrient. Applied to predation the function is:

$$\lambda = \lambda_m H / (L + H) \quad (4)$$

where λ_m is the maximum specific growth rate and L is the concentration of prey sufficient for growth at specific rate $\lambda_m/2$.

Both the Lotka-Volterra and the Monod functions for predator specific growth rate are dependent upon a single variable, the concentration of prey organisms. A third function, proposed by Contois (3) for bacterial growth as an alternative to that of Monod, when applied to predator growth takes the form:

$$\lambda = \lambda_m H / (LP + H) \quad (5)$$

In this case the specific growth rate is a function of both prey and predator density.

Using the ciliate protozoan Tetrahymena pyriformis as a predator and Klebsiella aerogenes as prey, Curds and Cockburn (4) found that of the three functional forms suggested for predator specific growth rate represented by equations (3) - (5), the Contois equation gave the best fit to their data. Dividing the numerator and denominator of equation (5) by P gives

$$\lambda = \lambda_m ((H/P) / (L + H/P)) \quad (5a)$$

showing that predator specific growth rate according to the Contois equation can be considered to be a function of the ratio of prey to predator population densities. Using catastrophe theory, analysis of results from experiments in which slime mould amoebae fed on E. coli indicated that it was this ratio that was the critical variable in the system (5).

The goal of the research we report here was to determine whether the specific growth rate of predatory amoebae of the cellular slime mould Dictyostelium discoideum feeding on the gut bacteria, Escherichia coli was dependent upon prey density alone or upon the ratio of prey to predator. Two experimental systems were employed, both based on the chemostat type of continuous culture. A chemostat is a continuously stirred tank reactor in which microorganisms grow in a homogeneous environment and are supplied with nutrient solution at the same volumetric rate at

which the culture is harvested. The advantages of such a system for studying microbial predator-prey dynamics have been described previously (6), but essentially, chemostat culture extends the period of time over which an experiment can be performed, reduces the effect of statistical fluctuations and sampling errors and has well-defined parameters which can be controlled by the experimenter while other aspects of the external environment can be kept constant.

Our first experimental system consisted of a single-stage chemostat to which nutrient solution for the bacterial prey was fed at a constant rate and in which the interaction between the prey and the predator took place. The equation of balance for the two populations can be written as:

$$\dot{P} = (\lambda - D) P \quad (6)$$

$$\dot{H} = (\mu - D) H - \frac{\lambda P}{W} \quad (7)$$

where D = dilution rate (the rate of flow through the culture vessel divided by its volume), μ is the specific growth rate of the prey and W is the yield of predator per unit of prey consumed, assumed to be constant.

When slime mould amoebae and bacterial prey are grown together in a chemostat, the population densities of both organisms fluctuate sinusoidally for several days (7, 8). We estimated the specific growth rate of the predator population in such cultures from the slope of the curve generated by plotting the logarithm of the predator density against time. This slope is

$$\dot{P}/P = \lambda - D \quad (8)$$

from which relationship λ could be simply calculated. Prey density was also measured so that the change in λ as a function of H and H/P could be determined.

Our second experimental system consisted of two chemostats linked in series. In the first vessel the bacterial prey was allowed to come to steady state and then fed into the second stage vessel which contained the amoebae. As the limiting nutrient source for the bacteria is virtually exhausted under steady state conditions, it was assumed that no further growth of prey occurred in the second vessel. In the second vessel the equation of balance for the predator is:

$$\dot{P} = (\lambda - D) P \quad (9)$$

so that at steady state

$$\lambda = D \quad (10)$$

By feeding bacteria to the predator population at different dilution rates and measuring the steady state prey density in the second vessel it is therefore possible to relate λ and H to each other.

Methods

Escherichia coli B/r and Dictyostelium discoideum NC4 were maintained routinely and grown in single-state chemostat culture as described previously (8). The outflow of chemostat cultures was passed along the same line as expelled air and by this means was forced into tubes resting in a refrigerated fraction collector. Fractions were collected at hourly intervals.

For two-stage continuous culture, the first stage vessel had a maximum capacity of 1 L while the vessel used for the second stage had a maximum capacity of either 1 L or 500 cm³, depending upon the volume appropriate to a particular experiment. The vessels were fitted with flat, flanged lids each bearing five access ports. Both vessels were mixed by means of magnetic stirrers and immersed in water maintained at 25°. Filter-sterilised air was supplied to both stages and the flow of nutrient to the first vessel and the flow from the first to the second vessel was regulated by peristaltic pumps. Two-stage chemostat experiments were performed by inoculating the first vessel with E. coli and incubating with the flow on until the system came to steady state. This was considered to have occurred when no significant change in the turbidity of the effluent cell suspension could be detected. At this time the second vessel was filled with culture from the first and inoculated with a suspension of D. discoideum spores. The culture in the second vessel was incubated under batch conditions for about 48 h during which time the spores germinated to form amoebae. Flow from the first vessel to the second was then initiated and the amoebae cultured on a continuous basis. Samples were taken directly from the culture vessels for analysis.

The cell number densities of the bacteria and the amoebae in both systems was measured on a Coulter Counter (Coulter Electronics Ltd., Harpenden, England). Mean cell volumes were estimated using a Coulter C1000 Channelyzer. A 30 μ m diameter aperture was used for the bacteria and a 50 μ m aperture for the amoebae. Samples were suspended either in culture medium or "Isoton" (Coulter Electronics Ltd) immediately prior to counting. Biomass was estimated either in terms of biovolume, the product of the mean cell volume and the number of cells present, or, for bacterial biomass where appropriate, as turbidity at 560 nm. Within the range of readings made there is a linear relationship between cell volume density and turbidity at 560 nm for E. coli. Single-stage continuous culture data was smoothed by the method of cubic splines using Nottingham Algorithms Routine EO2AAF. All computations were performed on a CDC 6600 digital computer.

Results

Single-stage chemostat culture. The single stage chemostat system represents a food chain in which glucose is converted to bacterial biomass which, in turn, is converted to amoebal biomass. As glucose is measured on a weight per unit volume basis it is appropriate that the other dependent variables of the system, H and P , be measured in the same terms, i.e. biomass per unit volume. The number densities of the prey and predator populations would be appropriate units provided that the average mass per bacterial or amoebal cell remained constant. Results of a typical single-stage experiment are shown in Figure 1. The change in the mean cell volume (MCV) of each species indicates quite clearly that cell mass does not remain constant. Therefore, we have used the biovolume density, the product of the number density and MCV, as estimates of H and P in our analysis of the data. That considerable differences exist between the system in terms of numbers and biovolumes is shown by inspecting phase plant plots of our results. There were constructed using smoothed data to plot predator density against prey density. Figure 2 shows the results obtained when number densities were used. An interdependence between the two variables is not readily apparent. On the otherhand, as shown in Figure 3, when biovolume densities were used a more readily interpretable relationship emerges. It is clear from the trajectory in phase space that the system damps slowly at first and then moves rapidly towards an equilibrium value. Figure 4 shows the change in P/P as a function of time, calculated from smoothed data, and Figure 5 is a plot of P/P against H constructed from the data in Figure 4.

Two-stage chemostat culture. In the two-stage continuous culture system, steady state in the second vessel which contained the amoebal population took more than two weeks to achieve. Steady state was accompanied by considerable clumping of the cells indicating, possibly, that the slime mould amoebae were aggregating. This condition was relieved only slightly by increasing the concentration of EDTA in the medium from 0.65 mM to 0.8 mM. Both the amount of time required to reach steady state and the tendency of the amoebae to form clumps of cells once steady state has been reached made collecting sufficient data to characterise the system with respect to the amoebal specific growth rate difficult. Therefore, steady-state data was augmented with estimates made near to steady state and results recorded in terms of the specific rate or predation, $\phi = -\dot{H}/P + D(H_1 - H_2)/P$, which is directly proportional to predator specific growth rate if the yield, W , is constant. The specific rate of predation was estimated by applying the following calculation:

$$\phi = D (H_1 - H_2)/P \quad (11)$$

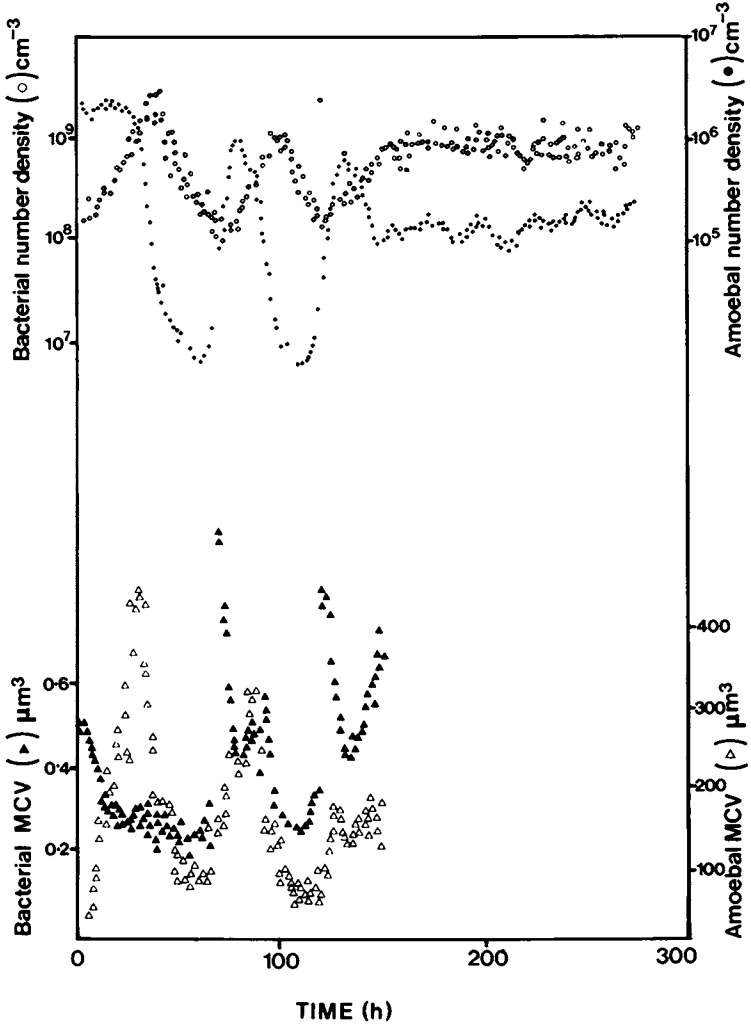


Figure 1. Change in mean cell volume and number density of *D. discoideum* amoebae and *E. coli* grown together in single-stage chemostat culture.

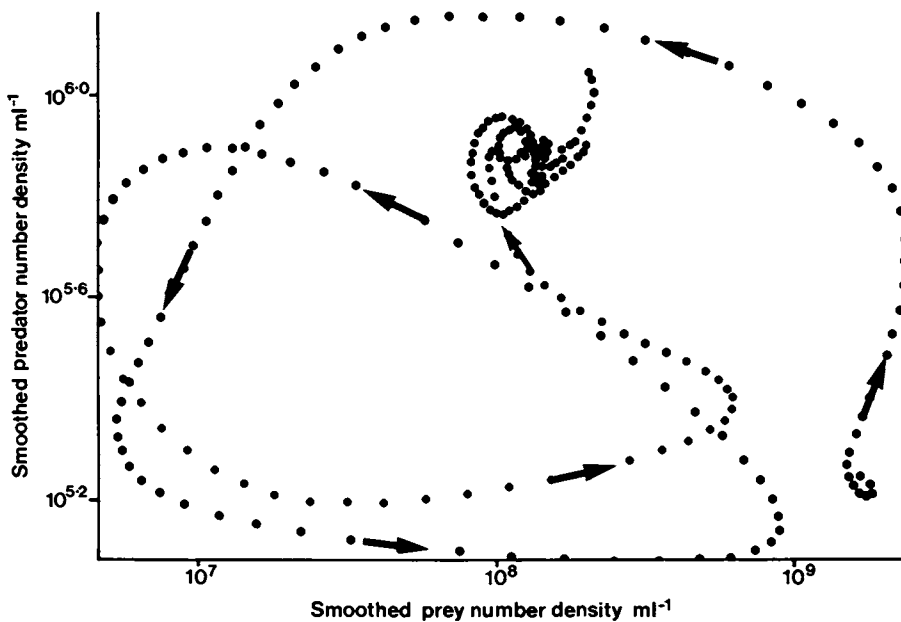


Figure 2. Phase plane plot of predator and prey number densities. Data from a single stage chemostat culture of *D. discoideum* and *E. coli* were smoothed by the method of cubic splines, and the smoothed data were used to construct this figure. The arrows indicate the direction of increasing time.

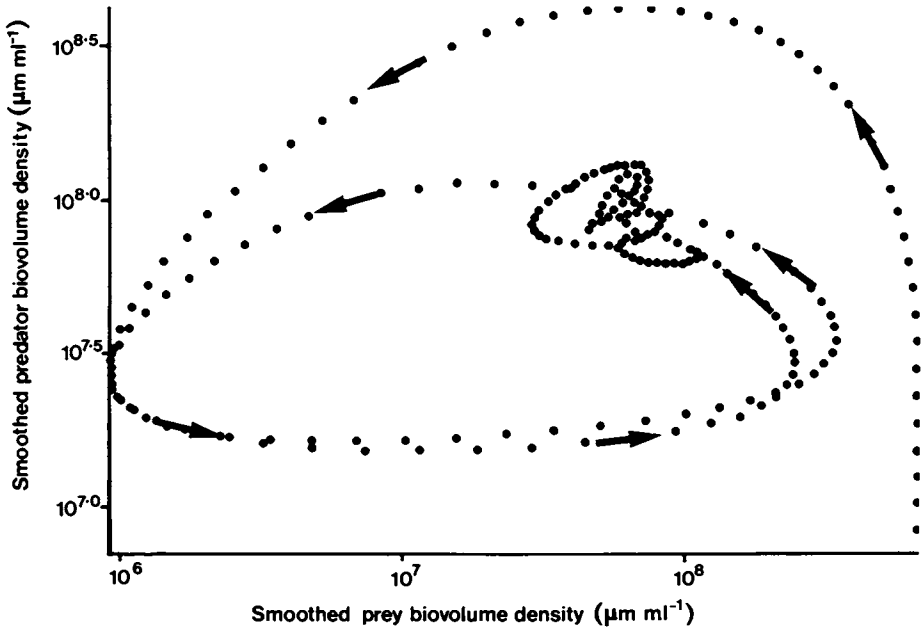


Figure 3. Phase plane plot of predator and prey densities constructed as for Figure 2, using biovolume density as the coordinates. The arrows indicate the direction of increasing time.

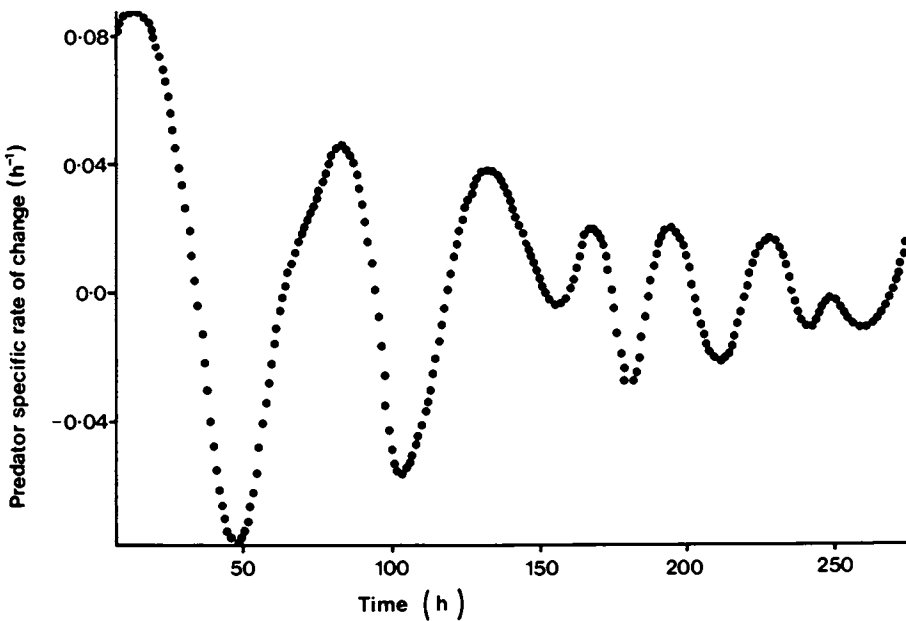


Figure 4. Change in the specific rate of change of *D. discoideum* in a single-stage chemostat as a function of time. Values were obtained from smoothed data. The specific growth rate of the amoebae is obtained by adding the dilution rate of the culture (0.065 h^{-1}) to the values on the ordinate.

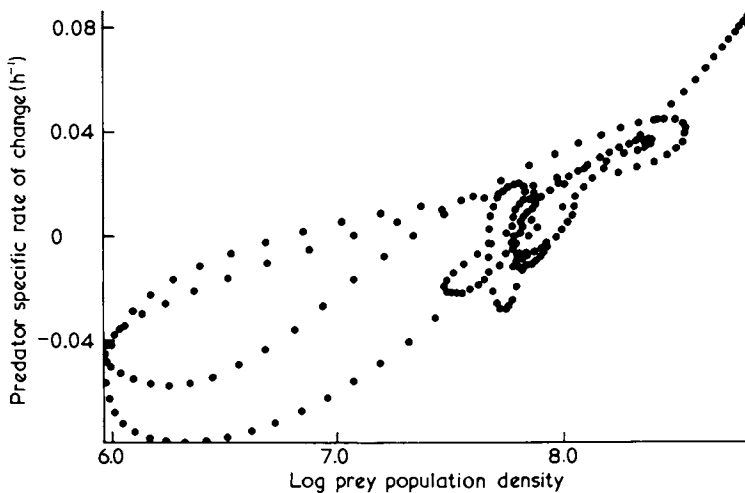


Figure 5. Specific rate of change of predator in a single-stage chemostat culture as a function of prey density. The specific growth rate of the predator is the sum of the specific rate of change and the dilution rate (0.065 h^{-1}).

where H_1 and H_2 are the population densities of the bacterial prey in the first and second stages of the continuous culture system respectively and D is the dilution rate of the second stage vessel. For the purposes of this calculation, bacterial density was estimated in terms of turbidity at 560 nm and it was assumed that the contribution by the amoebal population in the second vessel at this wavelength was negligible. The change in ϕ as a function of steady state prey density is shown in Figure 6.

Discussion

The three models we tested our experimental results against are given in equations (3), (4) and (5). The Lotka-Volterra equations predict a linear relationship between predator specific growth rate (or the specific rate of predation) and prey density; when λ is plotted against H according to the Monod function, the familiar rectangular hyperbola is generated. A hyperbolic relationship between λ and H/P is predicted by the Contois expression. Figures 5 and 6 show the way in which λ changes as a function of prey density taken from single- and double-stage chemostat cultures respectively. In neither case do the relationships indicated in equations (3) and (4), a straight line and a rectangular hyperbola, become apparent! Figure 7 shows λ plotted against the ratio of prey to predator, H/P , calculated from data from the two-stage experiment. Quite clearly, this relationship can be interpreted in terms of equation (5). Figure 8 shows a similar plot using data from single-stage experiments. Here it seems that a family of rectangular hyperbola are represented with H/P as the independent variable and with λ_m and L of equation (5) decreasing with time. It appears, therefore, that the specific growth rate of the amoebal predator is dependent not just on H , but upon the ratio of prey to predator present. The mechanism with which the amoebae are able to control their growth rate in this way is, of course, not known. We have suggested (5) that folic acid, which is secreted by the bacteria and is, therefore, a function of the prey population density, might be inactivated by the amoebae so that its concentration depends also on the density of predator present. This indeed appears to be the case as reported by Pan and Wurster (9). It is conceivable, therefore, that the concentration of folic acid in the media might serve to regulate the rate of growth of the predator population. Furthermore, the results indicate that the specific growth rate might depend explicitly on time. If such is the case then the differential equations describing the dynamics of the system are non-autonomous with time appearing on the right hand side of the equals sign and not autonomous as are the Lotka-Volterra equations and the vast majority of equations that have been suggested for describing microbial predator-prey interactions.

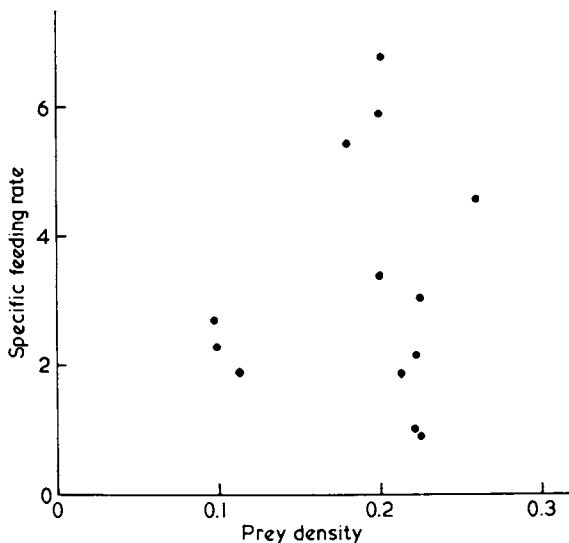


Figure 6. Data from a two-stage chemostat system showing the change in the specific feeding rate of *D. discoideum* in the second stage as a function of *E. coli* density. The specific feeding rate is directly proportional to specific growth rate providing that the yield of predator produced per unit of prey consumed is constant.

Prey density is measured in terms of absorbance at 560 nm in the second-stage vessel. Specific feeding rate was calculated as the product of the difference in turbidity between the cultures in the two vessels and the dilution rate, divided by the prey biovolume density. The units on the ordinate are therefore absorbance at 560 nm/mL culture $h^{-1} \mu m^{-3}$.

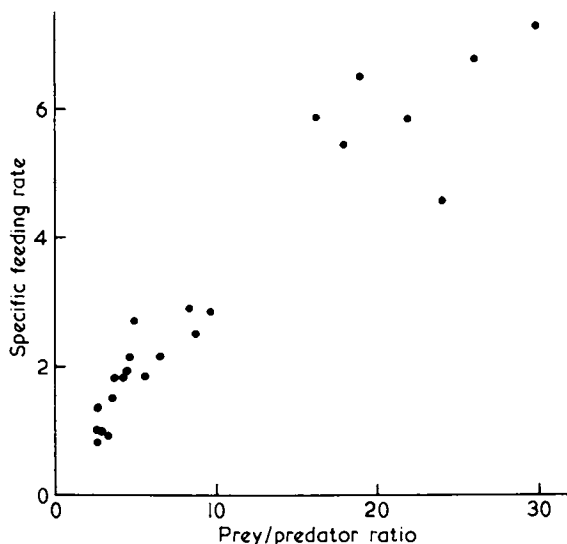


Figure 7. Specific feeding rate plotted against the ratio of prey to predator in the second vessel, estimated in terms of absorbance at 560 nm divided by the predator biovolume density ($\mu m^3 mL^{-1}$). Other conditions as in Figure 6.

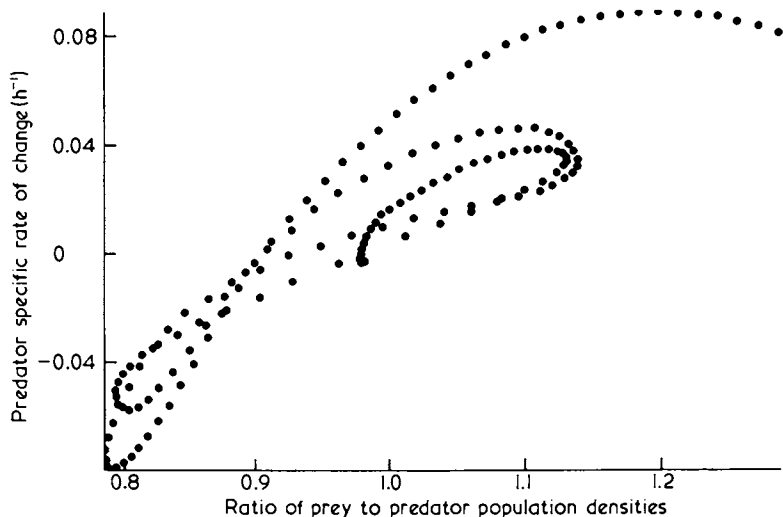


Figure 8. Specific rate of change of the predator population in a single-stage chemostat culture, plotted as a fraction of the ratio of prey to predator biovolume densities. The dilution rate of the culture was 0.065 h^{-1} .

Acknowledgments

This research was supported by the U.K. Natural Environmental Research Council and an SRC CASE studentship.

Literature Cited

1. Curds, C.R.; Bazin, M.J. "Advances in Aquatic Microbiology"; Droop, M.R.; Jannasch, H.W., Ed.; Academic: London, 1977; Vol. 1, p. 115.
2. Monod, J. Ann. Inst. Pasteur 1950, 79, 390.
3. Contois, D.E. J. Gen. Microbiol. 1959, 21, 40.
4. Curds, C.R.; Cockburn, A. J. Gen. Microbiol. 1968, 54, 343.
5. Bazin, M.J.; Saunders, P.T. Nature 1978, 275, 52-54.
6. Bazin, M.J.; Rapa, V.; Saunders, P.T. "Ecological Stability"; Usher, M.B.; Williamson, M.E., Ed; Chapman and Hall: London, 1974; p. 159.
7. Tsuchiya, H.M.; Drake, J.F.; Jost, J.F.; Fredrickson, A.G. J. Bacteriol. 1972, 100, 1147-1153.
8. Dent, V.E.; Bazin, M.J.; Saunders, P.T. Arch. Microbiol. 1976, 109, 187-194.
9. Pan, P.; Wurster, B. J. Bacteriol. 1978, 955-959.

RECEIVED June 29, 1982

Effects of Cell Motility Properties on Cell Populations in Ecosystems

DOUGLAS A. LAUFFENBURGER

University of Pennsylvania, Department of Chemical Engineering,
Philadelphia, PA 19104

Because most natural ecosystems cannot really be considered well-mixed, conclusions regarding dynamics of cell population growth and interactions drawn from well-mixed, chemostat studies may not necessarily be valid. Many microbial species, in fact, possess sophisticated movement behavioral properties by which distribution of a population in space is influenced by concentrations and gradients of chemicals commonly present in their environment. These chemotactic and chemokinetic properties can require significant devotion of genetic information and sometimes significant energy expenditure, yet are of little apparent use in artificial well-mixed systems. However, in non-mixed environments, the effects of chemosensory movement properties may be extremely important in determining the ability of a species to grow, or in deciding the outcome of competitive interactions. This paper summarizes the available experimental evidence that this is indeed the case, that movement properties can have crucial effects in microbial ecosystems. We then present some mathematical models that help explain and predict these effects.

0097-6156/83/0207-0265\$08.00/0
© 1983 American Chemical Society

Studies of microbial population dynamics have focused primarily on well-mixed, macroscopically homogeneous systems. This emphasis is easily discernible from the contents of this symposium volume. However, the situation in most naturally occurring microbial systems is far from ideal laboratory conditions, so that understanding gained about well-mixed systems may not provide the appropriate insight into ecological situations.

Environments which are not well-mixed can allow formation of spatial gradients of chemical concentrations and cell densities. Also, chemical diffusion and cell motility (i.e., self-propelled movement requiring energy expenditure) can replace convection as the dominant mode of transport. According to common categorization, half the orders of bacteria contain at least one motile species (1), including many of the commonly occurring species. Further, most motile bacteria exhibit chemotaxis, which is most simply defined as cell movement toward or away from chemicals (2), or as preferential cell movement toward higher or lower concentrations of a chemical stimulus (3). Actually, there are a number of different types of movement responses which lead to behavior of this general description (4). For peritrichously flagellated bacteria, which appear to be the most commonly encountered group (and on which this paper will accordingly focus), klinokinesis (in which the turning frequency of swimming bacteria is modulated by stimulus concentration) appears to be closest to observed behavior (5). This is illustrated in Figure 1. In the absence of a chemical stimulus gradient, these bacteria swim in roughly straight line steps called "runs" for a short time (about 1 second) and then stop and change direction, or "tumble", for about 1/10 second (6). The direction change is purely random, but the probability of tumbling is constant during a run, so that the run time distribution is Poissonian (6). This movement behavior is termed random motility. In the presence of a gradient, the direction change remains random but the tumbling probability decreases for a cell swimming toward higher attractant concentrations or lower repellent concentrations (6), leading to net migration in the direction of the gradient. This mechanism provides very efficient response (7); in an optimal gradient the net migration velocity is roughly half the linear cell swimming speed (8,9).

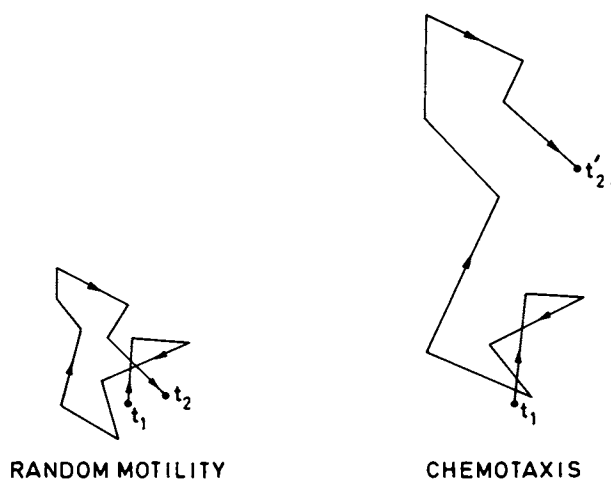


Figure 1. Illustration of typical movement of peritrichously flagellated bacteria. The left-hand figure shows movement of a cell in the absence of a chemical stimulus concentration gradient. The right-hand figure shows that the run length is increased when the cell moves in the direction of increasing attractant concentration, toward the top of the figure. The angles between respective runs in the two figures are identical. The increase in run length results in a greater drift in the direction of increasing attractant concentration for chemotactic movement than for random movement.

Stimulus concentrations are measured by occupancy of cell membrane receptors which can reversibly bind stimulus molecules according to Michaelis-Menten enzyme kinetics with dissociation constant K_d (10). Gradients are detected by a temporal sensing mechanism by which receptor occupancy over the entire cell is monitored during a run (11). A spatial sensing mechanism by which differences in receptor occupancy across the cell length is measured is impractical for such rapidly swimming cells, because of false apparent gradients due to cell motion itself (12).

A large variety of chemicals can serve as chemotactic stimuli. Approximately 20 attractant receptors and 10 repellent receptors have been identified for Escherichia coli and Salmonella typhimurium, the two most widely-studied species (13). These receptors are specific for one or two chemicals at high affinities (low K_d), but will also bind a range of related molecules with lower affinity (2). Table 1 lists a number of the well-known stimuli for a variety of species, although this is certainly incomplete as new responses are being discovered almost daily. In general, substances beneficial to an organism such as nutrients and oxygen (if aerobic) serve as attractants while toxic compounds or compounds causing pH extremes act as repellents (2). Some amino acids are attractants and others repellents, depending upon the species. Although there is not an exact correspondence between metabolizable compounds and attractants nor between unfavorable compounds and repellents (14), the observed responses can generally be rationalized in terms of particular species biochemical pathways and by recognition of some puzzling stimuli as analogues of other stimuli (2).

Speculation regarding a possible survival advantage of chemotaxis is thus not surprising. Approximately 40 genes are devoted specifically to the chemotactic response in E. coli and S. typhimurium (15), and a similar number of genes may be devoted to the motility apparatus. Such an investment must provide some benefit in the competitive world of microbial ecology. However, fundamental understanding of the circumstances in which a significant advantage due to motility and chemotaxis will actually be present is lacking, as are estimates of the magnitude of such an advantage. This understanding is lacking even for a single stimulus, and the problem becomes even more complex in any natural environment in which multiple

Table 1. Classification of Well-Known Bacterial Chemotactic Responses

Genus	Classes of Attractants	Classes of Repellents
Escherichia	sugars amino acids O ₂	pH extremes aliphatic alcohols
Pseudomonas	sugars amino acids nucleotides vitamins O ₂ ammonium ions	inorganic ions pH extremes amino acids
Bacillus	sugars amino acids O ₂	inorganic ions pH extremes metabolic poisons
Salmonella	sugars amino acids O ₂	aliphatic alcohols
Vibrio	amino acids O ₂	
Spirillum	sugars amino acids O ₂	inorganic ions pH extremes
Rhodospirillum	nucleotides sulfhydryl compounds	pH extremes poisons
Clostridium		O ₂
Bdellovibrio	amino acids	
Proteus	sugars amino acids O ₂	inorganic acids pH extremes
Erwinia	sugars	inorganic ions pH extremes
Sarcina		inorganic ions pH extremes
Serratia	sugars amino acids O ₂	inorganic ions pH extremes
Bordetella	O ₂	
Pasteurella	O ₂	
Marine bacteria	algal culture filtrates	heavy metals toxic hydrocarbons

Source: Refs. 36-38.

stimuli, probably both attractants and repellents, are present. Multiple signals are additive in some sense (16), and presumably the bacteria attempt to optimize their growth through preferential migration. From an engineering perspective, there is no quantitative basis for prediction of the effects of cell motility and chemotaxis on microbial population dynamics in any given situation at present. This paper is devoted to review of the small body of information available in this area at this time.

Experimental Observations

There exists only a small number of published experiments pertaining to the effects of cell motility on population growth. A well-known microbiology text gives one example without documentation: the competition between an aerotactic (i.e., chemotactically attracted by oxygen) Pseudomonas species and an immotile Acinetobacter species, for oxygen (17). When the growth medium is well-aerated the Acinetobacter predominate, thus showing superior growth kinetics on the rate-limiting substrate (presumably oxygen) since cell motility is apparently irrelevant. But in a non-mixed culture the Pseudomonas predominate. The chemotactic ability of the Pseudomonas species provides, in this situation, enough of a benefit to overcome its growth kinetic inferiority.

The first literature report in this area was by Smith and Doetsch (18), who studied competition between aerotactic Pseudomonas fluorescens and an immotile mutant strain of the same species, for oxygen (see Figure 2). In aerated mixed culture both strains grew to a roughly 1:1 ratio over a 24-hour period indicating that their growth kinetic properties were identical as expected. In non-aerated media, the aerotactic strain outgrew the mutant to a final ratio of over 10:1 after 24 hours. Unfortunately, the authors credited motility per se for this advantage, even though it is not clear whether random motility without chemotaxis is necessarily always beneficial.

In the course of studying the role of fimbriae in bacterial growth, Old and Duguid looked at competition for oxygen between two nonfimbriate strains of Salmonella typhimurium: one aerotactic and one immotile (19) (see Table 2). In aerobic shaken broth, the aerotactic strain multiplied by a factor of 46 within 48 hours, while the immotile strain multiplied by a factor of 52. Again the growth kinetic

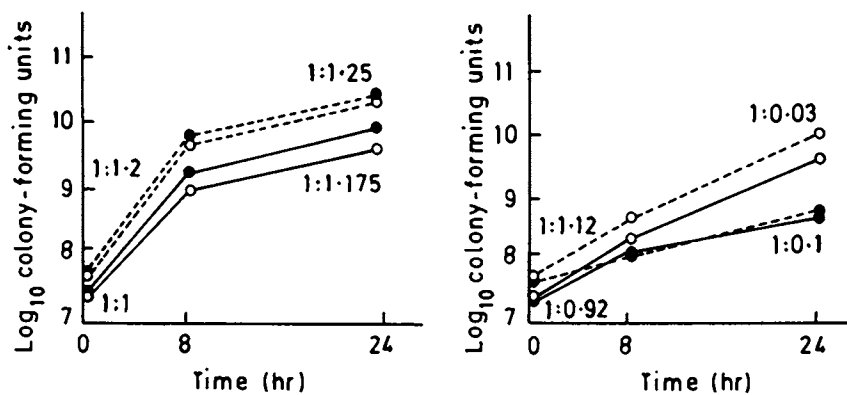


Figure 2. Multiplication of aerotactic (○) and immotile (●) strains of *Pseudomonas fluorescens* in two different experiments, each in aerated mixed culture (left) and nonaerated mixed culture (right). Reproduced, with permission, from Ref. 18. Copyright 1969, Society for General Microbiology.

Table 2. Growth in Mixed Cultures of Pairs of Variant Strains of *Salmonella typhimurium*

COMPETING STRAINS		Conditions of Growth	Time of Incubation hr	Amt of Growth	Viable Count (10^4 bacteria)/ml of	
Challenged (rha ⁻)	Challenging (rha ⁺)				Challenged bacteria	Challenging bacteria
S6352, fim ⁻ fla ⁺	S6358, fim ⁺ fla ⁺	Aerobic static broth	0	0.16	130	0.00033
			6	0.37	530	0.0053
			24	0.71	380	165
			48	1.84	1,030	880
S6351, fim ⁻ fla ⁻	S6355, fim ⁺ fla ⁻	Aerobic shaken broth	0	0.16	130	0.00033
			6	3.27	4,200	0.0012
			24	3.48	4,600	0.0029
			48	3.61	4,700	0.0093
S6351, fim ⁻ fla ⁻	S6353, fim ⁻ fla ⁺	Aerobic static broth	0	0.19	65	0.00017
			6	0.35	270	0.00080
			24	0.46	195	4.8
			48	0.48	86	74
			72	0.66	105	185
			96	1.41	190	450
S6351, fim ⁻ fla ⁻	S6353, fim ⁻ fla ⁺	Aerobic static broth	0	0.15	94	0.00024
			6	0.38	380	0.00080
			24	0.55	500	0.0016
			48	0.69	540	4.5
S6351, fim ⁻ fla ⁻	Aerobic shaken broth	Aerobic shaken broth	0	0.15	94	0.00024
			6	2.91	6,900	0.016
			24	3.00	3,800	0.011
			48	2.94	4,900	0.011

Reproduced with permission from Reference 19. Copyright 1970, American Society for Microbiology.

properties appeared nearly the same. In aerobic static broth, however, the aerotactic strain multiplied by a factor of 18,000 in 48 hours while the immotile strain multiplied by a factor of 6. Interpretation of this case is not straightforward, though, because pellicle formation was noted after 24 hours, complicating the situation.

More recently, Pilgram and Williams studied a slightly different case -- competition between chemotactic *Proteus mirabilis* and a nonchemotactic but randomly motile mutant of the species (20) (see Figures 3 and 4). In both pure and mixed cultures of periodically agitated amino acid broth, the two strains grew to a 1:1 ratio after 14 hours. On the other hand, in both pure and mixed cultures of semi-solid agar the ratio of chemotactic to randomly motile strains was greater than 5:1 after 14 hours.

The final experimental reports were by Freter *et al.* (21, 22, 23), who studied growth of *Vibrio cholerae* in mouse and rabbit large intestine (see Figure 5 and Table 3. Here three strains were compared: the chemotactic wild type, an immotile mutant strain, and a nonchemotactic but randomly motile mutant strain. In well-stirred continuous flow culture, all three strains grew in proportion. In the intestinal loops, the nonchemotactic strain was rapidly displaced by the chemotactic wild type. Most interestingly, in another experiment the randomly motile strain was also rapidly displaced by the immotile strain. Apparently, in this situation at least, motility without chemotaxis was a liability for the cells.

It is evident that theoretical analysis of motility and chemotaxis is necessary in order to provide quantitative interpretation of these results, and even qualitative explanation of the last, perhaps counter-intuitive, observation by Freter *et al.* This will be the concern of the next section of this paper. But it is important to emphasize at this point that the experimental results cited here demonstrate that the effects of cell movement properties can clearly be significant, and even dominant, in determining the competitive abilities of bacterial populations in non-mixed environments.

Theoretical Analyses

Early attempts at theoretical analysis of the effects of cell motility on population growth centered on uptake of nutrient by a single cell in a medium of infinite extent (12, 24, 25, 26). These analyses have

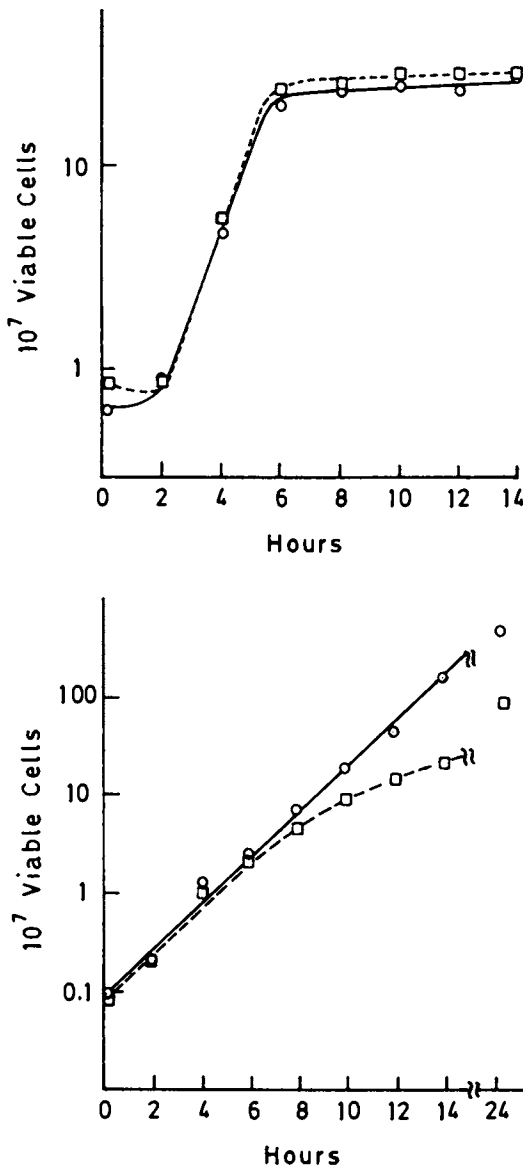


Figure 3. Growth of pure cultures of chemotactic (\circ) and nonchemotactic (\square) strains of *Proteus mirabilis* in periodically shaken amino acid broth (top) and soft-agar amino acid medium (bottom). Reproduced, with permission, from Ref. 20. Copyright 1976, National Research Council of Canada.

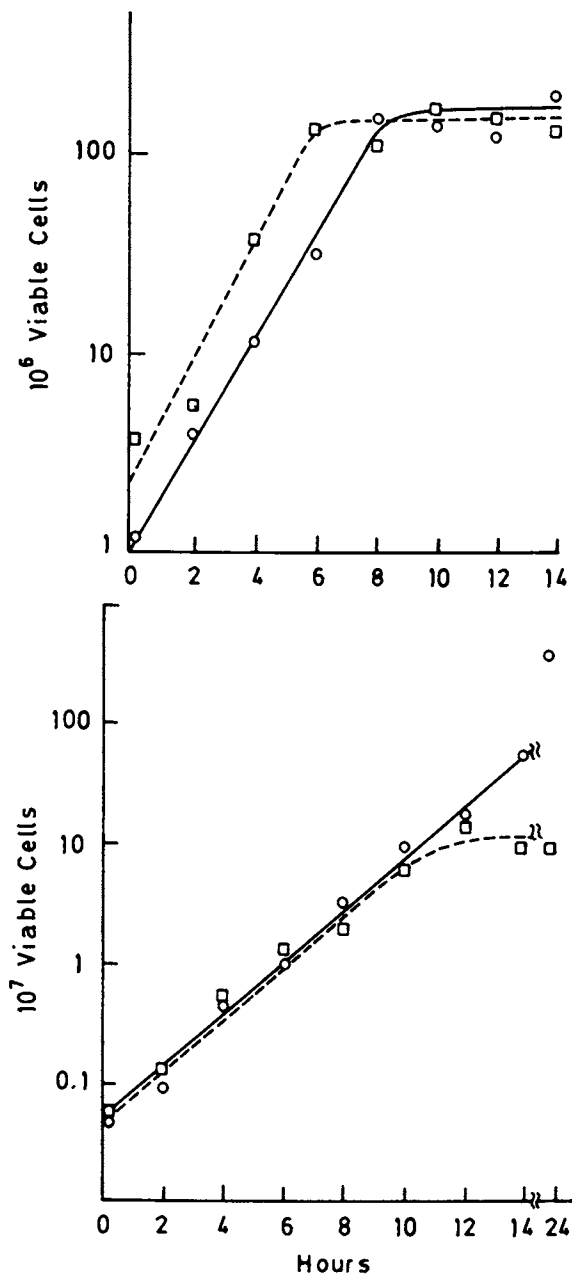


Figure 4. Growth of mixed cultures of chemotactic (\circ) and nonchemotactic (\square) strains of *Proteus mirabilis* in periodically shaken amino acid broth (top) and soft-agar amino acid medium (bottom). Reproduced, with permission, from Ref. 20. Copyright 1976, National Research Council of Canada.

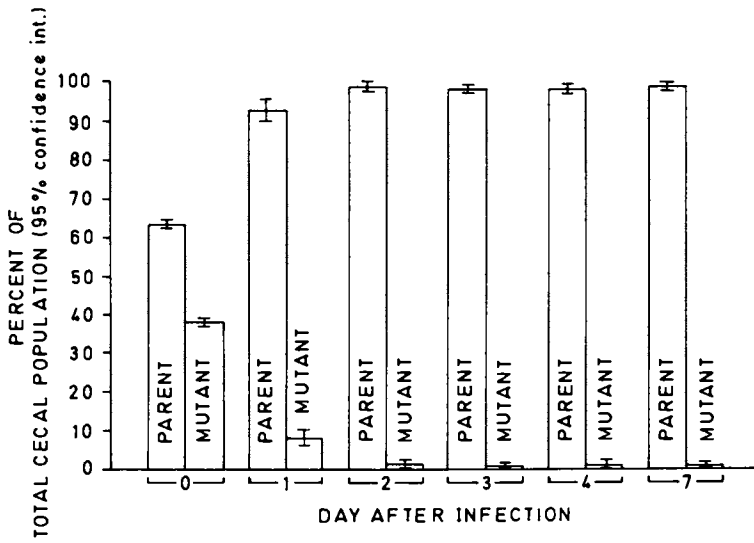


Figure 5. Time course of growth of chemotactic parent and randomly motile mutant strains of *Vibrio cholerae* in mouse large intestine. Reproduced, with permission, from Ref. 21. Copyright 1979, American Society for Clinical Nutrition.

Table 3. Displacement of Randomly Motile Mutant Strain of Vibrio cholerae by Immotile Mutant Strain in Mouse Large Intestine

Day after monoassociation	Percentage of non-motile vibrios in cecum (+ S.D.)	No. of mice cultured
0 (inoculum)	0.0	-
1	44 (+ 27)	6
2	50 (+ 35)	11
3	39 (+ 36)	3
5	96	1
10 or more	93 (+ 7.9)	11

Reproduced with permission from Reference 21. Copyright 1979, American Society for Clinical Nutrition.

invariably found that substrate uptake is ostensibly increased by movement, although the increase will be negligible for typical cell sizes, swimming speeds, and nutrient diffusivities. However, the result for a population may be quite different because the nutrient is subject to depletion by all the cells, and if the environment is not well-mixed the effect of movement will vary depending on the direction of movement. Since nutrient uptake relies essentially on diffusion to the cell surface (27), cell growth depends on the local nutrient concentration in which the cell is situated. Thus the chief effect of motility comes not from the act of movement itself, but from the fact that a cell can experience a new local nutrient concentration when it changes position.

We have accordingly developed mathematical models for the effects of cell motility at the population level (3, 28, 29, 30). Figure 6 illustrates the physical situation considered: "confined growth" of bacterial populations in a one-dimensional spatially finite non-mixed region, with the diffusible rate-limiting nutrient entering the region from a boundary. The equations governing a single bacterial population growing on a single nutrient are

$$\frac{\partial b}{\partial t} = - \frac{\partial J_b}{\partial x} + G_b$$

$$\frac{\partial s}{\partial t} = - \frac{\partial J_s}{\partial x} - G_s$$

over $0 < x < L$, where the notation is as follows:

$b(x,t)$ = viable cell density

$s(x,t)$ = nutrient concentration

J_b = viable cell flux

J_s = nutrient flux

G_b = net cell growth rate

G_s = nutrient consumption rate

The boundary conditions are

$$J_b = 0 \quad s = s_0 \text{ at } x = L$$

$$J_b = 0 \quad J_s = 0 \text{ at } x = 0$$

if the nutrient concentration at the source boundary remains constant.

For the net cell growth rate, we use Monod's model for growth and a first order rate of loss of viability:

$$G_b = \frac{ks}{K+s} b - k_e b$$

where k is the growth rate constant, K is the Monod constant, and k_e is the non-viability rate constant. The nutrient consumption rate is

$$G_s = \frac{1}{Y} \frac{ks}{K+s} b$$

where Y is the yield coefficient.

In order to permit analytical solution of the model equations, we replace these expressions by step-function approximations:

$$G_b = \begin{cases} (k - k_e) b & s > s_c \\ -k_e b & s \leq s_c \end{cases}$$

$$G_s = \begin{cases} \frac{1}{Y} kb & s > s_c \\ 0 & s \leq s_c \end{cases}$$

where s_c is a threshold nutrient concentration required to support net growth:

$$s_c = \left(\frac{k_e}{k - k_e} \right) K$$

This approximation allows direct analysis of the model predictions, and numerical computations show good quantitative agreement with the original expressions (31).

For the nutrient flux we can use Fick's law:

$$J_s = -D \frac{\partial s}{\partial x}$$

where D is the diffusivity. For the cell flux we use an expression originally formulated by Keller and Segel (32):

$$J_b = -\mu \frac{\partial b}{\partial x} + \chi b \frac{\partial s}{\partial x}$$

where μ is the random motility coefficient and χ is the chemotaxis coefficient. There are some estimates of μ and χ available (33, 34, 35), although a satisfactory analysis of a convenient assay for these parameters needs to be developed.

Defining dimensionless variables and parameters

$$u = \frac{s}{s_0} \quad v = \frac{b}{b_0} \quad \xi = \frac{x}{L} \quad \tau = \frac{Dt}{L^2} \quad b_0 = \frac{Ys_0 D}{kL^2}$$

$$\lambda = \frac{\mu}{D} \quad \kappa = \frac{kL^2}{D} \quad \theta = \frac{k_e L^2}{D} \quad \delta = \frac{\chi s_0}{\mu} \quad F(u) = \begin{cases} 1 & u > u_c \\ 0 & u \leq u_c \end{cases}$$

we obtain dimensionless model equations

$$\frac{\partial v}{\partial \tau} = \lambda \frac{\partial^2 v}{\partial \xi^2} - \delta \lambda \frac{\partial}{\partial \xi} \left(v \frac{\partial}{\partial \xi} \right) + [\kappa F(u) - \theta] v$$

$$\frac{\partial u}{\partial \tau} = \frac{\partial^2 u}{\partial \xi^2} - F(u) v$$

over $0 < \xi < 1$, with boundary conditions

$$\frac{\partial v}{\partial \xi} - \delta v \frac{\partial u}{\partial \xi} = 0 \quad u = 1 \text{ at } \xi = 1$$

$$\frac{\partial v}{\partial \xi} = 0 \quad \frac{\partial u}{\partial \xi} = 0 \text{ at } \xi = 0$$

Using these equations, the steady-state population

$$B = \frac{Ys_0 D}{kL^2} v$$

with

$$v = \int_0^1 v d\xi$$

has been analyzed for three cases so far: a) a single randomly motile population (3, 28), b) a single chemotactic population (3, 29), and c) two randomly motile populations growing in competition (30, 31). A steady state is set up by the balance between cell growth in a nutrient-rich zone and loss of viability in a nutrient-poor zone, mediated by cell flux from the nutrient-rich zone to the nutrient-poor zone (see Figure 7). The dimensionless position, ω , of the division between these two zones is the point at which $u = u_c = s_c/s_0$. ω is given by the largest root, less than unity, of the equation

$$\alpha \tanh \alpha \omega = \beta \tan \beta(1-\omega)$$

where $\alpha = (\theta/\lambda)^{1/2}$ and $\beta = ([\kappa - \theta]/\lambda)^{1/2}$.

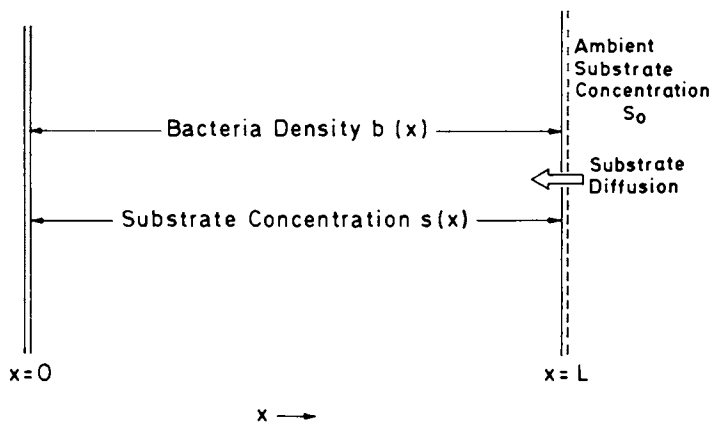


Figure 6. Illustration of confined-growth model system.

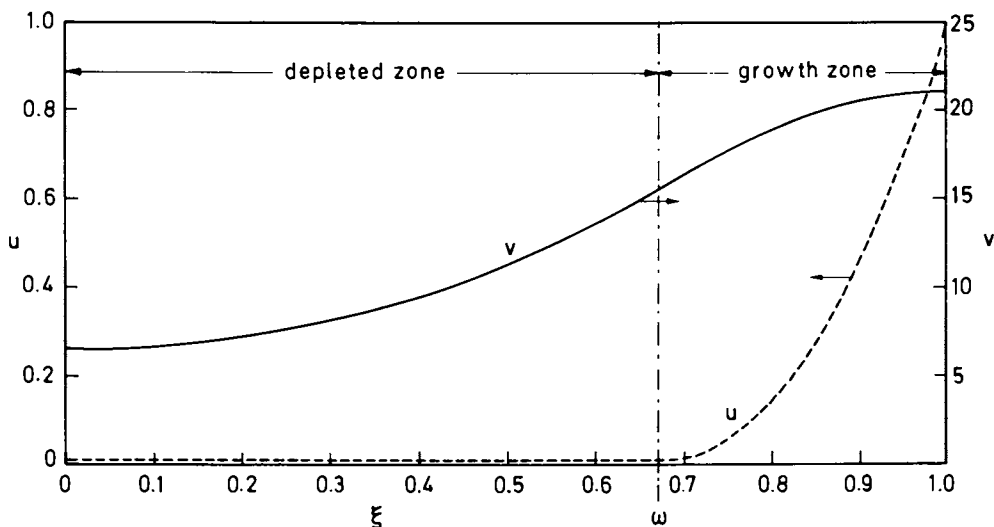


Figure 7. Typical steady state profiles of dimensionless bacterial density, v , and dimensionless substrate concentration, u . In the growth zone, $\omega < \xi < 1$, $u > u_c$, and bacterial growth can be supported. In the depleted zone, $0 < \xi < \omega$, $u = u_c$, and bacterial growth cannot be supported.

Thus, ω increases as κ increases and λ decreases. Although in natural systems such a steady state may not usually be attained, it is a good indication of the situation which will be approached if environmental conditions are not changed.

In the first case, single population growth of a nonchemotactic species ($\delta = 0$), the steady state population size B depends upon two quantities: λ/κ and κ/θ (see Figure 8). The latter quantity is the ratio of growth to nonviability rate constants, representing the growth potential at any given nutrient concentration. Figure 11 shows that for any value of λ/κ B increases as κ/θ increases. The former quantity is equal to μ/kL^2 , and thus is the ratio of the rate of cell movement across the region to the growth rate constant. Figure 11 also shows that for any value of κ/θ , B increases as λ/κ decreases. This is because random motility leads to dispersal of cells away from the nutrient-rich zone. From this result we expect that an immotile strain can outgrow a randomly motile strain, all other factors being equal, as was observed by Freter et al. (21). One can also see from Figure 11 that a species with smaller growth rate constant can outgrow a species with larger growth rate constant, if the random motility coefficient of the former species is small enough relative to that of the latter species. Figure 11 also shows that for λ/κ much greater than 1, B is independent of the random motility coefficient, because the system behaves essentially like a well-mixed system.

In the second case, single population growth of a chemotactic species, B additionally depends upon δ , the ratio of the chemotaxis coefficient to the random motility coefficient (see Figure 9). B increases as δ increases, because chemotaxis counteracts the random dispersal of cells away from the nutrient-rich zone (see Figure 10). The effect of chemotaxis becomes significant only when δ becomes greater than about 10^{-1} . These computations were done using a perturbation method, so that results for $\delta > 1$ are merely extrapolations. Numerical computations have shown the perturbation results to be accurate up to at least $\delta = 1.1$, however (31).

An interesting inference which can be drawn from Figure 12 is that there is a minimum value of δ that must be exceeded in order for motility to confer an advantage in this confined growth situation. If λ_1 represents the Brownian motion coefficient for an

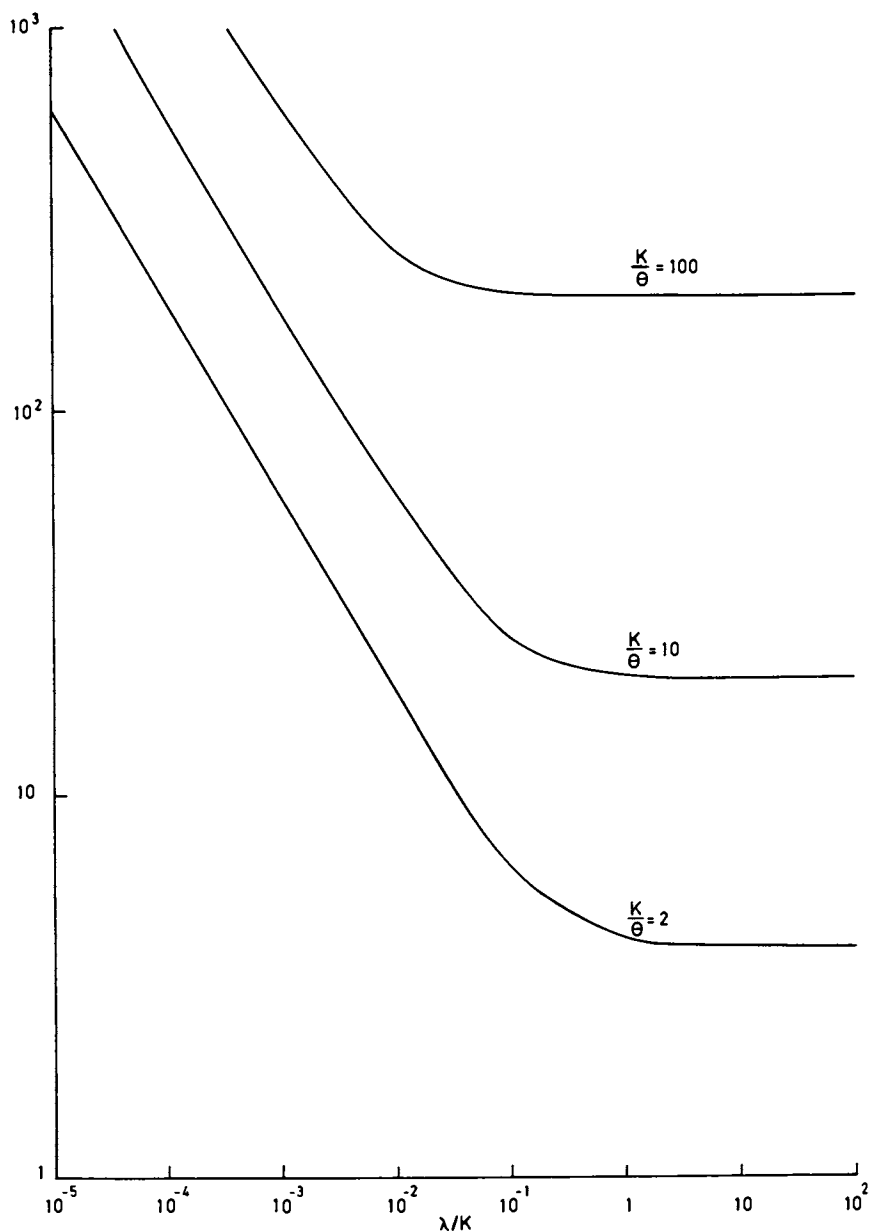


Figure 8. Plot of dimensionless total steady state bacterial density versus λ/κ for single randomly motile populations.

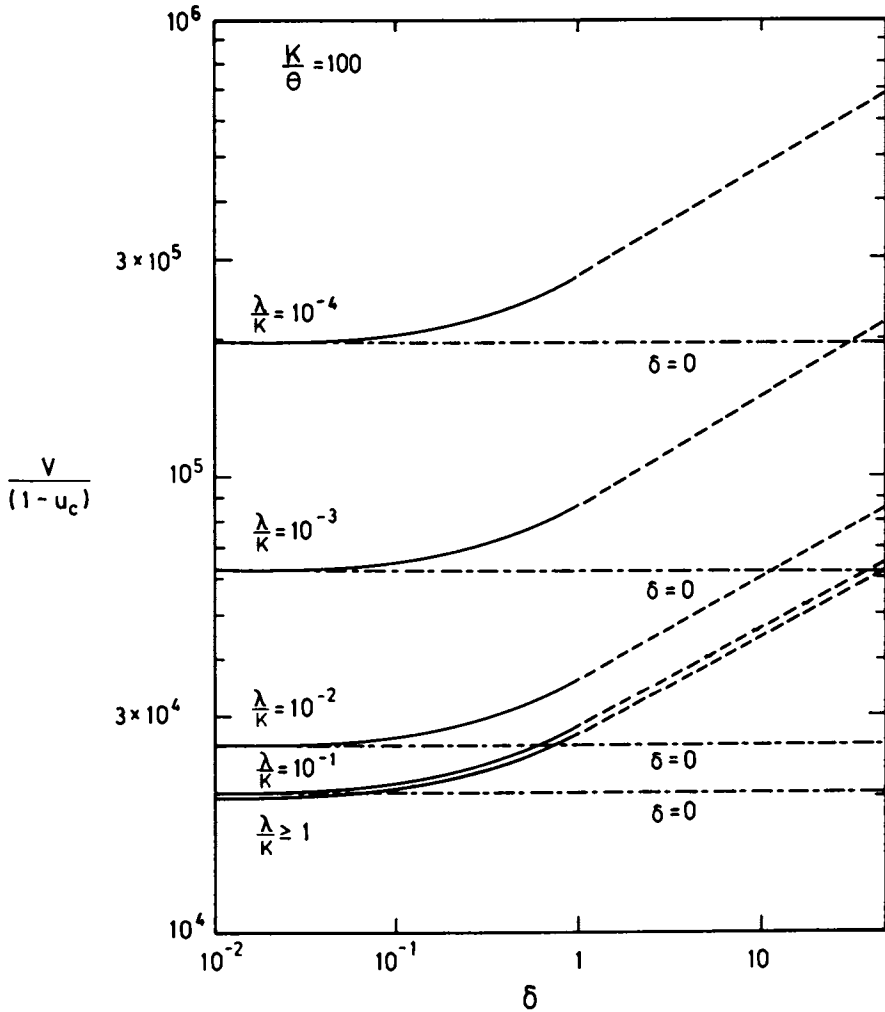


Figure 9. Plot of dimensionless total steady state bacterial density vs. δ for single chemotactic populations. Extrapolations of perturbation computations beyond $\delta = 1$ shown (---). Asymptotic values for $\delta = 0$ shown (- · - · -).

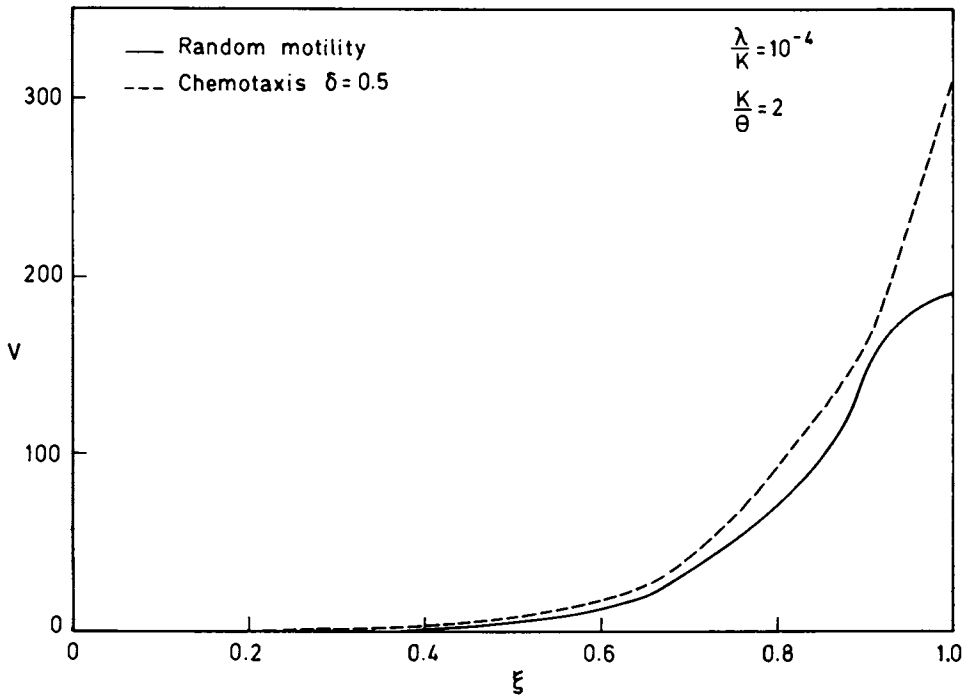


Figure 10. Typical steady state profiles of dimensionless bacterial density, v .

immotile species (33), then a chemotactic species must have a larger value, say $\lambda_2 > \lambda_1$. By itself this would yield a smaller value of B. Increasing δ from 0 increases B, and there will be a critical value, δ^* , at which B for λ_2 and δ becomes equal to B for λ_1 . Only for $\delta > \delta^*$ will the chemotactic strain outgrow the immotile strain. Thus, speculation that a motile chemotactic strain should always be superior to an immotile strain is not necessarily true.

These single population results suggest some important implications for competition between two or more populations growing together on a single rate-limiting nutrient. If one species has superior growth kinetic properties but the other has superior motility properties, we might expect coexistence to occur. Analysis of the third case, competition between two randomly motile populations, shows that this is indeed possible. There are now actually three permissible steady states: 1) coexistence, 2) species 1 only, and 3) species 2 only. For sake of clarity, let the two species have identical properties except that $k_1 > k_2$. Then species 1 will have a greater growth rate at all nutrient concentrations. In addition, the threshold concentration for net growth of species 2 must be greater than that of species 1; i.e., $u_{C_2} > u_{C_1}$. We can immediately see that a necessary condition for coexistence is that $\omega_2 > \omega_1$. The values of ω for each species are determined by the same equation as in the single population case, unaffected by the presence of the other species. We can, therefore, move directly to a graphical description of the steady-state behavior for our competition model. Figure 11 shows isoclines of ω in the plane of (κ, λ) values. If we specify values λ_1 and κ_1 for population 1, this yields a value for ω_1 . We can then immediately discover the permissible steady-states for any species 2 with parameter values λ_2 and κ_2 (see Figure 12). If $\kappa_2 < \kappa_1$, only species 1 can survive, unless λ_2 is such that $\omega_2 > \omega_1$ -- which would allow coexistence. If $\kappa_2 > \kappa_1$, only species 2 can survive, unless λ_2 is such that $\omega_2 < \omega_1$, which again allows coexistence.

So, the competition outcome can be predicted from the single population results, with one minor modification. Remember that the ω criterion is only a necessary condition for coexistence. It turns out that a second, slightly more restrictive condition is also required, to ensure that the cell densities and nutrient concentration remain positive everywhere (31). The difference between the two conditions is small

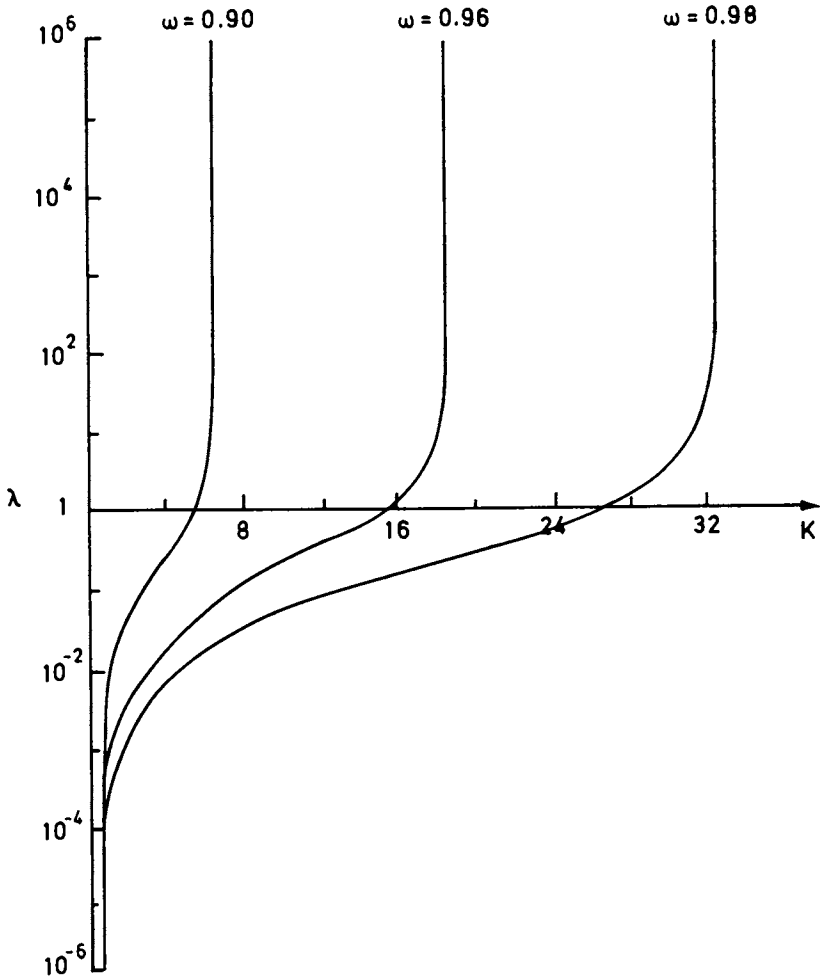


Figure 11. Sample plot of curves of constant ω in plane of (K, λ) .

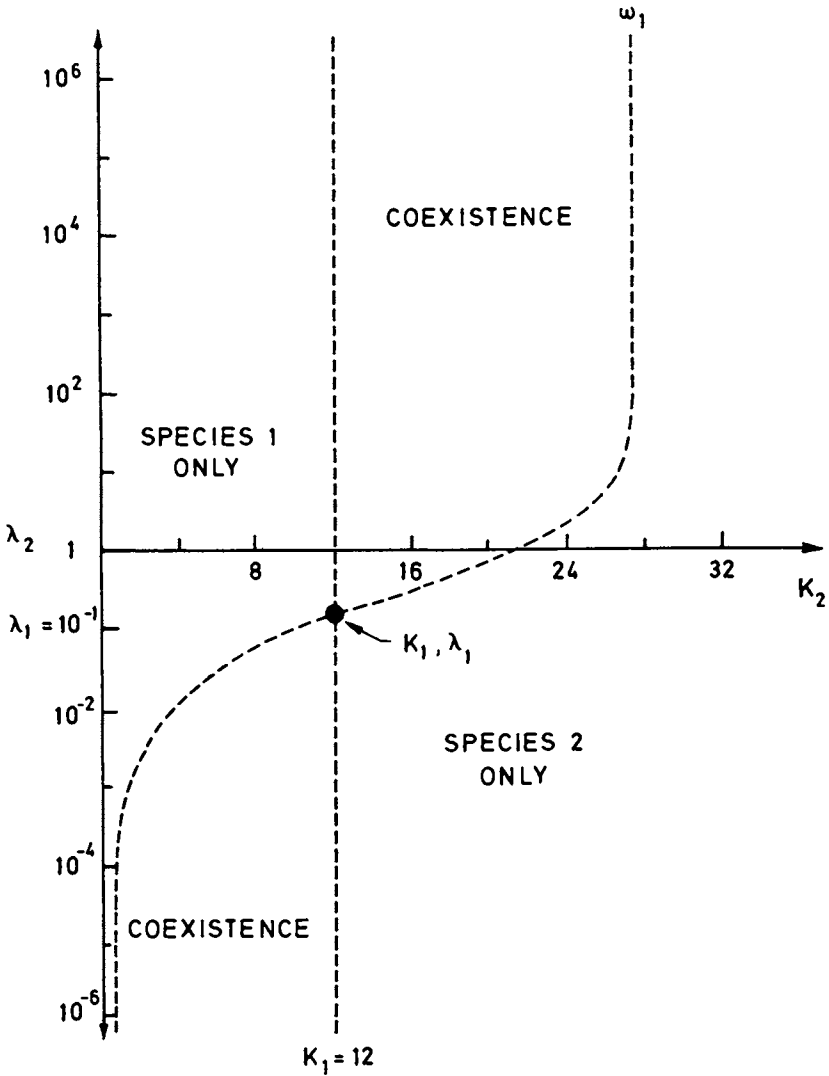


Figure 12. Illustration of predicted results for competition between two randomly motile populations with identical properties except for K and λ .

for typical parameter values, however, so that given the approximation involved in the model itself, we need not be too concerned with it.

When the cell densities are computed for a coexistence state, the species with smaller k can grow to a greater population size than the species with larger k , if its motility properties are sufficiently superior. This gives an explanation to the result cited by Stanier *et al* (17).

Similar results are expected when chemotaxis is present in competing populations, although the analysis has not yet been carried out. Chapman (5) formulated a model for competition of two chemotactic species in a traveling band, which predicted that superior chemotaxis could allow a species with inferior growth rate constant to exclude the other species. This result is consistent with our expectations; the model, however, is rather empirical.

Conclusions

Review of the literature reveals a small number of experiments that show that cell motility properties can have dramatic effects on population growth and competition in non-mixed systems. Simple mathematical models have been developed which provide qualitative explanation for all the observed phenomena, and yield quantitative prediction of the magnitude of effects which might be expected in a variety of situations.

Acknowledgments

This work has been partially supported by NSF Chemical and Biochemical Processes Program Grant CPE80-06701. D.A.L. would also like to thank Pat Thompson for typing this manuscript and Renate Schultz for many of the figures.

Literature Cited

1. Breed, R. S.; Murray, E. D. G.; Smith, N. R. "Bergey's Manual of Determinative Bacteriology"; Williams and Wilkins: Baltimore, 7th edition, 1957.
2. Koshland, Jr., D. E. "Bacterial Chemotaxis as a Model Behavioral System"; Raven Press: New York, 1980.

3. Lauffenburger, D. A. "Effects of Motility and Chemotaxis in Cell Population Dynamical Systems"; PhD Thesis, University of Minnesota, 1979.
4. Fraenkel, G. S.; Gunn, D. L. "The Orientation of Animals"; Dover: New York, 1961.
5. Chapman, P. A. "Chemotaxis of Bacteria"; PhD Thesis, University of Minnesota, 1973.
6. Berg, H. C.; Brown, D. A. Nature 1972, 239, 500-504.
7. Macnab, R. M.; Koshland, Jr., D. E. J. Mechanochem. Cell Motil. 1973, 2, 141-148.
8. Macnab, R. M. In "Biological Regulation and Development", vol. 2; R. Goldberger, ed.; Plenum Press: New York, 1980, pp. 377-412.
9. Dahlquist, F. W.; Elwell, R. A.; Lovely, P. S. J. Supramol. Struct. 1976, 4, 329-342.
10. Adler, J. Science 1969, 166, 1588-1597.
11. Macnab, R. M.; Koshland, Jr., D. E. Proc. Natl. Acad. Sci. USA 1972, 69, 2509-2512.
12. Berg, H. C.; Purcell, E. M. Biophys. J. 1977, 20, 193-219.
13. Hazelbauer, G. L.; Parkinson, J. S. In "Receptors and Recognition: Microbial Interactions"; J. Reissig, ed.; Chapman and Wall: London, 1977; pp. 60-80.
14. Adler, J. Annu. Rev. Biochem. 1975, 44, 341-356.
15. DeFranco, A. T.; Parkinson, J. S.; Koshland, Jr., D. E. J. Bacterial 1979, 139, 107-114.
16. Tsang, N.; Macnab, R. M., Koshland, Jr., D. E. Science 1973, 181, 60-63.
17. Stanier, R.; Adelberg, E.; Ingraham, J. "The Microbial World"; Prentice-Hall: Englewood Cliffs, New Jersey, 1976.
18. Smith, J. L.; Doetsch, R. N. J. Gen. Microbiol. 1969, 55, 379-391.

19. Old, D. C.; Duguid, J. P. J. Bacteriol. 1970, 103, 447-456.
20. Pilgram, W. R.; Williams, F. D. Can. J. Microbiol. 1976, 22, 1771-1773.
21. Freter, R.; Allweiss, B.; O'Brien, P. C. M.; Halstead, S. A. In "Proceedings of the 13th Joint Conference on Cholera", U.S. - Japan Cooperative Medical Sciences Program; U.S. Govt. Printing Office, Washington, D.C.; pp. 153-181.
22. Freter, R.; O'Brien, P. C. M.; Halstead, S. A. Adv. Exp. Med. Biol. 1978, 107, 429-437.
23. Freter, R.; O'Brien, P. C. M.; Macsai, M. S. Am. J. Clin. Nutr. 1979, 32, 128-132.
24. Carlson, F. D. In "Spermatozoan Motility"; D. W. Bishop, ed.; AAAS Publication No. 72: Washington, D. C., 1962.
25. Koch, A. L. Adv. Microb. Physiol. 1971, 6, 147-217.
26. Brunn, P. O. J. Biomech. Eng. 1981, 103, 32-37.
27. Purcell, E. M. Am. J. Physics 1977, 45, 3-11.
28. Lauffenburger, D. A.; Aris, R.; Keller, K. H. Microb. Ecol. 1981, 7, 207-227.
29. Lauffenburger, D. A.; Aris, R.; Keller, K. H. Biophys. J. (submitted for publication).
30. Lauffenburger, D. A.; Calcagno, B. Biotech. Bioeng. (submitted for publication).
31. Calcagno, B. "Analysis of Steady-State Growth and Competition of Motile Bacterial Populations in Non-mixed Environments", M.S. Thesis, University of Pennsylvania, 1981.
32. Keller, E. F.; Segel, L. A. J. Theor. Biol. 1971, 30, 225-234.
33. Segel, L. A.; Chet, I.; Henis, Y. J. Gen. Microbiol. 1977, 98, 329-337.

34. Segel, L. A.; Jackson, J. L. J. Mechanochem. Cell Motil. 1973, 2, 25-34.
35. Holz, M.; Chan, S. Biophys. J. 1979, 26, 243-262.
36. Barrachini, O.; Sherris, J. C. J. Path. Bact. 1959, 77, 565-574.
37. Seymour, F. W. K.; Doetsch, R. N. J. Gen. Microbiol. 1973, 78, 287-296.
38. Chet, I.; Mitchell, R. Annu. Rev. Microbiol. 1976, 30, 221-239.

RECEIVED June 1, 1982

Macroscopic Thermodynamics and the Description of Growth and Product Formation in Microorganisms

J. A. ROELS

Delft University of Technology, Netherlands Central Organization for Applied Scientific Research, T.N.O., P.O. Box 108, 3700 AC ZEIST, The Netherlands

From the point of view of macroscopic thermodynamics living organisms are energy transducers converting a source of energy, e.g. chemical substances or photons, into other forms of energy. As such they are subject to the constraints posed by the first and second laws of thermodynamics. As microorganisms are open systems and as such exist in a state outside equilibrium, non-equilibrium thermodynamics provide the perfect vehicle for a first approach to the description of their behaviour.

The concept of the thermodynamic efficiency of growth is developed and it is shown that, as a rule of thumb, the maximum observed efficiencies are about 0.65 irrespective the nature of the energy supplying process. A number of notable exceptions are shown to be most probably caused by limitations other than available energy.

The nature of growth and product formation is discussed in terms of the coupling of the transformation of a given amount of substrate energy into biomass energy to the energy obtained from a flow of electrons to a level of high to a level of low energy. The treatment is shown to result in a reliable rule of thumb for a first estimate of the order of magnitude of the growth yield of an organism feeding on a given energy supplying transformation process.

The biosphere on earth is, thermodynamically speaking, in a certain sense an open system. It receives energy from the sun in the form of radiation. The energy of the photons reaching earth is, in part, converted to chemical energy in a process called

0097-6156/83/0207-0295\$08.00/0
© 1983 American Chemical Society

photosynthesis. For the larger part this energy takes the form of carbohydrates, e.g. sugars, starches and cellulose. The components of the biomass of the primary producers are the starting point of a wide variety of transformations, which takes place under catalytic action of living organisms.

As a final result the solar energy is converted to less energy rich forms of radiation which transport energy to outer space or is used to decrease the entropy of the biosphere.

The reasoning developed above shows that the biosphere is a system, which is subject to a flow of energy. The energy enters the system at a low entropy level and leaves it at a substantially higher entropy level. As such the biosphere can maintain a state with an entropy lower than the maximum corresponding to thermodynamic equilibrium and processes known as "life" result (1).

A single organism or a species feeding on a given energy supplying process exists in much the same position as the biosphere as a whole. It is an open system through which energy flows from a low entropy state, e.g. chemical energy stored in compounds more reduced than CO_2 , to a high entropy state, e.g. heat at a low temperature level. As a result the organisms can maintain a state outside thermodynamic equilibrium and can continue performing the processes characteristic for their "life".

As organisms are systems which exist outside thermodynamic equilibrium and irreversible processes are taking place, the formalism of thermodynamics of irreversible processes constitutes the logical vehicle to treat their behaviour. In the present article the formalism will be briefly summarized for the purpose of its application to microorganisms engaged in growth and product formation. For a more thorough treatment of the basic formalism the reader is referred to the standard texts (2-4) and earlier work of the present author (5, 6).

Macroscopic thermodynamics and processes in open systems. (5, 6)

For the purpose of the present analysis of microbial metabolism, a given amount of microorganisms is considered to be an energy transducer. It is schematically represented in fig. 1. The system exchanges chemical energy and heat with the environment. For simplicity's sake the case of processes involving radiational energy is excluded. The basic formalism, however, can be easily extended to include these situations.

The state of the system can be characterized by a number of extensive quantities; these specify the amount of the various chemical substances and the amount of energy present in the system. For each extensive quantity, which can be attributed to the system, a balance equation can be formulated; it expresses the accumulation of the quantity inside the system as the sum of the changes of its amount due to transformation and transport processes respectively. Mathematically this can be expressed as:

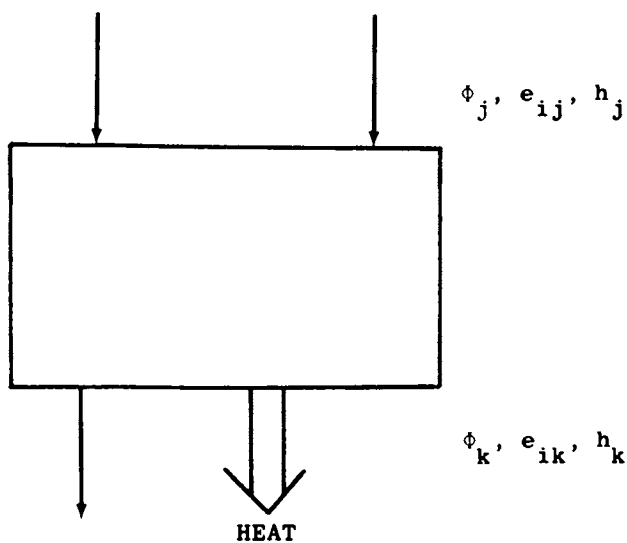


Figure 1. An open system for macroscopic analysis. It exchanges chemical substances and heat with the environment. The flow of chemical substances, Φ_i , is characterized by the elemental composition and the partial enthalpy of the chemical substances.

$$\frac{d}{dt} \int_V Q dV = \int_V r_Q dV + \int_S j_Q dS \quad (1)$$

In the formulation of eqn. (1) it is assumed that the volume and the surface area of the system do not change. In the present article the discussion will be restricted to systems in a stationary state, i.e. systems for which the time derivative appearing at the left hand side of eqn. (1) has become zero. In such a case eqn. (1) can be simplified to:

$$\int_V r_Q dV = - \int_S j_Q dS \quad (2)$$

With respect to the transformation processes open to a given non-equilibrium system the extensive quantities characterizing the system can be distinguished into two groups: conserved and non-conserved quantities. So-called conserved quantities cannot be produced or consumed in the transformation processes open to a given system. Therefore, the first term at the right hand side of eqn. (1) is necessarily zero and eqn. (2) can be simply written as:

$$\int_S j_Q dS = 0 \quad (3)$$

Equation (2) expresses the fact that for each conserved quantity the transport to a system in stationary state must exactly match transport from that system. For a non-conserved quantity such simplification is not possible.

The application of the formal macroscopic theory to transformation processes in open systems is based on the formulation of balance equations for a number of conserved quantities and an additional thermodynamic constraint allowing the formulation of a useful efficiency measure.

The elemental balance equations. In microbial conversion processes the amounts of the various atomic species are conserved. This observation results in the formulation of elemental balance equations. Using eqn. (3) the elemental balance equation for atomic species j can, again assuming a stationary state, be expressed as (5, 6):

$$\sum_{i=1}^n \phi_i e_{ij} = 0 \quad (4)$$

In eqn. (4) ϕ_i stands for the net molar flow of compound i to the system, e_{ij} stands for the number of moles of atomic species j in one mole of compound i . Equations of the type of eqn. (4) provide one constraint to the net exchange flows for each atomic species considered.

The thermodynamic constraints. The application of non-equilibrium thermodynamics to transformation processes is based on the formulation of two basic balance equations. The first one, a balance equation for energy, can, by virtue of the fact that the first law of thermodynamics assures energy to be a conserved quantity in any system, for a system in stationary state be expressed as:

$$\phi_E = 0 \quad (5)$$

in which ϕ_E is the net flow of energy towards the system. Thermodynamics show that, for an open system on which no work is performed by external force fields, the energy flow towards that system can be expressed as follows:

$$\phi_E = \phi_H + \sum_i \phi_i h_i \quad (6)$$

In this equation ϕ_H is the so-called heat flow of Prigogine (2) and the h_i are the partial molar enthalpies of the compounds exchanged with the environment.

If eqns. (5) and (6) are combined the familiar balance equation for enthalpy is obtained. It allows the calculation of the heat exchanged with the environment from the following equation:

$$\phi_H = - \sum_i \phi_i h_i \quad (7)$$

Equation (7) introduces one new unknown flow, the heat flow ϕ_H , and one additional constraint, hence the total number of unknown flows does not change by the application of the first law of thermodynamics.

A second restrictive equation results from the balance equation for entropy. For a system in stationary state the balance equation for entropy results in the following expression:

$$\Pi_S = - \phi_S \quad (8)$$

in which Π_S is the total entropy production in the system, ϕ_S is the flow of entropy to the system.

The second law of thermodynamics poses an important restriction to Π_S , which must necessarily exceed zero for any possible process:

$$\Pi_S > 0 \quad (9)$$

Furthermore, thermodynamics show that the entropy flow can be written as:

$$\phi_S = \phi_H/T + \sum_i \phi_i s_i \quad (10)$$

Combining eqns. (8) - (10) the following constraint is seen to derive from the second law of thermodynamics:

$$\phi_H/T + \sum_i \phi_i s_i < 0 \quad (11)$$

Equation (11) shows that the entropy flow towards a system in a stationary state outside thermodynamic equilibrium contains two contributions: one due to exchange of heat with the environment, the other resulting from the exchange of chemical substances. As can be seen eqn. (11) does not imply that heat should necessarily be produced (i.e. $\phi_H < 0$) in any process allowed by the second law, a statement, which can be shown (6) to be the rationale behind the Minkevich and Eroshin (7) efficiency, η .

Thermodynamics do not exclude processes in which heat is taken up (in fact endothermic processes are well known in chemical engineering) as long as it is compensated by a sufficiently large entropy flow associated with the exchange of chemical substances.

The combination of eqns. (11) and (7) allows the formulation of an alternative expression of the second law, it introduces the partial molar free enthalpy, g_i , (also termed Gibbs free energy):

$$\sum_i \phi_i g_i > 0 \quad (12)$$

The partial molar free enthalpy is defined by:

$$g_i = h_i - Ts_i \quad (13)$$

Equation (12) will be shown to allow the formulation of an efficiency measure, which can be used to analyse growth and product formation in microorganisms, its development will be undertaken in the next section.

The thermodynamic efficiency.

The energy and entropy content of chemical substances.
The thermodynamic theory outlined above can, in principle, be straightforwardly applied to the description of microbial growth and product formation. In order to perform such an analysis, thermodynamic data are needed regarding the compounds which are exchanged with the environment, i.e. the partial molar enthalpies

and entropies of the compounds involved in the processes in the system need to be known. In principle the partial molar quantities, enthalpy as well as entropy, are functions of the concentrations of each and every chemical compound present, i.e. definite values cannot be attributed to a single compound. In the approximation to the energetics of microbial growth presented here, ideality of the mixture of compounds involved will be assumed. This implies the partial molar thermodynamic quantities to be equal to the specific molar quantities, these latter quantities depend on intensive variables like temperature and pressure and the concentration of the compound considered only.

To a good degree of approximation, enthalpy can, at a given temperature and pressure, be assumed independent of the concentration of the compound under consideration. The free enthalpy is, however, by virtue of the entropy contribution to that quantity (eqn. 13), definitely concentration dependent. The following relationship holds:

$$g_i = g_i^0 + RT \ln C_i \quad (14)$$

in which g_i^0 is the free enthalpy at a given temperature and pressure and unit concentration of the compound, which is called standard free enthalpy. C_i is the concentration of compound i .

As a first approach, standard quantities, i.e. assuming unit concentrations, will be used in the present evaluation of growth and product formation.

One further convenient convention needs to be discussed. Energy, and hence also derived quantities like enthalpy and free enthalpy, cannot be attributed a definite value; its magnitude can only be defined with respect to a given reference state which is attributed a zero energy level. A convenient reference state for the evaluation of growth and product formation in microorganisms is obtained if CO_2 , H_2O , O_2 and N_2 are assigned a zero energy level. The energy of a compound thus becomes equal to its energy of combustion to CO_2 , H_2O and N_2 . This convention can be motivated by the fact that microorganisms can under no circumstances derive useful energy from processes in which only CO_2 , H_2O , O_2 and N_2 are involved.

The molar free enthalpies and enthalpies of combustion at standard conditions will be termed Δg_{ci}^0 and Δh_{ci}^0 , respectively. From eqn. (7) it is clear that the enthalpy of ci combustion, Δh_{ci}^0 , equals the heat of combustion.

The free enthalpy of combustion, Δg_{ci}^0 , is markedly dependent on the concentrations of the reactants involved (eqn. (14)) and most biological processes take place in aqueous solutions at a hydrogen ion concentration corresponding to a pH of 7 rather than at unit concentration of the H^+ -ion, corresponding to a pH of zero. The free enthalpies of combustion to liquid water, the HCO_3^- ion (the predominant form in which CO_2 exists at a pH of 7) and N_2 at a pH of 7 can thus be considered more relevant to biological

transformations. The free enthalpy of combustion under these conditions will be indicated Δg_{ci}^0 . The enthalpy of combustion is hardly affected by the pH. The free enthalpies and enthalpies of combustion are known to obey regularities (6, 8). These can be treated using the concept of the degree of reduction as introduced by Minkevich and Eroshin (7) and extended and generalized by the present author (5, 6). The generalized degree of reduction, γ_i , of a compound with respect to molecular nitrogen is defined by:

$$\gamma_i = 4 + a_i - 2b_i \quad (15)$$

In which a_i and b_i are the number of moles of H and O present in one C-mole (being the amount containing 12 grams of carbon) of compound i . For a component i the enthalpies and free enthalpies of combustion per C-mole, to be indicated Δh_{ci}^0 and Δg_{ci}^0 , respectively, are, to a first approximation, a unique function of the degree of reduction, γ_i , as introduced in eqn. (15). A statistical analysis of data for some 60 organic compounds of biological significance revealed the existence of the following regularities:

$$\Delta h_{ci}^0 = 115\gamma_i \quad (16)$$

$$\Delta g_{ci}^0 = 94.4\gamma_i + 86.6 \quad (17)$$

The residual error of the estimate is 18 kJ for both eqns. (16) and (17). Equation (16) states that the heat of combustion per C-mole is more or less directly proportional to the degree of reduction. As is apparent from eqn. (17) such a simple proportionality relation does not apply to free enthalpies of combustion.

Equations (16) and (17) show that systematic deviations between free enthalpies and heats of combustion must exist. For substrates of a low degree of reduction the free enthalpies of combustion exceed the heats of combustion, for substrates of a high degree of reduction the reverse applies. This phenomenon can be illustrated if the entropy contribution to the free enthalpy of combustion, $T\Delta s_{ci}^0$, is calculated. It is obtained from the equation:

$$\Delta g_{ci}^0 = \Delta h_{ci}^0 - T\Delta s_{ci}^0 \quad (18)$$

In fig. 2 the relation is shown between the said entropy contribution and the degree of reduction using data for a variety of organic compounds. A definite trend can indeed be shown to exist (apart from an incidental outlier): The entropy contribution increases with increasing degree of reduction. In view of the observation that free enthalpy changes at a pH of 7 may well be more relevant in microbiological processes, the entropy contribu-

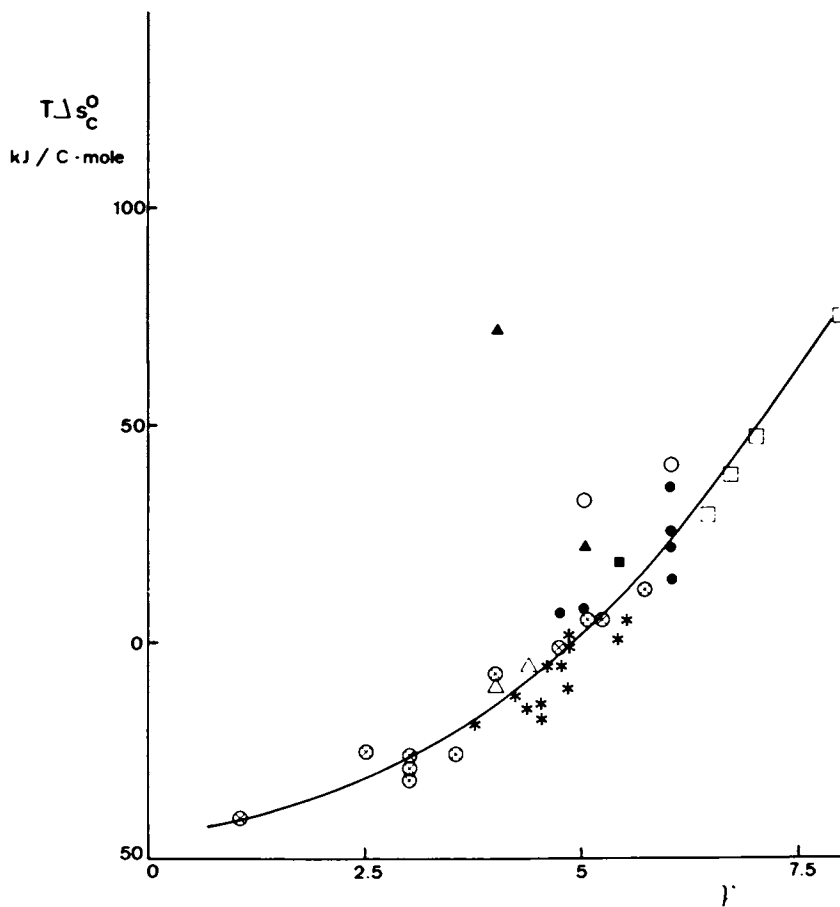


Figure 2. The entropy contribution, $T\Delta s_c^0$ (kJ/C·mole), to the free enthalpy of combustion at standard conditions, as a function of the degree of reduction, γ , of the compounds considered, for acids (\otimes), carbohydrates (Δ), alkanes (\square), ethene and ethyne (\circ), alcohols (\bullet), acetone (\blacksquare), aldehydes (\blacktriangle), and amino acids (*).

tion to the free enthalpy of combustion at a pH of 7, $T\Delta s^0$, was also calculated. These values are plotted as a function of the degree of reduction in fig. 3. The features of figs. 2 and 3 are seen to be very much alike, except for the acids, which have a markedly higher $T\Delta s^0$ at a pH of 7, i.e. their free enthalpy of combustion is lower at that pH. This difference between standard conditions and a situation in which the concentrations differ from unity, e.g. at a pH of 7, is characteristic for a limitation of the use of standard free enthalpy changes in the analysis of processes, where the concentrations at the locale of the process may differ from unity: the Δg_c^0 values can only be applied to an approximate analysis. For detailed considerations the Δg_c values at the concentrations at the locale of energy generation are needed. Still, as will be shown, the approximate analyses greatly contribute to the understanding of microbial energetics.

There also exist compounds of which the energy released on their combustion does definitely not follow the trends indicated by eqns. (16) and (17). Examples are oxygen and nitric acid which have a "heat of combustion" which is close to zero and a degree of reduction of -4 and -5 respectively. By virtue of this feature these compounds can serve as very efficient "electron acceptors".

The thermodynamic efficiency. The thermodynamic theory developed earlier was shown to result in eqn. (12), a restrictive equation regarding the flows of matter exchanged with the environment by an open system. On eqn. (12) a definition of the thermodynamic efficiency can be based if the dissipation, $T\Pi_s$, is compared to the total of the flows of free enthalpy entering the system. However, a problem which was already indicated above has to be tackled. The amount of energy cannot be specified in a unique way and it can only be defined with reference to a base level, which is arbitrarily attributed zero energy content. As soon as such a reference state has been chosen, the thermodynamic efficiency is easily calculated. The procedure is illustrated in fig. 4. The thermodynamic efficiency, η_{th} , is defined equal to the ratio of the free enthalpy gained if the compounds leaving the system were transformed to the reference state, to that, which would be obtained if this procedure were applied to the compounds entering the system. It is easily understood that η_{th} is constrained between zero, if all the free enthalpy entering the system is dissipated and unity if Δg_2^r equals Δg_1^r , i.e. if the dissipation equals zero. It is important to realize that the former constraint strongly depends on the correct choice of the reference state.

Applications of the theory

Aerobic growth without product formation. The application of the theory to aerobic growth without formation of products

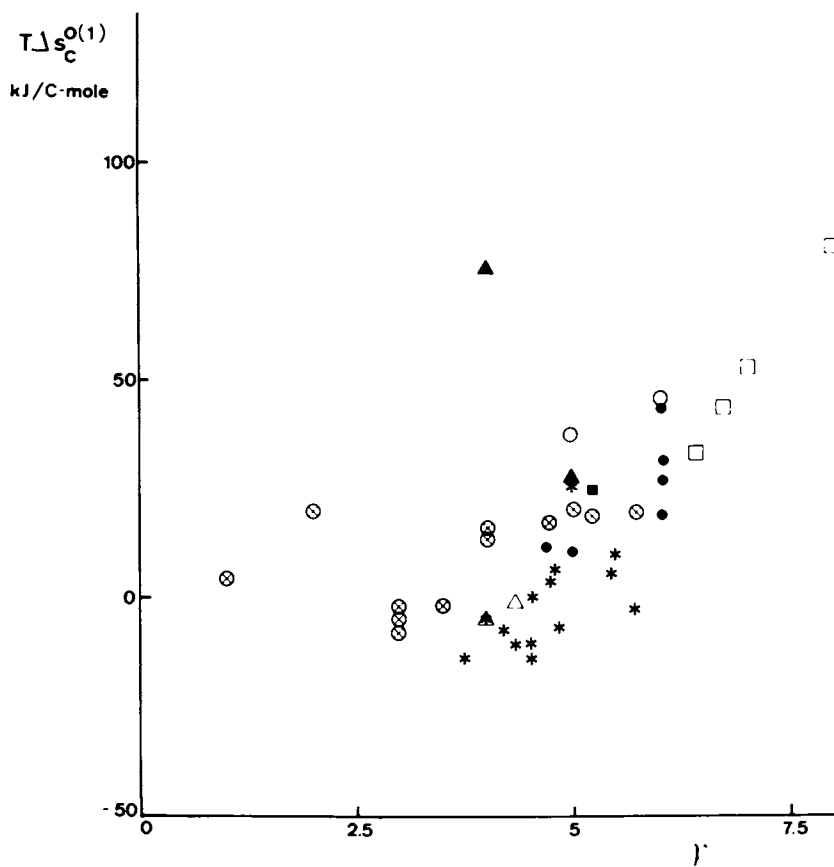


Figure 3. The entropy contribution, $T\Delta S_c^{O(1)}$ (kJ/C-mole), to the free enthalpy of combustion at a pH of 7, as a function of the degree of reduction, γ , of the compounds considered; symbols as in Figure 2.

will now be shown. Figure 5 shows the system and the exchange flows for this case. The elementary compositions and the heats of combustion of the compounds exchanged with the environment are indicated. Aerobic growth is for the present analysis assumed to involve uptake of a nitrogen source, a carbon source and oxygen and transport to the environment of carbon dioxide, water and new biomass. The biomass is assumed to be one compound, which can be characterized fully by its elemental composition. As the enthalpy as well as the free enthalpy of combustion, i.e. the enthalpy and free enthalpy content with respect to the reference state adopted in the present analysis, is zero for oxygen, carbon dioxide and water, it is easily understood that the thermodynamic efficiency can be defined as follows:

$$\eta_{th} = \frac{\phi_x \Delta g_{cx}^0}{\phi_s \Delta g_{cs}^0 + \phi_N \Delta g_{cN}^0} \quad (19)$$

in which ϕ_x , ϕ_s and ϕ_N are the flows of biomass (C-mole/hr), substrate (C-mole/hr) and nitrogen source (mole/hr) to or from the system (as indicated in figure 5). Δg_{cx}^0 and Δg_{cs}^0 are the free enthalpies of combustion of a C-mole of biomass and substrate respectively. Δg_{cN}^0 is the free enthalpy of combustion of a mole of the nitrogen source.

Equation (19) can also be written as:

$$\eta_{th} = \frac{\Delta g_{cx}^0}{\Delta g_{cs}^0 / Y'_{sx} + (c_1/c_4) \Delta g_{cN}^0} \quad (20)$$

In the formulation of this equation a balance for atomic nitrogen is used to relate the flows ϕ_N and ϕ_x . Y'_{sx} is a yield factor for biomass on substrate on a per C-mole s_x base; C-moles of biomass produced per C-mole of substrate consumed, thus it is defined by:

$$Y'_{sx} = \phi_x / \phi_s \quad (21)$$

Another useful efficiency measure is the so-called enthalpy efficiency of growth, η_H , it is by analogy obtained if the Δg_{ci}^0 in eqn. (20) are replaced by the respective Δh_{ci}^0 . As was already indicated the enthalpy efficiency does not have the fundamental properties of the thermodynamic efficiency as the restriction following from the application of the second law of thermodynamics (see eqn. (11)) does not pose an upper limit to ϕ_H . Hence, processes for which η_H exceeds unity can by no means be excluded. It can easily be shown that the efficiency measures developed above, i.e. η_{th} and η_H , allow the formulation of expressions for the dissipation $T\Pi_s$ and the heat production ($-\phi_H$). The following

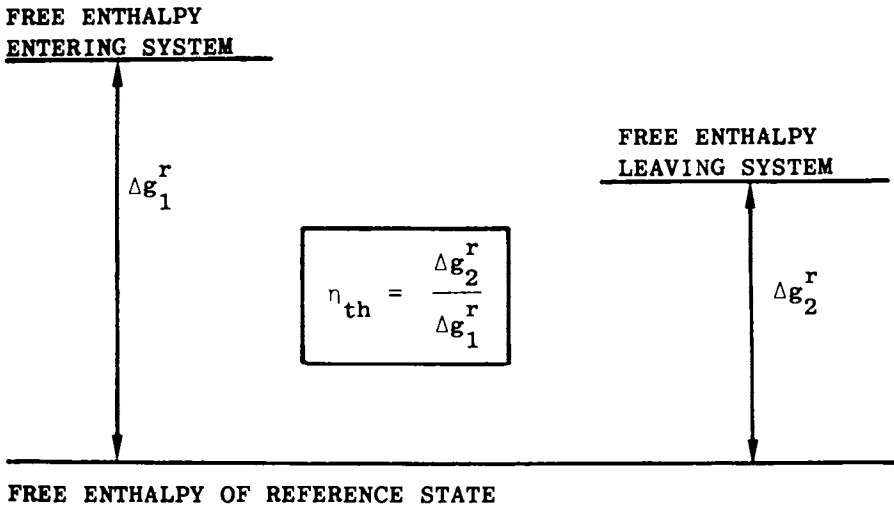


Figure 4. The thermodynamic efficiency, η_{th} , of a process. Δg_1^r and Δg_2^r are the amounts of free enthalpy gained when the compounds entering and leaving the system, respectively, are transformed to the reference state.

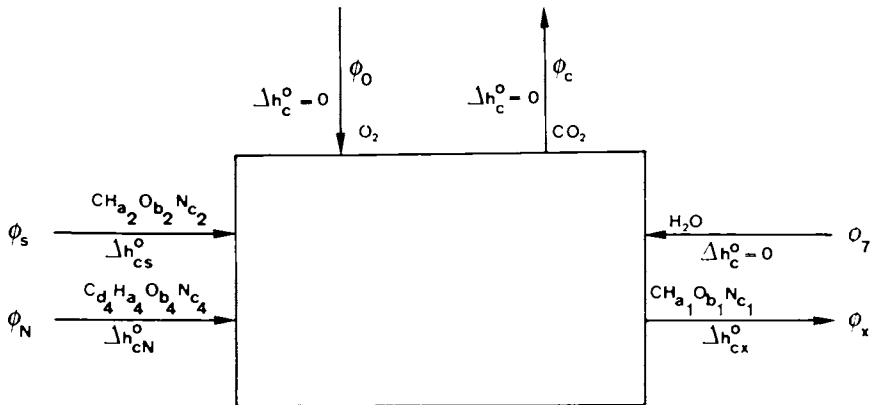


Figure 5. System and flows for thermodynamic analysis of aerobic growth without formation of products.

equations hold:

$$D = \phi_x \Delta g_{cx}^0 \{ (1 - \eta_{th}) / \eta_{th} \} \quad (22)$$

$$\phi_H = \phi_x \Delta h_{cx}^0 \{ (1 - \eta_H) / \eta_H \} \quad (23)$$

In eqn. (22) D equals the dissipation $T\Pi_s$.

For aerobic growth without product^s formation the absolute magnitude second term appearing at the left hand side of eqn. (11) can be shown to be small as compared to ϕ_H/T , i.e. the exchange of heat largely exceeds the exchange of "chemical entropy" (5, 6). This implies that D and ϕ_H are, to a good approximation equal and this, of course, also applies to η_{th} and η_H . In this case an analysis based on an enthalpy efficiency of growth is more or less valid and hence also the interpretation of the second law as to forbid processes with uptake of heat.

As has been shown earlier (6) the very fact that eqn. (16) is more or less valid implies that heat production and oxygen consumption, ϕ_o , are proportional according to the following equation:

$$\phi_H = 460 \phi_o \quad (24)$$

The approximate validity of this equation is easily understood as follows. The degree of reduction γ_e indicates the number of moles of electrons available for transfer to oxygen on complete combustion of a C-mole of a compound to CO_2 , H_2O and N_2 . On transfer to oxygen the energy of the electrons is dissipated, resulting in a heat production of 115 kJ per mole of electrons. On aerobic growth part of the energy content of the substrate and the nitrogen source is conserved in the form of newly synthesized biomass, the electrons corresponding to the remainder are transferred to oxygen and provide dissipation. As four moles of electrons are accepted by one mole of oxygen eqn. (16) shows 460 kJ to be generated for each mole of oxygen consumed.

The validity of eqn. (24) shows that a treatment can also be based on oxygen efficiency of growth (5-7).

A substantial body of data on aerobic growth without product formation supported by ammonia as a nitrogen source has recently been reviewed (9). From these data the values of η_{th} ($\approx \eta_H$) and the dissipation per unit biomass produced (D/ϕ_x , kJ/C-mole) were calculated. The results were averaged for each of the carbon sources considered and are shown in figs. 6 and 7.

Although, not unexpectedly, it is clear that considerable scatter is existent in both figs. 6 and 7, some global regularities seem to be present, which are indicated in the figures. For substrates with a degree of reduction lower than about 5, the thermodynamic efficiency averages 0.58 (the only significant outlier being the very low efficiency observed for growth supported by

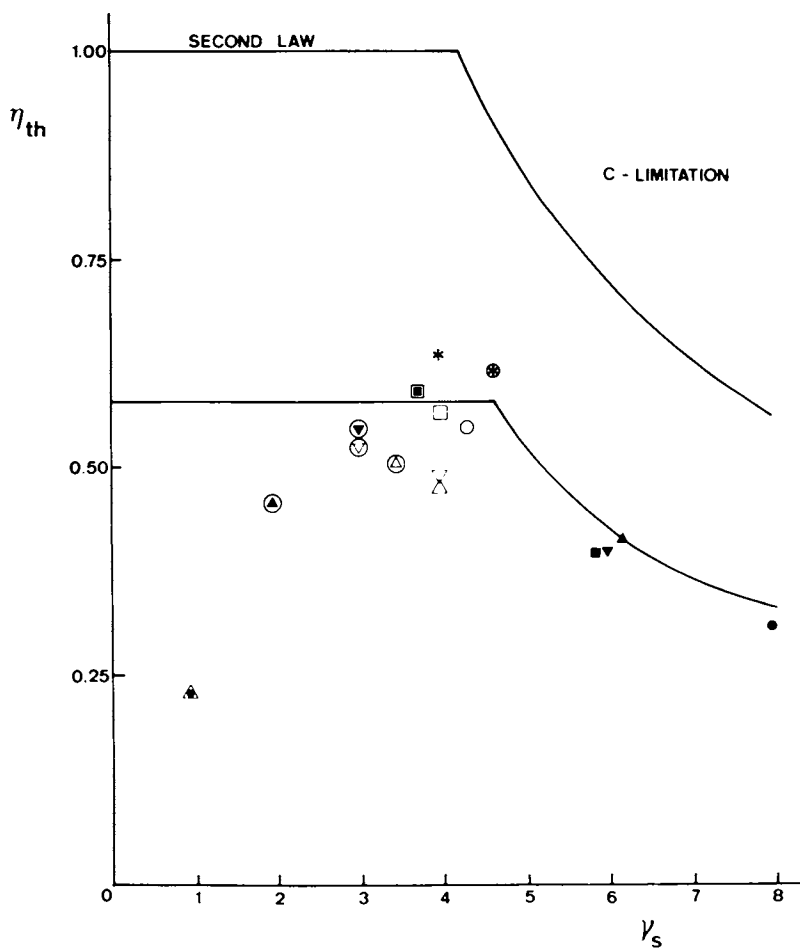


Figure 6. Thermodynamic efficiency, η_{th} , of aerobic growth with NH_3 as the nitrogen source, plotted as a function of the degree of reduction, γ , of the substrate. Theoretical limits due to the second law and C-limitation. Shown are averages of experimental data for methane (●), n-alkanes (▲), methanol (■), ethanol (▼), glycerol (⊗), mannitol (○), acetic acid (△), lactic acid (□), glucose (*), formaldehyde (▽), gluconic acid (■), succinic acid (⊕), citric acid (⊗), malic acid (⊖), formic acid (⊙), oxalic acid (▲).

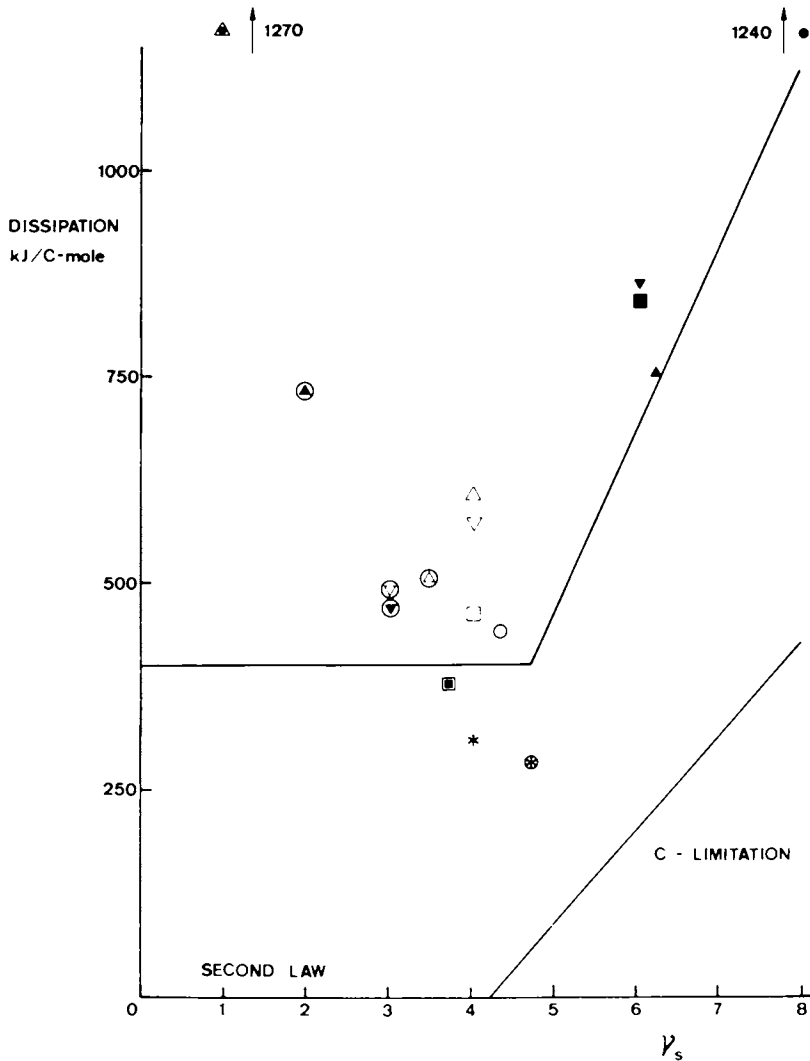


Figure 7. Dissipation of aerobic growth (kJ/C-mole of biomass produced) for aerobic growth with NH_3 as a nitrogen source as a function of the degree of reduction of substrate. Theoretical limits due to second law and C-limitation. Average of experimental data for various substrates, symbols as in Figure 6.

oxalic acid), this corresponds to a dissipation of roughly 400 kJ/mole of biomass produced. For substrates with a degree of reduction exceeding 5 the thermodynamic efficiency progressively decreases and the dissipation increases up to 1400 kJ/C-mole for the case of growth supported by methane.

In figs. 6 and 7 the restrictions of unit efficiency and zero dissipation respectively, as imposed by the second law are indicated as well as a limit imposed by a limitation of a different nature, i.e. carbon limitation. The latter limit merits a more thorough discussion. The degree of reduction, γ_x , of biomass from a variety of sources averages 4.8 (5,6,10) and hence by virtue of eqn. (16) its energy content is about 550 kJ/C-mole. If growth is supported by a substrate of a degree of reduction exceeding 4.8 its energy content will exceed the said 550 kJ/C-mole and hence, even if all substrate carbon were fixed in biomass, a thermodynamic efficiency lower than unity would be obtained. A complete exploitation of the energy present in the substrate would require fixation of additional low energy carbon e.g. from CO_2 . This is, however, excluded, as only one carbon source is assumed to be supplied.

On observation of fig. 6 it becomes clear that the trends observed in the experimental values of the thermodynamic efficiency mimic the shape of the theoretical restrictions at a level of about 60%. The deviation between the theoretical limit and the values actually observed is quite easily understood in general terms in the region of low degrees of reduction, where the energy available in the substrate rather than its carbon content limits the values of γ_{sx} . The theoretical limit of unity can never be reached as any process needs a non-zero dissipation to proceed at a non-zero rate (2-4). In fact the rate at which a process proceeds, e.g. the rate of growth of the amount of biomass, is to a certain extent increasing with increasing dissipation. Various optimality principles (11), may dictate an optimal thermodynamic efficiency of roughly the magnitude observed here (11, 12). The behaviour at high degrees of reduction is less easily understood on fundamental grounds. The thermodynamic efficiency could well approach the theoretical limit closer with a sufficiently large dissipation. Apparently other phenomena to which the formal macroscopic treatment provides no clues, limit the maximum conservation of substrate carbon in biomass to about 2/3 of the maximum. Obviously one has to resort to biochemical theory to obtain clues to the nature of the mechanisms underlying the phenomenon.

There exists still another useful quantity, which has been used to systematize the experimental data on the efficiency of growth supported by various carbon sources; it is Payne's yield on available electrons, $Y_{av/e}$ (13). It is defined as the amount of biomass produced per mole of electrons available for transfer to oxygen on complete combustion. Numerically the number of moles of electrons available for transfer to oxygen on

combustion of a C-mole of a given substrate is equal to the degree of reduction, γ , as defined by eqn. (15). As a first approximation, taking into account the fact that biomass from a variety of microbial sources can be well represented by the composition formula $\text{CH}_{1.8}\text{O}_{0.5}\text{N}_{0.2}$, $Y_{\text{av/e}}$ can be considered proportional to η_{th} (or rather η_{H}) (5, 6):

$$Y_{\text{av/e}} = 5.85 \eta_{\text{th}} \quad (25)$$

Figure 8 shows the data depicted in figs. 6 and 7 in a plot of $Y_{\text{av/e}}$ versus the degree of reduction γ . The trends and theoretical limits are also shown.

Growth with electron acceptors other than oxygen. In the preceding section a case was treated in which oxygen was the electron accepting moiety. Oxygen is, however, by no means the only compound, which can perform such function. Other examples are nitrate and sulphate. The characteristic feature of an electron acceptor is that free enthalpy is gained in the overall process of transfer of an electron from a given source (a substrate) to the acceptor. This free enthalpy is partly dissipated to provide the necessary irreversibility and it can be used to transfer carbon (-dioxide) from a low energy level to a high energy one. In table I a summary is provided of the energy becoming available on transfer of one mole of electrons from glucose to a given electron acceptor engaged in a given reduction process.

Table I. Free enthalpy gained at pH = 7 and standard conditions on transfer of one mole of electrons from glucose to a given electron acceptor (14)

electron acceptor	moles of electrons accepted	$\Delta g^0(1)$ kJ	$\Delta g_{\text{av/e}}^0(1)$ kJ/mole
N_2 (NH_4^+)*	6	79.1	13.2
S (HS^-)	2	27.7	13.9
SO_4^{2-} (HS^-)	8	150.7	18.8
SO_3^{2-} (HS^-)	6	171.9	28.7
NO_2^- (NH_4^+)	6	435.5	72.6
NO_3^- (NH_4^+)	8	598.4	74.8
NO_3^- (N_2)	5	559.5	111.9
O_2 (H_2O)	4	473.9	118.5

* In brackets reduced form of electron acceptor

The values of the free enthalpy gained per mole of electrons transferred are arranged in order of increasing magnitude. The "efficiency" of an electron acceptor thus increases from the top to the bottom of the table and faith in life's universal striving for more optimal growth would assume preference for the electron acceptors at the bottom of the table if two or more electron acceptors are simultaneously available.

Growth without externally supplied electron acceptors. In a number of cases growth is observed to take place without an identifiable separate electron acceptor being present. In such case the substrate or a substrate derived moiety is both donor and acceptor of electrons. For simplicity's sake only the case of anaerobic growth on a single carbon source with formation of a single product and NH_3 as the nitrogen source will be treated. It is easily understood that an analysis of anaerobic growth can be based on a balance on the degree of reduction as defined by eqn. (16). Table II shows the flows of the various compounds and their content of electrons available for transfer to oxygen on formation of ϕ_x C-moles of biomass.

Table II. A degree of reduction balance for anaerobic growth without external electron acceptors

molecular species	degree of reduction	flow	contribution to degree of reduction balance
substrate	γ_s	ϕ_x/Y''_{sx}	$\gamma_s \phi_x / Y''_{sx}$
N-source (NH_3)	3	$c_1 \phi_x$	$3c_1 \phi_x$
Biomass ($\text{CH}_{a1}\text{O}_{b1}\text{N}_{c1}$)	γ_x	ϕ_x	$-\gamma_x \phi_x$
Product	γ_p	ϕ_p	$-\gamma_p \phi_p$
CO_2	0	$\phi_x / Y''_{sx} - \phi_x - \phi_p$	0
H_2O	0	ϕ_w	0

By virtue of the fact that no external electron acceptors are present the contributions to the degree of reduction balance as shown in the last column of table 2 must add up to zero, it follows:

$$\phi_p = (\phi_x / \gamma_p) (\gamma_s / Y''_{sx} + 3c_1 - \gamma_x) \quad (26)$$

$$\phi_c = \phi_x \{ (1 - \gamma_s / \gamma_p) / Y''_{sx} - 1 - 3c_1 / \gamma_p + \gamma_x / \gamma_p \} \quad (27)$$

It becomes clear that on the anaerobic growth process an amount of product ϕ , given by eqn. (26), is formed. It corresponds to the transfer of $(\gamma/Y'' + 3c_1 - \gamma_x)\phi$ moles of electrons from the substrate to CO_2 , resulting in the formation of the product. Clearly, the driving force of the reaction, which must, amongst others, provide the necessary dissipation, must rest in the fact that the electrons in the substrate are at a higher free enthalpy level than those in the product. The mechanism of this process becomes clearer if eqns. (16) and (17) are observed closer. The enthalpy of combustion is, for compounds of different degree of reduction, apparently to a very good degree of approximation equal per mole of electrons available for transfer to oxygen. Hence, if enthalpy were, as in the case of aerobic growth, to be the source providing dissipation, anaerobic growth would to a degree of approximation involve only negligible dissipation and be impossible from the thermodynamic point of view. Equation (17), however, shows that the free enthalpy content of a substrate per mole of available electrons decreases, as a general tendency, with increasing degree of reduction. Hence, the dissipation necessary for efficient growth can be gained if a product of a higher degree of reduction is, with formation of CO_2 , formed from a substrate with a low degree of reduction (6). This can be shown to be the general tendency underlying anaerobic growth of the type treated here. The general tendency underlying aerobic growth is that, contrary to the situation in aerobic growth, that is driven by the enthalpy rather than the "chemical entropy" contribution to the dissipation, it involves a large contribution of "chemical entropy" dissipation at a generally minor contribution due to heat production. For practical purposes, this means that on these anaerobic processes close to 100% of the energy of combustion of the substrate supplied is conserved in the product and biomass formed, the irreversibility being provided by the contribution, $T\Delta s^0$.

The tendency sketched above only accounts for the main features, another important aspect being that anaerobic growth proceeds to compounds, which have a low enthalpy at a given degree of reduction, i.e. anaerobic growth is also driven by the deviations from eqns. (16) and (17) rather than by the general tendencies these equations describe.

The reason that the limited accuracy of eqns. (16) and (17) becomes important here, whilst being of virtually no importance in aerobic growth, rests in the fact that large flows of substrate and product are involved in anaerobic growth. Thus, dissipation becomes the difference of two large numbers and minor errors in these contributions become quite significant.

As a typical example of the features exhibited by anaerobic growth the following quantities are worthwhile. On anaerobic growth of a yeast on glucose with formation of ethanol typically about 90 kJ of heat are generated per C-mole of biomass produced; this value is substantially lower than the heat production on

aerobic growth of that same yeast, which typically amounts to 300 - 350 kJ/C-mole. The free enthalpy dissipation on anaerobic growth is, however, close to 300 kJ/C-mole produced, i.e. slightly lower than or equal to that on aerobic growth.

An earlier study performed by the present author (5, 6) showed that, if a realistic reference state for energy content is chosen, anaerobic growth proceeds as a general tendency with a thermodynamic efficiency of the same order of magnitude as that observed on aerobic growth. This provides the nucleus to a postulate that will be somewhat more closely investigated in the last section of this paper: Growth yields can as a rule of thumb be estimated from the assumption of a constant thermodynamic efficiency or, equivalently, a constant dissipation per unit biomass produced.

The constant efficiency hypothesis

For growth supported by different sources and sinks of electrons, e.g. aerobic growth, growth supported by electron acceptors other than oxygen or growth processes in which no external electron acceptors are present, widely varying substrate yields, e.g. expressed as Y''_{sx} , are observed. As was already indicated with reference to aerobic growth, matters can be generalized to a certain extent if yields are expressed in terms of $Y_{av/e}$, the yield expressed per mole of substrate electrons available for transfer to oxygen. However, as was pointed out in discussing table I, largely different amounts of energy may result from the transfer of one mole of electrons in dependence on the donor/acceptor combination. Table III provides a summary of literature data. For a number of growth processes the yield on available electrons, $Y_{av/e}$, as well as the $\Delta g_{av/e}^{0'}$, the free enthalpy obtained on transfer of one mole of electrons from the substrate to the electron acceptor (standard conditions and a pH = 7), are given.

Even a superficial study of table III clearly shows the existence of a relationship between $Y_{av/e}$ and $\Delta g_{av/e}^{0'}$. This relationship can be systematized as follows. If the thermodynamic efficiency, η_{th} , is known eqn. (22) allows the calculation of the dissipation per unit biomass produced. Furthermore it has to be recognized that the dissipation per mole of biomass produced can be calculated from:

$$D/\phi_x = \Delta g_{av/e}^{0'} (25.8/Y_{av/e} - 4.8) + 65.8 \quad (28)$$

In which the conversion factor 25.8 accounts for the conversion of g.DM. to C-moles, 4.8 is a correction accounting for the number of moles of available electrons conserved in one C-mole of biomass formed, and 65.8 accounts for the free enthalpy of combustion of the ammonia used in the process of

Table III. Yields on available electrons and energy available per mole of electrons transferred for various processes

substrate	electron acceptor	Y_{av}/e g.D.M./ mole	$\Delta g_{av}^0/e$ Source
Glycerol	O ₂	3.65	116.4 Average from (9)
Mannitol	O ₂	3.26	117.5
Acetic acid	O ₂	2.63	105.5
Lactic acid	O ₂	3.26	110.1
Glucose	O ₂	3.84	118.5
Formaldehyde	O ₂	2.98	124.0
Gluconic acid	O ₂	3.53	117.9
Succinic acid	O ₂	2.90	107.1
Citric acid	O ₂	3.09	111.0
Malic acid	O ₂	3.18	112.1
Formic acid	O ₂	3.17	118.0
Oxalic acid	O ₂	1.78	119.0
Succinic acid	NO ₃ ⁻	2.28	100.6 (15)
Succinic acid	NO ₂ ⁻	2.71	120.9 (15)
Succinic acid	O ₂	2.75	107.1 (15)
Gluconic acid	O ₂	3.26	117.9 (15)
Gluconic acid	NO ₃ ⁻	3.44	111.4 (15)
Glucose	Glucose→ethanol	0.88	9.5 from (6)
Glucose	Glucose→lactic acid	0.81-1.5	8.3
Glucose	Glucose→propionic/acetic acid	1.48	12.9
Glucose	Glucose→methane/acetic acid	1.63	14.4
Acetic acid	Acetic acid→methane	0.36	3.9
Methanol	Methanol→methane	0.91	13.0
Formate	Formate→methane	0.27	16.4
Propionic acid	Propionic acid→methane	0.41	4.0

growth. The biomass was assumed to have the standard composition $\text{CH}_{1.8}\text{O}_{0.5}\text{N}_{0.2}$ and to contain 5% ash.

If eqns. (28) and (22) are combined the following expression can be derived:

$$Y_{\text{av/e}} = \frac{25.8\Delta g_{\text{av/e}}^{0'}}{536(1 - \eta_{\text{th}})/\eta_{\text{th}} + 4.8\Delta g_{\text{av/e}}^{0'} - 65.8} \quad (29)$$

From eqn. (29) the solid line depicted in fig. 9, which corresponds to an η_{th} of 0.65, was calculated. Part of the experimental data depicted in table III are also indicated in the figure. As can be seen the general features of the experimental material follow the regularity of a constant efficiency of about 0.65. Of course, some deviations and outliers are present. This may be due to limitations of the experimental material as well as of the approximate nature of the calculations as the free enthalpy changes are based on standard conditions for compounds apart from the H^+ ion and water.

As a representative example the following analysis may prove illustrative. Aerobic growth of the yeast *S. cerevisiae* proceeds with a yield, $Y_{\text{av/e}}$, of about 3.75 (g DM/mole av/e). Equation (29) allows η_{th} for this case to be estimated at 0.63. ($\Delta g_{\text{av/e}}^{0'}$ equals 118.5). For anaerobic growth on glucose with formation of ethanol $\Delta g_{\text{av/e}}^{0'}$ equals 9.5 and if η_{th} would remain constant at 0.63 a $Y_{\text{av/e}}$ of 0.83 would be expected. This corresponds well to the experimental value of 0.88.

The analysis presented above may in some cases provide a useful alternative to the treatment of the efficiency of growth in terms of a Y_{ATP} or $Y_{\text{ATP}}^{\text{max}}$ value (16, 17), which involves the necessity of knowledge of the detailed biochemistry of the pathways used in the generation of metabolic energy. The treatment developed above does not need such information as it is based on an analysis of the energy flows to and from a system, without consideration of the detailed metabolic mechanism causing coupling of energy generation to biomass formation and dissipation processes in functioning living organisms.

Of course exceptions to the general rules developed above exist as is already apparent from the fact that the low efficiencies observed on aerobic growth on highly reduced compounds, where factors other than available energy are limiting, were, for obvious reasons, not included in the analysis performed in the present section.

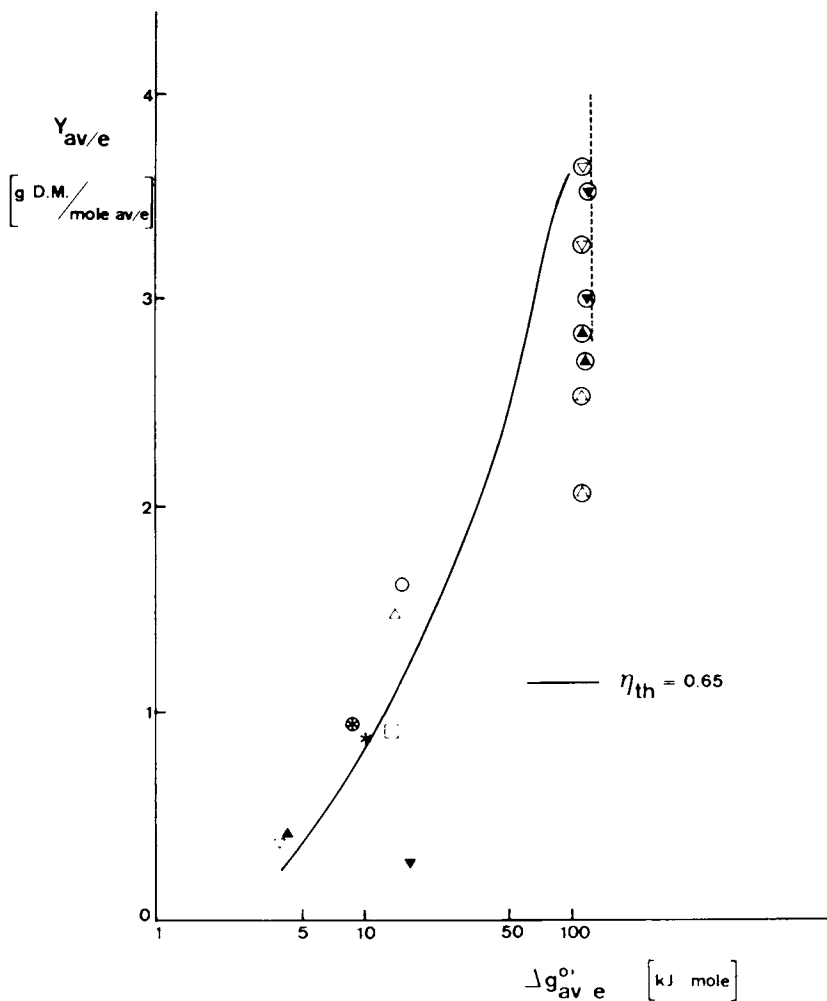


Figure 9. Relationship between yield on available electrons, $Y_{av/e}$ (g DM/mole) and the energy gained per mole electrons transferred to the electron acceptor, $\Delta g_{av/e}^{\circ}$ (kJ/mole). Expected relation if the thermodynamic efficiency were constant at 0.65 (—). Experimental data are shown for aerobic growth on glucose (---), succinate (\oplus), and gluconate (\odot). Data are shown for growth with NO_3^- as an electron acceptor on succinate (\otimes), and on gluconate (\odot). Anaerobic growth on glucose is shown with formation of ethanol (*), lactate (\ominus), propionic/acetic acids (Δ), and methane/acetic acid (\circ). Anaerobic growth is shown with formation of methane from acetic acid (∇), formic acid (\blacktriangledown), propionic acid (\blacktriangle), and methanol (\square).

List of symbols

a_i	number of moles of hydrogen per C-mole of compound i (-)	
a_4	number of moles of hydrogen per mole of N-source (-)	
b_i	number of moles of oxygen per C-mole of compound i (-)	
b_4	number of moles of oxygen per mole of N-source (-)	
C_i	concentration of compound i (moles/l)	
c_i	number of moles of nitrogen per C-mole of compound i (-)	
c_4	number of moles of nitrogen per mole of N-source (-)	
D	dissipation	(kJ/s)
d_4	number of moles of carbon per mole of N-source (-)	
e_{ij}	number of moles of atomic species j per mole of compound i	(-)
g_i	partial molar free enthalpy of compound i	(kJ/mole)
g_i^0	partial molar free enthalpy of compound i at standard conditions	(kJ/C-mole)
$\Delta g_{av/e}^0$	free enthalpy gained on transfer of one mole of electron from an electron donor to an electron acceptor at a pH = 7	(kJ/mole)
Δg_{ci}^0	partial free enthalpy of combustion of a C-mole of compound i at standard conditions	(kJ/C-mole)
$\Delta \bar{g}_{ci}^0$	partial molar free enthalpy of combustion of compound i at standard conditions	(kJ/mole)
Δg_{ci}^0	partial free enthalpy of combustion of a C-mole of compound i at a pH = 7	(kJ/C-mole)
h_i	partial molar enthalpy of compound i	(kJ/mole)
Δh_{ci}^0	partial heat of combustion of a C-mole of compound i at standard conditions	(kJ/C-mole)
$\Delta \bar{h}_{ci}^0$	partial molar heat of combustion of compound i at standard conditions	(kJ/mole)
j_Q	surface density of the rate of transport of Q	(kJ(mole)/m ² s)
Q	volume density of the amount of quantity Q	(kJ(mole)/m ³)
R	universal gas constant	(kJ/mole K)
r_Q	volume density of the rate of production of Q	(kJ(mole)/m ³ s)
S	surface area	(m ²)
s_i	partial molar entropy of compound i	(kJ/mole K)

Δs_{ci}^0	partial entropy of combustion of a C-mole of compound i at standard conditions	(kJ/C-mole K)
$\Delta s_{ci}^{0'}$	partial entropy of combustion of a C-mole of compound i at a pH = 7	(kJ/C-mole K)
T	absolute temperature	K
V	volume	m ³
Y_{sx}''	yield for biomass on substrate	(C-mole/C-mole)
$Y_{av/e}$	yield on the substrates' available electrons	(g.D.M./mole)
γ_i	degree of reduction of compound i	(-)
η	Minkevich and Eroshin's efficiency	(-)
η_H	enthalpy efficiency	(-)
η_{th}	thermodynamic efficiency	(-)
Π_S	entropy production rate	(kJ/Ks)
ϕ_i	rate of flow of compound i to the system	(mole/s)
ϕ_E	rate of flow of energy to the system	(kJ/s)
ϕ_H	heat flow to the system	(kJ/s)

Subscripts:

c	carbon dioxide
N	nitrogen source
o	oxygen
p	product
s	substrate
x	biomass

Literature Cited

1. Morowitz, H.J. Energy Flow in Biology 1968, Academic Press: New York
2. Prigogine I. Thermodynamics of Irreversible Processes Third Edition. Wiley: New York, 1967
3. Glansdorff, P., I. Prigogine Thermodynamic Theory of Structure Stability and Fluctuations; Wiley: New York, 1971
4. Haase, R. Thermodynamics of Irreversible Processes; Addison-Wesley. Reading (MA) 1969
5. Roels, J.A. Biotechnol. Bioeng. 1980, 22, 2457
6. Roels, J.A. Ann. New York Acad. Sci., 1981, 369, 113

7. Minkevich, I.G., Eroshin, V.K. Folia Microbiol., 1973, 18, 376
8. Kharasch, M.S. Bur. Stand. J. Res., 1929, 2, 359
9. Heijnen, J.J.; Roels, J.A. Biotechnol. Bioeng., 1981, 23, 739
10. Roels, J.A. Bioengineering Energetics and Kinetics, Elsevier North Holland (In prep.)
11. Stucki, J.W. Eur. J. Biochem.; 1980, 109, 269
12. Payne, W.J. Annu. Rev. Microbiol.; 1970, 24, 17
13. Caplan S.R. Curr. Top. Bioenerg.; 1971, 4, 1
14. Thauer, R.H.; Jungerman, K.; Decker, K. Bacteriol. Rev.; 1977, 41, 100
15. Van Verseveld, H.W. Influence of Environmental Factors on the Efficiency of Energy Conservation in Paracoccus denitrificans
Ph. D. Thesis, Free University of Amsterdam; Meppel Krips
Repro, 1979
16. Bauchop. T.; Elsdén, S.R. J. Gen. Microbiol. 1960, 23, 457
17. Stouthamer, A.H. Microbial Biochemistry, 1979, 21, 1

RECEIVED June 29, 1982

Ion Pumps as Energy Transducers

ERICH HEINZ

Cornell University Medical College, New York, NY 10021

Ionmotive forces, i. e. the electrochemical potential differences produced by ion pumps may serve to transmit energy released by exergonic reactions to drive endergonic processes, such as synthesis of energy-rich compounds or uphill transport of organic solutes. A typical example is the "chemiosmotic coupling" by a proton pump in oxidative and photosynthetic phosphorylation. The effectiveness of this coupling depends on its (energetic) efficiency as well as on its (kinetic) expeditiousness. The efficiency is mainly limited by inner and outer leakages to the transported ion species, the expeditiousness mainly by the delay in generating the protonmotive force. Whereas little is known about the various leakages to assess the efficiency, some preliminary information concerning the expeditiousness may be considered here. The generation of an ionmotive force, to the extent that it depends on ion gradients is a rather slow process. Electrogenic pumps, however, can more rapidly raise the electrical potential, prior to appreciable ion translocation by loading the static membrane capacity. Such rapid electric effects may significantly increase the expeditiousness of the coupling but only under the condition that the pump works at constant driving force. On the other hand, if the pump works at constant rate the rise of the protonmotive force is largely determined by the formation of ion gradients which rise more slowly and are less sensitive towards variations in energy input. Using a recently developed optical method of rapidly monitoring the PD, it could be shown that the light-driven proton pump of halobacterium halobium has the high expeditiousness predicted for an electrogenic pump working at constant driving force.

0097-6156/83/0207-0323\$06.00/0

© 1983 American Chemical Society

In order that energy be transferred between two different processes these have to be coupled. Homogenous coupling, i.e. between two chemical reactions within the same compartment is usually based on the principle of the "common intermediate" as is illustrated by the "classical" coupling between the dehydrogenation of triose-phosphate and the formation of adenosine triphosphate, for which diphosphoglycerate was identified as the "common intermediate" that links these two reactions. An analogous, though somewhat different principle underlies the coupling between two osmotic processes, e.g. in (secondary active) ion-linked cotransport, namely through a ternary complex supposedly formed by the two solutes with a carrier or a mobile gate. More complicated and less well understood is the corresponding principle of heterogenous coupling, between a chemical and an osmotic process in primary active transport, as has been discussed in more detail elsewhere (1). This coupling had mainly been considered a means of transferring chemical energy to drive an endergonic osmotic process, until Mitchell (2) postulated the reverse for mitochondrial and bacterial "oxidative phosphorylation" where the synthesis of energy rich phosphate should be energized by the downhill movement of H⁺-ions. In the evolving "chemiosmotic hypothesis" of oxidative phosphorylation two steps of heterogenous coupling occur in series: the first one links an oxidation-reduction reaction to the active extrusion of protons, thereby generating an electrochemical potential difference of H⁺-ions ("protonmotive force"); the second one links the passive reentry of protons, driven by this force, to the synthesis of energy-rich phosphate by means of the "proton translocating ATPase" (Fig. 1). There is good evidence that the same sequence of similar coupling steps occurs in the oxidative phosphorylation of aerobic bacteria (3) as well as in the light-driven phosphorylation of chloroplasts (4, 5), and halophilic bacteria (6). Various plausible models of such systems have since been devised and critically discussed (7, 8, 9). Though the postulated "chemiosmotic" coupling has not been proven yet beyond doubt, it is so far well enough supported by experimental evidence to justify the wide belief in its validity. It is nonetheless surprising that this coupling, which ultimately links two truly chemical reactions, does in contrast to the classical models not involve a common chemical intermediate, but rather two heterogenous coupling steps in series. In other words, energy is transferred from one chemical reaction to another one in osmotic form, with the help of two "chemiosmotic energy transductions". Whether this peculiar kind of coupling is a mere vestige or whether it has certain advantages as compared to other kinds of coupling, for instance, by being more effective, is hard to tell. Let us see how and under which conditions a greater effectiveness might come about.

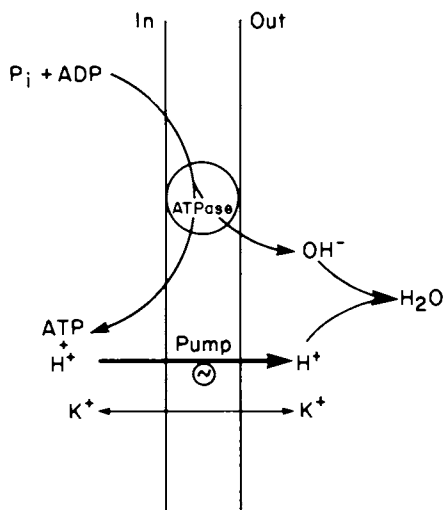


Figure 1. Chemiosmotic coupling in oxidative phosphorylation. The model is drawn according to Mitchell's hypothesis for mitochondria, but might also apply to other systems of phosphorylation.

A hydrogen ion pump transports the H^+ -ions from left to right, energized by an oxidation-reduction reaction, a light-driven photochemical mechanism, or any other appropriate energy source. This pumping is tantamount to pumping OH^- -ions in the opposite direction. A membrane-bound enzyme, the proton translocating *ATPase* catalyzes the interconversion of *ADP* and P_i and *ATP* by a heterophasic (or vectorial) reaction, i.e., a reaction in which the OH^- -ions, released by the synthesis or incorporated by the hydrolysis of *ATP*, can interact with the enzyme only from the phase contralateral to that from which the other reactants interact. In this way, the direction of the chemical reaction depends on the spatial direction of the H^- (or OH^-) gradient.

The overall effectiveness of any coupling mechanism may be assessed in terms of its (energetic) efficiency as well as in terms of its (kinetic) expeditiousness. The energetic efficiency is limited by the extent of unavoidable leakages, which are partly due to passive permeability of the membrane barrier to the transported solute (outer leakage) and partly reside in the transport mechanism itself (inner leakage) in that "slipping" and "back cycling" may permit the escape of unutilized input energy (1). Too little is known about the extent of leakages within the chemiosmotic mechanism of phosphorylation to compare its energetic efficiency with that of its chemical counterpart.

Not much more is known about the expeditiousness which, in this context, may be defined as the rate at which the protonmotive force rises after the onset of the pump, but some general predictions can be made. The expeditiousness is the higher the faster the pumping rate of protons is relative to the conductance of passive ions, which tend to shunt the electrogenic pump effect, in other words, to maintain electroneutrality. We see that the two components of the protonmotive force, the electrical and the chemical PD, are controlled by different factors and may therefore develop at different rates, as is illustrated by the following two extreme conditions:

If the passive conductance is extremely low, the electrical potential will be generated purely electrogenically, i. e. without appreciable net movement of passive ions. As the electric capacity of the membrane is rather low, $1\mu\text{F}/\text{cm}^2$, electrogenic expulsion of 300-400 protons per cell, passive shunting effect being negligible at this stage, should suffice to raise the electrical PD by 1 mvolt.

On the other hand, if the passive conductance is very high, it will keep electrical effects small but allow instead an equivalent rise of the chemical PD of protons. This rise will depend on the buffer capacity of the medium, which is normally much higher than the electrical capacity. From its value in the mitochondria we would estimate that about a million protons have to be expelled per 1 mvolt rise of the chemical PD, and hence of the protonmotive force. Obviously, the rise in chemical PD in this case is thousand or more times slower than the electrogenic one in the former case. At the rate assumed for the mitochondrial proton pump, we would predict that the critical protonmotive force, i. e. about 200 mvolts, could be reached within a few hundred milliseconds in the first case, but would take a few hundred seconds in the last case. It follows that the expeditiousness of the coupling, i. e. the speed at which this critical protonmotive force is reached after the initiation of the pump depends on the relative contribution of the initial pumping rate relative to the shunting pathways for passive ions.

To approach this problem quantitatively, we may for simplicity reasons follow the conventional procedure used by electrophysiologists in dealing with electrogenic pumps in their biological systems, etc. In the equivalent circuits used by them to visualize the electric phenomena of biological systems, an electrogenic ion pump is usually represented either as a constant voltage source or as a constant current source, based on the simplifying assumption that during the experimental observation either the driving force of the pump or the pumping rate remains fairly constant. The difference between these two alternatives corresponds with some crude approximation to the above discussed difference between two kinds of coupling models; the constant voltage source network most closely would account for the expeditiousness, but less stable coupling model, whereas the constant current source would do so for the more sluggish but more stable model. In most cases, it is difficult to tell a priori which of the two is correct as for either one some plausible explanation can be given. As a consequence, the treatment by electrophysiologists in this respect is not uniform, but as long as the steady state is concerned, either one may give reasonable answers. The difference between the two models becomes, however, crucial in transient states, for instance, immediately after the pump has been turned on or off.

Mitchell (8) was probably the first to investigate these questions, and by rigorous calculations, based on the assumption of constant pumping rate, he predicted that the electrical PD rises very fast but insignificantly high while the full development of the protonmotive force has to await the generation of a sufficiently high concentration gradient which would take more than 30 seconds. The same approach, except for the assumption that the driving force, rather than the rate of the pump remains constant, gave a greatly different result (10, 11). Depending on the pumping rate relative to the passive ion mobilities, the initial surge of the electrical potential may indeed be high enough to anticipate most of the final protonmotive force at static head (Fig. 2). Obviously, a constant pumping rate implies that the driving force is initially low but rises accordingly as the opposing protonmotive force grows. By contrast, at constant driving force, the pumping rate should initially be very high and later decline accordingly as the opposing protonmotive force rises. A priori, both models are in some way plausible and only the experiment can decide which one is the valid one.

So far, experimental tests are scarce, partly due to the difficulties to measure rapidly enough changes in electrical membrane potential (or protonmotive force) with small compartments such as mitochondria and bacteria. The usually applied chemical probes for potential changes are either too slow or too noisy. Recently, however,

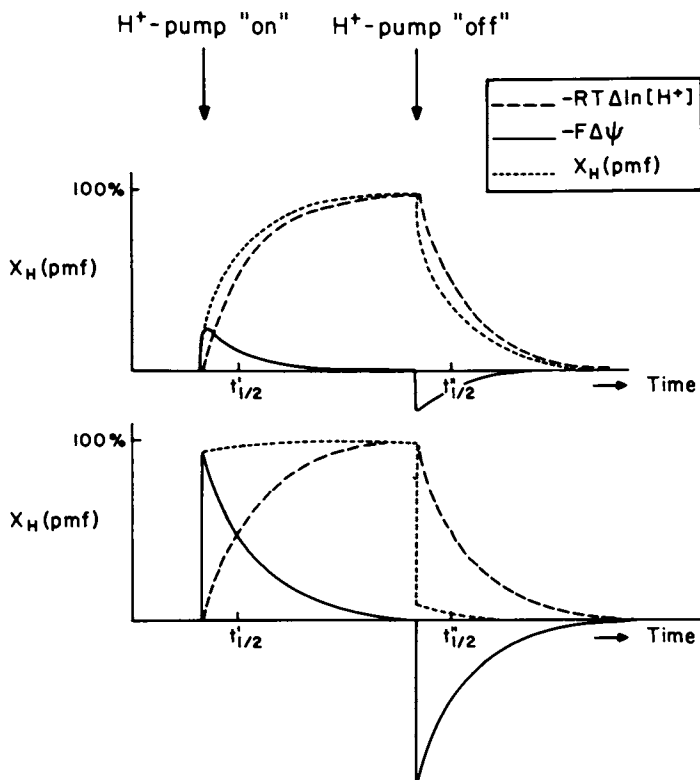


Figure 2. The calculated response of the protonmotive force, and its electrical and chemical components, to the sudden initiation or stopping of an electrogenic proton pump.

Ordinate: protonmotive force (X_H) in relative units. Abscissa: time. Solid line, electric PD; dashed line, chemical PD of H^+ ; dotted line, X_H . Top: constant rate of pumping (constant current source). Bottom: constant driving force of the pump (constant voltage source). It is seen that only under the condition of constant driving force is the initial rise of the electrical PD, and hence of the total protonmotive force, high enough to make pumping power available almost instantaneously after the start of the pump. It also is seen that the pump is more stable under constant pumping rate, because after the pump is turned off, the PMF drops almost instantaneously in the lower curve whereas it declines gradually in the upper curve. Reproduced, with permission, from Ref. 11. Copyright 1982, Academic Press, Inc.

a method that allows rapid monitoring of such changes based on a change in light absorption of the naturally present substance, bacteriorhodopsin, has been devised for the light-driven proton pumps in halobium (12). By this method, it could be shown with envelope vesicles of this bacterium, that after initiating the pump by illumination, the electrical potential (or the protonmotive force) rises with a half time of about 20 msec to a value close to 200 mv even though the buffer capacities of all permeant ions inside and outside was kept high enough to preclude appreciable changes in ion distribution during that time (13). This result closely agrees with what has been predicted on the basis of the constant driving force model, and thus confirms the hypothesis of the crucial role of the electrical potential for the expeditiousness of the coupling system.

This result also confirms that the pump is electrogenic, according to the following equation derived in terms of non-equilibrium thermodynamics (14):

$$F \left(\frac{\partial \Psi}{\partial A_{ch}} \right)_{\Delta \mu_{K^+}, \Delta \mu_{H^+}} = \frac{(\nu_K - \nu_H) L_T}{(\nu_K - \nu_H)^2 L_T + L_H^u + L_K^u}$$

$\Delta \Psi$ is the electric PD, A_{ch} the driving force of the pump and L_T the coefficient relating the overall pumping rate to A_{ch} . L_H^u and L_K^u are leakage coefficients of H^+ and K^+ , respectively. ν_K and ν_H are stoichiometric coefficients of the pump for the ions indicated. It is seen that at constant chemical potentials of the ions concerned the partial differential is different from zero only in the presence of an electrogenic pump, i.e. if $\nu_H \neq \nu_K$. Though buffer capacities of all permeant ions concerned were kept high enough to prevent the formation of any significant ion gradient during the time of observation a distinct electric response was registered upon illumination after a few milliseconds as would be inconsistent with an electrically silent H^+/K^+ pump ($\nu_H = \nu_K$).

Whether the high expeditiousness resulting from the electrogenic PD rise would be an advantage for any system is hard to predict. Owing to the low electric membrane capacity the ionmotive force at this stage, being predominantly electrogenic is very sensitive towards changing the driving force. By contrast a more slowly developing ionmotive force generated by ion translocation is certainly more stable as the energy stored in it would still be available for some time after the pump has stopped. If the system were to supply energy-rich compounds at a steady rate in spite of highly fluctuating energy input, obviously the slower but more stable arrangement would be more suitable. If, on the other hand, the system were to adjust its activity to a rapidly changing requirement at a rather steady input of energy, the more expeditious but less stable arrangement would be more suitable.

On the other hand, it is very likely that the electrogenic PD of a highly expeditious coupling system appears only as a wave of rather short duration, being replaced later by the chemical PD, which may predominate after the system has reached a stationary state (Fig. 2). Such is to be expected if the "buffer capacities" of the passive ions, chiefly K-ions, are big enough to prevent the formation of a more stable diffusion potential. Hence the protonmotive force generated by such a system may have a different composition in the stationary state from that during the initial electrical potential rise. In this way, the advantage of a high expeditiousness at the beginning may be combined with that of a higher stability obtained after some time of continuous pumping activity. Fig 2. also shows that the degree of stability at any stage should become apparent if the pump is suddenly stopped. After the pump has reached its (stable) stationary state, the protonmotive force at that stage would decay only slowly and would therefore be measurable immediately after the pump has stopped. In the initial stage, however, when the electrogenic component of the PMF dominates, the PMF should immediately disappear after stopping the pump, and thus escape detection. This may be the reason why the protonmotive force has often been found inadequate to support the chemiosmotic hypothesis of oxidative phosphorylation, as the electrogenic component is too labile to survive the disturbance associated with the usual measurements of electrical potential.

Acknowledgment

These studies were supported by a USPHS-NIH grant No. ROI GM 26554-01.

Literature Cited

1. Heinz, E., "Mechanics and Energetics of Biological Transport"; Springer Verlag: Heidelberg, New York, London, 1978
2. Mitchell, P., Nature, 1961, 191, 144-8
3. Maloney, P.C., Wilson, T.H., J. Membrane Biol, 1975, 25, 285
4. Junge, W., Ber. Dtsch. Bot. Ges., 1975, 88, 283-301
5. Witt, H.T., Biochim. Biophys. Acta, 1979, 505, 355-427
6. Stoeckenius, W., Lozier, R.H., Bogomolni, R.A., Biochim. Biophys. Acta, 1979, 505, 215
7. Mitchell, P., "Chemiosmotic Coupling in Oxidative and Photosynthetic Phosphorylation"; Glynn Research Ltd.: Bodmin, 1966
8. Mitchell, P., "Chemiosmotic Coupling and Energy Transduction"; Glynn Research Ltd.: Bodmin, 1968
9. Skulachev, V. P., "Membrane Energetics"; Lee, C. P., Schatz, G., Ernster, L., Eds; Addison-Wesley; p. 373

10. Heinz, E., "Electrogenic and Electrically Silent Proton Pumps in Hydrogen Ion Transport in Epithelia"; Shultz, I., Sachs, G., Forte, J.G., Ullrich, K.J., Eds; Elsevier/North Holland Biomedical, 1980, p. 41
11. Heinz, E., "Current Topics in Membranes and Transport"; Kleinzeller, A., Bronner, F., Eds; Academic, 1982; Vol 16, p. 249
12. Dancshazy, Z., Helgerson, S. L., Stoeckenius, W., in preparation
13. Helgerson, S. L., Dancshazy, Z., Stoeckenius, W., Heinz, E.; (Abstract); Biophys. J., 1982, 37, 266a
14. Heinz, E., "Electrical Potentials in Biological Membrane Transport"; (Monograph); Springer, 1981

RECEIVED June 29, 1982

Kinetics and Transport Phenomena in Biological Reactor Design

M. MOO-YOUNG

University of Waterloo, Department of Chemical Engineering,
Waterloo, Ont. N2L 3G1 Canada

H. W. BLANCH

University of California, Department of Chemical Engineering, Berkeley, CA 94720

The application of chemical engineering principles is useful in an analysis of the design and operation of bioreactors. However, classical approaches to the analysis are limited by the following special constraints:

1. The reactant mixture is relatively complex. Microbial biomass increases with the biochemical transformation and catalyst is synthesized as the reactions proceed.
2. The bulk densities of suspended microbial cells and substrate particles generally approach those of their liquid environment so that relative flow between the dispersed and continuous phases is normally low. This situation may be contrasted to the relatively heavy metallic catalyst particles generally used in chemical reactors.
3. The sizes of single microbial cells are very small (in the range of a few microns) compared to chemical catalyst particles: coupled with the above constraints it is generally difficult to promote high velocities and turbulent-flows conditions
4. Polymeric substrates or metabolites and mycelial growth often produce very viscous reaction mixtures which are generally pseudoplastic non-Newtonian; again, these conditions tend to limit desirably high flow dynamics in bioreactors.
5. Many multicellular microbial growths, especially fungal ones generally form relatively large cell aggregates such as clumps or pellets: compared to catalyst particles,

0097-6156/83/0207-0335\$06.00/0

© 1983 American Chemical Society

intraparticle diffusional resistances are often serious in these systems, e.g., leading to anaerobiosis.

6. Bioreactors frequently require critically close control of solute concentrations, pH, temperature, and local pressures in order to avoid damage or destruction of live or labile components which are essential to the process.
7. Very low concentrations of reactants and/or products in aqueous media are normally involved in bioreactors so concentration driving forces for mass transfer are often severely limited.
8. Microbial growth rates are substantially lower than chemical reaction rates so that relatively large reactor volumes and residence times are required.

As an illustration of some of the problems imposed by the above constraints, we note that an adequate oxygen supply rate to growing cells is often critical in aerobic fermentations. Because of its low solubility in water, gaseous oxygen, usually in the form of air, must be supplied continuously to the fermentation medium in such a way that the oxygen absorption rate at least equals the oxygen consumption rate of the cells. Even temporary depletion of dissolved oxygen could mean irreversible cell damage. In this respect, it is worth noting that the same microbial species may show large variations in its oxygen requirements, depending on the oxygen concentration to which they have been adapted.

Previous studies in which the oxygen supply to a submerged growing microbial culture was stopped, have shown a linear decrease in oxygen concentration with time over a large concentration range (Finn, 1954). Below a certain oxygen concentration, called the "critical oxygen tension," the decrease followed a hyperbolic pattern compatible with Michaelis-Menton kinetics. Often deviations from the linear and hyperbolic oxygen concentration decrease patterns are found. The rate controlling step in a fermentation process may shift the oxygen supply rate into the bulk liquid to the demand rate inside the cell if cell aggregates are formed which are larger than a few hundredths of millimeters. Usually, this is seen as an increased value of the critical oxygen tension or total absence of a linear part of the oxygen concentration decrease curve, showing dependence on the concentration driving force at the cell surface.

RATE-CONTROLLING STEPS

Figure 1 gives a generalized physical representation of a bioreactor subsystem involving two or more phases. An important example of this representation is an aerobic fermentation in which

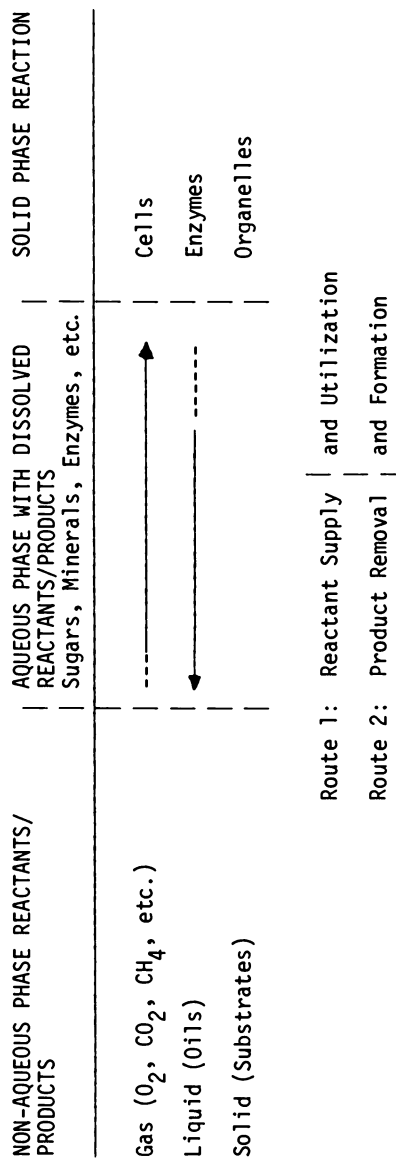


Figure 1. Generalization of biochemical reactor conditions illustrating the importance of aqueous phase transfer steps for mass and heat. Reproduced, with permission, from Ref. 38. Copyright 1981, Springer-Verlag.

a microbe utilizes oxygen (supplied by air bubbles which also desorb toxic carbon dioxide) and other dissolved nutrients (sugars, etc.) to grow and produce soluble extracellular metabolites. Eight resistances in the mass transfer pathways for the nutrients supply and utilization and for metabolite excretion and removal, are possible as indicated in the illustration at the following locations: (1) in a gas-film (2) at the gas-liquid interface (3) in a liquid-film at the gas-liquid interface (4) in bulk liquid (5) in a liquid-film surrounding the solid (6) at the liquid-solid interface (7) in the solid phase containing the cells (8) at the sites of the biochemical reactions. It should be noted that all the pathways except the last one are purely physical.

Figure 1 can represent a wide range of other practical situations. The continuous phase may be liquid or gas, the latter representing special cases such as "solid-state" fermentations (e.g., composting, trickle-bed reactors, and "Koji" processes) while the dispersed phase may be one or more of the following phases: solid (e.g., microbial cells, immobilized-enzyme particles, solid substrates); liquid (e.g., insoluble or slightly soluble substrates); gas (e.g., air, carbon dioxide, methane).

EFFECT OF INTERFACIAL PHENOMENA

If we consider a fluid particle (gas or liquid) moving relatively to a continuous liquid phase, there are two possible extremes of interfacial movement as classified below. (For convenience, we will consider a sphere).

- (a) There is no internal circulation within the particle. These particles behave essentially as if they are solid with rigid surfaces. We will refer to these as particles with "rigid" surfaces.
- (b) There is a fully developed internal circulation flow within the particle due to an interfacial velocity. The particle behaves as a part of an inviscid continuous phase with only a density difference. We will refer to these as particles with "mobile" surfaces.

Illustrations of velocity vectors for both kinds of these particles are illustrated in Figure 2. This concept has been useful in explaining many drop and bubble phenomena. For example, it has been found that trace amounts of surface-active materials can hinder the development of internal circulation by means of a differential surface pressure. Small bubbles rising slowly are apt to behave like particles with rigid surfaces. This phenomenon can lead to a decrease in k_L as the age of a bubble increases (Levich, 1956). Larger bubbles, rising more quickly, may sweep their front surface free of trace impurities and therefore escape

the contamination effect of surfactants as illustrated in Figure 3. These effects lead to significant variations of k_L with changing bubble size and agitation power (Calderbank and Moo-Young, 1961).

In fermentation practice, clean bubble systems are probably rarely achieved and it is conservatively safe to base a design on contaminated rigid interface behavior.

INTERPARTICLE TRANSFER RATES

Particles in stagnant Environments

For non-moving submerged particles (with rigid or mobile surface) in a stagnant medium, mass transfer occurs only by radial diffusion. $Re = Gr = 0$, whence it can be shown that:

$$Sh = Nu = 2 \quad (1)$$

As the lower limit for Sh , we will see that this value usually vanishes for bubble mass transfer, but it may become significant when applied to small light particles, e.g., microbial cells. Pseudostagnant liquid environments can exist in viscous fermentations and/or with well dispersed single cells as illustrated in case (a) of Figure 3.

Moving Particles with Rigid Surfaces

A range of these cases can occur in packed-bed, trickle-bed or free-rise or free-fall dispersed-phase reactor systems. For creeping flow, $Re < 1$, (e.g., certain packed-bed immobilized-enzyme reactors) theory developed by Levich (1962) and others show that:

$$Sh = 0.99 Re^{1/3} Sc^{1/3} = 0.99 Pe^{1/3} \quad (2)$$

In the regime $10 < Re < 10^4$ (e.g., certain trickle-bed reactors)

$$Sh = 0.95 Re^{1/2} Sc^{1/3} \quad (3)$$

At high agitation intensities, turbulence is expected to affect the mass transfer rates at solid particle surfaces. However, in these cases the actual particle velocity is unknown and conventional Reynolds numbers cannot be deduced.

An appropriate Re -number expression characteristic of local isotropic turbulence can be derived using the root-mean-square fluctuating velocity postulated by Batchelor (1951).

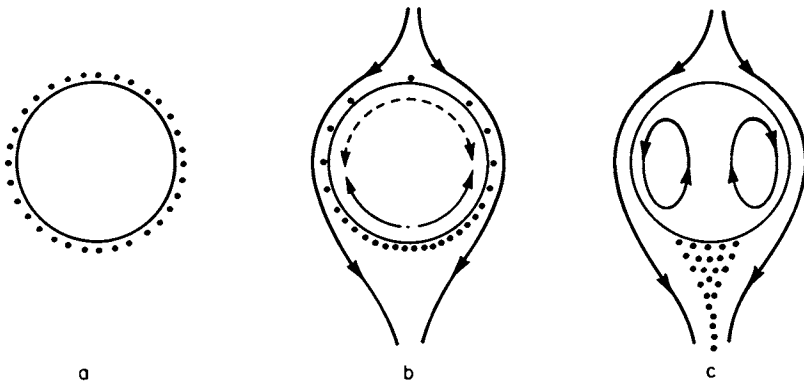


Figure 2. Surfactant effects on bubble drop surface-flows. Key: a, zero relative particle velocity; b, low relative particle velocity; and c, high relative particle velocity. Reproduced, with permission, from Ref. 38. Copyright 1981, Springer-Verlag.

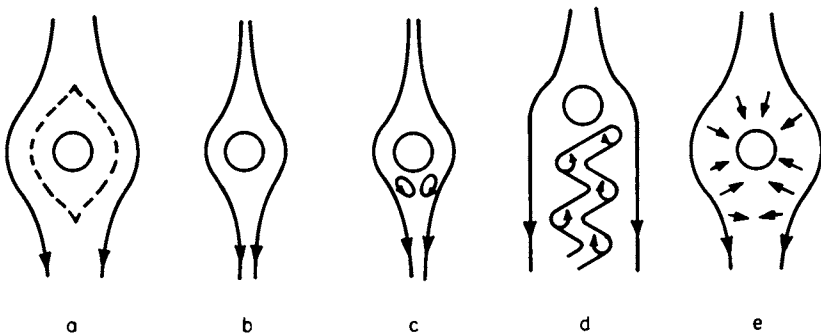


Figure 3. Possible conditions of the momentum boundary layer around a submerged solid sphere with increasing relative velocity. Key: a, envelope of pseudo-stagnant fluid; b, streamline flow; c, flow separation and vortex formation; d, vortex shedding; e, localized turbulent eddy formation. Reproduced, with permission, from Ref. 38. Copyright 1981, Springer-Verlag.

$$\text{Re}_e = \frac{d^{4/3} \rho^{2/3} (P/V)^{1/3}}{\mu} \quad (4)$$

Calderbank and Moo-Young (1961) developed a correlation for rigid-surface particle mass transfer in bioreactors in terms of the energy input to the system as follows:

$$\text{Sh} = 0.13 \text{Re}_e^{3/4} \text{Sc}^{1/3} \quad (5)$$

where k_L is seen to be dependent on $(P/V)^{1/4}$, a dependence which may be masked by the effect of power on interfacial area, as discussed later.

Moving Particles with Mobile Surfaces

Mobile surface fluid particles show a behavior which is less sphere-like than that of rigid-surface particles. By viscous interaction with the continuous phase, oscillating shape variations of liquid drops and gas bubbles occur, and for $\text{Re}_e > 1$, mobile surface fluid particles in free-rising or falling conditions move in a wobbling or spirial-like manner, which has a marked influence on mass transfer rates. As before, we can arrive at different correlations for different bulk flow regions. These are summarized below:

$$\text{Sh} = 0.65 \left(\frac{\mu}{\mu + \mu_d} \right)^{1/2} \text{Pe}^{1/2} \quad (6)$$

For higher Re -numbers, Higbie (1935) gave an equation which takes the form:

$$\text{Sh} = 1.13 \text{Pe}^{1/2} \quad (7)$$

Refinements between the two extremes are possible.

In thick viscous liquids ($\mu > 70$ cp) large spherical-cap bubbles are frequently encountered and the relevant correlation is:

$$\text{Sh} = 1.31 \text{Pe}^{1/2} \quad (8)$$

Non-Newtonian Flow Effects

When the liquid phase exhibits non-Newtonian behavior, the mass transfer coefficient will change due to alterations in the fluid velocity profile around the submerged particles. The trends for both mass transfer and drag coefficient are analogous. As before for Newtonian fluids, two types of interfacial behavior need to be considered.

For mobile-surface particles in power-law fluids, Hirose

and Moo-Young (1969) have obtained a correlation factor for k_L for single bubbles, based on small pseudoplastic deviations from Newtonian behavior ($0.7 < n < 1.0$). They also provide some data on drag coefficients as functions of the power-law and Bingham plastic fluids, with mobile interfaces, using perturbation analysis, and provided correlation factors for the enhancement of mass transfer.

For rigid surface behavior, the mass transfer coefficients can be obtained from the results of Wellek and Huang (1970). Moo-Young and Hirose (1972) showed that an additional effect of "interfacial slip" by additives can occur in practice.

Effect of Bulk Mixing Patterns

In addition to the determination of the mass transfer coefficient, k_L , and the interfacial area, a , the development of gas and liquid phase mass balance equations for the species transferred depends on the flow behavior of both gas and liquid phase.

In low viscosity liquids it is reasonably well established that in small stirred-tanks the liquid phase can be considered to be "perfectly mixed" (Westerterp, et al., 1963). Under these conditions, the gas phase has also generally been assumed to be well mixed in tanks operating above critical impeller speed. In large tanks, however, the situation is less clear, and care must be taken to establish the behavior of both phases. In cases where the degree of gas absorption is high, the assumptions of well mixed or plug-flow of the gas phase may predict significantly different gas absorption rates. Shaftlein and Russell (1968) present design equations for various models of gas and liquid flows.

INTRAPARTICLE BIOREACTION RATES

General Concepts

In some biochemical systems the limiting mass transfer step shifts from a gas-liquid or solid-liquid interface (as discussed earlier) to the interior of solid particles. The most important cases are solid substrates and cell aggregates (such as microbial flocs, cellular tissues, etc.) and immobilized enzymes (gel-entrapped or supported in solid matrices). In the former, diffusion of oxygen (or other nutrients) through the particle limits metabolic rates, while in the latter, substrate reactant or product diffusion into or out of the enzyme carrier often limits the overall global bioreaction rates.

Generalized mass balances for the above scenarios can be

set up and various cases where mass transfer resistance within the particle may become important can be identified.

Oxygen Transfer in Mold Pellets

Marshall and Alexander (1960) discovered that for several pellet-forming fungi a "cube root" growth curve fit their data significantly better than the standard exponential growth model. It was suggested that this was probably due to the effects of intraparticle diffusion; a nutrient was not diffusing into the particle fast enough to maintain unrestricted growth. It was soon realized that oxygen was the limiting nutrient.

Phillips (1966) measured oxygen diffusion in pellets of Penicillium chrysogenum by first assuming that diffusion is the mechanism that supplies oxygen to the interior of the microbial pellet and that the mass transfer resistance outside the pellet is comparatively small. Yano et. al. (1961) and Koyayashi, et al. (1973 b) did the same with Aspergillus niger pellets. By taking into account the effect of intraparticle diffusion, Kobayashi and Suzuki (1976) were able to characterize the kinetic behavior of the enzyme galactosidase within mold pellets of Mortierella vinacea.

Kobayashi, et al. (1973 b) studied three cases: (1) uniform respiration activity throughout mycelial pellets, (2) respiration activity as a function of age distribution within the pellet, (3) respirative activity adaptation to the local oxygen concentration within the pellet. In case 1, it was found that the effectiveness factor (E_f) is equal to the ratio of the specific respiration rate of a pellet to the respiration rate of well dispersed filamentous mycelia. The theoretical and experimental results for each case are given in Figure 4. It is seen that the three cases considered gave similar results and it is difficult to discriminate between them with the limited experimental data available.

Immobilized Enzyme Kinetics

Intraparticle diffusion can have a significant effect on the kinetic behavior of enzymes immobilized on solid carriers or entrapped in gels. In their basic analysis of this problem, Moo-Young and Kobayashi (1972) derived a general modulus and effectiveness factor. The results also predicted possible multiple steady-states as well as unstable situations for certain systems. While these results are very interesting it should be remembered that they are primarily mathematical and await extensive experimental support data.

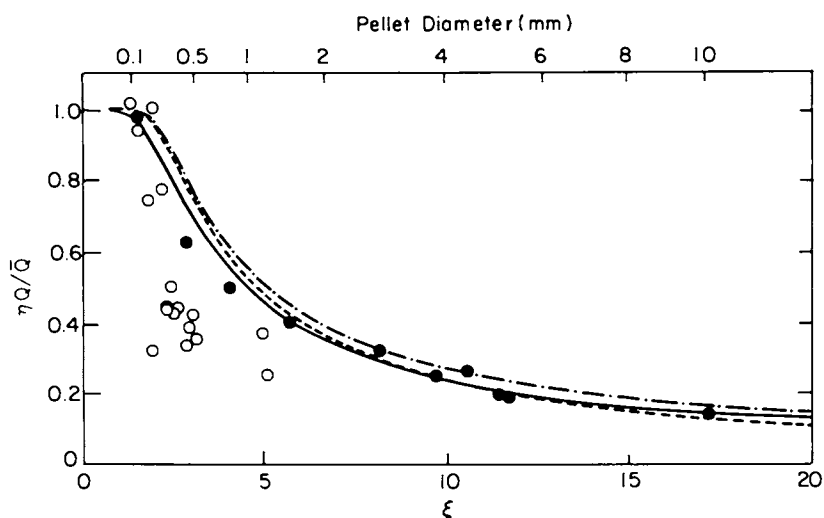


Figure 4. Oxygen transfer in mold pellets. Comparison between theoretical curves relating η to ξ , Case 1 (- · -), Case 2 (- - -), and Case 3 (—) of Ref. 20. \circ , data of Yano et al. \bullet , data of Kobayashi et al. Conditions: $c = 1.9 \times 10^{-4} \mu\text{mol mm}^{-3} \text{O}_2$; $K_m = 3.0 \times 10^6 \mu\text{mol mg}^{-1} \text{min}^{-2} \text{O}_2$; $\xi = R(\rho\bar{Q}/2D_r c)^{1/2}$.

Enzymatic Degradation of Insoluble Substrates

When the substrate in a bioreactor is a water-soluble material (e.g., cellulose, oils), the effects of intraparticle mass transfer may be important. In such systems, extracellular enzymes can break down substrate eventually into water soluble components, as products, or as intermediates for consumption by micro-organisms (Okazaki and Moo-Young, 1978).

If a solid substrate is sufficiently porous, the enzyme can diffuse into it and degradation can proceed inside the material. The water-soluble substrate fragments must also diffuse out of the solid matrix through these same pores into the bulk solution where they may be subject to further enzymatic attack. The reaction may concurrently proceed at the exterior of the matrix surface and for substrates of low porosity this is where much of the degradation takes place. As before, utilization of the effectiveness factor and general modulus is convenient in solving the relevant differential equations.

BIOREACTOR EQUIPMENT PERFORMANCEBubble-Columns

Pneumatically agitated gas-liquid reactors may show wide variations in height to diameter ratios. In the production of baker's yeast, a tank-type configuration with a ratio of 3 to 1 is common industrially. Tower type systems have height to diameter ratios of 6 to 1 or more. As would be expected, the behavior of both gas and liquid phases may be quite different in these cases. In general the gas phase rises through the liquid phase in plug-flow, under the action of gravity, in both types of system.

A variety of correlations for $k_L a$ are available in the literature for bubble-columns. Generally they are of the form

$$k_L a = \text{const. } v^n \quad (9)$$

where n is usually in the range of 0.9 to unity. Yoshida and Akita (1965) correlate the overall mass transfer coefficients in bubble columns in the form:

$$\frac{k_L a D^2}{T} = 0.6 \left(\frac{\mu}{\rho D_L} \right)^{1/2} \left(\frac{g T \rho}{\sigma} \right)^{0.62} \left(\frac{g T^3 \rho^2}{\mu} \right)^{0.31} \phi^{1.1} \quad (10)$$

A recent review of bubble-columns by Schugerl, et al. (1977, 1978) examines single and multistage columns and a variety of liquid phases. A correlation for $k_L a$ is proposed for porous and perforated plate spargers (cgs units):⁴

$$k_L a = 0.0023 (v_s/d_B)^{1.58} \quad (11)$$

Many of the available correlations for $k_L a$ have been obtained on small scale equipment, and have not taken cognizance of the underlying liquid hydrodynamics. Bhavaraju, et al. (1978) propose a design procedure based on the difference in bubble size close to the orifice and in the liquid bulk. Provided the liquid is turbulent, the equilibrium bubble size in the bulk will be independent of the size at formation. The height of the region around the orifice where the bubble formation process occurs is a function of sparger geometry and gas flow rate and in laboratory scale equipment this height may be significant fraction of the total liquid height (up to 30%). In plant scale equipment, however, this generally represents less than 5% of the total liquid height. Thus, correlations developed on small scale apparatus need to be reviewed in light of the varying interfacial area with column height.

Systems with Stationary Internals

Several laboratory scale devices which include internal elements to enhance mass transfer rates have appeared. These include draft-tubes, multiple sieve plates staged along the length of the column, and static mixing elements.

A considerable literature exists on draft-tube columns, where liquid is circulated due to a bulk density difference between the inner core and the surrounding annular space. The downcoming liquid in the annular space entrains air bubbles, and thus holdup in the central core and annular region will be different. Several reports on small scale airlift columns as bioreactors have appeared. Chakravarty, et al. (1973) examined gas holdup at various positions in a 10 cm diameter column. A rectangular airlift has been reported (Gasner, 1974) and airlifts with external recirculation (Kanazawa, 1975) have been proposed. The overall mass transfer correlations for airlift devices are usually expressed as:

$$k_L a = \text{const. } V_s \quad (12)$$

Industrially, plant scale airlift devices have been used by Japanese, British, French and USA companies mainly for SCP production and waste treatment

Static mixing elements have been incorporated into airlift devices with the objectives of providing additional mixing and hence greater mass transfer capabilities. Static mixers are becoming increasingly more common in oxidation ponds for

biological wastewater treatment. Here, fine bubbles may be produced as the gas-liquid mixture passes through the mixing element. These are usually 18-24 inches in diameter, and are placed over sparger pipes. A fairly intense liquid circulation can be developed by such mixers due to entrainment by the gas-liquid jet rising from the mixing element.

Mechanical Stirred Tanks

Non-Viscous Systems

The previous sections dealt with gas-liquid contacting without mechanical agitation in such devices as bubble-columns and airlift towers. To obtain better gas-liquid contacting, mechanical agitation is often required. The discussion is confined to baffled sparged stirred-tanks with impellers. Aeration by surfaction impellers are sometimes used in one wastewater treatment facilities (Zlokarnik, 1978).

For particulates, such as cells, insoluble substrates, or immobilized-enzymes, the interfacial area can be determined from direct analyses such as by microscopic examination. For gas bubbles and liquid drops, a can be evaluated from semi-empirical correlations. Two cases are identified:

(a) For "coalescing" air-water dispersions,

$$a = 0.55 \left(\frac{P}{V}\right)^{-0.4} v_s^{0.5}$$

and

$$d_B = 0.27 \left(\frac{P}{V}\right)^{-0.17} v_s^{0.27} + 9 \times 10^{-4}$$

(b) For "non-coalescing" air-electrolyte solution dispersions,

$$a = 0.15 \left(\frac{P}{V}\right)^{0.7} v_s^{0.3}$$

and

$$d_B = 0.89 \left(\frac{P}{V}\right)^{-0.17} v_s^{0.17}$$

In the equation, (P/V) is in Watts/m³, and v_s is in m/s.

American Chemical
Society Library
1155 16th St., N.W.

It is seen that there is a significant effect of electrolytes on the correlations. Electrolytes and surfactants inhibit bubble coalescence resulting in the formation of smaller bubbles and increased interfacial area than normally found in the clean water system.

A very high gas flow rate, liquid blow-out from the vessel may occur. In addition, the above equations are applicable provided that the impeller is not flooded by too high a gas flow rate and there is no gross surface-aeration due to gas back-mixing at the surface of the liquid. Equations are available to calculate these criteria (Calderbank, 1959; Westerterp, 1963).

The efficiency of gas-liquid contacting has already been presented in terms of the fundamentals of k_L and a separately; the overall correlations should therefore have universal applicability. Several investigations have developed overall correlations. They usually take the form

$$k_L a = \text{const.} \left(\frac{P}{V}\right)^m v_s^n \quad (17)$$

and their ranges of applicability are compared to bubble columns and airlift devices in Figure 5.

In recent years, extensive studies have been carried out using physical rather than chemical reaction measurements for the evaluation of $k_L a$. On this basis, Smith Van't Riet and Middleton (1977) found that in general, the following correlations apply to a wide variety of agitator types, sizes and D/T ratios:

(a) For "coalescing" air-water dispersion

$$k_L a = 0.01 \left(\frac{P}{V}\right)^{0.475} v_s^{0.4} \quad (18)$$

(b) For "non-coalescing" air-electrolyte solution dispersions

$$k_L a = 0.02 \left(\frac{P}{V}\right)^{0.475} v_s^{0.4} \quad (19)$$

Both equations are in SI units $k_L a$ in s^{-1} , (P/V) in W/m^3 , v_s in m/s . The accuracy of the correlations is $\pm 20\%$ and $\pm 35\%$ with 95% confidence for the above two equations, respectively.

From Figure 5, it is seen that for comparable power

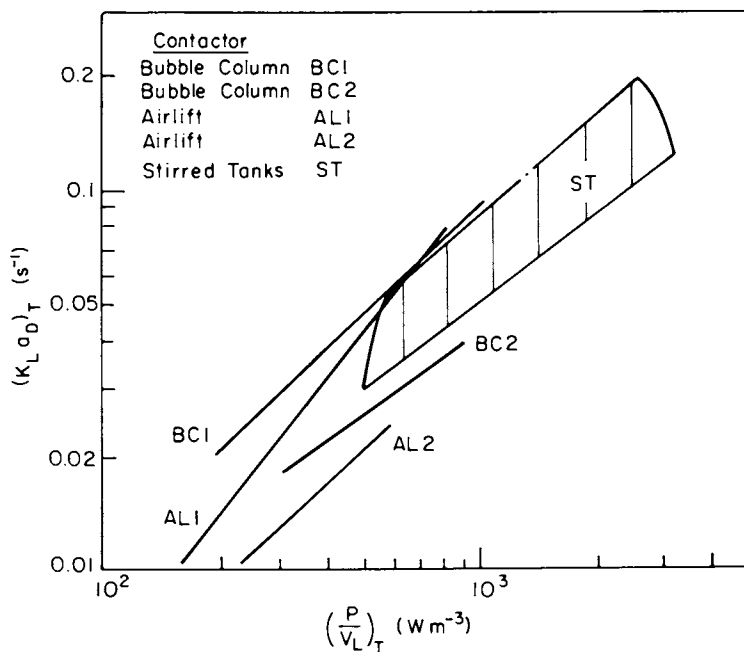


Figure 5. Aeration efficiencies of various gas-liquid contacting devices (air-electrolyte systems). Reproduced, with permission, from Ref. 38. Copyright 1981, Springer-Verlag.

inputs, the magnitude of $k_L a$ obtained is about the same whether mixing is done mechanically in stirred-tanks or pneumatically in bubble-columns or airlift devices. However, only mechanically agitated systems are capable of attaining high values of $k_L a$ required (e.g., in some antibiotic fermentations and the activated sludge method of treating wastewater). Non-mechanically agitated systems would result in liquid blowout before reaching these high aeration rates.

It should be stressed that none of the overall correlations for $k_L a$ had universal applicability. The problem is that any scale-up procedure based on equalizing $k_L a$ of both scales according to a given correlation may cause other physical criteria to be violated. Also, depending on biological demands and tolerances, other criteria may be more important. For example, increasing the $k_L a$ can sometimes result in damage to the organisms in highly turbulent fermentation broth.

Viscous Systems

Two types of viscous fermentations need to be distinguished:

(a) mycelial fermentations (e.g., molds, actinomycetes) where the viscosity is due to the microbial network structure dispersed in continuous aqueous phase.

(b) polysaccharide fermentations where the viscosity is due to polymers in the continuous aqueous phase resulting in an essentially homogeneous, viscous liquid.

The first type of fermentation broth can be simulated by material such as paper pulp, which has a macroscopic structure analogous to fungal hyphae, suspended in water. The second type may be simulated by aqueous polymer solutions of known properties.

Sideman, et al. (1966) have proposed the following form of a general correlation for the liquid phase mass transfer coefficient.

$$\frac{k_L a D^2}{D_L} = A \left(\frac{\mu_a}{\rho D_L} \right)^\alpha \times \left(\frac{\mu_a V}{\sigma} \right)^\beta \left(\frac{D^2 N \rho}{\mu_a} \right)^\gamma \left(\frac{\mu_d}{\mu_a} \right)^\delta \quad (20)$$

Additional dimensionless groups be incorporated to account for geometric variables, e.g. H_L/T , D/T . The above equation can be altered to relate $k_L a$ to the specific power input.

Loucaides and McManamey (1973) examined rates in paper pulp suspensions simulating filamentous fermentation media. Tank geometries and impeller geometries were both varied; vessel

volumes ranging from 5 to 72 liters. Analogous to the results for non-viscous solutions, $k_L a$ as found to correlate well with variations in tank diameter.

$$k_L a = C_1 (T/H_L) N D \bar{T}^{-.5} + C_2 \quad (21)$$

By varying the impeller blade dimensions, variations in power per unit volume were made at a constant impeller speed. At low power per unit volumes there was a linear increase in $k_L a$, which correlated with P/V with an exponent of 0.9 to 1.2. Beyond the breakpoint, the exponent relating the P/V dependence was 0.53. In both regions, the $k_L a$ depend on the superficial gas velocity to the 0.3 power. These results are similar to those reported earlier by Blakebrough and Sambamurthy (1966), and Hamer and Blakebrough (1963), obtained in smaller scale vessels, also using paper pulp suspensions. Other references on the aeration of viscous non-Newtonian fermentation broth are Banks (1977), and Blanch and Bhavaraju (1976).

NOMENCLATURE

a	specific interfacial area (based on dispersion volume)
C	Concentration of solute in bulk liquid (generally)
C	Concentration of solute in bulk media (for intraparticle diffusion case)
D	Dilution rate; impeller diameter
D_L	Liquid phase diffusivity
d	Diameter of particle as an equi-volume sphere
d_B	Bubble diameter
E_f	Effectiveness factor
H_L	Liquid height in reactor
k_L	Liquid phase mass transfer coefficient

Continued on next page

$k_L a$	Volumetric liquid phase mass transfer coefficient
m	An exponent
N	Speed of agitator
P	Agitator power requirements for ungasged systems
P_g	Agitator requirements for gas-liquid dispersions
T	Temperature; tank diameter
V	Volume of reactor contents
V_s	Superficial gas velocity
VVM	Volume of air per unit volume of medium per minute

Greek Letters

μ	Viscosity (dynamic) of continuous phase
μ_a	Apparent viscosity (dynamic)
μ_d	Viscosity (dynamic) of dispersed phase
ν	Kinematic viscosity of continuous phase
ρ	Density of continuous phase
ϕ	Holdup of dispersed phase.

Abbreviations for Dimensionless Groups

Gr	Grashof number for mass transfer (based on particle environment density difference)
Nu	Nusselt number
Pe	Peclet number (single particles)
Pr	Prandtl number
Re	Reynolds number for particles
Re_e	Reynolds numbers for isotropic turbulence
Sh	Sherwood number
Sc	Schmidt number

Literature Cited

1. Banks, G.T., in "Topics in Enzymes and Fermentation Biotechnology", Wiseman (Ad.), John Wiley and Sons, 1977, 1, 72.
2. Batchelor, G.K., Proc. Camb. Phil. Soc., 1951, 47, 359
3. Bhavaraju, S.M., Mashelkar, R.A., Blanch, H.W., AIChE J., 1978, 24 1063; AIChE J., 24, 1070
4. Bhavaraju, S.M., Russell, T.W.F., Blanch, H.W., AIChE J., 1978, 24, 454
5. Blakebrough, N., Sambamurthy, K., Biotechnol. Bioeng., 1966 8, 25.
6. Blanch, H.W., Bhavaraju, S.M., Biotechnol. Bioeng., 1976, 18, 745.
7. Calderbank, P.H., Trans. Inst. Chem. Engrs., 1959, 37, 173.
8. Calderbank, P.H., Moo-Young, M. Chem. Eng. Sci., 1961 16, 39.
9. Calderbank, P.H., Moo-Young, M., Trans. Inst. Chem. Engrs., 1961, 39, 337.
10. Chakravarty, Y., Begum, S., Singh, A.D., Baruah, J.N. Iyengar, M.S., Biotechnol. Bioeng. Symp., 1973, No. 4 363.
11. Finn, R.K., Bact. Rev., 1954, 18, 245.
12. Gasner, L.L., Biotechnol. Bioeng., 1974, 16, 1179
13. Hadamard, J., Compt. Rend. Acad. Sci., 1911, 152, 1735.
14. Hamer, G., Blakebrough, N., J. Appl. Chem., 1963, 13, 517
15. Higbie, R., Trans. Amer. Inst. Chem. Engrs., 1935, 31, 365.
16. Hirose, T., Moo-Young, M., Can. J. Chem. Eng., 1969, 47, 265.
17. Kanazawa, M., in "SCP II," Tannenbaum and Wang (Eds.), MIT Press, 1975.
18. Kobayashi, H., Suzuki, M., Biotechnol. Bioeng., 1976, 18, 37.
19. Kobayashi, T., Moo-Young, M., Biotechnol. Bioeng., 1973 a, 15, 47.

20. Kobayashi, T., van Dedem, B., Moo-Young, M., Biotechnol. Bioeng., 1973 b., 15, 27.
21. Levich, V.G., "Physicochemical Hydrodynamics," 1962, Prentice-Hall.
22. Loucaides, R., McManamey, W.J., Chem. Eng. Sci., 1973, 28, 2165.
23. Marshall, K.C., Alexander, M., J. Bacteriol., 1960, 80, 412.
24. Moo-Young, M., Hirose, T., Can. J. Chem. Eng., 1972, 50 128.
25. Moo-Young, M. Kobayashi, T., Can. J. Chem. Eng., 1972, 50, 128.
26. Okazaki, M., Moo-Young, M., Biotechnol. Bioeng., 1978, 20, 637.
27. Phillips, H.H., Biotechnol. Bioeng., 1966, 8, 456.
28. Schugerl, K., Oels, U., Lucke, J., Adv. Biochem. Eng., 1977, 7, 1.
29. Schugerl, K., Lucke, J., Lehman, J., Wagner, F., Adv. Biochem. Eng., 1978, 8, 63.
30. Shaftlein, R.W., Russell, T.W.F., Ind. Eng. Chem., 1968, 60(5), 13.
31. Sideman, S., Hortacsu, O., Fulton, J.W., Ind. Eng. Chem., 1966, 58(7), 32.
32. Smith, J., Van't Riet, K., Middleton, J., Second European Conf. on Mixing, April 1977, Preprint.
33. Wellek, R.M., Huang, C.C., Ind. Eng. Chem. Fund., 1970, 9, 480.
34. Westerterp, K., Chem. Eng. Sci., 1963, 18, 157.
35. Yano, T., Kodama, T., Yamada, K., Agr. Biol. Chem., 1961, 25, 589.
36. Yoshida, F., Akita, K., AIChE J., 1965, 11, 9.
37. Zlokarnik, M., Adv. Biochem. Eng., 1978, 8, 133.
38. Moo-Young, M., Blanch, H.W., Adv. Biochem. Eng., 1981, 18, 2.

RECEIVED June 29, 1982

Reactor Design Fundamentals

Hydrodynamics, Mass Transfer, Heat Exchange, Control, and Scale-up

ALES PROKOP

Kuwait Institute for Scientific Research, Biotechnology Department,
P.O. Box 24885, Kuwait

For the convenience of discussing the above subject it is helpful to adopt a systems approach (analysis and synthesis), i.e., the decomposition of a system into several orders of structural and functional hierarchy, including biological and physical levels (such as molecular, cellular, population, reactor and technological line), and to select from a number of elementary events systemic phenomena playing a decisive role at each level of hierarchy. This approach allows an integral description during process synthesis while maintaining the specific properties of each level. The bioreactor level is distinguished by the following fundamental events and functions: bioreactor hydrodynamics, mass transfer, heat exchange, bioreactor control and its scale-up. This review will emphasize reactors employed in microbial protein production and the systems approach is intended as a methodological aid in process research and development.

Recently, the author advocated the application of the systems approach in the analysis and synthesis of a biotechnological process (1). The hierarchy of a biological system involves structural, functional, descriptive, control and dynamic organization. Structural and functional hierarchies of a biotechnological process are depicted in Tables I and II. In Table II a compartmental level is omitted. This is possible as long as the translocation of substances between organelles and cytoplasm is not important. The scheme of functions should be understood in both directions, i.e., from higher levels to lower (analysis) and vice versa (synthesis), representing basic and applied research. The first

On leave from: Institute of Microbiology, Czechoslovak Academy
KISR 620 of Sciences, 142 20 Prague 4, Czechoslovakia

0097-6156/83/0207-0355\$06.50/0
© 1983 American Chemical Society

Table I Structural and Functional Hierarchies
of a Biotechnological Process

Level	Structural Elements	Function
Molecular	Atoms, molecules	Synthesis of macromolecules
Organelles	Macromolecules	Duplication of organelles, metabolic manifestation of cells
Cell	Organelles	Translocation of substances, complex biochemical reactions, morphological differentiation, cell cycle
Population	Cells	Growth and multiplication, interaction between cells
Reactor	Elementary zones of reactor	Mass transfer, heat exchange, diffusion, etc.
Biotechno- logical process (line)	Unit equipment	Unit operations

Internat. J. General Systems 1982, 8(1), Table VII (1)

Table II Hierarchy of Functions of Biotechnological Processes

-
- 1 Molecular Level
 - 1.1. Catabolic and anabolic manifestations of living systems
 - 1.1.1. Energy formation
 - 1.1.2. Synthetic processes
 - 1.1.3. Macromolecular decay
 - 1.2. Control mechanisms
 - 1.2.1. Reaction mechanisms
 - 1.2.2. Epigenetic control
 - 1.2.3. Biochemical differentiation
 - 1.2.4. Reproduction mechanisms
 - 2 Structural Hierarchy of Cells (Compartments)
 - 2.1. Translocation of substances
 - 2.2. Complex biochemical network
 - 2.3. Morphological differentiation
 - 2.4. Cell cycle
 - 2.5. Genetic phenomena at level of organelles
 - 3 Population
 - 3.1. Dispersed growth
 - 3.1.1. Pure culture
 - 3.1.2. Mixed culture
 - 3.2. Aggregated growth
 - 4 Bioreactor and Other Equipment
 - 4.1. Macro- and micro-mixing of equipment contents
 - 4.2. Mass transfer
 - 4.3. Heat exchange
 - 4.4. Bioreactor control and of other equipment
 - 4.5. Scale-up
 - 5 Technological Line
 - 5.1. Batch processes
 - 5.2. Continuous processes
-

Internat. J. General Systems 1982, 8(1), Table VIII (1)

level (molecular) in Table II is considered quasihomogeneous (reactions occurring in a solution), the second is represented by a cell considered as a two-phase system, composed of organelles homogeneously dispersed in the cytoplasm. The population level is manifested by different morphological states (dispersed and aggregated) of a population. The levels of the reactor and technological line are distinguished by fundamental functions typical for chemico-technological processes.

The reactor level is distinguished by the following fundamental events and functions: macro- and micro-mixing of reactor (equipment) contents and the corresponding mass transfer and heat exchange involve the determination of elementary zones of reactor, mass transfer and heat exchange between them and also between individual phases (liquid, gaseous, solid); bioreactor control and scale-up (2). If non-homogeneities of reactor performance in space and time are expected, local dynamic balances of mass, heat and momentum transport, incorporating all phases, are required. As a solution to momentum transport (Navier-Stokes equation) is usually not available for bioreactor velocity field, we are left with mass and heat balances. A local balance describing mixing, flow and interface transfer, including reaction is known as the dispersed model (3):

$$\frac{\partial C_{ij}}{\partial t} + \nabla C_{ij} u + \nabla D \nabla C_{ij} + r_{ij} - \sum_{k=1}^f (k \neq j) k_k a_k (C_{iks} - C_{ik}) = 0 \quad (1)$$

where subscript i denotes system component, j is the number of a phase in the f -phase system, k is a phase other than j , subscript iks denotes concentration near the interfacial area on side j , and u is the local velocity of phases j . The last term denotes the transport between phases. A limited application of this system of partial differential equations was made for a stirred-tank reactor (STR) with a neglect of transfer term (4) as well as for a tubular reactor (5).

Hydrodynamics

Elementary regions of bioreactor. A more simple description of the flow characteristics of a reactor than that by a local mass balance is done by introducing the residence time distribution concept (RTD), which provides macro-mixing characteristics (determination of the elementary regions of the reactor). In fact, using the residence time concept a particular situation may be described by mixed-type models considering "the reactor as

consisting of interconnected flows between and around these regions" (6). The following kinds of elementary regions are used in the construction of mixed models: two types of ideal zones (plug-flow and perfectly stirred = backmixed), dispersed plug flow and deadwater. In addition to these regions, the following kinds of flow may be used: by-pass, recycle and cross-flow. The above non-idealities in mixing may be described either by means of dispersed or discrete (stage-wise) models, the latter considering a series of ideally mixed vessels.

Residence time distribution. The above distribution of liquid, gaseous and solid (cells) phases is usually measured by a stimulus-response experiment. Frequently, radioactive tracers are used (7,8). In the absence of microorganisms and for liquid RTD, a pH tracer is quite convenient (9). The application of a discrete-type model for interpreting tracer data is in (8).

Micro-mixing characteristics. It is well established that the RTD concept does not characterize all aspects of mixing. To clarify this a concept of segregation has been introduced (10). Micro-mixing falls, then, between two limiting cases of maximum mixedness and complete segregation, and is typical for reactor zones smaller than the elementary regions defined above, usually at the level of individual cells, bubbles, molecules and their clumps. Micro-mixing characteristics, however, cannot be extracted from RTD data. Fortunately, the reactor performance is not often too sensitive to micro-mixing. For example, for growth of yeasts on hydrocarbons, where one can assume an influence of the degree of oil drop and cell segregation, the differences between complete segregation and maximum mixedness is appreciable only for longer cultivation times (11). Some progress can be expected from theoretical and experimental investigation of the effect of the gas phase (bubble) segregation on mass transfer and oxygen utilization efficiency in connection with different reactor designs. For almost all practical cases maximum substrate conversion is achieved at maximum mixedness.

Mass Transfer

Mass transfer involves establishing a transfer between the elementary regions of the reactor and between individual phases (interfacial mass transfer coefficients: gas phase mass transfer, liquid phase mass transfer, mass transfer with reaction, liquid-solid mass transfer), as well as other elementary phenomena and processes connected with mass transfer: gas phase phenomena and processes (gas hold-up, bubble size, interfacial area and bubble coalescence/redispersion), volumetric mass transfer and power consumption during mass transfer (2).

Interfacial mass transfer coefficients. Theoretical and experimental investigations of many authors have shown that during the absorption of sparingly soluble gases such as oxygen, the gas phase coefficient (k_G) is several orders in magnitude higher than the liquid phase mass transfer coefficient (k_L). Because of the above fact and also due to the high value of Henry's Law constant for oxygen, the liquid phase mass transfer coefficient determines the overall rate of mass transfer. In dealing with interfacial phenomena, two extreme cases are encountered: mass transfer by molecular diffusion and convection from rigid immobile spheres, represented by gas bubbles with contaminated surfaces and described by the Frössling equation (e.g., in (12)), and mass transfer by convection from mobile spheres, described by the Boussinesq equation (e.g., in (13)). In practice, the latter system is rarely achieved since fermentation media with electrolytes, proteins, products of metabolism and cell lysis and other surface-active material may hinder the development of internal circulation of gas bubbles. Various theoretical and experimental correlations for predicting k_L for bubbles with immobile interfaces have been presented in reviews (14, 15) involving situations with creeping flow (typical for air-lift reactors) and low-high Re numbers, and also effects of non-Newtonian fluid on mass transfer from moving bubbles. These correlations are of importance in polysaccharide and antibiotic productions. The effect of surface-active compounds on k_L and α is differential because of their different influence on surface tension (increase or decrease). These phenomena have not yet been incorporated into a sufficiently general theory.

Mass transfer with reaction. The preceding situation involved only a physical mass transfer between gas-liquid or solid-liquid interfaces. In the presence of microorganisms, oxygen uptake by respiring cells within the relatively stagnant liquid region adjacent to bubbles submersed in a cell suspension may lead to enhanced oxygen transfer rates. Using an enhancement concept of Astarita, Blanch (16) presented rules for its prediction: the diffusion time for the oxygen of gas bubbles ascending through a liquid, estimated from bubble diameter and ascending air velocity, d_B / u_B , should be greater or at least of the same order as the reaction time, evaluated from dissolved oxygen concentration, oxygen uptake rate and biomass density, $C_L / (Q_0 X)$. Sobotka et al. (17) have shown that the cell flotation $C_L / (Q_0 X)$ mechanism can be successfully utilized to obtain a better fit for experimental growth data, considering gas-solid (cells) absorption of oxygen (it may amount up to a half of total absorption) in addition to the prevailing typical oxygen path to cells via dissolved oxygen (Figure 1). Conclusion of this work, providing enhanced absorption (reduced bubble slip velocity due to electrolyte, alcohols and other surface-active compounds; oxygen limitation of growth; high respiration rate; high cell density at the interface) are in full

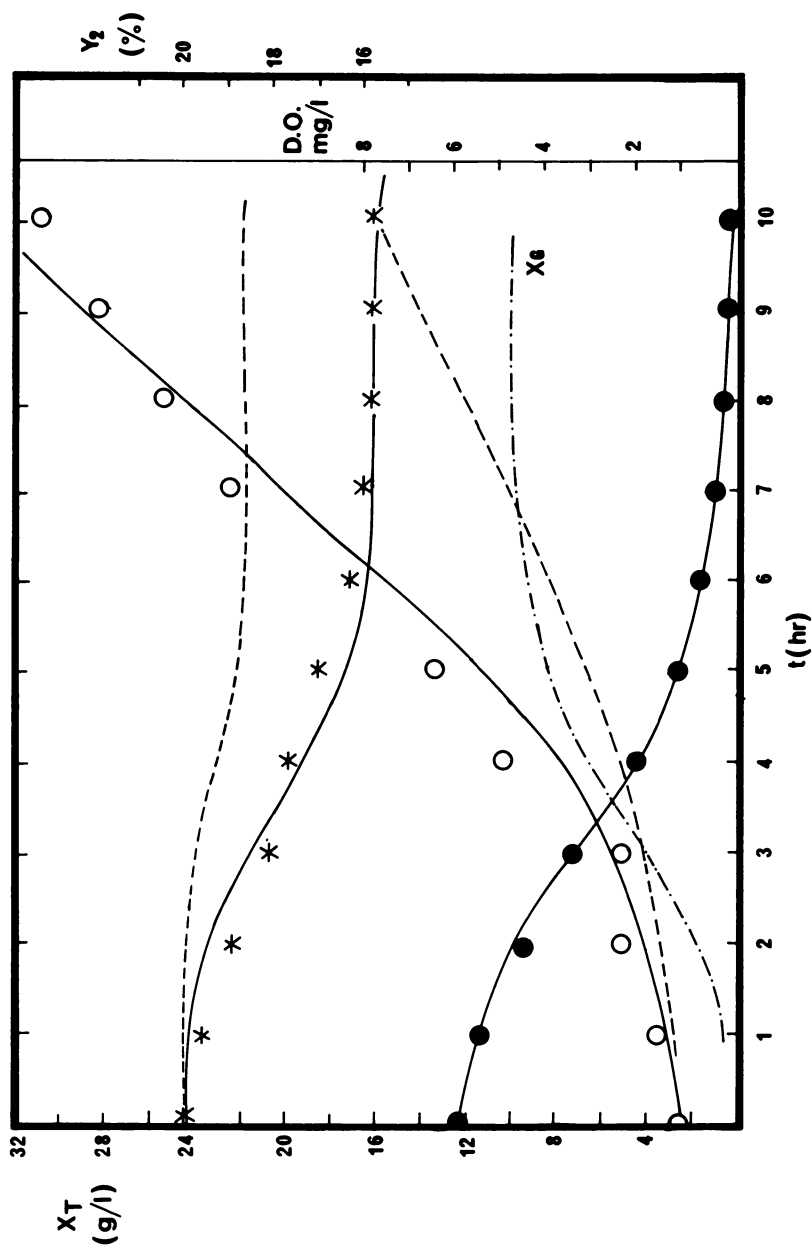


Figure 1. Fitting data to one-phase (liquid) and two-phase (liquid and gas) oxygen uptake models. Key: *, oxygen in outlet gas (Y_2 scale); O, biomass concentration (X_T scale); ●, dissolved oxygen concentration; dashed line, one-phase model; solid line, two-phase model; X_G , biomass concentration at the interface. Reprinted, with permission, from Ref. 17. Copyright 1981, John Wiley & Sons, Inc.

accord with Blanch's argumentation. Enhanced absorption is, in fact, only apparent, because of the parallel pathway of oxygen utilization.

Intraparticle mass transfer. For some practical situations mass transfer limiting step is localized in the interior of a solid phase. This is the case for certain mycelial fermentations where the oxygen transfer via pellet or mycelial clump interior may limit growth or production processes. This situation, employing the effectiveness concept, is reviewed by Moo-Young and Blanch (14). In the following, some other elementary phenomena and processes connected with mass transfer are reviewed.

Gas phase phenomena and processes. These include gas hold-up, bubble size, interfacial area and bubble coalescence/redispersion. Gas hold-up and bubble size depend on the gas flow rate, on physico-chemical properties of cultivation broth, on the reactor configuration and on operation conditions. The initial bubble diameter at orifice is an order of magnitude smaller than the equilibrium bubble size and, at some distance from the gas distributor, the size of bubbles is dependent only on broth properties and on local turbulence. In bubble column, on the other hand, different regions can be observed, where bubble diameter is either determined by orifice characteristics or by a particular turbulence. A distinction must be made between coalescing media (water) and non-coalescing media with electrolytes, alcohols and other surface-active additions. In media with a clean interface (coalescing), an average equilibrium size of bubbles, determined by an extent of parallel processes of coalescence and redispersion, is higher because of enhanced coalescence. Under these conditions, the secondary bubbles, arising from primary ones at the orifice, coalesce easily at some distance from that space. On the other hand, dispersion of gas bubbles is enhanced in the presence of electrolytes or alcohols. This effect is explained on the basis of complex phenomena connected with water structure changes near the interface (18). The influence of electrolytes and alcohols is differentiated: the concentration of electrolytes at the fresh interface decreases with bubble age whereas that of alcohols increases. These phenomena have, no doubt, an impact on reactor design as bubble path and age can considerably influence gas hold-up and interfacial area (mechanically-mixed reactors vs. vertical multi-stage reactors or bubble columns). However, no sound theoretical basis has been put forward for generalizing the effect of alcohols, electrolytes and other surface-active compounds. Similarly, no quantitative description of a bubble behaviour during mass transfer in the presence of microorganisms, including bubble coalescence and redispersion and cell adsorption and desorption, has been suggested. Even a simple measurement of bubble size or of total interfacial area in a cell suspension

presents a problem. The same applies to an assessment of coalescence/redispersion rates and mechanisms although some methods for coalescence frequency measurement have been suggested (19, 20). Some further theoretical considerations and correlations for predicting bubble size, gas hold-up and interfacial area were reviewed (16, 15). Gas hold-up and pressure drop are of importance in a rational design of air-lift reactors (21).

Volumetric mass transfer coefficient $k_L a$. This represents the most important design parameter because $k_L a$ and a are difficult to measure under real conditions. The $k_L a$ measurement methods were reviewed by Sobotka et al. (22). The most reliable values are obtained by balance methods. The model of Sinclair and Ryder (23) may serve as a good example of the application of the above general balance equation (1) with a double substrate limitation of growth (carbon source and dissolved oxygen). The fitting of this model, composed of gaseous and dissolved oxygen, substrate and biomass balances, to growth data provides a possibility of estimating $k_L a$ as one of several evaluated model parameters. An extension of this model with a provision for an alternative oxygen uptake from the gaseous phase has been proposed by Sobotka et al. (17).

For $k_L a$ prediction in bubble columns, an empirical equation of Akita and Yoshida (24), which describes fairly well various data obtained from large scale equipment, can be used:

$$Sh (a D_c) = 0.6 \epsilon_G^{1.1} , Sc^{0.5} . Bo^{0.62} . Ga^{0.31} \quad (2)$$

containing dimensionless Sherwood, Schmidt, Bodenstein and Grashof numbers, interfacial area a , bubble column diameter D_c and gas hold-up ϵ_G . A similar equation may be applicable to bubble columns provided with the two-phase nozzle (ejector), as indicated from $k_L a$ vs. ϵ_G dependence (Figure 2). Two-phase nozzles and multi-orifice spargers are suited for industrial reactors because of high volumetric mass transfer coefficients. The main feature of two-phase nozzle is in preserving the energy of the jet, utilized for the production of a high interfacial area, by suppressed coalescence in suitable media and by a suitable guide tube (momentum transfer tube, (26)). The industrial applications involve those in SCP production (27) and in waste water treatment (28). The correlation of the type of eq.(2) can, perhaps, be of use in predicting $k_L a$ for stirred-tank reactors, based on a single measured value (gas hold-up). Correlations based on power input and superficial velocity are the most frequent (29).

Effect of viscosity on $k_L a$ and power consumption during mass transfer. The effect of viscosity on $k_L a$ is of importance in several highly viscous Newtonian and non-Newtonian fermentations. Some correlations describing $k_L a$ decrease with viscosity have

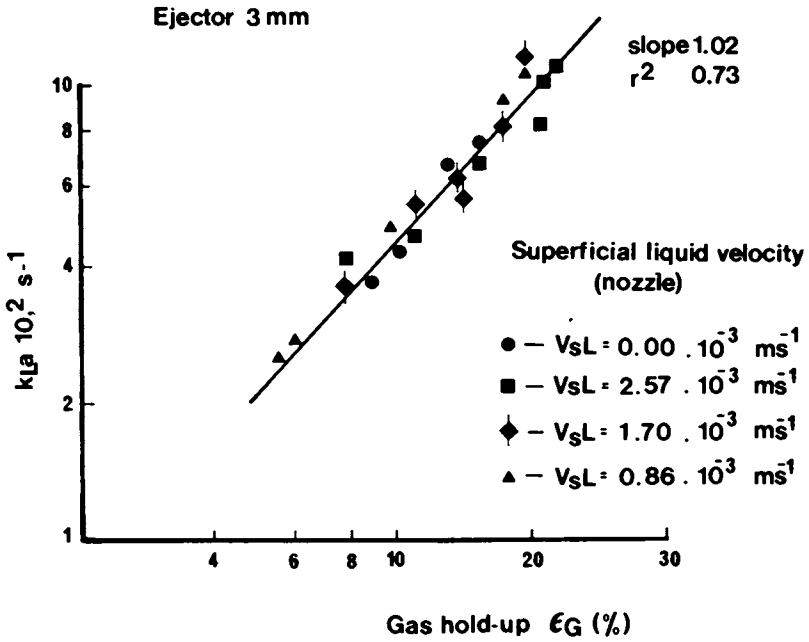


Figure 2. The k_{La} dependence on ϵ_G , bubble column with two-phase nozzle (3 mm ID), electrolyte solution plus ethanol (0.1% v/v) (25).

been summarized in (15). From this paper, the Henzler's correlation for 1-2% CMC solutions in bubble columns (flow behaviour representative for penicillin fermentation) is useful:

$$\frac{k_L a}{u_G} \left(\frac{v}{g} \right)^{1/3} \cdot Sc^{0.3} = 0.012 \left(\frac{v_{sG}^2}{(v_g)^{2/3}} \right)^{-0.45} \quad (3)$$

where v_{sG} is the superficial air velocity and v kinematic viscosity. Reuss^{SG} et al. (30) suggested a much simpler equation for stirred-tank reactor:

$$k_L a \frac{V_L}{\dot{V}_G} = f \left(\frac{P_g}{\dot{V}_G \rho_L (v_g)^{2/3}} \right) \quad (4)$$

involving two dimensionless groups (\dot{V}_G is volumetric air flow rate, V_L reactor volume). Power consumption in gassed systems, P_g , is then calculated from:

$$P_g/P_o = 0.0312 Re^{0.064} Fr^{-0.156} Na^{-0.38} \left(\frac{D_T}{d_i} \right)^{0.8} \quad (5)$$

involving Reynolds and Froude numbers of impeller, aeration number Na and ratio of tank and impeller diameter. The applicability of eq.(4) for predicting $k_L a$ during fermentation of *P.chrysogenum* and *A.niger* is shown in Figure 3. Thus, the basic physical properties of cultivation broths (in this case viscosity) are incorporated into correlations for transport phenomena together with key design parameters ($k_L a$ and power consumption).

Nishikawa et al. (31) have recently proposed the two-region model (bubbling- and agitation-controlled) for estimating $k_L a$ in a mixed reactor. Exponents for viscosity terms are different for different regions. Predictions by dimensionless correlations are applicable for both non-Newtonian and Newtonian liquids.

For bubble columns fitted with a two-phase nozzle and electrolyte solutions, $k_L a$ can be predicted from power for aeration E_a and from power for liquid circulation via nozzle E_p (Figure 4).

Heat Exchange

Heat exchange involves heat generation and transfer in and between elementary regions of a bioreactor and that of individual phases of a reactor (2). A rational start for these considerations is the general local heat balance, similar to that of mass transfer:

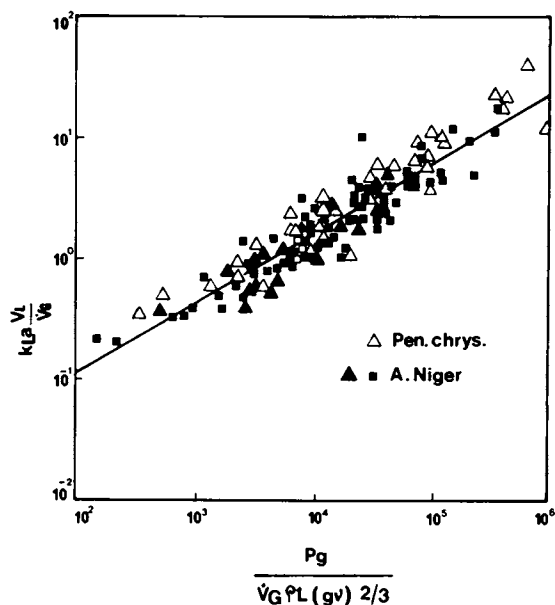


Figure 3. Correlation of Reuss as applied for k_{La} estimate during mold fermentations. Reprinted, with permission, from Ref. 30. Copyright 1981, Pergamon Press Ltd.

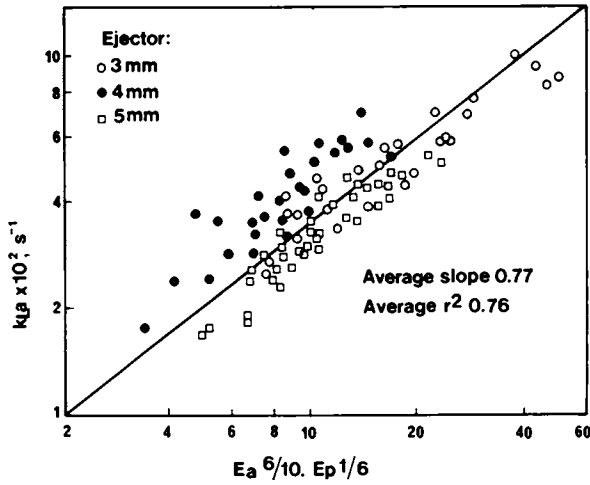


Figure 4. The $k_L a$ dependence on E_a and E_p ; bubble column with two-phase nozzles (3–5 mm ID), electrolyte solution plus ethanol (0–0.1% v/v) (25).

$$\frac{\partial \rho_j C_{pj} T_j}{\partial t} + \nabla \rho_j C_{pj} T_{ij} + \nabla k_{ej} \nabla T_j + \sum \Delta H_{rij} r_{ij} - \sum_{k=1(k \neq j)} k_k a_k (T_{js} - T_j) = 0 \quad (6)$$

where ρ is specific density, C_p is molar heat, T is absolute temperature, k_e is effective thermal conductivity, ΔH is heat of reaction, h_e is heat transfer coefficient and T_{ij} is the temperature at the interface area. The first term of this balance is an accumulation term accounting for heat capacity; the second term is heat transport due to convection, which is important in tubular reactors. The third term represents heat backmixing and can be important in bioreactions occurring in relatively stagnant zones or in a deep layer of solid substrates or cell clumps. The fourth term characterises heat generation due to a reaction and the fifth is the interface heat transfer. In bioreactors that are thoroughly mixed only the accumulation and heat generation terms are significant and the temperature field is uniform. The boundary conditions of this simplified equation are represented by the overall heat transfer from the cultivation broth to the cooling or heating (sterilization) medium.

The amount of heat generated in a bioreactor can be easily evaluated from the above simplified heat balance, resulting in a volumetric rate of heat generation, Q_f ($J \cdot l^{-1} \cdot h^{-1}$). Cooney et al. (32) obtained Q_f by means of dynamic calorimetry. For a rough estimation of Q_f , applicable under oxygen limitation and with cells as the sole reaction product, Minkevich and Eroshin (33) derived a theoretical formula:

$$Q_f = 818 N a_{-1}^m = 818 k_L a \frac{y_2}{H} \quad (7)$$

where $N a_{-1}^m$ is the maximum oxygen transfer of a bioreactor (in $g \cdot l^{-1} \cdot h^{-1}$), y_2 is the mole fraction of oxygen in the exit gas and H is Henry's constant. The coefficient 818 has the meaning of heat generation per 1 g of oxygen consumed. Cooney et al. (32) using direct measurements, found this coefficient to be $822 J \cdot g^{-1}$ oxygen. Eq. (7) seems to be useful for predicting the design of heat exchangers. Q_f is also correlated to biomass yield and productivity (μX):

$$Q_f = \left(k_1 - \frac{k_2}{Y_{x/s}} \right) \mu X \quad (8)$$

where k_1 and k_2 are constants that can be derived from the heats of combustion of substrate and cells. Thus, Q_f can be assessed

for a given substrate and expected yield and productivity (34).

The overall heat transfer coefficient is composed of a minimum of three contributions, the major of which is the coefficient of heat transfer from gas-liquid phase to heat exchanger-wall. Pollard and Topiwala (35) reported values of heat transfer coefficients in gas-liquid bioreactors for various configurations of heat exchanger (coil, jacket). These authors questioned the application of currently used correlations obtained in liquid media (36) to gas-liquid systems. The introduction of air affects the heat transfer coefficient. A novel theory for predicting heat transfer in bubble column reactors was put forward by Deckwer (37). Blakebrough and McManamey (38) measured the heat transfer of mold fermentations in an air-lift reactor. The effects of non-Newtonian aerated liquids on heat transfer coefficient were shortly reviewed by Pace and Righelato (39).

Process Synthesis at Reactor Level

The overall description (model) of a reactor is obtained through process synthesis by combining models of reactor hydrodynamics, mass transfer and heat exchange with an appropriate cell (subcellular) or population model (1). Description of a population should take into consideration possible dispersed or aggregated (the distinct morphological appearances of a culture: pellets, mycelium, flocks, growth on reactor wall in the form of microbial film) forms of population. Biomass support particles are gaining appreciable importance in aerobic (40) as well as in anaerobic processes.

The description hierarchy acquires different ways: physical processes in mass and energy balances; information processing and control; optimization of the system at the reactor level or as a whole (41). The most elaborate concept of descriptive hierarchy, including a set of programs, was published and routinely used by Klir (42). As descriptive hierarchy usually follows structural and functional hierarchy, it is thus assured that the modelled object possesses enough structural and functional features, otherwise the reactor control by means of such models would not satisfactorily respond to changing conditions.

Reactor Control

Reactor control concerns the system properties from the control viewpoint, and the determination of criteria of control and optimization. System properties include dynamic properties such as the nature of system response to small and large disturbances. Regular transient reactor operation may be of future importance even for some product formation processes (43). Elucidation of input operating variables affecting a process is then valuable for reactor control. In this connection the parametric

sensitivity of these variables, defined as a relative or absolute change in an optimization criterion on their change (44), is required. The decisive parameters seriously affecting the system are defined in this way. The criterion of control and optimization is conveniently set up, e.g., as the maximum biological titre, maximum productivity, lowest running costs, etc.

Control and dynamic hierarchies may serve as a good guideline for setting up proper control. Control hierarchy of biological levels is in Table III, control loops and goal functions (control and optimization criteria) of biological levels are in Table IV. The complexity of biological phenomena is reflected in the presence of multiple local goal functions of different subsystems, which may act in an accord or oppositely. Note that Table IV has been developed for ecosystems. The implementation of control hierarchy in the modelling and control of biological systems has not yet been carried out. The control hierarchy is connected with the dynamic hierarchy of time characteristics (relaxation times of individual subsystems). The relaxation time is considered to be the time for a change from one state to another (due to reaction, diffusion, change in the adjoining level, etc.). Table V presents average relaxation times of some cellular subsystems. As appears from this table, slow (and limiting) processes give rise to structural elements, serving as basis for fast processes. Usually, responses of higher levels of the system to disturbances coming from the superior level are slower than responses at the next lower level. Besides relaxation times of biological subsystems of cells, the selection of systemic phenomena may proceed via an utilization of, e.g., cell generation time, rate of substrate consumption, respiration rate, oxygen transfer and of the homogenization time of a reactor, to mention some.

The above discussion may involve both control and dynamics of steady state (single and multiple), unsteady state (transition between two states) and unstable operations of the bioreactor resulting from typical non-linear response of biological systems. In spite of the fact that the stability analysis of non-linear systems is quite advanced, experimental confirmation of multiple steady states and instabilities lags behind (for a review of theory and experiments see (45)). An excellent example of experimental demonstration of unstable operation of a continuous reactor is in (46).

Reactor Scale-Up

On the basis of a reactor model, involving enough structural and functional features of biological and engineering (physical) properties of a biotechnological process, new criteria for a scale-up may evolve. The employment of only one criterion, taken from one arbitrary level of a hierarchy, in the modelling and subsequent scale-up frequently fails, as is apparent from numerous

Table III Control Hierarchy of Biological Levels

Control Level	Dynamic Behaviour	The Highest Control Mechanism
1	Mass and energy change (steady number of structural elements and steady parameters)	Direct and feed-back control
2	Functional dynamics (steady number of structural elements, changing parameters)	Adaptation
3	Structural dynamics (changing number of structural elements)	Organization
4	Developmental dynamics (changing goal function)	Development

Internat.J.General Systems 1982, 8(1), Table IV (1)

Table IV Control Loops and Goals of Biological Levels

	S t r u c t u r a l H i e r a r c h y		
	Cellular	Population	Trophic
Goal function	Optimization of individual subsystems by controlling biochemical pathways	Optimization of subsystems of a cell by controlling individual subsystems	Optimization of structural elements of population
Direct and feed-back	Simple kinetics	Stabilization of ratio of individual subsystems	Stabilization of a number of individuals
Adaptation	Multiple kinetics	Physiological adaptation of subsystems	Adaptation of trophic levels
Organization (selection)	Change-over from one to another biochemical pathway	Change in function of subsystems	Change in ratio of structural elements of different populations
Development	Change in goal function of a subsystem	Change in goal function of individual cells	Change in goal function of ecosystem

Internat. J. General Systems 1982, 8(1), Table V (1)

Table V Dynamic Hierarchy of Biological Subsystems

System (Subsystem)	Relaxation Time, s
Cell multiplication, DNA replication	$10^2 - 10^4$
mRNA synthesis on operon	$10^3 - 10^4$
Translocation of substances into cells	$10^1 - 10^3$
Protein synthesis in polysomes	$10^1 - 10^2$
Allosteric control of enzyme synthesis	10^0
Glycolysis in cytoplasm	$10^{-1} - 10^1$
Oxidative phosphorylation in mitochondria	10^{-2}
Enzymatic reaction and turnover	$10^{-6} - 10^{-3}$
Bond between enzyme and substrate	10^{-6}

Internat. J. General Systems 1982, 8(1), Table VI (1)

examples of applications of engineering criteria (e.g., in (29)). The neglect of biological features of biotechnological processes frequently leads to an unresolved case of simultaneous maintenance of the numerical values of all dimensionless groups of physical parameters (mass transfer, power input per unit volume, mixing time, etc.). For example, a single criterion of constant mixing time would violate an invariance of gas phase dynamics. Macro-mixing of the fluid phase determines, to a considerable extent, the behaviour of the gas phase, i.e., the residence time distribution of gas bubbles. In reactor scale-up, a considerable difference in gas phase residence time can be expected as the liquid flow paths (loops) grow with increasing reactor scale. The maintenance of mixing time would result in an increase in oxygen utilization efficiency. Some limited experimental data for different reactor designs are available in (47).

Qualitatively new criteria, which may be derived from the scheme of the hierarchical functions of a biotechnological process, suggest a need for maintaining similarity between systems of different sizes of laboratory and plant levels, i.e., the identity of values of parameters and constants (1,2). Such a scale-up procedure would require a repetition of systemic features of decisive levels of hierarchy involving those of biotechnological and physical nature on the laboratory and plant scale and would assume the invariance of the systemic phenomena of a given level with respect to the scale. The methodology of scale-up via modelling and simulation is yet to be developed.

Conclusions

Further development of reactor design is hampered by a lack of appropriate theory of some elementary phenomena. This situation leads to empirical correlations that may be of some practical use. Systems approach aids in creating a guideline for rational bioreactor design, especially on the basis of sound biological theory.

Literature Cited

1. Prokop, A. Internat.J.General Systems 1982, 8(1)
2. Prokop, A. Acta Biotechnologica (DDR) 1981, 1(3) 269-278.
3. Bird, B.; Stewart, W.E.; Lightfoot, B.N. "Transport Phenomena"; J.Wiley: New York, 1980.
4. Turian, R.M.; Fox, G.E.; Rice, P.A. Can.J.Chem.Eng. 1975, 53, 431-437.

5. Deckwer, W.-D. Chem. Ing. Technik 1977, 49, 213-233.
6. Levenspiel, O. "Chemical Reaction Engineering. An Introduction to the Design of Chemical Reactors"; J.Wiley: New York, 1962.
7. Prokop, A.; Erickson, L.E.; Fernandez, J.; Humphrey, A.E. Biotechnol. Bioeng. 1969, 11, 945-966.
8. Laine, J.; Kuoppamäki, R. Ind. Eng. Chem., Proc. Des. Develop. 1979, 18, 501-506.
9. Einsele, A. Chem. Rundschau 1976, 29, 53-55.
10. Danckwerts, P.V. Chem. Eng. Sci. 1958, 8, 93-102.
11. Bajpai, R.K.; Ramkrishna, D.; Prokop, A. Biotechnol. Bioeng. 1977, 19, 1761-1772.
12. Skelland, A.H.P. "Diffusional Mass Transfer"; J.Wiley: New York, 1974.
13. Aiba, S.; Toda, K. J. Gen. Appl. Microbiol. 1964, 10, 157-162.
14. Moo-Young, M.; Blanch, H.W. "Advances in Biochemical Engineering"; Fiechter, A., Ed.; Springer: Berlin, 1981; Vol. 19, pp. 1-69.
15. Deckwer, W.-D. "Advances in Biotechnology"; Moo-Young, M.; Vezina, C.; Robinson, W.C., Eds.; Pergamon Press: Oxford, 1981; Vol. 1.
16. Blanch, H.W. "Annual Reports on Fermentation Processes"; Perlman, D., Ed.; Academic Press: New York, 1979; Vol. 3, pp. 47-74.
17. Sobotka, M.; Votruba, J.; Prokop, A. Biotechnol. Bioeng. 1981 23, 1193-1202.
18. Zieminski, S.A.; Whittermore, R.C. Chem. Eng. Sci. 1971, 26, 509-520.
19. Koetsier, W.T.; Thoenes, D. Proc. 5th Europ. 2nd Internat. Symp. on Chemical Reaction Engineering; Amsterdam, May 2-4, 1972, Elsevier: Amsterdam, 1972; pp. (B3-15)-(B3-24).
20. Hassan, I.T.M.; Robinson, C.W. Chem. Eng. Sci. 1980, 35, 1277-1289.
21. Hsu, Y.C.; Dudukovic, M.P. Chem. Eng. Sci. 1980, 35, 135-141.
22. Sobotka, M.; Prokop, A.; Dunn, I.J.; Einsele, A. "Annual Reports on Fermentation Processes"; Tsao, G.T., Ed; Academic Press: New York, 1981; Vol. 5.
23. Sinclair, C.G.; Ryder, D.N. Biotechnol. Bioeng. 1975, 17, 375-389.
24. Akita, K.; Yoshida, F. Ind. Eng. Chem., Proc. Des. Develop. 1973, 12, 76-80.
25. Prokop, A.; Janík, P.; Sobotka, M.; Krumphanzl, V. Biotechnol. Bioeng., submitted.
26. Nagel, O.; Kürten, H.; Sinn, R. Chem. Ing. Technik 1970, 42, 474-479.
27. Dimling, W.; Seipenbusch, R. Process Biochem. 1978, 13(3), 9-12, 14-15, 34.
28. Leistner, G.; Müller, G.; Sell, G.; Bauer, A. Chem. Ing. Technik 1979, 51, 288-294.
29. Aiba, S.; Humphrey, A.E.; Millis, N.F. "Biochemical Engineering"; Tokyo University Press: Tokyo, 1973, 2nd Ed.

30. Reuss, M.; Bajpai, R.K.; Lenz, R.; Niebelschütz, H.; Papalexion, A. "Advances in Biotechnology"; Moo-Young, M.; Vezina, C.; Robinson, W.C., Eds.; Pergamon Press: Oxford, 1981; Vol.1.
31. Nishikawa, M.; Nakamura, M.; Hashimoto, K. J.Chem.Eng.Japan 1981, 14, 227-232.
32. Cooney, C. .; Wang, D.I.C.; Mateles, R.I. Biotechnol.Bioeng. 1968, 11, 269-281.
33. Minkevich, I.G.; Eroshin, V.K. Folia Microbiol. 1973, 18, 376-385.
34. Wang, H.Y.; Mou, S.-G.; Swartz, J.R. Biotechnol.Bioeng. 1976, 18, 1811-1814.
35. Pollard, R.; Topiwala, H.H. Biotechnol.Bioeng. 1976, 18, 1517-1535.
36. Edwards, M.F.; Wilkinson, W.L. Chem.Engr.(London) 1972, 265, 328-335.
37. Deckwer, W.-D. Chem.Eng.Sci. 1980, 35, 1341-1346.
38. Blakebrough, N.; McManamey, W.J.; Tart, K.R. Trans.Instrn.Chem. Engrs. 1978, 56, 127-135.
39. Pace, G.W.; Righelato, R.C. "Advances in Biochemical Engineering"; Fiechter, A., Ed.; Springer: Berlin, 1980; Vol.15, pp.41-70.
40. Atkinson, B.; Black, G.M.; Pinches, A. Process Biochem. 1980, 15(4), 24-26, 29-32.
41. Mesarovic', M.D.; Macko, D.; Takahara, Y. "Theory of Hierarchical, Multilevel Systems"; Academic Press: New York, 1970.
42. Klir, G.J. "Theoretical Systems Ecology; Advances and Case Studies"; Halfon, E., Ed.; Academic Press: New York, 1979; pp.291-323.
43. Pickett, A.M.; Topiwala, H.H.; Bazin, M.J. Process Biochem. 1979, 14(11), 10, 12, 14-16.
44. Ditmar, P.; Khartman, K.; Ostrovskii, G.M. Theoret.Osnovy Khim. Tekhnol. 1978, 12, 104-111 (in Russian).
45. Prokop, A. "Continuous Cultivation of Microorganisms"; Sikyta, B.; Fencl, Z.; Poláček, V., Eds.; Institute of Microbiology: Prague, 1980, pp. 173-187.
46. DiBiasio, D.; Lim, H.C.; Weigand, W.A. AIChE Journal 1981, 27, 284-292.
47. Ovaskainen, P.; Lundell, R.; Laiho, P. Process Biochem. 1976 11(4) 37-39, 55.

RECEIVED June 1, 1982

Immobilized Cells

Catalyst Preparation and Reaction Performance

J. KLEIN and K.-D. VORLOP

Technical University of Braunschweig, Institute of Chemical Technology,
Federal Republic of Germany

Immobilized cells have proven to be effective catalysts in the enzymatic conversion of organic compounds. Such catalysts are typically prepared by entrapment of cells in polymeric carriers, and the methods of ionotropic gelation and polycondensation of epoxids will be described. Depending on enzymatic activity and particle size the transformation may proceed in the reaction or diffusion controlled regime. Quantitative estimation of the effectiveness factor-Thiele modulus relation will be presented for different reaction types. This includes the experimental determination of the catalytically active cell concentration and the effective diffusivity in the porous polymeric carrier. Transport limitation can also be a controlling factor in the experimental determination of the operational stability of such biocatalysts.

A large number of products in the pharmaceutical and food industry is obtained from fermentation processes. Examples are amino acids, stereoregular organic acids, antibiotics, ethanol, etc. In a classical fermentation process the product formation is strictly coupled to cell growth resulting in a possibly unfavorable byproduction of biomass. Furthermore these processes are typically performed as batch operations.

As has been shown already on an industrial scale, fermentation can be substituted by heterogeneous catalysts with resting microbial cells immobilized in polymeric carriers. Repeated use of the once formed biomass, continuous process operation, and elimination of costly separation steps of product solution from biomass are obvious advantages of this new technology. Some principal aspects of a) immobilization methodology, b) catalyst effectiveness, and c) operational stability shall be outlined in this contribution.

0097-6156/83/0207-0377\$06.00/0
© 1983 American Chemical Society

Polymer Entrapment

Various methods have been proposed for whole cell immobilization including adsorption and covalent attachment to a preformed carrier, crosslinking, flocculation, microencapsulation, and entrapment. Physical entrapment in a porous matrix is by far the most flexible and most commonly used technique. Considering the fact that the polymer network has to be formed in the presence of the finally entrapped biological material, the performance criteria of chemical and physical nature are as follows:

(1) The network formation has to proceed under mild conditions (pH and temperature) in an aqueous environment;

(2) the network has to be chemically stable under various reaction conditions (pH, buffer solution, ionic and nonionic substrates, etc.);

(3) the size and the porosity of the polymeric carrier (preferably as beads) has to be controlled;

(4) the possibility for a large variation of biomass content in the catalyst should be given;

(5) the catalyst beads should be mechanically stable to be used in various reactor configurations (packed bed, fluidized bed, stirred tank).

Appropriate polymeric carriers can be obtained from polymeric, oligomeric, and monomeric precursors. Due to unwanted chemical interaction of such chemicals with the cell material larger size of these precursors is favorable. The ionotropic gelation, starting from polyelectrolytes and the polycondensation, starting from oligomeric epoxy resins, are typical problem solutions.

Ionotropic Gelation of Polyelectrolytes

This method of network formation is defined as a crosslinking reaction of polyelectrolytes with lower molecular weight multivalent counterions. Considering the polymeric component, anionic (e.g., alginate, CMC (1) or cationic (chitosan (2)) substances can be used. This variety of polymers and the appropriate counterions are summarized in Figure 1. The choice of the polymer is determined by the pH region of the respective biocatalytic reaction, since all ionotropic gels are reversible structures which can be redissolved by increase (alginate) or decrease (chitosan) of pH beyond certain limits. A second important criterion is the ionic composition of the reaction medium and the possibility of insoluble byproduct or complex formation with the network forming ions.

In a typical alginate entrapment process the cells are suspended in a 3% sodium alginate solution and this viscous suspension is precipitated dropwise in a 1% CaCl_2 solution. After 30 minutes stable Ca-alginate gels are formed where the cells are immobilized in a macroporous structure. Following to this precipitation process a partial drying step can be applied which results in a homogeneous shrinking of the particles, thus increasing con-

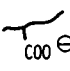
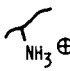
POLYELECTROLYTES	MULTIVALENT COUNTERIONS
<p>POLYANIONS</p>  COO^- $x \oplus$ <p>ALGINATE CARBOXYMETHYL-CELLULOSE CARBOXY-GUAR-GUM COPOLY-STYRENE-MALEIC ACID</p>	<p>Ca^{2+}, Fe^{2+}, Zn^{2+} ... Al^{3+}, Fe^{3+}</p>
<p>POLYCATIONS</p>  NH_3^+ $x \ominus$ <p>CHITOSAN</p>	<p>$\text{Fe}(\text{CN})_6^{4-}$, $\text{Fe}(\text{CN})_6^{3-}$ POLY-PHOSPHATE POLY-ALDEHYDO-CARBONIC ACID POLY-1-HYDROXY-1-SULFONATE-PROPEN-2 ALGINATE</p>

Figure 1. Summary of polymer-counterion systems to be used in ionotropic gelation for whole cell entrapment. Reprinted, with permission, from Ref. 13. Copyright 1982, Plenum Publishing Corp.

siderably the mechanical stability as well as the packing density of the entrapped cells itself. All these factors are very advantageous for the biocatalytic application. The flexibility of the alginate-method can be demonstrated according to the following parameter boundary values: polymer concentration from 0.5 to 8%, CaCl_2 concentration from 0.05 to 2%, cell concentration (on wet weight basis) from 0.1 to 100%, bead diameters from 0.1 to 5 mm, and preparation temperatures from 0 to 80° C. Cells of different structure; e.g., aerobic (1) or anaerobic microbes (3), plant cells (4), mammalian cells (5), can be entrapped and thus stabilized without considerable toxicity problems.

A problem of practical importance is the scale up of the immobilization process from amounts of several grams to several hundred liters. While small amounts can easily be prepared using one capillary orifice, a bundle of such capillary in a sieve plate type construction will give larger amounts of identical particles, if the capillary characteristics are not changed. These devices are shown in Figure 2.

Polycondensation of Epoxy Resins

In this case covalent networks of high mechanical and chemical stability are obtained as a result of crosslinking reaction of epoxides with multifunctional amines (6). The main problems of this technique are the toxicity of the amino-component and the usually low porosity of the polymeric network. The toxicity, measured by the viability of immobilized yeast cells, could be minimized a) by proper selection of epoxy and amino components and b) by introduction of a pregelling time in the order of 15 minutes before mixing the cells with the condensating oligomers (7). The porosity of the matrix is introduced by the immobilized cells itself and by an intermediate preparation of an interpenetrating network with an ionotropic gel. The ionotropic gelation is also used to control the particle shape and size. A complete scheme of such an immobilization process is shown in Figure 3. Again quite high concentrations (up to 70% on wet weight basis) of cells can be finally incorporated in such a polymeric structure.

The viability of the yeast cells, and thus the reduced toxicity of the entrapment method, can be demonstrated by cell growth in the matrix, which gives rise to a corresponding activity increase for ethanol production from glucose (7). This behavior is shown in Figure 4. The factor of activity increase compared to the initial value increases with decreasing initial loading; however, it is obvious that an upper limit of activity will finally be reached. The reason for this phenomenon, as well as for the activity decrease with increasing incubation time, will become obvious from the discussions of the following chapter.

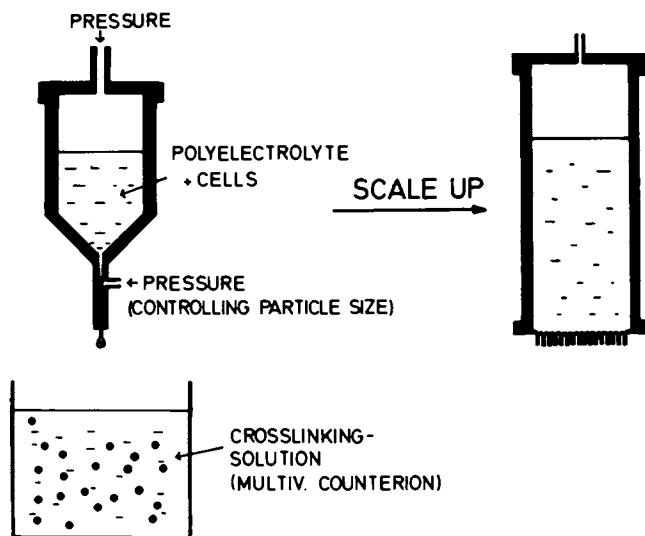


Figure 2. Scheme for catalyst bead formation by ionotropic gelation, including scale-up device.

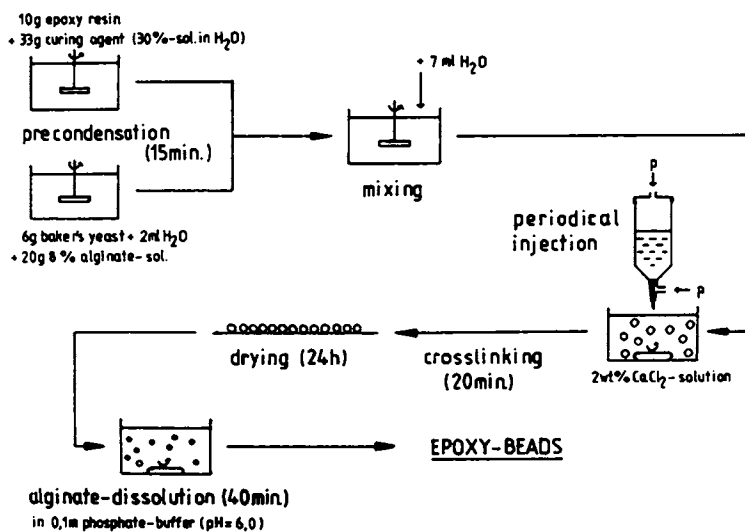


Figure 3. Process scheme for preparation of biocatalysts by cell entrapment in epoxy beads. Reprinted, with permission, from Ref. 14. Copyright 1982, Science and Technology Letters.

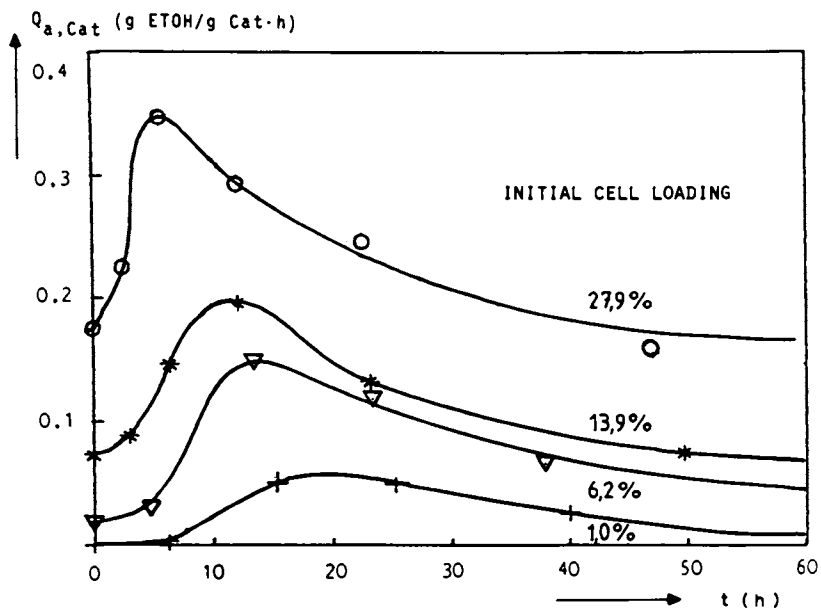


Figure 4. Dependence of biocatalytic activities for the batch fermentation of ethanol from glucose with immobilized yeast cells as a function of incubation time (time for cellgrowth in the carrier) for various initial cell loadings in epoxy carriers.

Effectiveness of Immobilized Cell Catalysts

It is a well known fact in heterogeneous catalysis, that the catalytic activity is generally not directly proportional to the concentration of active sites but depends also on hydrodynamic conditions in the surrounding of the particles, on particle size and matrix porosity. It is furthermore well understood, that various transport phenomena have to be taken into account, mainly diffusional transport processes which necessarily are preceding to the reaction step itself.

A dimensionless number, usually called Thiele-modulus, can be used to quantitatively account for transport-reaction coupling phenomena. Assuming the validity of Michaelis-Menten rate equation - which is justified for simple enzymatic reactions in whole cells too - the following expression for the Thiele modulus has been derived (8):

$$\phi = \frac{R}{3} \sqrt{\frac{v'}{2K_M \cdot D_e}} \left(\frac{S}{K_M + S} \right) \left[\frac{S}{K_M} - \ln \left(1 + \frac{S}{K_M} \right) \right]^{-1/2} \quad (1)$$

where R is the particle radius, v' the rate of reaction, K_M the Michaelis constant, S the substrate concentration and D_e the effective substrate diffusivity in the porous catalyst particle. On the other hand the effectiveness factor η is defined as the ratio of the effective reaction rate v_e to the maximum reaction rate v_{\max} which would be observed without transport limitation

$$\eta = \frac{v_e}{v_{\max}} \quad (2)$$

For immobilized cell catalysts there are two possibilities to obtain this factor. Firstly, the particles of larger radius can be grinded down to such a small size that pore diffusion becomes negligible. In this case $v_{\max} = v_{e,R \rightarrow 0}$. Due to the size and the simple entrapment of the catalytic species loss from the matrix may be considerable. Therefore, secondly, the free cell activity can be used in the denominator, if the exact concentration of catalytically active immobilized cells (X_{act}) is known. Since

$$v = -\frac{1}{X} \cdot \frac{d(S)}{dt} \quad (3)$$

is the specific reaction rate of the freely suspended cells, the equation

$$v_{\max} = v \cdot X_{\text{act}} = v' \quad (4)$$

holds, which furthermore defines v' in Eqn. (1). Based on numerical calculations typical functions

$$\eta = f(\phi) \quad (5)$$

have been developed, which interrelate the two dimensionless parameters and which can be checked experimentally.

To evaluate the applicability of Eqn. (5), the parameters in Eqns. (1-4) have to be determined independently. This has been done for the cleavage reaction of Penicillin G to 6APA with immobilized *E. coli* cells immobilized in epoxide beads (9).

The radius R: The radius of particles obtained from ionotropic gelation is usually controlled within very narrow limits and the size can easily be determined by microscopic measurements.

Reaction Kinetics: The reaction rates have been measured at pH = 7.8 and T = 37° C, using a 5% Pen G substrate concentration. Titration with 0.1 molar NaOH has been used to determine the amount of product formation. The K_M values of free and immobilized cells have been obtained from the Lineweaver-Burk plots as shown for some examples in Figure 5. Following to irreversible deactivation of enzymes during the process of immobilization, the inequality $X_{act} < X_{immobil.}$ holds. The following approach has been developed for the determination of X_{act} : in a certain experiment, in a first approximation $X_{act} = X_{imm.}$; i.e., 100% of all immobilized cells are assumed to be active. In this case, $\eta = 0.23$ has been determined. If $X_{act} < X_{imm.}$, η will become larger, due to the decrease of the denominator in Eqn. (2). In the same way a series of ϕ -values can be calculated from Eqn. (1) on the basis of different v' -values. The corresponding sets of values for different assumptions of X_{act} are listed in Table I:

Table I. Calculated η - and ϕ - values based on different assumptions of residual cell activity after immobilization.

$X_{act}/X_{imm.}$			
%	η calc.	ϕ calc.	
10	2.36	0.59	
20	1.18	1.34	
30	0.79	1.44	
40	0.59	1.63	
50	0.47	2.11	
60	0.39	2.32	
70	0.34	2.50	
80	0.30	2.68	
90	0.26	2.84	
100	0.24	3.00	

The true value of X_{act} has to satisfy Eqn. (5), which has been

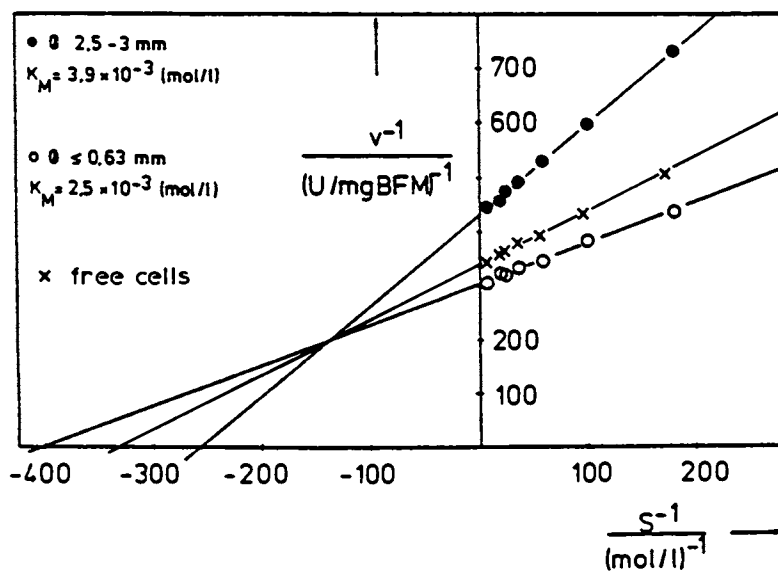


Figure 5. Determination of the Michaelis constant, K_M , for 6 APA formation from penicillin G with immobilized *E. coli* cells. Conditions: pH 7.81, 37°C, 5% penicillin G solution, epoxy carrier.

generally calculated (8). Plotting all data from Table I together with the function Eqn. (5) in Figure 6 gives a point of intersection, which determines the true pair of η/ϕ -values and thus X_{act} . Comparison of several immobilized cell preparations gave practically identical results, showing that a value $X_{act} = 0.43X_{imm}$ is a typical one for this epoxide-immobilization procedure.

Effective Pore Diffusivity: The effective pore diffusivity of penicillin G has been determined experimentally in a batch experiment (10). Mixing a certain number of catalyst beads having a homogeneous substrate concentration S_a (g/l), with a certain volume of fresh, non-conducting water, the diffusion process can be followed by the conductivity and the concentration increase in the supernatant liquid. If S_e is the substrate concentration in the particle at $t \rightarrow \infty$ and S the concentration at time t , R the particle radius (cm) and D_e the effective diffusivity (cm^2/sec) the diffusion coefficient can be obtained from the slope plotting $\ln(S - S_e)/(S_a - S_e)$ vs. t , following to Eqn. (6):

$$\frac{S - S_e}{S_a - S_e} = \frac{6}{\pi^2} \sum_{n=1}^{\infty} \frac{1}{n^2} \exp. \frac{-\pi^2 D_e \cdot t}{R^2} \quad (6)$$

Such a plot is shown in Figure 7.

Comparison of Theory and Experiment: If the simple model of transport limitation due to pore diffusion holds, all experimentally determined pairs of η and ϕ should fall on the non-dotted $\eta = f(\phi)$ - function shown in Figure 6. Using the independently determined parameters as described before such values have been determined for a number of catalyst preparations used in the penicillin G cleavage reaction. The excellent agreement between calculation of Eqn. (5) and experimental determination can be seen from Figure 8. In this series of experiments two different strains of *E. coli* cells have been used, the one of them having been obtained by genetic engineering leading to a tenfold activity increase compared to the conventional strain ATCC 11 105 (1).

Catalyst Optimization: In another reaction example the application of the Thiele-modulus concept for the optimization of catalyst composition could be demonstrated. Here the oxidation of glucose to gluconic acid, catalyzed by *Acetobacter simplex* cells has been studied, where oxygen is the rate limiting substrate. In this case a Ca-alginate matrix has been used for cell immobilization. Using simplified equations for the calculation of D_e and furthermore assuming $X_{act} = X_{imm}$, (12), the relation between relative activity (η in %) and particle diameter could be calculated for different cell concentrations. As can be shown in Figure 9, a good agreement with experimental data is obtained.

The absolute activity for gluconic acid production is obtained if the specific activity of the different preparations is multiplied with the cell concentration. The non-dotted curve in Figure 10 is the result of this calculation, which gives a good

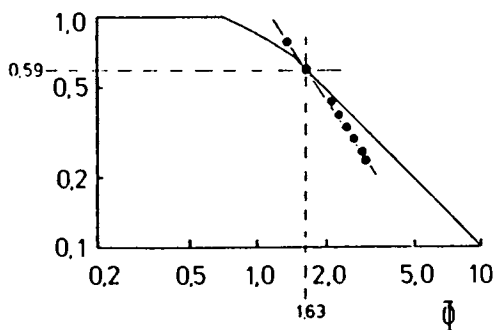


Figure 6. Determination of catalytically active cell concentration, X_{act} , on the basis of the effectiveness factor/Thiele modulus relation.

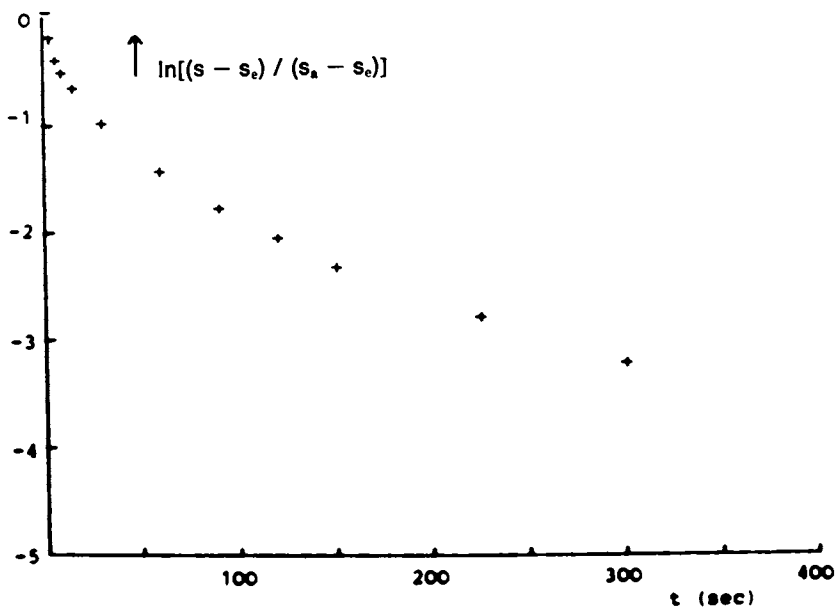


Figure 7. Plot of time dependence of solution concentration from a batch diffusion experiment for the determination of the effective substrate diffusivity, D_e .

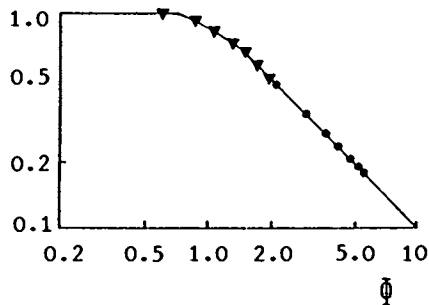


Figure 8. Comparison of calculated and experimentally determined effectiveness factor and Thiele modulus values for 6 APA formation from penicillin G with immobilized *E. coli* cells. Conditions: pH 7.8, 37°C, 5% penicillin G solution, epoxy-carrier. Key: ▼, ATCO 11 105; ●, *E. coli* 5 K (pHM 12).

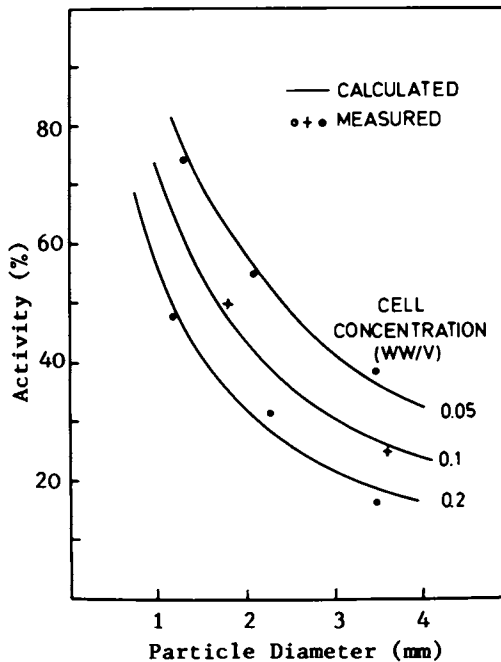


Figure 9. Dependence of residual activity (effectiveness of immobilized cells) on particle size and cell loading for the production of gluconic acid from glucose with calcium alginate immobilized *Acetobacter simplex* cells.

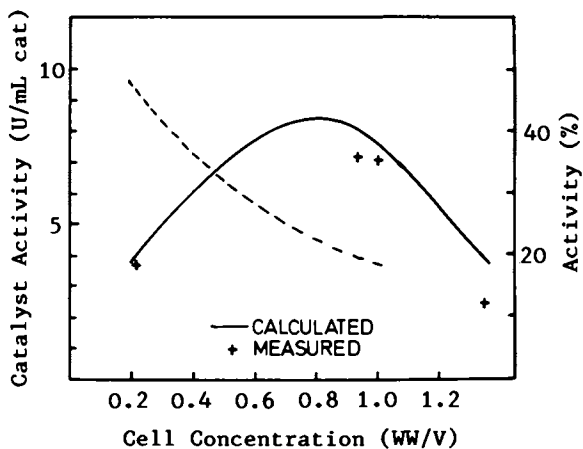


Figure 10. Catalytic effectiveness (activity in %) and absolute catalytic activity as a function of cell concentration for gluconic acid production from glucose with calcium alginate immobilized *Acetobacter simplex* cells. Reprinted, with permission, from Ref. 13. Copyright 1982, Plenum Publishing Corp.

correlation to experimental data shown in the same graph. The maximum in this curve gives the optimum value of cell loading and can be explained by the increased blocking of pore space for oxygen transport with an increasing number of immobilized cells. In the same sense the curvature of the reactivity curves of Figure 4 should be recalled.

Catalyst Deactivation and Operational Stability

Coming back to the penicillin G cleavage reaction, long time experiments with epoxide-immobilized *E. coli* cells have been reported earlier (6). Without any correction an effective half-life value $t_{1/2}$ of catalytic activity of 43 days has been determined. Repeated experiments confirmed the abrupt change of slope in the activity-time curve of consecutive batch reactions. In another experiment, where the cells have been immobilized in a low concentration at the surface of a macroporous epoxy-carrier, a straight line activity-time function has been found with a much smaller value $t_{1/2} = 11$ days (9). It therefore becomes obvious, that transport limitation due to much higher cell loading and longer diffusion pathways in a bead-type carrier might be responsible for the two different slopes.

The experimental data are shown in Figure 11a, together with a dotted line, extrapolating the reaction controlled regime to zero time. On the other hand some model calculations have been performed under the assumption that, at the beginning of the experiment, the reaction rate is in the diffusion controlled regime. Then only a restricted spherical shell close to the bead surface is participating in the substrate conversion. If superimposed on the reaction a time dependent catalyst deactivation occurs, the reactive shell should move to the center of the catalyst particle where active cells are available to substitute for the deactivated cells closer to the surface.

Assuming different rate equations for the time dependent deactivation reaction the graphs in Figure 11b are obtained. Without achieving quantitative agreement in such a simplified calculation, we believe that the good qualitative agreement of the non-dotted lines in Figure 11b with the experimental curve in Figure 11a supports our considerations in principle. The general conclusion is that one should be very careful in deriving intrinsic half-life values of immobilized cells from overall operational stability data of biocatalytic conversion. Diffusional limitation will always lead to artificially higher values.

Acknowledgements

The fruitful cooperation with Professor F. Wagner and his research group as well as the financial support from the BMFT under Grant No. PTB 8150 is gratefully acknowledged.

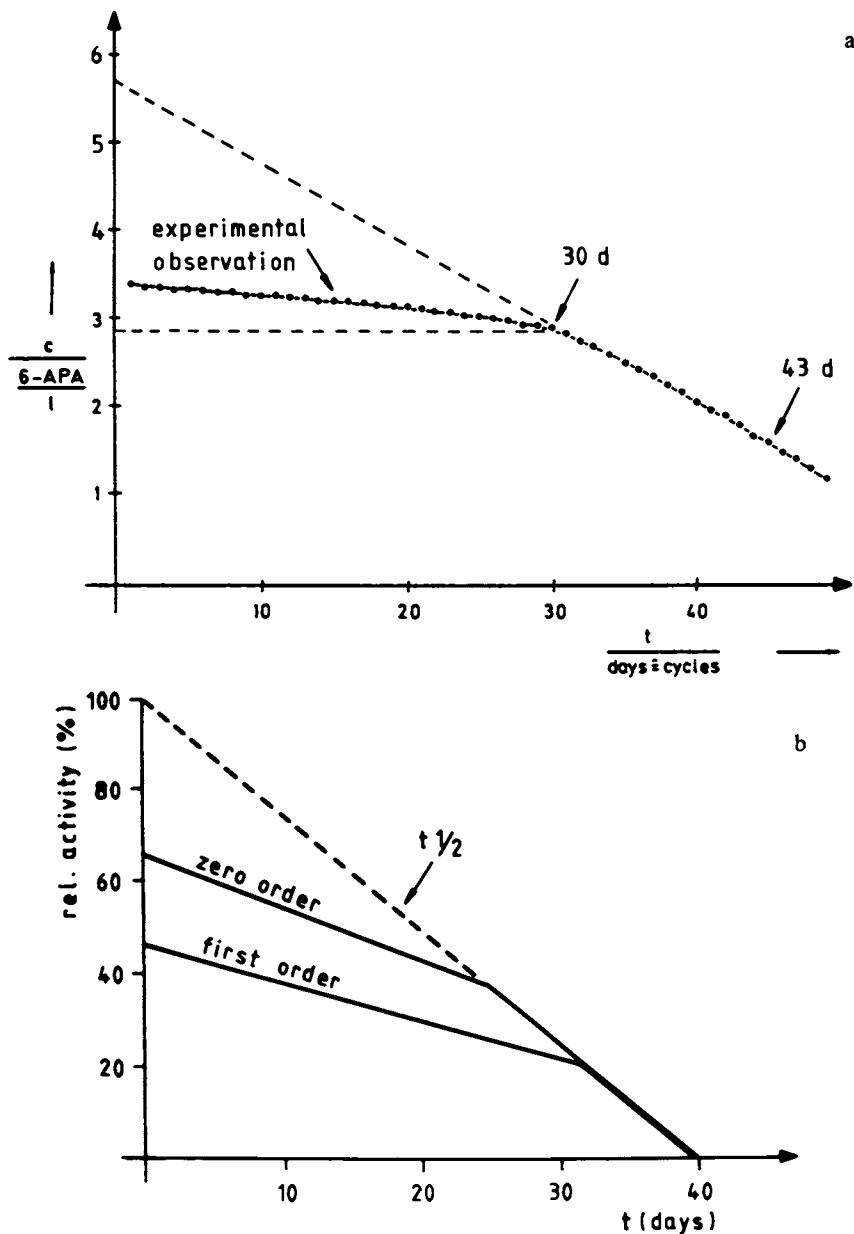


Figure 11. Operational stability functions of *E. coli* cells immobilized in epoxy carrier for consecutive batch operation in the production of 6 APA from penicillin G. Top, experimental data; bottom, model calculations for the superposition of 6 APA formation and conversion dependence catalyst deactivation reaction in the diffusion controlled regime.

Literature cited

1. Klein, J.; Hackel, U., and Wagner, F. ACS Symposium Series, 1979, 106, 101
2. Vorlop, K.-D., and Klein, J. Biotechnol. Letters 1981, 3, 65
3. Scherer, P.; Kluge, M.; Klein, J., and Sahm, H., Biotechnol. Bioeng. 1981, XXIII, 1057
4. Scheurich, P.; Schnabl, H.; Zimmermann, U., and Klein, J. Biochem & Biophys. Acta 1980, 598, 645
5. Pilwat, G.; Washausen, P.; Klein, J., and Zimmermann, U., Z. Naturforschung 1980, 35c, 352
6. Klein, J., and Eng, H., Biotechnol. Letters 1979, 1, 171
7. Kressdorf, B., Diplom Thesis, Technical University Braunschweig 1981
8. Bischoff, K.B., AICHE J. 1965, 11, 351
9. Eng, H., PhD. Thesis, Technical University, Braunschweig 1980
10. Klein, J., and Washausen, P., DECHEMA Monograph. Vol. 84, Verlag Chemie, Weinheim 1979, p. 300
11. Klein, J., and Wagner, F., Enzyme Engineering Vol. 5,; H. Weetall and G. Royer, ed., Plenum Publ. Corp., New York 1980, p. 359
12. Vorlop, K.-D.; Klein, J., and Wagner, F. 6th Intern. Fermentation Symposium, London (Canada), 1980, paper F 12.1.12.p.
13. Klein, J., and Manecke, G., Enzyme Engineering Vol. 6, Plenum Publ. Corp., New York 1982.
14. Klein, J., and Kressdorf, B., Biotechnol. Letters 1982, 4, 375.

RECEIVED August 18, 1982

Dissolved Oxygen Contours in *Pseudomonas ovalis* Colonies

H. R. BUNGAY, P. M. PETTIT, and A. M. DRISLANE

Rensselaer Polytechnic Institute, Troy, NY 12181

Pseudomonas ovalis colonies of various sizes grown on agar supplemented with glucose developed patterns of dissolved oxygen in the colonies and surrounding agar. Proximity to glucose from the agar determines the demand for oxygen, so regions of a colony that are distant from the agar tend to have ample dissolved oxygen. A control colony on unsupplemented agar was rich in dissolved oxygen. As colony size increased on agar with added glucose, regions quite low in dissolved oxygen developed.

Our group has investigated oxygen transfer in a number of microbial systems such as slimes, pellets, flocs, and films (1). A logical extension is the study of colonies because many microorganisms grow attached to surfaces. Although colonies are often bathed by nutrient media, it seemed convenient and interesting to work with bacteria growing on a solid surface that supplied nutrients. Studies of oxygen transfer in microbial systems often employ *Pseudomonas ovalis* because this bacterium has a high demand for oxygen as it converts glucose to gluconic acid. We have at times used oxygen microelectrodes drawn to tips one micrometer in diameter, but a tip of about four micrometers is more rugged and is adequate for studying colonies that are several millimeters in diameter.

Materials and Methods

Colonies of *Pseudomonas ovalis* Strain ATCC 8209 were grown in petri dishes on nutrient agar (8 g. Difco nutrient broth + 15 g. Difco Bacto-agar/L.) with supplemental glucose. Agar was poured into petri dishes to a height of about 0.5 cm. Dilute suspensions of organisms were streaked onto the agar carefully to avoid distorting the surface.

0097-6156/83/0207-0395\$06.00/0

© 1983 American Chemical Society

The apparatus has been reported previously (1). The micro-manipulator had coarse control in the X and Y axes and a precise vernier for the Z axis. A reference plane was established by lowering the microprobe until electrical contact was established at points several millimeters away from the colony in all directions. The colony was traversed by the microprobe at the center line, at several locations progressing toward the edge, and adjacent agar was also probed. Small, medium, and large colonies were selected.

Results and Discussion

First electrical contact with the colony was not reproducible, and an uncertainty of about 5 micrometers exists. Furthermore, the signal from the microelectrode tended to be wildly erratic near the point of first contact. First contact with the agar remote from the colony was also somewhat erratic. While no proof is offered, it is thought that outer cells or a thin film of moisture can draw away from the electrode as a result of electrical stimulation. When advanced a few microns past the point of first electrical contact, the microelectrode delivered a stable signal.

Profiles from typical traverses are in Figure 1. From such profiles, locations of a given oxygen concentration were taken to construct the contour lines for Figure 2. Colonies were assumed to be symmetrical, so only one side was probed. Note that the abscissa changes, and the colonies for Figure 2C and 2D are much larger than those for 2A and 2B. The colonies did not tend to sit exactly on the plane of the agar; this may be error because the precision of positioning the microelectrode is great compared to possible bumps in the agar surface. However, as the shape of the curve for first electrical contact was usually peculiar at the edges of the colony, it is likely that growth and metabolism distort the agar.

No supplemental glucose was in the agar for the colony for Figure 2A. Compared to a colony of similar size on agar plus glucose (Figure 2B), the colony with little demand for oxygen is rich in oxygen throughout. Shape of the colony changes as it grows; height remains fairly constant as the colony spreads. Outer portions of a colony are rich in oxygen, and steep gradients exist toward the agar surface. Oxygen can diffuse through the air interface of the colony or can enter the surrounding agar and diffuse toward the colony as the contours indicate. Glucose is a larger molecule than oxygen and diffuses more slowly. The shape of the contour lines and their steepness near the agar indicate regions of rapid metabolic activity. It should be possible to relate the contours to rate of glucose diffusion through the colony.

This new method for investigating colonial growth and mass transfer can be extended to various organisms and different media.

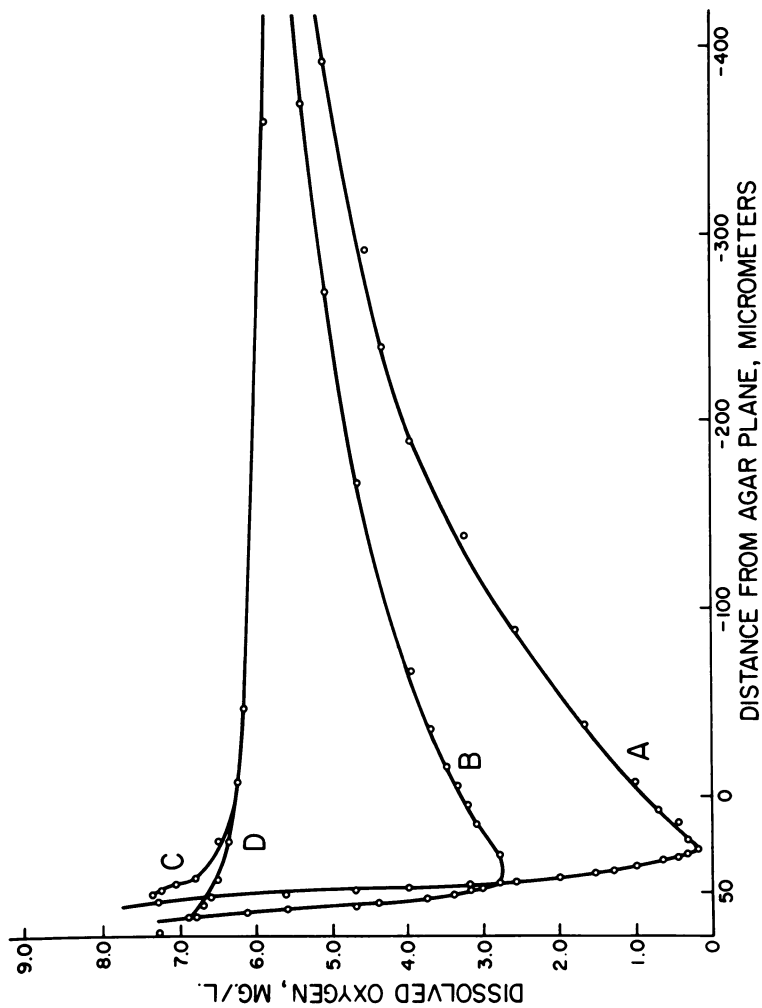


Figure 1. Dissolved oxygen profiles from typical traverses of a microelectrode through a *P. ovalis* colony. Colony diameter, 1.5 mm; 40 mg/L glucose. Key: A, center line of colony; B, 0.5 mm from center; C, 0.75 mm from center; D, 1.0 mm from center.

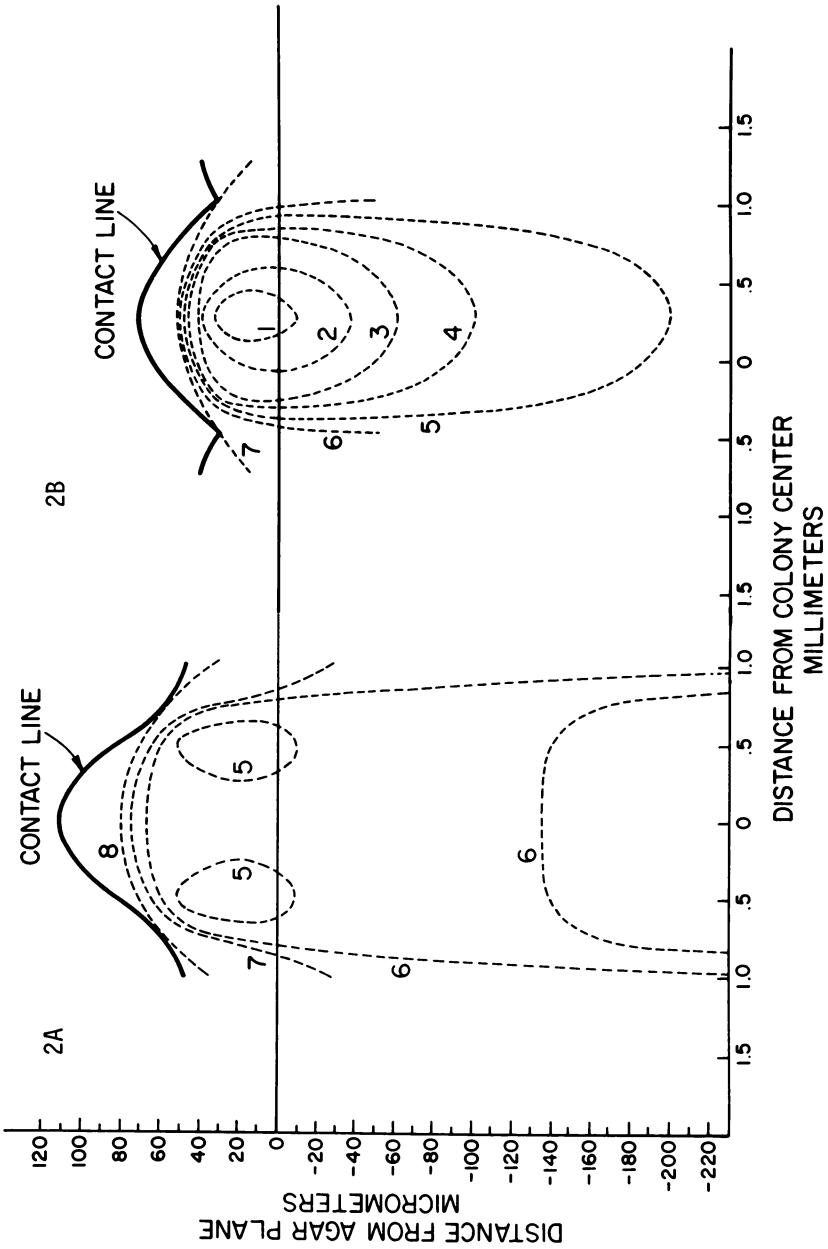


Figure 2A and B. Contours of dissolved oxygen in colonies of *P. ovalis* of different sizes. Note that the colonies are much smaller than those shown in Figures 2C and 2D. Continued on next page.

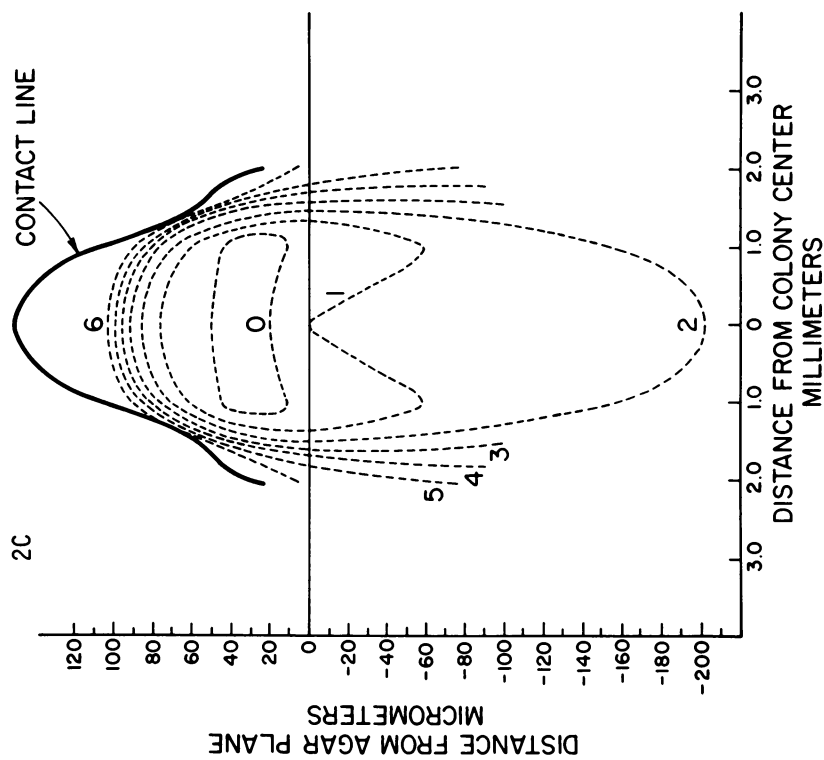


Figure 2C. Contours of dissolved oxygen in a colony of *P. ovalis*. Continued on next page.

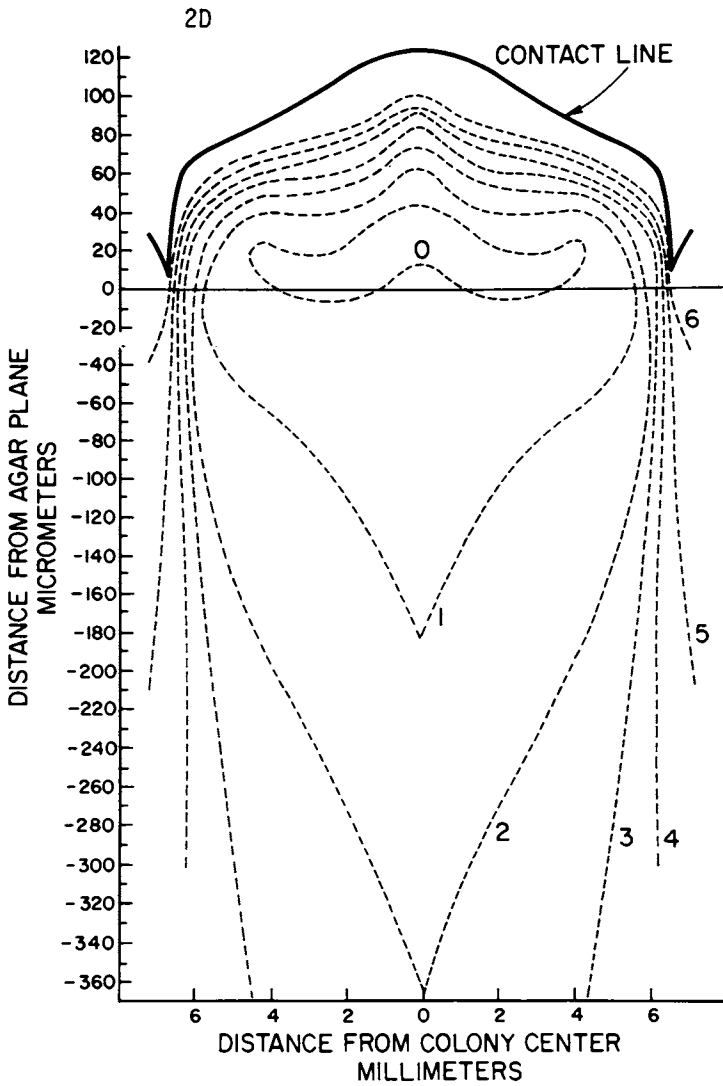


Figure 2D. Contours of dissolved oxygen in a colony of *P. ovalis*.

The release of oxygen from colonies of photosynthetic organism would be particularly interesting. Measurement of dissolved oxygen contours provides new perspectives to the analysis of colonial growth (2). Furthermore, better understanding of mass transfer to colonies has economic value for better operation of processes dependent on attached organisms. For example, trickling filters for biological waste treatment, purification of streams by slimes, and fouling of cooling towers by slimes involve colonial growth.

Acknowledgement

This project was supported by the National Science Foundation through Grant #CPE-7920121.

Literature Cited

1. Whalen, W.J.; Bungay, H.R.; Sanders, W.M. Environ. Sci. Technol. 1969, 3, 1297.
Sanders, W.M.; Bungay, H.R.; Whalen, W.J. AIChE Symp. 107 1971, 69.
Huang, M.Y.; Bungay, H.R. Biotechnol. Bioengr. 1973, 15, 1193.
Bungay, H.R.; Masak, R.D. Biotechnol. Bioengr. 1981, 23, 1155.
Bungay, H.R.; Chen, Y.S. Biotechnol. Bioengr. 1981, 23, 1893.
2. Pirt, S.J. J. Gen. Microbiol. 1967, 47, 181.
Cooper, A.L.; Dean, A.C.R.; Hinshelwood, C. Proc. Royal Soc. 1968, 175, B171.
Palumbo, S.A.; Johnson, M.G.; Rieck, V.T.; Witter, L.D. J. Gen. Microbiol. 1971, 66, 137.

RECEIVED June 1, 1982

Stochastic Growth Patterns Generated by *Phycomyces* Sporangiohores

R. IGOR GAMOW and DAVID E. CLOUGH

University of Colorado, Department of Chemical Engineering, Boulder, CO 80309

The giant aerial sporangiohore of the fungus *Phycomyces blakesleeanus* rotates as it elongates tracing out a left-handed spiral. A number of years ago our laboratory became fascinated with the nature of this spiral growth for it appeared to us that it must accurately reflect the molecular architecture of the growing plant cell wall. Fine structure kinetic analysis of both the rotational and the elongational components of spiral growth revealed what appeared to be random growth irregularities. We now show by using time series analysis that the apparent rotation and elongation irregularities are truly stochastic and, most surprisingly, are not correlated.

During the past 100 years a number of laboratories have studied the growing "antics" of the giant, single-celled sporangiohore of the filamentous fungus, *Phycomyces blakesleeanus*. "Antics" is appropriate here since, in terms of describing the variety of growth patterns that the mature sporangiohore produces, it certainly appears to be the "clown" of the plant world. Even left to its own devices and not subjected to any sensory inputs, it is happy in a dark, damp room at about 22°C; its behavior is still quite extraordinary because of its phenomenal growth rate of three millimeters per hour (50 $\mu\text{m}/\text{min}$) simultaneously coupled with a rotation rate of 12 to 15 degrees per min. Shown on the TV monitor in Figure 1 is the upper part of a mature *Phycomyces* sporangiohore consisting of a cylindrical stalk, about 100 μm in diameter crowned with a spherical spore sack, about 500 μm in diameter.

Biophysicists have long been fascinated with this organism because of its unique sensory apparatus. Both the direction of growth and the rate of growth are quantitatively controlled by a variety of well-defined stimuli: they respond to both the intensity and the direction of either visible or UV light, to a variety of wind gradients, and to touch. The organism elicits complex

0097-6156/83/0207-0403\$06.00/0

© 1983 American Chemical Society



*Figure 1. The video recorder and TV monitor of the video microscope. On the screen of the monitor is shown a mature stage IV/b *Phycomyces sporangioaphore*.*

olfactory responses, it grows away from gravity, and finally, it senses the presence of distant objects and thus avoid growing into them. Details concerning these behaviors have been described in a number of review articles (1-4). The last behavior listed, the avoidance response, appears to be a combination of two independent sensory inputs, olfaction and wind (5, 6). As a result of all these studies concerning the sensory apparatus, more is known about the two-dimensional growth patterns produced by the Phycomyces sporangiophore than any other plant system. It is thus all the more surprising that the detailed fine structure of the spiral growth is only now beginning to be known. In general, the older Phycomyces literature considered spiral growth to be analogous to a rotating screw, i.e. the faster the screw would rotate, the faster it would elongate, and to the first approximation this is true. But detailed fine structure measurements of rotation and elongation rates within the growing zone clearly showed that this analogy is a poor one. Cohen and Delbrück (7) in 1958 first realized that a material section of the growing zone, GZ, is not equivalent to the entire GZ but each section of the GZ is in steady state flux characteristic of that particular section. They also found that the degree of rotation and elongation was not uniformly distributed within the GZ. In 1974 Ortega, Harris and Gamow (8) determined the ratio of rotation to elongation as a function of growing zone position and found that this ratio increased as measurements were taken towards the lower edge of the growing zone.

Most recently, Gamow and Böttger (9), using either high resolution 35 mm photography or a video TV microscope, have found that when the minute-per-minute rotational and elongational growth rates were simultaneously measured, both rates were quite irregular and "appeared" to be random. In addition, it "appeared" that little or no correlation existed between the irregularities in the rotation rate and the elongation rate. In this paper we have treated these growth data, both rotation and elongation, to what is popularly known as time series analysis. We have concluded from these analyses that not only are the measured irregularities in rotation and elongation purely random white noise, but that they are, in addition, not correlated. We would expect that on a microscopic scale, all growth processes would be stochastic, but what is surprising is that the macroscopic growth kinetics of a Phycomyces sporangiophore is also stochastic.

Materials and Methods

Wild-type Phycomyces blakesleeanus sporangiophores, NRRL1555(-), originally obtained from M. Delbrück, were grown in shell vials containing 5.0% potato dextrose agar (PDA) with 1.0% yeast extract. The shell vials were incubated under diffuse incandescent light in a high-humidity room with a temperature range

between 22° and 27°C. Before each experiment the sporangiophores were dark adapted in red light for at least 20 minutes. All experiments were carried out with a water-filtered red light source.

The apparatus used to simultaneously measure minute-by-minute the net rotation and the net elongation of a stage IVb GZ was first described by Cohen and Delbrück (7) and then modified by Gamow and Böttger (9). The mature stage IVb sporangiophore in a glass shell vial was firmly secured to a stage that rotated clockwise once every 60 seconds. To ensure that the GZ of the sporangiophore was vertical (parallel to the axis of rotation of the stage), a double knee was inserted between the stage and the vial. The rotating stage allowed us to measure the angular velocity of any particle situated above, below, or in the GZ. Because the net rotation of a mature stage IVb sporangiophore is in the same direction as the rotating stage (clockwise), a particle either above or in the GZ takes less than 60 seconds to complete one revolution. By determining how much less, we calculated the angular velocity of the particle in respect to the observer. (For instance, if a particle completes one revolution in 58 seconds, we can easily calculate that the entire region below the particle must have a total angular velocity of $12^\circ/58 \text{ sec}$ or $12.4^\circ/\text{min.}$) For our present experiments, we used a glass bead approximately 15 μm in diameter. The bead was placed on the stalk approximately 50 μm below the sporangium; this region of the stalk shows no elongation. The GZ, with the attached glass bead, was observed continuously through a TV video camera attached to a low-powered ($\times 10$ microscope). An electronic timer with a digital printout records the time with a resolution of 10 milliseconds.

Experimental Controls. The rotational velocity of a particle placed just below the GZ was measured in order to determine the rotation measurement error. Velocity measurements of a particle below the GZ make an excellent control since all the parameters are the same except the innate rotation of the GZ itself. We measured the rotation rate for such a particle once every minute for 56 consecutive minutes and determined that the standard deviation was $\pm 1.7^\circ$ per minute (9). The beauty of our rotation-measuring method is that the measurements are virtually insensitive to parallax problems and to the hunting problem mentioned below. Calculating elongational velocities, on the other hand, is beset with numerous difficulties. Although the photographs are not necessary in order to calculate the angular velocities, they are needed in order to measure the elongational velocities. To determine our error for the elongational measurement, an artificial sporangiophore was constructed. The artificial sporangiophore consisted of a straight 0.5 mm diameter wire attached to a motor-driven micrometer screw. A small spur gear on the motor-shaft of a synchronous clock motor (1 rpm) drives a larger spur gear on a metric micrometer head with a gear ratio of 1:8. The

micrometer screw was advancing at 63 $\mu\text{m}/\text{min}$. The artificial *Phyco* was photographed next to a calibrated scale placed in the ocular of the microscope. From a series of minute-per-minute photographs, we determined that the standard deviation of our error was $\pm 1.4 \mu\text{m}$ per min (9). This photographic method is highly dependent on using straight sporangiohores to avoid parallax errors. Perfectly straight-growing sporangiohores are nearly impossible to obtain since they show both fast, 5 to 7.5 min, and slow, 30 to 60 min oscillations; a term used to describe these oscillations is hunting (10). In order to verify that our measurements were not significantly influenced by either a parallax problem or sporangiohore hunting, we placed an additional marker below the growing zone and calculated directly the change in length between the two markers. The data obtained in this manner were no different from data obtained using the calibrated scale with reasonably straight sporangiohores. From a series of photographs taken with a one-minute interval, small bends were seen to occur in the GZ, but since the bend angle between any pair of photographs was less than a degree, the error in terms of bending is negligible. We have determined that hunting causes a bending rate of about 0.5 degree/min, and in a continuous set of measurements lasting for 38 minutes, the bending angle will not vary more than five degrees from the vertical. From a single pair of photographs, we cannot eliminate the possibility that the growing zone is bent directly towards or directly away from the camera, but since we find no significant bends from a large random sample of photographs, we have discounted this possibility.

A TV video camera in conjunction with a TV monitor and video cassette recorder (Figure 1) has an enormous advantage over the conventional 35 mm photography. Firstly, since an entire experiment can be stored on a TV cassette and thus becomes part of a permanent *Phycomyces* library, we can rerun any given experiment, many lasting several hours, at any future date. Secondly, the reliability of measurements is enhanced since replicates may be taken and the taped experiment may be stopped or rewound to check results.

Experimental Results and Stochastic Modeling. Measurements of rotational and elongational growth rates for a typical experiment are shown in Figure 2. The sample interval is one minute, and there are 110 measurements. It certainly appears that both the growth and rotation series are highly irregular in terms of their growth rates. It is difficult to see any systematic behavior and there is little apparent correlation between the two. These qualitative observations must be quantified.

Estimates of the autocorrelation function and the partial autocorrelations for the rotational growth curve in Figure 2 are presented in Figures 3 and 4. The autocorrelation function often depicts dependence of a measurement value on recent previous values whereas the partial autocorrelations show the significance

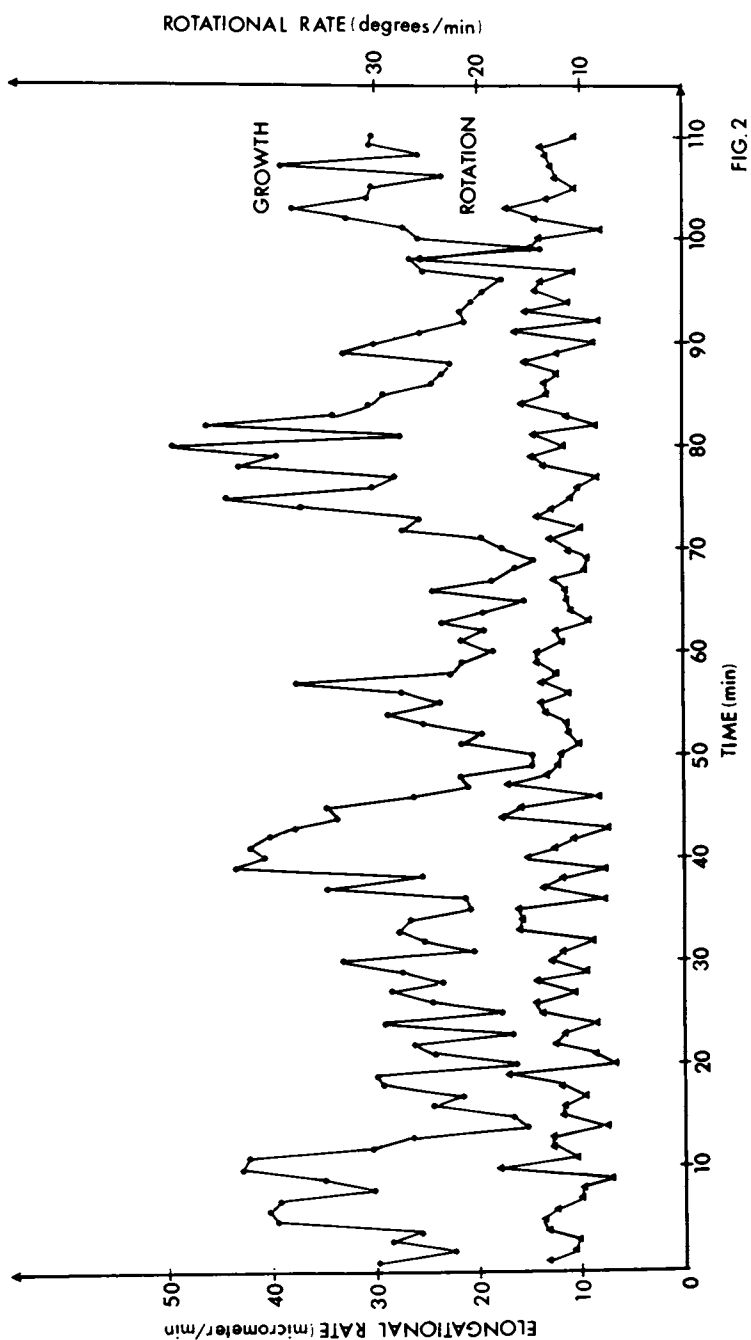


FIG. 2

Figure 2. The simultaneously measured elongation and rotation rates of a mature sporangiophore, plotted as a function of time.

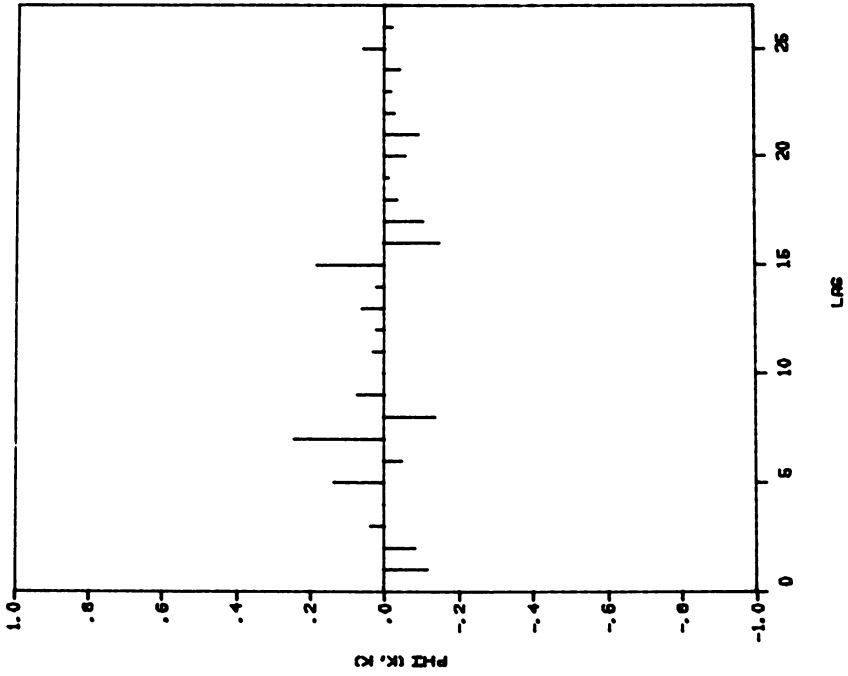


Figure 4. Partial autocorrelation of a rotational growth series.

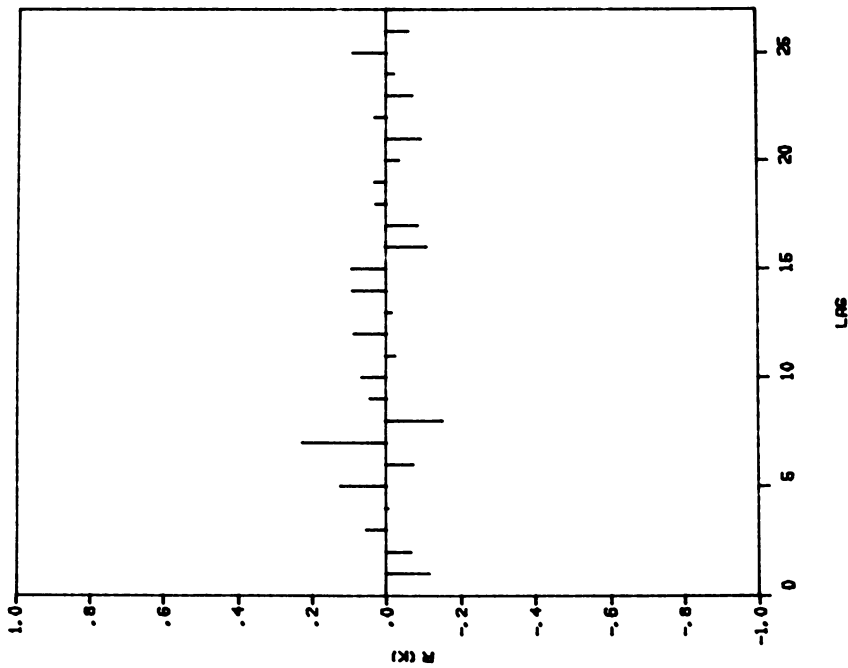


Figure 3. Autocorrelation function of a rotational growth series.

of adding additional terms to an autoregressive model of the series. In Figure 3, there is little significance and no real pattern apparent. Two standard-error limits for this sample size are about ± 0.2 , and only the autocorrelation estimate at lag 7 exceeds these limits. The same observations can be made of Figure 4. The implication is that the variations in rotational growth are "white," that is, random and uncorrelated (with earlier variations). To confirm this, a cumulative periodogram of the frequency spectrum was computed and is presented in Figure 5. Since the solid curve follows the 45°-dashed-line, this proves that the rotational series is essentially white, quantifying the conjecture made in a previous paper (9).

The autocorrelation function and partial autocorrelation for the elongational growth series are presented in Figures 6 and 7. Systematic behavior is evident in the regular pattern of the autocorrelation function and the significance of the partial autocorrelations at lags 1 and 2. This directly suggests that a second-order autoregressive model is appropriate for this series (11). The model form is

$$g_k + a_1 g_{k-1} + a_2 g_{k-2} = e_k$$

where g_i is the i^{th} element of the series,
 a_1, a_2 are model parameters, and
 e_i is the i^{th} model error or residual.

Least squares estimation was applied to this series for the second-order model above, and the following parameter values were determined:

$$\begin{aligned} a_1 &= 0.570 \\ \text{and} \\ a_2 &= 0.412 \end{aligned}$$

Such a model describes an underdamped oscillatory behavior with a sinusoidal period of 11 minutes and damping coefficient of 0.44. This period of oscillation corresponds to the "hunting" swings of the sporangiophore; therefore, it appears that our model accounts for the gross mechanical behavior of Phycomyces and its interaction with our measurement system.

It is possible to remove this systematic behavior from the data and examine local variations in elongational growth rate by studying the residual series of the above model. This residual series was analyzed and found to be essentially white: the cumulative periodogram is presented in Figure 8. This is in contrast to the periodogram of the original elongational series, see Figure 9, which shows significant deviation from the 45° line. We can summarize the analysis of both growth series by stating that local growth behavior exhibited by the sporangiophore is random

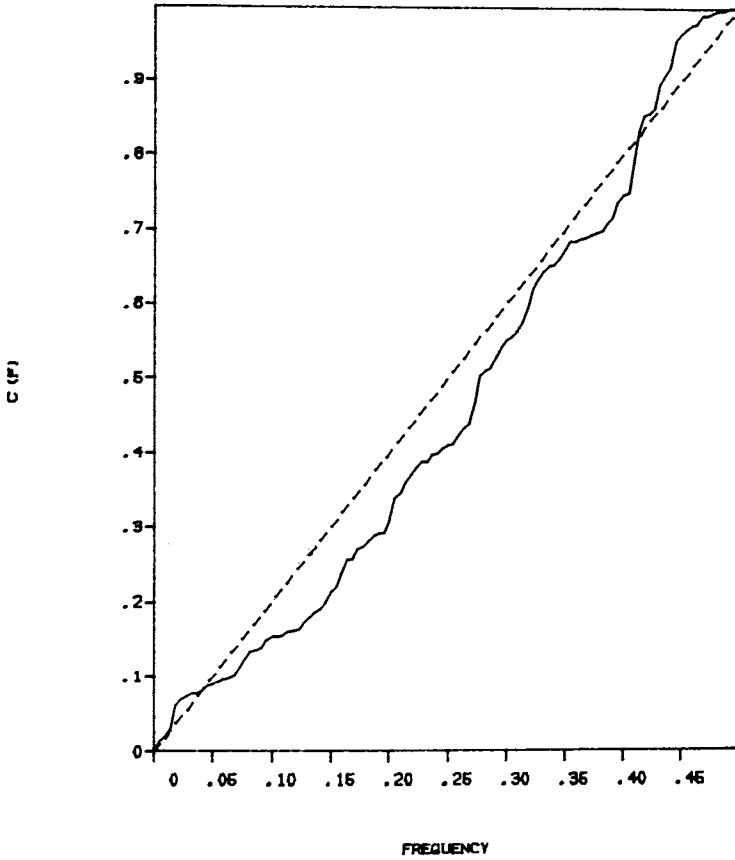


Figure 5. Cumulative periodogram of a rotational growth series.

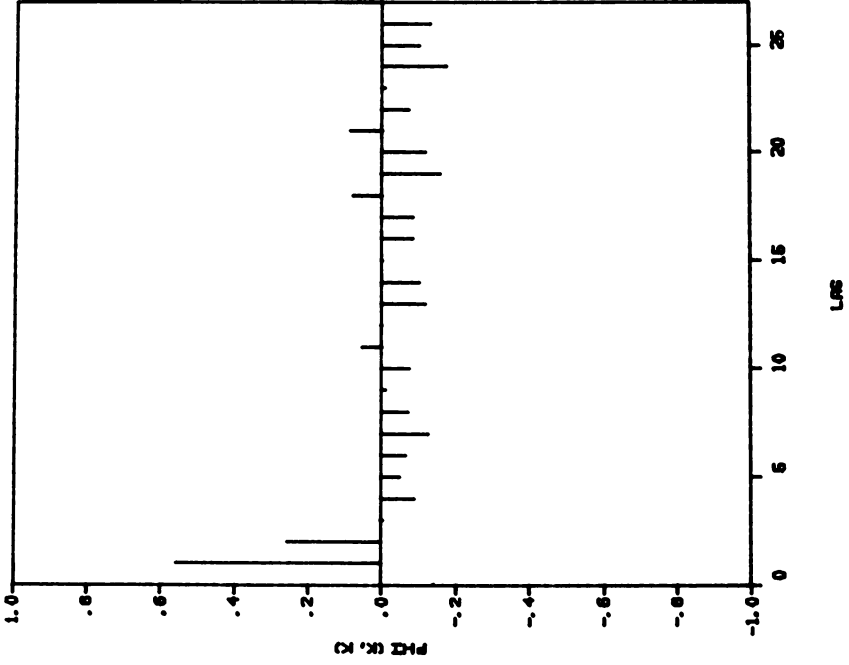


Figure 7. Partial autocorrelation of an elongational growth series.

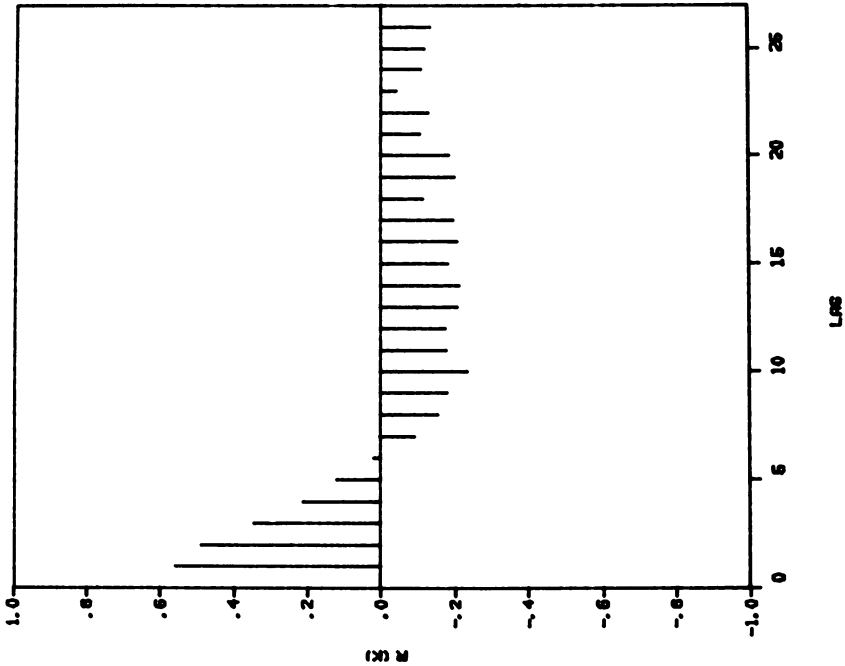


Figure 6. Autocorrelation function of an elongational growth series.

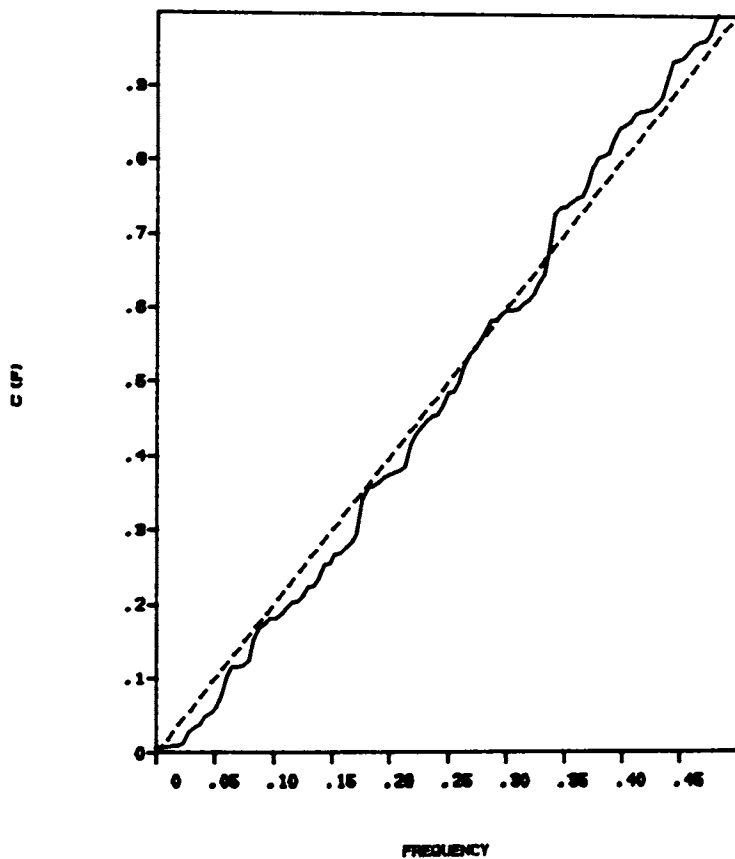


Figure 8. Cumulative periodogram of an elongational residual series.

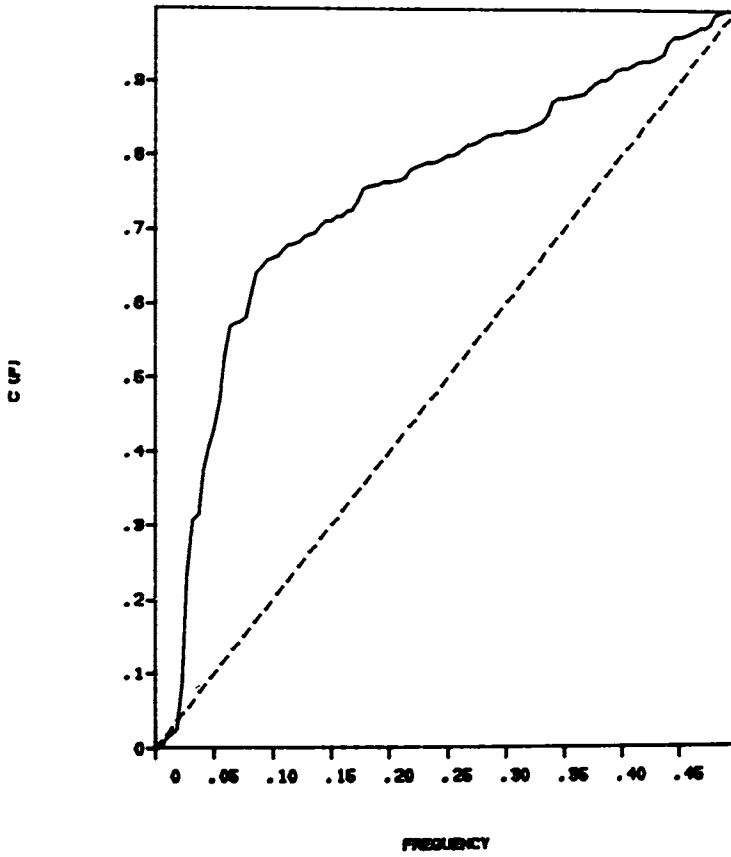


Figure 9. Cumulative periodogram of an elongational growth series.

and uncorrelated when the elongational rate and rotational rate series are studied separately.

It is tempting to relate the noisy growth patterns since similar mechanisms may underlie elongation and rotation. A plot of the cross-correlation function between the rotational series and the elongational residual series is shown in Figure 10. The result is perhaps unexpected, since there is no significant correlation between the two series, that is, the noisy growth patterns appear independent. The limits shown on the figure are for one standard error, and one would expect a significant cross-correlation to exceed two standard errors.

Conclusions

We have shown that stochastic variations in the rotational and elongational growth rates of *Phycomyces* are random and uncorrelated. Systematic behavior in elongational growth was attributed to the slower "hunting" motion of the sporangiophore. The irregular patterns in rotational and elongational growth do not appear to be interdependent nor related to the same major source or stimulus.

Discussion

All organisms that possess a rigid exoskeleton such as the arthropods, insects and crustaceans must have evolved one of many possible strategies in order to increase in size, i.e. to uniformly increase in volume. The arthropods simply molt their old exoskeleton and then redeposit a new one after a short burst of intensive growth. Plants in general, but fungi in particular, have devised a slightly different strategy to enable them to grow even though they are also encased in a rather rigid cell wall. The new synthesized cell wall, termed the primary wall, appears as an end result of giant carbohydrate microfibrils being deposited on the inner surface of the existing primary cell wall. In addition, it has been shown that the longitudinal axis of these newly laid down polymers is perpendicular to the net direction of growth of the cell wall itself. Cell wall thickening resulting from newly deposited microfibrils is constantly being counterbalanced by cell wall extension. The driving mechanism of cell wall extension is the large pressure difference, the cell's turgor pressure, between the inside of the cell wall and its external environment. Because the polymers are laid down perpendicularly to its net direction of growth, during cell wall extension they are passively reoriented towards the cell's longitudinal axes, and in addition, transported toward the outer surface of the cell wall. The model described above is basically known as the multinet theory of cell wall growth first proposed by Roelofsen and Houwink (12) and experimentally verified in *Nitella* by Gertel and Green (13).

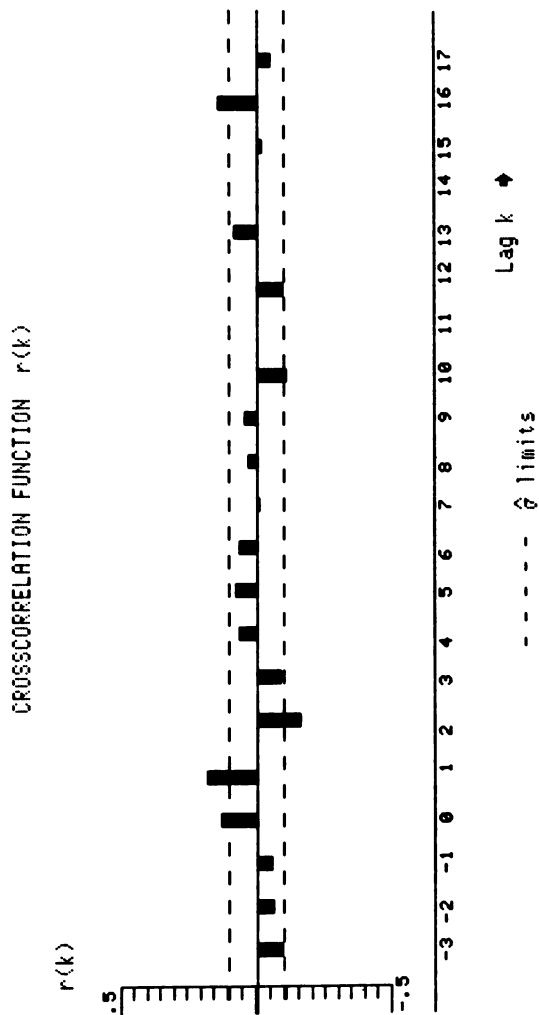


Figure 10. Cross-correlation between local variations in rotational and elongational growth.

Since these newly laid down microfibrils are in constant motion, the primary cell wall behaves much like a visco-elastic fluid. Bartnicki-Garcia (14) in 1970 proposed that the newly synthesized cell wall is in a constant state of flux in terms of synthesis and degradation resulting from the presence of synthesizing and lytic enzymes, respectively. In 1974 Ortega and Gamow (15) proposed that the orientation of microfibrils, or bundles of microfibrils, could account for both cell elongation and cell rotation. They also deduced that the magnitude of the ratio of rotation to elongation must be a function of the microfibril angle, the angle being measured in respect to the longitudinal axis of the growing cell wall. This model predicted that the fibrils located in the lower region of the growing zone, those which would have already maximally reorientated towards the longitudinal axis, would show maximum rotation to elongation ratios, and this prediction was experimentally verified.

Our present results contradict the simple reorientation theory as presented above since it clearly predicts that any irregularity in the growth rate would be directly coupled with an irregularity in the rotation rate. Our present data would be consistent with a reorientation model in which the maximum rotation and elongation occur in different regions of the GZ. Recent fine structure studies in our laboratory have confirmed the 1958 report by Cohen and Delbrück that the maximum elongation rate occurring in the region of the growing zone is distinctly different from that occurring in the region of maximum rotation rate. Our present analysis is consistent with this finding because if both rotation and elongation are stochastic in terms of growth irregularities, we would not expect to find a correlation if the rotation and elongation occurred in different and independent regions of the growing zone.

Lastly, we are intrigued by the sinusoidal behavior, having a period of 11 minutes, in the elongation rate. At this time we have no way of determining whether this oscillation is real in the sense that the net rate of growth oscillates with this period or whether we are observing the well-known hunting behavior (10); *Phycomyces* sporangiohores show both a fast, 5 to 7.5 min, and a slow, 30 to 60 min, oscillation. Our guess would be that the 11-minute period we have observed is a direct result of the measurement error caused by the sporangiohore's hunting behavior. In order to confirm this speculation, we would require faster sampling rates for both elongation and rotational growth. Such an increase in sampling rate would also facilitate more detailed study of the stochastic growth behavior. We believe an extension of our present measurement technique would allow for this. This would be to couple a computer-based pattern recognition system to our microscopic video equipment. By having the computer follow motion of several tracking particles, a high resolution profile of both growth rates is feasible. Such an extension to our present apparatus would require less than \$100,000 in capital funding.

Appendix: A Brief Description of Time Series Analysis

The techniques of time series analysis have been applied across a broad spectrum of fields, notably business and economics, engineering, and meteorology. They have gained wide acceptance partly due to the high yield of modeling information one achieves through the application of a straight-forward, easy-to-use methodology. There are two common scenarios:

- 1) analysis of a single time series, usually a sampled measurement signal, to determine its systematic and random character
- 2) analysis of two or more time series to assess and quantify connective relationships (one must be careful with claims of "cause-and-effect" here--additional information on structure is usually required)

It is desirable, from a practical standpoint, to model time series in as simple a form as possible. Such are linear models with a minimal number of parameters. There are two primary steps to the modeling process: identification of the model form and estimation of the model's parameters. These steps are appropriately followed by testing of the model's ability to fit or predict new data.

It is typical of a single time series that measurements will show some dependence on their recent past history--many processes are inertial in behavior. The autocorrelation function (or its estimate from the series' data) will reveal such dependence, and the partial autocorrelations will help show how far into the past this "autoregressive" model must extend. The model thus selected can be fit to the data by one of many regression techniques, e.g. linear least squares. The residuals, those components of the data which are not explained by the autoregressive model, form another series. If the residual series is uncorrelated (to itself), this indicates a random behavior which we can neither predict nor regulate--we just have to live with it as uncertain behavior. Often, however, it is possible to model the residuals also in a similar, autoregressive manner--which would indicate that although we cannot regulate these quantities, we can do some prediction. This structure of the residual series is usually built back into the original model, and the terminology used for the residual description is "moving average." It is then best to refit the entire model by regression. A general form for the autoregressive-moving average model is

$$g_k + a_1 g_{k-1} + \dots + a_n g_{k-n} = e_k + c_1 e_{k-1} + \dots + c_p e_{k-p}$$

where e_k is now an uncorrelated residual. The above model may appear imposing; however, the appropriate values for n and p are usually less than three.

Connection between two series is manifested in the cross-correlation function (or its estimate). When a cause-and-effect,

"input-output" relationship is justified, a model of the form

$$g_k + a_1 g_{k-1} + \dots + a_n g_{k-n} = b_0 x_{k-d} + b_1 x_{k-d-1} + \dots + b_m x_{k-d-m} + e_k + c_1 e_{k-1} + \dots + c_p e_{k-p}$$

may be proposed which includes the autoregressive dependence of the output variable (g_k), a "cause" dependence on values of the input variable (x_k) and a description of residual (e_k) behavior as before. Selection of model form (which may include a delay of d sample intervals between the input and output variables) is facilitated by study of the cross-correlation function and impulse response function estimates in addition to the autocorrelation function and partial autocorrelations. Once the model form is selected, regression techniques are used to fit the parameters.

Two model-checking methods are common, and they are often applied to a "new" set of data. First, the residuals are analyzed for lack of correlation or "whiteness." White noise has the characteristic that all frequencies contained in it should be present in equal strength. The cumulative periodogram is the integral of a spectrum estimate; therefore, for white noise, it should be the integral of a constant or a linear ramp function. The "whiteness" of the residuals can be analyzed by plotting their cumulative periodogram and observing closeness to the ideal ramp line. Another common diagnostic technique is to determine the statistical efficiency of adding one or two parameters (and terms) to the model. This will check if the minimal parametric model chosen is truly parsimonious. The statistical F-test based on the extra-sum-of-squares principle is useful for this efficiency test.

Literature Cited

1. Bergman, K.; Burke, P. V.; Cerda-Olmedo, E.; David, C. N.; Delbrück, M.; Foster, K. W.; Goodell, E. W.; Heisenberg, M.; Meissner, G.; Zalokar, M.; Dennison, D. S.; Shropshire, W.; Jr. Bacterial Rev. 1969, 33, 97-157.
2. Shropshire, W., Jr. Phys. Rev. 1963, 43, 38-67.
3. Cerda-Olmedo, E. Ann. Rev. Microbiol. 1977, 31, 535-47.
4. Foster, K. W. Ann. Rev. Biophys. Bioeng. 1977, 6, 419-43.
5. Cohen, R. J.; Fried, M. G.; Atkinson, M. M. Biochem. and Biophys. Res. Comm. 1979, 86, 877-84.
6. Gamow, R. I.; Böttger, B. J. Gen. Physiol., in press.
7. Cohen, R.; Delbrück, M. J. Cell Comp. Physiol. 1958, 52, 361-88.
8. Ortega, J. K. E.; Harris, J.; Gamow, R. I. Plant Physiol. 1974, 53, 485-90.
9. Gamow, R. I.; Böttger, B. J. Gen. Physiol. 1981, 77, 65-75.

10. Dennison, D. S. Science 1959, 129, 775-7.
11. Box, G. E. P.; Jenkins, M. "Time Series Analysis: Forecasting and Control"; Revised Edition; Holden-Day: San Francisco, CA, 1976.
12. Roelofsen, P. A.; Houwink, A. L. Acta. Bot. Neerl. 1953, 2, 218-25.
13. Gertel, E. T.; Green, P. B. Plant Physiol. 1977, 60, 247-54.
14. Bartnicki-Barcia, S. In "Phytochemical Phylogeny;" Hasborne, J. B., Ed.; Academic Press, Inc.; New York, NY, 1970; p. 81.
15. Ortega, J. K. E.; Gamow, R. I. J. Theoret. Biol. 1974, 47, 317-32.

RECEIVED June 1, 1982

Growth Characteristics of Microorganisms in Solid State Fermentation for Upgrading of Protein Values of Lignocelluloses and Cellulase Production

D. S. CHAHAL

Devinder Chahal Enterprises, Inc., 312-1800 Baseline Road,
Ottawa, Ontario Canada K2C 3N1

Solid state fermentation (SSF) is considered to require no complex controls, and to have many advantages over liquid state fermentation. Upgrading of protein values of lignocelluloses and cellulase production by SSF holds great promise. Pretreatment of lignocelluloses with alkali or steam is necessary to break lignin and carbohydrate bonds for successful growth of microorganisms in SSF. Filamentous fungi seem to be the most suitable organisms for SSF. Fungal hyphae can penetrate into plant cell lumina through pits, cracks, or by boring holes through the cell wall. Once inside the cell lumen, the fungus utilizes the cell wall from inside. It is postulated that sequence of synthesis of cellulases in the fungal hyphal tip is triggered by physical signals sent by cellulose. Finally, the substrate is completely utilized to produce fungal biomass rich in protein and/or cellulases, depending on the microorganism.

"Solid State Fermentation" (SSF) is defined as a process whereby an insoluble substrate is fermented with sufficient moisture, but without free water. In the liquid state or slurry state fermentation, on the other hand, the substrate is solubilized or suspended as fine particles in a large volume of water. In most liquid state fermentations (LSF) or submerged fermentations substrate concentrations ranging from 0.5 to 5% are used. Now, in a number of fermentations the concentration of the substrate has gone up to 10% to increase the productivity per unit time.

Solid state fermentation is considered to require no complex controls and to have many advantages over the LSF (1). The SSF for upgrading the protein values of lignocelluloses, (agricultural, forestry and animal wastes) is becoming a focus of activity for some researchers (2,3,3a,4). Recently it has been calculated (5) that high cellulase activity per unit volume of fermentation broth is the most important factor in obtaining sugar

0097-6156/83/0207-0421\$06.50/0

© 1983 American Chemical Society

concentrations of 20-30% from hydrolysis of cellulose in a process for ethanol production from cellulosic materials. It has also been confirmed (6) that cellulase activity per unit volume can be increased by increasing the cellulose concentration in the medium. But it is not possible to handle more than 6% cellulose in conventional fermenter because of rheological problems. In order, therefore, to increase the cellulose concentration higher than 6%, SSF seems to be the most attractive alternative (5). Toyama (7) has already shown that sugar syrup of 22% concentration can be obtained by hydrolyzing delignified rice straw or bagasse with the concentrated cellulases obtained by Trichoderma reesei in SSF. Recently, interest in the production of amylases and cellulases by SSF is increasing because a great demand of these enzymes is envisaged in the near future. These enzymes are required to convert starch and cellulose into glucose for further fermentation into ethanol to alleviate the shortage of liquid fuel in the world (5). But the survey of such literature indicated that very little is known about the growth characteristics and behavior of microorganisms in SSF.

Origin of Solid State Fermentation

The origin of SSF is lost in the mist of antiquity when relationship of microorganism were established with their host (animals or plants; living or dead). In nature microorganisms grow in close association with solid substrates to obtain their nutrition saprophytically or parasitically. One of the earliest records of SSF traced out by Chang (8) was the cultivation of paddy straw mushroom, Volvariella volvacea, in the Canton region of China's Kwangtung province during the Chow Dynasty, about 3000 years ago. However, until 20 years ago, almost no scientific research has been done on this species. The other early record of SSF was growing of "Shiitake" (Lentinus edodes) by the Chinese and Japanese on wood logs about 20 centuries ago (9). The spores are inoculated in wood logs and are left to incubate for many months before the mushrooms are harvested for eating. Agaricus campestris (A. bisporus), a commonly cultivated mushroom in Europe and Western countries, has been grown in caves in France since the time of Louis XIV (1683-1715) (10). Of great historical relevance to modern technology is the Japanese "Koji" process, i.e. growing of Aspergillus oryzae on rice (or other cereals) in solid state. Production of "Koji" has been in practice in Japan at least since the eighth century for production of Saké - the most traditional alcoholic drink in Japan. The Koji process was introduced to the Western World by Takamine in 1891 for the production of fungal diastase on a large scale (11). The Koji process is now being exploited for the production of amylases and cellulases (7,12).

Another early solid state fermentation was the discovery of gallic acid production in gall nuts piled in a heap and moistened with water. It was van Teigham (1867) who first established that Aspergillus niger was responsible for this fermentation (9).

The records for the production of Roquefort cheese from sheep's milk in caves of Southern France go back about a thousand years. It was established by Thom (13) that the special characteristics of Roquefort cheese was due to the growth of a fungus, Penicillium roqueforti. This organism grows deep into cheese blocks under limited O_2 supply - a perfect example of solid state fermentation. The special flavour of Camembert cheese is due to the growth of Penicillium camemberti on the surface of cheese blocks.

Nature of the Substrate

The SSF can only be applied to insoluble substrates like cereal grains, oil seeds, and lignocelluloses (agricultural crop residues and forestry wastes). The cereal grains and oil seeds are composed of easily available form of carbohydrates (starches), proteins, minerals, etc. Thus a wide variety of microorganisms are able to grow on these substrates in SSF. However, mild pretreatments are still required to make them suitable substrates. Cereals like rice grains are used as such without any treatment whereas wheat grains require pearling before use. During this process the surface of wheat grains is abraded to provide suitable sites for colonization by the microorganisms. In case of corn and soybean the grains are broken into five or six pieces to provide suitable surface for the growth of the microorganisms, as the hard seed coats are very difficult for many microorganisms to colonize. Oats have to be dehulled for better growth. All these grains are very suitable for the production of aflatoxins and various fermented oriental foods (1).

The most serious problem encountered in SSF of grains, especially rice, is that the substrates become sticky and form compact masses in which movement of air is restricted. The grains also agglomerate into compact masses due to fungal growth on their surfaces. Therefore, timely and proper agitation is required to break such agglomerates and provide better aeration.

Production of aflatoxins and fermented oriental foods on grains is much easier than the use of lignocelluloses. The carbohydrates of lignocelluloses are not easily available and drastic pretreatments are required. Moreover, lignocelluloses are also not as rich in proteins and other nutrients as are grains. Lignocelluloses are very complex substrates and are composed of three major components: hemicelluloses, cellulose, and lignin. Only a few microorganisms, like white-rot fungi (Polyporus versicolor), are able to grow on such materials (14). The white-rot fungi have complete enzyme systems to utilize all three components. Similarly, it has been shown that Pleurotus ostreatus (15) and Stropharia rugosoannulata (4) can utilize all three components of wheat straw. On the other hand, many microorganisms cannot utilize hemicelluloses; of those that can, most are unable to metabolize cellulose.

Lignin in the plant cell wall not only encrusts the cellulose microfibrils in a sheath-like manner, but is bonded physically and chemically to the plant polysaccharides (16). Lignin-carbohydrate bonds form metabolic blocks that greatly limit the action of microbial hemicellulases and cellulases. Physically, lignin forms a barrier suppressing the penetration by polysaccharide-digesting enzymes (17). Unless the lignin is depolymerized, solubilized, or removed, the cellulose and the hemicelluloses cannot be metabolized by most microorganisms. As mentioned earlier, only white-rot and brown-rot fungi (Basidiomycetes) are able to utilize carbohydrates from lignocelluloses but they are very slow growing (4,14,15,18,19). Therefore, these fungi are not very promising, from the economic point of view as candidates to ferment lignocelluloses for the production of animal feed or cellulases. The case is similar with other basidiomycetes especially mushrooms. Agaricus bisporus, Lentinus edodes, Volvariella volvacea, and Pleurotus ostreatus take a long time (1-2 months) to produce fruiting bodies (mushrooms). Mushroom growing, however, is justified because of their economic value as food delicacies.

Pretreatment of Lignocelluloses

Pretreatment of lignocelluloses is the first requirement for the growth of the microorganisms which are unable to grow on the untreated substrate but which, otherwise, grow rapidly and make certain products i.e. Trichoderma reesei for cellulases; and Chaetomium cellulolyticum for single-cell protein (SCP) production. Pretreatments that increase the digestibility of lignocelluloses for production of SCP and cellulases have been discussed in detail by various workers (20,21,22). Only those pretreatments which could make the substrate most suitable for SSF are discussed very briefly below:

Grinding/Ball-Milling. Grinding/ball-milling of lignocelluloses to a very small particle size results in the exposure of more surface area for the growth of microorganisms and also reduces crystallinity (23). The main problem in using fine powder of lignocellulose for SSF is to supply good aeration, as the moist fine powder of lignocellulose would form a compact mass by its own weight. Improper aeration will reduce the growth of the organism considerably. Frequent agitation and forced aeration may be necessary to keep up the growth of the organism.

Alkali. Sodium hydroxide and aqueous ammonia cause extensive swelling and separation of structural elements, and lead to the formation of cellulose II whose X-ray pattern differs considerably that of from cellulose I. Five to six grams of sodium hydroxide per 100 grams of wood seem to be necessary for the maximum effect (24,25). This level of alkali is essentially equivalent to the combined acetyl and carbonyl contents of wood. This leads to the

postulate that the main consequence of alkali treatment is the saponification of intermolecular ester bonds, thus promoting the swelling of wood beyond water-swollen dimensions and favouring increase enzymatic and microbiological penetration into the cell-wall fine structure (22). Both sodium hydroxide and ammonia treatments proved to be very useful in increasing the in vitro digestibility of lignocelluloses (21) as well as their utilization as carbon source for SCP production in SSF (26). These pretreatments also retain the fibrous structure of cellulose. The fibrous structure is very conducive for the growth of the organisms because of easy penetration of enzymes, fungal hyphae and air in the substrate.

Steam. Steam treatment of lignocelluloses under high pressure (27-30) is now becoming an important pretreatment to make the substrate easily accessible to hydrolytic enzymes (31-33). The substrate is also sterilized, and changed into a fibrous form. A fibrous substrate is better than the powdered form for SSF.

The chemical changes in steam-treated wood depend on the temperature, pressure, and time of exposure to steam. Hemicelluloses are hydrolyzed to soluble sugars by organic acids, mainly acetic acid derived from acetylated polysaccharides present in wood (28). Under more drastic conditions, secondary reactions occur which result in the formation of furfural, hydroxymethyl furfural, and their precursors by dehydration of pentoses and hexoses, respectively. It has been reported (34) that phenolic-like compounds increased from 0.43 to 5.3% in steam-pretreated bagasse. Since phenolic-like compounds and furfurals are usually toxic to most microorganisms (35,36), such treated lignocelluloses may not be good substrates for SSF, because the toxic compounds are in a concentrated form when the substrate is in moist form. Therefore, washing out of the toxic compounds from steam-treated substrates will be necessary before using them for SSF. Toxic compounds, on the other hand, are diluted with water in slurry state fermentation and have little effect on the growth of microorganisms. There was no adverse effect of these toxic compounds on *T. reesei* for cellulase production in slurry of 4% steam treated wood (32).

Sodium Chlorite (NaClO_2). Sodium chlorite, a strong oxidizing agent, has been used for removing lignin during the preparation of "Holocellulose", the total carbohydrate portion of lignocellulose (37). Georing and Van Seot (38) demonstrated that in vitro digestibility of straws is increased with NaClO_2 treatment. Chahal et al. (39) reported that protein productivity increased considerably on NaClO_2 - delignified wheat straw fermented with *Cochliobolus specifier*. This treatment, by removing lignin, exposes the surface of hemicelluloses and cellulose for enzymatic attack and also creates capillaries in the substrate cell wall for deep penetration of enzymes and hyphae. However, this process of delignification is not economically attractive because of the high cost of chemicals involved (38). Sodium

chlorite treated substrate, on the other hand, is composed of hemicelluloses and cellulose, which would be a good substrate for the production of hemicellulases (especially xylanases) and cellulases simultaneously in monoculture or mixed culture. There is a great future for such an enzyme system (mixture of hemicellulases and cellulases) for the complete hydrolysis of lignocelluloses into monomer sugars.

Choice of Microorganism

In nature, bacteria grow best only when in a liquid phase, or at least when the nutrients are in free water. Likewise, single-celled fungi, the yeasts, grow well when the nutrients are in a soluble form. Such microorganisms may not be able to grow successfully in SSF where substrate carbon is not available in soluble form. A limited success in converting lignocellulosic materials into animal feed by using bacteria (Cellulomonas sp., Alcaligenes faecalis) or yeasts (Aureobasidium pullulans and Candida utilis) has been reported in semi-solid state fermentation (3, 3a). Low protein yields in the final product might be attributed to the fact that in such system the unicellular organisms (bacteria and yeasts) were unable to penetrate deep into the tissue for complete utilization of the substrate.

Streptomycetes have not been tried for SSF so far but Hesseltine (1) has reported that he has seen a preparation in which Streptomyces aureofaciens was grown on millet seeds, to be used in swine feed mixes in the U.S.S.R.

On the other hand, filamentous fungi typically grow in nature on solid substrates, such as, wood, seeds, stems, roots and leaves of plants, without the presence of free water (1). High protein contents of 20-24% in the finished product have been recorded by Chahal et al. (2) in SSF of corn stover with Chaetomium cellulolyticum. High protein content in the final product has been attributed to the fact that the hyphae of C. cellulolyticum have the power to penetrate deep into the intercellular and intracellular spaces for better utilization of the substrate (40). Most filamentous fungi have such intrusion power. Aist (41) has given a good review of the penetration of fungal hyphal tips into plant cell walls. He concluded that the mechanism of fungal penetration into substrates could be mechanical and/or enzymatic. It is, therefore, evident that the choice of the microorganisms for successful SSF is limited to filamentous organisms - fungi and actinomycetes.

Mechanism of Fungal Growth During Solid State Fermentation

Fungal hyphae are septate, tubular, uniseriate filaments, on average 10-15 μm in diameter. The growth in length occurs at the tip and is confined to this area, so that in septate hyphae when a cell is cut off from the apex it is no longer capable of any

significant increase in length. There is thus no increase in interseptal distances, although there may be increases in diameter and wall thickness. The older portion of the hypha disintegrates, whereas the apex continues to grow into new sites in the substrate. Autoradiographs made of hyphae which have been fed with brief pulses of tritiated wall precursors demonstrated that incorporation is highest in the apical 1 μm and falls off rapidly after the first 5 μm , however, there is still appreciable incorporation from 5-75 μm behind the tip (42).

Hyphal walls are usually two layered with an inner layer of microfibrillar materials, usually chitin or cellulose, or both and an outer layer of amorphous glucan. The chitin is composed of β -1, 4 linked N-acetyl glucosamine residues and cellulose is composed of β -1,4 linked glucose units. The glucans of the outer layers of cell walls are composed of highly branched β -1, 3 linked glucan with β -1, 6 linked branches. These compounds give rigid cell walls to the hyphae. The rigid nature of the wall behind the apex and the complex system of branching ensure that the older rearward part of the hypha is firmly anchored in the substrate and enable the hyphal tip to exert very considerable forward mechanical pressure as it extends under turgor (42). Coupled with the production of extracellular enzymes and the much branched hyphal system, the fungi can thus completely permeate even the hardest substrate.

Fungal Growth in Solid Substrate in Nature. In nature, according to the study of Cowling (43), fungal growth on solid substrate can be of three general types exhibited by wood-inhabiting fungi:

Wood-Staining Fungi. These fungi are of two types:

- (a) surface molds, such as, Trichoderma lignorum, that develop on the external surface of the substrate; and
- (b) penetrating fungi, Ceratocystis spp. that develop deep within wood, most conspicuously in ray parenchyma. These fungi just grow on reserve food and do not affect the strength of the substrate cell walls. They merely produce stains in wood due to the presence of pigments in their hyphae.

Soft-Rot Fungi. These fungi attack the exposed surfaces of wood and wood products that are more or less constantly saturated with water. These fungi are confined to cylindrical cavities created by themselves within the secondary walls of wood cells. Bailey and Vestal (44) reported for the first time that the soft-rot fungi attack the wood parallel to the orientation of cellulose molecules in the secondary walls of the cell. Similarly, spiral cracking along the angle of the fibrils of cellulose in the secondary wall of Douglas fir wood cells caused by Fomes pini was observed by Proctor (45). Soft-rot fungi such as Chaetomium spp. and Xylaria spp. are a little more aggressive than wood-stain fungi, in that they are able to penetrate deeper into the substrate, but they remain restricted along the

orientation of the cellulose fibrils. They are unable to cause complete decay of the affected tissue because of their poor cellulase systems.

Typical Wood-Destroying Fungi. Two groups of these fungi are distinguished on the basis of color and texture of the decayed wood: white-rot fungi, such as Polyporus versicolor, produce light colored wood mainly because of the utilization of lignin along with polysaccharides, while brown-rot fungi, such as, Poria monticola, produce brown colored wood mainly because of utilization of polysaccharides although some lignin is also degraded.

Both white- and brown-rot fungi inhabit the wood cell lumina and penetrate from one cell to another, either through natural openings, such as pits, or directly by boring a hole. Proctor (45) reported that the fungal hyphae penetrate the wood cell wall by an enzymatic mechanism rather than by mechanical force but Aist (41) supported the idea that the penetration of fungal hyphal tips into plant cell wall could be a mechanical and/or enzymatic mechanism. The bore-holes are formed because of the close contact of surface of hyphal tip against wood cell wall surface. The cellulase system produced at the tip is able to solubilize wood cell wall fibers, thereby making room for further penetration by the hyphal tip. This process continues till the hyphal tip enters into the next cell lumen. The fungal attack goes on from one cell to the other till the whole tissue is decayed.

The highly localized nature of the dissolution involved in the formation of these bore-holes by the white-rot fungus, Polyporus versicolor, is illustrated in Figure 1 (43). The hyphae responsible for formation of the holes are autolyzed as soon as the tip of the hypha reaches the lumen where it gets more suitable conditions for further development. That could be the main reason why the dissolution of wood cell wall remains restricted to a size a little bigger than the diameter of penetrating hypha. Where the hypha stays for long time, dissolution beyond the bore-hole is noticed, as shown in Figure 2 (43). The remnants of hyphae are also seen in the bore-hole. Figure 2 shows that dissolution extends more longitudinally than transversally. This indicates that it is easier for the cellulase system to move along the orientation of the fibres in the cell wall. Figure 2 also shows more dissolution on the extreme left and extreme right sides of cell walls, the surfaces of the lumina of two adjacent cells. This dissolution is due to the cellulase system produced by the hyphae growing in the cell lumina. The development of hyphae within the wood cell lumen shown in Figure 3 (46) also shows dissolution of secondary wall along the hyphae forming erosion troughs, which indicates that initial dissolution of cellulose occurs very close to the surface of fungal hyphae. A similar type of growth behavior (penetration of hyphae through cell wall, via pores of tracheids and ray cells) was also shown by another wood-inhabiting fungus, Phanerochaete chrysosporium (47).

It is clear from these observations (43,45,46) that the most active cellulase system is produced on the surface of the fungal hypha which is able to produce a bore-hole when it is penetrating the cell wall transversely and where the enzyme system has restricted movement, and produces erosion troughs initially along the hyphae when attacking the inner surface of the cell lumen. But in the latter situation the enzyme system is able to penetrate quickly and deeply along the orientation of fibrils in the secondary walls, ahead of the hyphal surface and to cause considerable decay. The tangential section in Figure 4 shows almost complete dissolution of secondary walls of the two adjacent fiber trachied cells, leaving behind only the middle lamella, which are resistant to cellulase system, being highly lignified (43). The fungal hypha in cross section is also seen on the right side of the Figure 4. Figure 4 clearly indicates that it is easier for the organism to utilize the cell wall starting from the inside surface of the cell lumen towards the outside, the middle lamella.

It is inferred from the growth behavior of the typical wood-inhabiting fungi that the most active cellulase system was produced on the surface of fungal hypha when it was in close contact with cellulose. The cellulase system produced under such conditions was able to hydrolyze native cellulose with high crystallinity, on the other hand the enzyme system produced by T. reesei in LSF was not very effective in hydrolyzing cellulose until the crystallinity was reduced by various physical or chemical pretreatments as indicated in the recent evaluation of enzymatic hydrolysis of cellulose (5). In LSF the fungal hyphae and cellulose particles do not remain in close contact with each other for long time due to high agitation in the conventional fermenter. That might be the reason that enzyme produced in LSF is not so effective for hydrolysis of crystalline cellulose. It is, therefore, likely that cellulase system produced in SSF will not only have high cellulase activity per unit of fermentatbn broth (5), but will also be most active in hydrolyzing the crystalline cellulose.

Observations on the Fungal Growth in Solid State Fermentation. Fungal growth in solid state fermentatbn of sodium hydroxide-treated corn stover has been reported by Chahal et al. (40) in detail. They have reported that Chaetomium cellulolyticum proved to be the best organism for upgrading the protein values of corn stover for animal feeding. The organism grew profusely on corn stover within five days. Visual examination indicated that the mycelium impregnated the entire substrate.

Microscopic examination of the substrate particles showed that cells of the substrate tissue were loosely held together and tended to separate easily when pressed. It indicated that sodium hydroxide treatment solubilized lignin and weakened the bonds of adjacent cells. Figure 5 shows broken ends of cells on the sides

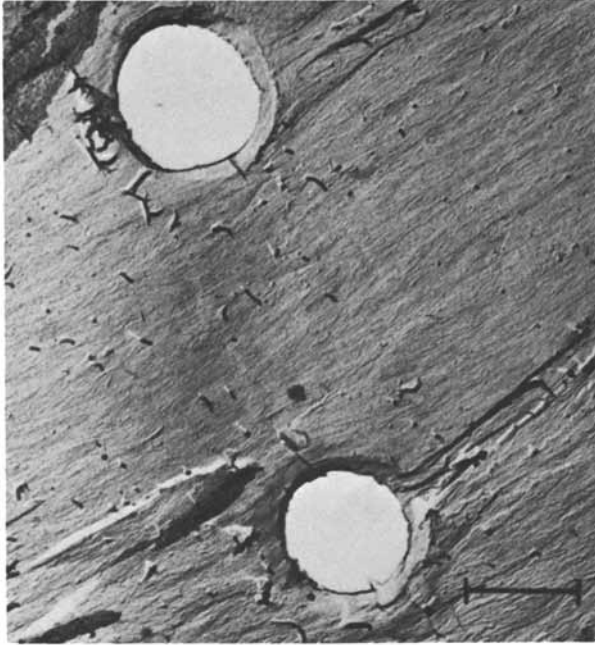


Figure 1. Bore holes in spruce tracheid made by the hyphae of white rot fungus *Polyporus versicolor* ($\times 20,250$). Reproduced, with permission, from Ref. 43. Copyright 1965, Syracuse University Press.

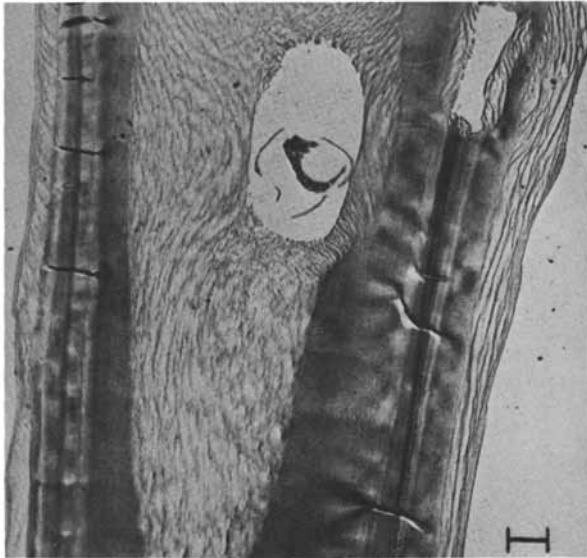


Figure 2. Advanced stage of decay around bore hole and inner side of secondary wall of two fiber tracheids of sweetgum sapwood, $\times 2700$. Reproduced, with permission, from Ref. 43. Copyright 1965, Syracuse University Press.

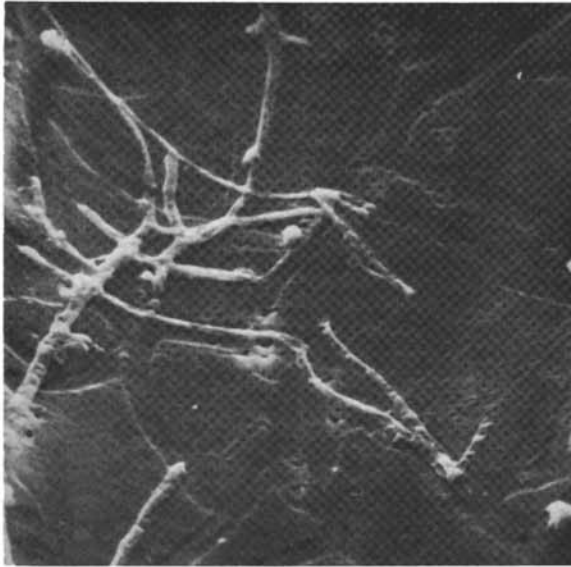


Figure 3. Trough formed by decaying of secondary wall of birch vessels in the vicinity of the fungal hyphae of Polystictus versicolor. Reproduced, with permission, from Ref. 46.

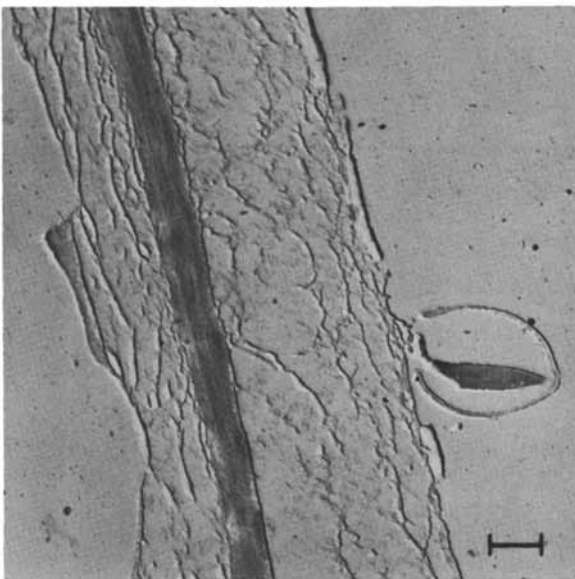


Figure 4. Almost complete utilization of secondary walls of two adjacent cells leaving middle lamella intact. Reproduced, with permission, from Ref. 43. Copyright 1965, Syracuse University Press.

as well as on the ends of the substrate particle. Such broken and exposed cells were the first sites to be attacked by the organism. Figure 6 shows mycelial growth on such broken exposed cells on the lateral side of the substrate particle.

When such substrate particles, colonized by the organism, were pressed slightly under a cover slip, they disintegrated easily. The disintegrated material contained some substrate cells showing penetration by hyphae and development of mycelial growth in the cell lumina at various stages. In Figure 7 penetration of a single hypha into the lumen of a thin longitudinal fiber cell is clearly seen. As soon as the hypha establishes itself in the lumen a thick mycelial mass is developed within the cell (Figure 8). It was concluded from these observations that the hyphae of C. cellulolyticum entered into the cell lumen through natural openings, mechanical breaks, or spaces (created by solubilization of hemicelluloses and lignin during sodium hydroxide-treatment) in the cell wall of the substrate tissue. Once inside the cell lumen, the hypha digested the cell wall starting from the inside towards the outside. Ultimately, the cell collapsed leaving behind mycelial biomass rich in protein. Reese (48) has also reported that in attacking cotton, many fungi penetrated through the fiber wall into the lumen and did most of their digesting from within (Figure 9). Similarly Bravery (46) has reported the growth of Polystictus versicolor in the wood cell lumen and has shown that digestion of the cell is initiated from inside to outside (Figure 3).

Postulated Mechanism of Fungal Growth in Solid State

Microorganisms may possess the potential ability to perform many metabolic activities which are not obligatory for the maintenance of cellular function and which come into play only under certain special environmental conditions. Such activities are typically concerned with energy-yielding metabolism (49). Liberation of hydrolytic enzymes is an active function of living fungal cells (50). During growth on cellulose, enzymes are liberated, chiefly at the hyphal tip. They diffuse to the substrate and digest it. The hydrolysis products enter into the fungus cytoplasm. The hypha then grows into the digested region and maintains continual intimate contact with the substrate (48).

Whether cellulases are adaptive or constitutive enzymes has not been resolved so far. It has been reported that T. reesei can produce cellulases in the presence of inducers such as cellobiose, sophorose, cellulose (51,52,53). On the other hand, recently a small quantity of cellulase production has been reported by hypercellulase mutants of T. reesei while growing in glucose medium under normal growth conditions (54, 55). There is evidence (48) that glucose is not a true inducer but is metabolized to an inducer, probably a β -glucoside. It appears that the β -1, 4 glucosidic linkage must be present in soluble compounds that act

as inducers of cellulase. But in nature when the fungal tip makes its contact with cellulose for the first time, no such solutes (inducers) are available to trigger the synthesis of cellulase within the cell. It is known (49) that the enzymatic machinery for the performance of these facultative metabolic activities is usually synthesized by cells only in response to a specific chemical signal from the environment. Cellulose, being insoluble, cannot enter into the cell to send any chemical signals for the synthesis of cellulases. Under such conditions (in the absence of soluble inducers), it is plausible that a mere physical contact of cellulose with the fungal hyphal tip is enough to send some sort of physical (instead of chemical) signals through the wall of the fungal cell to the nucleus to synthesize specific RNA to produce the required inducer (probably a β -glucoside) as mentioned earlier (48). It has also been pointed out earlier that a close contact between cellulose and the organism is necessary to trigger cellulase synthesis (56,57). As early as 1960, it was pointed out by Mandels and Reese (52) that soluble products of enzyme action are natural inducers of the enzymes that attack insoluble substrates. On this theory they assumed that small amounts of inducible enzymes (cellulases) are produced even in the absence of inducer (cellobiose). When the insoluble substrate (cellulose) is present, it is hydrolyzed and the soluble products (especially cellobiose) thus enter the cell and induce more enzymes (cellulases). The above assumption also supports the postulate that a mere physical contact of the organism with cellulose may be responsible to trigger the synthesis of cellulases.

The postulated mechanism of metabolism of cellulose by a complete cellulase complex produced at the tip of the fungal hypha is based on the observation recorded by various workers (40-50,52,56,57,58). The mechanism given in Figure 10 is explained as follows:

1. Plausibly physical signals are transmitted from cellulose to the fungal cell nucleus to trigger the synthesis of the first enzyme (E_1), which causes splitting of fibrils and microfibrils from the crystalline portion of cellulose fiber. The action of E_1 here is the same as explained by Reese (48) for C_1 . The C_1 is still a controversial enzyme and is confused with exo-1,4- β -D-glucan cellobiohydrolase. The most important role of C_1 to split glucose polymer chains from crystalline cellulose proposed in 1950 (59) is still retained here as well as by Reese (60). Therefore, there is every possibility that close contact of cellulose and the organism is most important to produce $C_1(E_1)$ enzyme, if not, for other components of cellulases (exo- and endo-gluconases).
2. Subsequent synthesis of the second enzyme (E_2) is triggered. E_2 is composed of three components: (1) Endo 1, 4- β -D-glucan glucohydrolase (endo-gluconase) with random attack on

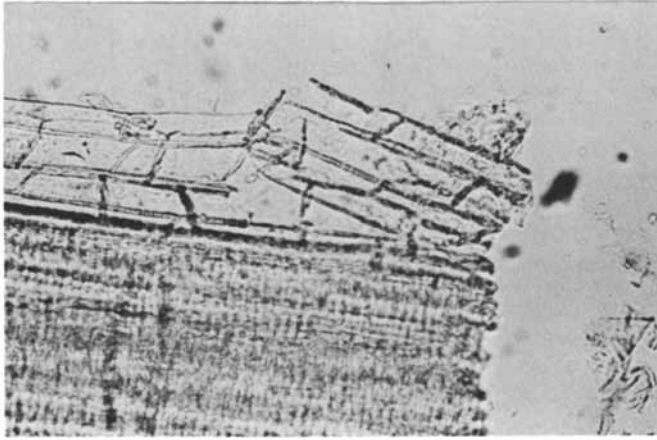


*Figure 5. Growth of *Chaetomium cellulolyticum* in NaOH-treated corn stover. Substrate particles showing broken cells, first sites for attack by the organism ($\times 94.5$). From Ref. 40.*

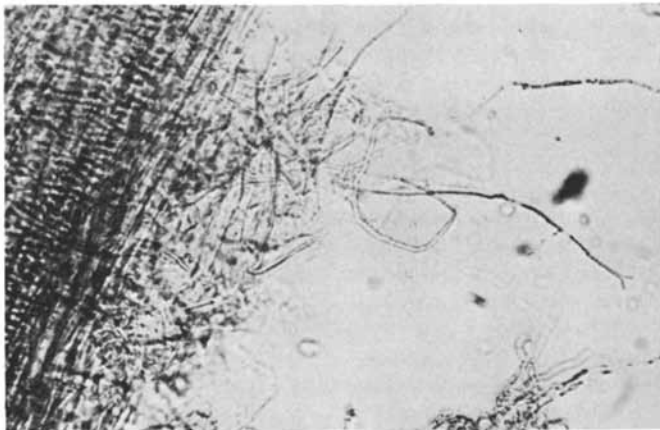


Figure 6. Hyphal growth on sites like those shown in Figure 5. From Ref. 40.

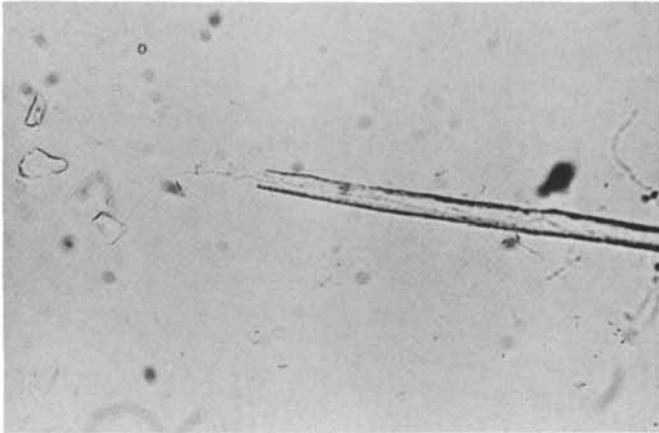


Figure 7. Penetration by a single hyphae into cell lumen through the broken end ($\times 94.5$). From Ref. 40.

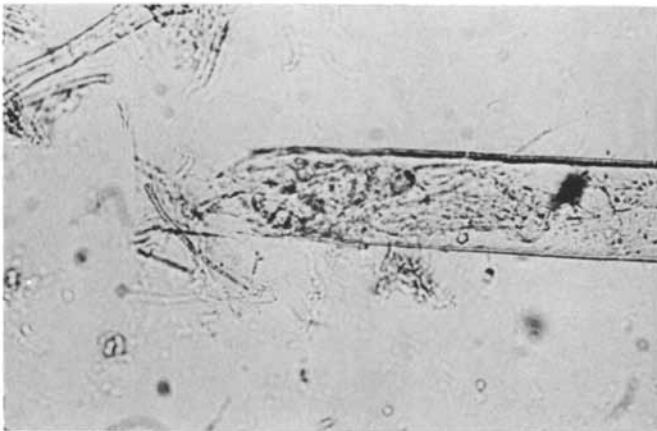


Figure 8. Mycelial biomass developed in the cell lumen ($\times 94.5$). From Ref. 40.

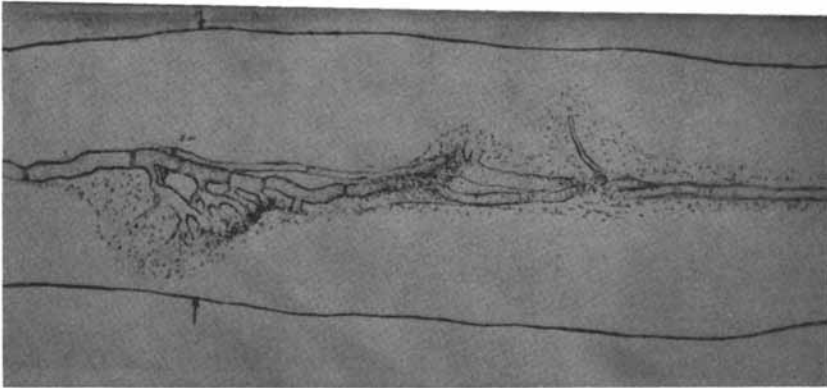


Figure 9. Memnoniella echinata in the lumen of cotton fiber showing utilization of secondary wall from inside towards outside. Reproduced, with permission, from Ref. 49. Copyright 1959, University of Washington Press.

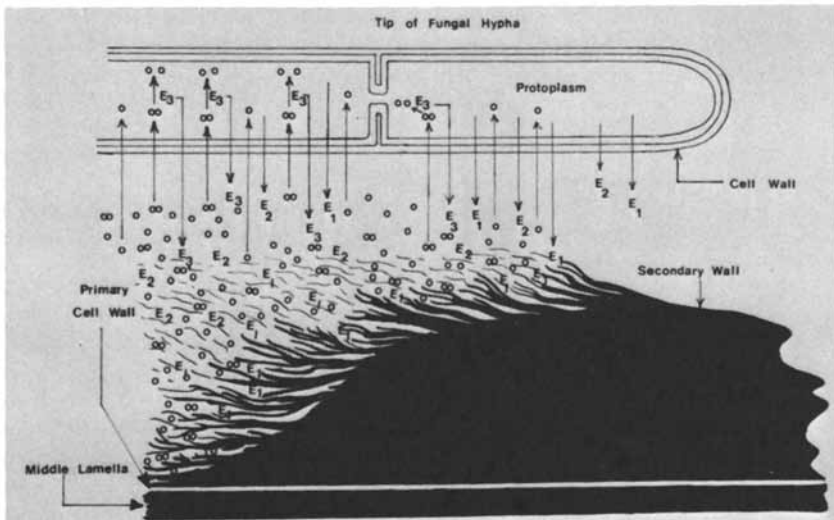


Figure 10. Utilization of secondary wall from the inside of the lumen of wood cell, as explained in the text.

glucose polymer chains to break it into smaller chains (oligomers). Some glucose units are also released during this reaction. (ii) Exo-1, 4- β -D-glucan glucohydrolase (exo-glucanase) removes glucose units from the non-reducing end of glucose polymer chains. (iii) Exo-1,4- β -D-glucan cellobiohydrolase (exo-glucanase) removes cellobiose from non-reducing ends of glucose polymer chains. This compound enzyme E_2 releases a mixture of oligomers, cellobiose and glucose. The sequence of synthesis of these three components of E_2 is another controversial point in cellulase system.

3. Cellobiose is absorbed by the fungal cells where it triggers the synthesis of the third enzyme, β -glucosidase (E_3) to break cellobiose into glucose units. The E_3 is an intracellular enzyme but a small quantity is also secreted outside of the fungal cell. Large quantities of E_3 are usually released by the older cells or after the autolysis of the older cells. Thus E_3 hydrolyzes cellobiose into glucose units inside as well as outside the fungal cells.

Finally some of the glucose released from cellulose is catabolized to release energy needed for various metabolic processes and some is metabolized to synthesize fungal biomass, extracellular cellulases and β -glucosidase. The final product may be a fungal biomass rich in protein (to be used as SCP) as in the case of C. cellulolyticum or it may be very little biomass with more extracellular cellulases (to be used for hydrolysis of cellulosic materials into glucose) as in the case of T. reesei.

Physiological Aspects

Temperature. During SSF the temperature in the substrate rises due to heat generated by metabolism. The rise in temperature is directly related to the depth of the substrate and the metabolic activities of the organisms. It has been recorded (61) that during composting of straw for mushroom growing, the temperature of the outer layer of the compost heap (one meter high) is around 37°C, while in the inner portion the temperature rises as high as 60-77°C. On the other hand, in the innermost region the temperature reaches only 32-49°C because of low microbial activity, due to anaerobic conditions in that region.

Edwards (62) had reported that one Kg (dry weight) of organic matter (cellulose) when consumed by microorganism produced 0.597 Kg of water, 1.465 Kg of CO₂ and 14,960 BTU. Some of the heat (about 59%) is used to evaporate water produced during the metabolic activity while the remaining (41%) is left in the substrate to be dissipated. This amount of energy, if not dissipated immediately, as it is released, will reduce the productivity or may kill the organism.

Aeration. Aeration has the following functions in SSF:

- (i) To supply O_2 for aerobic metabolism.
- (ii) To control the temperature.
- (iii) To remove CO_2 , water vapours, and volatile metabolites produced during metabolism.

The problem of aeration will increase correspondingly with the increase in the thickness of the substrate layer. Proper aeration in the SSF also depends on the air spaces available in the substrate. Fibrous materials can provide more air spaces than finely powdered substrate. Aeration seems to be a very critical requirement. Ochratoxin production by Aspergillus ochraceus in a rotating drum fermenter stopped when the air flow rate was greater than 0.1 liter/Kg/minute(63). In contrast, the increase in air flow rate through a column of corn inoculated with Aspergillus flavus increased the rate of production of aflatoxin (64-65). Similarly it was reported that β -galactosidase and invertase production by Aspergillus niger on wheat bran was increased considerably when the aeration was increased.

Moisture. In nature, vegetables and fruits contain about 60-80% moisture. This much moisture is sufficient to encourage the growth of microorganisms (66,67). But Christensen (68) reported that Eurotium halophilicum can grow on wheat grains at 13-14% moisture. Morton and Eggins (69) have also reported that some fungi like Absidia corymbifera, Fusarium solani and Chaetomium trilaterale can grow and penetrate in wood at a 14% moisture level at 35°C.

Growth of soft-rot fungi in situations of extreme dryness has been recorded by Duncun and Esllyn (70). A basidiomycete, Serpula lacrymans is well known to colonize dry timber in buildings causing the conditions known as "dry rot". This is achieved by the fungus initiating growth in timber with a high water content and then using the energy and nutrients gained to produce rhizomorphs which can explore dry timber many meters away from the initial colony. Though such rhizomorphs can transport water, further water is produced at the site of action by the utilization of the timber with the evolution of CO_2 (71).

Various levels of moisture in SSF have been reported for different products. About 75% moisture in straw was used for SCP production (2,3,3a) whereas for aflatoxin production it was 33.3% in rice and 48.4% in straw (1). Thus moisture level in the SSF depends on the nature of the substrate, organism and the type of end product.

pH. Most fungi are able to grow in a wide pH range of 5-8. Adjustment of pH during the growth in SSF is very difficult. Some of the substrate (straws, grains) have good buffering capacity and there may not be any need to adjust the pH during SSF. But maintenance of pH around 4.5 is very crucial for cellulase production with T. reesei (5).

Osmotic Pressure. Raising the osmotic potential of a material by addition of salt or sugar or both to a level higher than that occurring in the cytoplasm is a well tried method of

microbial inhibition and is widely used in preservation of foods, such as meats and fruits. Sugar concentrations in the regions of 50-70% are usually adequate; salt is added to 20-25% level (71). However, there are some osmophilic and halophilic organisms (Saccharomyces rouxii, S. mellis and Aspergillus glaucus series) which can grow in concentrated sugar solutions (71). High concentrations of salts (nutrients) are used in SSF for SCP production from straw (2). Therefore, the microorganisms capable of withstanding high osmotic pressure will be more suitable under such conditions, otherwise, the required nutrients are to be added in frequent small doses to avoid high osmotic potential in the substrate.

Characteristics of an Organism for SCP and Cellulase Production

Production of SCP and cellulases in SSF on a large scale will depend on the thorough understanding of growth characteristics and behavior of SCP and cellulase producing organisms under such conditions before the application of biochemical engineering to scale up the processes. The organism for successful SSF should have the following primary qualities:

1. It is able to utilize mixtures of various polysaccharides.
2. It should have complete enzyme systems to switch over its metabolism from one polysaccharide to another polysaccharide (found in complex substrates) without any lag phase.
3. It is able to penetrate deep into the thick layer of the substrate as well as into the cells of the substrate.
4. It is able to grow in high concentrations of nutrients.
5. It grows in a vegetative form and does not sporulate during the fermentation time.
6. It should be fast growing to avoid chances of contamination by other fast-growing organisms.
7. It is able to grow in low moisture content of the substrate.
8. It is able to grow in the presence of phenolic and toxic compounds produced during the pretreatment of the substrate.

Acknowledgement

The author is very grateful to Dr. D.J. Kushner, professor of Microbiology, University of Ottawa, Ottawa, Ontario, Canada for his invaluable suggestions and for editing the manuscript.

Literature Cited

1. Hesseltine, C.W. Biotechnol. Bioeng. 1972, 14, 517-532.
2. Chahal, D.S.; Vlach, D.; Moo-Young, M. in: "Advances in Biotechnology", Vol. II, General Editor M. Moo-Young, pp. 327-332, 1981. Pergamon Press, Toronto.
3. Han, Y.W.; Anderson, A.W. Appl. Microbiol. 1975, 30, 930-934.

- 3a. Yu, P.L.; Han, Y.W.; and Anderson, A.W. Proc. West. Sec. American Soc. Animal Sci. 1976, 27, 189-191.
4. Zadrazil, F. European J. Appl. Microbiol. 1977, 4, 273-281.
5. Chahal, D.S. "Enzymatic Hydrolysis of Cellulose - State-of-the Art". N.R.C. Canada, Report. 1982, pp. 101.
6. Nystrom, J.M. and DiLuca, P.H. Proc. of Bioconversion Symp. I.I.T., New Delhi, 1977, 293-304.
7. Toyama, N. Biotechnol. Bioeng. Symp. No. 6, 1976, 207-219.
8. Chang, S.T. "The Chinese Mushroom". The Chinese University of Hong Kong, Shatin, N.T. 1972.
9. Miall, L.M. in "The Filamentous Fungi" vol. 1, ed. Smith, J.E.; Berry, D.R. Edward Arnold. 1975; 104-121.
10. Hayes, W.A.; Nair, N.G. in "The Filamentous Fungi"; vol. 1, ed. Smith, J.E.; Berry, D.R. Edward Arnold. 1975; 212-248.
11. Takamine, J.J. Indust. Eng. Chem. 1914, 6, 824-828.
12. Wood, B.J.B.; Min, Y.F. in "The Filamentous Fungi"; vol. 1, ed. Smith, J.E.; Berry, D.R. Edward Arnold. 1975; 265-280.
13. Thom, C. "The Penicillia" Pailliere, Tindal & Cox, London, 1930.
14. Cochrane, V.W. "Physiology of Fungi" John Wiley and Sons, Inc. New-York. 1958; p. 524.
15. Detroy, R.W.; Lindenfelser, L.A.; St. Julian Jr., G.; Orton, W.L. Biotechnol. Bioeng. Symp. No. 10. 1980, 135-148.
16. Higuchi, T. Adv. Enzymology. 1971, 34, 207-277.
17. Kirk, T.; Haskin, J.M. ACS Symp. Ser. 69, 1973, 124-126.
18. Chahal, D.S.; Gray, W.D. in "Biodeterioration of Materials - Microbiological and Allied Aspects". eds. Walter, A.H.; Elphic, J.S. Elsevier Publ. Co. Barking, Essex, England. 1968, p. 584-593.
19. Kuhlman, E.G. Canadian J. Botany, 1970, 48, 1787-1793.
20. Chahal, D.S. in "Advances in Agricultural Microbiology" ed. Subba Rao, N.S. Oxford and IBH Publ. Co., New Delhi 1982 (in Press).
21. Millett, M.A.; Baker, A.J.; Sattar, L.D. Biotechnol. Bioeng. Symp. No. 6 1976, 125-153.
22. Tarkow, H.; Feist, W.D. Adv. Chem. Ser. 95, 1969, 197-218.
23. Fan, L.T.; Lee, Y.-H.; Beardmore, D.H. Biotechnol. Bioeng. 1980, 22, 177-199.
24. Fiest, W.C.; Baker, A.J.; Tarkow, H. J. Animal Sci., 1970, 30, 832-835.
25. Millett, M.A.; Baker, A.J.; Fiest, W.C.; Mellenberger, R.W.; Sattar, L.D. J. Animal Sci., 1970, 31, 781-788.
26. Chahal, D.S.; Moo-Young, M. Develop. Indust. Microbiol. 1981, 22, 143-159.
27. Bender, R. U.S. Patent No. 4, 136, 207, 1979.
28. Casebier, R.L.; Hamilton, J.K.; Hergert, H.L. Tappi, 1969, 52, (12) 2369-2377.
29. Lora, J.H.; Wayman, M., Tappi, 1978, 61, (6) 47-50.
30. Noble, G. "Final Report submitted to U.S. Dept. Energy, Fuels from Biomass Program", Iotech Corporation Ltd. Ottawa,

- Ont. Canada. 1980, p. 356.
31. Alcohol Fuels Process R/D Newsletter, U.S. Dept. Energy, SERI, Winter 1980.
 32. Chahal, D.S., McGuire, S., Pikor, H., and Noble, G., in "Symposium: Fuel and Chemicals from Biomass", ACS Annual Meeting, 1981.
 33. Wayman, M., Lora, J.H., and Gulbinas, E. 1979, ACS Symp. Series 90, "Chemistry for Energy", 183-201.
 34. Campbell, C.M.; Wayman, O.; Stanley, R.W.; Kazmstra, L.D.; Oldrich, S.E.; Hoa, E.B.; Nakayama, T.; Kohler, G.O.; Walker, H.G.; Graham, R.; Proc. West. Sec. American Soc. Animal Sci. 1973, 24, 173-184.
 35. Harris, E.E.; Hajny, G.J.; Hannan, M.; Rogers, S.C. Indust. Eng. Chem. 1946, 38, 896-904.
 36. Leonard, R.H.; Hajny, G.J. Indust. Eng. Chem. 1945, 37, 390-395.
 37. Green, J.W. "Methods Carbohydrate Chemistry", 1963, 3, 9-20.
 38. Georing, H.K.; Van Soet, P.J. J. Dairy Sci. 1968, 51, 974 (Abstract).
 39. Chahal, D.S.; Moo-Young, M.; Dhillon, G.S. Canadian J. Microbiol. 1979, 25, 793-797.
 40. Chahal, D.S.; Moo-Young, M.; Valach. Mycologia. 1982, (communicated).
 41. Aist, J.R. in "Physiological Plant Pathology" eds. Heitefuss, R.; Williams, P.H. Springer-Verlag, New York, 1976.
 42. Hudson, H.J. "Fungal Saprophytism". Edward Arnold Publishers Ltd. London. 1980 p. 76.
 43. Cowling, E.B. in "Cellular Ultrastructure of Woody Plant" ed. Cote Jr. W.A. Syracuse University Press. 1965, p. 181-189.
 44. Baily, I.W.; Vestal, M.R. J. Arnold Arboretum, 1937, 18, 196-205.
 45. Proctor, P., Jr. "Penetration of the Walls of Wood Cells by the Hyphae of Wood-destroying Fungi". Yale University, School of Forestry Bull. No. 47. 1941, pp. 31.
 46. Bravery, A.F. in "Biological Transformation of Wood by Microorganisms" ed. Liese, W. Springer-Verlag, New York, 1975, p. 129-142.
 47. Eriksson, K.-E. and Vallander, L. in "Lignin Biodegradation: Microbiology, Chemistry, and Potential Applications". vol. II pp. 213-224. Eds. T.K. Kirk, T. Higuchi, H. Chang. CRC Press, Inc., Boca Raton, Florida, 1980.
 48. Reese, E.T. in "Marine Boring and Fouling Organisms" ed. Ray, D.L. University of Washington Press, Seattle, Washington, 1959, p. 265-300.
 49. Stanier, R.Y.; Doudoroff, M.; Adelberg, F.A. "The Microbial World". Printice-Hall, Inc. 1970.
 50. Mandels, G.R. J. Bacteriol., 1956, 71, 684-688.
 51. Mandels, M. and Reese, E.T. J. Bacteriol., 1957, 73, 269-278.

52. Mandels, M. and Reese, E.J. J. Bacteriol. 1960, 79, 816-826.
53. Mandels, M. and Reese, E.T. J. Bacteriol. 1962, 83, 400-408.
54. Chahal, D.S., McGuire, S., Pikor, H., and Noble, G. Biomass. 1982. In press.
55. Shoemaker, S.P., Raymond, J.C., and Brunch, R. in "Trends in the Biology of Fermentations for Fuels and Chemicals". Plenum Press, New York. 1981. In press.
56. Berg, B. and Hofsten, A. J. Appl. Bacteriol. 1976, 35, 201.
57. Rautela, G.S. and Cowling, E.B. Appl. Microbiol. 1966, 14, 892.
58. Chahal, D.S.; Overend, R.P. In "Advances in Agricultural Microbiology" ed. Subba Bao, N.S. 1982, Oxford and IBH Publ. Co. New Delhi (in press).
59. Reese, E.T., Siu, S.G.H., and Levison, H.S., 1950, 59, 485.
60. Reese, E.T. 1976, Biotechnol. Bioeng. Symp. No. 6, 9-20.
61. Hayes, W.A. In "Composting" ed. Hayes, W.A. The Mushroom Growers' Association. 1977, 1-20.
62. Edwards, R.L. In "Composting" ed. Hayes, W.A. The Mushroom Growers' Association. 1977, 32-36.
63. Lindenfelser, L.A.; Ciegler, A. Appl. Microbiol. 1975, 29, 323.
64. Silman, R.W., Conway, H.C.; Anderson, R.A.; Bagley, F.B. Biotechnol. Bioeng. 1979, 21, 1799.
65. Silman, R.W. Biotechnol. Bioeng. 1980, 22, 411-420.
66. De Groot, R.C. Economic Botany, 1972, 26, (1) 85-89.
67. Liska, J.A. Unasyuva. 1971, 25, (2-4), 71-79.
68. Christensen, C.M.; Papavizas, G.C.; Benjamin, C.R. Mycologia, 1959, 51, 636-640.
69. Morton, L.H.G.; Eggins, H.O.W. Material und Organismen. 1976, 11, (4). 279-294.
70. Duncan, C.G.; Eslyn, W.E. Mycologia, 1966, 58, 642-645.
71. Eggins, H.O.W.; Allsopp, D. In "The Filamentous Fungi" vol. 1. ed. Smith, J.F.; Berry, D.R. Edward Arnold, 19 p. 301-319.

RECEIVED June 1, 1982

Molecular Size Distribution of Starch During Enzymatic Hydrolysis

J. E. ROLLINGS¹, M. R. OKOS, and G. T. TSAO

Purdue University, West Lafayette, IN 47907

An appropriate means of determining the molecular size and molecular size distribution of starch during hydrolysis is via aqueous size exclusion chromatography. This method employs a strong alkaline mobile phase and porous stationary gel supports which are stable to the basic solutions. The separation range of molecular sizes is extended to span from 2×10^7 to 5×10^2 hydrodynamic volume (dl/mole) by coupling size exclusion chromatographic columns in a manner that will maintain both linearity in molecular size separation with elution volume and high separation efficiency.

This method is used to establish that molecular size distribution, reaction extent and reaction rate strongly depend upon the crystalline state of the substrate and the activity of the enzyme. The susceptibility of starch to hydrolysis by α -amylase is closely related to the crystalline states of the substrate. Starch crystals are present both in the natural granule structure and in retrograded starch. Due to thermal deactivation, the highest overall conversion achieved for a given amount of enzyme is obtained at temperatures below the upper limits of the gelatinization range of starch. The initial rate of the reaction is greatest at temperatures above the gelatinization range.

From these results, a plausible physical model of starch structure during hydrolysis is presented. The model states that various crystalline states of the constituent starch molecules are present throughout the course of degradation. These crystalline states are associated with the natural state of the

¹ Current address: Worcester Polytechnic Institute, Worcester, MA 01609

starch granule as well as with recrystallized states caused by retrogradation. In order to properly describe enzymatic starch liquefaction, these crystalline states must be accounted for.

Recently, much attention has been given to the production of liquid sweeteners as an alternative to cane sugar using inexpensive starch-containing natural materials as the primary feed stock. This situation exists in the United States as this country is not self sufficient in the production of cane, but must rely heavily on importation mainly from South America and the Caribbean. The main source of starch in the United States comes from corn (*Zea mays*) and the liquid sweetener commercially produced from this material is called high fructose corn syrup (HFCS). The current method of production of HFCS is via wet milling which exploits the physical properties of the whole corn constituents (oil, starch, gluten, and fiber) for their separation coupled with enzymatic hydrolysis of the starch fraction to monosaccharides.

The majority of reported research articles have dealt with low molecular weight starch conversion reactions such as glucose isomerization and "limit" dextranization (1-4). Only a few reports have dealt with enzymatic hydrolysis of high molecular weight starch (5-8) in spite of the obvious importance of this step of the process; starch liquefaction. A number of technical difficulties have prevented quantitative monitoring of changes in the molecular properties of starch undergoing hydrolysis. Bulk chemical or physical measurements will not reveal the essential changes occurring during starch liquefaction or provide sufficient information for modeling the operation. Recently, a size exclusion chromatographic (SEC) apparatus has been described which is capable of providing the required information (9,10). It is the aim of this report to demonstrate that aqueous SEC can be employed to study enzymatic starch liquefaction and provide a clear picture of the physical and chemical events occurring during this important depolymerization process.

Experimental

Purified corn starch prepared by wet milling was obtained from Sigma Chemical Company, St. Louis, MO (lot no. 68C-0244) and used as substrate. A commercial grade, endo-acting α -amylase used to hydrolyse the starch substrate was a gift of Novo Laboratories, Wilton, CT (Thermamyl-high temperature stable enzyme). A stock enzyme solution was prepared by diluting the commercial grade liquid enzyme (1:19) with 0.01 M acetate buffer pH 6.0 and stored at 40°C. This enzyme solution was used for the hydrolysis experiments as described below. All chemicals used in this study were reagent grade or better.

The reactor used for starch hydrolysis was a standard two liter Ace Glassware, four-port batch reactor. The central port was used to house the agitator shaft in a jacketed column. The agitator was powered by a variable speed motor operating at 140 rpm. The three side ports were used to house the internal thermistor, a NBS thermometer, and a teflon plug for the sampling port. The reactor was thermostated both internally and externally in a well-mixed oil bath. This thermostated system was found to achieve a desired temperature within three hours and to maintain the temperature within $\pm 0.3^\circ\text{C}$ continuously thereafter. A schematic representation of the apparatus is shown in Figure 1.

Starch hydrolysate samples were extracted from the batch reactor at timed intervals and assayed by either traditional end group analysis as described previously (11) or by SEC. The SEC apparatus used in these studies is shown in Figure 2. No single chromatographic resin column is capable of resolving more than two and one half decades in molecular weight for random coil polymers (12). During liquefaction, starch molecules range in molecular size from approximately 10^8 dl/g to approximately 10^2 dl/g (9). In order to extend the molecular size range and thereby obtain a maximal amount of molecular information from each experiment, a two-column SEC system was developed which is capable of separating 4.5 - 5.0 decades in molecular size for water soluble polymers (10). This system consists of a 25.6 cm long Sepharose CL-6B column coupled with a 17.85 cm long Sepharose CL-2B column. Each column was 8 mm in inside diameter. The chromatographic resins packed in these columns were fractionated by a wet sieving technique to obtain beads of

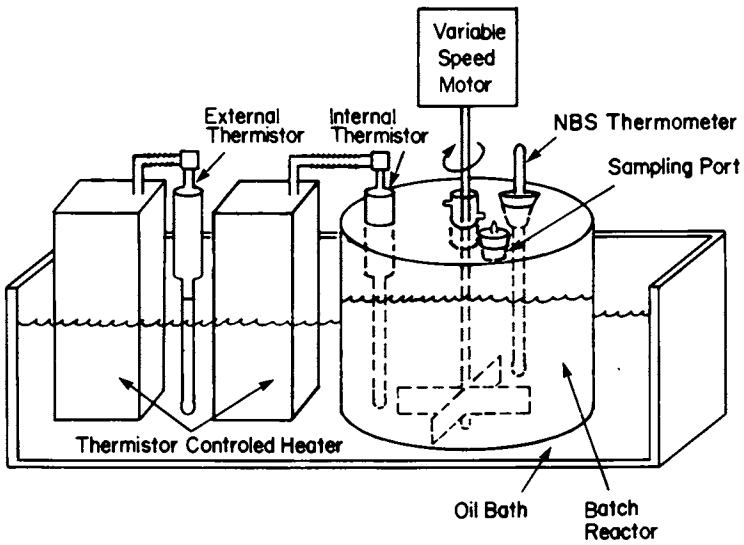


Figure 1. Schematic diagram of batch reactor.

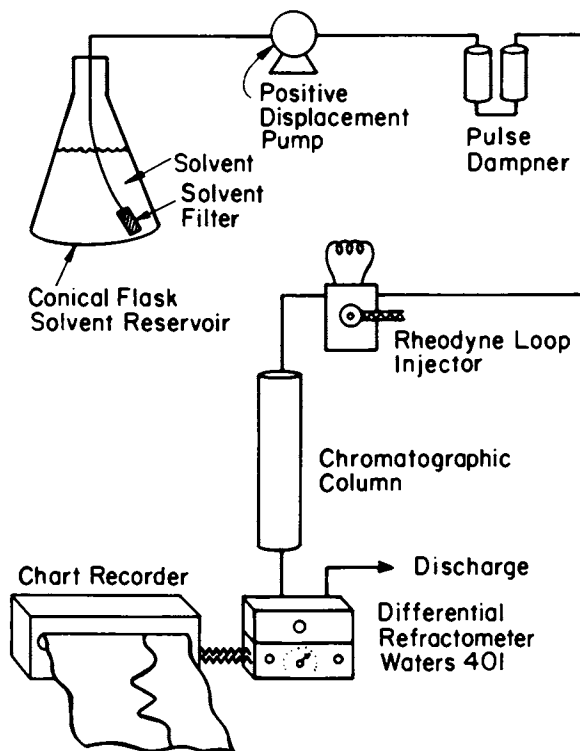


Figure 2. Size exclusion chromatographic (SEC) apparatus.

American Chemical
Society Library
1155 16th St., N.W.

40-60 μm in size (9). This was done to increase the fractionation efficiency to approximately 3000 theoretical plates per meter and shorten the elution time to less than two hours. The eluent and starch solvent was 0.5 N NaOH. A constant eluent flow rate of 6.5 ml per hour was maintained using a slow-flow mini pump (Milton Roy: Laboratory Data Control, Riviera Beach, FL).

The SEC columns were calibrated using narrow molecular weight distribution water soluble polymer standards; sodium polystyrene sulfonate, NaPSS (Pressure Chemical Company, Pittsburgh, PA) and dextrans (Pharmacia Fine Chemicals, Piscataway, NJ). The universal calibration curve proposed by Grubisic et al. (13) was found not to be applicable for these polymer standards. The alternative calibration procedure of Coll and Prusinowski (14) which incorporates excluded volume effects in the numerical value of the Flory parameter was found to be applicable for this system (15). The calibration curve for the two-column network system described above is shown in Figure 3. The K_{AV} parameter used on the abscissa of Figure 3 is a normalized elution volume parameter defined by Equation 1,

$$K_{AV} = \frac{V_e - V_o}{V_t - V_o} \quad (1)$$

where V_e is the peak retention volume of the sample, V_o is the void volume of the column, and V_t is the total interstitial volume of the column.

Results and Discussion

In order to describe the kinetics of enzymatic starch depolymerization, information on reaction rate, reaction extent, and product distribution profiles are required. Traditional end-group analysis can be used to a limited extent in the first two areas, but will not provide information about the last important subject. Hence, SEC profiles can provide sufficient insight into the mechanism of starch degradation.

Effect of Temperature on Reaction Rate. The initial rate of starch hydrolysis was investigated at five temperatures (40°C, 57.5°C, 67.5°C, 80°C and 95°C) using three different substrate concentrations (0.44%, 0.88%, and 1.76% wt/vol) by

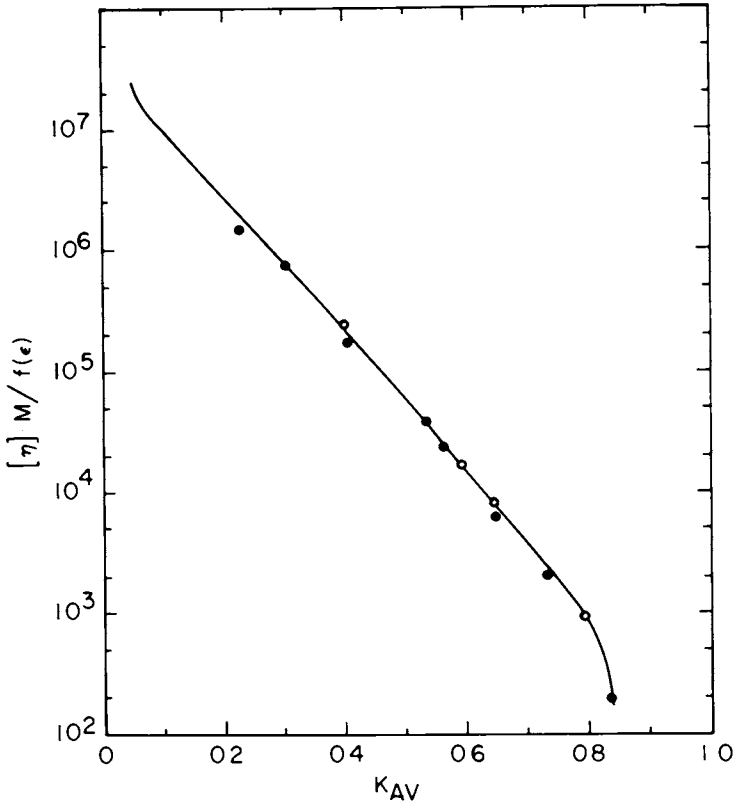


Figure 3. C-P calibration curve of SEC column network.

monitoring the production of reducing sugars (dextrose equivalence, D.E.). At each isotherm, the initial rate data were shown to follow Michaelis-Menten kinetics (11) consistent with the observations of previous reports (16,17). Hence, Lineweaver-Burk plots could be generated from the data yielding values of apparent maximum initial velocities at each of the temperatures. This information is plotted in Figure 4 with an assumed Arrhenius dependency, which for this system clearly does not exist. The salient features of this study are that there exists nearly a three fold order of magnitude increase in the apparent maximum velocity as the starch substrate is modified due to the gelatinization phenomena. At the highest temperature tested, the rate of the reaction decreases. This is due to thermal deactivation of the enzyme. This large increase in the reaction rate indicates that the overriding effect involves the physical state of the starch granule. Non-gelatinized starch is highly crystalline (18) and thus the susceptibility of starch to be enzymatically hydrolyzed under these conditions is much lower than for starch granules that have been disrupted by heating in aqueous suspension. Through the process of gelatinization, the original internal ordering of the starch molecules within the granules is disrupted, the granule imbibes large amounts of water and swells. Eventually due to combined action of shearing within the reactor and osmotic swelling, granule integrity is completely lost. Large starch molecules may then reassociate (retrograde) producing a gel matrix. It cannot be assumed that the progress of the reaction will follow the same sequence if the substrate is in various physical states. It is therefore of interest to follow the molecular weight distribution profiles during the course of the reaction at various states of macromolecular aggregation. The aqueous SEC apparatus described above was specifically developed for this purpose. This technique was shown to be approximately 10^4 times more accurate than reducing sugar measurements for low degree of conversion starch hydrolysis reactions (10).

Effect of Temperature on Hydrolysis Extent and Product Distribution. It was shown above that slow initial rate of reaction is characteristic of operating at low temperatures (below the gelatinization range of starch) whereas rapid initial rates are

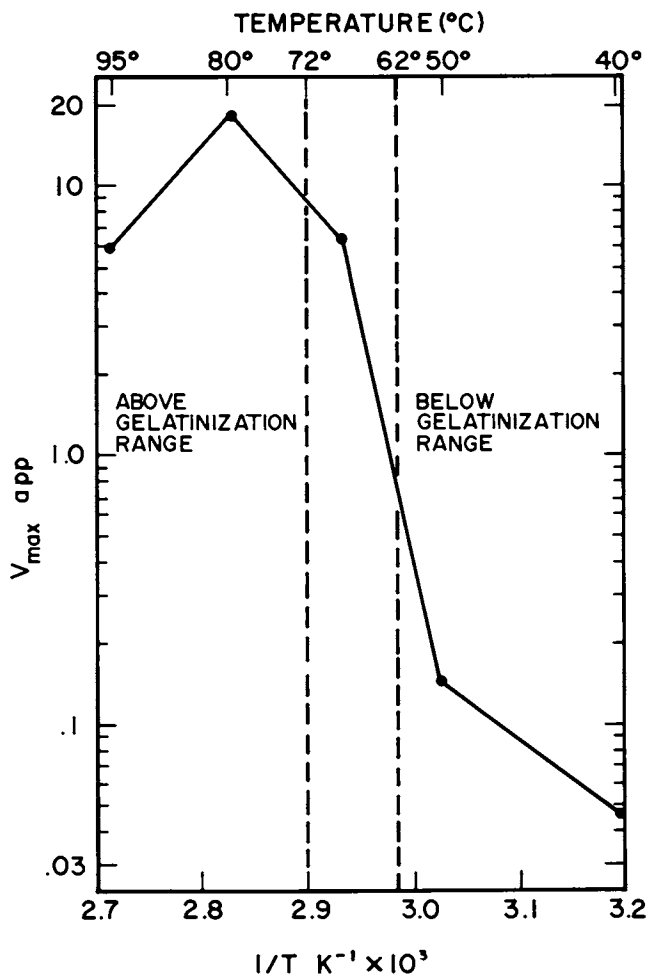


Figure 4. Arrhenius plot of $V_{max\ app}$.

observed at high temperatures (above the gelatinization of starch). However, the distributions of macromolecular components during hydrolysis at various temperatures have not been reported and are thus of interest.

SEC profiles of hydrolysis products of enzyme-treated starch as a function of reaction time at 60°C and 80°C are shown in Figures 5 and 6 respectively. In both cases, a common enzyme dose of one ml of the 1:19 stock Novo Thermamyl solution was mixed with a slurry of 15 gms starch dry basis in 75 ml water and added to the reactor. The final volume was 1500 ml.

At 60°C, below the gelatinization (melting) range of the granules, the product distribution is extremely non-random (see Figure 5). Only during the initial stages of reaction is any significant amount of intermediate molecular size products (i.e., between hydrodynamic volume 10^7 and 10^3 dl/mole) detected. Throughout the time course of liquefaction, the majority of the molecular species present are either very high in molecular weight (excluded from the SEC column) or low molecular weight end products. Low molecular weight products continuously accumulate while high molecular weight materials disappear without detection of any significant amount of intermediate molecular weight material. This situation could result if the enzyme is allowed to act only on relatively short, exposed chains of starch present in the crystalline matrix of the granule, or if longer chain molecules freed from the granule are more susceptible to enzyme hydrolysis than the molecules associated with the granule and are therefore preferentially degraded. Alternatively this situation could also arise if the available starch is simply overloaded with enzyme. Other authors suggest that preferential "pitting" may occur due to differing degrees in substrate susceptibility. The reaction under these conditions does proceed to completion although requiring approximately ten hours for the conversion.

Above the gelatinization range (80°C, see Figure 6) the product distribution during reaction is considerably different than 60°C. Again, the distribution of molecular sizes is not random. During the early stages of the reaction, in addition to the very high molecular weight and low molecular weight products, a large fraction of intermediate molecular weight dextrans (between hydrodynamic value 10^7 and 10^3 dl/mole, see Figure 5) are present.

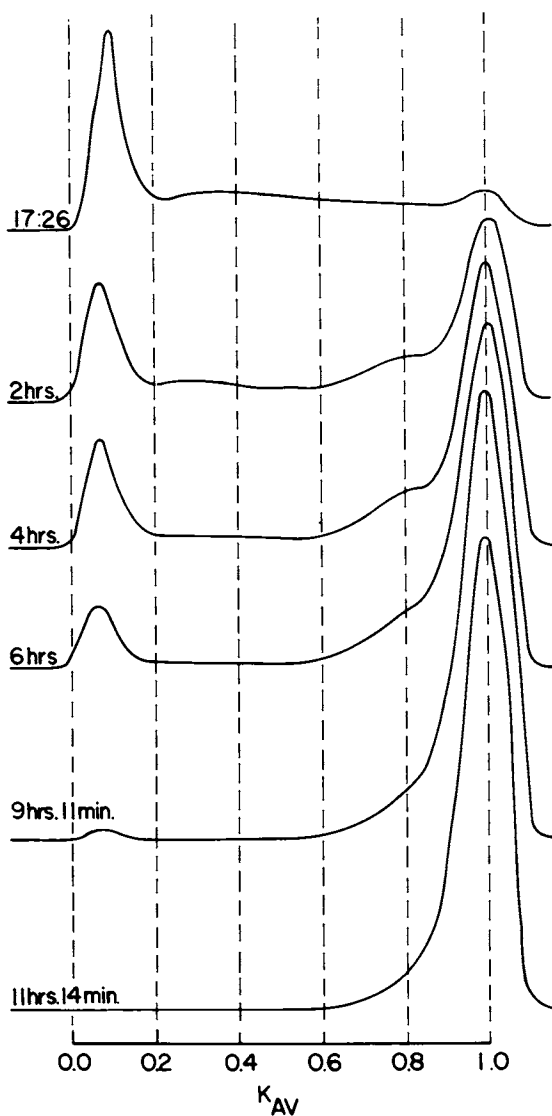


Figure 5. Chromatograms of starch hydrolyzed at 60°C at indicated times during reaction. Top curve, 17 min: 26 s.

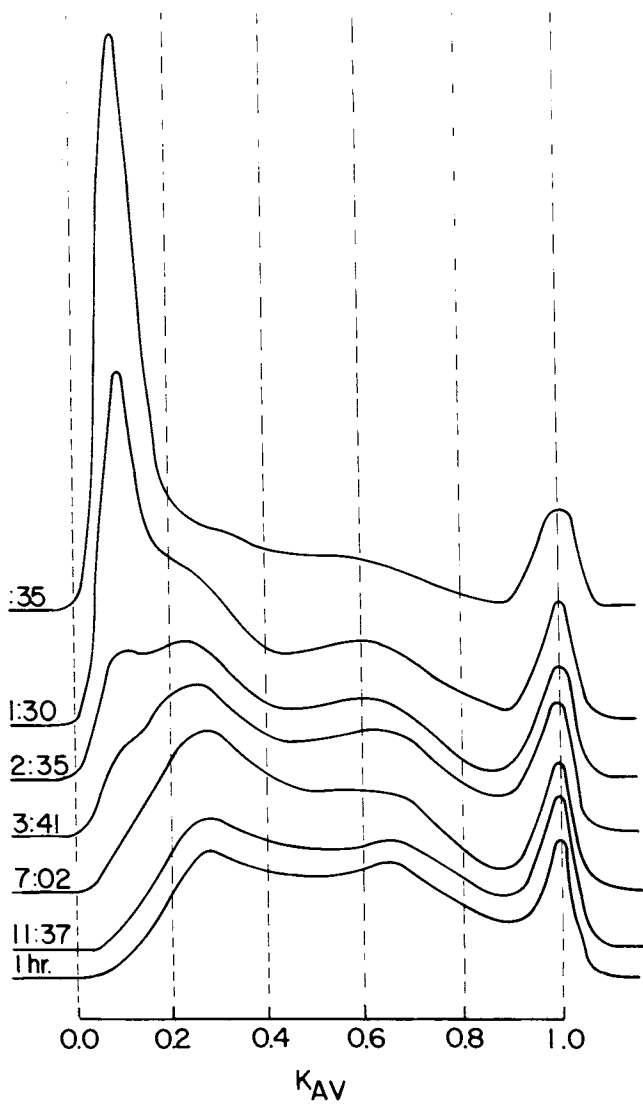


Figure 6. Chromatograms of starch hydrolyzed at 80°C at indicated times during reaction. Times indicated as min: s.

At one and one-half minutes into the reaction, two discrete intermediate molecular weight peaks are detected at K_{AV} values of 0.25 and 0.60. These values correspond to approximate molecular weights of 5×10^5 and 10^4 respectively (9). Throughout the remaining time course of the reaction these peaks persist, though their K_{AV} values increase slightly (to 0.275 and 0.65 respectively) with increasing time characteristic of a reduction in their molecular weight values. This is apparently due to gradual end-wise depolymerization of these intermediates. This indicates that under these reaction conditions, certain intermediate products are more resistant to enzymatic attack, and therefore appear as discrete chromatographic peaks. Discrete peaks could result if certain molecular size starch molecules are either preferentially produced (as by-products) or are resistant to enzymatic attack, and therefore appear as discrete chromatographic peaks. Previous reports of such intermediates during starch liquefaction have not been found.

No further changes in the chromatographic tracings are seen beyond eleven and one-half minutes at 80°C, which shows that thermal deactivation of the enzyme has stopped the progress of the reaction. The reaction does not proceed to completion under these conditions.

The final product distribution of a starch solution hydrolyzed at 95°C under the same conditions as the other two isotherms was determined and is shown together with the similar data at 80°C, 65°C, and 60°C in Figure 7. Four distinct peaks are observed: one at the low molecular weight limit, and two intermediate molecular weight peaks at K_{AV} values of 0.2 and 0.6 respectively. This is the same type of chromatographic behavior observed during the initial stages of reaction at 80°C. Under all thermal states tested, a non-random distribution exists.

Effect of Starch Recrystallization on Hydrolysis Extent, Product Distribution, and Reaction Rates. Since retrograded (recrystallized) starch is thought to be more resistant to enzymatic depolymerization than unretrograded starch (22,23), it is of interest to compare the hydrolysis of retrograded starch to non-retrograded starch. Extremely retrograded starch was prepared by freeze-drying pregelatinized starch, and ball-milling this material to a

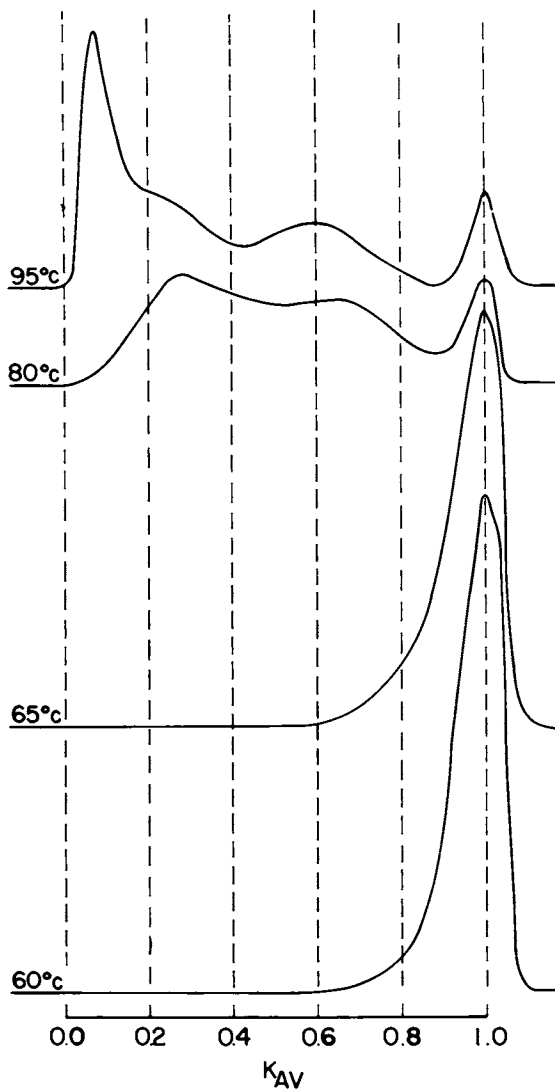


Figure 7. Comparison of final product distribution of starch hydrolyzed at 95°C, 80°C, 65°C, and 60°C.

fine powder. This material was enzymatically hydrolyzed at 80°C, and the molecular size distribution was determined by size exclusion chromatography. The chromatographic profiles are shown in Figure 8. The chromatographic profile of unreacted, pregelatinized, freeze-dried, ball-milled starch ("0" time chromatogram) shows that significant depolymerization occurred during the ball-milling operation. During the course of enzymatic depolymerization of this recrystallized starch, four distinct peaks are present: one near the exclusion limit of the column set, one at the end products, and two intermediate peaks. These intermediate peaks are detectable as early as two and one-half minutes into the reaction. The peaks appeared at K_{AV} values of approximately 0.25 and 0.6, the same values observed when non-pregelatinized starch was reacted at 80°C. These K_{AV} values for the two intermediate peaks increased slightly with increasing reaction time, again consistent with the results shown at 80°C for non-pregelatinized starch. Thus the resistant, intermediate molecular size starch products formed after severe retrogradation during freezing are quite similar to the groups formed when a non-pregelatinized starch is enzymatically depolymerized under the same conditions. No change in the chromatographic profiles is detected after eleven minutes and the reaction does not proceed to completion.

Conclusion

The present investigation has provided new insight into the physical events occurring during enzymatic starch depolymerization. Degradation of starch under the conditions tested does not proceed by a random process. Granule structure affects the molecular weight distribution profiles of the starch hydrolysates. Starch hydrolysates produced at temperatures below the gelatinization range of the substrate are composed mainly of high molecular weight material or low molecular weight end products. At 80°C, above the melting range of the granules, a large amount of intermediate molecular size components exist in addition to the high and low molecular weight groups. These intermediate products are approximately 5×10^5 and 10^4 in molecular weight and are the same size components seen in the hydrolysis of highly recrystallized starch reacted at the same isotherm. This suggests that the recrystalli-

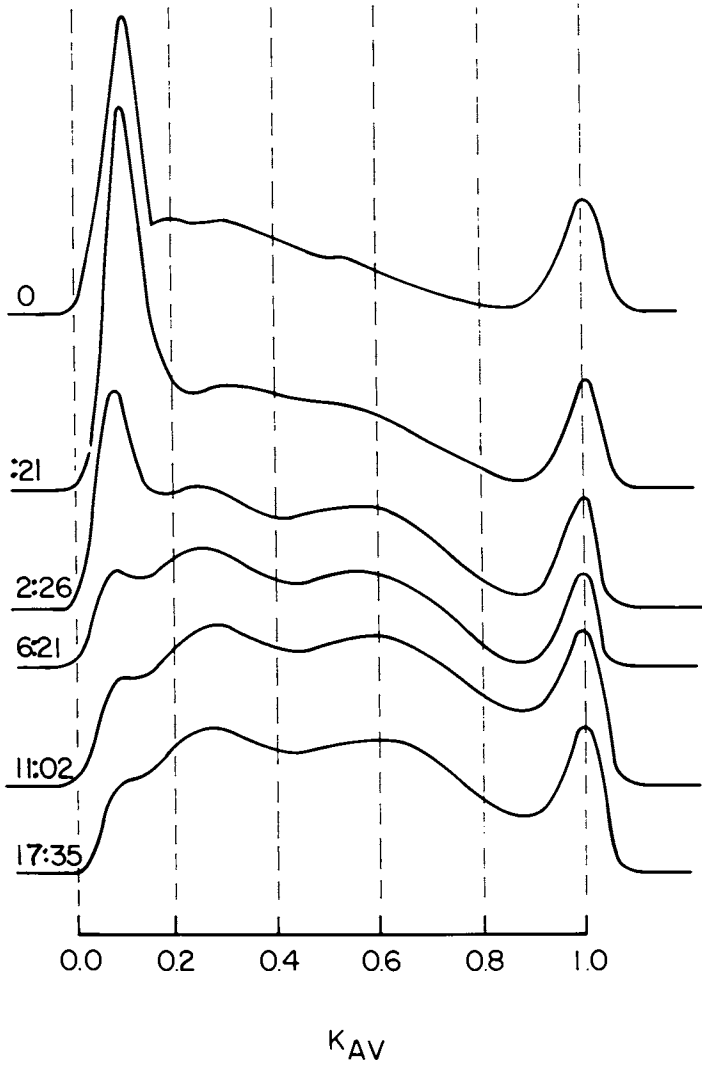


Figure 8. Chromatograms of pregelatinized starch hydrolyzed at 80°C at indicated times (min: s) during reaction.

zation process will occur even at high temperature operation.

Although the initial rate of the reaction is greatest at temperatures above the gelatinization range of the substrate, the final extent of conversion is greatest at low temperature operation for a common amount of enzyme loading. This situation exists due to thermal deactivation of the catalyst. Optimal operation of a starch liquefaction operation must account for both the rate of increased substrate susceptibility caused by the disruption of the internal macromolecular ordering within the granule and the loss of enzymatic activity due to thermal deactivation.

A physical model of starch gelatinization, retrogradation, and liquefaction can be presented from these results. It is clear that molecular recrystallization via retrogradation process will occur quite rapidly for pregelatinized starch. It is therefore not possible to study the enzymatic hydrolysis of starch without considering retrogradation effects. The physical picture for the overall process is summarized in Figure 9. The initial population of starch granules is suspended in aqueous solution. When subjected for a period of time at or above the gelatinization temperature range of the material, some of the starch granules melt. The molecular components of the granule will then reassociate to form crystalline bodies, some of which may be more or less resistant to enzymatic hydrolysis than other crystal types. The enzyme will hydrolyze susceptible bond linkages to low molecular weight oligosaccharides as a function of time and concentration.

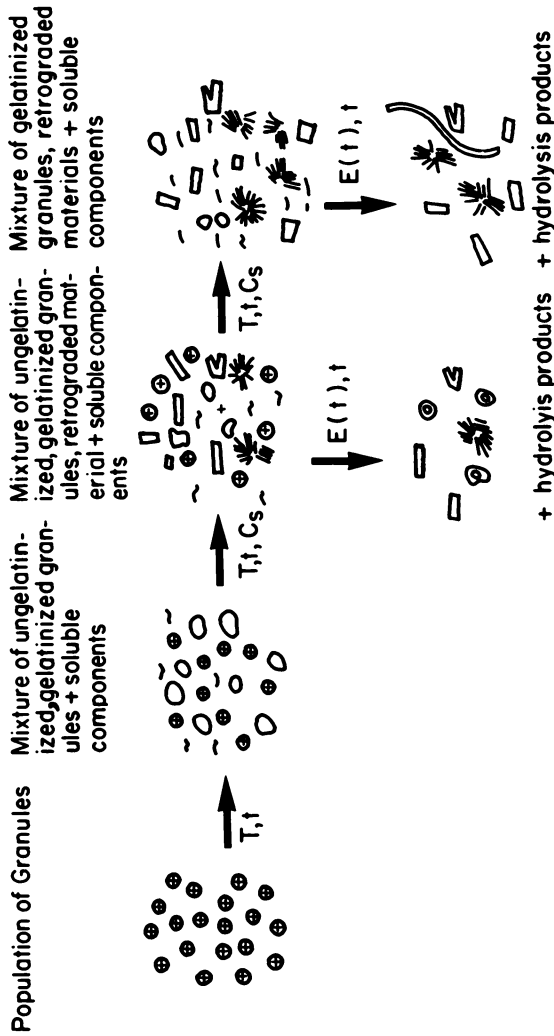


Figure 9. Physical model of gelatinization, retrogradation, and liquefaction.

Literature Cited

1. Marsh, D.R.; Lee, Y.Y.; Tsao, G.T. *Biotechnol. Bioeng.* 1973, 15, 483.
2. Lee, D.D.; Lee, Y.Y.; Reilly, P.J.; Collings, E.V.; Tsao, G.T. *Biotechnol. Bioeng.* 1976, 18, 253.
3. Wight, A.W. *Die Starke* 1976, 28, 311.
4. John, M. and Dellweg, H. *Sept. and Pur. Meth.* 1973, 2, 231.
5. Cruz, A. Ph.D. Thesis, Princeton University, Princeton, NJ, 1976.
6. Henriksnas, H. and Bruun, H. *Die Starke* 1978, 30, 233.
7. Henriksnas, H. and Lovgren, T. *Biotechnol. Bioeng.* 1978, 20, 1303.
8. Bondetskii, K.M. and Yarovenko, V.L. *Bioorgan. Khimiia* 1975, 1, 614.
9. Rollings, J.E. Ph.D. Thesis, Purdue University, Lafayette, IN, 1978.
10. Rollings, J.E.; Bose, A.; Okos, M.R.; and Tsao, G.T. *J. Appl. Polym. Sci.* (accepted).
11. Rollings, J.E. M.S. Thesis, Purdue University, Lafayette, IN, 1978.
12. Yau, W.W.; Kirkland, J.J.; and Bly, D.D. "Modern Size Exclusion Chromatography"; John Wiley and Sons, NY, 1979, 97.
13. Grubisic, Z.; Rempp, R.; and Benoit, H. *J. Polym. Sci. Part B* 1967, 5, 753.
14. Coll, H. and Prusinowski, P. *J. Polym. Sci. Part B* 1967, 5, 1153.
15. Bose, A.; Rollings, J.E.; Caruthers, J.M.; Okos, M.R.; and Tsao, G.T. *J. Applied Polym. Sci.* (accepted).
16. Rosendal, P.; Nielsen, B.H.; and Lange, N.K. *Die Starke* 1979, 31, 368.
17. Roels, J.A. and vanTilburg, R. *Die Starke* 1979, 31, 338.
18. Sterling, C. *J. Texture Studies* 1978, 9, 225.
19. Chabat, J.F.; Allen, A.E.; and Hood, L.F. *J. Food Sci.* 1978, 43, 727.
20. Hollinger, L.F. and Marchessault, R.H. *Biopolymers* 1975, 14, 265.
21. Mussulman, W.C. and Wagoner, J.A. *Cereal Chem.* 1968, 45, 162.
22. Watson, S.A. in "Methods in Carbohydrate Chemistry, Vo. IV" R.L. Whistler, ed.; Academic Press, NY, 1964.
23. Boruch, W.M. and Pierzgalski, T. *Die Starke* 1979, 31, 149.

RECEIVED June 1, 1982

Thermochemical Optimization of Microbial Biomass-Production and Metabolite-Excretion Rates

ALICIAN V. QUINLAN

Massachusetts Institute of Technology, Department of Mechanical Engineering,
Cambridge, MA 02139

The temperature that maximizes the rate of many microbial processes is known to vary with medium composition. As a result, the operating temperature of biological reactors should be varied to keep such process rates maximal as their chemical milieux vary. The laws relating optimum operating temperature to medium composition are not well known. This relation was theoretically investigated for processes whose rates saturate in substrate concentration. The Michaelis-Menten reaction mechanism was modified to describe microbial biomass production and metabolite excretion in both batch and continuous reactors. Monod rate laws whose macro-coefficients depend on dilution rate as well as temperature were derived. Conditions for which these coefficients may fall, rise, or show a minimum with rising temperature and dilution rate were enumerated. The optimum temperature was shown to vary with both substrate concentration and dilution rate. The pattern of variation was explained in terms of the thermal sensitivities of the coefficients. The validity of the theoretical results was discussed relative to published data and found promising but in need of experimental testing.

The rates of microbially mediated processes typically show a single rate maximum as temperature rises (1-7). Changes in a microorganism's chemical environment can shift the temperature at which the thermal rate maximum occurs (3-7). As a consequence, given the chemically changing milieux of biological reactors, their operating temperatures would have to be varied to optimize process rates (8,9). In biological reactors, substrate concentration is the most important chemical variable. So, it's most desirable to know how the optimum operating temperature depends on substrate concentration.

0097-6156/83/0207-0463\$07.25/0
© 1983 American Chemical Society

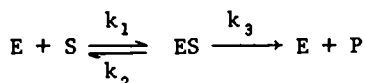
Quinlan (8-10) has analyzed how changes in substrate concentration affect the optimum temperature of processes that saturate in substrate concentration according to a generic Michaelis-Menten reaction mechanism. For such processes, the optimum temperature was shown to vary linearly with the logarithm of substrate concentration. This logarithmic relation results when both the maximum-velocity and half-saturation coefficients show Arrhenius temperature dependencies, with the latter's falling faster. Such dependencies are commonly seen in batch reactors (11-14), but not always (13,14).

Although applicable to many processes, this analysis (8-10) is not generally applicable to microbially mediated processes. It's restricted to batch reactors and can't account for the influence of mass inflow and outflow in continuous reactors. It also can't explain why some maximum-velocity and half-saturation coefficients determined in continuous reactors tend to show non-Arrhenius temperature dependencies (15-19) and why others seem to vary with dilution rate (20,21).

In this paper, the Michaelis-Menten reaction mechanism will be modified to eliminate these and other shortfalls. The modified reaction mechanism will then be used to explore the influence of substrate concentration on the optimum temperature of biomass-production and metabolite-excretion rates. The influence of dilution rate will also be examined. The scope of analysis will still be confined to processes whose rates saturate in substrate concentration.

Reaction Mechanism

The Michaelis-Menten reaction mechanism describes the enzyme-catalyzed conversion of substrate into product as follows (2, 22-24):



This reaction mechanism assumes one molecule each of substrate (S) and free enzyme (E) reversibly combine ($K_m \equiv k_2/k_1$) to form (k_3) product (P) with a concomitant recycling of free enzyme.

In biological reactors, microbial biomass plays a role analogous to the enzyme's role. Let Y be the average number of substrate consumption sites per microorganism. Then,

$$Y \equiv C/N \quad (1)$$

where C is the concentration of consumption sites in the microbial population and N is the concentration of microorganisms in the population. Similarly, let β be the average biomass per microorganism, with

$$\beta \equiv B/N \quad (2)$$

where B is the biomass concentration of the population. Solving equations (1) and (2) for N and equating the resulting expressions yields

$$B = (\beta/\gamma)C \quad (3)$$

Equation (3) states that the biomass concentration of a microbial population is directly proportional to the concentration of substrate consumption sites in the population.

As for the enzyme, the substrate consumption sites may be partitioned into two portions: those capable of consuming substrate (C_c) and those not capable (C_n). An equivalent biomass may be assigned to each portion through equation (3):

$$B_c \equiv (\beta/\gamma)C_c \quad (4a)$$

$$B_n \equiv (\beta/\gamma)C_n \quad (4b)$$

The total biomass of a microbial population can then also be partitioned into two portions so that

$$B \equiv B_c + B_n \quad (5)$$

In this context, B_c plays a role analogous to free enzyme, and B_n , to enzyme-substrate complex.

In conformance with this interpretation of B_c , substrate is assumed to be consumed at a rate jointly proportional to its concentration S and B_c , i.e., at a mass flow rate cSB_c . Similarly, the metabolite of interest is assumed to be excreted at a rate proportional only to B_n , i.e., at a mass flow rate eB_n . In this case, the microscopic rate coefficients c and e play roles analogous to those of k_1 and k_2 , respectively.

Furthermore, saturated and unsaturated consumption sites are assumed to cycle as complexed and free enzyme do, but with no concomitant release of substrate or metabolite into the medium. Saturated sites are assumed to unsaturate at a rate proportional only to their own concentration, i.e., at a mass flow rate uB_n . On the other hand, unsaturated sites are assumed to saturate at a rate jointly proportional to substrate concentration and their own, i.e., at a mass flow rate sSB_c . If each consumption site becomes saturated when one substrate molecule occupies it, then the microscopic saturation and consumption coefficients are equal. This is the case assumed by the Michaelis-Menten reaction mechanism. However, if n molecules are required for saturation of one site, then $s = (1/n)c$.

The modified reaction mechanism must also account for biomass wastage (and the concomitant loss of consumption sites) through respiration, excretion, death, etc. Biomass wastage is assumed to take place at a rate proportional to the biomass concentration of the population, i.e., at a mass flow rate $wB = wB_c + wB_n$.

Finally, substrate is added to a continuous reactor at a mass flow rate dS_0 , where S_0 is the concentration of inflowing substrate and d is a dilution rate equal to the ratio of the volumetric inflow rate to the volume of fluid in the reactor. For a constant fluid volume, inflowing substrate also displaces substrate, biomass, and metabolite at mass flow rates equal, respectively, to dS , $dB = dB_c + dB_n$, and dM .

At this point, all the necessary mass concentrations and flows have been defined. The resulting reaction mechanism is schematized in Figure 1. The solid lines represent the mass flows, and the dashed lines show which concentrations influence their rates. A yield coefficient Y must be introduced to make the units of S and M compatible with those of B_c and B_n . Each unit of S consumed is assumed to produce Y units of B . Similarly, each unit of M excreted is assumed to deplete Y units of B .

Rate Laws

The rate of change of each concentration shown in Figure 1 may be obtained by summing all its mass inflows and outflows:

$$dS/dt \equiv \dot{S} = d(S_0 - S) - cSB_c/Y \quad (6)$$

$$dB_c/dt \equiv \dot{B}_c = (c - s)SB_c + uB_n - (w + d)B_c \quad (7)$$

$$dB_n/dt \equiv \dot{B}_n = sSB_c - (u + w + d)B_n \quad (8)$$

$$dM/dt \equiv \dot{M} = eB_n/Y - dM \quad (9)$$

Also, equations (7) and (8) may be added together to yield:

$$dB/dt \equiv \dot{B} = cSB_c - (w + d)B \quad (10)$$

The rates of biomass production and metabolite excretion can be shown to saturate in substrate concentration if B_c is assumed to adjust much more slowly to changes in S than B_n does. So, on the time scale of changes in B_c , $\dot{B}_n \approx 0$, and from equation (8):

$$B_n \approx SB_c/K \quad (11a)$$

where
$$K \equiv (u + w + d)/s \quad (11b)$$

Now, from equations (5) and (11a):

$$B_c \approx BK/(K + S) \quad (12a)$$

$$B_n \approx BS/(K + S) \quad (12b)$$

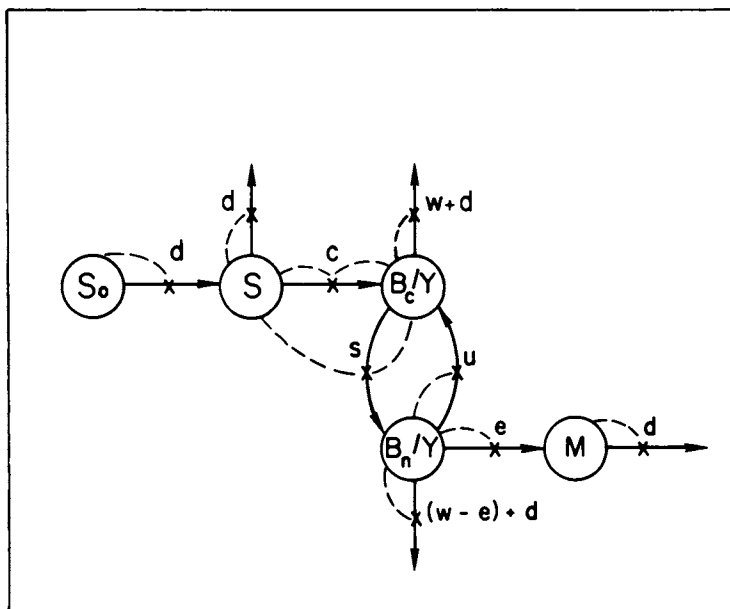


Figure 1. Reaction mechanism assumed to govern the rates of microbial biomass production and metabolite excretion in batch ($d = 0$) and continuous ($d > 0$) reactors. Symbols defined in text and in legend of symbols. $B \equiv B_c + B_n$.

Substrate Depletion. Substitution of equation (12a) into (6) yields the familiar continuous-culture equation for substrate depletion (17,18):

$$\dot{S} \approx d(S_0 - S) - \mu_m(B/Y)S/(K + S) \quad (13a)$$

where $\mu_m \equiv cK \quad (13b)$

The second term in equation (13a) represents the rate of substrate consumption, or nutrient uptake. It saturates in substrate concentration according to a Monod rate law where both K and μ_m/Y are known to vary with temperature and dilution rate (11-21).

Biomass Production. Similarly, substitution of equation (12a) into (10) yields the net biomass production equation commonly used for continuous culture systems (17,18):

$$\dot{B}/B \approx \mu_m S/(K + S) - (w + d) \quad (14)$$

The first term in equation (14), representing the gross rate of biomass production, is identical with the function Monod (25) originally adopted "to express conveniently the relation between exponential growth rate and concentration of an essential nutrient." Such a rectangular hyperbolic function has been derived many times from various reaction mechanisms (26-30), but none has addressed the present case of continuous culture systems where μ_m and K have been observed to vary with temperature and dilution rate. Now, through equations (11b) and (13b), the temperature variation of μ_m and K is attributable to the microscopic rate coefficients c, s, u, w , and their variation with dilution rate is explicit.

To estimate the values of the micro-coefficients c, s, u, w as functions of temperature, equation (14) can be rewritten as

$$\dot{B}/B \approx V_B(S - S_T)/(S + K) \quad (15a)$$

where $V_B \equiv \mu_m - (w + d) \quad (15b)$

$$\equiv (c - s)K + u \quad (15c)$$

$$S_T \equiv (w + d)K/V_B \quad (15d)$$

Equation (15a) represents a Monod rate law with a threshold substrate concentration S_T (Figure 2). It can be linearized to a generalized Eadie-Augustinsson equation (31-33):

$$v \approx V_B - K(v/S) - V_B S_T(1/S) \quad (16)$$

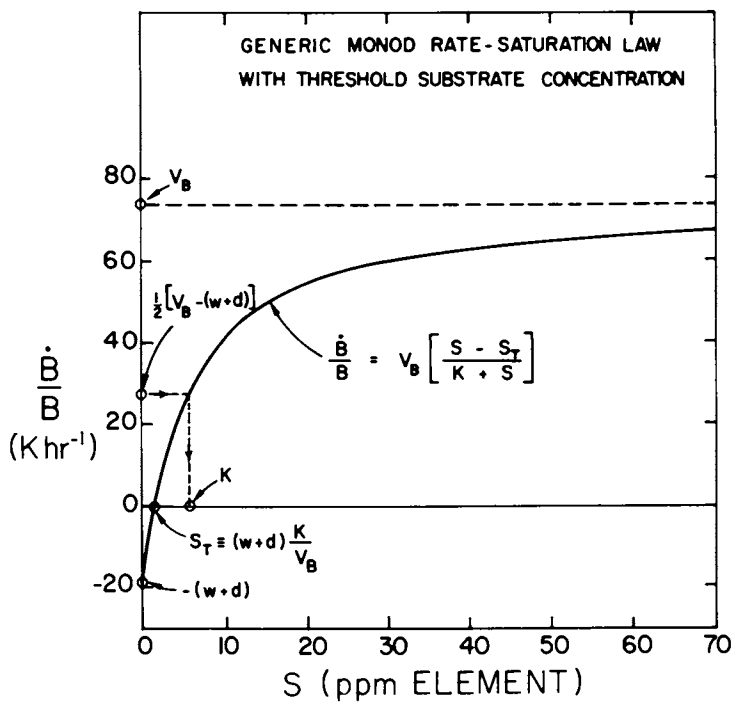


Figure 2. Properties of the rate law for net biomass production in batch ($d = 0$) and continuous ($d > 0$) reactors. Symbols defined in text and in legend of symbols.

where v is the specific net biomass production rate \dot{B}/B measured in the reactor at particular values of substrate concentration, temperature, and dilution rate. A linear regression of v versus v/S and $1/S$ will yield values for the macro-coefficients V_B , K , and S_T as functions of temperature and dilution rate. The values of the micro-coefficients as functions of temperature can then be estimated from equations (11b), (15c), and (15d) assuming $c = s$.

Metabolite Excretion. Substitution of equation (12b) into (9) yields a pure Monod rate law for metabolite excretion:

$$(\dot{M} + dM)/(B/Y) \approx V_M S/(S + K) \quad (17a)$$

where $V_m \equiv e \quad (17b)$

Thermal Sensitivity of the Macro-Coefficients

Temperature influences the macro-coefficients (K, μ_m, V_B, V_m, S_T) through the temperature dependencies of the micro-coefficients (c, e, s, u, w). Each of the micro-coefficients is assumed to obey an Arrhenius temperature law of the form (34):

$$k = A \exp(-E_A/RT_K) \quad (18)$$

- where
- $k \equiv$ a positively-valued micro-scopic rate coefficient
 - $A \equiv$ a positively-valued coefficient that is practically independent of temperature
 - $E_A \equiv$ a positively-valued apparent activation energy (cal. mol⁻¹)
 - $R \equiv$ the gas constant (1.987 cal. mol⁻¹ K⁻¹)
 - $T_K \equiv$ degrees Kelvin

Within the temperature range 0 - 50°C, equation (18) may be approximated as follows (10):

$$k \approx \alpha \exp(T/\theta_\alpha) \quad (19a)$$

$$\alpha \equiv A \exp(-1.843 \times 10^{-3} E_A) \quad (19b)$$

$$T \equiv \text{degrees Celsius}$$

$$\theta_\alpha \equiv 1.481 \times 10^5/E_A \quad (19c)$$

This approximation considerably simplifies the investigation of thermo-chemical rate-optimization conditions.

To illustrate some interesting aspects of the thermal sensitivity of the macro-efficients, specific temperature dependencies were assumed for the five micro-coefficients. The assumed dependencies are shown in Figure 3. The parameter values were chosen so in batch culture ($d = 0$) all five macro-coefficients would always rise with temperature (Figures 4-6) and K would rise more rapidly with temperature than V_B and V_M in the temperature range 20-30°C. This thermal sensitivity pattern is often seen in batch culture (e.g., 11-14).

Half-Saturation Coefficient K . For batch culture, equation (11b) reduces to:

$$K|_{d=0} = (u + w)/s \quad (20)$$

If s rises more rapidly with temperature than both numerator terms, then the batch-culture half-saturation coefficient should always decrease as temperature increases. If s rises more rapidly than the numerator term dominant at low temperatures but more slowly than the term dominant at high temperatures, it should show a temperature minimum. If s rises more slowly than both numerator terms (Figure 3), it should always rise with temperature (Figure 4, $d = 0$).

The thermal sensitivities of the batch-culture half-saturation coefficients for several microbial processes (11-14) have been observed to resemble the linear portion of the $d = 0$ curve in Figure 4. However, a few deviations from this pattern have been seen where the half-saturation coefficients showed either a negative slope or a maximum (13). Only the thermal maximum is inconsistent with equations (18) - (20).

For continuous culture,

$$K|_{d>0} = K|_{d=0} + (1/s)d \quad (21)$$

According to equation (21), the continuous-culture half-saturation coefficient equals the batch-culture half-saturation coefficient augmented by a term that increases linearly with dilution rate. However, the magnitude of this term should decrease exponentially with increasing temperature because of the factor $1/s$. Thus, at low temperatures where the dilution term may dominate the batch-culture half-saturation coefficient, the continuous-culture half-saturation coefficient may decline with increasing temperature. It should grow with temperature only when the batch-culture half-saturation coefficient has a positive slope and dominates the dilution term. In this case, it may have a thermal minimum (Figure 4, $d > 0$). Moreover, for the range of dilution rates where the locus of minima (dashed line, Figure 4) parallels the

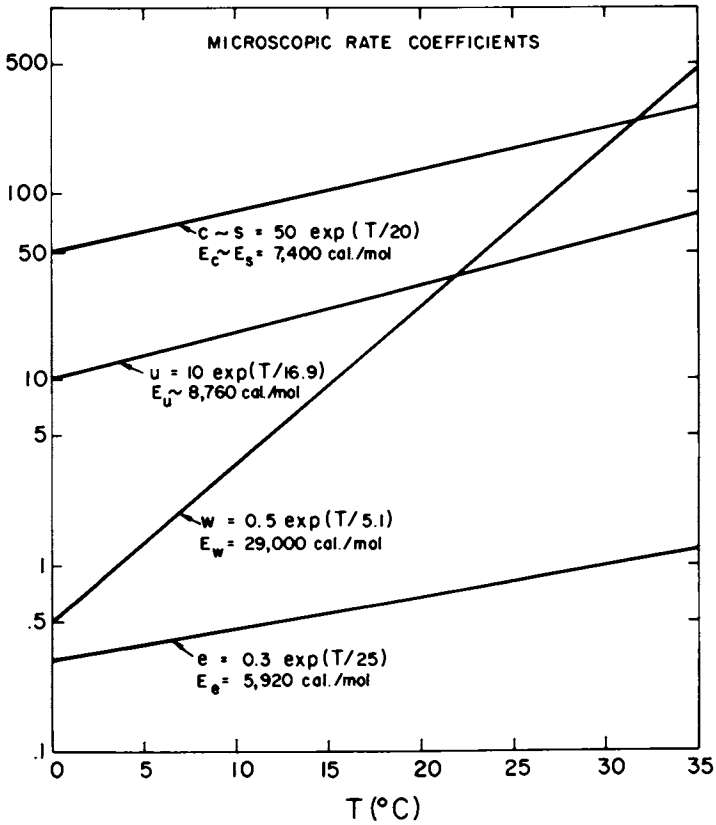


Figure 3. Temperature dependencies assumed for the five microscopic rate coefficients defined in Figure 1. The microcoefficients c and s have units $(\text{ppm element})^{-1} \text{Khr}^{-1}$, e , u , and w have units Khr^{-1} .

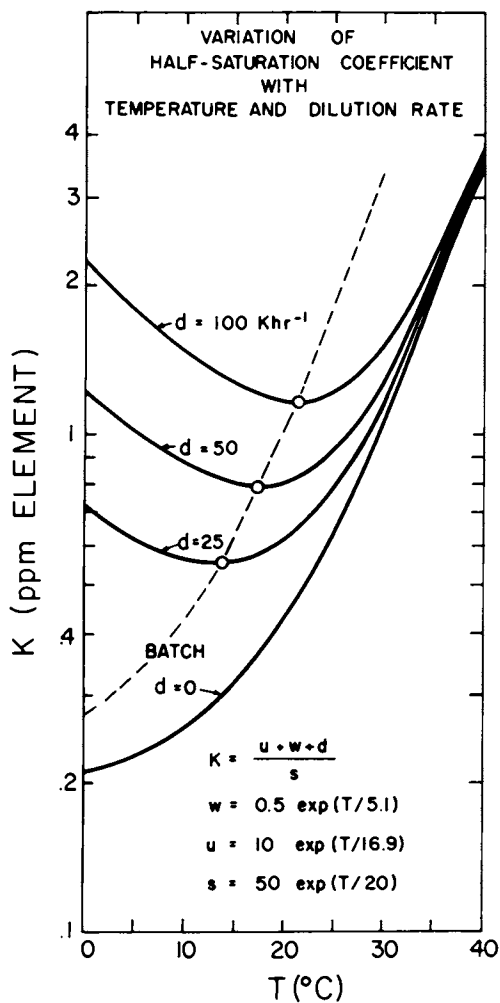


Figure 4. Theoretical thermal sensitivity of the half-saturation coefficient in batch ($d = 0$) and continuous ($d > 0$) culture with the parameter values specified in Figure 3. Dashed line, locus of thermal minima (\circ).

$d = 0$ curve, the temperature that minimizes the half-saturation coefficient rises linearly with the logarithm of the dilution rate.

In continuous culture, the half-saturation coefficient has been observed to respond to rising temperatures by declining monotonically (15-17) and by showing a minimum (18,19). Both cases are consistent with the $d > 0$ curves in Figure 4.

In contrast, experiments probing its response to rising dilution rates haven't shown clear-cut trends because of extremely large measurement uncertainties (20,21). In one instance, no trend could be detected (20). In another, the mean values showed a maximum, but linear and saturation curves could also be drawn through the \pm one-standard-deviation uncertainty ranges for each mean value (21). Better data are clearly needed to test the linear dependence on dilution rate predicted by equations (11b) and 21).

Maximum-Specific-Growth-Rate Coefficient μ_m . In batch culture, equations (11b) and (13b) combine to yield:

$$\mu_m \Big|_{d=0} = cu/s + cw/s \quad (22)$$

The batch-culture maximum-specific-growth-rate coefficient should fall with increasing temperature if s rises more rapidly than both cu and cw . It should show a minimum if s rises more rapidly than the numerator of the term dominant at low temperatures but less rapidly than the other term. It should always increase if s rises less rapidly than the numerators of both terms. When $c = s$, it also should always increase (Figure 5, $d = 0$).

The data (11-14) available to test the predicted thermal sensitivity of the batch-culture maximum-specific-growth-rate coefficient were obtained from substrate consumption experiments. From equation (13a), the maximum-velocity coefficient for substrate consumption is μ_m/Y . Data presented in this form must be multiplied by a yield coefficient Y to convert to μ_m . If the yield coefficient is assumed to be practically constant, then μ_m/Y should show the same thermal sensitivity pattern as μ_m . The thermal sensitivity of μ_m/Y in batch culture is well described by the linear portion of the $d = 0$ curve in Figure 5, and so is that of μ_m as long as Y is nearly constant.

In continuous culture, the maximum-specific-growth-rate coefficient is according to equations (11b), (13b), and (22):

$$\mu_m \Big|_{d > 0} = \mu_m \Big|_{d = 0} + (c/s)d \quad (23)$$

The continuous-culture μ_m should increase linearly with dilution rate, and the influence of the dilution term should grow with rising temperature if s rises more slowly than c . If $c = s$, the continuous-culture μ_m should asymptotically approach the dilution

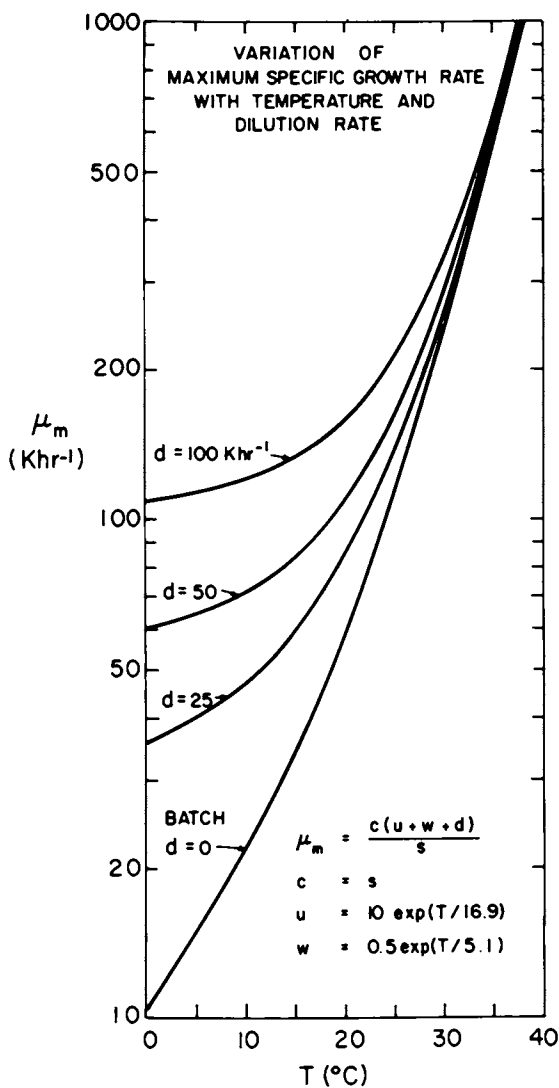


Figure 5. Theoretical thermal sensitivity of the maximum specific growth-rate coefficient in batch ($d = 0$) and continuous ($d > 0$) culture with the parameter values specified in Figure 3.

rate as temperature falls and the batch culture μ_m as temperature rises (Figure 5, $d > 0$).

The linear portions of the $d > 0$ curves in Figure 5 resemble the thermal sensitivities observed for μ_m (17,18) and μ_m/Y (15,16, 19) in continuous culture. Moreover, in agreement with equation (23) μ_m/Y has been observed to increase linearly with dilution rate (20). It has also been seen to decrease slightly with increasing dilution rate (21), which disagrees with equation (23).

Maximum-Velocity Coefficients V_B , V_M . According to equations (11b) and (15c), the maximum-velocity coefficient for biomass production depends on the microscopic rate coefficients as follows:

$$V_B = (1/s) [(c - s)w + cu] + [(c - s)/s]d \quad (24)$$

In general, depending especially on the relative sizes of c and s , this maximum-velocity coefficient may vary in a complicated fashion with both temperature and dilution rate. However, as c approaches s in value, the influence of all the micro-coefficients but u vanishes, and in the limit of $c = s$,

$$V_B = u \quad (25)$$

In this special case only, the maximum-velocity coefficient for biomass production would show the same exponential temperature dependence in continuous culture as it does in batch culture.

The maximum-velocity coefficient for metabolite excretion as given by equation (17b) is identically equal to e . As a result, it should generally rise exponentially with temperature and be insensitive to dilution rate. Thus, the maximum-velocity coefficient for metabolite excretion in batch culture should also be identical to that seen in continuous culture.

No thermal sensitivity data could be found for V_B or V_M . So, the validity of equations (17b), (24), and (25) awaits testing.

Threshold Coefficient S_T . For batch culture and the special case $c = s$, the thermal sensitivity of the threshold coefficient is determined as follows by equations (15d), (20), and (25):

$$S_T \Big|_{d=0} = (w/s) + (w/u) (w/s) \quad (26)$$

At temperatures where u dominates w , the batch-culture threshold coefficient should fall exponentially with temperature if s rises more rapidly with temperature than w . At temperatures where w dominates u , it should also fall exponentially with rising temperature if su rises more rapidly than w^2 . If both terms decrease as temperature rises, it should always diminish as temperature rises. If the term dominant at low temperatures falls

with rising temperature and the other term increases, it should have a thermal minimum. If both terms rise with temperature, it should always rise with temperature (Figure 6, $d = 0$).

None of the batch-culture thermal sensitivity experiments reported any values for S_T , so the validity of equation (26) and the $d = 0$ curve in Figure 6 can't be judged now.

For continuous culture and the special case $c = s$, equations (11b), (15d), and (26) determine the thermal sensitivity of the threshold coefficient as follows:

$$S_T \Big|_{d > 0} = S_T \Big|_{d = 0} + (1/s) [1 + 2 (w/u)] d + (1/su)d^2 \quad (27)$$

According to equation (27), the continuous-culture threshold coefficient is a quadratic function of dilution rate when $c = s$; however, the magnitude of the quadratic term decreases exponentially with rising temperature because of the factor $1/su$. The linear term will vanish too if su rises more rapidly with temperature than w does. The continuous-culture threshold coefficient should increase when the batch culture threshold coefficient rises with temperature and dominates the dilution terms. It should have a thermal minimum if a declining term dominates at low temperature and an increasing term dominates at high temperature (Figure 6, $d > 0$). The temperature at which this minimum occurs rises almost linearly with the logarithm of the dilution rate as long as the locus of minima (dashed line, Figure 6) parallels the $d = 0$ curve.

In continuous reactors, the threshold coefficient is identical with the steady state substrate concentration (17,18). For increasing temperatures, it has been observed to fall (17,18) and show a minimum (18). These responses are consistent with the $d > 0$ curves shown in Figure 6. It has also been observed to increase nonlinearly with dilution rate until washout occurred (17,18). In both instances, the slope at low dilution rates decreased with rising temperature. The observed responses to increasing dilution rate are also consistent with equation (27).

At this point, it would appear that one can account for most of the observed effects of temperature and dilution rate on the macro-coefficients by simply assuming temperature dependencies such as those shown in Figure 3 for the micro-coefficients in equations (20) - (27). These equations with the parameter values specified in Figure 3 will now be used to analyze the thermal sensitivity of the net biomass production and metabolite excretion rates.

Thermal Sensitivity of Process Rates

Rate Isotherms. Depending on substrate concentration, three thermal sensitivity patterns may be seen in both batch and continuous reactors when the net biomass production rate (as specified by equations (11b) and (15) and Figures 3, 4, and 6) is plotted

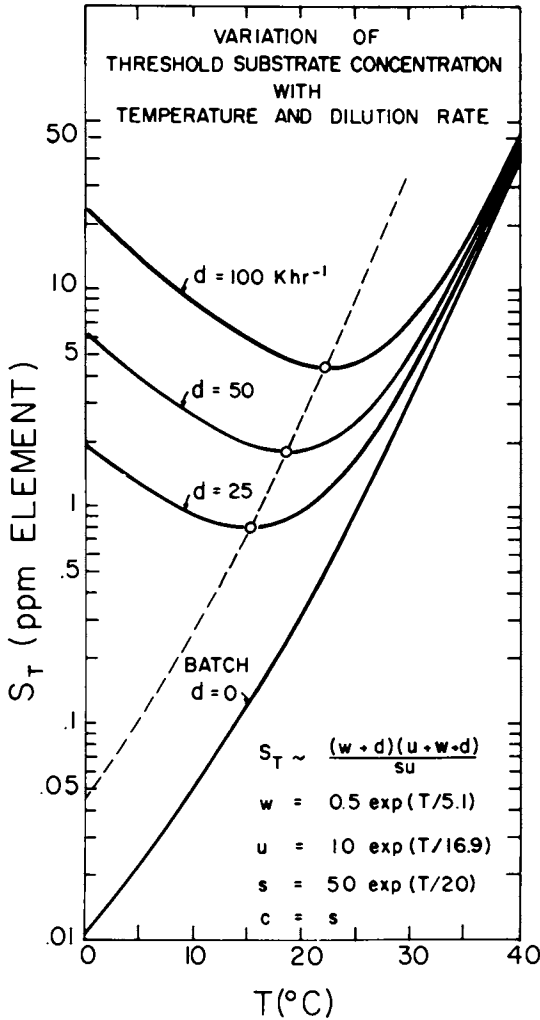


Figure 6. Theoretical thermal sensitivity of the threshold coefficient in batch ($d = 0$) and continuous ($d > 0$) culture with the parameter values specified in Figure 3. Dashed line, locus of thermal minima (\circ).

versus substrate concentration with temperature as a parameter (Figure 7). At low substrate concentrations ($S < 1.2$), the rate diminishes as temperature rises and hence shows a negative thermal sensitivity; whereas, at high substrate concentrations ($S > 4.4$), the rate increases with temperature and thus has a positive thermal sensitivity. At intermediate substrate concentrations ($1.2 < S < 4.4$), the rate first rises and then falls with increasing temperature. In other words, at moderate substrate concentrations, the thermal sensitivity switches sign from positive to negative, which means the rate goes through a maximum as temperature rises. Moreover, the maximum rate is determined by a higher temperature isotherm as substrate concentration increases. As a consequence, the optimum temperature should rise when substrate concentration increases.

The rate isotherms for metabolite excretion (as specified by equations (11b) and (17) and Figures 3 and 4) show the same three thermal sensitivity patterns as the net biomass production rate isotherms. Thus, the rate of metabolite excretion may also have an optimum temperature that shifts to higher values as substrate concentration rises.

Rate Isoconcentrates. The increase of optimum temperature with increasing substrate concentration is plainly seen by plotting rate versus temperature with substrate concentration as a parameter (Figures 8 and 9). The families of rate isoconcentrates for net biomass production and metabolite excretion also appear qualitatively similar. However, the maxima of corresponding isoconcentrates occur at quite different temperatures. For example, when $S = 1$ ppm, the optimum temperature for the net biomass production rate would be about 16°C (Figure 8) and that for the metabolite excretion rate would be about 28°C (Figure 9). Note that if the operating temperature of the reactor were set at the optimum temperature for the metabolite excretion rate, the net biomass production rate would be severely suboptimal (Figure 8). But if it were set at the optimum temperature for the net biomass production rate, the metabolite excretion rate would be only slightly suboptimal (Figure 9).

Shift of Optimum Temperature. Figure 10 shows how the temperature that maximizes the rate of each process varies with both substrate concentration and dilution rate. In this regard, the thermal sensitivities of the two processes differ substantially.

The optimum operating temperature for the net biomass production rate is nearly insensitive to dilution rate, but increases almost linearly with the logarithm of substrate concentration when this concentration exceeds the minimum value of the threshold coefficient (Figure 6).

In contrast, the optimum operating temperature for the metabolite excretion rate is strongly affected by both dilution rate and substrate concentration. As substrate concentration

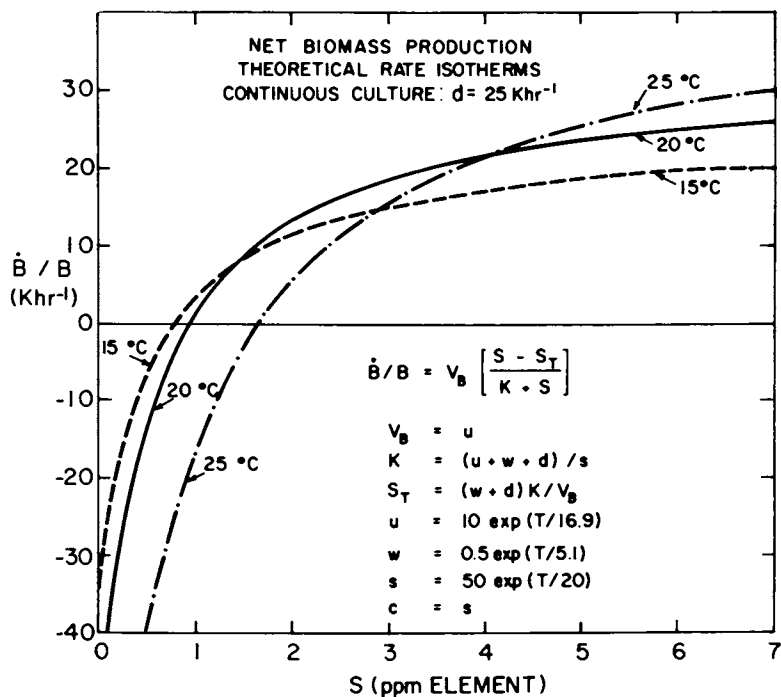


Figure 7. Predicted influence of substrate concentration on the rate of net biomass production, with temperature as a parameter. Parameter values correspond to Figures 3-6. Note shift of optimum temperature to higher values with increasing substrate concentration.

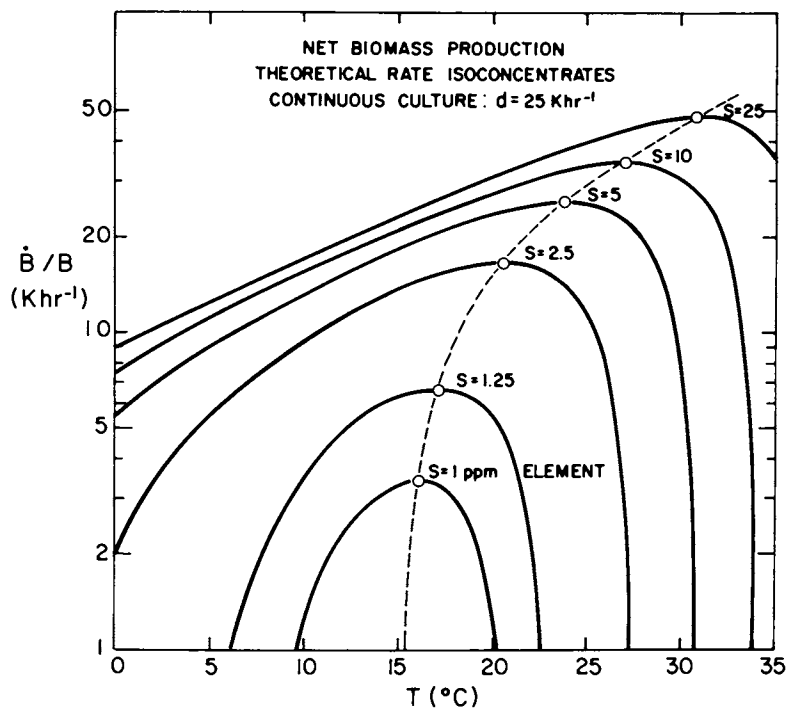


Figure 8. Predicted influence of temperature on the rate of net biomass production with substrate concentration as a parameter. Parameter values correspond to Figures 3-7. Dashed line, locus of thermal rate maxima (O). Note shift of optimum temperature to higher values as substrate concentration rises.

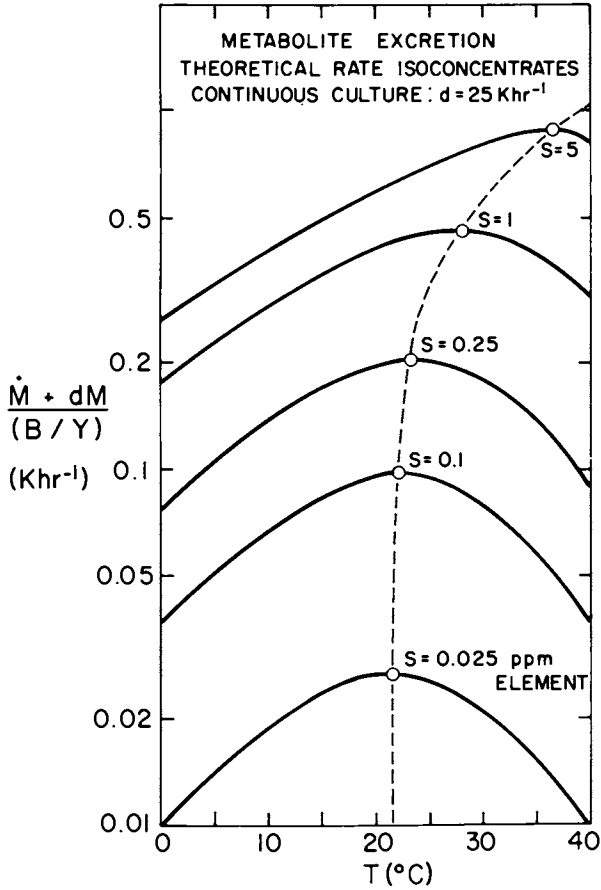


Figure 9. Predicted influence of temperature on the rate of metabolite excretion with substrate concentration as a parameter. Solid lines, curves generated from Equations 11b and 17 with the parameter values given in Figures 3 and 4. Dashed line, locus of thermal rate maxima (○).

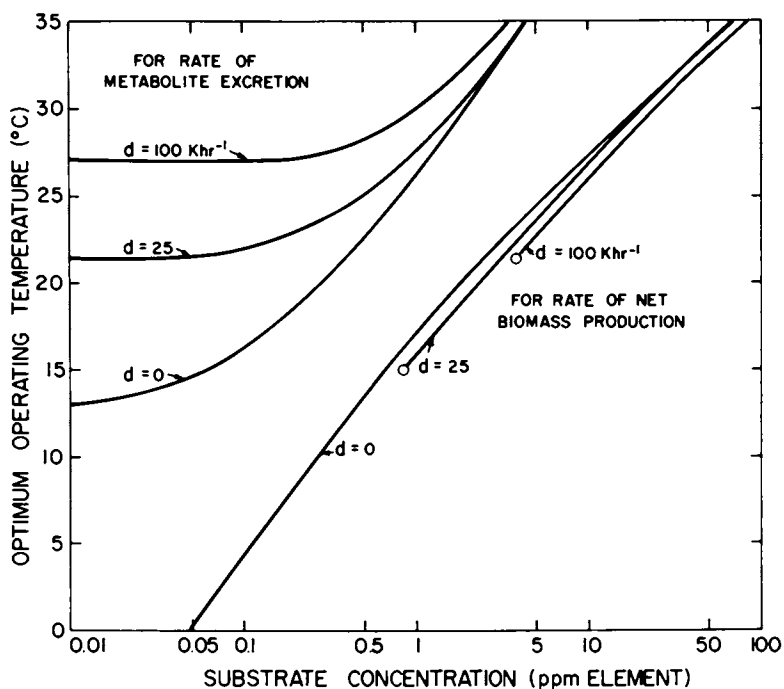


Figure 10. Predicted influence of substrate concentration and dilution rate on the temperature that maximizes the rates of net biomass production and metabolite excretion in batch ($d = 0$) and continuous ($d > 0$) culture.

becomes very low, the optimum temperature asymptotically approaches a minimum value characteristic of each dilution rate. The minimum optimum temperature is the temperature at which the slope of the half-saturation coefficient (Figure 4) equals that of the maximum-velocity coefficient, namely, the microscopic excretion rate coefficient e . As substrate concentration increases, the influence of the dilution rate progressively diminishes, and the optimum temperature curves converge. At high substrate concentrations, the optimum temperature increases almost linearly with the logarithm of substrate concentration.

Thermo-Chemical Optimization of Process Rates

At this point, the goal of this paper has been achieved. The two families of curves shown in Figure 10 constitute thermo-chemical rate-optimization constraints between reactor temperature, substrate concentration, and dilution rate. When any two of these three variables are fixed, each family specifies what value the third must have to maximize its rate. The separation of the two families means that both rates cannot be simultaneously maximized. As a result, an optimization strategy may be needed, such as operating at the optimum temperature of the process whose rate is most sensitive to temperature.

Summary and Conclusions

This paper showed how changes in substrate concentration and dilution rate may shift the optimum temperature of microbial processes whose rates saturate in substrate concentration according to Monod rate laws. The optimum temperature shift was attributed to the effects of temperature and dilution rate on the macro-coefficients in the Monod rate laws. Equations describing these effects were derived from a suitably modified Michaelis-Menten reaction mechanism. With only a few exceptions, these equations agreed with published data when Arrhenius temperature dependencies were assumed for the micro-coefficients in the reaction mechanism. As a consequence, these equations and the optimum temperature curves may be considered as plausible, experimentally testable hypotheses. They deserve careful quantitative testing because they promise to unify heretofore fragmentary and seemingly contradictory batch and continuous culture data. Such unification is needed to develop a rational methodology for optimizing the design and operation of biological reactors in which substrate concentration, temperature, and dilution rate are economically important variables.

Legend of Symbols

- A \equiv pre-exponential factor in Arrhenius temperature law; same units as k.
- B \equiv total biomass concentration in reactor; equals sum of B_c plus B_n ; mg dry weight per liter.
- B_c \equiv biomass concentration associated with substrate consumption sites capable of consuming substrate; mg dry weight per liter.
- B_n \equiv biomass concentration associated with substrate consumption sites not capable of consuming substrate; mg dry weight per liter.
- C \equiv total concentration of substrate consumption sites in microbial population; equals sum of C_c plus C_n ; number of sites per liter.
- C_c \equiv concentration of substrate consumption sites capable of consuming substrate; number of sites per liter.
- C_n \equiv concentration of substrate consumption sites not capable of consuming substrate; number of sites per liter.
- E \equiv concentration of free enzyme.
- E_A \equiv apparent activation energy; cal./mol.
- ES \equiv concentration of enzyme-substrate complex.
- K \equiv half-saturation coefficient; same units as S.
- K_m \equiv the Michaelis-Menten half-saturation coefficient.
- M \equiv concentration of metabolite of interest; same units as S.
- N \equiv concentration of microorganisms in reactor; number of organisms per liter.
- P \equiv concentration of product(s).
- R \equiv gas constant = $1.987 \text{ cal. mol}^{-1} \text{ K}^{-1}$.
- S \equiv substrate concentration in reactor; ppm of an element.
- S_0 \equiv inlet substrate concentration; same units as S.

Continued on next page

- S_T \equiv threshold coefficient; steady-state substrate concentration that must be exceeded for a positive net biomass production rate; same units as S .
- T \equiv temperature; $^{\circ}\text{C}$.
- T_K \equiv temperature; $^{\circ}\text{K}$.
- V_B \equiv maximum possible specific rate of net biomass production in the reactor; time^{-1} (e.g., Khr^{-1}).
- V_M \equiv maximum possible rate of gross metabolite formation; time^{-1} (e.g., Khr^{-1}).
- Y \equiv yield coefficient; ppm dry weight produced per ppm element consumed or excreted.
- c \equiv microscopic substrate-consumption rate coefficient; $(\text{ppm element})^{-1} \text{time}^{-1}$.
- d \equiv dilution rate (flow/volume); rate at which substrate, biomass, and metabolite displaced from culture vessel; time^{-1} .
- e \equiv microscopic metabolite-excretion rate coefficient; time^{-1} .
- k \equiv generic microscopic rate coefficient, e.g., c, f, s, u, w .
- k_1 \equiv microscopic rate coefficient for formation of enzyme-substrate complex.
- k_2 \equiv microscopic rate coefficient for disassociation of enzyme-substrate complex.
- k_3 \equiv microscopic rate coefficient for formation of product.
- n \equiv number of substrate molecules needed to fill a substrate consumption site.
- s \equiv microscopic substrate-saturation rate coefficient; $(\text{ppm element})^{-1} \text{time}^{-1}$.
- u \equiv microscopic unsaturation rate coefficient; time^{-1} .
- w \equiv microscopic wastage rate coefficient; time^{-1} .
- α \equiv value of generic microscopic rate coefficient at 0°C ; same units as k .

- β \equiv average biomass per microorganism; mg dry weight per organism.
- γ \equiv average number of substrate consumption sites per organism; number of sites per organism.
- μ_m \equiv maximum specific growth rate coefficient; time⁻¹.
- θ_α \equiv retardation temperature; °C.

Acknowledgments

The research reported in this paper was supported in part by the Department of Mechanical Engineering at M.I.T. through a grant from the Thermo Electron Fund.

The figures were drawn by Michele Halverson, and the text was prepared for publication by Anna M. Piccolo. The author greatly appreciates their efforts in her behalf.

Literature Cited

1. Dorn, F.L.; Rahn, O. Arch. Mikrobiol. 1939, 10, 6-12.
2. Aiba, S.; Humphrey, A.E.; Millis, N.F. "Biochemical Engineering;" 2nd ed.; Academic: New York, 1973; pp. 93-94, 103-110, 115-117.
3. Johnson, F.H.; Eyring, H.; Steblay, R.; Chaplin, H.; Huber, C.; Gherardi, G. J. Gen. Physiol. 1945, 28, 463-537.
4. Koffler, H.; Johnson, F.H.; Wilson, P.W. J. Am. Chem. Soc. 1947, 69, 1113-1117.
5. Hromatka, O.; Kastner, G.; Ebner, H. Enzymologia 1953, 15, 337-350.
6. Deppe, K.; Engel, H. Zentralbl. Bakteriol. Parasitenkd. Infek. Hyg. Abt. II 1960, 113, 561-568.
7. McCombie, A.M. J. Fish. Res. Bd. Canada 1960, 17, 871-894.
8. Quinlan, A.V. Water Res. 1980, 14, 1501-1507.
9. Quinlan, A.V. J. Franklin Inst. 1980, 310, 325-342.
10. Quinlan, A.V. J. Thermal Biol. 1981, 6, 103-114.
11. Knowles, G.; Downing, A.L.; Barrett, M.J. J. Gen. Microbiol. 1965, 38, 263-278.
12. Laudelout, H.; van Tichelen, L. J. Bact. 1960, 79, 39-42.
13. Stratton, F.E.; McCarty, P.L. Environ. Sci. Technol. 1967, 1, 405-410.
14. Novak, J.T. J. Water Poll. Control Fed. 1974, 46, 1984-1994.
15. Lawrence, A.W.; McCarty, P.L. J. Water Poll. Control Fed. 1969, 41, R1-R17.

16. Lawrence, A.W. "Anaerobic Biological Treatment Processes;" *Adv. Chem. Ser.* 105; American Chemical Society: Washington, DC, 1971; pp. 163-189.
17. Topiwala, H.; Sinclair, C.G. *Biotechnol. Bioeng.* 1971, 13, 795-813.
18. Muck, R.E.; Grady, C.P.L., Jr. *ASCE J. Environ. Eng. Div.* 1974, 100, 1147-1163.
19. Charley, R.C.; Hooper, D.G.; McLee, A.G. *Water Res.* 1980 14, 1387-1396.
20. Caperon, J.; Meyer, J. *Deep-Sea Res.* 1972, 19, 619-632.
21. Eppley, R.W.; Renger, E.H. *J. Phycol.* 1974, 10, 15-23.
22. Michaelis, L.; Menten, M.L. *Biochem.Z.* 1913, 49, 333-369.
23. Briggs, G.E.; Haldane, J.B.S. *J. Biol. Chem.* 1925, 19, 338-339.
24. Bailey, J.E.; Ollis, D.F. "Biochemical Engineering Fundamentals;" McGraw-Hill: New York, 1977; pp. 92-98, 345-347.
25. Monod, J. *Ann. Rev. Microbiol.* 1949, 3, 371-394.
26. Holling, C.S. *Mem. Ent. Soc. Can.* 1965, 5-60.
27. Caperon, J. *Ecology* 1967, 48, 715-722.
28. Smith, F.E. "Eutrophication: Causes, Consequences, Correctives;" Rohlich, G.A., Ed.; National Academy of Sciences: Washington, DC, 1969; pp. 631-645.
29. Odum, H.T. "Modelling of Marine Systems;" Nihoul, J.C.J., Ed.; Elsevier: Amsterdam, 1975; pp. 133-135.
30. Quinlan, A.V. "Energy and Ecological Modelling;" Mitsch, W.J., Bosserman, R.W., Klopatek, J.M., Eds.; Elsevier: Amsterdam, 1981; pp. 635-640.
31. Eadie, G.S. *J. Biol. Chem.* 1942, 146, 85-93.
32. Augustinsson, K.-B. *Acta Physiol. Scand.* 1948, 15 (suppl. 52), 99-100.
33. Dowd, J.E.; Riggs, D.S. *J. Biol. Chem.* 1965, 240, 863-869.
34. Arrhenius, S. "Quantitative Laws in Biological Chemistry;" Bell: London, 1915; pp. 49-60.

RECEIVED July 7, 1982

Kinetics of Yeast Growth and Metabolism in Beer Fermentation

IVAN MARC and JEAN-MARC ENGASSER

Institut National Polytechnique de Lorraine, Laboratoire des Sciences du Génie
Chimique, CNRS-ENSIC, Nancy 54042 France

MANFRED MOLL and BRUNO DUTEURTRE

Centre de Recherche TEPRAL, Champigneulle 54250 France

An experimental and theoretical kinetic study of yeast growth and flocculation, sugar and amino acid uptake, ethanol, CO₂ and other metabolite production during beer fermentation is presented. Cellular growth, and consequently amino acids uptake and some metabolites production, stops after about 100 hours of fermentation. Yeast flocculation, which starts when glucose is totally removed from the medium, then becomes a predominant phenomenon. Fermentable sugars are sequentially taken up, maltose and maltotriose being repressed by glucose. Ethanol and CO₂ production rate remain essentially proportional to the total rate of sugar uptake both during the growth and flocculation phase. The increase with temperature of substrate uptake, yeast growth and flocculation, and metabolite production rate is simply described by Arrhenius type of relationships.

The conversion by yeast of sugars and amino acids into aromatic compounds represents a central process in brewing. A quantitative understanding of the microbial events taking place during the transformation of wort into beer is essential when considering the automatic control of this fermentation.

A first kinetic modeling of yeast growth, sugar and amino acid uptake and aromatic metabolite production was previously proposed (1,2). On the basis of recent experimental results we propose a new model which takes into account the evolution of the yeast viability during the fermentation, and describes in greater detail the flocculation phase and the production of CO₂. The kinetic study is specially aimed at establishing relationships between the wort initial composition, the final beer quality and various process parameters, such as temperature, pressure and inoculum size.

0097-6156/83/0207-0489\$06.00/0

© 1983 American Chemical Society

EXPERIMENTAL

The experimental part of this work was performed at the TEPRAL Beer Research Center in Champigneulle, France. Beer production was carried out either in laboratory tubular fermentors, 1,80 m height and 4,5 cm inner diameter, containing 2 liters of medium, or in 1000 liters cylindro-conical pilot plant fermentors without mechanical agitation. Standard industrial wort and yeast *Saccharomyces uvarum* 0019 were used. The initial dissolved oxygen concentration in the wort was fixed at 8 ppm. The temperature was maintained constant at either 10° C or 14° C during the whole fermentation. The overhead pressure was 1 atm with the laboratory fermentor and 2,2 atm with the pilot plant.

Samples of 80 cm³ and 4 liters were periodically withdrawn from the laboratory and pilot vessel, respectively. Yeast concentration was determined either from the dry weight or with a Coulter counter. The various sugars, glucose, fructose, maltose, saccharose, maltotriose were analyzed by high pressure liquid chromatography. The concentration of the twenty amino acids were determined by ion exchange chromatography. Ethanol was assayed by microcalorimetry and other metabolites by gas chromatography.(3)

THE KINETIC MODEL

In conventional fermentation models the central equation usually expresses cellular growth as a function of substrate, product and cellular concentration in the medium. Product formation is then related to cell growth or cellular concentration, whereas substrate uptake rate may include several contributions from cellular growth, maintenance and product formation. Moreover, these models most often are based on constant yields.

In view of the experimental results (4) it is clear that the conventional approach cannot be used to model beer fermentation. First, the fermentation medium contains several sugars which are assimilated at different rates. The uptake of each sugar may be limited by its own concentration and inhibited by the presence of others. Second, the investigated beer fermentation from a kinetic point of view is complicated by yeast flocculation which becomes predominant during the second stage of the process, and which is affected by one of the fermentable sugars, namely glucose. Third, the various yields between fermentable sugars uptake, yeast growth, ethanol and CO₂ formation are not constant during the course of the fermentation. Finally, the rate of aromas production is related to either yeast growth rate or sugars uptake rate.

In order to describe the influence of the initial wort composition on the fermentation process the proposed model is based on separate rate equations for the various sugars uptake. Production of yeast, ethanol and carbon dioxide is then related to the total uptake of fermentable sugars with variable yields. The rate of amino acids uptake and other metabolites production is expressed as a function of growth rate or sugars uptake rate with constant or variable yields.

Yeast growth and flocculation. Distinction is made between the total yeast produced during the growth phase and the suspended yeast concentration in the fermentation medium. The increase in total yeast concentration in the fermentor is directly related to the total rate of fermentable sugar consumption.

$$\frac{d(X_T)}{dt} = - R_{X/S} \frac{d(\text{TFS})}{dt} \quad (1)$$

(X_T) being the total yeast concentration

(TFS) the total fermentable sugar concentration

$R_{X/S}$ the yeast to sugar yield

The experimentally observed decrease of $R_{X/S}$ during the fermentation has previously been attributed to the decrease in intracellular sterol concentration as a result of yeast growth in the absence of oxygen. We found it most convenient to mathematically relate the decrease of $R_{X/S}$ to the increase of the ethanol concentration in the medium, (Eth) , as :

$$R_{X/S} = Y_{X/S} \frac{1}{1 + \frac{(\text{Eth})^4}{K_E}} \quad (2)$$

with $Y_{X/S}$ the initial yeast to sugar yield

K_E the ethanol inhibition constant.

Yeast flocculation, an essential phenomenon in beer fermentation, is influenced by the medium composition, especially by the glucose concentration, and is delayed by the mixing effect of CO_2 production. The time variation of the suspended yeast concentration is thus taken as the difference between the growth and flocculation rate as :

$$\frac{d(X_S)}{dt} = \frac{d(X_T)}{dt} - \left[K_f \frac{1}{1 + \frac{(\text{Gl})}{K_{\text{Gl}}^f}} - k_m r_{\text{CO}_2}^d \right] (X_S) \quad (3)$$

with (X_S) the suspended yeast concentration

k_f the yeast flocculation constant

(Gl) the glucose concentration

K_{Gl}^f the inhibition constant of flocculation by glucose

k_m the mixing constant by CO_2

$r_{\text{CO}_2}^d$ the rate of CO_2 desorption

Sugars consumption. Saccharose is first hydrolysed into glucose and fructose at the cell surface, then the four fermentable sugars, glucose, fructose, maltose and maltotriose are assimilated at different rates depending on the medium composition. Glucose is taken up the fastest as the maltose, maltotriose and fructose intracellular transports are inhibited by glucose. Assuming that the substrates are mainly consumed by the suspended yeasts, the following rate expressions are proposed to describe the time variation of fermentable sugars :

$$\frac{d(\text{Gl})}{dt} = - V_{\text{Gl}} \frac{(\text{Gl})}{K_{\text{Gl}} + (\text{Gl})} (X_S) - \frac{180}{342} \frac{d(\text{Sac})}{dt} \quad (4)$$

$$\frac{d(\text{Mal})}{dt} = - V_{\text{Mal}} \frac{(\text{Mal})}{K_{\text{Mal}} + (\text{Mal})} \frac{1}{1 + \frac{(\text{Gl})}{K_{\text{Gl}}^i}} (X_S) \quad (5)$$

$$\frac{d(\text{Sac})}{dt} = - k_{\text{sac}} (\text{Sac}) (X_S) \quad (6)$$

$$\frac{d(\text{Mlt})}{dt} = - V_{\text{Mlt}} \frac{(\text{Mlt})}{K_{\text{Mlt}} + (\text{Mlt})} \frac{1}{1 + \frac{(\text{Gl})}{K_{\text{Gl}}^{i'}}}} (X_S) \quad (7)$$

$$\frac{d(\text{Fr})}{dt} = - V_{\text{Fr}} \frac{(\text{Fr})}{K_{\text{Fr}} + (\text{Fr})} \frac{1}{1 + \frac{(\text{Gl})}{K_{\text{Gl}}^{i''}}}} (X_S) - \frac{180}{342} \frac{d(\text{Sac})}{dt} \quad (8)$$

with (Gl), (Mal), (Sac), (Mlt), (Fr) the glucose, maltose, saccharose, maltotriose and fructose concentration.

V_{Gl} , V_{Mal} , V_{Mlt} , V_{Fr} the maximal rate of glucose, maltose, maltotriose and fructose consumption.

K_{Gl}^i , $K_{\text{Gl}}^{i'}$, $K_{\text{Gl}}^{i''}$ glucose inhibition constants

k_{sac} , K_{Gl} , K_{Mal} , K_{Mlt} , K_{Fr} kinetic constants.

The time variation of the total fermentable sugar concentration is calculated by adding the previously defined rates of variation of the concentration of the individual sugars.

Amino acids consumption. Two rate expressions were used. For threonine, serine, methionine, isoleucine, leucine, lysine, the rate of consumption is proportional to the rate of yeast growth, but can be limited by the amino acid concentration

$$\frac{d(\text{AA})}{dt} = - V_{\text{AA}} \frac{(\text{AA})}{K_A + (\text{AA})} \frac{d(X_T)}{dt} \quad (9)$$

(AA) being the amino acid concentration in the medium
 V_{AA} the maximal rate of amino acid consumption
 K_{AA} a kinetic constant.

For other amino acids, such as aspartic acid, glutamic acid, alanine, valine, tyrosine, phenylalanine, histidine, arginine, an additional inhibitory effect of threonine demonstrated by experiments with threonine enriched wort, is considered

$$\frac{d(AA)}{dt} = -V_{AA} \frac{(AA)}{K_A + (AA)} \frac{1}{1 + \frac{(Thr)}{K_{Thr}}} \frac{d(X_T)}{dt} \quad (10)$$

with K_{Thr} the inhibition constant by threonine.

Ethanol production. Ethanol production is assumed directly related to the total rate of fermentable sugar consumption

$$\frac{d(Eth)}{dt} = -R_{E/S} \frac{d(TFS)}{dt} \quad (11)$$

The ethanol to sugar yield, $R_{E/S}$, was found to slightly increase during the fermentation as a result of the decrease of the growth yield. Based on a carbon balance of the sugar conversion into yeast, ethanol and CO_2 , the variation of $R_{E/S}$ can be related to the previously expressed variation of $R_{X/S}$ as

$$R_{E/S} = Y_{E/S} \left[1 + \frac{0,45 (Y_{X/S} - R_{X/S})}{0,52 Y_{E/S} + 0,27 Y_{CO_2/S}} \right] \quad (12)$$

with $Y_{E/S}$ and $Y_{CO_2/S}$ as the initial ethanol to sugar and CO_2 to sugar yield, respectively.

Other metabolite production. The rate of production of aromatic compounds - higher alcohols, esters, ethers, acids - is assumed proportional to the rate of yeast growth. Some, like diketones, are reassimilated or chemically transformed after excretion, so that the following general equation was used :

$$\frac{d(M)}{dt} = Y_{M/X} \frac{d(X_T)}{dt} - k_M (M) \quad (13)$$

with (M) the metabolite concentration
 $Y_{M/X}$ a proportionality constant between metabolite and yeast production
 k_M a first order transformation constant.

CO₂ production. The rate of carbon dioxide production is taken proportional to the total rate of sugar consumption. Produced CO₂ is either dissolved, or transformed into bicarbonate, or is desorbed into the gas phase when the dissolved concentration exceeds the saturation concentration. The desorption of CO₂ is enhanced by the natural convection resulting from the rising of CO₂ bubbles. It is thus assumed that the desorption rate is proportional to the rate of CO₂ production, i.e. approximately to the rate of fermentable sugar uptake. Consequently the rate of variation of dissolved CO₂ is written as :

$$\frac{d(\text{CO}_{2d})}{dt} = - R_{\text{CO}_2/S} \frac{d(\text{TFS})}{dt} - \frac{d(\text{HCO}_3^-)}{dt} + k_d \left[(\text{CO}_{2d}) - (\text{CO}_2)^* \right] \frac{d(\text{TFS})}{dt} \quad (14)$$

with (CO_{2d}) the dissolved CO₂ concentration

(CO₂)^{*} the saturation CO₂ concentration

(HCO₃⁻) the bicarbonate concentration

k_d the desorption constant

The CO₂ to sugar yield, R_{CO₂/S}, was observed to slightly increase during the fermentation. As previously for the variable ethanol to sugar yield, the value of R_{CO₂/S} can be related to the initial CO₂ to sugar yield, Y_{CO₂/S} and the variable yeast to sugar yield as

$$R_{\text{CO}_2/S} = Y_{\text{CO}_2/S} \left[1 + \frac{0,45 (Y_{X/S} - R_{X/S})}{0,52 Y_{E/S} + 0,27 Y_{\text{CO}_2/S}} \right] \quad (15)$$

Bicarbonate is considered in equilibrium with dissolved CO₂, with the pH decreasing from 5 to 4.2 during the fermentation. Desorbed CO₂ leaves the fermentor when the overhead pressure reaches the maximal tank pressure. Under these conditions

$$Q_{\text{CO}_2} = - k_d \left[(\text{CO}_{2d}) - (\text{CO}_2)^* \right] \frac{d(\text{TFS})}{dt} \quad (16)$$

Q_{CO₂} being the CO₂ flow rate leaving the fermentor.

The resulting set of differential equations is numerically integrated by standart Runge Kutta procedure. The different parameters of the model are determined to obtain the best agreement between the theory and the experimental results.

RESULTS AND DISCUSSION

Experiments were first performed in laboratory tube fermentors to study the yeast growth phase. The time change of total fermentable sugar concentration, total and suspended yeast concentration during beer fermentation is shown in Figure 1. As seen, despite a

high level of fermentable sugars, yeast growth considerably slows down and flocculation becomes a predominant phenomenon after 80 hours of fermentation. When the initial wort is enriched in glucose, one observes in Figure 2, that yeast growth rate is not influenced, but flocculation is delayed until glucose consumption is completed, which confirms previously reported dependence of flocculation on glucose concentration (5).

Figure 3 shows the experimentally determined and the calculated time variation of suspended yeast concentration in pilot plant fermentor at two different temperatures. As seen, decreasing the temperature decreases the initial growth rate, delays the onset of flocculation and decreases the rate of flocculation. A satisfactory modeling is provided by equations 1 to 3 using a yeast to sugar yield decreasing from 0,065 to 0,018 with increasing ethanol concentration, and an Arrhenius type of temperature dependence of the maximal rates of sugar consumption and of the flocculation constant.

The experimentally measured and the calculated decrease with time of the five fermentable sugars at 14° C in the pilot plant fermentor are represented in Figure 4. As expected, glucose, saccharose, fructose, maltose and maltotriose are removed at different rates from the medium. Glucose, which is partly produced by the saccharose hydrolysis, is taken up the fastest, the initial assimilation of maltose and maltotriose being repressed by the presence of glucose.

Figure 5, which represents the experimental and theoretical results obtained for four of the twenty considered amino acids, shows that amino acids present in the wort are consumed at very different rates. Proline is practically not taken up, whereas threonine is totally consumed after 70 hours of fermentation. Others, like leucine and valine, are partially assimilated during the yeast growth phase. It has been verified that amino acids are not limiting at the end of the growth phase.

Ethanol production, which is shown in Figure 6 at 10° C and 14° C, is adequately related to the fermentable sugars consumption by equations 11 and 12, with an ethanol to sugar yield increasing slightly from 0,46 to 0,485. The time variation of two of the other investigated metabolites, acetolactate and phenyl ethanol, as experimentally observed and calculated from equation 13, is represented in Figure 7.

Finally Figure 8 shows the measured change with time of dissolved CO₂ concentration, fermentor overhead pressure, and CO₂ outlet flow rate at 14° C in the pilot plant. As demonstrated by the good agreement between the experimental points and the calculated curves, equations 14 to 16 provide an adequate modeling of CO₂ production, dissolution and desorption.

CONCLUSIONS

The experimental and theoretical results of this study are expected to improve the quantitative understanding of beer ferment-

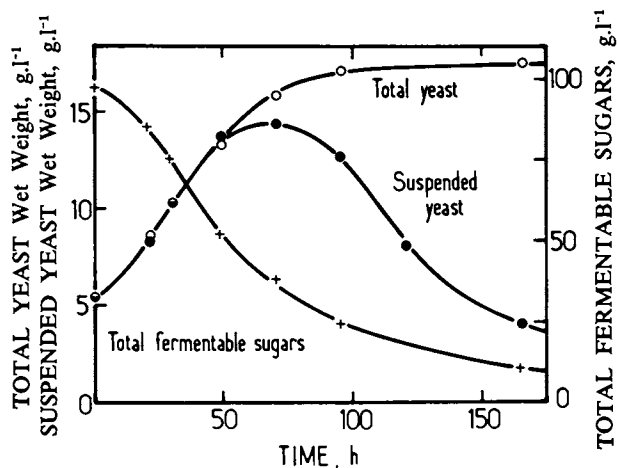


Figure 1. Time variation of total yeast, suspended yeast, and total fermentable sugar concentrations in a laboratory scale fermentation. Key: \circ , total yeast; \bullet , suspended yeast; $+$, total fermentable sugar.

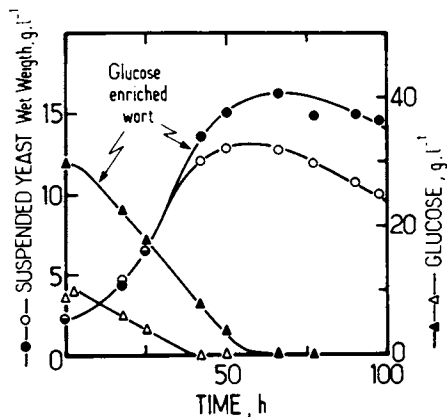


Figure 2. Time variation of glucose and suspended yeast concentration with standard and glucose-enriched (+ 20 g/L) wort.

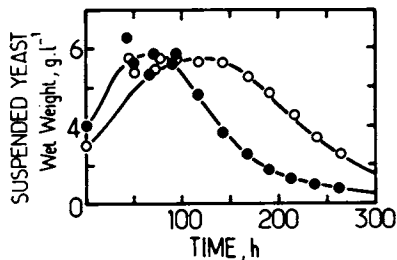


Figure 3. Experimental and theoretical yeast growth and flocculation kinetics at 14°C (\bullet) and 10°C (\circ).

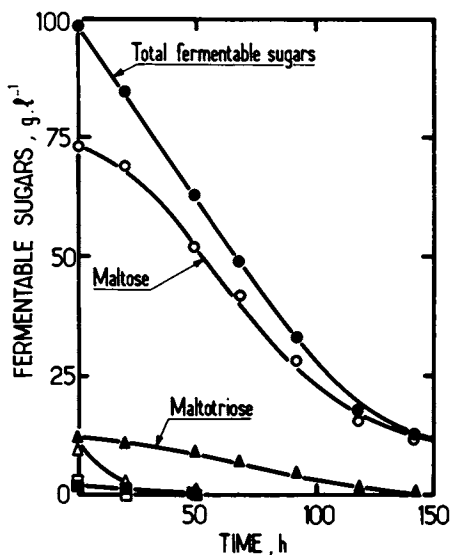


Figure 4. Experimental and theoretical kinetics of uptake of sugars at 14°C. Key: □, saccharose; ■, fructose; △, glucose; ▲, maltotriose; ○, maltose; ●, total fermentable sugars.

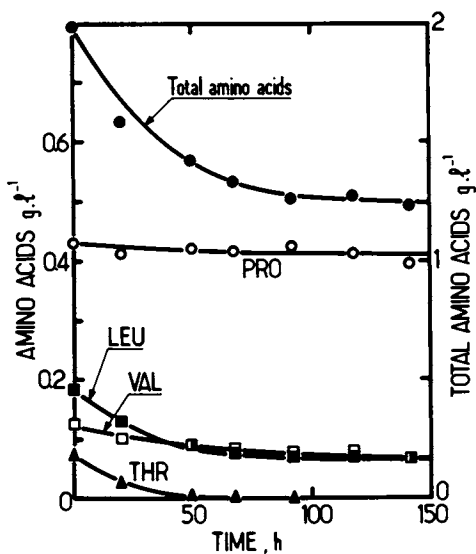


Figure 5. Experimental and theoretical kinetics of uptake of amino acids at 14°C. Key: ▲, threonine; □, valine; ■, leucine; ○, proline; ●, total amino acids.

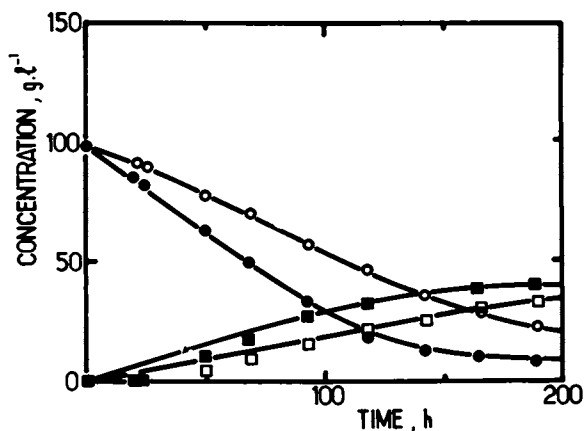


Figure 6. Experimental and theoretical kinetics of ethanol production (■ and □) and total fermentable sugar consumption (● and ○) at 14°C and 10°C. Open symbols, 10°C; solid symbols, 14°C.

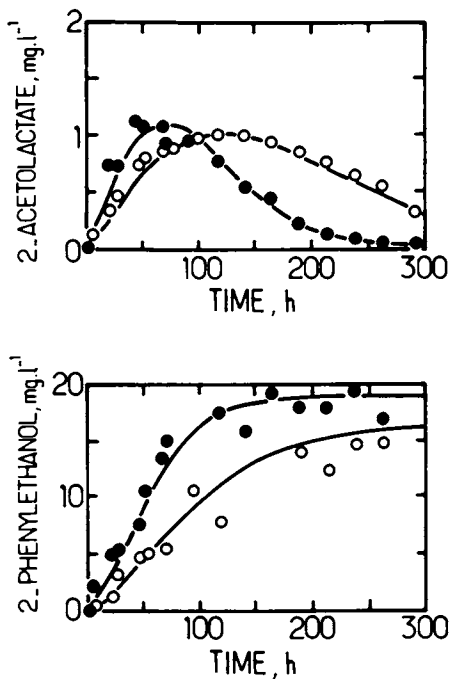


Figure 7. Experimental and theoretical time variation of acetolactate and phenylethanol concentration at 10°C (○) and 14°C (●).

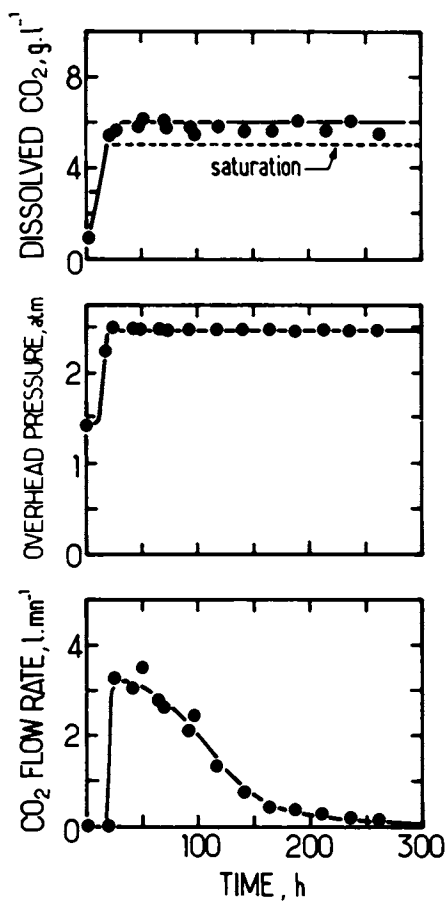


Figure 8. Experimental and theoretical time variation of dissolved CO₂, overhead pressure, and CO₂ exit flow rate at 14°C.

tation. An essential finding of both laboratory and pilot plant experiments is the decrease in cellular growth activity during the course of the fermentation, the growth phase ending after about 100 hours of fermentation. This fall in cellular viability is not caused by sugar or amino acids limitations. It may partly result from ethanol accumulation in the medium, or as suggested by other studies (6), from limitations in intracellular sterols which are no longer synthesized under anaerobic conditions. According to our results, the rate of sugar uptake is directly proportional to the suspended yeast concentration, the rate of amino acids uptake and of some aromatic metabolites production is directly related to the yeast growth rate, whereas ethanol and CO₂ production is essentially proportional to the total rate of sugar consumption.

As demonstrated by the good agreement between experiments and theory, the time variation of the different species in the fermentation medium can be adequately described by a relatively simple model based on yeast metabolism and the physical processes of yeast flocculation, CO₂ desorption and CO₂ mixing. Essential in the model is the introduction of a yeast to sugar yield depending on the measurable ethanol concentration to represent the loss of cellular viability.

Further experimental and theoretical investigations are being done to study in greater detail the possible influence of other key process parameters, pitching rate, pressure, wort aeration, on the fermentation process and the final beer quality.

LITERATURE CITED

1. Tepper, P. ; Marc, I. ; Engasser, J.M. ; Moll, M. ; Duteurtre, B. in Current Developments in Yeast Research (G. Stewart and I. Russel, eds) 1981, p. 129, Pergamon Press, Toronto
2. Engasser, J.M. ; Marc, I. ; Moll, M. ; Duteurtre, B. Proc. 18 th Eur. Brew. Conv. 1981, p. 579
3. Lehuede, J.M. ; Flayoux, R. ; Moll, M. ; 9 th Technicon International Symposium, Paris, 1979, p. 1
4. Marc, I. , Thesis Nancy, 1982
5. Amri, M.A. ; Bonaly, R. ; Duteurtre, B. ; Moll, M. Eur. J. Appl. Microbiol. 1979, 7, 227-234
6. Haukeli, A.D. ; Lie, S. Proc. 17 th Eur. Brew. Conv. 1979, p. 35.

RECEIVED June 29, 1982

Growth Inhibition Kinetics for the Acetone-Butanol Fermentation

JEANINE M. COSTA and ANTONIO R. MOREIRA¹

Colorado State University, Department of Agricultural and Chemical Engineering,
Fort Collins, CO 80523

The inhibitory effect of each fermentation product on the cell growth rate and the kinetics of product formation was studied for the acetone-butanol fermentation with Clostridium acetobutylicum ATCC 824. Inhibition of cell growth was studied by challenging cultures with varying concentrations of each product. There was a threshold concentration which must be reached before growth inhibition occurred. This concentration was found to vary with each inhibitor. Above the threshold concentration, there was a linear decrease of the growth rate with an increase in product concentration.

Due to the rising costs associated with producing chemicals from fossil fuels, alcohol fermentations based on renewable resources are becoming more and more attractive as an alternative route for obtaining commodity chemicals. However, a problem common to many of these fermentations is the relatively low concentration of the desired product in the final fermented broth. Bacterial ethanol fermentations stop at alcohol levels in the range of 5-8 weight percent (1). A more dramatic toxic effect is observed in the acetone-butanol fermentation. The total solvents concentration is 2-3 weight percent at the point where solvent levels are toxic to the producing Clostridium (2). Butanol, butyric acid, and acetic acid are the most toxic products of the acetone-butanol fermentation. It has been previously shown (3) that at butanol concentrations in the range of 0.10-0.15 M, 50% inhibition is observed simultaneously for the maximum specific growth rate, the nutrient uptake rate, and the membrane-bound ATPase activity. This end-product toxicity results in large

¹ Current address: International Flavors and Fragrances, Inc., Union Beach, NJ 07735

energy expenditures for product recovery as well as in large capital investments due to the large size equipment required to reach an economically attractive scale of production. Consequently, kinetic data is needed to develop a basic understanding of these fermentation processes and to permit an optimal design for the fermentor systems to be used for the production of these chemicals. This paper addresses the kinetics of end-product inhibition of cell growth in the acetone-butanol fermentation.

Materials and Methods

Microorganism and Culture Conditions. Clostridium acetobutylicum strain ATCC 824 was used in this study. Maintenance cultures were grown in corn mash medium for 72 hours at 37 C and then refrigerated at 4 to 5 C. The corn mash medium consisted of 5% (w/v) corn meal with 0.05% cysteine added to ensure for anaerobic conditions. The media was boiled with the appropriate volume of distilled water for one hour. The mash was then distributed into screw cap tubes (16 x 125 mm) and autoclaved for 15 minutes at 121 C.

The microorganism was routinely transferred anaerobically in screw cap tubes with 10 ml of medium comprised of 50% (v/v) thioglycollate 135C medium (Difco Laboratories, Detroit, Michigan) and 50% (v/v) soluble medium containing the following components in g/l: KH_2PO_4 , 0.75; K_2HPO_4 , 0.75; MgSO_4 , 0.20; $\text{MnSO}_4 \cdot \text{H}_2\text{O}$, 0.01; $\text{FeSO}_4 \cdot 7\text{H}_2\text{O}$, 0.01; NaCl, 1.00; cysteine, 0.50; yeast extract, 5.00; glucose, 60; asparagine. $\cdot\text{H}_2\text{O}$, 2.00; $(\text{NH}_4)_2\text{SO}_4$, 2.00.

Growth Challenge Studies. The effect of the fermentation products on the growth rate of Cl. acetobutylicum was determined by the following procedure. A 24-hour old culture was used as a 5% inoculum to flasks containing 200 ml of 2% (w/v) glucose soluble medium. After 10-12 hours, these cells were used as a 20% (v/v) inoculum for flasks containing soluble media with 2% (w/v) glucose. After a lag phase of 30-45 minutes, the cultures were challenged with various concentrations of ethanol, butanol, and acetone. Growth was monitored by hourly measurements of optical density at 560 nm.

The procedure for determination of growth rates in the presence of acetic and butyric acid was modified as follows. The inoculum was prepared by using cells from a corn tube as a 10% (v/v) inoculum for thioglycollate/soluble medium containing 20 g/l MES buffer (2-[N-morpholino] ethanesulfonic acid), (Sigma Chemical Co., St. Louis, MO). After 10-12 hours, these cells were used as a 20% (v/v) inoculum for flasks containing soluble media (20 g/l glucose + 20 g/l MES buffer). After a lag phase of 30-45 minutes, the cells were challenged with various concentrations of acetic and butyric acid.

pH Controlled Fermentation. A 7-liter New Brunswick Micro-ferm fermentor (New Brunswick Scientific, Edison, NJ) with a working volume of 4 liters was used in this study. The agitation speed was maintained at 200 rpm during the fermentation. The pH of the fermentation started at 6.2 and was allowed to fall to pH 5.0. The pH was thereafter maintained at 5.0 by the addition of 1 N NaOH on a demand basis. The temperature was controlled at 37 C.

Analysis. The cell density was measured at 560 nm using a Bausch and Lomb Spectronic 20 spectrophotometer.

Fermentation samples were collected and centrifuged immediately under refrigeration at 15,000 rpm for 10 minutes. The supernatants were stored in plastic vials and immediately frozen for subsequent analysis. The cell pellet was washed twice with distilled water. The cells were then resuspended in distilled water and placed in tared containers. The cell dry weight was determined after drying for 24 hours at 80 C.

The concentration of products in the supernatants was determined on a Varian model 2400 gas chromatograph equipped with a flame ionization detector. The chromatograph had installed a 6 ft x 1/8 in stainless steel teflon lined column packed with Chromosorb W-AW coated with 10% AT-1000. The temperature of the column was programmed from 100 C to 180 C at a rate of 20 C/min. Helium was used as the carrier gas at a flow rate of 30 ml/min. The flame ionization detector temperature was 230 C. A 10% (w/w) n-propanol solution containing 4% (w/w) H₂SO₄ was used as an internal standard.

The glucose concentration of the fermentation samples was measured by the DNSA (dinitrosalicylic acid) method (4) using glucose as a standard. Samples were diluted to contain less than 1 g/l glucose.

Results and Discussion

Product Challenged Growth Studies. To study the inhibitory factors of the acetone-butanol fermentation, the growth rates of Cl. acetobutylicum in the presence of each fermentation product were determined. The end products used in this study included ethanol, butanol, acetone, acetic acid, and butyric acid. From the slopes of the least squares regression lines of optical density vs. time data, the maximum specific growth rates in the presence of varying concentrations of each inhibitor (μ_m^i) were determined. The results for each fermentation product are shown in Figures 1 - 3. There appears to be a threshold concentration which must be reached before growth inhibition occurs. This concentration was found to vary with each inhibitor studied. Above the threshold concentration, the growth inhibition can be described by a linear relationship of the form:

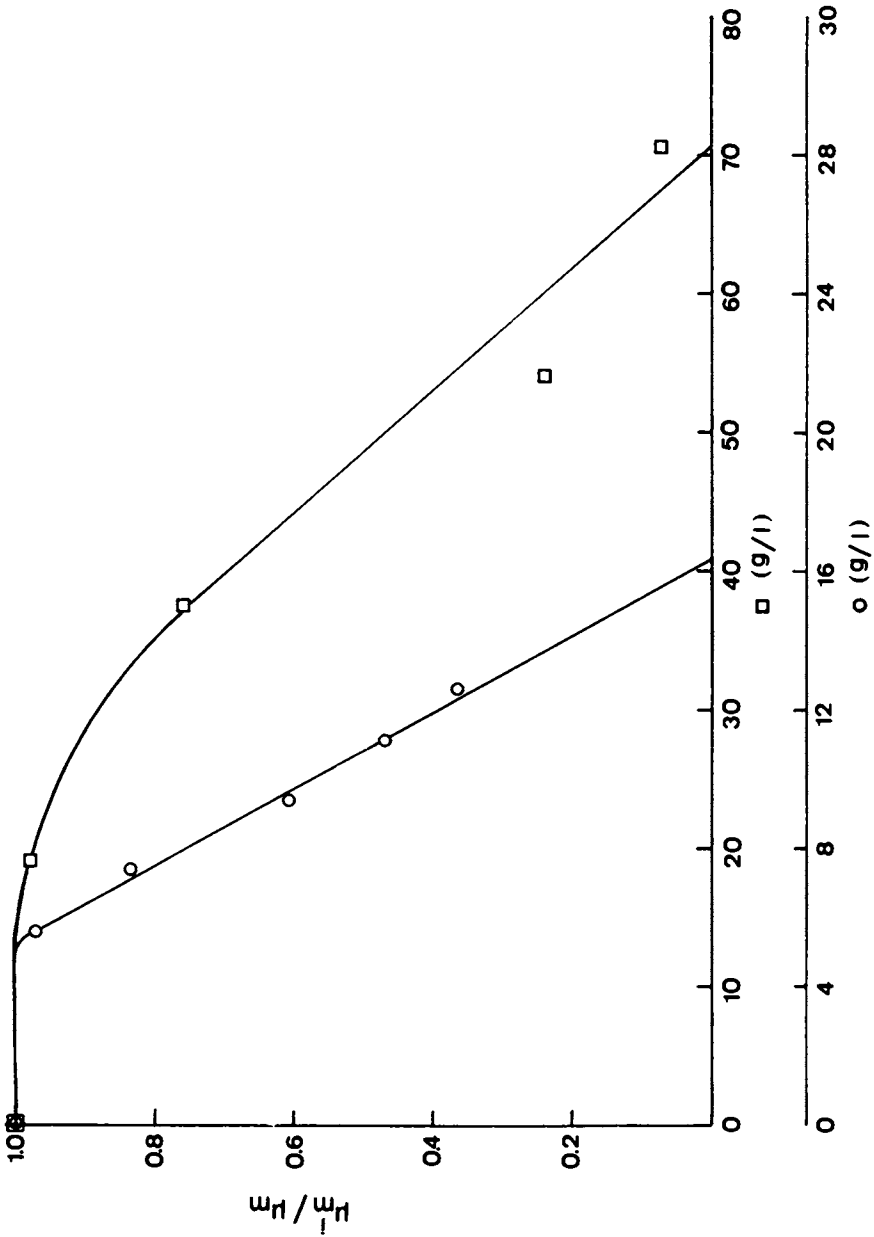


Figure 1. Maximum specific growth rates of *Cl. acetobutylicum* when challenged with various concentrations of ethanol and butanol. Key: \square , ethanol; \circ , butanol.

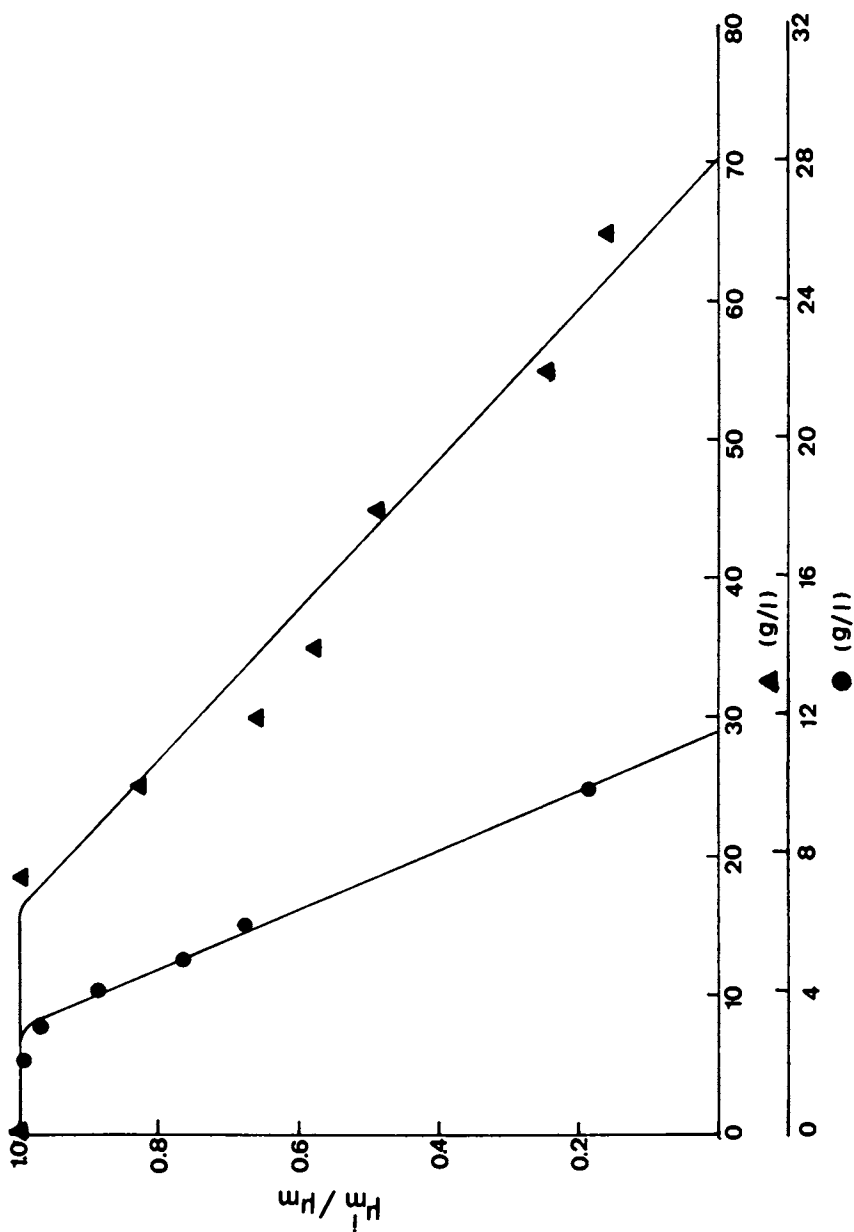


Figure 2. Maximum specific growth rates of *Cl. acetobutylicum* when challenged with various concentrations of acetone and acetic acid. Key: ▲, acetone; ●, acetic acid.

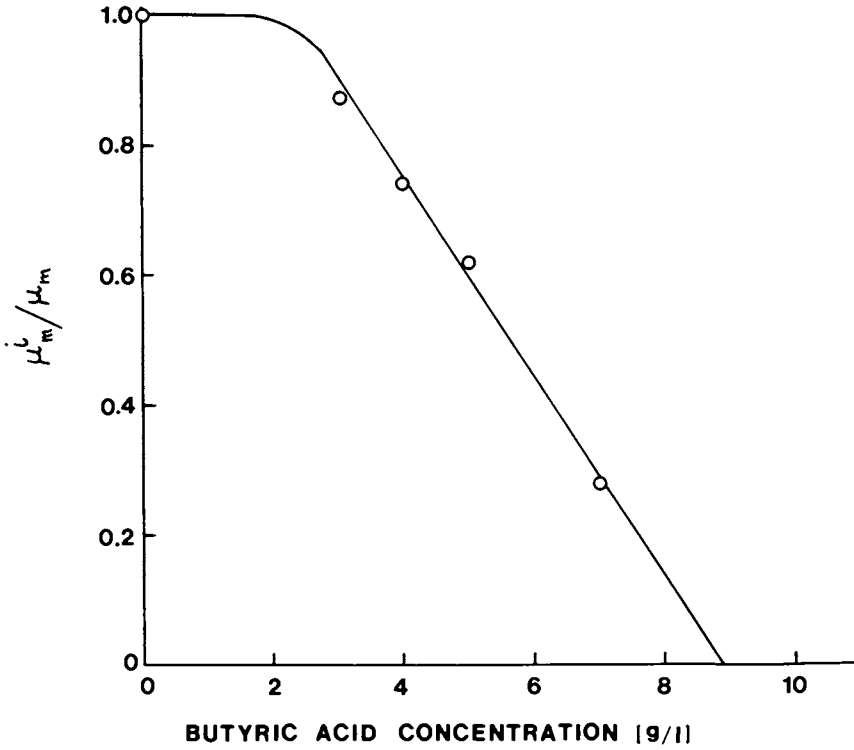


Figure 3. Maximum specific growth rate of *Cl. acetobutylicum* when challenged with various concentrations of butyric acid.

$$\mu_m^i = \mu_m \left[1 - \frac{1}{K_p} (P - P_o) \right] \quad \text{for } P \geq P_o \quad (1)$$

Concentrations causing a 50% reduction in growth rate were also determined. A summary of the inhibition data obtained is given in Table I.

Table I. Summary of Growth Inhibition Data

Product	K_p (M)	P_o (M)	Conc. at which growth was inhibited by 50%	
			<u>M</u>	<u>g/l</u>
Butyric Acid	0.07	0.02	0.07	6.0
Butanol	0.15	0.06	0.15	11.0
Acetic Acid	0.19	0.05	0.13	8.0
Acetone	0.98	0.26	0.88	43.5
Ethanol	1.01	0.26	1.10	51.0

The inhibition constant K_p for each product was calculated from the slope of the least squares regression line of μ_m^i/μ_m vs. P data. The inhibition constants for ethanol and acetone are approximately ten times greater than that for butanol, acetic acid, and butyric acid. This is indicative of the relatively low toxicity of acetone and ethanol as compared with the other fermentation products.

For each fermentation product, the P_o value was plotted against the K_p value as shown in Figure 4. The threshold concentration was found to increase linearly with an increasing K_p value. The equation of this line was determined to be:

$$K_p = 3.94 P_o - 0.03 \quad (2)$$

by a least squares regression analysis. The correlation coefficient was found to be 0.997.

Similar growth challenge experiments were performed using tert-butyl alcohol and n-hexanol. Although tert-butyl alcohol and n-hexanol are not products of this fermentation, the K_p and P_o values obtained for these two alcohols were found to lie on the straight line shown in Figure 4. Linden *et al.* (3) have shown that the end product toxicity in the acetone-butanol fermentation occurs by altering membrane functionality. The linear relationship between K_p and P_o may indicate that the inhibition of each of these various compounds occurs by the same mechanism.

The results of a 39-hour batch fermentation are shown in Figure 5. The levels of acetone and ethanol typically observed during a fermentation (5 g/l and 1.5 g/l respectively) were

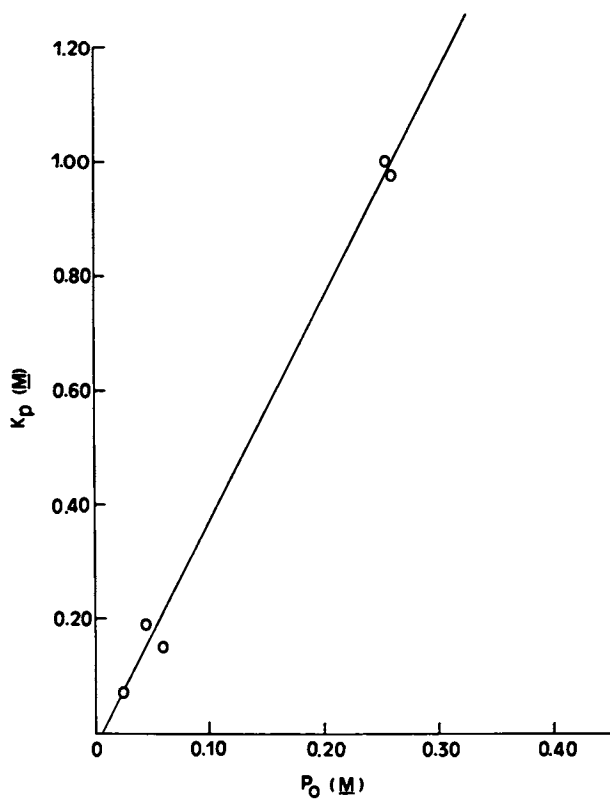


Figure 4. Relationship between K_p and P_o from the product inhibition studies.

found to be noninhibitory to cell growth. The highest concentrations of butyric acid and acetic acid which have been observed during fermentation are in the range of 3.5 to 4.0 g/l. These levels of acids approach those causing 50% inhibition of growth. Typical butanol concentrations observed during a fermentation are 11-12 g/l. Butanol is the only product that reaches levels actually causing 50% growth inhibition.

Recent results reported by Leung and Wang (5) show acetic and butyric acid concentrations causing 50% inhibition of growth, which are about twice the levels obtained in this work. The apparent disagreement between the two sets of data could be due to the different methods used in each case to stabilize the pH of the fermentation media during an acid challenge.

The methodology used in this study involved the use of a biological buffer, MES (2-[N-morpholino] ethanesulfonic acid) to stabilize the pH. Cells grown in two control flasks, one containing MES buffer and the other without MES buffer showed no difference in growth rates. This indicates that MES has no effect on the growth rate of the organism.

The methodology to stabilize the pH of the fermentation media reported by Leung and Wang (5) involved the preparation of 200 g/l solutions of acetate and butyrate by titration with NaOH. In this manner, the cells were exposed to Na⁺ concentrations in the range of 2-7 g/l. The high concentrations of Na⁺ may have an osmotic or membrane stabilizing effect which may account for the higher tolerance to acids. However, in spite of these discrepancies, this investigation supports the conclusion that the concentration of butanol is an important parameter in the acetone-butanol fermentation.

Attempts to model the cell growth curve during a batch fermentation by considering the inhibition due to each product separately resulted in much higher growth rates than were actually observed. Two factors could contribute to this discrepancy. On the one hand, the product inhibition experiments were carried out using each fermentation product separately. However, in an actual fermentation the products are present together. Thirteen hours into the fermentation, as shown in Figure 5, the concentration of each product is below the threshold concentration when growth inhibition was determined to occur. This indicates that no growth inhibition should be observed. However, the cell growth rate at this time was determined to be one-half of the maximum specific cell growth rate. This indicates that some synergism occurs among the several fermentation products and it is probably the total concentration of products which is important in determining the toxic effect on growth rate.

The other factor could be the difference in toxic effects of produced solvents as opposed to added solvents. Novak *et al.* (6) have shown that ethanol produced during a batch fermentation of *Saccharomyces cerevisiae* is more inhibitory than ethanol added to the fermentation. Therefore, it is possible that the inhibition

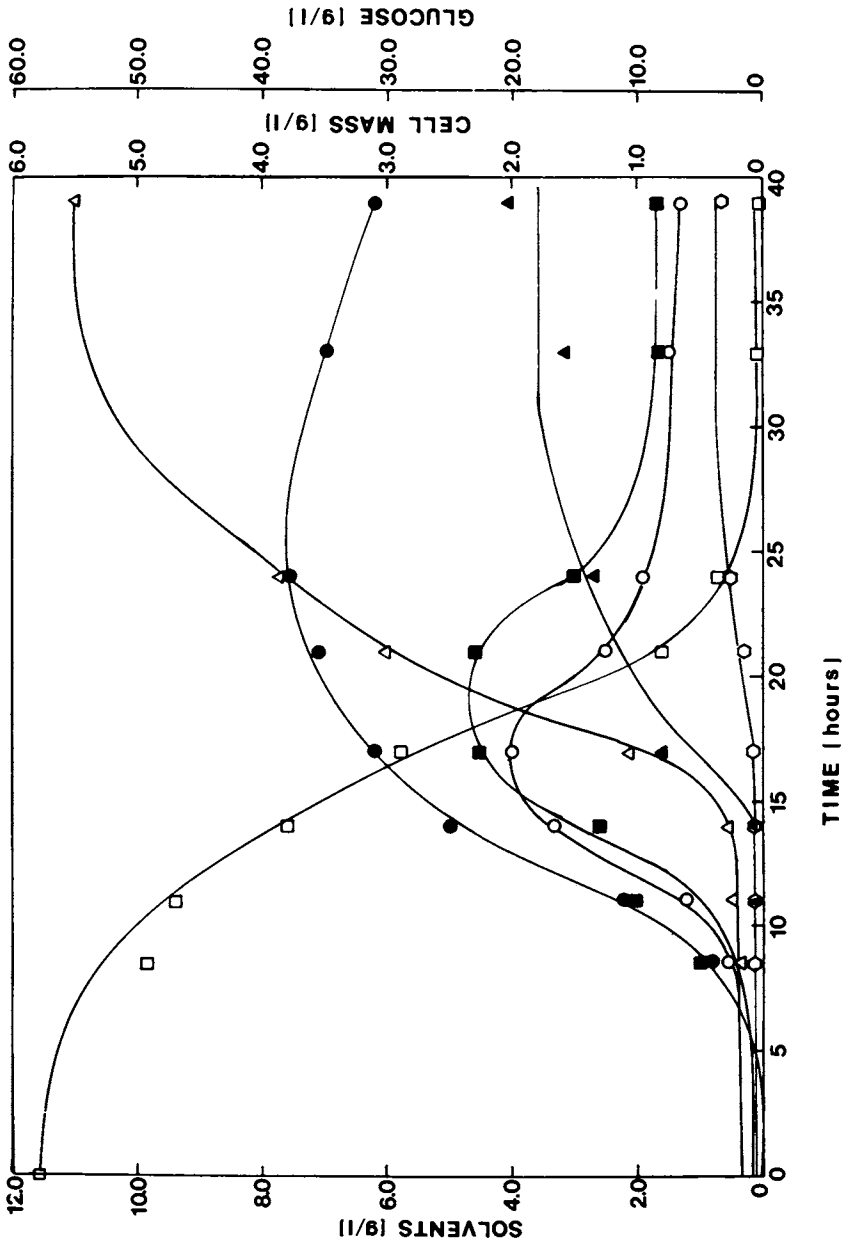


Figure 5. Batch production of solvents by *Cl. acetobutylicum* grown on soluble medium with pH controlled at 5.0. Key: □, glucose; ■, acetic acid; △, butanol; ○, butyric acid; ●, cell mass; ▲, acetone; ○, ethanol.

parameters determined in this study, based on added solvents, might be less severe than the actual values due to the solvents produced during the fermentation.

Conclusions

From these studies of growth inhibition and fermentation kinetics in the acetone-butanol fermentation, the following conclusions may be made:

1. At levels normally observed during fermentation
 - a. Butanol, acetic acid, and butyric acid are inhibitory to cell growth.
 - b. Acetone and ethanol show no inhibition effects.
2. For each fermentation product there is a threshold concentration below which no growth inhibition occurs and above which a linear decrease in growth rate is observed with an increase in product concentration.
3. There is a linear relationship between the threshold concentration (P_0) and the inhibition constant (K_P) for each fermentation product.
4. Preliminary observations seem to indicate that the growth inhibition caused by solvents produced during fermentation is different from the inhibition caused by externally added solvents.

Legend of Symbols

K_P	inhibition constant (M)
P	product concentration (M)
P_0	threshold product concentration (M)
μ_m	maximum specific growth rate (hr^{-1})
μ_m^i	maximum specific growth rate in presence of inhibitor (hr^{-1})

Acknowledgments

Partial support for this research was provided by the U.S. Department of Energy under Subcontract No. XK- ϕ -9059-1. The authors also wish to acknowledge Dr. James C. Linden for helpful discussions.

Literature Cited

1. Reed, G.; Pepler, H. J. "Yeast Technology;" Avi Publishing Co.: Westport, 1973; 185.

2. Steel, R. "Biochemical Engineering: Unit Processes in Fermentation;" Macmillan: New York, 1958; 125.
3. Linden, J. C.; Ulmer, D. C.; Moreira, A. R. "A Mechanism for Aliphatic Alcohol-Induced Toxicity in Clostridium acetobutylicum," presented at the 182nd National Meeting American Chemical Society, Division of Microbial and Biochemical Technology New York, New York. 1981.
4. Miller, G. C. Anal. Chem. 1959, 31, 426.
5. Leung, J. C. Y.; Wang, D. I. C. Proc. 2nd World Congress of Chemical Engineering. 1981, 1, 348.
6. Novak, M.; Strehaiano, P.; Moreno, M.; Goma, G. Biotechnol. Bioeng., 1981, 23, 201.

RECEIVED August 2, 1982

INDEX

- A**
- Acetone-butanol fermentation, growth inhibition kinetics
 experimental methods502, 503
 growth challenge experiments503-508
 pH controlled509, 510f
- Activator mechanisms of gene regulation 10f
- Aerobic growth without product formation, thermodynamic theory304-311
- Agrobacterium tumefaciens*, as example of demand theory 22
- Airlift columns—*See* Reactor equipment performance, systems with stationary internals
- Allosteric inhibitors 74
- Amensalism
 mixed cultures 209
 scheme for 211f
- Anaerobic growth, thermodynamic theory 314
- Antagonism in mixed cultures 209
- Antibiotics
 optimizing fermentation processes53-67
 production, penicillin 65
- Antiterminator mechanisms of gene regulation 11f
- B**
- Bacillus brevis*
 optimization of fermentation processes53-67
 in vivo inactivation of enzymes in 55
- Bacillus cereus*, competition in mixed cultures 208
- Bacteria, enteric, as example of demand theory 15
- Baker's yeast—*See* *Saccharomyces cerevisiae*
- "Bang-bang" policy 168
- Beer fermentation
 comparison of kinetic theory and experiment 494-500
 kinetic analysis490-494
 kinetics of yeast growth and metabolism 489-500
- Biocatalysts—*See* Immobilized cell catalysts
- Biochemical engineering—*See* Biotechnology
- Biomass production
 rate equations 468-469f
 thermochemical optimization463-488
- Bioreactor—*See* Reactor
- Bioreaction rates—*See* Reaction rates
- Biotechnology
 functional hierarchies 355-357t
 history 3
 structural hierarchies 355-357t
- Bubble columns
 mass transfer345, 346
 performance as bioreactor345, 346
- Butanol-acetone fermentation—*See* Acetone-butanol fermentation
- C**
- Candida tropicalis*, competition in mixed cultures 208
- Carbon source management in optimizing fermentations180-198
- Catalysts—*See* Immobilized cell catalysts
- Cell control system, cybernetic perspective165-176
- Cell cycle, models 137
- Cell division cycle, *Saccharomyces cerevisiae*151, 152f
- Cell mass production, optimization180-186
- Cell, as control system165-176
- Cellulase production by solid state fermentation421-442
- Cellulose, hydrolysis of, kinetic analysis of enzyme reaction 37
- Chaetomium cellulolyticum*, growth on corn stover429-432
- Chemiosmotic coupling324, 325f
See also Ion pumps
- Chemiosmotic hypothesis of oxidative phosphorylation 324
- Chemosensory movement properties—*See* Chemotaxis
- Chemotactic responses of various species268, 269f
- Chemotaxis265, 266

- Chemotaxis—
Continued
 and competition in mixed cultures .. 276t
 Chromatography, size exclusion,
 procedure 445-449
Clostridium acetobutylicum, acetone-
 butanol fermentation 501-512
 Clumping, mass transfer in viscous
 systems with microbial network
 structure 351
Colpoda steinii, feeding behavior
 in mixed cultures 215, 216, 219
 Commensalism, in mixed cultures 210-212
 Competition in mixed cultures 205-209
 effect of cell motility 286-289
 mathematical models 206-209
 Continuous culture
Hansenula polymorpha 187, 188f
 single-cell protein production 185-188
 Continuous reactors
 rate laws 466, 468
 reaction mechanism 464-467f
 Control
See also Regulation
 of reactor in reactor design 370-373t
 Cooper-Helmstetter model 137, 138, 140
 Cornell model 100-102t, 114-121f
 predictions 116-121f
 Crowding in mixed cultures 222, 223
 Cybernetic approach, diauxic growth .. 164
 Cybernetic perspective
 cell control system 165-176
 microbial growth 161-178
 Cytometry, flow 135, 139f
- D**
- Demand theory
Agrobacterium tumefaciens as
 example 22
 enteric bacteria as example 15
 gene regulation 3, 7
 development 13
 and physiology 16t
 Depolymerization of cell wall, kinetic
 analysis of enzyme reaction 35
 Design—*See* Reactor design
 Diauxic growth
 dissolved oxygen as indicator 171f
 example of cybernetic approach 164
Dictyostelium discoideum
 feeding behavior in mixed cultures 215
 predator for *Escherichia coli* 254
Didinium nasutum, feeding behavior
 in mixed cultures 214, 215
 DNA synthesis in bacteria 140
- E**
- Eccrinolysis in mixed cultures 214
 Ecology, and demand theory of
 gene regulation 15
 Ecosystems, effects of cell motility
 on populations 265-293
 Efficiency
 energetic, of ion pumps 326
 ion pumps 323, 326
 thermodynamic, for non-
 equilibrium 300-304
 Electrodes, enzyme 46, 48, 50f
 Electrogenic pumps—*See* Ion pumps
 Enteric bacteria
 demand theory 15
 gene regulation 15, 18t-21t
 and demand theory of gene
 regulation 15
 relation to gene control 3
 Enzymatic hydrolysis of starch 443-461
 effect of starch recrystallization 457, 458f
 effect of temperature 448
 Enzyme activity
 mechanisms of regulation 73t
 physiological patterns affecting 71, 72t
 Enzyme amount
 mechanisms of regulation 77-83
 physiological mechanisms of
 regulation 75
 physiological patterns of
 regulation 76, 77
 Enzyme electrodes 46, 48, 50f
 Enzyme inactivation in vivo 55, 57
 Enzyme systems, kinetics 27-52
 Henri equation 27-32
 Enzyme-catalyzed reactions, kinetics
 immobilized enzymes 38
 particulate substrates 32-37
 soluble substrates 27-32
 Enzymes
See also specific enzymes
 degradation of insoluble substrates,
 mass transfer 345
 immobilized cells as catalysts—*See*
also Immobilized cells
 preparation and reaction
 performance 377-392
 comparison of kinetics, with
 soluble enzymes 40f, 42t, 43
 kinetics 38-48, 343, 345
 production, strategies for
 optimization 189-191
 production of heparinase by
Flavobacterium heparinum 191-192f
 strategies for optimization ... 191-192f

- Enzymes—*Continued*
 production of maltase by
 Saccharomyces italicus 189–191
 production optimization 186–192
 reducing in vivo inactivation 53–67
- Escherichia coli*
 immobilized in epoxide beads, as
 immobilized cell catalyst 384–388f
 mathematical models 98, 99
 transient response 123
 mechanisms of enzyme regulation 80, 82
 mechanisms of regulation of
 enzyme activity 74
 model of single-cell kinetics 138–143
 in mixed cultures 209
 and parasitism in mixed cultures 221
 physiological patterns in enzyme
 regulation 76, 77
 population, mathematical growth
 model 138–143
 as prey for *Dictyostelium*
 discoideum 254
 regulation of enzyme activity in 73f
 structural genes 84
- F**
- Feeding
 See also Predation
 in mixed cultures 214–220
 mathematical model 219
- Fermentation—See Solid state
 fermentation
- Fermentation processes,
 optimization 179–198
 through control of in vivo inactivation
 of biosynthetic enzymes 53–67
- Flavobacterium heparinum*
 optimization of production 191, 192f
- Flow cytometry
 cell division of *Schizosaccharomyces*
 pombe 144, 146, 147f
 and frequency function 137, 139f
 measurement and analysis 155
- Flow in reactors, effect on interparticle
 mass transfer rates 339–342
- Frequency function, experimental
 determination 137, 139f
- Fungal growth, mechanism in solid
 state fermentation 426–437
- G**
- Gene control models 3–25
- Gene regulation
 in enteric bacteria 15, 18f–21f
 demand theory 3, 7
- Gene regulation mechanisms
 activator 10f
 antiterminator 11f
 negative 14f, 80
 positive 14f, 80
 proterminator 12f
 repressor 9f
- Generalist microorganism,
Thiobacillus A2
 as example 232, 234f, 235f
- Generalists in microbial population
 interactions 229–251
- Generalists and specialists—See
 Specialists and generalists
- Glucose oxidation, as example of
 immobilized enzyme reaction 45, 47f
- Gramicidin S synthetase
 factors affecting inactivation 57–61
 inactivation in vivo 55, 56f, 59, 60
 mechanism 62, 63f
 kinetics of inactivation 57, 58f
- Growth inhibition—See Kinetics,
 growth inhibition
- Growth of microorganisms in solid
 state fermentation of lignocel-
 luloses for protein and cellulase
 production 421–442
- Growth in multiple substrate
 systems 166–176
- Growth patterns of *Phycomyces*
 sporangiophores 403–420
 measurement 406–407
- Growth
 mathematical models of
 single cells 93–133
 and product formation 179–198
 microbial, cybernetic
 perspective 161–178
 and product formation 179–198
 organisms with rigid
 exoskeletons 415–417
- H**
- Halobium, measurement of potential
 changes in membrane 329
- Hansenula polymorpha*
 continuous culture 187, 188f
 single-cell protein source 187, 188f
 strategy for optimization of
 growth 187, 188f
- Henri equation, enzyme conversion
 of soluble substrates 27–32

- Heparinase, optimization of
production 191-192f
- Heat transfer in reactor design 368, 369
- History
biotechnology 3
enzyme kinetics 28
mathematical models of
cell population 94-96
solid state fermentation 421-423
- Hydrodynamics in reactor design 358-359
- Hydrolysis of cellulose, kinetic
analysis of enzyme reaction 37
- Hydrolysis of particulate substrate,
kinetic analysis of enzyme
reaction 32
- Hydrolysis of starches by amylase,
kinetic analysis of enzyme
reaction 36
- Hypomicrobium*, and *Pseudomonas*
interactions in mixed cultures 214
- I**
- Immobilized cell catalysts
deactivation 390, 391
effectiveness and Thiele
modulus 383-386
effectiveness, cleavage of peni-
cillin G by *Escherichia*
coli 384-388f
operational stability 390, 391
preparation entrapment
in polymeric carriers by ionic
gelation of poly-
electrolytes 379f, 380, 381f
in polymeric carriers by polycon-
densation of epoxy
resins 380-382f
- Immobilized enzymes
enzyme electrode as example 46, 48, 50f
kinetics 38-48, 343, 345
comparison with soluble
enzymes 39-43
pancreatic lipase 43
optimization 386
- Immobilized cell catalysts, prepa-
ration and reaction
performance 377-392
- Inhibition of product—*See*
Acetone-butanol fermentation
- Interfacial phenomena, effect in
reactor design 338-340f
- Interparticle mass transfer rates 342
- Intraparticle bioreaction rates 342
- Ion pumps
coupling models 327
energy transducers 323-331
- Ion pumps—*Continued*
measurement of potential changes
by light absorption 329
- Isoleucine, pathway for formation 85f, 86f
- Isosteric inhibitors 74
- K**
- Kinetic(s)
in biological reactor design 335-354
of enzyme systems 27-52
Henri equation 27-32
expeditiousness of ion pumps 323-331
growth inhibition, acetone-
butanol fermentation 501-512
experimental methods 502, 503
growth challenge experiments 503-508
pH controlled 509, 510f
of immobilized enzymes 343, 345
single-cell models 135-138
of yeast growth and metabolism
in beer fermentation 489-500
- Kinetic analysis
biological systems by power-
law formalism 4-7
derivation 5-7
evidence 6
complex biological systems 4
enzyme reactions
hydrolysis of cellulose 37
hydrolysis of particulate
substrate 32
hydrolysis of starch by amylase 36
general methods 3-25
- Klebsiella aerogenes*
physiological patterns of
enzyme regulation 76, 77
as prey for *Tetrahymena*
pyriformis 254
- L**
- Lactobacillus plantarum*, commensal
interaction in mixed cultures 212
- Lignocelluloses, fermentation—*See*
Solid state fermentation
- M**
- Maltase, optimization of production 189-191
- Mass transfer
See also Transport, Transfer
in reactor design 359-365
with reaction 360, 361f
effect of viscosity 365-367f
gas phase phenomena 326
interfacial coefficients 360
intraparticle 362

- Mass transfer in reactor
 design—*Continued*
 volumetric coefficient 363, 364f
- Mathematical models
 of beer fermentation kinetics 490–494
 comparison with experiment 494–500
 cell motility 265
 of cell population
 Cornell model 123, 125f
 description and history 94–96
 of commensalism in mixed
 cultures 212
 of competition in mixed
 cultures 206–209
 of competition of *Thiobacillus*
 A2, *T. neapolitanus* and
Spirillum G7 243f–245f
 comparison with experiment 245–250
 Cornell single-cell model
 examples of ideal model 96–99
 predictions 116–121f
 transient response 118, 122–125
 rationale 93, 94, 96
 metabolism 135–158
 of *Escherichia coli* 98, 99
 effect of cell motility on popu-
 lation 277–289
 of feeding behavior in mixed
 cultures 219
 of growth of single cells 93–133
 of interactions of mixed
 cultures 201–227
 of population growth, *Escherichia*
coli 138–143
 predator–prey dynamics 253–254
- Mechanisms of gene regulation
 activator 10f
 antiterminator 11f
 proterminator 12f
 repressor 9f
- Medium conservation equations 135
- Metabolic models, single-cell 135–158
- Metabolite excretion rates
 equations 470
 thermochemical optimization 463–488
- Metabolite flow
 enzymic mechanisms of
 regulation 73f
 physiological patterns of
 regulation 72
- Metabolite production
 optimization 186–192
 penicillin by *Penicillium*
chrysogenum 193–196
- Metabolite production—
Continued
 strategies for optimization 193–196
- Microbial growth
 cybernetic perspective 161–178
 and product formation,
 optimizing 179–198
 Microbial populations 135–158
 Microbial regulatory mechanisms 71–92
Micrococcus lysodeikticus
 comparison of immobilized and
 soluble enzymes in lysis 42
 kinetic analysis of enzymatic lysis 35
- Microorganisms as energy
 transducer 297f
- Mixed cultures
 competition of chemotactic
 strains 276f
 effect of cell motility 265–293
 effect of motility on compe-
 tition 286–289
 interactions 201–227
 interactions of specialists and
 generalists 229–251
 predator–prey dynamics 253–254
Thiobacillus A2 and *Spirillum G7* 237
Thiobacillus A2 with *T. neapoli-
 tanus*, *Spirillum G7*, or
 both 230–249
- Mixing in reactors
 See also Reactor equipment per-
 formance, mechanically
 stirred tanks
 effect on interparticle mass
 transfer rates 342
- Models
 See also Mathematical models
 cell cycle 137
 gene function 3–25
 stochastic, of *Phycomyces*
 sporangiophores 407–415
- Molecular size distribution of
 starch during enzymatic
 hydrolysis 443–461
- Motility
 chemotactic responses of various
 species 268, 269f
 effect in mixed cultures 265–293
 experimental observations 270–276f
 mathematical model 277–289
 peritrichously flagellated
 bacteria 266, 267f
- Multiple substrate systems,
 growth 166–176
- Mutation
Escherichia coli strains as immo-
 bilized cell catalysts 386, 388f

- Mutation—*Continued*
 and parasitism in mixed cultures .. 221
Saccharomyces italicus 189, 191f
 scheme for producing strain of
Serratia marcescens 87-90
 as tool for biochemical engineer .. 83-90
 Mutualism in mixed cultures 213-214
- N
- Negative mechanisms of gene
 expression regulation 13
- O
- Optimal strategy in micro-
 organisms 161-178
 Optimization
 immobilized cell catalyst, Aceto-
 bacter simplex 386, 388f, 389f
 microbial growth and product
 formation 178-198
 of cell mass 186-192
 of enzymes 186-192
 of metabolites 186-192
 thermochemical, of microbial
 biomass-production and
 metabolite-excretion rates .. 463-488
 and in vivo inactivation of bio-
 synthetic enzymes 53-67
 Optimum temperature for biological
 processes, relation to substrate
 concentration 463-488
 Osmotic processes—*See* Chemios-
 motic coupling
 Oxidation, glucose, immobilized
 enzyme reaction 45, 47f
 Oxygen transfer in mold pellets .. 343, 344f
 Oxygen, dissolved
 contours in *Pseudomonas ovalis*
 colonies 395-401
 as indicator in diauxic growth 171f
- P
- Pancreatic lipase, comparison of
 kinetics of immobilized and
 soluble enzymes 43
Paramecium and *Didinium nasutum*
 in mixed cultures 214, 215
 Parasitism in mixed cultures 221
 Penicillin G, cleavage by *Escherichia*
coli, immobilized cell
 catalyst 384-388f
 Penicillin production
 computer control 193-196
 Penicillin production—
Continued
 strategies for optimization 193-196
 Phosphorylation, chemiosmotic
 hypothesis of oxidative 324, 325f
Phycomyces sporangiophores
 growth patterns 403-420
 sensory apparatus 403-420
 Physiology and demand theory 16t
Polyporus versicolor, destruction
 of wood 428-429
 Population(s)
 dissolved oxygen in *Pseudo-*
monas ovalis colonies 395-401
 interactions in mixed culture .. 201-227
 classification 202
 of mixed specialists and
 generalists 229-251
 relation to single-cell operation 137
 Population analysis, for single-cell
 metabolic models 135-158
 Population balance
 equations 135, 136, 146
Poria monticola, destruction of
 wood 428
 Positive mechanisms of gene
 expression regulation 13
 Power-law formalism, for kinetic
 analysis of biological systems ... 4-7
 derivation of 5-7
 evidence for 6
 Predation dynamics, microbial 253-264
 Predator-prey dynamics
Dictyostelium discoideum as
 predator for *Escherichia*
coli 255-263f
 mathematical model 253-254
 Process synthesis at reactor level,
 in reactor design 367
Propionibacterium shermanii, com-
 mensal interaction in mixed
 cultures 212
 Protein amount, physiological pat-
 terns of regulation 76, 77
 Protein formation, mechanisms of
 regulation 77-83
 Protein
 microbial, reactor design 355
 single-cell
 continuous culture 185-187
Hansenula polymorpha 187, 188f
 strategies for optimizing
 production 185-187
 from lignocelluloses by solid
 state fermentation 421-442
 Proterminator mechanisms of
 gene regulation 12f

- Protocooperation in mixed cultures 213-214
- Proton pumps—*See* Ion pumps
- Pseudomonas* and *Hyphomicrobium*, interactions in mixed cultures 214
- Pseudomonas ovalis* colonies, dissolved oxygen contours 395-401
- R**
- Reactor design
- See also* Reactor design fundamentals
- constraints 335, 336
- effect of flow 339-342
- effect of interfacial phenomena 338, 340*f*
- effect of interparticle transfer rates 339-342
- kinetics and transport phenomena 335-354
- effect of mixing 342
- rate controlling steps 336-338
- stagnant reactor 339
- systems approach 355-358
- Reactor design fundamentals 335-376
- heat transfer 368, 369
- hydrodynamics 358-359
- mass transfer 359-365
- process synthesis at reactor level 369
- reactor control 369-373*t*
- scale-up 370
- Reactor equipment performance
- bubble columns 345, 346
- mechanically stirred tanks 347-351
- systems with stationary internals 346
- Reaction mechanism
- modified Michaelis-Menten ... 464-467*f*
- for process whose rates saturate in substrate concentration 464-467*f*
- Reaction performance, immobilized cells as catalysts—*See* Immobilized cells
- Reaction rate laws
- development, for processes whose rates saturate in substrate concentration 466, 468-477
- thermal sensitivity 470-477
- Reaction rates, intraparticle 342-345
- Reactors
- effect of start-up conditions on growth of *Schizosaccharomyces pombe* 146, 147*f*
- microbial, population balance equations 135, 136
- Regulatory mechanisms, microbial ... 71-92
- Repressor mechanisms of gene regulation 9*f*
- S**
- Saccharomyces cerevisiae*
- cell division cycle 151, 152*f*
- fed-batch fermentation 181-184
- computer control 181-184
- strategy for fermenter operation 181-184
- mathematical model of growth kinetics 150-154
- Saccharomyces italicus*
- mutation 189, 191*f*
- optimization of maltase production 189, 191*f*
- Scale-up in reactor design 370, 374
- Schizosaccharomyces pombe*
- cell cycle 145*f*
- flow cytometer measurements 144, 146, 147*f*
- mathematical model of growth kinetics 142, 144-150
- trajectory tracking kinetics 149*f*, 150
- Serratia marcescens*
- mutation for production of isoleucine 87*f*
- production of isoleucine 84-86*f*
- Sewage treatment 250
- See also* *Thiobacillus* A2, T. *neapolitanus*, *Spirillum* G7
- Single-cell kinetics, steady-state models 138
- Single-cell metabolic models 135-158
- Single-cell protein
- continuous culture 185-187
- optimizing production 185-187
- source, *Hansenula polymorpha* 187, 188*f*
- Size distribution of starch
- determination by size exclusion chromatography 445-449
- during enzymatic hydrolysis 443-461
- Size exclusion chromatography, procedure 445-449
- Size of starch
- effect of recrystallization 457, 458*f*
- effect of temperature 448
- Solid state fermentation
- of grains 423
- of lignocellulose 421-442
- choice of microorganisms 426
- mechanism of fungal growth 426-437
- physiological aspects 437, 438
- pretreatment of lignocelluloses 424-426
- requirements 437, 438
- Spirillum* G7 as example 232, 234*f*, 235*f*
- Thiobacillus neapolitanus* as example 232, 234*f*, 235*f*
- Specialists and generalists
- growth rate 230, 231

- Specialists and Generalists—*Continued*
 model bacteria 233*t*
 Specialists in microbial population
 interactions 229–251
Spirillum G7
See also Thiobacillus A2
 as example of specialist 232, 234*f*, 235*f*
 metabolism 233*t*
 specific growth rates 236*t*
 SSF—*See* Solid state fermentation
 Starch, effect of recrystallization
 on molecular size 457, 458*f*
 Starch, effect of temperature on
 molecular size 448
 Starch, hydrolysis of
 as example of kinetic analysis
 of enzyme reaction 36
 physical model 459, 460*f*
 Starch, molecular size distribution
 during enzymatic hydrolysis 443–461
 Steady-state models of single-cell
 kinetics 138
 Strategies
 optimizing microbial growth and
 product formation 179–198
 survival, specialist and generalist
 populations 250
 Symbiosis in mixed cultures 222
 Systems approach to reactor design—
See Reactor design

T

- Tetrahymena pyriformis*
 feeding behavior in mixed
 cultures 215–221
 predator for *Klebsiella aerogenes* .. 254
 Thermal sensitivity of process rates,
 relation of substrate con-
 centration 477–484
 Thermal sensitivity of reaction rate
 laws 470
 Thermochemical optimization—*See*
 Optimization, thermochemical
 Thermodynamic(s)
 macroscopic, and growth and
 product formation of micro-
 organisms 295–322
 of microorganisms 296
 nonequilibrium, of ion pumps 329
 nonequilibrium, for living
 organisms 295–322
 aerobic growth without
 product formation 304–311
 growth with electron acceptors
 other than oxygen 312–313

- Thermodynamics—
Continued
 thermodynamic constraints 299
 balance equations 298
 Thermodynamic constraints 299
 Thermodynamic efficiency 300–304
 of growth, constant efficiency
 hypothesis 316
Thiobacillus A2
 specific growth rates 236*t*
 competition with both *T. neapolitanus*
 and *Spirillum* G7
 232, 237–241*f*, 247, 249*f*
 mathematical model 242–245*f*
 as example of generalist 232, 234*f*, 235*f*
 metabolism 233*t*
Thiobacillus neapolitanus
See also Thiobacillus A2
 as example of specialist 232, 234*f*, 235*f*
 metabolism 233*t*
 specific growth rates 236*t*
 Time-series analysis 418, 419
 applied to *Phycomyces blakeslee-*
anus sporangiophores 403–420
 Trajectory tracking kinetics, in
Schizosaccharomyces pombe 149*f*, 150
 Transfer rates in reactors
 dependence on flow and mixing 339–342
 interparticle 339–342
 Transfer, mass
 in airlift columns 346
 in bubble column reactors 345, 346
 in mechanically stirred reactors 347–351
 Transfer, oxygen
 in mold pellets 343–344*f*
 in *Pseudomonas ovalis* colonies 395–401
 Transient experiments, test of
 mathematical models 143*f*
 Transient response in single cell,
 mathematical model 118, 122–125*t*
 Transport phenomena, in biological
 reactor design 354–354

U

- Urease electrode 46

- Valine, pathway for formation 85*f*, 86*f*

Y

- Yeast growth and metabolism in beer
 fermentation
 comparison with experiment 494–500
 kinetics 489–500
 theory 489–494